



HAL
open science

Les macrophages périvasculaires cérébraux comme modulateurs de la réponse inflammatoire post-ischémique

Damien Levard

► **To cite this version:**

Damien Levard. Les macrophages périvasculaires cérébraux comme modulateurs de la réponse inflammatoire post-ischémique. Médecine humaine et pathologie. Normandie Université, 2021. Français. NNT : 2021NORMC424 . tel-03555391

HAL Id: tel-03555391

<https://theses.hal.science/tel-03555391>

Submitted on 3 Feb 2022

HAL is a multi-disciplinary open access archive for the deposit and dissemination of scientific research documents, whether they are published or not. The documents may come from teaching and research institutions in France or abroad, or from public or private research centers.

L'archive ouverte pluridisciplinaire **HAL**, est destinée au dépôt et à la diffusion de documents scientifiques de niveau recherche, publiés ou non, émanant des établissements d'enseignement et de recherche français ou étrangers, des laboratoires publics ou privés.



Normandie Université

THÈSE

Pour obtenir le diplôme de doctorat

Spécialité SCIENCES DE LA VIE ET DE LA SANTE

Préparée au sein de l'Université de Caen Normandie

Les macrophages périvasculaires cérébraux comme modulateurs de la réponse inflammatoire post-ischémique

**Présentée et soutenue par
DAMIEN LEVARD**

**Thèse soutenue le 15/12/2021
devant le jury composé de**

MME AGNES NADJAR	Chargé de recherche HDR, Université Bordeaux 2 Victor Segalen	Rapporteur du jury
MME SUSANNE WEGENER	Professeur, University Hospital Zurich	Rapporteur du jury
M. ANTOINE DRIEU	Chercheur, Université de Washington - USA	Membre du jury
M. COSTANTINO IADECOLA	Professeur, Weill Cornell Medical College	Membre du jury
M. DENIS VIVIEN	Professeur des universités PraticienHosp, Université Caen Normandie	Président du jury
MME MARINA RUBIO	Ingénieur HDR, Université Caen Normandie	Directeur de thèse

Thèse dirigée par MARINA RUBIO, Physiopathologie et imagerie des troubles neurologiques



UNIVERSITÉ
CAEN
NORMANDIE



Normande de Biologie Intégrative,
Santé, Environnement



La science pour la santé
From science to health

Résumé

L'AVC ischémique est l'une des principales causes de décès et d'invalidité permanente dans le monde. Les processus inflammatoires induits par l'AVC ont été proposés comme des contributeurs clés de la physiopathologie de l'AVC ischémique. Alors que le rôle de la microglie dans l'AVC ischémique a été largement étudié, celles des macrophages associés aux bordures du SNC (BAMs) restent largement inconnues. Notre hypothèse, basée sur les études décrites précédemment et sur la localisation privilégiée des BAMs à l'interface entre le compartiment vasculaire et le parenchyme cérébral, était que les BAMs pouvaient jouer un rôle majeur dans la réponse inflammatoire déclenchée par l'AVC, *via* la médiation du recrutement et l'infiltration des leucocytes. De plus, sur la base d'études précédentes, nous avons fait l'hypothèse que les BAMs pourraient moduler les réponses inflammatoires induites par l'AVC de manière différente en fonction de l'état inflammatoire basal du cerveau, en particulier au cours du vieillissement.

Pour tester cette hypothèse, nous avons étudié l'AVC chez des souris jeunes et âgées avec ou sans déplétion antérieure des BAMs. Nos résultats ont montré que le déficit fonctionnel de l'AVC était aggravé chez les souris âgées déplétées en BAMs. Cette aggravation du résultat fonctionnel s'accompagnait (i) d'une augmentation de l'expression de la P-sélectine endothéliale, (ii) d'une augmentation du roulement et de l'adhésion des leucocytes à la paroi vasculaire, et (iii) d'une infiltration accrue de leucocytes dans l'hémisphère lésé. Ces réponses immunitaires exacerbées étaient présentes à la fois dans la phase aiguë et subaiguë après le début de l'AVC, suggérant ainsi que la présence de BAMs assure un contrôle à long terme de la réponse immunitaire après un AVC. En utilisant le séquençage ARN à partir de BAMs isolés, nous montrons que les BAMs modifient leur phénotype transcriptomique au cours du vieillissement pour surexprimer des gènes impliqués dans la régulation de la réponse immunitaire innée et adaptative et de la présentation des antigènes.

Nos résultats montrent que les BAMs acquièrent au cours du vieillissement un rôle central dans l'orchestration de la réponse neuroinflammatoire déclenchées par un AVC, et que leur présence garantit une bonne régulation de la réponse immunitaire.

Abstract

Ischemic stroke is one of the main causes of death and permanent disability worldwide. Stroke-induced inflammatory processes, including the activation of resident glial cells as well as the invasion of circulating leukocytes, have been proposed as key contributors of the ischemic stroke pathophysiology. While the responses of microglia to ischemic stroke have been extensively studied, those of border-associated macrophages (BAMs) remain largely unknown. In this study, we hypothesized that BAMs could influence stroke-induced inflammatory responses, particularly during aging and thus final stroke recovery.

We thus compared stroke outcome in young and old mice subjected to thromboembolic stroke with or without a previous depletion of BAMs. Our results show that functional outcome following stroke was worsened in depleted mice without modification of the lesion volumes, exclusively in aged mice. This worsening in the functional outcome was accompanied by (i) an increase of endothelial P-selectin expression, (ii) an increased leukocyte rolling and adhesion to the vessel wall, and (iii) an increased leukocyte infiltration in the injured hemisphere. These exacerbated immune responses were present at both the acute and the sub-acute phase (up to 5 days) after stroke onset, thus suggesting that the presence of BAMs ensures a long-term control of the immune response after stroke. Using cell sorted RNAseq, we show that BAMs change their transcriptomic phenotype during aging, overexpressing genes implicated in the regulation of both innate and adaptive immune responses and antigen presentation.

Taken together, our results reveal that BAMs acquire during aging a central role in orchestrating the neuroinflammatory response triggered by stroke, and that their presence guarantees good regulation of the immune response.

Table des matières

Table des abréviations (fr/en)

Index des figures

INTRODUCTION

Les accidents vasculaires cérébraux	1
<i>Historique</i>	1
<i>Définition</i>	2
<i>Classification</i>	3
<i>Traitement</i>	4
<i>Facteurs de risque</i>	5
<i>Physiopathologie de l'AVC ischémique</i>	6
Excitotoxicité	6
Apoptose	7
Inflammation	8
L'inflammation cérébrale et les accidents vasculaires cérébraux	11
<i>Historique</i>	11
<i>Brève présentation du système immunitaire</i>	12
<i>Mécanismes d'action de l'inflammation</i>	14
<i>L'inflammation cérébrale après AVC : description et principaux acteurs</i>	16
Microglie	16
Astrocytes	17
Cellules endothéliales et molécules d'adhésion	18
Neutrophiles	19
Lymphocytes T	20
Cicatrisation et réparation tissulaire	21
<i>Essais cliniques immunomodulateurs</i>	24
Anakinra	24
Minocycline	24
Natalizumab	25
Enlimomab	25
Fingolimod	25

<i>Voies d'entrée des cellules inflammatoires</i>	27
<i>L'inflammation dans les modèles expérimentaux</i>	29
Filament intraluminal	29
Électrocoagulation	30
Photothrombose	31
Thomboembolique	32
<i>Influence des facteurs de risque de l'AVC sur l'inflammation cérébrale</i>	35
<i>Impact du vieillissement sur l'accident vasculaire cérébral</i>	38
<i>Le priming inflammatoire, point commun aux différentes comorbidités</i>	42
Les macrophages résidents du système nerveux central	45
<i>La microglie</i>	47
Historique	47
Caractérisation	48
Rôles	49
Surveillance de l'environnement	49
Entretien physiologique du système nerveux central, ou « <i>Housekeeping</i> »	49
Protection et défense du SNC	49
<i>Les macrophages associés aux bordures du système nerveux central</i>	52
Description anatomique des interfaces entre le système nerveux central et la périphérie	52
Les méninges	53
L'espace périvasculaire	53
Les plexus choroïdes	54
Les macrophages périvasculaires	56
Historique	56
Origine	59
Caractérisation moléculaire et fonctionnelle	60
Rôles en condition physiologique	65
Intégrité de la BHE	65
Présentation d'antigènes	65
Drainage du LCR	67
Implications des PVM dans les pathologies cérébrales	67
Rôle des PVM dans les altérations de la BHE	67
Rôle des PVM dans les pathologies amyloïdes	68
Rôle des PVM dans les infections du SNC	69
Rôle des PVM dans la sclérose en plaque	70

Rôle des PVM dans les maladies cérébrovasculaires et facteurs de risques associés	71
Les macrophages méningés	74
Les macrophages des plexus choroïdes	75
OBJECTIFS	79
RÉSULTATS	81
DISCUSSION	129
Les BAMs acquièrent au cours du vieillissement un rôle central en tant que régulateurs de la réponse neuroinflammatoire	131
Les BAMs changent de phénotype durant le vieillissement	132
<i>Timing</i> de mesure des déficits post-AVC et limite du modèle	135
Liens entre réaction inflammatoire, volume de lésion ischémique et déficits neurologiques	138
Limite de la méthode de déplétion et différentes voies d'entrées dans le SNC des leucocytes périphériques	139
Interaction entre les BAMs et les fibroblastes du SNC	141
Conclusion	144
AUTRES TRAVAUX	146
RÉFÉRENCES BIBLIOGRAPHIQUES	236

Table des abréviations (fr/en)

ACM / MCA : artère cérébrale moyenne / *middle cerebral artery*

AD : maladie d'Alzheimer / *Alzheimer disease*

ADN : acide désoxyribonucléique / *deoxyribonucleic acid*

AIF : *apoptosis-inducing factor*

APP : protéine précurseur de l'amyloïde / *amyloid precursor protein*

ARN : acide ribonucléique / *ribonucleic acid*

ATP : adénosine triphosphate / *adenosine triphosphate*

AVC : accident vasculaire cérébral / *stroke*

A β : peptide amyloïde bêta / *amyloid beta peptide*

BAMs/CAMs : macrophages associés aux bordures du SNC / *CNS border associated macrophages*

Bcl-2 : *B-cell lymphoma 2*

BCSFB : barrière sang-liquide céphalorachidien / *blood-cerebrospinal fluid barrier*

BHE : barrière hémato-encéphalique / *blood-brain barrier*

CAA : angiopathie amyloïde cérébrale / *cerebral amyloid angiopathy*

CCR2 : *C-C chemokine receptor type 2*

CDX : groupe de différentiation X / *cluster of differentiation X*

ChP : plexus choroïde / *choroid plexus*

ChPM : macrophages des plexus choroïdes / *choroid plexus macrophages*

Csfr1 : *colony stimulating factor 1 receptor*

Cx3cr1 : *CX3C chemokine receptor 1*

DAMPS : motifs moléculaires associés aux dégâts / *damage-associated molecular patterns*

DC : cellules dendritiques / *dendritic cells*

DNase : désoxyribonucléase / *deoxyribonuclease*

EAE : encéphalomyélite auto-immune expérimentale / *experimental autoimmune encephalomyelitis*

EMP : *erythromyeloid progenitors*

FGP : *fluorescent granular perithelial cells*

GFAP : protéine acide fibrillaire gliale / *glial fibrillary acidic protein*

GFP : protéine fluorescente verte / *green fluorescent protein*

HexB : *beta-hexosaminidase subunit beta*

HIVE : encéphalite associée au virus de l'immunodéficience humaine / *human immunodeficiency virus encephalitis*

HLA-DR : *human leukocyte antigen – DR isotype*

HSC : cellules souches hématopoïétiques / *hematopoietic stem cells*

ICAM-1 : *intercellular adhesion molecule-1*

ICV : injection intracérébroventriculaire

IL-X : *interleukin-X*

INSERM : Institut National de la Santé et de la Recherche Médicale / *National Institute of Health and Medical Research*

IRM / MRI : imagerie par résonance magnétique / *magnetic resonance imaging*

LCR / CSF: *liquid céphalorachidien / cerebrospinal fluid*

Lyve-1 : *lymphatic vessel endothelial hyaluronan receptor 1*

MCP-1 : *monocyte chemoattractant protein 1*

MHC II : complexe majeur d'histocompatibilité de classe II / *class II major histocompatibility complex*

MM : macrophages méningés / *meningeal macrophages*

MMP9 : *matrix metalloproteinase 9*

NETs : *neutrophils extracellular traps*

NK : *natural killer*

NLR : *Node-like receptors*

NMDA : N-méthyl-D-aspartate

NOS : oxyde nitrique synthase / *nitric oxide synthase*

NOX2 : *NADPH oxidase 2*

P2ry12 : *purinergic receptor P2Y12*

PVM : macrophages périvasculaire / *perivascular macrophages*

ROS : radicaux libres oxygénés / *reactive oxygen species*

SHR : *spontaneously hypertensive rat*

SigleCH : *sialic acid binding Ig-like lectin H*

SIV : virus d'immunodéficience simienne / *simian immunodeficiency virus*

SNC : système nerveux central / *central nervous system*

TGF- β : *transforming growth factor- β*

TLR : *Toll-like receptors*

Tmem119 : *transmembrane protein 119*

TNF : facteur de nécrose tumorale / *tumor necrosis factor*

TOAST : *Trial of ORG 10172 in Acute Stroke Treatment*

tPA : activateur tissulaire du plasminogène / *tissue-type plasminogen activator*

TRITC : *Tetra methyl Rhodamine Iso Thio Cyanate*

VCAM-1 : *vascular cell adhesion molecule-1*

VEGF : *vascular Endothelial Growth Factor*

VIH / HIV : virus de l'immunodéficience humaine / *human immunodeficiency virus*

Index des figures

<i>Figure 1 : La mort du roi George Ier, frappé d'une attaque d'apoplexie au cours d'un voyage, en 1727.</i>	1
<i>Figure 2 : L'AVC représente la première cause de handicap acquis de l'adulte.</i>	2
<i>Figure 3 : Les deux principaux types d'accidents vasculaires cérébraux.</i>	4
<i>Figure 4 : Planisphère montrant le taux d'AVC attribuable à des facteurs de risque modifiables en 2013.</i>	5
<i>Figure 5 : Excitotoxicité et apoptose causés par les flux de calcium intracellulaire.</i>	8
<i>Figure 6 : Les 5 caractéristiques de l'inflammation.</i>	12
<i>Figure 7 : Représentation schématique des composants des systèmes immunitaires innés et acquis.</i>	13
<i>Figure 8 : Représentation schématique du mécanisme d'action de la réaction inflammatoire.</i>	15
<i>Figure 9 : Étapes de la transmigration leucocytaire : implication des molécules d'adhésion endothéliales.</i>	19
<i>Figure 10 : Image en microscopie électronique à balayage de NETs libérés par un neutrophile dans un caillot de fibrine.</i>	20
<i>Figure 11 : Illustration de la réaction inflammatoire après un accident vasculaire cérébral ischémique.</i>	23
<i>Figure 12 : Traitements immunomodulateurs testés en clinique dans le cadre de l'AVC ischémique.</i>	26
<i>Figure 13 : Comparaison de l'AVC humain et des modèles expérimentaux d'AVC chez les rongeurs.</i>	34
<i>Figure 14 : Le vieillissement induit des modifications physiologiques pouvant impacter l'AVC ischémique.</i>	41
<i>Figure 15 : Priming microglial induit par le vieillissement et le stress chronique.</i>	43
<i>Figure 16 : Anatomie et marqueurs des différentes populations de macrophages résidents du SNC.</i>	46
<i>Figure 17 : Illustrations de cellules microgliales réalisées par Pío del Río Hortega.</i>	48
<i>Figure 18 : Représentation de 3 rôles de la microglie.</i>	51
<i>Figure 19 : Anatomie des barrières entre le SNC et la périphérie.</i>	55
<i>Figure 20 : Observation de macrophages périvasculaires autour de vaisseaux sanguins de cerveaux de rats par Masao Mato.</i>	57
<i>Figure 21 : Chronologie des découvertes majeures, des premières descriptions des interfaces du SNC jusqu'aux études des BAMs.</i>	58
<i>Figure 22 : Origine ontogénique des macrophages du système nerveux.</i>	60
<i>Figure 23 : Caractérisation immunohistologique des PVM.</i>	61
<i>Figure 24: Mécanisme d'action du clodronate</i>	63
<i>Figure 25 : Localisation anatomique des macrophages périvasculaires (PVM) et méningés (MM).</i>	64
<i>Figure 26 : Mécanisme de présentation d'antigène par la voie MHCII.</i>	66
<i>Figure 27 : L'Aβ circulant est retrouvé dans les PVM, module le stress oxydatif et le dysfonctionnement du couplage neurovasculaire.</i>	69
<i>Figure 28 : Macrophages périvasculaires infectés par le SIV dans le cerveau des macaques.</i>	70
<i>Figure 29 : Les PVM modulent l'effet aggravant de la consommation chronique d'alcool sur l'AVC ischémique chez la souris.</i>	72
<i>Figure 30 : Rôles des PVM dans les pathologies cérébrales.</i>	73
<i>Figure 31 : Différentes populations de macrophages aux interfaces du SNC.</i>	76

<i>Figure 32 : Altérations des différentes populations de leucocytes du SNC (hors microglie) lors du vieillissement</i>	134
<i>Figure 33 : Déficits fonctionnels mesurés à l'aide d'un test de préhension automatisé</i>	137
<i>Figure 34 : Voies d'infiltration cérébrale méningée et par les plexus choroïdes pour les leucocytes dans la neuroinflammation post-AVC.</i>	140
<i>Figure 35 : Localisation des fibroblastes dans le cerveau de souris adulte et organisation des cicatrices gliales et fibrotiques.</i>	142

INTRODUCTION

INTRODUCTION

Les accidents vasculaires cérébraux

Historique

Hippocrate, le « père de la médecine », a reconnu pour la première fois un accident vasculaire cérébral il y a plus de 2 400 ans. Il a appelé ce phénomène « apoplexie », qui est un terme grec qui signifie « frappé violemment ». Bien que ce nom décrive le côté soudain de la pathologie, il ne traduit pas nécessairement ce qui se passe réellement dans le cerveau.

Des siècles plus tard, dans les années 1600, un médecin du nom de Jacob Wepfer a découvert que quelque chose perturbe l'approvisionnement en sang dans le cerveau des personnes décédées d'apoplexie. Dans certains cas, il y avait un saignement massif dans le cerveau, tandis que dans d'autres cas les artères étaient bouchées (Engelhardt, 2017).

Dans les décennies qui ont suivi, la science et la médecine ont continué à faire des progrès concernant les causes et les symptômes de l'apoplexie. L'un des résultats de ces progrès a été la division de l'apoplexie en catégories basées sur la cause de la maladie. Après cela, l'apoplexie est devenue connue sous des termes tels que l'infarctus cérébral ou l'accident vasculaire cérébral (AVC).



Figure 1 : La mort du roi de Grande-Bretagne George Ier, frappé d'apoplexie au cours d'un voyage, en 1727.

Illustration du Cassell's Illustrated History of England, vol.4 (1865).

Définition

Un accident vasculaire cérébral (AVC) est un déficit neurologique soudain qui a pour origine un trouble vasculaire. Parfois appelé « attaque cérébrale » l'AVC induit des symptômes variables en fonction de la zone lésée, de sa gravité et du type d'AVC : perte de motricité, perte de sensibilité, trouble du langage, perte de connaissance et décès.

Les handicaps courants post-AVC comprennent les déficiences motrices telles que l'hémiplégie (faiblesse du côté gauche ou droit du corps), l'hémiplésie (paralysie du côté gauche ou droit du corps) et la parésie faciale centrale (Amarenco *et al.*, 2009). Les troubles du langage et de la parole sont également courants, tels que l'aphasie globale ou mixte (troubles de la compréhension du langage) et la dysarthrie (troubles de la parole) (Beal, 2010). D'autres handicaps incluent des niveaux de conscience altérés, des troubles de la vision et une diminution du flux sanguin vers certaines parties du cerveau (Khoshnam *et al.*, 2017). Tous ces handicaps ont des effets drastiques sur la qualité de vie des patients victimes d'un AVC.

En France, on dénombre chaque année plus de 140 000 nouveaux cas d'accidents vasculaires cérébraux, soit un toutes les quatre minutes. L'AVC représente la première cause de handicap physique acquis chez l'adulte, la deuxième cause de démence (après la maladie d'Alzheimer) et la deuxième cause de mortalité avec 20% des personnes qui décèdent dans l'année suivant l'AVC (Inserm).



Figure 2 : L'AVC représente la première cause de handicap acquis chez l'adulte.

Inserm.fr/accident-vasculaire-cerebral-avc

Classification

Les AVC existent principalement sous deux formes selon la nature du désordre vasculaire : ischémique, la plus commune, dans 80 % à 85% des cas, ou hémorragique dans 15% à 20% des cas.

Les AVC hémorragiques, ou hémorragies cérébrales, sont causés par la rupture d'une artère cérébrale du cortex ou des méninges qui l'entourent. La cause principale est souvent la rupture d'un anévrisme, une dilatation anormale de la paroi artérielle. L'hémorragie peut également être due à un traumatisme ou une tumeur. Par ailleurs, une maladie comme l'angiopathie amyloïde cérébrale peut être responsable d'hémorragies spontanées.

Les AVC ischémiques, également appelés infarctus cérébraux, sont quant à eux causés par l'obstruction du flux sanguin par un caillot, qui peut avoir plusieurs origines. Selon la classification TOAST ([Chung et al., 2014](#)), l'athérosclérose est la cause la plus fréquente (30 %) des cas d'AVC. Un thrombus se forme au contact d'une plaque d'athérome (accumulation de lipides, glucides, produits sanguins, tissus adipeux) qui se fragmente et se détache pour obstruer une artère distale. L'ischémie cérébrale peut également être d'origine cardioembolique ; dans ces cas une cardiopathie (arythmie cardiaque le plus souvent) va être responsable de la libération d'un thrombus dans la circulation artérielle. Ce sont les grosses artères, telles que l'artère cérébrale moyenne (ACM) et la carotide qui sont les plus souvent touchées dans ces deux principaux sous-types d'AVC ischémiques.

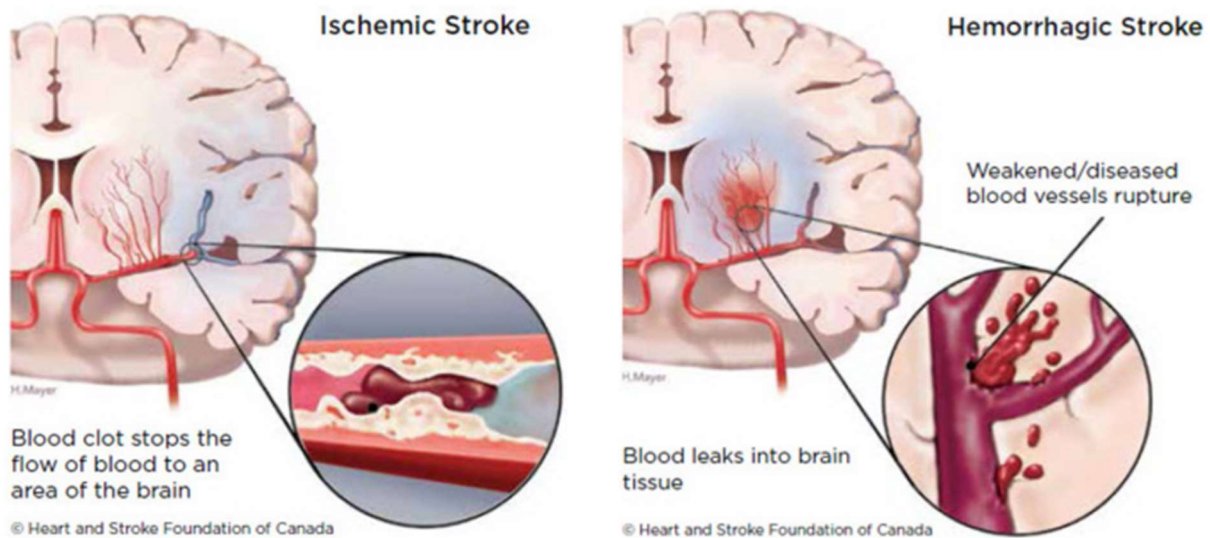


Figure 3 : Les deux principaux types d'accidents vasculaires cérébraux.

Heart and Stroke Foundation of Canada.

Traitement

Il n'existe à l'heure actuelle que deux traitements approuvés en clinique pour l'AVC ischémique aigu : la thrombolyse du caillot par administration intraveineuse d'activateur tissulaire du plasminogène (tPA, Actilyse) et l'élimination du caillot par thrombectomie mécanique endovasculaire. L'utilisation de ces traitements reste cependant limitée. En effet, en pratique le traitement pharmacologique par administration de tPA est limité à une courte fenêtre thérapeutique de 4h30 après apparition des symptômes (Khoshnam *et al.*, 2017), avec un risque accru d'hémorragie cérébrale au-delà de ce délai. Par ailleurs, la thrombectomie endovasculaire peut être réalisée jusqu'à 24 heures après le début des symptômes en fonction des critères d'imagerie, à condition de disposer du matériel et du personnel nécessaire (Thomalla and Gerloff, 2019; Casetta *et al.*, 2020). Des traitements préventifs, tels que des anticoagulants et des médicaments hypotenseurs et hypocholestérolémiants, peuvent également être administrés, car il existe un risque accru de subir un deuxième AVC dans les jours suivants l'AVC initial (Hossmann, 2006). L'administration rapide de ces traitements peut aider à atténuer les effets des incapacités que l'AVC peut causer.

Facteurs de risque

Le vieillissement est le facteur de risque non modifiable majeur, bien que l'AVC peut survenir à tout âge. En effet, si l'âge moyen de survenue de l'AVC est de 74 ans, 25% des patients ont moins de 65 ans et 10% moins de 45 ans. En 2013, on estimait que d'ici 2050 plus de 1,5 milliard de personnes auront plus de 65 ans, ce qui augmentera fortement la prévalence des AVC (Krishnamurthi *et al.*, 2013).

Outre le vieillissement, les principaux facteurs de risque d'AVC sont l'hypertension, l'hypercholestérolémie, la sténose carotidienne et la fibrillation auriculaire. En effet, des essais cliniques ont montré que le traitement de ces affections réduit l'incidence des AVC (Hart, Pearce and Aguilar, 2007; Raman *et al.*, 2013; Collins *et al.*, 2016). De plus, le tabagisme, la consommation excessive d'alcool et le diabète sont également des facteurs de risque importants, ainsi que la pollution de l'air, la sédentarité ou l'obésité (Peters, Huxley and Woodward, 2014; Zhang *et al.*, 2014; Mons *et al.*, 2015). On estime que les dix principaux facteurs de risques modifiables représentent environ 90% du risque d'AVC dans la population. Ainsi, tous ces facteurs, s'ils étaient modifiés, pourraient réduire drastiquement l'incidence des AVC (Hankey, 2017).

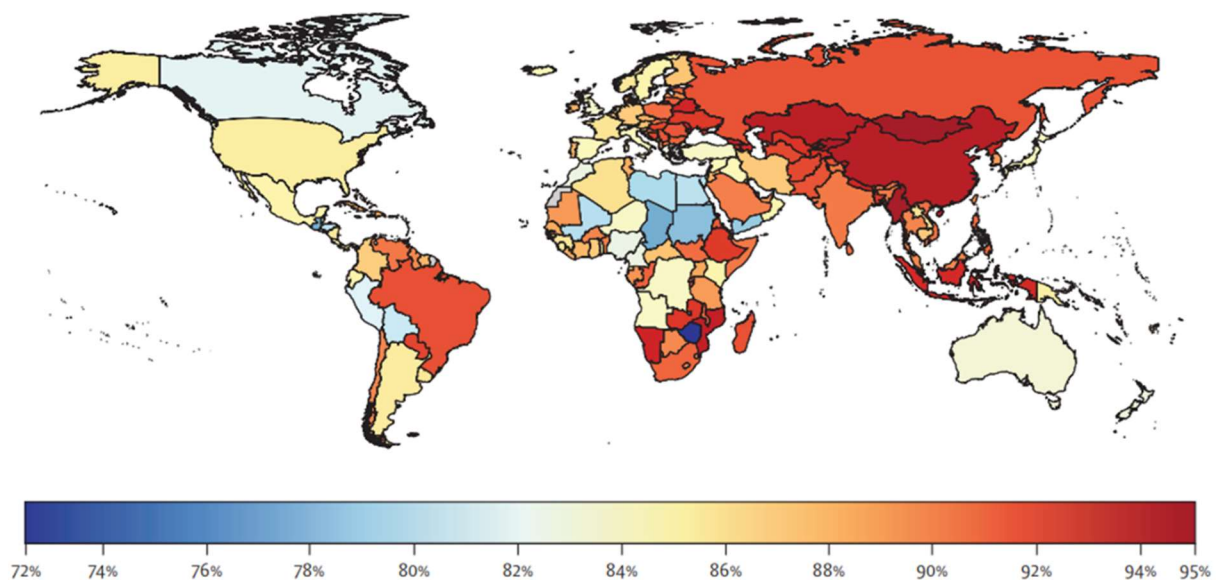


Figure 4 : Planisphère montrant le taux d'AVC attribuable à des facteurs de risque modifiables en 2013.

D'après "Global burden of stroke and risk factors in 188 countries, during 1990–2013: a systematic analysis for the Global Burden of Disease Study 2013" (Feigin *et al.*, 2016).

Physiopathologie de l'AVC ischémique

Lors d'un AVC ischémique, l'interruption du flux sanguin induit une privation d'oxygène pour les neurones, qui se trouvent alors privés d'énergie.

L'AVC ischémique focal est caractérisé par un cœur ischémique, au sein duquel la mort cellulaire survient quelques minutes après l'occlusion artérielle. Le tissu cérébral dans cette région est généralement considéré comme irrécupérable. La région péri-lésionnelle entourant le cœur ischémique est appelée pénombre (tissu à risque), dans lequel il y a une réduction partielle de l'apport sanguin en raison de la présence de vaisseaux collatéraux. La récupération de la pénombre par recanalisation rapide est corrélée avec de meilleurs résultats neurologiques chez les patients victimes d'un AVC, et le tissu dans cette zone est la cible principale de médicaments neuroprotecteurs en développement (Candelario-Jalil and Paul, 2021).

Après le début de l'ischémie plusieurs processus conduisent à la mort des cellules : excitotoxicité, stress oxydatif, inflammation et apoptose. Ces différents processus pathologiques sont liés entre eux et se déclenchent mutuellement ; ils ont un effet sur l'ensemble des cellules du système nerveux central (SNC), aboutissant à la mort cellulaire et à l'apparition de troubles neurologiques (Khoshnam *et al.*, 2017).

Excitotoxicité

L'excitotoxicité a été le premier mécanisme moléculaire impliqué dans les lésions ischémiques cérébrales à être identifié et étudié en détails. L'excitotoxicité désigne la libération rapide et massive de glutamate, un acide aminé excitateur, à la suite du déficit énergétique (Chamorro *et al.*, 2016)

La consommation d'oxygène du cerveau par rapport à son poids est très élevée (environ 20% de l'oxygène de l'organisme) et doit générer suffisamment d'adénosine triphosphate (ATP) *via* la chaîne respiratoire mitochondriale pour maintenir et restaurer les gradients ioniques des cellules (Claassen *et al.*, 2021). Au niveau cellulaire, le manque d'oxygène causé par l'ischémie provoque un dysfonctionnement de la phosphorylation oxydative et de la synthèse d'ATP, conduisant à la consommation en seulement quelques

minutes de tout l'ATP disponible. Le manque d'ATP induit entraîne un arrêt de la pompe Na^+/K^+ ATPase, causant une dépolarisation de la membrane plasmique, une entrée massive de sodium dans les cellules et une libération de potassium dans l'espace extracellulaire.

De plus, l'arrêt de la pompe à calcium Ca^{2+} -ATPase provoque une augmentation massive de la concentration de calcium intracellulaire, qui active plusieurs protéines des voies de signalisation de mort cellulaire telles que les lipases et DNAses (Khoshnam *et al.*, 2017). L'afflux d'ions calcium dans les neurones provoque la libération de glutamate en excès. Cet excès de glutamate sur-stimule les récepteurs du glutamate des autres neurones, en particulier les récepteurs N-méthyl-D-aspartate (NMDA-R). L'accumulation de glutamate active également des voies de signalisation activant des enzymes cytotoxiques, notamment des protéases, nucléases et caspases, amenant à la mort du neurone (Chamorro *et al.*, 2016).

Apoptose

L'apoptose est aussi connue sous le nom de mort cellulaire programmée. Elle est importante durant le développement et tout au long de la vie en conditions physiologiques pour le renouvellement cellulaire. L'apoptose intervient également dans la physiopathologie de l'AVC. Différents stimuli vont activer des voies de signalisation mitochondriales et déclencher des signaux de mort cellulaire par des voies apoptotiques.

Pendant l'ischémie, l'activation des récepteurs NMDA et l'accumulation de calcium intracellulaire provoque également le clivage du domaine d'interaction de la protéine Bcl-2. Au niveau de la membrane mitochondriale, la Bcl-2 tronquée interagit avec des protéines pro-apoptotiques et ouvre les pores mitochondriaux. L'ouverture des pores favorise la libération du cytochrome C mitochondrial et du facteur d'induction de l'apoptose (AIF, *apoptosis-inducing factor*). Cela entraîne une cascade d'activation des caspases, provoquant des dommages à l'acide désoxyribonucléique (ADN) et la mort cellulaire par apoptose (Nikoletopoulou *et al.*, 2013). Il a été rapporté que les protéines caspases sont particulièrement activées dans la zone péri-lésionnelle de l'ischémie et que leur inhibition pourrait protéger le tissu cérébral (Li *et al.*, 2000).

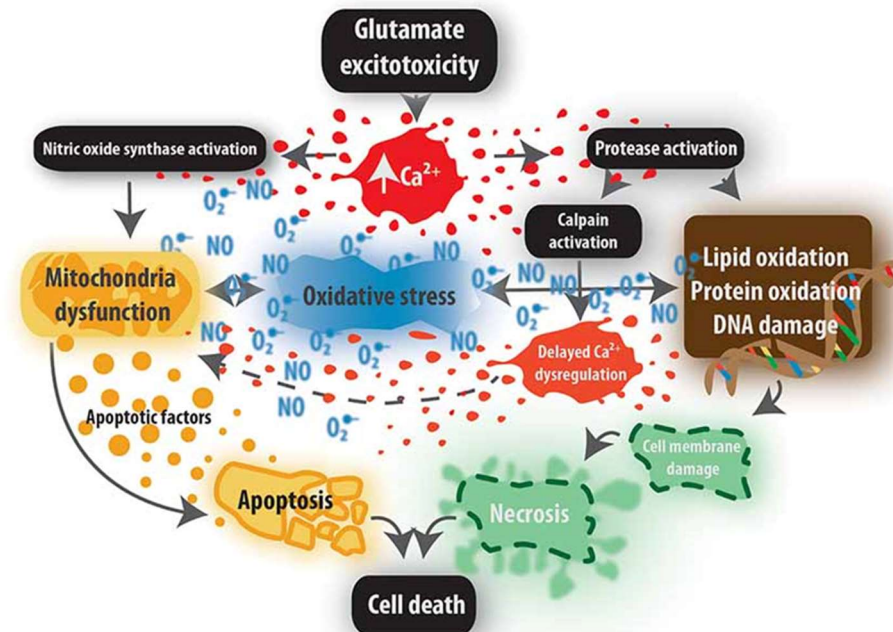


Figure 5 : Excitotoxicité et apoptose causés par les flux de calcium intracellulaire.

Des concentrations élevées de Ca^{2+} intracellulaire conduisent à l'activation d'enzymes telles que les protéases et l'oxyde nitrique synthase (NOS). Il en résulte un dysfonctionnement des mitochondries, un stress oxydatif et une oxydation de macromolécules essentielles, contribuant à l'apoptose ou à la nécrose. D'après "Ischemia-Triggered Glutamate Excitotoxicity From the Perspective of Glial Cells" (Kirdajova 2020)

Inflammation

L'inflammation est la réaction du système immunitaire en réponse à une agression. Cela joue un rôle central dans la physiopathologie des maladies cérébrovasculaires, et en particulier de l'AVC ischémique. Juste après le début de l'ischémie, la réponse inflammatoire est initiée par plusieurs signaux envoyés par les cellules en souffrance dans le tissu. La réponse inflammatoire est un processus complexe, hautement régulé, qui implique de nombreux types cellulaires différents, des médiateurs inflammatoires et des récepteurs cellulaires. Les mécanismes détaillés de la réaction inflammatoire spécifique à l'AVC ischémique sont présentés dans la section suivante.

- ❖ Un AVC est un déficit neurologique soudain qui a pour origine un trouble vasculaire.
- ❖ Il existe deux formes d'AVC : ischémiques dans 80% des cas et hémorragique dans 20% des cas.
- ❖ Lors d'un AVC ischémique, l'interruption du flux sanguin par un caillot induit une privation d'oxygène pour les neurones, qui se trouvent alors privés d'énergie.
- ❖ Le vieillissement est le facteur de risque non modifiable majeur, même si l'AVC peut survenir à tout âge.
- ❖ Plusieurs processus conduisent à la mort cellulaire : excitotoxicité, stress oxydatif, apoptose et inflammation

- ❖ *Stroke is a sudden neurological deficit that originates from a vascular disorder.*
- ❖ *There are two forms of stroke: ischemic in 80% of cases and hemorrhagic in 20% of cases.*
- ❖ *In an ischemic stroke, the interruption of blood flow by a clot causes oxygen deprivation for neurons, which are then deprived of energy.*
- ❖ *Aging is the major unmodifiable risk factor, although stroke can occur at any age.*
- ❖ *Several processes lead to cell death: excitotoxicity, oxidative stress, apoptosis and inflammation*

L'inflammation cérébrale et les accidents vasculaires cérébraux

Historique

L'inflammation est connue depuis plusieurs milliers d'années, et des descriptions de ce phénomène peuvent même être trouvées dans des papyrus de l'Égypte antique. Du latin *inflammatio*, pour « allumer » ou « mettre le feu », le terme a probablement été introduit par l'auteur romain Aulus Cornelius Celsus au 1^{er} siècle après JC. Dans son traité *De medicina*, Celsus aurait été le premier à décrire les 4 principaux symptômes de l'inflammation : « *rubor et tumor cum calore et dolore* », c'est-à-dire rougeur et gonflement avec chaleur et douleur. La base physiologique de ces quatre signes cardinaux a été fondée bien plus tard par Augustus Waller (1846) et Julius Cohnheim (1867), grâce aux progrès de la microscopie. En analysant des tissus lésés, ils ont observé la vasodilatation, la fuite de plasma et la migration des leucocytes hors des vaisseaux sanguins vers les tissus environnants (Medzhitov, 2010).

Le 5^{ème} signe de l'inflammation, *functio laesa* (perturbation fonctionnelle) a été ajouté par Rudolph Virchow en 1858 dans son livre *Cellularpathologie*. Il a participé à établir les bases cellulaires de la pathologie ; une rupture radicale avec la vision traditionnelle de la médecine depuis l'époque d'Hippocrate, qui décrivait la maladie comme un déséquilibre des quatre humeurs (Medzhitov, 2010). Une autre étape importante a été la découverte de la phagocytose par Elie Metchnikoff décrite dans sa théorie de l'immunité cellulaire en 1892. Selon lui, l'inflammation était un processus de défense régulé par les phagocytes ; une invasion du tissu par ses propres leucocytes. Metchnikoff a souligné le rôle clé des neutrophiles et des macrophages dans la défense de l'organisme et dans le maintien de l'homéostasie tissulaire, révélant les côtés bénéfiques de l'inflammation qui n'était plus considérée uniquement comme une maladie (Parnes, 2008). Aujourd'hui il est courant de faire la distinction entre inflammation aiguë et chronique, la première faisant référence à des processus sains et normaux de protection et de réparation, la seconde à des processus dégénératifs nocifs. La compréhension que nous avons de ces phénomènes a depuis évolué, mais l'idée générale reste essentiellement la même.

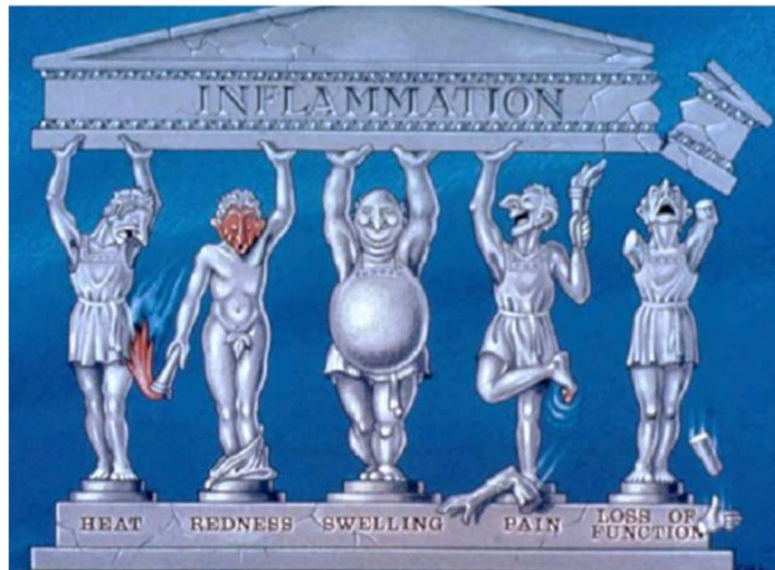


Figure 6 : Les 5 caractéristiques de l'inflammation.

Les 4 premières observées sont chaleur, rougeur, gonflement et douleur. Plus tard a été ajouté le déficit fonctionnel. D'après « *Anti-inflammatory lipid mediators and insights into the resolution of inflammation* » (Lawrence et al., 2002).

Brève présentation du système immunitaire

L'inflammation est la réaction du système immunitaire à une agression externe ou interne. Le système immunitaire comprend des structures, des cellules et des molécules qui, ensemble, sont chargés de défendre l'organisme contre les agents pathogènes ou les traumatismes physiques. Il est classiquement divisé en deux parties : le système immunitaire inné et le système immunitaire acquis.

Le système immunitaire inné est caractérisé par des réponses rapides et non spécifiques. Il joue un rôle essentiel dans la prévention ou la limitation de l'invasion de microorganismes, l'élimination des débris ainsi que la cicatrisation et le remodelage tissulaire. Ce système comprend les barrières anatomiques (la peau, les muqueuses, etc.), des gradients physiologiques (la température, le pH, etc.), des cellules lymphoïdes innées (lymphocytes *Natural Killer*), mais aussi des cellules phagocytaires (neutrophiles, macrophages, cellules dendritiques). Pour détecter les signaux de danger ou les pathogènes et déclencher une réponse immunitaire, ces cellules utilisent des récepteurs de reconnaissance de motifs tels que les récepteurs de types NOD (NLR, *Node-like receptors*), des récepteurs Toll-like (TLR, *Toll-*

like receptors) et des récepteurs *scavengers* (« éboueurs » en français) (Postolache *et al.*, 2020).

L'immunité acquise ou adaptative implique d'autres cellules, les lymphocytes T et B, ciblant des antigènes spécifiques et ayant une mémoire de l'exposition antérieure de l'organisme à ces antigènes, permettant une réponse plus rapide et ciblée. Les lymphocytes T ont des fonctions cytotoxiques ou régulatrices, et sont activés ou réactivés en reconnaissant des antigènes qui leur sont présentés par les complexes majeurs d'histocompatibilité. Les lymphocytes B produisent des immunoglobulines et ont des interactions réciproques avec les lymphocytes T et les cellules de l'immunité innée (Postolache *et al.*, 2020).

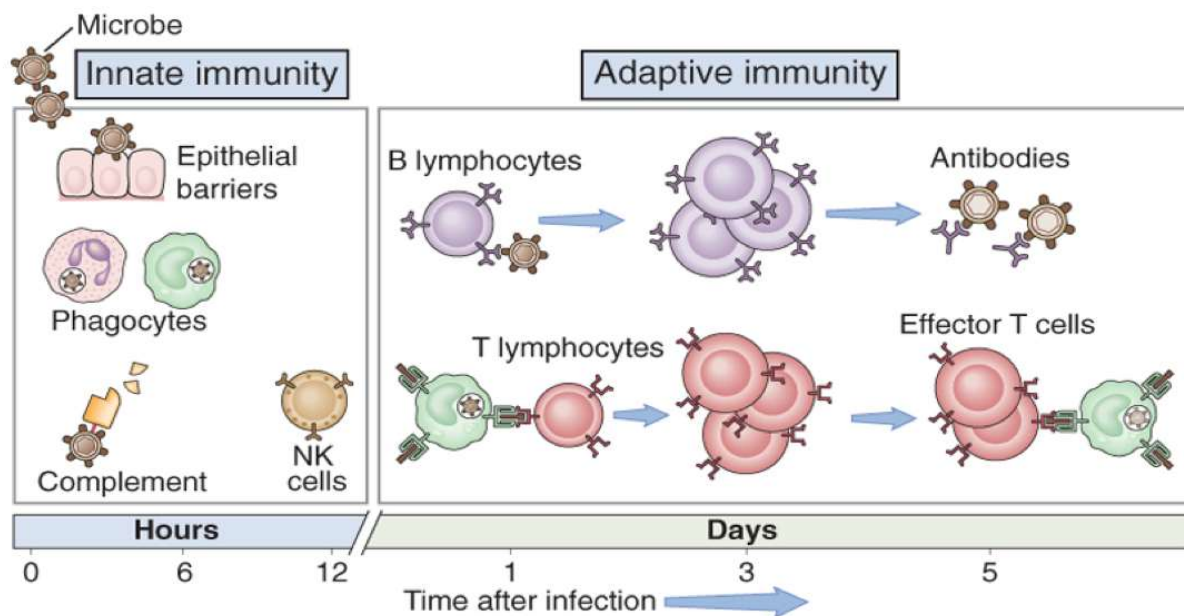


Figure 7 : Représentation schématique des composants des systèmes immunitaires innés et acquis.

D'après "Abbas & Lichtman : Basic Immunology, 3rd Edition. 2008 by Saunders."

Mécanismes d'action de l'inflammation

Classiquement, la réponse inflammatoire aiguë déclenchée par une infection ou une lésion tissulaire entraîne l'acheminement de composés sanguins (plasma et leucocytes) au site d'infection ou de lésion (Majno and Joris, 2004). Cette réaction a notamment bien été caractérisée pour les infections bactériennes, dans ce cas de figure elle est déclenchée par les récepteurs TLR et NLR du système immunitaire inné (Barton, 2008). Cette reconnaissance initiale de l'infection est médiée par les macrophages et mastocytes résidents dans le tissu, conduisant à la production d'une variété de cytokines, des médiateurs inflammatoires. Ces médiateurs provoquent localement un exsudat inflammatoire : les protéines plasmatiques et les leucocytes (en particulier les neutrophiles), qui sont normalement restreints dans les vaisseaux sanguins, accèdent au tissu extravasculaire au niveau du site de l'infection. Lorsqu'ils atteignent la zone cible, les neutrophiles sont activés, soit par contact direct avec l'agent pathogène, soit par l'action des cytokines sécrétées par les cellules résidentes du tissu lésé. Les neutrophiles tentent d'éliminer le pathogène en libérant le contenu toxique de leurs granules, qui comprennent des radicaux libres oxygénés (ROS, *reactive oxygen species*) et des enzymes de dégradation (Nathan, 2006; Barton, 2008).

Une réponse inflammatoire aiguë réussie entraîne l'élimination des agents infectieux suivie d'une phase de résolution de l'inflammation et de réparation tissulaire, qui est principalement médiée par les macrophages résidents et recrutés dans les tissus. Le passage des médiateurs sécrétés de pro- à anti-inflammatoire inhibe le recrutement des neutrophiles

et favorise le recrutement des monocytes qui éliminent les cellules mortes et initient le remodelage tissulaire (Serhan and Savill, 2005).

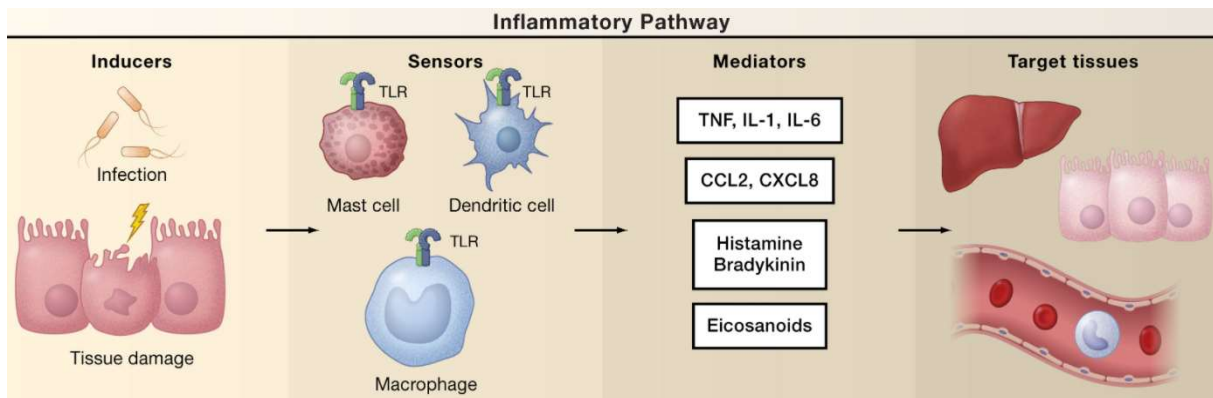


Figure 8 : Représentation schématisée du mécanisme d'action de la réaction inflammatoire.

D'après « Inflammation 2010: New Adventures of an Old Flame » (Medzhitov 2010).

Si la réponse inflammatoire aiguë ne parvient pas à éliminer les pathogènes, le processus inflammatoire persiste et acquiert de nouvelles caractéristiques. L'infiltrat de neutrophiles est remplacé par des macrophages dérivés des monocytes sanguins, et en cas d'infection également par les lymphocytes T. Si l'effet combiné de ces cellules est encore insuffisant, un état inflammatoire chronique s'installe. En plus des agents pathogènes persistants, l'inflammation chronique peut résulter d'autres causes telles que le vieillissement, des réponses auto-immunes contre des antigènes du soi ou des corps étrangers non-dégradables (Medzhitov, 2008).

L'inflammation cérébrale après AVC : description et principaux acteurs

Lors d'un AVC, la réaction inflammatoire est une cascade de réactions orchestrées qui s'initie immédiatement après l'occlusion du vaisseau et va évoluer et perdurer durant les jours et les semaines suivantes (Anrather and Iadecola, 2016). Ce processus a été profondément étudié au cours de la dernière décennie, en particulier la phase aiguë correspondante aux premières 48 heures après la survenue de l'AVC (Iadecola and Anrather, 2011; Anrather and Iadecola, 2016; Drieu *et al.*, 2018; Levard *et al.*, 2020). La réponse inflammatoire est initiée lors des premières lésions cellulaires par la libération de facteurs moléculaires associés aux dommages (DAMPs, *damage-associated molecular patterns*), ainsi que des cytokines inflammatoires. Ces molécules activent des récepteurs à la surface de la microglie (des cellules immunitaires résidentes du cerveau) et des astrocytes. Ensuite, l'activation des cellules endothéliales des vaisseaux aggrave la dégradation de la barrière hémato-encéphalique (BHE), permettant aux leucocytes périphériques d'atteindre la zone lésée (Gadani *et al.*, 2015; Shi *et al.*, 2019). De plus, en raison de la perturbation de la BHE, les cytokines et les DAMPs pénètrent dans la circulation sanguine et induisent une réponse immunitaire systémique. Cependant, après cette suractivation précoce du système immunitaire survient plus tardivement un état d'immunodépression qui prédispose aux infections post-AVC, notamment aux infections pulmonaires ou urinaires (Prass *et al.*, 2003; Meisel *et al.*, 2005). Ainsi, de nombreuses recherches tentent toujours de comprendre le rôle du système immunitaire et de développer de potentiels médicaments immunomodulateurs en traitement de l'AVC.

Microglie

L'activation des cellules microgliales est l'une des premières étapes du déclenchement de la réponse immunitaire innée après un AVC. Ces cellules peuvent adopter différents phénotypes, couvrant un large spectre de pro- à anti-inflammatoire, et sont connues pour répondre très rapidement aux lésions neuronales dans la zone lésée (Szalay *et al.*, 2016). Lors de l'AVC, les gradients ioniques et l'activité neuronale sont altérés en seulement quelques minutes en raison du manque de nutriments causé par l'interruption du flux sanguin. Les

cellules microgliales détectent les changements de gradients ioniques et les métabolites purinergiques relâchés par les cellules en souffrance grâce à leurs prolongements qui surveillent l'environnement (Cserép *et al.*, 2019). Lors de la phase aigüe, après le début de l'AVC, les cellules microgliales au cœur de la lésion détectent les DAMPS *via* leurs récepteurs TLR. Cette liaison conduit notamment à l'activation de la voie NF- κ B et à l'activation des cellules microgliales. Une fois activées, elles produisent des interleukines (IL) pro-inflammatoires comme les IL-1 et IL-6, ainsi que du TNF (TNF, *tumor necrosis factor*) qui exacerbe la réponse inflammatoire de la part des astrocytes et des cellules endothéliales (Xu *et al.*, 2020). A l'état activé, les cellules microgliales augmentent leur expression de *clusters* de différenciation (CD) en surface, comme les CD11b, CD45 et CD68, correspondant à un phénotype phagocytaire visant à l'élimination des débris cellulaires.

Astrocytes

Les astrocytes sont le type cellulaire le plus abondant dans le SNC et jouent un rôle essentiel à son bon fonctionnement. En tant que partie intégrante de l'unité neurovasculaire, les astrocytes assurent de nombreuses fonctions essentielles. Notamment la formation de la BHE grâce aux pieds astrocytaires formant la *glia limitans*, en interaction avec les cellules endothéliales. Ils participent également au soutien structurel, à la régulation du métabolisme neuronal ou au maintien de l'environnement extracellulaire (Liu and Chopp, 2016).

Ces cellules sont également des acteurs clés dans la réaction inflammatoire induite par l'ischémie. Les cytokines libérées par les neurones et les cellules microgliales entraînent une hyperréactivité des astrocytes. L'activation et la prolifération des astrocytes induisent la synthèse de facteurs inflammatoires supplémentaires tels que la protéine acide fibrillaire gliale (GFAP), la protéine chimiotactique des monocytes 1 (MCP-1), l'IL-1 β ou la vimentine qui vont entraîner une gliose réactive et former par la suite la cicatrice gliale (Jayaraj *et al.*, 2019). De plus, des métalloprotéases matricielles (MMP) comme MMP9 fragilisent l'interaction entre les pieds astrocytaires et les cellules endothéliales en dégradant la lame basale (del Zoppo, 2010). Ainsi, il a été supposé que cette rupture de la BHE constitue une voie d'entrée majeure pour l'invasion des leucocytes périphériques et leur migration transendothéliale.

Cellules endothéliales et molécules d'adhésion

L'intégrité de la BHE est sensiblement altérée après l'AVC, et les vaisseaux cérébraux deviennent plus perméables aux molécules et cellules qui sont normalement empêchées de passer du sang vers le parenchyme cérébral. De plus, la sécrétion des différentes cytokines favorise le recrutement des leucocytes circulants à la zone de lésion, avec successivement les neutrophiles, les monocytes/macrophages et les lymphocytes (Veltkamp and Gill, 2016). En effet, des molécules d'adhésion sont exprimées à la surface luminale des cellules endothéliales des vaisseaux pour permettre la transmigration des leucocytes. Les leucocytes circulants commencent par rouler sur la paroi du vaisseau grâce aux sélectines exprimées par les cellules endothéliales activées. Ensuite ils adhèrent fortement à la paroi en se liant avec des molécules d'adhésion cellulaires (ICAM-1, *intercellular adhesion molecule-1* ; VCAM-1, *vascular cell adhesion molecule-1*) (Gauberti and Martinez de Lizarrondo, 2021). Comme les autres cellules inflammatoires, les leucocytes libèrent des facteurs pro-inflammatoires dans la région ischémique. Les neutrophiles sont les premières cellules circulantes à envahir le tissu ischémié, suivis des monocytes, tandis que les lymphocytes semblent arriver quelques jours plus tard (Levard *et al.*, 2020). Alors que ce phénomène a été relativement bien décrit dans plusieurs modèles animaux, le profil temporel et spatial du recrutement des leucocytes, après l'AVC chez l'Homme en clinique, nécessite toujours une meilleure caractérisation (Gelderblom *et al.*, 2009; Veltkamp and Gill, 2016; Drieu *et al.*, 2019).

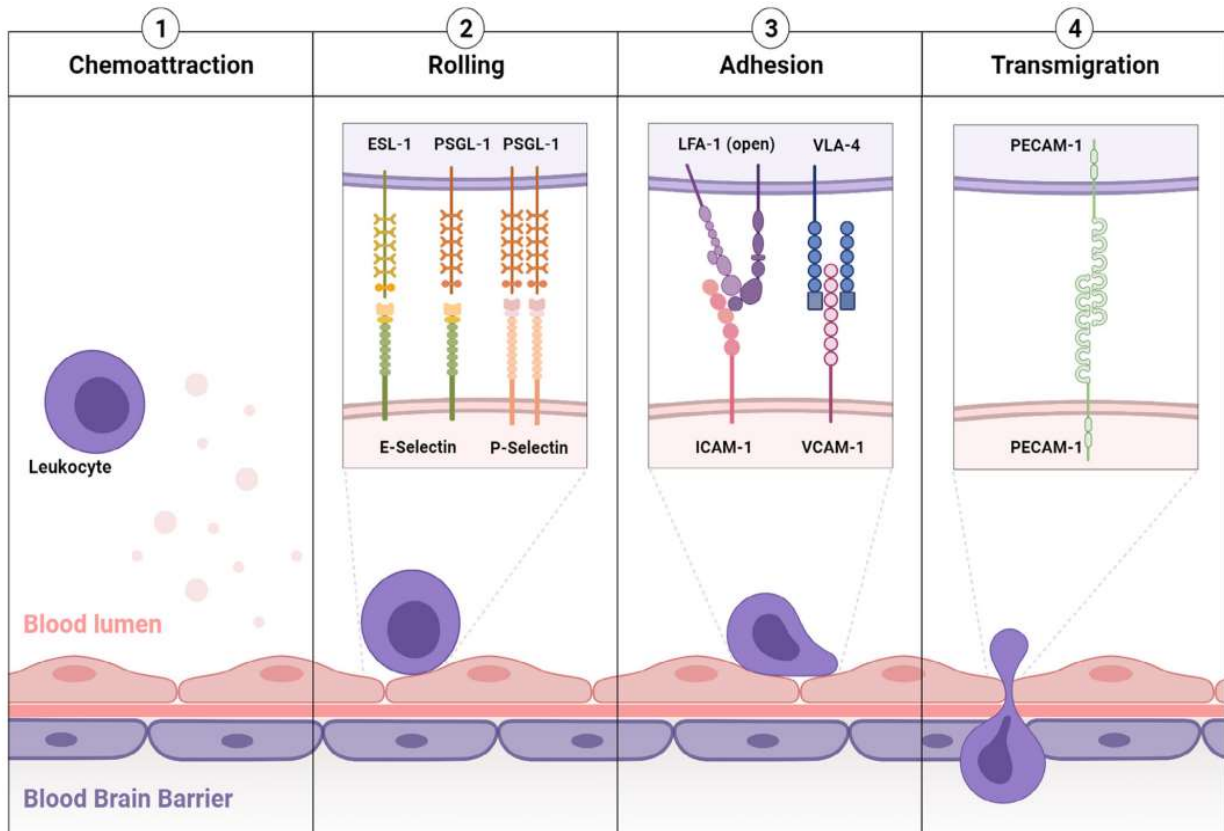


Figure 9 : Étapes de la transmigration leucocytaire : implication des molécules d'adhésion endothéliales.

D'après "Molecular MRI of Neuroinflammation: Time to Overcome the Translational Roadblock" (Gauberti et de Lizarrondo 2021).

Neutrophiles

Les neutrophiles sont des leucocytes polynucléaires, généralement les premiers leucocytes à être recrutés sur un site inflammatoire, et sont capables d'éliminer des agents pathogènes par de multiples mécanismes (Kolaczowska and Kubes, 2013). Une fois infiltrés, les neutrophiles facilitent le recrutement des autres leucocytes par la dégranulation de leur contenu riche en cytokines et enzymes protéolytiques (Mayadas, Cullere and Lowell, 2014). De plus, les neutrophiles pourraient contribuer à aggraver les dommages ischémiques en endommageant la matrice extracellulaire par les enzymes protéolytiques et des radicaux libres libérés, ainsi qu'en obstruant la circulation des microvaisseaux (Amki et al., 2020). Les neutrophiles sécrètent également des pièges extracellulaires (NETs, *Neutrophils extracellular traps*), constitués par des réseaux de fibres composés d'ADN capables d'activer les plaquettes et de contribuer à la consolidation du thrombus (Rayasam et al., 2018). Des études sur des modèles expérimentaux ainsi que des études cliniques ont montré que les neutrophiles

infiltrent le parenchyme cérébral dans les premières heures suivant le début de l'AVC (Gelderblom *et al.*, 2009; Cai *et al.*, 2019; Drieu *et al.*, 2020). Des données cliniques montrent également que les NETs sont augmentés chez les patients ayant subi un AVC, et que le ratio neutrophiles/lymphocytes pourrait être un marqueur pronostic en phase aiguë (Vallés *et al.*, 2017; Xue *et al.*, 2017).

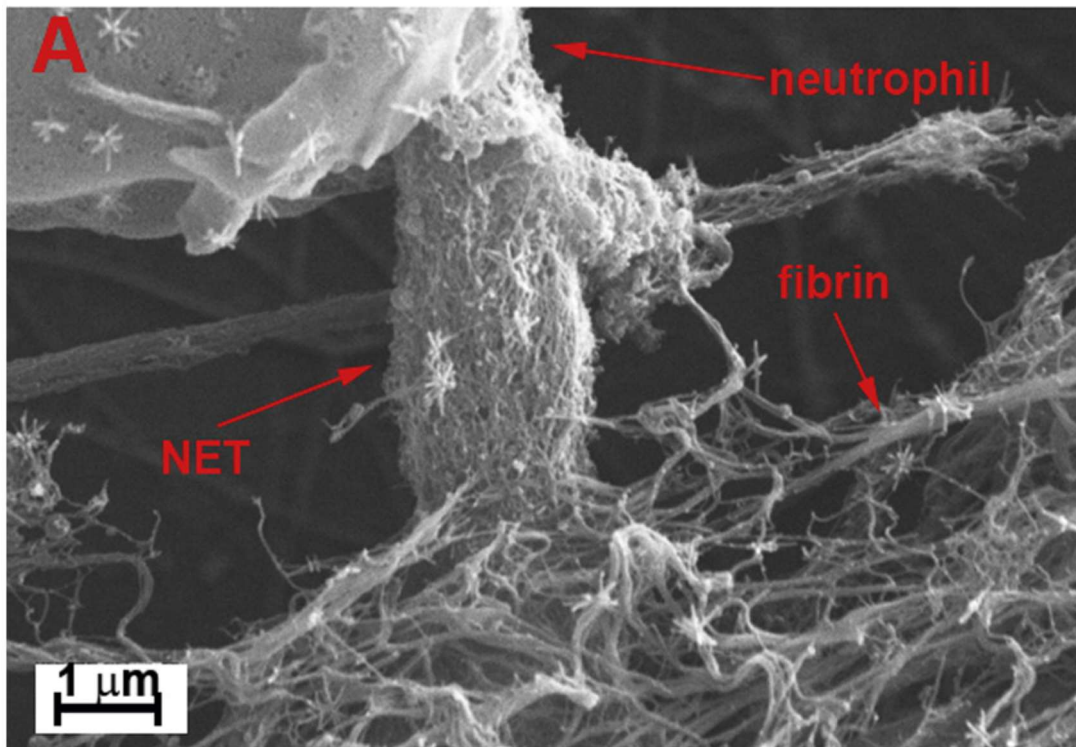


Figure 10 : Image en microscopie électronique à balayage de NETs libérés par un neutrophile dans un caillot de fibrine.

D'après "Networks that stop the flow: A fresh look at fibrin and neutrophil extracellular traps" (Varjú & Kolev, 2019).

Lymphocytes T

Les lymphocytes T jouent un rôle central dans le système immunitaire adaptatif, et sont très importants pour la bonne communication avec l'immunité innée. Ils sont identifiés par l'expression à leur surface des récepteurs des cellules T (TCR, *T cells receptor*) (Gu *et al.*, 2015). Les implications de la réponse immunitaire adaptative dans l'AVC ischémique sont encore très mal connues, et des résultats à la fois bénéfiques et délétères ont été rapportés selon le type de sous-population lymphocytaire. L'infiltration des cellules $\gamma\delta$ T, CD8+ T et *Natural killer* (NK) contribue aux lésions cérébrales aiguës, tandis que les cellules régulatrices

T et B pourraient être protectrices (Feng *et al.*, 2017). Des modèles expérimentaux ont permis de montrer que l'infiltration lymphocytaire dans le tissu ischémique survient plus tardivement, quelques jours après le début de l'AVC (Drieu *et al.*, 2018, 2019). Des échantillons humains *post-mortem* révèlent également que l'infiltration des lymphocytes dans la zone ischémique se produit à partir de 3 jours et peut être présente jusqu'à plusieurs années plus tard (Mena, Cadavid and Rushing, 2004).

Cicatrisation et réparation tissulaire

La réaction inflammatoire est également nécessaire pour le nettoyage et la réparation tissulaire qui s'opère tardivement après la lésion. Après la phase aiguë de l'AVC ischémique, l'inflammation initiale s'auto-régule et laisse place au remodelage structurel et à la réorganisation fonctionnelle (Xu *et al.*, 2020). La fin de la phase aiguë se caractérise d'abord par l'élimination des cellules mortes et débris tissulaires, la création d'un milieu anti-inflammatoire et la production de facteurs de survie cellulaires (Malone *et al.*, 2019). Cette phase, réalisée de concert par de nombreux types cellulaires, allant des cellules immunitaires aux neurones et astrocytes vise à restaurer l'intégrité des tissus et implique le remodelage de la matrice ainsi que la genèse de nouvelles cellules. Ensemble, ces cellules produisent des facteurs de croissance et des protéases permettant le remodelage du site de lésion (Iadecola and Anrather, 2011).

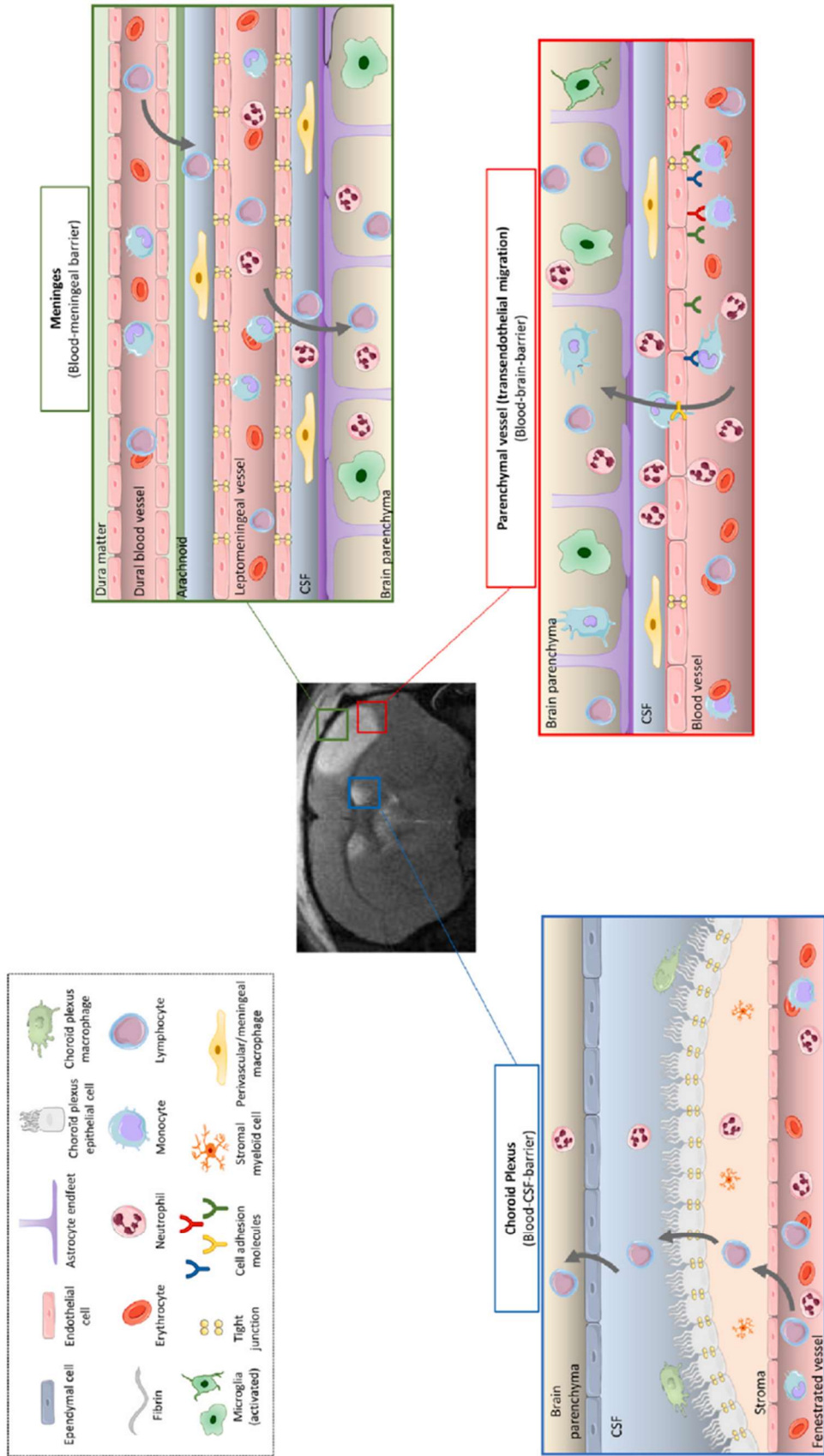


Figure 11 : Illustration de la réaction inflammatoire après un accident vasculaire cérébral ischémique.

Réponses inflammatoires/immunitaires après un AVC ischémique. Dans le cerveau sain, trois barrières principales protègent le parenchyme des agents pathogènes externes : la barrière hémato-encéphalique (BHE) autour des vaisseaux cérébraux, la barrière hémato-méningée dans les méninges et la barrière sang-liquide céphalo-rachidien (LCR) du plexus choroïde (ChP). Les cellules immunitaires circulent librement dans le sang et quelques lymphocytes patrouillent dans le LCR pour l'immunosurveillance. Dans le parenchyme cérébral, la microglie au repos examine l'environnement avec ses processus. Après un AVC, la microglie passe d'une forme de repos à un état activé, adoptant un phénotype phagocytaire et sécrétant des facteurs pro-inflammatoires. La BHE est perturbée, les cellules endothéliales sont activées et expriment les molécules d'adhésion. Les jonctions serrées entre les cellules endothéliales disparaissent. Cela permet le roulement et l'adhésion des leucocytes du côté luminal du vaisseau sanguin, puis la transmigration du compartiment vasculaire vers le parenchyme cérébral. Les leucocytes peuvent également envahir le cerveau à travers les méninges et les ChP. Une fois infiltrés dans les tissus, les neutrophiles sécrètent des facteurs pro-inflammatoires qui vont recruter des monocytes/macrophages, et plus tard des lymphocytes vers le parenchyme.

D'après "Filling the gaps on stroke research: Focus on inflammation and immunity" (Levard et al., 2021)

Essais cliniques immunomodulateurs

Étant donné que les mécanismes inflammatoires ont commencé à attirer de plus en plus l'attention dans la recherche sur les AVC ischémiques, quelques médicaments ayant pour but de moduler l'inflammation ont atteint le stade d'essai clinique de phase II ou de phase III.

Anakinra

Plusieurs essais cliniques randomisés ont testé l'utilisation de l'anakinra, un antagoniste recombinant des récepteurs à l'IL-1Ra, dans le but d'inhiber les effets déclenchés par la cytokine pro-inflammatoire. Ce composé était historiquement utilisé pour traiter la polyarthrite rhumatoïde et d'autres maladies inflammatoires similaires. Après des essais précliniques prometteurs sur des modèles animaux, des études ont montré que l'anakinra était bien toléré chez les patients victimes d'AVC ischémique aigu (*Emsley et al., 2005*). Cependant, même si l'anakinra a significativement diminué les niveaux plasmatiques d'IL-6 pro-inflammatoire et de protéine C-réactive, les patients n'ont pas montré de réduction des niveaux d'invalidité à 3 mois par rapport au placebo. De plus, il a été suggéré qu'une possible interaction négative entre l'IL-1Ra et le tPA pourrait masquer l'effet bénéfique de l'anakinra (*Smith et al., 2015*). Plus d'études précliniques et cliniques seraient nécessaires pour confirmer ou non son utilisation comme traitement de l'AVC.

Minocycline

Un autre composé bien documenté comme protecteur dans les modèles d'AVC ischémiques est la minocycline, un dérivé de la tétracycline. Cette molécule exerce de nombreux effets anti-inflammatoires, notamment en inhibant l'expression de cytokines, de MMP, mais aussi en ciblant l'activation microgliale au niveau cérébral. Une étude a montré une bonne innocuité chez des patients dans les premières heures après l'apparition des symptômes, et ce jusqu'à 24 heures suivant le début de l'AVC (*Kohler et al., 2013*). Cependant, dans cette étude elle n'a pas amélioré la proportion de patients sans incapacité à 3 mois après l'AVC. En revanche, une méta-analyse regroupant plusieurs essais a démontré l'efficacité du traitement, suggérant la minocycline comme agent neuroprotecteur prometteur pour les patients (*Malhotra et al., 2018*).

Natalizumab

Plusieurs stratégies ont été suivies pour tenter d'éviter l'infiltration des cellules immunitaires périphériques vers le SNC à travers les vaisseaux. Parmi celles-ci on retrouve le natalizumab, un anticorps humanisé anti-CD49d qui bloque la liaison de l'intégrine $\alpha 4$ et atténue l'infiltration leucocytaire, utilisé dans le traitement de la sclérose en plaques ou la maladie de Crohn (Polman *et al.*, 2006; Guagnozzi and Caprilli, 2008). Des résultats prometteurs ont été obtenus chez l'animal. Puis, dans un premier essai clinique le natalizumab semblait être non-toxique et avoir des bénéfices dans la récupération des fonctions cognitives à 3 mois chez des patients, bien qu'il n'y ait pas d'impact sur la croissance de la lésion ischémique (Elkins *et al.*, 2017). Par la suite, dans la phase IIb, l'essai n'a malheureusement pas montré de bénéfices et le développement du natalizumab ne sera pas poursuivi dans le traitement des AVC ischémiques (Malone *et al.*, 2019).

Enlimomab

Une cible pharmacologique alternative a été proposée pour atténuer le recrutement et la migration des leucocytes à travers la BHE. En effet, enlimomab est un anticorps humanisé qui cible la liaison entre l'intégrine $\beta 2$ des leucocytes et la molécule d'adhésion endothéliale ICAM-1. Bien que des résultats positifs aient été obtenus en recherche préclinique, un essai clinique de phase III n'a pas réussi à reproduire ces résultats chez les patients. Au contraire, le groupe traité par l'anticorps présentait une mortalité plus élevée que le groupe placebo (Enlimomab Acute Stroke Trial Investigators, 2001).

Fingolimod

Le fingolimod est un agoniste de haute affinité pour les récepteurs de la sphingosine-1-phosphate, qui empêche la sortie des lymphocytes des ganglions lymphatiques, réduisant ainsi le taux de lymphocytes dans la circulation et réduisant leur infiltration dans le SNC (Mandala *et al.*, 2002). Il est ainsi utilisé dans le traitement de la sclérose en plaques ou de l'encéphalite. Dans plusieurs modèles animaux d'AVC chez les rongeurs, le fingolimod réduit la taille de la lésion, le déficit neurologique ou le nombre de cellules apoptotiques autour de la zone ischémisée (Liu *et al.*, 2013). Lorsqu'il est administré chez des patients victimes d'AVC, le fingolimod ne cause pas d'effet indésirable et est efficace pour limiter les lésions secondaires, réduire la perméabilité vasculaire, atténuer les déficits neurologiques et favoriser

la récupération (S. Zhang *et al.*, 2017). De plus, la combinaison du fingolimod avec l'altéplase entraîne une diminution des lymphocytes circulants, des volumes de lésions, des hémorragies et des déficits neurologiques (Zhu *et al.*, 2015; S. Zhang *et al.*, 2017). Ainsi, le fingolimod est

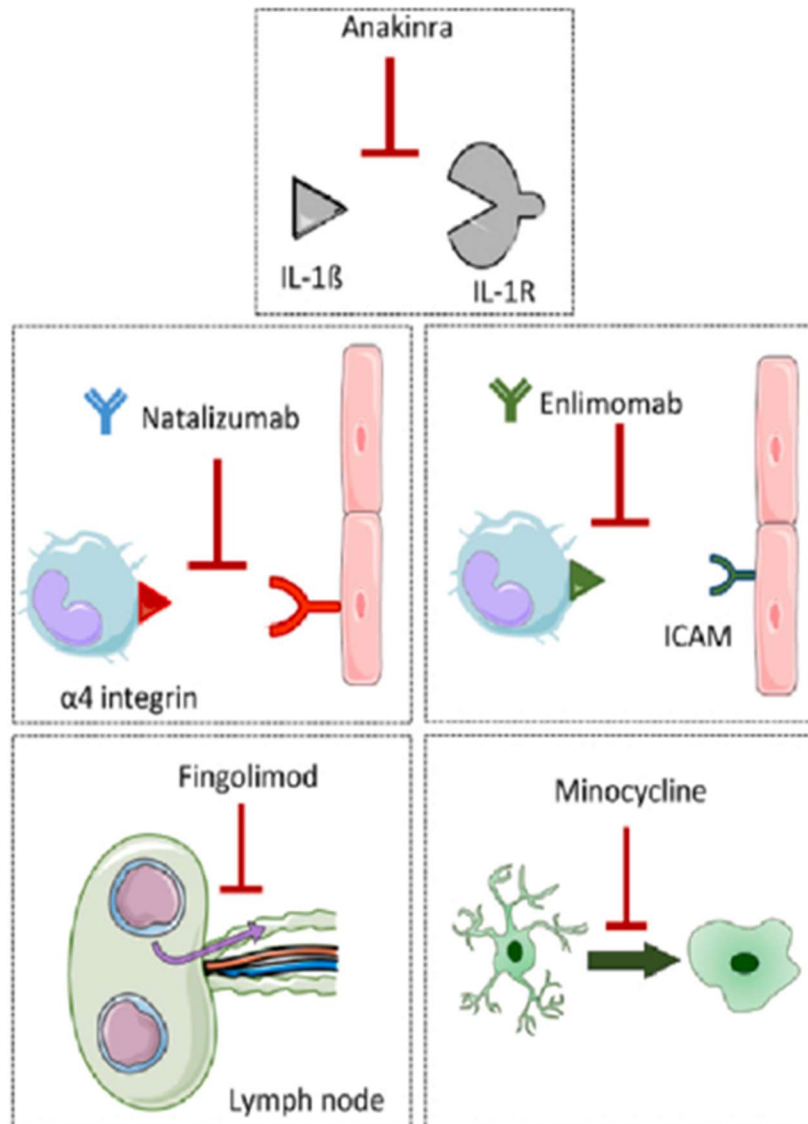


Figure 12 : Traitements immunomodulateurs testés en clinique dans le cadre de l'AVC ischémique.

L'anakinra est un antagoniste de la cytokine pro-inflammatoire interleukine-1. Le natalizumab agit en bloquant la liaison de l'intégrine $\alpha 4$ à la molécule d'adhésion VCAM pour réduire l'infiltration leucocytaire. L'enlimomab est un anticorps ciblant la molécule d'adhésion ICAM. La minocycline inhibe l'activation microgliale parmi d'autres propriétés anti-inflammatoires. Le fingolimod est un agoniste de haute affinité pour plusieurs des récepteurs de la sphingosine-1-phosphate qui empêche la sortie des lymphocytes des ganglions lymphatiques, limitant ainsi l'infiltration des lymphocytes vers le cerveau.

D'après "Filling the gaps on stroke research: Focus on inflammation and immunity" (Levard *et al.*, 2021).

certainement l'immunothérapie la plus convaincante contre l'AVC, bien que d'autres essais à plus grande échelle soient nécessaires (Malone *et al.*, 2019).

Voies d'entrée des cellules inflammatoires

Au cours des dernières années, la recherche de stratégies anti-inflammatoires pour le traitement de l'AVC s'est concentrée sur la limitation de la migration transendothéliale des cellules immunitaires périphériques dans le parenchyme cérébral, dans le but de réduire la gravité des AVC. Ces études sont basées sur l'idée de la transmigration des cellules inflammatoires à travers la BHE des vaisseaux cérébraux, mais de nouvelles preuves suggèrent maintenant qu'il existe d'autres voies potentiellement plus importantes : la migration au niveau des méninges, ou à travers des plexus choroïdes (ChP) (Benakis, Llovera and Liesz, 2018).

Les ChP sont à l'origine connus comme le principal producteur de liquide céphalo-rachidien (LCR), qui remplit les ventricules cérébraux, les espaces sous-arachnoïdiens et les espaces périvasculaires. Cette structure cérébrale hautement vascularisée réside dans les ventricules cérébraux et est formée d'une couche de cellules épithéliales formant une barrière étanche entre le sang et le LCR (BCSFB, *blood-cerebrospinal fluid barrier*) qui entoure un stroma de tissu conjonctif parcouru par des capillaires sanguins fenestrés. En plus de ce rôle de barrière, de plus en plus d'études indiquent que les ChP régulent des processus immunitaires spécifiques du SNC, comme la surveillance immunitaire et le trafic de cellules périphériques (Gherzi-Egea *et al.*, 2018). En effet, il a été montré par Ge et collaborateurs que les ChP répondent à une lésion ischémique corticale par l'expression de molécules d'adhésion et de chimiokines, et que les macrophages dérivés de monocytes sanguins peuvent infiltrer l'hémisphère ischémié par les ChP et le LCR (Ge *et al.*, 2017). De plus, une autre étude a démontré que les ChP constituent une voie d'infiltration majoritaire des lymphocytes T vers le cortex dans un modèle d'ischémie permanente par électrocoagulation, *via* un mécanisme dépendant de CCR2 (Llovera *et al.*, 2017).

Par ailleurs, plusieurs études récentes ont soulevé le fait que les méninges pourraient être un autre lieu majeur de l'infiltration des leucocytes dans le parenchyme cérébral. Des analyses en immunohistochimie ainsi qu'en cytométrie en flux ont révélé que des lymphocytes $\gamma\delta$ T s'accumulent dans les méninges très rapidement après la survenue d'un AVC avant

d'infiltrer la zone ischémique (Gelderblom, Arunachalam and Magnus, 2014; Benakis *et al.*, 2016). De plus, les lésions ischémiques induisent la croissance de vaisseaux lymphatiques méningés dans un modèle de photothrombose, et l'absence de ces vaisseaux impacte le devenir de l'AVC dans un modèle d'occlusion transitoire par filament (Yanev *et al.*, 2020). Ces observations sont d'autant plus intéressantes qu'une étude de Cugurra et collaborateurs a révélé en 2021 que les méninges sont parcourues par des populations de leucocytes provenant directement de la moelle osseuse par des canaux en travers du crâne. Ces cellules immunitaires ne sont pas dérivées du sang et ont un phénotype immunorégulateur dans le cas d'une lésion cérébrale (Cugurra *et al.*, 2021).

L'ensemble de ces études récentes révèle la diversité auparavant méconnue des voies d'invasion des populations de leucocytes après un AVC, et aide à mieux comprendre les échecs des différents essais cliniques avec des molécules agissant sur la transmigration endothéliale comme l'enlimomab et le natalizumab. Comprendre comment les cellules immunitaires migrent vers le cerveau *via* ces voies alternatives peut nous aider à développer des approches plus efficaces pour les thérapies anti-inflammatoires contre l'AVC. Comme évoqué précédemment, plusieurs essais cliniques ont été initiés avec l'enlimomab (anticorps anti-ICAM-1), le natalizumab (anti-CD49d) ou le fingolimod (FTY720). Alors que le fingolimod pourrait réduire le volume de l'infarctus et améliorer la récupération, le natalizumab et l'enlimomab n'ont pas montré d'effet sur leurs critères d'évaluation principaux (Enlimomab Acute Stroke Trial Investigators, 2001; Fu *et al.*, 2015; Elkins *et al.*, 2017). Ces divergences pourraient être dues au concept incomplet selon lequel les lymphocytes s'infiltrent dans le cerveau principalement par la voie transendothéliale des capillaires parenchymateux, sans tenir compte des méninges et des ChP. En effet, le natalizumab et l'enlimomab visaient à inhiber l'entrée des lymphocytes dans le SNC en bloquant des molécules d'adhésion spécifiques, nécessaires à la migration transendothéliale à travers les vaisseaux parenchymateux. Cependant, VCAM ainsi que ICAM-1 ne sont pas exprimés sur les vaisseaux des ChP (Steffen *et al.*, 1996). Par conséquent, les lymphocytes dans le système vasculaire des ChP n'ont pas accès à ces molécules d'adhésion et le blocage de celles-ci n'affectera pas la voie d'infiltration (Benakis, Llovera and Liesz, 2018). En revanche, le Fingolimod agit en favorisant la rétention lymphocytaire dans le thymus et les ganglions lymphatiques (Mandala *et al.*, 2002) et réduit ainsi le nombre de lymphocytes circulants indépendamment de

l'expression des molécules d'adhésion au niveau des différentes voies de migration. Cela pourrait expliquer pourquoi, actuellement, le seul résultat positif sur l'efficacité du traitement n'est obtenu qu'avec ce médicament chez les patients ayant subi un AVC (Benakis, Llovera and Liesz, 2018). Cela pourrait également expliquer les résultats prometteurs obtenus avec le traitement à la minocycline. En effet, la minocycline exerce des effets anti-inflammatoires sur plusieurs cibles qui ne dépendent pas forcément de la voie de migration des cellules immunitaires périphériques, notamment l'activation microgliale (Malhotra *et al.*, 2018). Ainsi, des cibles thérapeutiques devraient être identifiées en se concentrant sur des composés qui agissent directement sur les cellules immunitaires circulantes plutôt que sur les différentes molécules d'adhésion, afin de maximiser l'efficacité sur l'ensemble des voies d'entrée.

L'inflammation dans les modèles expérimentaux

Les modèles précliniques d'AVC sont nécessaires pour étudier les processus pathologiques et les différents mécanismes cellulaires et moléculaires déclenchés par l'ischémie, ainsi que pour tester de potentielles cibles thérapeutiques. Cependant, il existe une grande diversité de modèles, avec différents types de lésions induisant leurs propres réponses inflammatoires. Chaque modèle d'AVC présente ses avantages et ses inconvénients expérimentaux, et présente plus ou moins de ressemblance avec la réalité clinique. Ainsi, une attention particulière doit être portée sur la sélection du modèle expérimental le plus adapté et la meilleure combinaison de modèles, en particulier pour les études de nouveaux médicaments anti-inflammatoires.

Filament intraluminal

Le modèle expérimental d'AVC le plus fréquemment utilisé est le modèle d'occlusion de l'artère cérébrale moyenne (MCA, *middle cerebral artery*) à l'aide d'un filament intraluminal (Sommer, 2017). Pour induire l'occlusion de l'artère, un filament de nylon est introduit dans l'artère carotide interne et avancé jusqu'à l'origine de la MCA, obstruant le flux sanguin. Le modèle filament ne nécessite pas de craniotomie et peut être utilisé pour modéliser soit une ischémie permanente (Yan, Chopp and Chen, 2015; Pedragosa *et al.*, 2018)

soit une ischémie transitoire par retrait du filament, permettant une reperfusion contrôlée à différents temps, entre 30 minutes et 120 minutes (Yan, Chopp and Chen, 2015; Buscemi *et al.*, 2019). Ce modèle est caractérisé par un grand volume de lésion incluant le cortex et le striatum, mais également par des durées d'occlusions plus longues entraînant des lésions encore plus importantes ainsi que de la mortalité (Hata *et al.*, 2000). De plus, il induit souvent des dommages à l'hypothalamus, qui se produisent rarement dans les AVC ischémiques humains (Uzdensky, 2018).

Dans ce modèle, la reperfusion rapide et soudaine entraîne des lésions secondaires retardées, appelées lésions d'ischémie-reperfusion, dont l'existence chez l'Homme a été remise en question même après thrombectomie mécanique (Gauberti *et al.*, 2018). En effet, il a été montré qu'environ 70% du volume de lésion dans ce modèle expérimental est en fait dû à la formation de microthrombi après le retrait du filament (Gauberti *et al.*, 2014). Cette reperfusion rapide contraste avec la reperfusion progressive qui se produit dans de nombreux AVC ischémiques humains non traités (Hossmann, 2012).

Une réaction inflammatoire est bien présente dans ce modèle avec une rupture de la BHE, une production de cytokines inflammatoires et le recrutement de leucocytes, bien qu'il ait été observé que cette réaction est moins importante que dans d'autres modèles permanents (Zhou *et al.*, 2013). Des centaines de molécules anti-inflammatoires ont été testées dans ce modèle et beaucoup ont montré des effets bénéfiques. Malheureusement, aucune n'a jusqu'à présent montré de réel avantage clinique.

Électrocoagulation

L'occlusion de la MCA par électrocoagulation est un autre modèle d'AVC fréquemment utilisé. Ce modèle consiste en l'occlusion permanente par une stimulation électrique qui induit une coagulation de l'artère. L'électrocoagulation est généralement suivie d'une dissection de l'artère pour éviter tout risque de recanalisation. Une craniotomie est nécessaire pour accéder à la MCA. La lésion induite est plus petite que pour le modèle filament et se limite à la zone corticale (Howells *et al.*, 2010). De plus, le volume et la localisation de la lésion correspondent à la majorité des AVC ischémiques humains, proportionnellement à la taille du cerveau (Llovera *et al.*, 2014).

La réaction inflammatoire décrite dans ce modèle est plus importante que dans le modèle filament, bien qu'elle puisse être surestimée en raison des effets de la stimulation électrique. L'activation microgliale est en effet plus importante, de même que l'infiltration leucocytaire. L'inflammation est également exacerbée en termes d'expression de cytokines pro-inflammatoires et de molécules d'adhésion (Zhou *et al.*, 2013). Un désavantage de ce modèle est que seuls des déficits légers peuvent être détectés dans les tests comportementaux classiques, et la récupération fonctionnelle est rapide dans les premiers jours après l'induction de l'AVC, rendant difficile l'évaluation fonctionnelle à long terme dans ce modèle (Llovera *et al.*, 2014).

Photothrombose

Le modèle d'AVC par photothrombose utilise l'illumination focale des vaisseaux cérébraux à travers le crâne après l'injection d'un colorant photosensible (Watson *et al.*, 1985). Le colorant photosensible (Rose Bengale ou érythrosine B) est administré par voie intrapéritonéale chez la souris, ou par voie intraveineuse chez le rat. Ensuite, la photo-activation du colorant conduit à la formation de radicaux libres oxygénés, entraînant des dommages endothéliaux et l'agrégation des plaquettes dans l'ensemble des vaisseaux illuminés par le laser (Kim, Sugawara and Chan, 2000). Ce modèle ne nécessite pas de craniotomie, puisque la source lumineuse peut être appliquée directement à travers le crâne. Elle produit une lésion corticale bien définie et de petite taille (Labat-gest and Tomasi, 2013). Un autre avantage de ce modèle est qu'il ne nécessite pas de manipulation mécanique des vaisseaux sanguins telles que la ligature ou l'insertion des filaments, ce qui réduit les risques.

Il a été observé dans ce modèle une activation microgliale, une infiltration lymphocytaire et une augmentation du niveau de cytokines pro-inflammatoires jusqu'à 14 jours après l'induction de l'AVC (Feng *et al.*, 2017). De plus, ce modèle induit des déficits sensorimoteurs à long terme avec une survie élevée, ce qui peut être utile pour étudier les processus inflammatoires tardifs impliqués dans la récupération et la régénération après AVC (Lunardi Baccetto and Lehmann, 2019).

Néanmoins, l'inconvénient majeur du modèle est la différence avec la pathologie de l'AVC. La lésion causée par la photothrombose présente simultanément un œdème

cytotoxique et vasogénique, des lésions microvasculaires et une rupture de la BHE (Lee *et al.*, 1996). Par ailleurs, ce modèle provoque une lésion ischémique très localisée, sans la zone de pénombre ischémique péri-infarct généralement présente dans la pathologie de l'AVC.

Thromboembolique

Il existe plusieurs modèles thromboemboliques. Par exemple, un caillot préalablement formé par du sang autologue ou hétérologue peut être dirigé vers la base de la MCA (Ansar *et al.*, 2014). Un caillot peut également être créé par l'application de chlorure de fer ou d'aluminium directement sur l'artère (Bonnard and Hagemeyer, 2015). Un autre modèle d'AVC thromboembolique, développé au sein de notre unité, consiste à injecter de la thrombine directement dans la MCA à l'aide d'une micropipette, ce qui provoque la formation *in situ* d'un caillot riche en fibrine (Orset *et al.*, 2007). Ces caillots riches en fibrines peuvent être lysés spontanément (partiellement ou totalement) comme cela se produit chez beaucoup de patients non traités. Le volume et la localisation de l'infarctus dans les modèles chlorure de fer et thrombine correspondent également à des lésions ischémiques observées dans la majorité des AVC humains (Drieu *et al.*, 2019). De plus dans le modèle thrombine, la lésion est généralement corticale et bien définie avec la présence d'une zone péri-lésionnelle qui peut être sauvée par la fibrinolyse précoce (Orset *et al.*, 2007, 2016; Macrez *et al.*, 2011). En effet, le modèle thrombine est le seul à avoir montré des bénéfices similaires à la clinique après traitement au tPA. En revanche, les caillots formés dans le modèle chlorure de fer ou aluminium sont riches en plaquettes et ne peuvent pas être lysés par le tPA (Martinez de Lizarrondo *et al.*, 2017).

Nous avons récemment publié une description longitudinale détaillée de la réponse inflammatoire induite dans le modèle par injection de thrombine chez la souris. Celle-ci consiste en une réponse myéloïde précoce dans les premières heures avec un pic à 48 heures après l'induction de l'AVC, et toujours présente, dans une moindre mesure, 5 jours après. Les lymphocytes T s'infiltrent plus tardivement, à partir de 48h après le début de l'AVC. Ces réponses cellulaires s'accompagnent d'une activation des cellules endothéliales entre 24 et 48 heures, et qui n'est plus présente plus tard. Alors que les lésions ischémiques sont maximales entre 24 et 48 heures, la dégradation de la BHE augmente progressivement atteignant un maximum 5 jours après l'AVC (Drieu *et al.*, 2018, 2019).

En ce qui concerne les problèmes de translation, les modèles thromboemboliques semblent plus proches de la physiopathologie humaine et peuvent ainsi fournir une opportunité d'étudier non seulement les médicaments fibrinolytiques mais aussi les stratégies ciblant l'inflammation et les réponses immunitaires déclenchées après l'apparition d'un AVC. En effet, le modèle d'AVC induit par la thrombine a montré des similitudes avec les résultats obtenus dans plusieurs essais cliniques. En plus des résultats mentionnés sur le tPA, le Natalizumab, qui a montré son efficacité dans plusieurs autres modèles avant d'échouer en clinique, n'est pas bénéfique dans le modèle thrombine, mais la minocycline a montré des résultats prometteurs comme chez l'homme (Malhotra *et al.*, 2018; Drieu *et al.*, 2019).

L'inconvénient majeur de ce modèle est, comme pour le modèle d'électrocoagulation, le faible déficit comportemental observé. A l'heure actuelle, seuls des déficits fonctionnels mineurs peuvent être détectés dans les premiers jours suivant l'AVC, et la récupération apparaît en quelques jours. Cela rend donc actuellement difficile l'évaluation de la récupération à long terme. Des travaux sont maintenant en cours au sein de notre laboratoire afin de caractériser des déficits fonctionnels et/ou cognitifs observables, ce qui permettrait l'étude de la réponse inflammatoire tardive et les effets sur la régénération et la récupération.

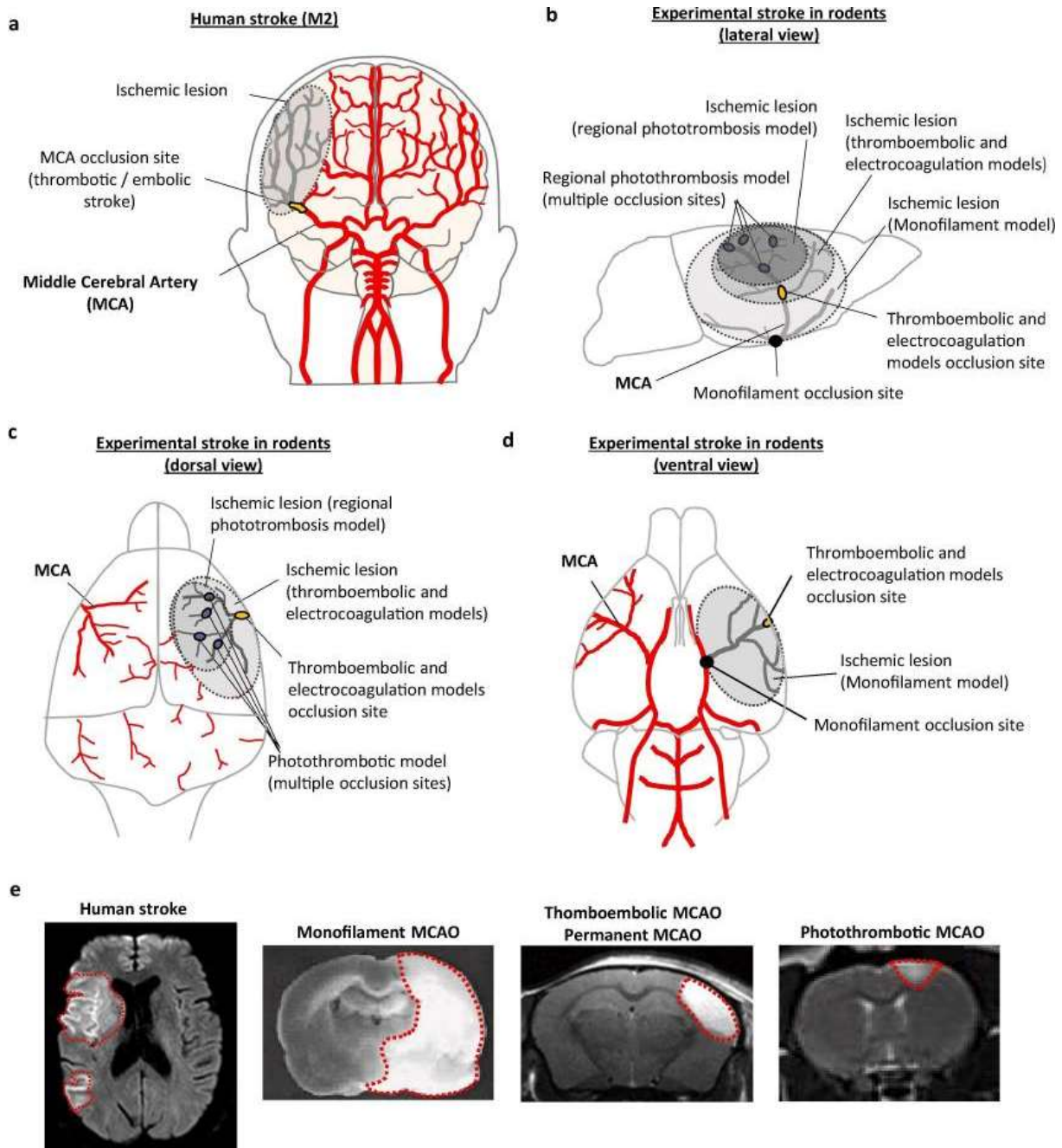


Figure 13 : Comparaison de l'AVC humain et des modèles expérimentaux d'AVC chez les rongeurs.

a) Vue schématique du système vasculaire cérébral humain avec représentation du sous type d'AVC le plus fréquent : une occlusion du segment M2 de l'artère cérébrale moyenne (MCA). b, c, d) Vues schématiques du système vasculaire cérébral du rongeur en vue b) latérale, c) dorsale et d) ventrale, avec représentations des sites de lésions dans les différents modèles d'AVC expérimentaux. e) Comparaison des lésions ischémiques visualisées par imagerie à résonance magnétique (IRM) dans l'AVC humain (occlusion M1-M2) et différents modèles expérimentaux. D'après "Filling the gaps on stroke research: focus on inflammation and immunity" (Levard et al., 2021).

Influence des facteurs de risque de l'AVC sur l'inflammation cérébrale

Plusieurs facteurs affectant la physiopathologie de l'AVC sont trop souvent négligés, dans la recherche préclinique notamment d'un point de vue inflammatoire. Le principal facteur aggravant est le vieillissement, qui sera discuté plus loin dans ce manuscrit de manière plus approfondie. On peut également citer les différences liées au sexe et les comorbidités telles que l'hypertension, le diabète et la consommation d'alcool. Une meilleure inclusion de ces facteurs dans les études précliniques augmenterait la robustesse et le potentiel translationnel des résultats.

Par exemple, malgré le fait que ce soient les femmes qui aient un risque plus élevé d'AVC, notamment après 65 ans (Appelros, Stegmayr and Terént, 2009), et qui présentent le plus de déficit fonctionnels (Guzik and Bushnell, 2017), il se trouve que la vaste majorité des données précliniques ait été obtenue chez de jeunes souris et rats mâles. Les quelques études menées en préclinique ont montré que les femelles présentent des tailles de lésion plus petites que les mâles du même âge. En effet, l'œstrogène a été décrit comme protecteur, le traitement avec cette hormone réduisant la mort neuronale et les cytokines pro-inflammatoires après l'AVC chez des animaux mâles (Wise *et al.*, 2001; Liu *et al.*, 2012).

Outre le vieillissement et le sexe qui sont des facteurs de risques non-modifiables, il existe d'autres comorbidités modifiables liées à l'AVC qui peuvent également être prises en compte. L'hypertension est le facteur de risque modifiable le plus classiquement lié aux AVC, affectant un tiers des adultes en France et même 65% des plus de 65 ans (Agence Nationale de santé publique). L'hypertension augmente le stress oxydatif, l'inflammation endothéliale, aggrave les déficits neurologiques et augmente la mortalité (Guzik and Bushnell, 2017). Bien qu'un nombre grandissant d'études soutienne l'existence d'interactions étroites entre la neuroinflammation et l'hypertension, les mécanismes restent encore vagues (Calvillo *et al.*, 2019). L'inclusion de modèles d'hypertension chez les rongeurs dans la recherche préclinique sur l'AVC, tels que les rats spontanément hypertendus (SHR), le modèle d'hypertension induite par une supplémentation en sel ou le modèle d'hypertension induite par l'angiotensine II aiderait à améliorer la translation des résultats à l'Homme.

De même que l'hypertension, les troubles du métabolisme du glucose sont des facteurs de risque majeurs de l'AVC, notamment le diabète de type 1 et de type 2 (Guzik and Bushnell, 2017). Ces troubles sont très fréquents chez les patients ayant subi un AVC, en effet 25 à 40% d'entre eux souffrent de diabète (Kernan *et al.*, 2014). Une méta-analyse d'études prospectives a montré que le diabète multiplie par 2,27 le risque d'AVC ischémique (Sarwar *et al.*, 2010). Dans les modèles animaux, le diabète induit une inflammation chronique se manifestant entre autres par la génération de ROS, l'expression de cytokines pro-inflammatoires et l'expression de molécules d'adhésion vasculaire. Il semble que l'augmentation des processus pro-inflammatoires due au diabète soit exacerbée après un AVC, entraînant une augmentation des dommages ischémiques (Shukla *et al.*, 2017).

Des études au sein de notre laboratoire se sont intéressés à la consommation excessive d'alcool, un problème majeur de santé publique dans le monde. Dans l'Union Européenne 89% des hommes et 82% des femmes consomment de l'alcool au moins une fois par an, et parmi eux 15,3% des hommes et 3,4% des femmes consomment plus de 6 verres par jour (Rehm *et al.*, 2013). Aux États-Unis, la consommation excessive d'alcool tue environ 95 000 personnes chaque année (*Excessive Drinking is Draining the U.S. Economy*, 2020). L'alcool a une influence sur le risque de survenue d'un AVC : une consommation d'alcool « légère à modérée » (0-2 verres/jour) est associée à un risque moindre d'AVC ischémique, tandis que des doses plus élevées sont associées à un risque accru (Larsson *et al.*, 2016). De plus, le risque d'AVC associé à une consommation excessive d'alcool avant 75 ans prédomine sur des facteurs de risque considérés comme « majeurs » par rapport à l'AVC que sont l'hypertension et le diabète (Kadlecová *et al.*, 2015). Cependant, l'impact de la consommation d'alcool sur l'issue de l'AVC est moins connu. Les études cliniques actuelles sont controversées et ont décrit, soit aucun effet (Gattringer *et al.*, 2015) soit un effet aggravant de la consommation excessive d'alcool sur la gravité de l'AVC (Ducroquet *et al.*, 2013). Les mécanismes médiateurs de cette aggravation ne sont pas encore bien compris, mais des données cliniques et précliniques ont montré qu'une consommation excessive d'alcool peut avoir un impact sur l'inflammation (Imhof *et al.*, 2001; Alho *et al.*, 2004; He and Crews, 2008).

Une étude translationnelle a été réalisée dans notre unité, en collaboration avec l'Hôpital Universitaire de Saint-Jacques-de-Compostelle en Espagne. Cette étude a porté sur l'impact de la consommation d'alcool sur la gravité et l'issue neurologique de l'AVC

ischémique chez des patients et des rongeurs, et a mis en évidence un effet aggravant de la consommation chronique d'alcool lié à la réponse inflammatoire précédant l'AVC. Les résultats cliniques de cette étude ont montré que les patients victimes d'AVC ischémique qui consommaient des quantités excessives d'alcool avaient des déficits neurologiques significativement plus sévères et un haut pourcentage de détérioration neurologique précoce, et que ces aggravations étaient liées à une inflammation systémique plus élevée par rapport aux patients qui ne consommaient pas d'alcool. De manière intéressante, cette inflammation périphérique augmentée existe au niveau « basal » (en absence d'AVC) chez des sujets consommant de l'alcool de manière excessive. Chez les souris, les résultats ont montré que l'alcool a aussi un effet aggravant sur les lésions ischémiques. En termes de mécanismes, cette étude a montré que l'alcool induit un état inflammatoire basal altéré au niveau cérébral : un *priming* inflammatoire. Ce *priming* induit par l'alcool affecte le parenchyme cérébral mais également les compartiments périvasculaires et vasculaires. Dans le parenchyme, il est caractérisé notamment par un profil d'activation non conventionnel des cellules microgliales et une augmentation de l'expression du TGF- β . Au niveau périvasculaire, l'alcool provoque une augmentation du nombre des macrophages périvasculaires. En cas d'atteinte cérébrale comme dans le cas d'un AVC, la réponse inflammatoire est exacerbée à tous les niveaux : la réaction microgliale et l'infiltration leucocytaire sont augmentées ; dans le compartiment vasculaire cérébral, ce *priming* se traduit par une augmentation des niveaux d'expression de la molécule d'adhésion P-sélectine à la surface des cellules endothéliales accompagnée d'une augmentation d'adhérence des leucocytes à la paroi des vaisseaux sanguins à la suite d'un AVC (Drieu *et al.*, 2020).

Impact du vieillissement sur l'accident vasculaire cérébral

L'âge est le facteur de risque non modifiable le plus important pour de nombreuses maladies humaines, et le facteur de risque le plus important pour l'AVC ischémique. En effet, à chaque décennie de vie l'incidence des AVC fait plus que doubler (Virani *et al.*, 2020). L'incidence annuelle des AVC augmente d'un facteur 100 entre 50 et 80 ans, du fait notamment d'une plus grande prévalence des facteurs de risque vasculaire au cours du vieillissement. Cette constatation est d'autant plus vraie chez la femme dont l'espérance de vie, supérieure à celle de l'homme, l'expose à un risque accru d'AVC (Béjot *et al.*, 2014). En effet, l'âge avancé est associé à de profonds changements physiopathologiques dans le SNC et la périphérie, ce qui augmentent la susceptibilité du cerveau aux lésions ischémiques.

Au cours du vieillissement du cerveau humain s'opèrent des changements structurels et fonctionnels des différents composants de l'unité neurovasculaire qui entraînent des altérations significatives de la perfusion cérébrale et de la perméabilité de la BHE. En effet, des études chez l'Homme ont montré une réduction de 25 à 40% du débit sanguin cérébral et de la consommation d'oxygène chez les sujets âgés (Ainslie *et al.*, 2008; De Vis *et al.*, 2015), ainsi qu'une perméabilité accrue de la BHE à des traceurs injectés par voie intraveineuse (Montagne *et al.*, 2015; Chagnot, Barnes and Montagne, 2021).

Des études cliniques ont montré que malgré des taux similaires de recanalisation artérielle, les patients âgés victimes d'AVC ayant reçu une thrombolyse ont plus de déficit que les individus plus jeunes. De plus, dans la population âgée le tissu dans la zone de pénombre est plus vite dégradé et converti en cœur ischémique (Mishra *et al.*, 2010; Sharma *et al.*, 2020). Conformément aux résultats cliniques, les études précliniques sur des modèles animaux montrent que les rongeurs âgés développent des déficits neurologiques plus graves, une moindre récupération fonctionnelle à long terme, des lésions de la BHE exacerbées ainsi qu'une mortalité accrue par rapport aux animaux jeunes (Brown, Marlowe and Bjelke, 2003; DiNapoli *et al.*, 2008; Crapser *et al.*, 2016; Candelario-Jalil and Paul, 2021). En revanche, il est intéressant de noter que concernant la taille de la lésion ischémique, des résultats divergents ont été observés. Par rapport au groupe jeune, certaines études montrent que les animaux âgés ont des volumes de lésion plus importants (DiNapoli *et al.*, 2008; Suenaga *et al.*, 2015;

Ma *et al.*, 2020), tandis que d'autres montrent l'inverse (Liu *et al.*, 2010; Liu and McCullough, 2012).

Le vieillissement s'accompagne d'un niveau inflammatoire basal augmenté dans plusieurs organes, qui peut être désigné par l'appellation « *inflammaging* » ou « *priming inflammatoire* » (Hu *et al.*, 2019). Au niveau du SNC, les cellules microgliales sénescents présentent un phénotype pro-inflammatoire chronique (elles sont dites plus « activées »), ont une capacité phagocytaire diminuée, et produisent des niveaux élevés de ROS et de médiateurs pro-inflammatoires (Mosher and Wyss-Coray, 2014, 2014; Marschallinger *et al.*, 2020). A l'aide du séquençage des acides ribonucléiques (ARN), des études ont confirmé l'augmentation de la transcription de gènes pro-inflammatoires par les cellules microgliales de souris âgées de 18 mois par rapport à celles âgées de 2 mois, après un AVC expérimental. En réponse à l'AVC, les souris âgées ont montré une altération par les cellules microgliales de la transcription de gènes impliqués dans la chimiotaxie des cellules immunitaires, le remodelage des tissus et les interactions intercellulaires, ce qui peut contribuer à une vulnérabilité accrue et une moins bonne récupération chez les animaux âgés après l'AVC (Jiang *et al.*, 2020; Shi *et al.*, 2020). Dans l'ensemble, ces modifications microgliales associées au vieillissement rendent davantage pro-inflammatoire le microenvironnement du SNC. Une neuroinflammation exacerbée dans le cerveau âgé pourrait aggraver les conséquences de l'AVC ischémique et interférer avec la réparation tissulaire et la récupération fonctionnelle.

Comme expliqué précédemment, l'infiltration des cellules immunitaires périphériques est un événement majeur dans la physiopathologie de l'AVC. Parmi les cellules infiltrées, les neutrophiles sont les premiers à intervenir et ils participent à aggraver les lésions en libérant des enzymes protéolytiques et des ROS (Perez-de-Puig *et al.*, 2015). Une étude combinant des données cliniques de patients et des données expérimentales a montré d'une part que chez les patients ayant subi un AVC ischémique, l'âge était associé à des taux plus élevés de cytokines activant les neutrophiles, et d'autre part, que les souris âgées présentaient des niveaux plus élevés de cytokines activant les neutrophiles et une génération accrue de ROS par rapport aux jeunes souris. Enfin, la déplétion des neutrophiles via un anticorps monoclonal spécifique, après un AVC ischémique, a entraîné des bénéfices à long terme sur les résultats fonctionnels chez les animaux mâles et femelles âgés, sans aucun bénéfice observé chez les jeunes (Roy-O'Reilly *et al.*, 2020). Ces résultats démontrent que le vieillissement est associé à

une pathogénicité accrue des neutrophiles dans les accidents vasculaires cérébraux ischémiques, et que les thérapies ciblant les neutrophiles peuvent conférer un plus grand bénéfice chez les sujets âgés.

Juste après le début de l'AVC, les différents mécanismes pathologiques conduisent à la production excessive de ROS, créant un stress oxydatif (Heo, Han and Lee, 2005). De plus, le vieillissement est associé à un dysfonctionnement mitochondrial qui augmente le stress oxydatif. Les dommages oxydatifs des ROS aux cellules endothéliales cérébrales contribuent à une réaction inflammatoire et des lésions tissulaires exacerbées après l'AVC chez les sujets âgés (Candelario-Jalil and Paul, 2021).

Par conséquent, la réalisation d'études précliniques avec des modèles d'AVC chez des rongeurs âgés pourrait fournir plus d'informations sur les effets protecteurs potentiels des médicaments, augmentant l'impact translationnel et la pertinence des résultats.

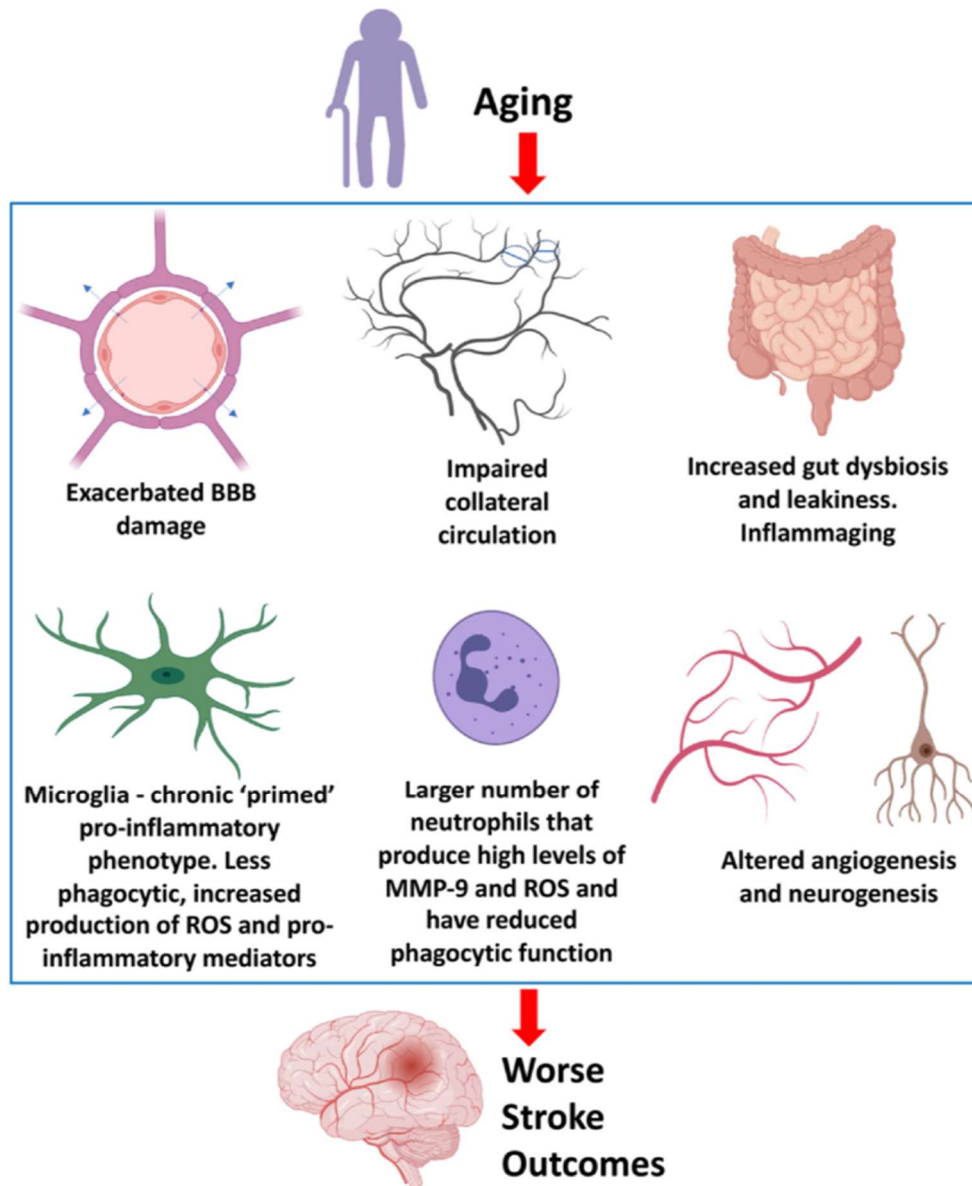


Figure 14 : Le vieillissement induit des modifications physiologiques pouvant impacter l'AVC ischémique.

L'âge avancé est associé à de nombreux changements physiopathologiques à la fois dans le SNC et en périphérie qui modifient la réponse aux lésions cérébrales ischémiques. D'après "Impact of aging and comorbidities on ischemic stroke outcomes in preclinical animal models: A translational perspective" (Candelario-Jalil 2021).

Le *priming* inflammatoire, point commun aux différentes comorbidités

De nombreuses comorbidités impliquées dans l'AVC, que ce soient des facteurs modifiables ou le vieillissement, partagent certains mécanismes qui convergent vers la présence d'un *priming* inflammatoire au niveau cérébral. Le terme « *priming* » est utilisé pour décrire la propension d'un type cellulaire particulier à réagir de manière exagérée à un stimulus secondaire, tel qu'une infection. Ce terme provient de l'étude des macrophages, utilisé pour la première fois pour décrire une réponse inflammatoire exacerbée à la suite d'un stimulus inflammatoire initial (Pace *et al.*, 1983). Dans cette étude, la réponse accrue des macrophages péritonéaux au lipopolysaccharide (LPS) après l'induction du *priming* avec l'interféron gamma (IFN γ) était caractérisé par une production plus importante d'IL-1 β et d'oxyde nitrique synthase inductible (iNOS), par rapport aux macrophages de souris non *primées*.

Au niveau du SNC, le *priming* a surtout été décrit par le phénotype et la réactivité des cellules microgliales : après avoir subi un stimulus initial, les cellules microgliales présentent une réponse inflammatoire exagérée à un deuxième stimulus (Haley *et al.*, 2019). Le *priming* microglial a été montré pour la première fois expérimentalement dans un modèle murin de maladie à prions. Dans ce modèle, les souris malades ont montré une réponse inflammatoire microgliale accrue après l'administration périphérique ou centrale de LPS par rapport aux souris contrôles (Cunningham *et al.*, 2005). Des observations similaires du *priming* microglial ont été rapportées après une infection bactérienne systémique (Püntener *et al.*, 2012). Les stimuli inflammatoires d'initiation du *priming* et l'atteinte secondaire peuvent même être temporellement séparés. En effet, une inflammation chronique *in utero* peut entraîner des altérations de la réactivité microgliale plus tard dans la vie adulte (Knuesel *et al.*, 2014). Des études ultérieures ont depuis montré que le *priming* inflammatoire cérébral peut être également déclenché par des stimuli chroniques, notamment le stress, le diabète, l'hypertension, la consommation chronique d'alcool et même le vieillissement (Muriach *et al.*, 2014; Norden, Muccigrosso and Godbout, 2015; Winklewski *et al.*, 2015; Drieu *et al.*, 2020).

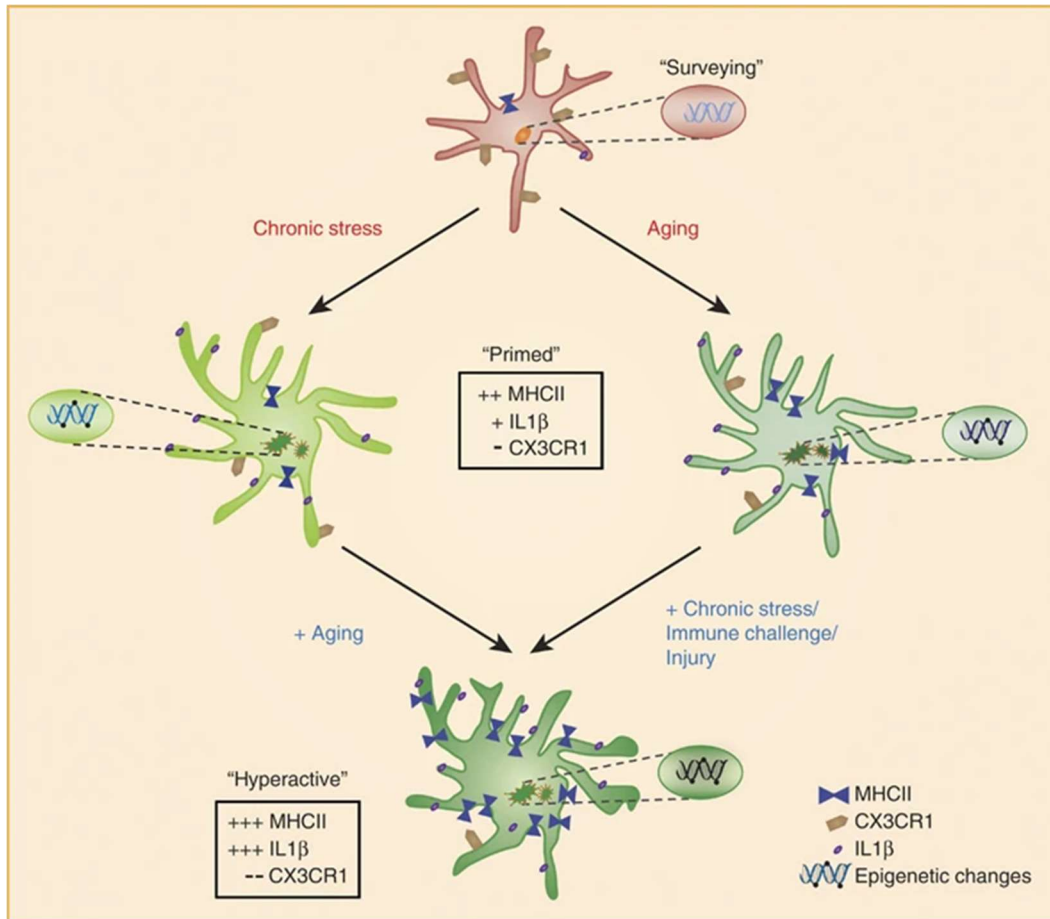


Figure 15 : Priming microglial induit par le vieillissement et le stress chronique.

En conditions homéostatiques, les cellules microgliales sont dynamiques, surveillant le microenvironnement cérébral. La microglie primée est caractérisée par des processus déramifiés, un corps cellulaire sphérique et un cytoplasme fragmenté. Des changements biochimiques sont associés à ces altérations morphologiques, tels qu'une expression élevée des molécules de présentation d'antigène (MHCII), des récepteurs Toll-like et des cytokines pro-inflammatoires (IL-1 β). La microglie du cerveau âgé montre également une activité phagocytaire déficiente et une mobilité réduite. Lors de l'exposition à de nouveaux stimuli, la microglie primée prend un état « hyperactif » marqué par une réponse pro-inflammatoire exagérée et une résistance aux mécanismes de régulation.

D'après "Microglia Priming with Aging and Stress" (Niraula et al., 2016).

- ❖ L'inflammation est la réaction du système immunitaire à une agression externe ou interne. Cette réaction entraîne l'acheminement de leucocytes sanguins au site de lésion afin d'éliminer la menace et initier la réparation tissulaire.
- ❖ Lors d'un AVC, la réaction inflammatoire s'initie immédiatement après l'occlusion et participe aux dégâts causés par la pathologie.
- ❖ Il existe plusieurs modèles animaux de l'AVC, qui diffèrent en termes de réaction inflammatoire post-AVC.
- ❖ De nombreuses molécules anti-inflammatoires ont montré des effets bénéfiques en laboratoire, mais aucune n'a montré de réelle efficacité lors des essais cliniques.
- ❖ De nombreuses comorbidités impliquées dans l'AVC, notamment le vieillissement, partagent la présence d'un *priming* inflammatoire au niveau cérébral.
- ❖ La réalisation d'études précliniques avec des modèles d'AVC chez des rongeurs âgés pourrait fournir plus d'informations sur les effets protecteurs potentiels des médicaments anti-inflammatoires, augmentant l'impact translationnel et la pertinence des résultats.

- ❖ *Inflammation is the immune system's response to external or internal aggression. This reaction causes leukocytes to flow from the blood to the site of injury to eliminate the threat and initiate tissue repair.*
- ❖ *The inflammatory reaction starts immediately after the occlusion and contributes to the damages caused by stroke.*
- ❖ *There are many different experimental models of stroke that differ in terms of the inflammatory response.*
- ❖ *Many anti-inflammatory molecules have been tested and have shown beneficial results in preclinical research, but none has shown real efficacy in clinical trials.*
- ❖ *Many comorbidities involved in stroke, including aging, have in common the presence of an inflammatory priming in the brain.*
- ❖ *Conducting preclinical studies with stroke models in elderly rodents could provide more information on the potential protective effects of anti-inflammatory drugs, increasing the translational impact and relevance of the results.*

Les macrophages résidents du système nerveux central

Au cours de l'évolution, le système nerveux s'est centralisé, formant le cerveau et la moelle épinière. Le SNC des vertébrés est le système le plus complexe du corps et est essentiel pour les réponses aux stimuli environnementaux, le contrôle des fonctions corporelles et le stockage des informations. De plus, la capacité de régénération très limitée du SNC signifie que des perturbations mêmes légères de ce système peuvent entraîner de graves complications. Ainsi, pour protéger le SNC des agents pathogènes envahissants et des facteurs circulants qui pourraient perturber l'homéostasie, il a été nécessaire durant l'évolution de le séparer de la périphérie, ce qui a conduit au développement d'un système immunitaire spécialisé dans le système nerveux des vertébrés (Ransohoff and Brown, 2012).

En effet, le SNC se compose non seulement de milliards de neurones, astrocytes et oligodendrocytes, mais aussi de cellules immunitaires résidentes qui représentent environ 10% de l'ensemble du SNC (Prinz *et al.*, 2021). Ces cellules immunitaires résidentes font principalement partie de l'immunité innée. Ce sont des macrophages, des cellules myéloïdes spécialisées trouvées soit dans le parenchyme cérébral, la microglie, soit aux interfaces du SNC tels que les leptoméninges, les espaces périvasculaires et les plexus choroïdes. Alors qu'ils étaient au départ principalement considérés pour leur fonction de phagocytose, on sait aujourd'hui que leurs fonctions s'étendent bien au-delà de la simple élimination des débris cellulaires. Les cellules immunitaires innées du cerveau et de la moelle épinière s'avèrent être dotées d'une grande plasticité, d'une longue durée de vie, et sont impliquées dans de nombreux mécanismes physiologiques et pathologiques. Elles sont maintenant considérées comme des cibles de choix pour moduler les maladies du SNC.

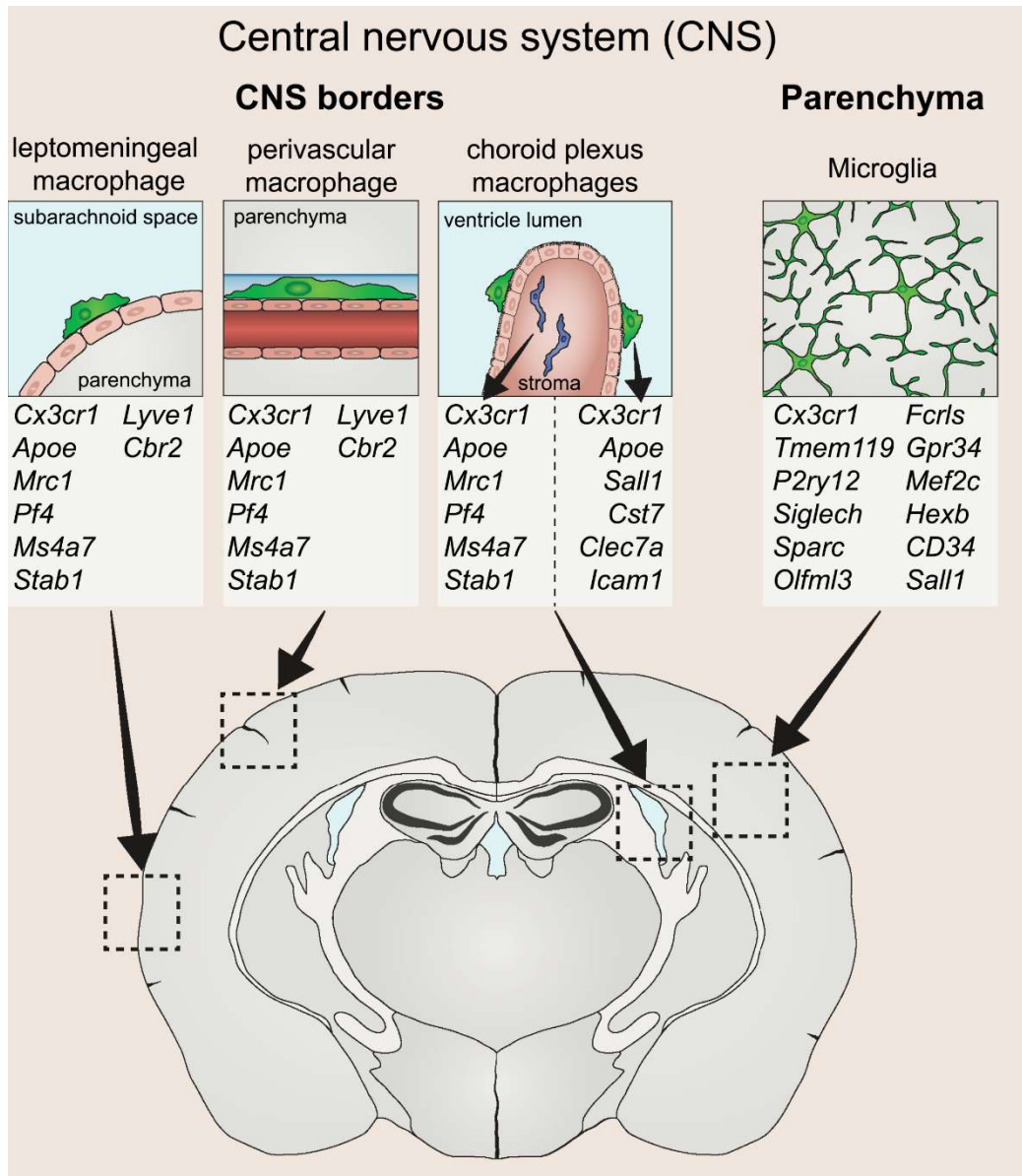


Figure 16 : Anatomie et marqueurs des différentes populations de macrophages résidents du SNC.

Les macrophages leptoméningés sont situés dans l'espace sous-arachnoïdien, à l'extérieur de la pie-mère. Les macrophages périvasculaires résident dans l'espace périvasculaire, entre les vaisseaux sanguins et le parenchyme cérébral. Dans les plexus choroïdes au sein des ventricules cérébraux, deux populations de macrophages sont retrouvées : les cellules de Kolmer de l'épipleux, sur la surface apicale de l'épithélium en contact direct avec le LCR, et les macrophages du stroma, à l'intérieur de la structure des plexus. La microglie est la population de macrophages résidents dans le parenchyme cérébral. Chaque population de macrophages exprime des gènes caractéristiques.

Adapté de "The origin, fate and function of macrophages in the peripheral nervous system-an update" (Amann and Prinz, 2020).

La microglie

Historique

Au début du XIXe siècle, des anatomistes tentaient de mieux comprendre la structure du cerveau en appliquant différents colorants pour étudier la morphologie des neurones. Les cellules gliales n'avaient alors pas encore été décrites. En 1856, le célèbre pathologiste allemand Rudolph Virchow a inventé le terme *glia* (du grec « glue ») pour décrire l'ensemble du compartiment non-neuronal du SNC. Virchow voyait la glie comme une sorte de tissu conjonctif acellulaire, et a découvert ensuite que ce tissu contient également des cellules. Cependant, la microglie était encore inconnue à cette époque et n'a été découverte en tant que type cellulaire à part entière qu'en 1919 par le neuroscientifique espagnol Pío del Río Hortega (Prinz, Jung and Priller, 2019).

En effet, il ya un peu plus de cent ans, Hortega a publié une méthode pour colorer les cellules gliales et les distinguer des autres cellules du SNC (Del Río Hortega, 1918). Il a alors nommé la microglie, « micro » désignant la petite taille de leur corps cellulaire (environ 7-10 μm). Il appellera ces cellules le « troisième élément » du SNC, les neurones et les astrocytes étant respectivement premier et deuxième. Il a ensuite commencé à décrire leur fonction phagocytaire, leur plasticité, leur distribution et leur hétérogénéité (Sierra et al., 2016).

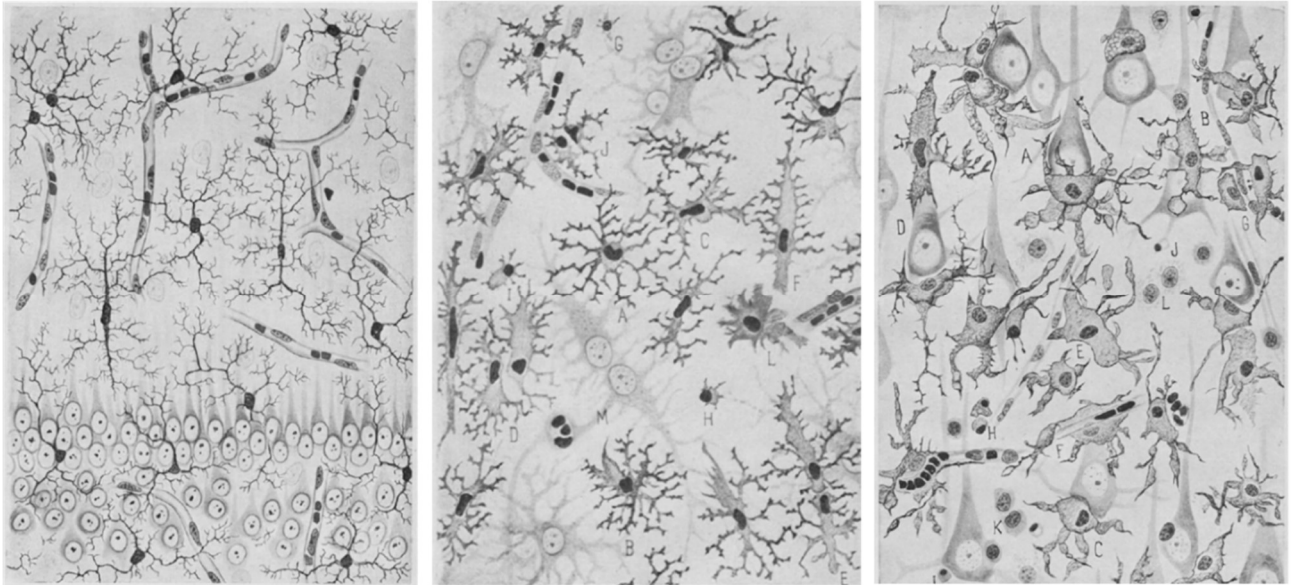


Figure 17 : Illustrations de cellules microgliales réalisées par Pío del Río Hortega.

A gauche : Microglie dans l'hippocampe d'un cerveau de lapin. On note la morphologie des cellules, avec un petit corps cellulaire et des prolongements fins et ramifiés. Au centre : Cellules microgliales dans le cerveau de lapin, à proximité d'une blessure produite deux jours auparavant. On note le changement de morphologie, avec un corps cellulaire grossi et des prolongements hyper-ramifiés. A droite : Cellules microgliales dans le cortex cérébral de lapin, au cœur d'une lésion produite deux jours auparavant. On voit bien le changement de morphologie, avec des très gros corps cellulaires et très peu de prolongements. On parle de phénotype améboïde.

Adapté de "The Big-Bang for modern glial biology: Translation and comments on Pío del Río-Hortega 1919 series of papers on microglia" (Sierra et al., 2016).

Caractérisation

La microglie constitue 5 à 12 % des cellules du SNC, selon les régions cérébrales (Lawson et al., 1990). Ce sont les principales cellules immunitaires résidentes du cerveau et sont impliquées dans l'homéostasie et dans la défense contre les agents pathogènes et les troubles du SNC (Ransohoff and El Khoury, 2015). Des études ont confirmé l'intuition d'Hortega selon laquelle elles sont mésenchymateuses, myéloïdes, originaires du sac vitellin et capables de s'auto-renouveler indépendamment des cellules souches hématopoïétiques (Kierdorf et al., 2013; Tay et al., 2017). Jusqu'à récemment, on pouvait identifier les cellules microgliales avec des marqueurs myéloïdes comme Cx3cr1, CD11b, Iba1 et F4/80. De plus, de récentes analyses de séquençage ARN (RNAseq) ont identifié un nouvel ensemble de marqueurs spécifiques à la microglie dans le cerveau sain, notamment HexB, P2ry12, S100A8, S100A9, Tmem119, Gpr34, Siglech, TREM2 et Olfml37 (Hickman et al., 2013).

Rôles

Les cellules microgliales exercent principalement trois fonctions essentielles : (i) surveiller leur environnement, (ii) effectuer un entretien physiologique (« *Housekeeping* ») et (iii) protéger contre les blessures et les agents pathogènes. Ces fonctions sont essentielles et assurées à divers stades de développement ; aux stades embryonnaires, à l'âge adulte et jusqu'au vieillissement (Hickman *et al.*, 2018).

Surveillance de l'environnement : Les cellules microgliales forment un réseau couvrant tout le SNC. Alors qu'elles ont longtemps été supposées inertes, leurs prolongements minces et dynamiques sont en mouvement constant, ce qui leur permet de scanner et de surveiller la zone entourant leur corps cellulaire en permanence. Ainsi, une centaine de gènes sont impliqués dans la détection des changements de leur microenvironnement (leur « *sensome* »), notamment P2yr12, AXL et MER (Se *et al.*, 2006; Hickman *et al.*, 2013). Une bonne surveillance est une condition préalable à la microglie pour remplir ses autres fonctions d'entretien et de défense de l'organisme.

Entretien physiologique du système nerveux central, ou « *Housekeeping* » : Ces fonctions comprennent le remodelage synaptique (une fonction critique pour le développement du SNC), l'homéostasie et la neurodégénérescence (Zhan *et al.*, 2014; Vasek *et al.*, 2016), la migration vers les sites de mort neuronale pour phagocyter les cellules mortes, mourantes et les débris (Fuhrmann *et al.*, 2010; Krasemann *et al.*, 2017), et le maintien de l'homéostasie de la myéline (Healy *et al.*, 2017). L'interaction avec les astrocytes est une autre fonction microgliale importante impliquée dans l'homéostasie, l'inflammation et éventuellement la neurodégénérescence (Liddelow *et al.*, 2017). Parmi les gènes impliqués dans l'entretien du SNC figurent ceux codant pour les récepteurs des chemokines et des chemoattractants, les gènes impliqués dans la phagocytose (récepteurs scavengers et Trem2), ainsi que les gènes impliqués dans l'élagage et le remodelage synaptique (C1q et Cx3cr1) (Hickman *et al.*, 2013). Des dysfonctionnements de ces mécanismes peuvent également mener à la neurodégénérescence.

Protection et défense du SNC : La microglie assure la défense du SNC contre les agents pathogènes infectieux, les protéines nuisibles telles que le peptide bêta-amyloïde (A β)

ou l' α -synucléine agrégée, les prions, ou encore les tumeurs métastatiques ou primaires. Pour remplir ces fonctions, la microglie exprime des récepteurs aux fragments cristallisables (Fc), des TLR, des récepteurs viraux et des peptides antimicrobiens (Hickman *et al.*, 2018). En réponse à de tels stimuli, la microglie peut initier une réponse neuroinflammatoire ; on parle alors d'activation microgliale. Lors de son activation la microglie adopte des changements morphologiques et phénotypiques. Elle peut alors présenter de très nombreuses ramifications, mais aussi perdre tous ses prolongements et adopter une forme plus grosse et ronde ; on parle alors de phénotype améboïde (Perry, Nicoll and Holmes, 2010). Cela comprend aussi la production de cytokines inflammatoires telles que le TNF et l'IL-1 (El Khoury *et al.*, 2003; Hickman, Allison and El Khoury, 2008), et éventuellement des chemokines comme CCL2 (El Khoury *et al.*, 2007, p. 2) pour recruter des cellules supplémentaires afin d'aider à éliminer les agents nocifs et rétablir ainsi l'homéostasie cérébrale.

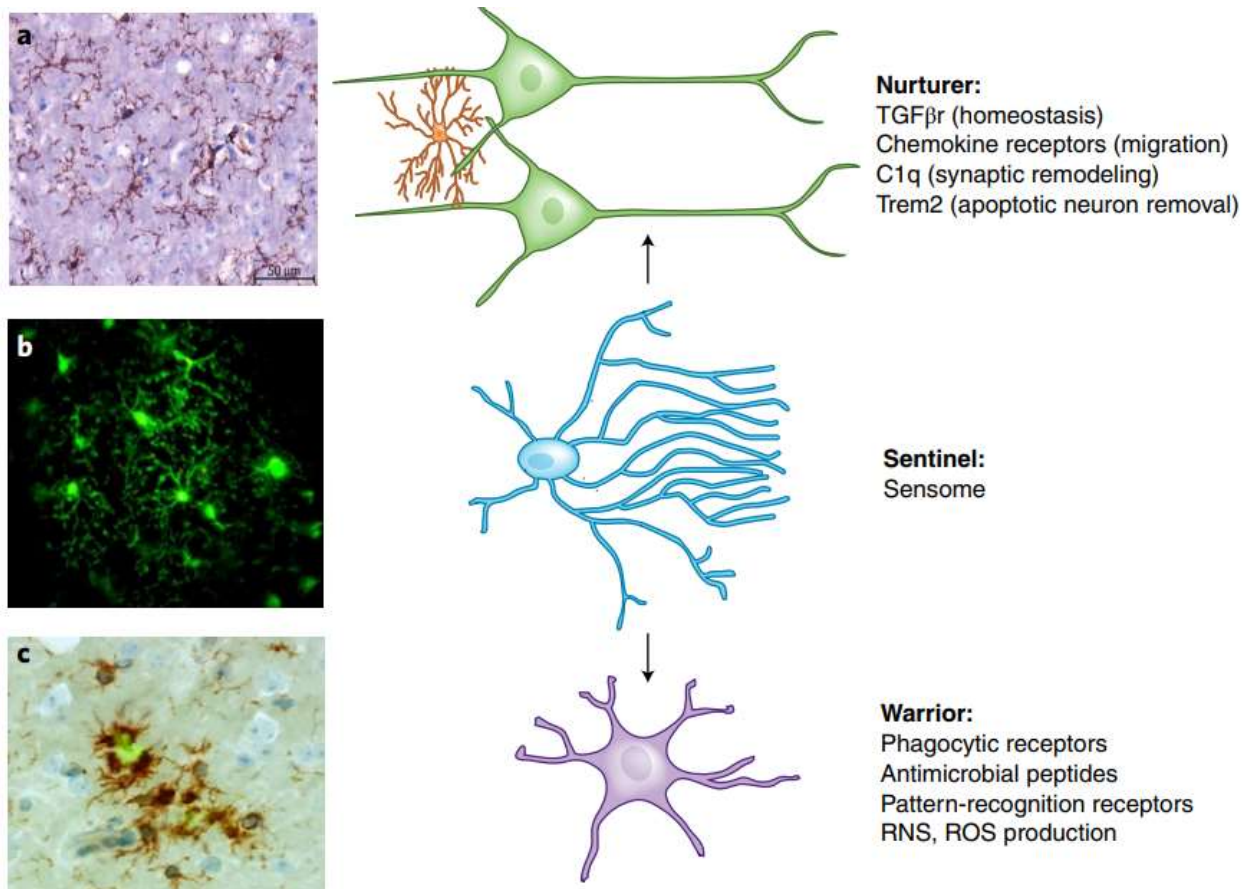


Figure 18 : Représentation de 3 rôles de la microglie.

a, Rôle de soutien/entretien du SNC. Des cellules microgliales marquées pour le CD11b (en haut, à gauche) dans un cerveau sain, les cellules sont bien ramifiées et régulièrement espacées dans tout le parenchyme. Elles maintiennent l'homéostasie du milieu, participent au remodelage et à la migration synaptique, et éliminent les neurones apoptotiques. *b*, Rôle de sentinelle, de surveillance du milieu. Microphotographie (au milieu, à gauche) extraite d'une vidéo de microscopie à deux-photons dans un cerveau de souris Cx3cr1-GFP avec les cellules microgliales fluorescentes vertes. Sur la vidéo originale, les prolongements des cellules sont en mouvement constant et scannent l'environnement. Dans le cas d'une lésion focale induite par un laser, la microglie va tout de suite détecter le problème et se polariser vers le site de lésion. *c*, Rôle de défense du SNC. La microglie marquée pour le CD11b (marron) s'accumule autour des dépôts amyloïdes colorés avec la thioflavine-S (vert). La densité de cellules est alors plus importante et la morphologie devient plus ronde et moins ramifiée.

D'après « Microglia in neurodegeneration » (Hickman et al., 2018).

Les macrophages associés aux bordures du système nerveux central

Description anatomique des interfaces entre le système nerveux central et la périphérie

Dans le parenchyme cérébral et la moelle épinière, les cellules microgliales sont les seules cellules immunitaires résidentes. Le SNC a longtemps été considéré comme un organe privilégié sur le plan immunitaire, sans système lymphatique ni surveillance immunitaire par des cellules circulantes en conditions physiologiques (Engelhardt, 2006; Galea, Bechmann and Perry, 2007). Cependant ces théories ont été remises en question récemment par la (re)découverte d'un système de drainage lymphatique spécialisé observé au niveau de la dure-mère, une des couches des méninges qui englobent le SNC (Furukawa *et al.*, 2008; Louveau *et al.*, 2017, 2018; Ahn *et al.*, 2019; Papadopoulos, Herz and Kipnis, 2020). De nombreuses études sont actuellement en cours pour élucider ces mécanismes. Quoiqu'il en soit, il est clair que le SNC présente une séparation immunitaire avec la périphérie, avec un accès limité et hautement régulé pour les cellules immunitaires circulantes, les métabolites et les molécules de signalisation (Daneman and Engelhardt, 2017).

Ainsi, des structures anatomiques hautement spécialisées existent pour protéger le SNC de la périphérie. Les principales sont les méninges, l'espace périvasculaire, et les plexus choroïdes. Ces structures forment des interfaces, qui agissent à la fois comme des barrières mais aussi des passerelles hautement régulées, soutenant le privilège immunologique du SNC et lui conférant un accès restreint aux cellules et molécules extérieures.

Ces interfaces peuvent également servir de sites d'entrée pour des agents pathogènes, d'infiltration de cellules immunitaires ou de dépôt de molécules pathologiques. Ainsi ces dernières années, il existe un intérêt croissant pour le rôle de ces interfaces dans les maladies neuroinflammatoires, neurodégénératives et les infections (Daneman and Engelhardt, 2017; Erickson and Banks, 2018).

Toutes ces structures anatomiques possèdent des populations de macrophages résidents connus comme les « macrophages associés aux bordures » du SNC (BAMs, *border-*

associated macrophages ; ou encore CAMs, *CNS-associated macrophages*). L'ensemble des BAMs regroupe ainsi (i) les macrophages de l'espace périvasculaire (PVM, *perivascular macrophages*), (ii) les macrophages méningés (MM) et (iii) les macrophages des plexus choroïdes (ChPM) (Amann and Prinz, 2020; Ivan et al., 2021).

Les méninges

Les méninges sont les membranes protectrices qui entourent le SNC. Elles sont au nombre de trois, de la plus externe à la plus interne : la dure-mère, l'arachnoïde et la pie-mère. Ces deux dernières forment ensemble les leptoméninges (Weller, 2005). La dure-mère est une couche dense et étroitement associée au crâne. L'arachnoïde, la couche intermédiaire, est principalement constituée de tissu conjonctif non vascularisé (Clarke, 1944; Nabeshima et al., 1975). L'espace sous arachnoïdien entre l'arachnoïde et la pie-mère est un compartiment rempli de LCR. La pie-mère est étroitement associée avec le parenchyme du SNC. En plus d'une grande variété de cellules immunitaires périphériques qui circulent dans cet espace, les méninges sont peuplées de deux sous-populations de macrophages méningés (MM), les macrophages durs et leptoméningés (Wilson, Weninger and Hunter, 2010; Ransohoff and Engelhardt, 2012).

L'espace périvasculaire

Les vaisseaux sanguins du cerveau sont entourés d'un compartiment périvasculaire rempli de LCR, également connu sous le nom d'espace de Virchow-Robin. Rudolp Virchow a été le premier à fournir une description détaillée de ces espaces, et plus tard Charles-Philippe Robin a confirmé ces observations et fut le premier à décrire les espaces périvasculaires comme des canaux en conditions physiologiques (Cherian et al., 2016). En effet, ce compartiment suit le parcours des vaisseaux de l'espace méningé à travers le SNC et est situé entre la membrane basale abluminale des vaisseaux et la membrane de la *glia limitans* (Lam et al., 2017). Au point où les artères pénétrantes deviennent des artérioles, puis des capillaires, les deux membranes basales fusionnent et restreignent l'espace périvasculaire. L'espace périvasculaire sert de système de drainage pour les substances et déchets du LCR, et sert également de barrière pour limiter l'entrée de cellules périphériques directement dans le parenchyme. Au sein de cet espace résident des macrophages périvasculaires, ou PVM.

Les plexus choroïdes

Les ChP forment une structure composée de cellules épithéliales liées par des jonctions serrées entourant un stroma hautement vascularisé. Ils sont situés dans les ventricules cérébraux et créent une interface entre le sang et le LCR. La fonction principale des plexus choroïdes est de réguler le contenu et le volume du LCR. En effet, ils produisent le LCR mais filtrent également les déchets métaboliques (Lun, Monuki and Lehtinen, 2015). De plus, les plexus choroïdes sont de plus en plus considérés comme une porte d'accès importante du SNC pour les cellules immunitaires périphériques. Au sein des plexus choroïdes, deux différentes populations de macrophages existent : les macrophages des épiplexus, ou cellules de Kolmer, au contact du LCR, et les macrophages résidents dans le stroma des plexus choroïdes (Ransohoff and Engelhardt, 2012).

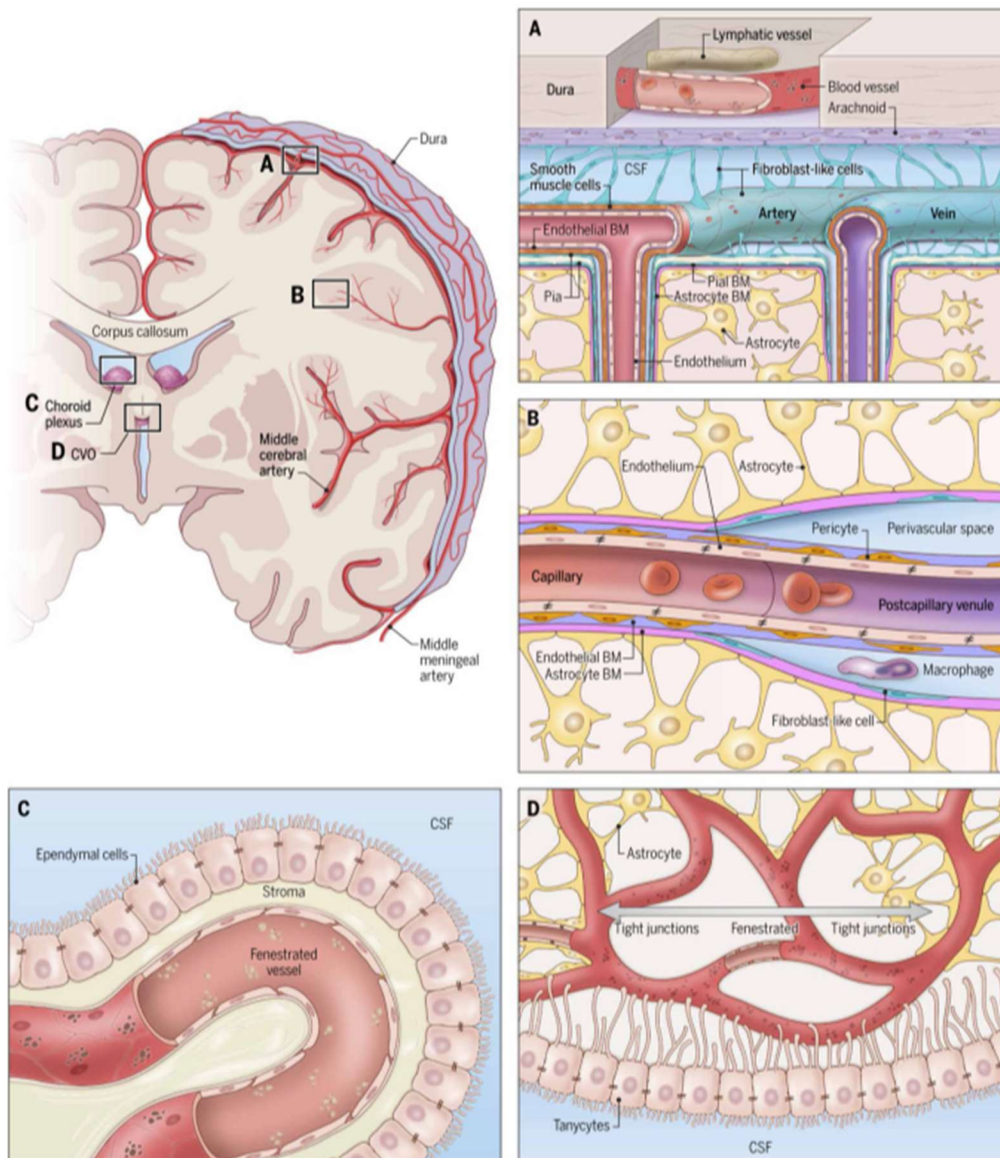


Figure 19 : Anatomie des barrières entre le SNC et la périphérie.

Représentation coronale du cerveau et de la dure-mère en relation avec les artères cérébrales moyennes et méningées moyennes. A, Anatomie vasculaire méningée. La dure-mère contient des vaisseaux lymphatiques et des vaisseaux sanguins fenêtrés qui manquent de jonctions serrées. Les vaisseaux sanguins leptoméningés de la pie-mère sont dépourvus d'enveloppe astrocytaire mais leurs cellules endothéliales sont reliées par des jonctions serrées. Les artères piales pénètrent dans le parenchyme et se recouvrent des pieds astrocytaires. B, Venule capillaire et post-capillaire dans le parenchyme cérébral. La venule est entourée de l'espace périvasculaire rempli de LCR, tandis que la membrane basale endothéliale est accolée à la membrane basale astrocytaire autour des capillaires. C, Les vaisseaux des plexus choroïdes sont fenêtrés et manquent de jonctions serrées. Les cellules épithéliales recouvrant les plexus sont liées par des jonctions serrées chargées de former une barrière entre le sang et le LCR. D, Les vaisseaux sanguins des organes circumventriculaires sont fenêtrés et manquent de jonctions serrées.

D'après de "The anatomy and immunology of vasculature in the central nervous system" (Mastorakos and McGavern, 2019).

Les macrophages périvasculaires

Historique

En 1980, Masao Mato a montré que du bleu trypan et de la peroxydase injectés dans les ventricules cérébraux sont captés par des cellules allongées autour des vaisseaux sanguins du cerveau (Mato, Ookawara and Kurihara, 1980). Ces cellules, d'abord définies comme des « péricytes granulaires », ont ensuite été appelées cellules « périthéliales granulaires fluorescentes » (FGP pour *fluorescent granular perithelial cell*), ou cellules de Mato. Ces cellules ont tout de suite été caractérisées par leur activité phagocytaire, c'est à dire leur capacité à éliminer des déchets métaboliques du LCR et du parenchyme cérébral, de par la présence d'inclusions globulaires dans leur cytoplasme et l'expression de récepteurs *scavengers* (Mato et al., 1986). Il a également été décrit que les cellules FGP étaient capables d'incorporer des lipides circulants, et que la quantité de ces dépôts lipidiques augmentait avec l'âge (Mato et al., 1982). Ces cellules étaient décrites dans l'espace périvasculaire autour des artérioles et veinules de 10 à 35 µm de diamètre, et différentes des péricytes intégrés dans la membrane basale des capillaires (Mato et al., 1996). Cependant, l'identité précise de ces cellules n'était pas très bien définie. En effet, des cellules « périvasculaires fluorescentes » (Fleischhauer, 1964) ainsi que des cellules « microgliales péricytiques » (Mori and Leblond, 1969) avaient déjà été décrites, créant une confusion dans les différentes dénominations.

En 1988, Hickey et Kimura ont poursuivi la description de ces cellules « microgliales périvasculaires », capables de présenter des antigènes aux lymphocytes. Ces cellules, positives pour l'antigène ED2, présentent une forme allongée et sont situées autour des vaisseaux sanguins cérébraux (Hickey and Kimura, 1988). Cependant, Graeber et collaborateurs ont suggéré que ces cellules périvasculaires ED2⁺ étaient différentes de la microglie, négative pour ED2 (Graeber, Streit and Kreutzberg, 1989). L'antigène ED2 a ensuite été identifié comme CD163, une glycoprotéine membranaire appartenant à la famille des récepteurs *scavengers* avec une haute affinité pour l'hémoglobine (Fabriek et al., 2007). Les cellules périvasculaires CD163⁺ sont également positives pour le marqueur phagocytaire CD68, et négatives pour l'actine des cellules musculaires lisses, confirmant que ces cellules sont des macrophages et non des péricytes ou des cellules musculaires (Kim et al., 2006). De plus, elles sont positives pour les protéines du complexe majeur d'histocompatibilité de classe II (MHC II) et plusieurs

molécules de co-stimulation telles que les CD80, CD86 et CD40, suggérant un rôle dans la reconnaissance et la présentation d'antigènes (Fabriek *et al.*, 2005). L'ensemble de ces résultats ont alors établi les PVM comme une population distincte des cellules myéloïdes résidentes, situées dans l'espace périvasculaire entourant les vaisseaux sanguins du SNC.

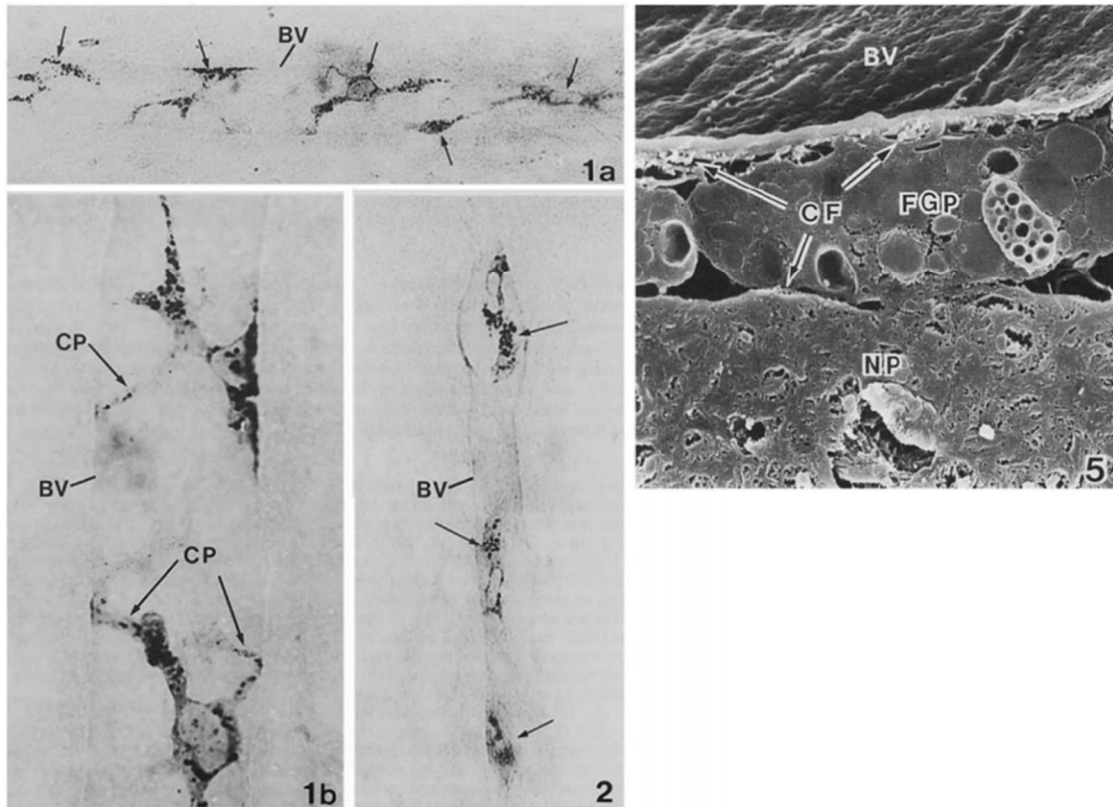


Figure 20 : Observation de macrophages périvasculaires autour de vaisseaux sanguins de cerveaux de rats par Masao Mato.

1a,b,2, PVM régulièrement disposés (flèches) autour d'un petit vaisseau sanguin (BV, blood vessel) du cortex cérébral. Ils ont une forme hexagonale et sont pourvus de projections cytoplasmiques allongées (CP, cytoplasmic projections). 5, PVM (alors appelés FGP, fluorescent granular perithelial cells) localisé entre un vaisseau sanguin (BV) et un neuropile (NP). Des fibres de collagène (CF, collagen fibers) sont réparties dans les interstices entre le PVM et les vaisseaux sanguins ou neuropile.

D'après « Tridimensional observation of fluorescent granular perithelial (FGP) cells in rat cerebral blood vessels » (Mato *et al.*, 1986).

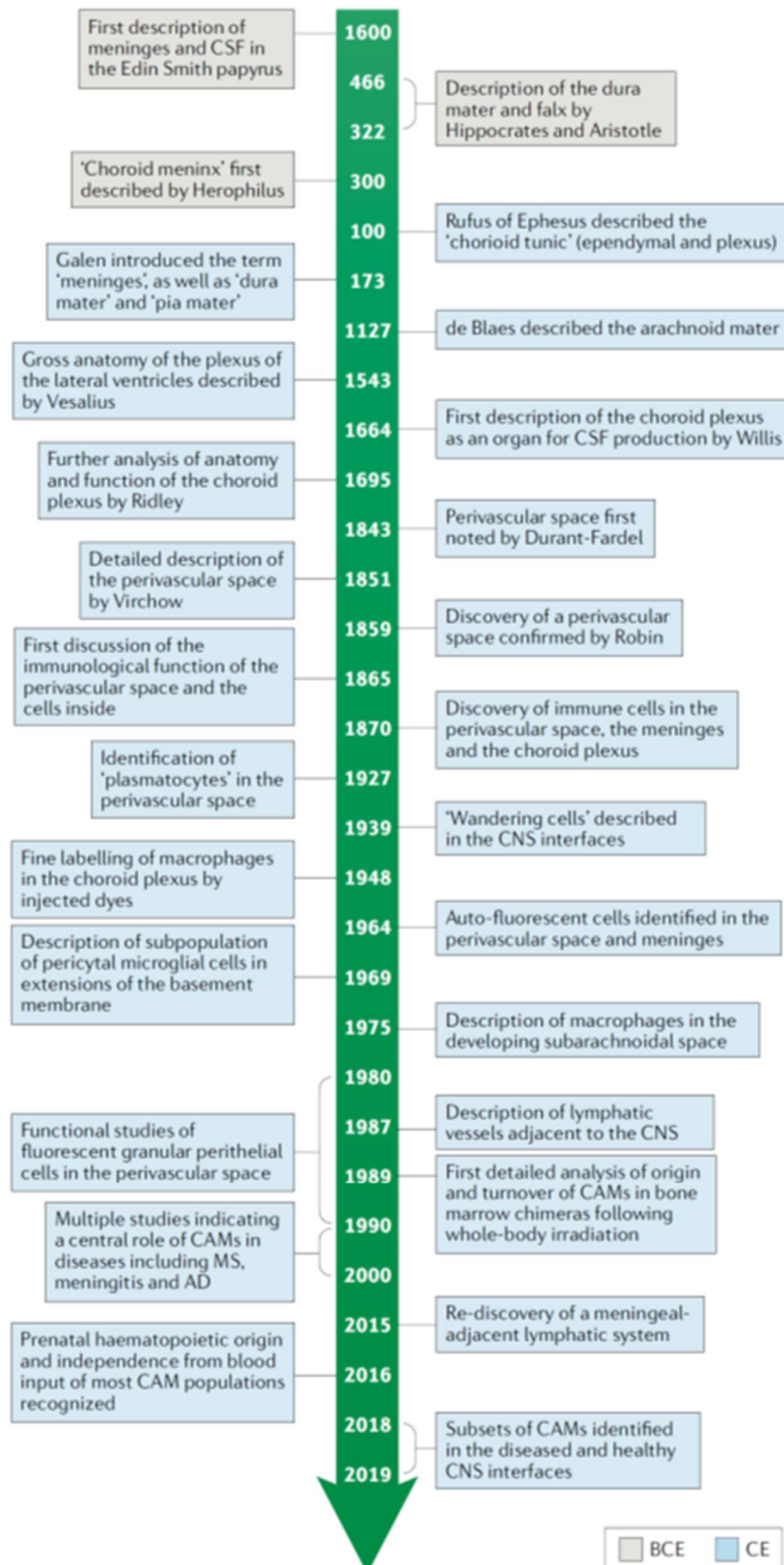


Figure 21 : Chronologie des découvertes majeures, des premières descriptions des interfaces du SNC jusqu'aux études des BAMs.

D'après "Macrophages at CNS interfaces: ontogeny and function in health and disease" (Kierdorf et al., 2019).

Origine

Depuis le système de classification de van Furth et collaborateurs en 1972, les macrophages tissulaires étaient considérés comme des cellules ayant une vie relativement courte continuellement remplacés par des monocytes circulant dans le sang, dérivés de la moelle osseuse (van Furth *et al.*, 1972). Ce concept a radicalement évolué avec des preuves que les macrophages peuvent être dérivés de précurseurs embryonnaires et être maintenus sur le long terme sans contribution des cellules souches hématopoïétiques (HSC, *hematopoietic stem cells*) (Ajami *et al.*, 2007; Amann and Prinz, 2020). Plusieurs études au cours de la dernière décennie ont revisité et clarifié l'ontogénie des macrophages résidents des différents tissus et organes. Il a été montré qu'au cours du développement embryonnaire les tissus sont très tôt peuplés par des macrophages qui se développent à partir de progéniteurs érythromyéloïdes (EMP, *erythromyeloid progenitors*) dans le sac vitellin extra-embryonnaire (YS, *yolk sac*) ou dans le foie fœtal (Ginhoux *et al.*, 2010; Hoeffel *et al.*, 2015). Dans plusieurs tissus, comme le foie ou les alvéoles pulmonaires, ces cellules dérivées embryonnaires subsistent après la naissance et forment des populations de macrophages résidents qui s'auto-entretiennent sans contribution des cellules dérivées de la moelle osseuse, au moins en conditions physiologiques d'homéostasie (Hashimoto *et al.*, 2013; Amann and Prinz, 2020).

Dans le parenchyme du SNC, les cellules microgliales semblent exclusivement dérivées des EMP du YS, et se renouvellent tout au long de la vie sans apport extérieur (Ajami *et al.*, 2007; Kierdorf *et al.*, 2013; Tay *et al.*, 2017). Concernant les BAMs, il a été montré récemment que les PVM et MM sont également dérivés des EMP et ne sont pas remplacés par des cellules dérivées de la moelle osseuse après la naissance (Goldmann *et al.*, 2016; Utz *et al.*, 2020). Dans les plexus choroïdes, la situation est plus complexe car il existe en réalité au moins deux sous-populations de macrophages : les macrophages du stroma et les cellules de l'épipleux de Kolmer à la surface apicale de l'épithélium de plexus (Prinz and Priller, 2014). Alors que les macrophages du stroma sont continuellement remplacés par des cellules périphériques dérivées de la moelle osseuse, les macrophages de l'épipleux semblent être dérivés des EMP sans contribution périphérique (Goldmann *et al.*, 2016; Hove *et al.*, 2019).

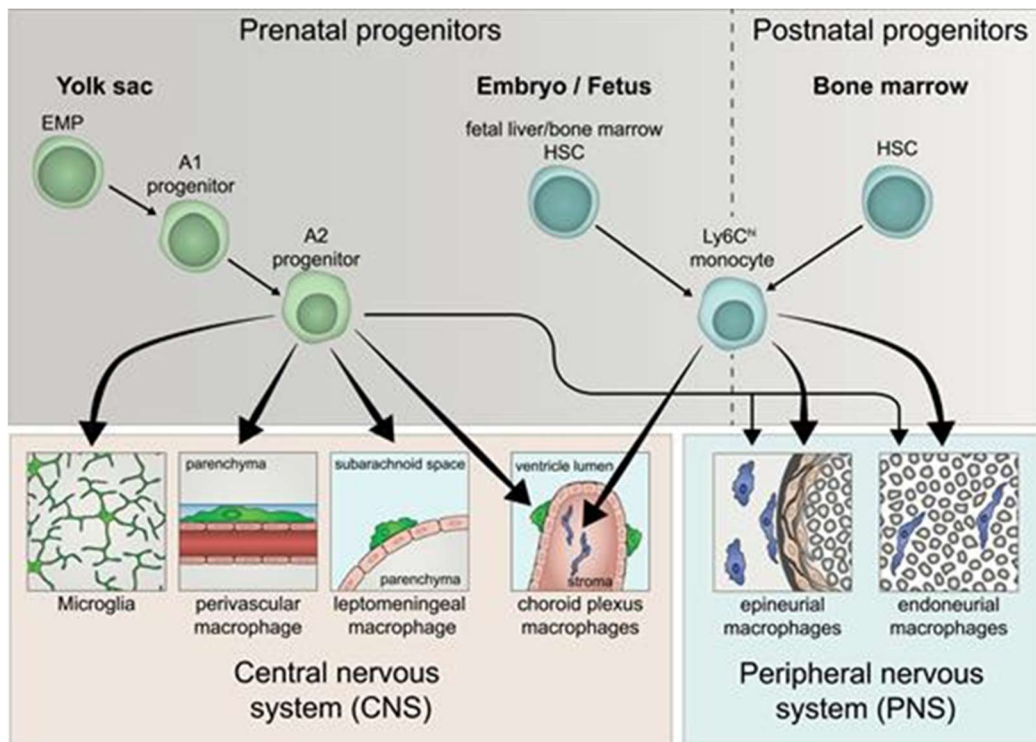


Figure 22 : Origine ontogénique des macrophages du système nerveux.

Les macrophages tissulaires peuvent être dérivés de différents précurseurs prénataux ou postnatals. Les EMP (vert clair) se développent dans le sac vitellin extra-embryonnaire et donnent naissance à la microglie, aux macrophages périvasculaires, aux macrophages méningés et aux cellules épiplexiques de Kolmer (vert). À partir des stades ultérieurs du développement fœtal, les HSC (bleu clair) dans le foie fœtal ou la moelle osseuse donnent naissance à des macrophages tissulaires via les monocytes Ly6C^{hi} (bleu clair). Ces monocytes dérivés du fœtus donnent naissance à des macrophages dans le SNP et contribuent également aux macrophages du stroma dans le ChP (bleu).

D'après « The origin, fate and function of macrophages in the peripheral nervous system—an update » (Amann & Prinz, 2020)

Caractérisation moléculaire et fonctionnelle

Comme tous les leucocytes, les PVM expriment CD45 et CD11b. Ils partagent également avec la microglie l'expression de Cx3cr1, Iba-1 (également appelé Aif1) et Csf1 (*colony-stimulating factor 1 receptor*). Par rapport à la microglie, le niveau d'expression de CD45 est plus élevé dans les PVM, alors que Cx3cr1 et Iba-1 sont bien moins exprimés. De plus, les PVM n'expriment pas le récepteur purinergique P2RY12 spécifique de la microglie (Goldmann *et al.*, 2016). Dans le SNC de la souris, les PVM sont également positifs pour le récepteur du mannose CD206, impliqué dans la reconnaissance d'agents pathogènes et

l'endocytose (Galea et al., 2005). L'expression de CD206 est observée dans l'ensemble des BAMs (PVM, MM, ChPM) mais n'est pas présente dans les cellules microgliales ou les leucocytes périphériques infiltrant le parenchyme (Galea et al., 2005; Goldmann et al., 2016). Lyve-1, le récepteur de l'hyaluronane et marqueur des vaisseaux lymphatiques, est également exprimé par les PVM, contrairement aux monocytes et à la microglie. Cependant, ce marqueur n'est pas aussi sensible que CD206 pour identifier les PVM (Yang, Guo and Zhang, 2019). Des études plus récentes, dont l'une utilise la cytométrie de masse couplée au séquençage d'ARN, ont révélé que la combinaison de CD38 et MHC II était une signature moléculaire fiable des BAMs (Mrdjen et al., 2018). Finalement, il n'y a pas un seul marqueur spécifique des PVM, mais souvent une combinaison de deux ou trois d'entre eux en fonction du contexte et de la méthode utilisée. Par exemple, $CD11b^+CD45^{high}CD206^+$ peut être un bon moyen de les identifier spécifiquement en cytométrie en flux, en condition physiologique.

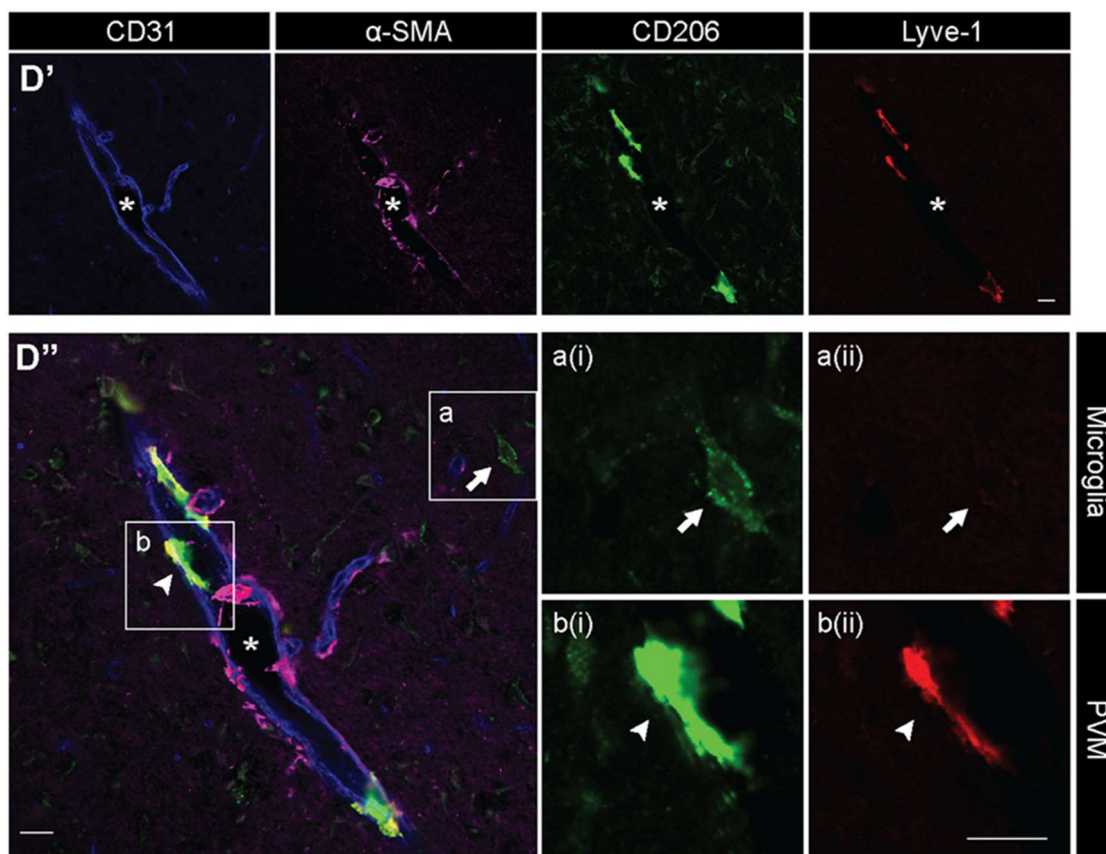


Figure 23 : Caractérisation immunohistologique des PVM.

D'après "Brain perivascular macrophages: Recent advances and implications in health and diseases" (Yang, Guo and Zhang, 2019).

L'activité phagocytaire des PVM est également utilisée pour les identifier. En effet, les PVM peuvent être marqués par une injection intracérébroventriculaire de traceurs comme des dextrans fluorescents. Une fois injecté dans le ventricule cérébral, le traceur diffuse dans le LCR et dans les espaces périvasculaires où il sera phagocyté par les PVM, conduisant à un marquage granulaire reflétant le stockage intracellulaire dans les phagosomes (Bechmann *et al.*, 2001; Drieu *et al.*, 2020). Cette capacité de phagocytose est d'ailleurs largement exploitée pour étudier les fonctions des PVM dans différents mécanismes et pathologies. En effet, les PVM peuvent être ciblés en utilisant l'injection intracérébroventriculaire de liposomes contenant du clodronate (Polfliet, Goede, *et al.*, 2001). Les liposomes injectés dans les ventricules cérébraux sont phagocytés dans le LCR par les PVM et MM. Une fois libéré dans le cytosol, le clodronate agit comme un analogue cytotoxique de l'ATP, bloquant la consommation mitochondriale d'oxygène et menant à la mort cellulaire de la cellule par apoptose (Lehenkari *et al.*, 2002). Chez la souris, l'injection intracérébroventriculaire de clodronate supprime la plupart des PVM et MM sans affecter la microglie où les cellules périphériques, à l'exception d'une réduction transitoire du nombre de cellules de Kupffer dans le foie. La déplétion des PVM est transitoire et la population commence à se reconstituer après environ 14 jours (Polfliet, Goede, *et al.*, 2001). Concernant la source d'où proviennent les cellules qui vont reconstituer la population de PVM et MM après la déplétion, on ne sait pas encore s'il s'agit de cellules myéloïdes circulantes, de précurseurs résidents dans le cerveau, ou d'un mélange de ces deux hypothèses (Yang, Guo and Zhang, 2019). Il est aussi possible qu'il existe d'autres sources, encore hypothétiques. En effet, une étude récente a décrit la moelle osseuse du crâne comme nouvelle source directe de cellules myéloïdes pour le SNC (Cugurra *et al.*, 2021). De futures études devraient déterminer si cela peut également constituer une origine des populations de BAMs.

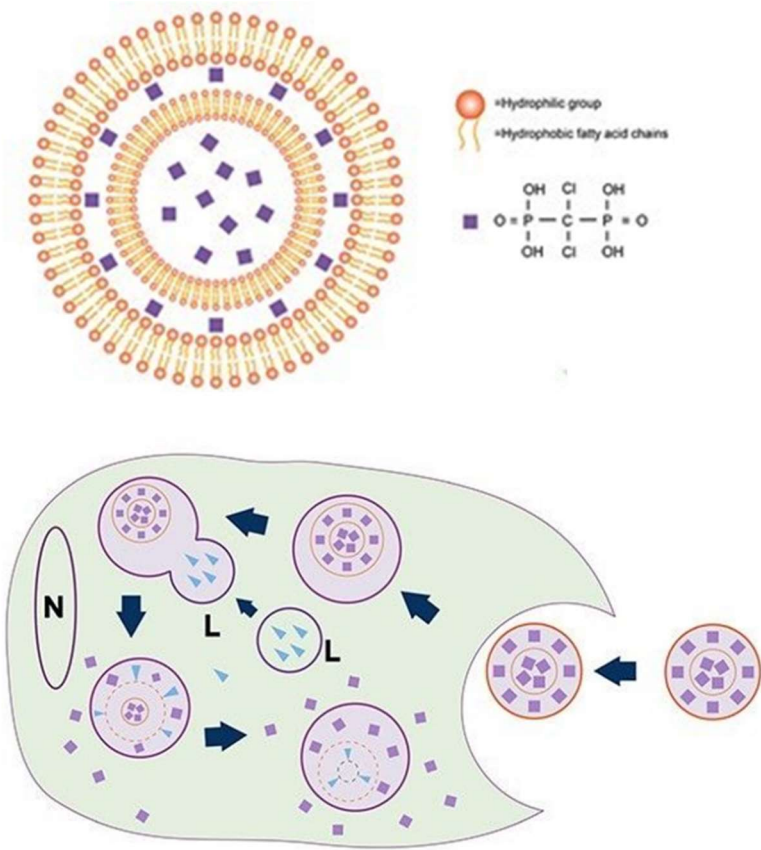


Figure 24: Mécanisme d'action du clodronate
(clodrosome.com)

Pour résumer, la combinaison de différents marqueurs, la localisation anatomique périvasculaire et la fonction phagocytaire permettent une identification spécifique des PVM. Bien qu'encore très peu connus, les PVM (et plus généralement les BAMS) constituent un champ de recherche en pleine expansion. En effet, leur localisation stratégique à l'interface du SNC, du sang et du système immunitaire fait d'eux de potentiels acteurs majeurs de la physiopathologie cérébrale.

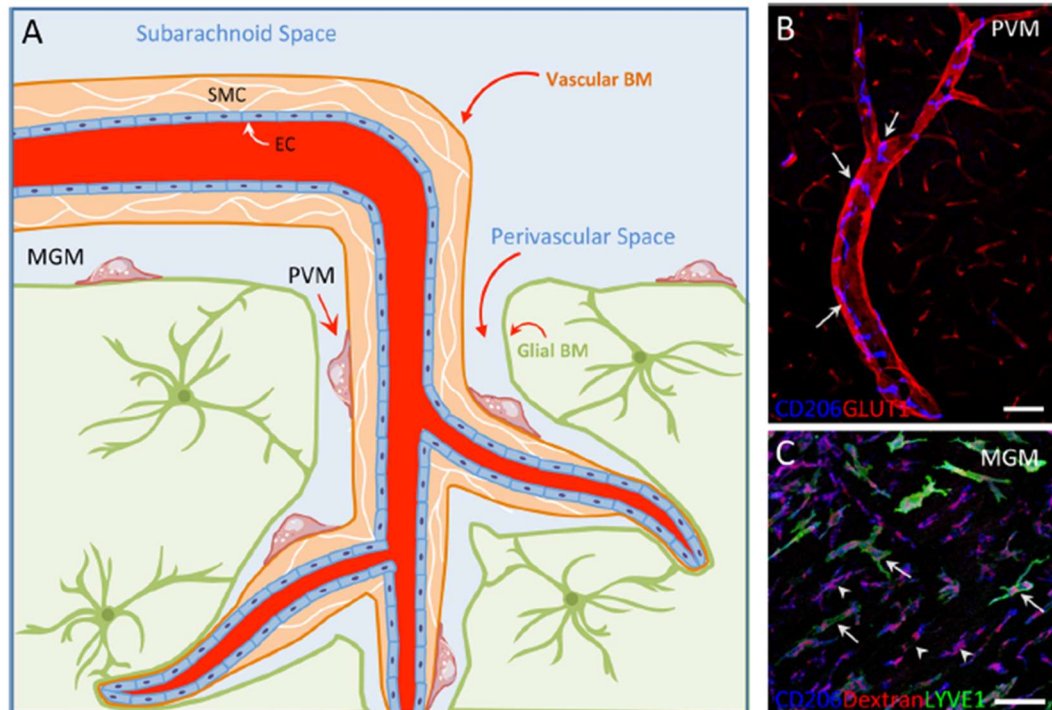


Figure 25 : Localisation anatomique des macrophages périvasculaires (PVM) et méningés (MM).

A, Les PVM sont situés dans l'espace périvasculaire entourant les artères et les veines dans le tissu cérébral, tandis que les MM sont localisés dans les méninges. L'espace périvasculaire est délimité par la membrane basale vasculaire (Vascular BM) du côté abluminal de la paroi vasculaire et par la membrane basale de la glia limitans (Glial BM) du côté parenchymateux. Au niveau des capillaires, les deux membranes fusionnent en obstruant l'espace périvasculaire. B, Les PVM peuvent être identifiés comme des cellules périvasculaires positives pour CD206 (flèches). C, Les MM sont CD206 positifs et, comme les PVM, sont capables de phagocyter le TRITC-dextran injecté dans les ventricules cérébraux (pointes de flèche). Barres d'échelle 50 μ m.

D'après "Brain perivascular macrophages: characterization and functional roles in health and disease" (Faraco et al., 2017).

Rôles en condition physiologique

Intégrité de la BHE

En conditions physiologiques, les PVM contribuent à l'intégrité de la BHE. Il a été montré qu'ils peuvent phagocyter des protéines sériques de 10 à 70 kDa et jouent un rôle essentiel dans la restriction du passage des macromolécules du sang vers le cerveau. Ce rôle est également observé dans des organes circumventriculaires du cerveau dépourvus de jonctions serrées avec une perméabilité plus élevée de la BHE, comme l'*area postrema* (Willis, Garwood and Ray, 2007). De même, les PVM des organes périphériques restreignent la perméabilité vasculaire, notamment au niveau des artères mésentériques et cochléaires (W. Zhang *et al.*, 2012; He *et al.*, 2016). Cette propriété est également observée dans un modèle de co-culture de BHE *in vitro*, composé de cellules endothéliales, de PVM et de péricytes (D. J. Zhang *et al.*, 2017). À l'inverse, il semble que les PVM peuvent contribuer à la fragilisation et l'ouverture de la BHE dans certaines pathologies.

Présentation d'antigènes

Les molécules du MHC II sont une classe de molécules que l'on retrouve normalement à la surface des cellules présentatrices d'antigènes telles que les cellules dendritiques (DC), les monocytes/macrophages, ou les lymphocytes B. Cela permet à ces cellules de présenter des antigènes aux lymphocytes T qui peuvent enclencher la réponse ciblée grâce à la reconnaissance de signatures spécifiques. On passe d'une réponse immunitaire non spécifique, ou innée, à une réponse immunitaire spécifique, adaptative (Roche and Furuta, 2015). Depuis 1988, il est décrit que les PVM (alors appelés « microglie périvasculaire ») expriment le MHC II dans le cerveau des souris et sont capables de présenter des antigènes aux lymphocytes (Hickey and Kimura, 1988). De plus, l'expression de MHC II par les PVM peut être augmentée en conditions pathologiques, comme dans une EAE (Encéphalite Autoimmune Expérimentale, modèle murin de sclérose en plaques), ou un modèle transitoire d'occlusion de l'artère cérébrale moyenne (Hickey and Kimura, 1988; Henning *et al.*, 2009). Des PVM exprimant le MHC II ont également été observés après autopsie de cerveaux humains atteints de sclérose en plaques (Hickey and Kimura, 1988). Plus récemment, des études de séquençage ARN et de cytométrie de masse ont montré que les expressions de MHC II, mais également de

CD74 (impliqué dans la formation et le transport du MHC II) sont augmentées durant le vieillissement, renforçant le rôle des PVM dans l'immunité acquise (Mrdjen *et al.*, 2018; Jordão *et al.*, 2019).

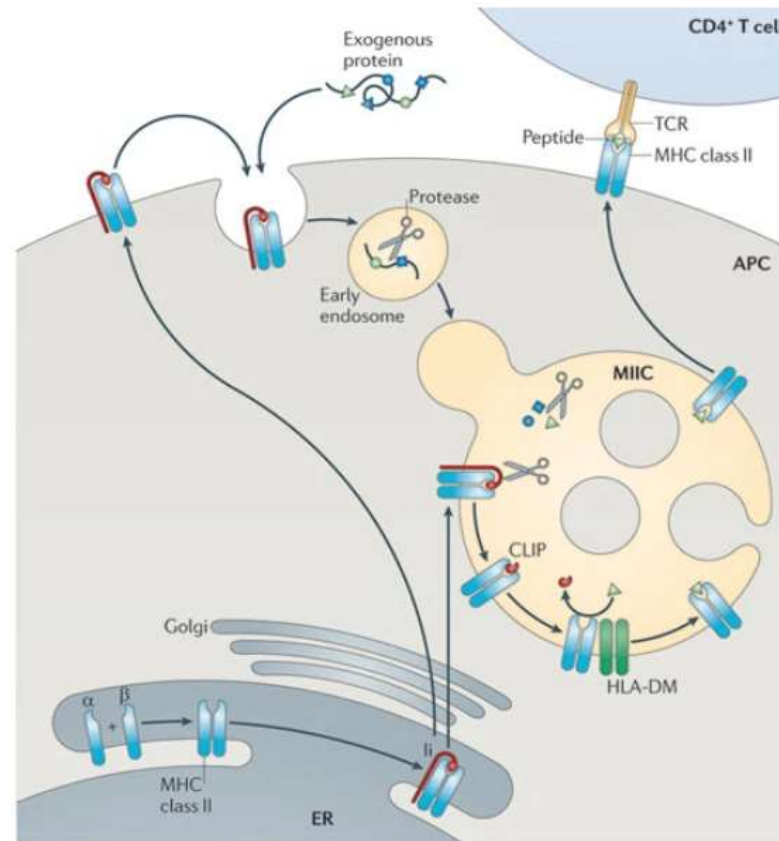


Figure 26 : Mécanisme de présentation d'antigène par la voie MHCII.

L'hétérotrimère du MHCII est transporté à travers l'appareil de Golgi jusqu'au compartiment du MHC de classe II (MIIC), directement et/ou via la membrane plasmique. Les protéines Ii et celles endocytosées sont dégradées par les protéases résidentes dans le MIIC. Le fragment de peptide Ii associé à la classe II (CLIP) est échangé contre un peptide antigénique. Les molécules du MHCII sont ensuite transportées vers la membrane plasmique pour présenter des peptides antigéniques aux cellules T CD4⁺. APC, cellule présentatrice d'antigène; TCR, récepteur des cellules T.

D'après "Towards a systems understanding of MHC class I and MHC class II antigen presentation" (Neeffjes *et al.*, 2011)

Drainage du LCR

Compte tenu de leur emplacement stratégique au sein de l'espace périvasculaire, les PVM sont en permanence au contact du LCR. Ils participent ainsi à l'élimination des déchets du SNC grâce à leur grande capacité de phagocytose, qui est d'ailleurs utilisée pour marquer et/ou cibler ces cellules (Kida et al., 1993; Faraco et al., 2017). En effet, les PVM peuvent aussi phagocyter des traceurs injectés directement dans le parenchyme, ce qui démontre leur capacité à filtrer le fluide interstitiel sortant du SNC (Carare et al., 2008; Engelhardt et al., 2016). De plus, les PVM participent à la régulation du tonus vasculaire et de la pression artérielle (Iyonaga et al., 2019), ce qui pourrait être un moteur de la circulation et du drainage lymphatique du LCR (Rasmussen, Mestre and Nedergaard, 2018). Ainsi, les PVM semblent être des acteurs de la dynamique des fluides du SNC. Le rôle exact des PVM dans le drainage lymphatique doit être abordé dans les recherches futures. Les PVM sont situés à l'interface entre le cerveau et la périphérie. Ils expriment des récepteurs *scavengers* qui leur confèrent une grande activité de phagocytose, agissant comme surveillant immunitaire, fournissant un soutien structurel et fonctionnel à la BHE et au drainage lymphatique. Ces rôles sont tous importants pour l'homéostasie cérébrale.

Implications des PVM dans les pathologies cérébrales

Rôle des PVM dans les altérations de la BHE

La BHE joue un rôle essentiel dans le maintien de l'homéostasie cérébrale, et son dysfonctionnement est mis en cause dans de nombreuses pathologies. Plusieurs études ont ainsi observé une accumulation de PVM corrélée avec la perméabilisation de la BHE dans diverses conditions pathologiques. Par exemple, une étude de tissu cérébral humain a montré que des patients épileptiques présentaient un plus grand nombre de PVM CD163⁺ que les témoins. Dans le modèle expérimental d'épilepsie chez le rat, les auteurs ont observé une perméabilité de la BHE dont la gravité est corrélée avec l'augmentation du nombre de PVM et l'expression de CCL2 dans l'hippocampe (Broekaart et al., 2018). Dans un modèle de lésion de la BHE chez la souris induite par l'expression transgénique de la protéine tat1-86 du virus de l'immunodéficience humaine (VIH), le nombre de PVM s'est vu multiplié par 5 notamment dans le putamen (Leibrand et al., 2017). De la même façon, dans un modèle de traumatisme

crânien chez le rat, le nombre de PVM était augmenté plusieurs jours après la lésion (Z. Zhang *et al.*, 2012).

Il est compliqué de définir le rôle précis des PVM dans le maintien ou bien la perméabilité de la BHE. Il semblerait que les PVM maintiennent l'intégrité de la BHE en conditions physiologiques, tout en participant à sa perturbation dans certaines pathologies. Il est également possible que les PVM s'accumulent autour des vaisseaux dont la BHE est endommagée dans le but de limiter la perméabilité et amorcer une réparation tissulaire.

Rôle des PVM dans les pathologies amyloïdes

La fonction phagocytaire des PVM est essentielle dans la régulation des dépôts amyloïdes, intervenant notamment dans la maladie d'Alzheimer (AD) et l'angiopathie cérébrale amyloïde (CAA). En effet, ces pathologies sont caractérisées notamment par l'accumulation de peptides A β dans le parenchyme cérébral ou le long des vaisseaux sanguins cérébraux (Kierdorf *et al.*, 2019). Dans une étude utilisant des souris Tg CRND8 (surexpression de mutations de l'APP, protéine précurseur amyloïde), la déplétion des PVM entraînait une augmentation de l'accumulation vasculaire d'A β et de la sévérité de la CAA (Hawkes and McLaurin, 2009). Dans une autre étude s'intéressant à SR-B1, un récepteur qui régule l'efflux de cholestérol des tissus périphériques vers le foie, il a été montré que ce récepteur était exprimé exclusivement par les PVM dans un modèle murin d'Alzheimer. La délétion génétique de ce récepteur entraîne une formation accélérée des plaques amyloïdes parenchymateuses et vasculaires, ainsi qu'une aggravation des déficits cognitifs (Thanopoulou *et al.*, 2010). De plus, une étude de Park et collaborateurs décrit le rôle des PVM dans la dysfonction du couplage neurovasculaire induite par A β , par le biais du stress oxydatif médié par CD36. En effet, la délétion spécifique de CD36 et NOX2 dans les PVM permet d'atténuer le dysfonctionnement du couplage neurovasculaire dans 3 modèles différents de pathologie A β (Park *et al.*, 2017).

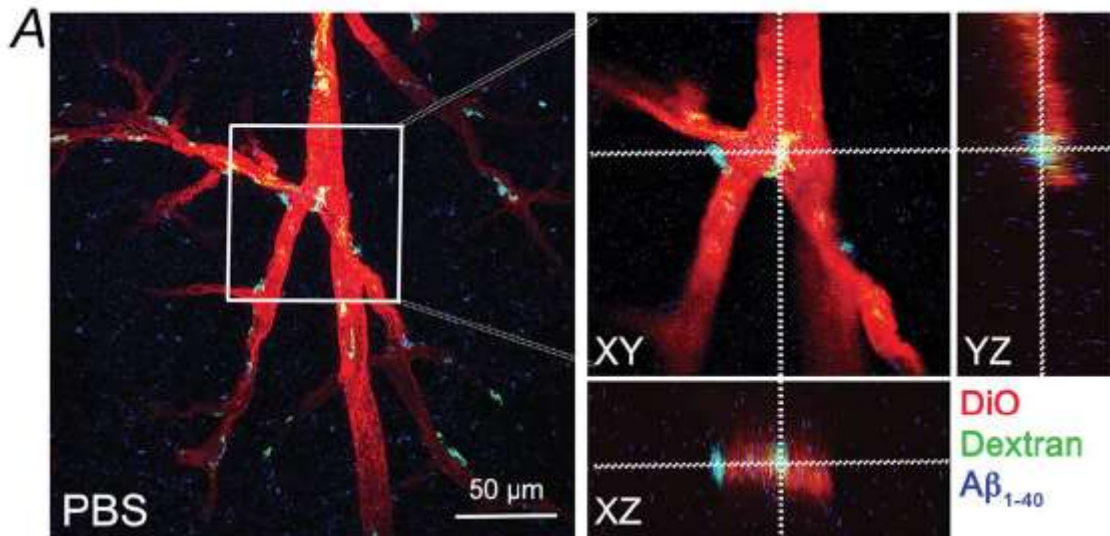


Figure 27 : L'A β circulant est retrouvé dans les PVM, module le stress oxydatif et le dysfonctionnement du couplage neurovasculaire.

Chez une souris contrôle traitée avec du PBS, l'A β_{1-40} (marqué au Cy5, bleu) infusé dans l'artère carotide colocalise avec les PVM (marqués au dextran, vert) entourant les vaisseaux sanguins cérébraux (marqués avec DiO, rouge), et résultant en la couleur cyan dans l'image fusionnée. D'après "Brain Perivascular Macrophages Initiate the Neurovascular Dysfunction of Alzheimer A β Peptides" (Park et al., 2017).

Rôle des PVM dans les infections du SNC

Les PVM interviennent dans la perturbation de la BHE causée par les infections bactériennes et virales. Dans un modèle de méningite à *Streptococcus pneumoniae* chez le rat, la déplétion des PVM et MM induit une aggravation de la pathologie, associée à une augmentation du nombre de bactéries dans le LCR, une plus grande production de chemokines pro-inflammatoires et une augmentation de l'expression de la molécule d'adhésion vasculaire VCAM-1, suggérant un rôle protecteur des PVM (Polfliet, Zwijnenburg, et al., 2001). D'un autre côté, dans un modèle d'encéphalite virale chez la souris, la déplétion des PVM et MM réduit l'infiltration de granulocytes ainsi que de lymphocytes T CD4/CD8, et diminue la morbidité, suggérant plutôt un rôle délétère des PVM (Steel et al., 2010).

Les PVM sont aussi étudiés dans la physiopathologie de l'encéphalite associée au VIH (HIVE), une complication courante du SIDA. Les PVM sont en effet les principales cibles de

l'infection au niveau cérébral, et une augmentation du nombre de PVM a été observée il y a déjà plusieurs décennies (Lane *et al.*, 1996). En utilisant des modèles de macaques rhésus infectés par le virus de l'immunodéficience simienne (SIV), un proche cousin du VIH, plusieurs études ont montré la présence d'ARN et de protéines de SIV spécifiquement dans les PVM (Chakrabarti *et al.*, 1991; Williams *et al.*, 2001; Thompson *et al.*, 2009). De plus, peu de protéines virales sont détectées lors de l'infection initiale, mais une grande quantité est retrouvée dans les stades terminaux, suggérant que les PVM participent activement à la production virale et au développement de l'infection (Williams *et al.*, 2001). Ainsi, il semble que les PVM soient les premières cibles de ces virus au niveau cérébral, et qu'ils servent de réservoir viral durant l'infection.

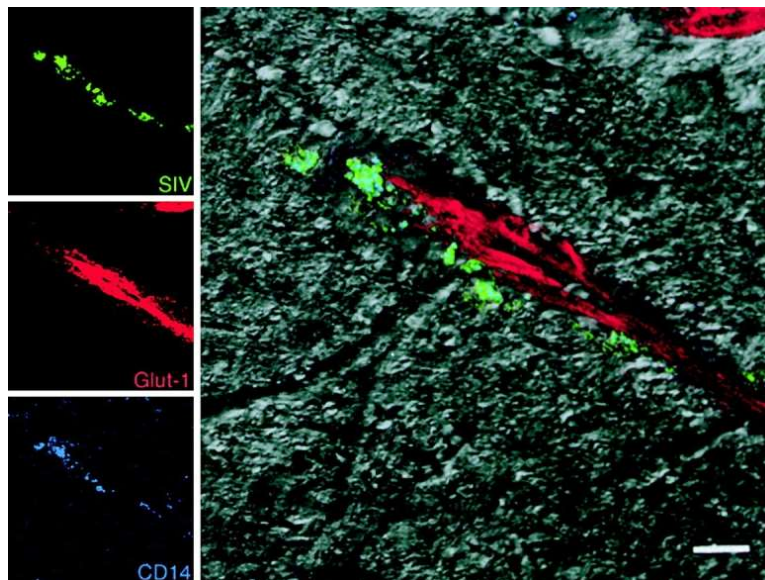


Figure 28 : Macrophages périvasculaires infectés par le SIV dans le cerveau des macaques.

Des macrophages périvasculaires (CD14, bleu) qui sont positifs pour la protéine virale (SIV-p28, vert) apparaissent bleu-vert près d'un vaisseau du SNC (Glut-1, rouge).

D'après "Perivascular macrophages are the primary cell type productively infected by simian immunodeficiency virus in the brains of macaques: implications for the neuropathogenesis of AIDS" (Williams *et al.*, 2001).

Rôle des PVM dans la sclérose en plaque

La sclérose en plaques (SEP, ou MS pour *multiple sclerosis*), est une maladie démyélinisante auto-immune du SNC. Elle est caractérisée par des lésions démyélinisantes

associées à des infiltrats périvasculaires de leucocytes et des lésions axonales (Kierdorf *et al.*, 2019). Dans des échantillons de cerveaux humains atteints de SEP, des accumulations de PVM et MM ont été observées, en particulier au niveau des zones de lésion. Ces cellules étaient positives pour HLA-DR, un récepteur MHC II, suggérant un rôle dans la présentation d'antigènes (Zhang *et al.*, 2011). De la même façon, chez des rats soumis à une EAE, le nombre de PVM et de MM est augmenté avant l'apparition des symptômes et l'infiltration de leucocytes périphériques. Dans cette étude, la déplétion des BAMS par injection intracérébroventriculaire de liposomes contenant du clodronate aurait permis d'atténuer légèrement les symptômes neurologiques de l'EAE, suggérant un rôle délétère des PVM et MM (Polfliet *et al.*, 2002). Une autre étude de l'EAE sur des rats a montré que les PVM de la moelle épinière surexprimaient des molécules d'adhésion et chemokines telles qu'ICAM-1, VCAM-1, MCP-1 et MIP-1, ce qui pourrait être un des mécanismes d'aggravation de la maladie (Hofmann *et al.*, 2002). Une analyse en cytométrie en flux haute dimension a confirmé que les BAMS augmentent leur expression de CD38 et MHC II au pic de l'EAE (Mrdjen *et al.*, 2018). Ces résultats confirment que les PVM exercent une fonction de présentation d'antigènes et peuvent moduler la réponse immunitaire.

Rôle des PVM dans les maladies cérébrovasculaires et facteurs de risques associés

Jusque récemment, aucune étude ne s'était intéressée au rôle des PVM dans la physiopathologie de l'AVC ischémique. Ces dernières années, des études sur un modèle d'occlusion de l'artère cérébrale moyenne chez le rat ont montré que les PVM CD163⁺ pouvaient proliférer, acquérir un phénotype inflammatoire après l'ischémie, et jouer un rôle dans l'attraction des leucocytes et l'intégrité de la BHE. De plus, une accumulation de PVM CD163⁺ a été observée *post-mortem* dans des cerveaux de patients atteints d'AVC (Pedragosa *et al.*, 2018; Rajan *et al.*, 2020).

Concernant l'AVC hémorragique, une étude a montré que les MM et PVM étaient responsables du nettoyage des espaces sous-arachnoïdiens et périvasculaires et de l'élimination des érythrocytes dans un modèle d'hémorragie sous-arachnoïdienne chez la souris (Wan *et al.*, 2021).

L'hypertension artérielle est un facteur de risque de plusieurs maladies neurovasculaires, notamment l'AVC. Une étude a montré que les PVM contribuent aux troubles neurovasculaires et cognitifs induits par l'hypertension. En effet, dans un modèle murin d'hypertension, l'angiotensine II de la circulation active les récepteurs à l'angiotensine de type 1 à la surface des PVM, conduisant ceux-ci à produire des ROS grâce à la NOS. Les ROS produits par les PVM causent des altérations du couplage neurovasculaire et des troubles cognitifs, qui sont atténués par la déplétion des PVM (Faraco *et al.*, 2016).

De précédents travaux au sein de notre unité se sont intéressés à l'impact de la consommation excessive d'alcool, un autre facteur de risque de maladies cérébrovasculaires, sur la neuroinflammation, notamment dans le cadre de l'AVC. La consommation excessive d'alcool entraîne un état inflammatoire exacerbé dans le cerveau, appelé « *priming inflammatoire* », caractérisé par une augmentation du nombre de PVM et de l'activation microgliale. Il a été montré que ce *priming* inflammatoire aggrave les lésions ischémiques, et que les PVM sont liés à ce phénomène. Dans cette étude, la déplétion des PVM avant l'AVC permet de réduire la lésion ischémique ainsi que la neuroinflammation consécutive à l'AVC (Drieu *et al.*, 2020).

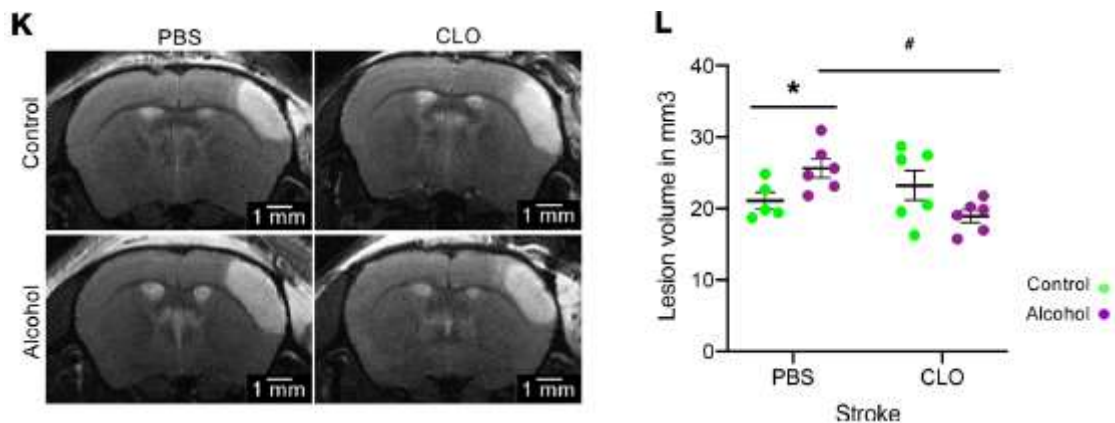


Figure 29 : Les PVM modulent l'effet aggravant de la consommation chronique d'alcool sur l'AVC ischémique chez la souris.

D'après "Alcohol exposure–induced neurovascular inflammatory priming impacts ischemic stroke and is linked with brain perivascular macrophages" (Drieu *et al.*, 2020).

Les mécanismes de régulation mis en place par les PVM dans ces pathologies sont encore très mal connus. De futures études devraient explorer les différents phénotypes et

rôles précis des PVM et autres BAMs dans les maladies cérébrovasculaires, en particulier dans des modèles incluant des facteurs de risque et comorbidités.

Disease	Model	PVM manipulation	Effect of PVM
Cerebrovascular diseases			
Ischemic stroke	MCA stroke patients	N/A	Possibly contribute to long-term poststroke demyelination
Ischemic stroke	tMCAO	CLO	Participate in granulocyte recruitment, promote VEGF expression, increase BBB permeability, promote neurological dysfunction
Myocardial infarction	SD rats subjected to coronary artery ligation	CLO	Mediate sympathetic activation by releasing proinflammatory cytokines
Hypertension	Mice received angiotensin II administration, BPH mice	CLO, bone marrow chimeras	Mediate neurovascular and cognitive dysfunction through oxidative stress
High-fat diet	Mice fed with high-fat diet	Vegfa ^{lox/lox} LysM ^{Cre+/-}	Induce VEGF and GLUT1 expression, maintain brain glucose uptake and prevent cognitive dysfunction
Aβ pathologies			
CAA	TgCRND8 transgenic mice	CLO, chitin (stimulate PVM turnover)	Promote Aβ clearance
CAA	J20 transgenic mice	SR-B1 ^{+/-} and SR-B1 ^{-/-}	Promote Aβ clearance, improve neurocognitive function
Alzheimer's disease	Aβ topical perfusion, iv administration, Tg2576 transgenic mice	CLO, bone marrow chimeras	Mediate neurovascular dysfunction dependent on CD36 and NOX2
Infectious diseases			
Bacterial meningitis	Wistar rats received <i>Streptococcus pneumoniae</i> intracisternal injection	CLO	Protective, facilitates leukocyte infiltration
Viral encephalitis	Breeding pairs of macrophage fas-induced apoptosis (MAFIA) mice, intranasal injection of VSV	CLO	Detrimental facilitates leukocyte infiltration
AIDS and SIVE	Rhesus macaques infected with SIV and HIV human brains	N/A	Express viral DNA, RNA and proteins, reservoir of latent infection
Autoimmunity			
Multiple sclerosis	Lewis rats injected with MOG	CLO	Promote development of symptoms
Multiple sclerosis	Lewis rats injected with MBP or transferred with autoimmune T cells primed by MBP	N/A	Strongly activated and secrete chemokines for monocyte/macrophage recruitment
Multiple sclerosis	Recipient mice transferred with autoimmune T cells primed by MOG	l ^{ab} ^{lox/lox} Cx3cr1 ^{CreERT2}	Not necessary for reactivation of primed autoimmune T cells

Figure 30 : Rôles des PVM dans les pathologies cérébrales.

D'après "Brain perivascular macrophages: Recent advances and implications in health and diseases" (Yang et al., 2019).

Les macrophages méningés

Les méninges sont constituées de trois couches, de la plus externe à la plus interne : la dure-mère, l'arachnoïde et la pie-mère. Comme décrit précédemment, plusieurs populations de macrophages résident dans ces différents espaces, regroupées sous le terme de macrophages méningés, ou MM. L'espace sous arachnoïdien est rempli de LCR et héberge plusieurs types de cellules immunitaires, dont les macrophages leptoméningés qui peuvent représenter jusqu'à 1/3 des cellules présentes (Oehmichen, 1976). On les trouve également dans l'espace sous pial, entre la pie-mère et la *glia limitans*, au plus proche du parenchyme (McMenamin et al., 2003; Prinz, Erny and Hagemeyer, 2017). Les macrophages leptoméningés (entre l'arachnoïde et la pie-mère) sont des cellules à longue durée de vie qui proviennent du sac vitellin extra-embryonnaire. Tout comme les PVM, ils expriment les récepteurs *scavengers* CD206 et CD163 ainsi que Lyve-1 et MHCII. Ils ont un rôle de sentinelle, surveillant en permanence la composition du LCR en antigènes, métabolites et agents pathogènes.

Des macrophages résidents sont également présents dans la dure-mère, la couche la plus externe des méninges. Les macrophages durs forment une population hétérogène, avec la majorité des cellules exprimant fortement MHC II et une minorité de cellules exprimant plus fortement Lyve-1 (Mrdjen et al., 2018). Contrairement aux PVM et aux macrophages leptoméningés, les macrophages durs ont une origine mixte : une partie dérivant du sac vitellin extra-embryonnaire et l'autre provenant de la moelle osseuse. Dans le cas d'une inflammation, de nouveaux macrophages sont recrutés localement à partir de monocytes sanguins (Coles et al., 2017). De plus, les macrophages durs peuvent réguler l'angiogenèse des vaisseaux lymphatiques méningés par la libération de VEGF-C (Hsu et al., 2019).

Il est important de noter que le LCR imprégnant l'espace sous arachnoïdien est sensiblement le même qui circule dans les espaces périvasculaires des vaisseaux parenchymateux, bien que ses flux exacts et les voies d'élimination soient sujets à importants débats. En conséquence, l'administration dans le LCR de traceurs ou de substances actives (par exemple les liposomes de clodronate) conduit au ciblage à la fois des MM et des PVM. Ainsi, dans la plupart des études s'intéressant au rôle des PVM, les deux types cellulaires sont en fait ciblés sans distinction. Il est donc jusqu'à maintenant difficile de dissocier les différents

rôles de ces deux populations. C'est d'autant plus important que ces dernières années plusieurs études ont révélé l'implication majeure des méninges dans la neuroinflammation et l'immunité, avec certainement un rôle bien spécifique des MM (Cugurra *et al.*, 2021; Rustenhoven *et al.*, 2021).

Les macrophages des plexus choroïdes

Les plexus choroïdes sont situés dans le troisième et quatrième ventricule, ainsi que dans les ventricules latéraux. Ils produisent le LCR, maintiennent un équilibre homéostatique et forment une barrière fonctionnelle pour le trafic des cellules immunitaires. Différents macrophages peuplent les ChP (ChPM), avec une densité inférieure par rapport aux autres BAMs (Korin *et al.*, 2017). Il existe au moins deux différentes populations de macrophages : les macrophages « épiplexiques », ou cellules de Kolmer au contact du LCR, et les macrophages résidant dans le stroma des plexus choroïdes (Ransohoff and Engelhardt, 2012). Comme les autres BAMs, les ChPM sont décrits comme des présentateurs d'antigènes CD163⁺ MHCII⁺ riches en lysosomes (McMenamin *et al.*, 2003). Situés à l'interface sang-LCR, les ChPM participent activement à l'immunité et à la fonction de barrière des ChP.

La dynamique des mouvements des ChPM a été récemment décrite *in vivo* par microscopie à deux-photons. Les macrophages du stroma ont des corps cellulaires relativement stationnaires mais surveillent l'environnement avec leurs processus cellulaires dotés d'une forte motilité. Leurs processus sont en contact avec les vaisseaux sanguins fenestrés du stroma des ChP, et ils sont capables de phagocyter des dextrans injectés dans la circulation sanguine. En revanche, les cellules de l'épiplexus présentent une grande mobilité du corps cellulaire, se déplaçant rapidement à la surface apicale des ChP (Shiple *et al.*, 2020; Cui, Xu and Lehtinen, 2021). Une telle mobilité n'a pas été observée chez les autres BAMs.

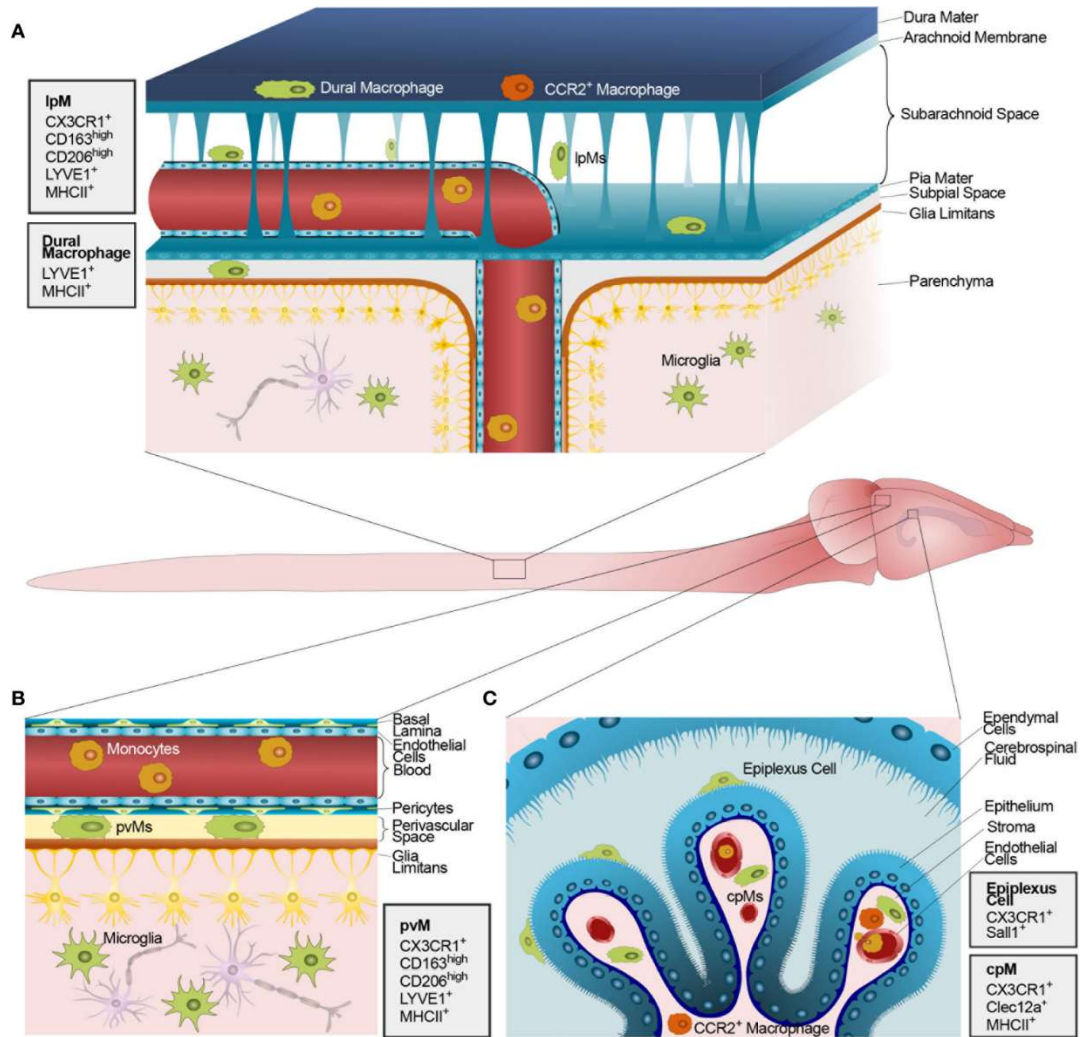


Figure 31 : Différentes populations de macrophages aux interfaces du SNC.

D'après "Dwellers and Trespassers: Mononuclear Phagocytes at the Borders of the Central Nervous System" (Ivan et al., 2021).

- ❖ Le SNC contient différentes populations de cellules myéloïdes résidentes : la microglie présente dans le parenchyme et les macrophages associés aux bordures (BAMs), aux interfaces du SNC.
- ❖ Les BAMs sont divisés en trois sous-populations : les macrophages périvasculaires (PVM) entre le parenchyme et les vaisseaux sanguins, les macrophages méningés (MM) et les macrophages des plexus choroïdes (ChPM).
- ❖ Les BAMs sont impliqués dans la réaction inflammatoire, par la production de cytokines et le maintien de l'intégrité de la BHE.
- ❖ Parmi les BAMs, les PVM pourraient jouer un rôle majeur dans l'inflammation post-AVC en raison de leur emplacement stratégique à l'interface entre les vaisseaux sanguins, le parenchyme cérébral et le système immunitaire circulant.

- ❖ *The CNS contains different populations of resident myeloid cells: the microglia present in the parenchyma and the border-associated macrophages (BAMs), at the interfaces of the CNS.*
- ❖ *BAMs are divided into three subpopulations: perivascular macrophages (PVM) between the parenchyma and blood vessels, meningeal macrophages (MM) and choroid plexus macrophages (ChPM).*
- ❖ *BAMs are involved in the inflammatory response, through the production of cytokines and the maintenance of the integrity of the BBB.*
 - ❖ *Among BAMs, PVM could play a major role in post-stroke inflammation due to their strategic location at the interface between blood vessels, brain parenchyma and the circulating immune system.*

OBJECTIFS

Les PVM semblent donc participer activement à l'inflammation cérébrale, qui est un acteur central de la physiopathologie des AVC ischémiques. Alors que la réponse des cellules microgliales a été largement étudiée, celle des PVM reste très méconnue.

Notre hypothèse, basée sur les études décrites précédemment et sur la localisation privilégiée des PVM à l'interface entre le compartiment vasculaire et le parenchyme cérébral, est que les PVM peuvent jouer un rôle majeur dans la réponse inflammatoire déclenchée par l'AVC, *via* la médiation du recrutement et l'infiltration des leucocytes.

De plus, sur la base d'études précédentes, nous faisons l'hypothèse que les PVM pourraient moduler l'AVC et les réponses inflammatoires induites par l'AVC de manière différente en fonction de l'état inflammatoire basal du cerveau, en particulier au cours du vieillissement.

L'objectif de ce travail est donc d'étudier le rôle des PVM dans la réponse inflammatoire déclenchée par un AVC ischémique, dans un contexte « naïf » - chez des animaux jeunes -, ainsi que chez des animaux présentant un *priming* inflammatoire cérébral dû au vieillissement. Ainsi, cette étude permettra de répondre à plusieurs questions :

- Les PVM ont-ils un impact sur le volume de lésion ischémique ?
- Les PVM ont-ils un impact sur l'inflammation vasculaire suite à l'ischémie cérébrale ?
- Les PVM ont-ils un impact sur l'infiltration de cellules immunitaires suite à l'ischémie ?
- Les PVM ont-ils un impact sur le déficit fonctionnel post-ischémie ?
- Les PVM changent-ils de phénotype au cours du vieillissement ?
- Les PVM ont-ils un impact différentiel sur l'AVC en fonction de l'âge ?

RÉSULTATS

Border-associated macrophages (BAMs) play a central role in the regulation of the neuroimmune response following stroke in aged mice

Damien Levard ¹, Célia Seillier ¹, Gaetan Riou ², Lukas Amman ³, Marco Prinz ³, Denis Vivien ^{1,4},
Marina Rubio ^{1,*}

¹ Normandie University, UNICAEN, INSERM UMR-S U1237, Physiopathology and Imaging of Neurological Disorders (PhIND), GIP Cyceron, Institut Blood and Brain @ Caen-Normandie (BB@C), 14000 Caen, France

² Normandie University, UNIROUEN, Inserm, U1234, FOCIS Center of Excellence PAn'THER, Rouen University Hospital, Department of Immunology and Biotherapy, Rouen, France

³ Institute of Neuropathology, Medical Faculty, University of Freiburg, Breisacher Str. 64, Freiburg, Germany

⁴ Department of Clinical Research, Caen-Normandie University Hospital, CHU, Avenue de la côte de Nacre, Caen, France

Abstract

Ischemic stroke is one of the main causes of death and permanent disability worldwide. Stroke-induced inflammatory processes, including the activation of resident glial cells as well as the invasion of circulating leukocytes, have been proposed as key contributors of the ischemic stroke pathophysiology. While the responses of microglia to ischemic stroke have been extensively studied, those of border-associated macrophages (BAMs) remain largely unknown. In this study, we hypothesized that BAMs could influence stroke-induced inflammatory responses, particularly during aging and thus final stroke recovery. We thus compared stroke outcome in young and old mice subjected to thromboembolic stroke with or without a previous depletion of BAMs. Our results show that functional outcome following stroke was worsened in depleted mice without modification of the lesion volumes, exclusively in aged mice. This worsening in the functional outcome was accompanied by (i) an increase of endothelial P-selectin expression (measured by molecular MRI and IHC), (ii) an increased leukocyte rolling and adhesion to the vessel wall (measured by two-photon *in vivo* imaging), and (iii) an increased leukocyte infiltration (measured by flow cytometry and IHC) in the injured hemisphere. These exacerbated immune responses were present at both the acute and the sub-acute phase (up to 5 days) after stroke onset, thus suggesting that the presence of BAMs ensures a long-term control of the immune response after stroke. Using cell sorted RNAseq, we show that BAMs change their transcriptomic phenotype during aging, overexpressing genes implicated in the regulation of both innate and adaptive immune responses and antigen presentation. Taken together, our results reveal that BAMs play a central role in the regulation of the neuroimmune response following stroke, especially during aging, and that BAMs guarantee a long-term fine-tuning of the immune responses after stroke.

List of abbreviations used in the text:

ALS: amyotrophic lateral sclerosis

ATP: adenosine triphosphate

BAMs: CNS border-associated macrophages

BBB: blood brain barrier

CD: cluster of differentiation

ChPM: choroid plexus macrophages

CLO: clodronate liposomes

CNS: central nervous system

COLA6A1: collagen type VI alpha 1

COLIV: collagen type IV

DAPI: 4',6-diamidino-2-phenylindole

FACS: fluorescence-activated cell sorting

FITC: fluorescein isothiocyanate

GFAP: glial fibrillary acidic protein

GFP: green fluorescent protein

IHC: immunohistochemistry

Ly6G: lymphocyte antigen 6 complex locus G6D

MCAo: middle cerebral artery occlusion

MHCII: major histocompatibility complex class II

MM: meningeal macrophages

MPIOs: microparticles of iron oxide

MRI: magnetic resonance imaging

PBS: phosphate buffered saline liposomes

Psel: P-selectin

PVM: perivascular macrophages

RNA: ribonucleic acid

RNAseq: RNA sequencing

SPP1: secreted phosphoprotein 1

Introduction

Ischemic stroke is one of the main causes of death and permanent disability worldwide (Katan and Luft, 2018). Lack of adequate blood supply to a brain region causes brain damages and triggers sterile inflammation and innate immune responses (Anrather and Iadecola, 2016). Stroke-induced inflammatory processes are a response to the tissue damage due to the absence of blood supply and have been proposed as a key contributors to all the stages of the ischemic stroke pathophysiology (Drieu *et al.*, 2018).

The CNS contains different subsets of resident myeloid cells including microglia and border-associated macrophages (BAMs), i.e., macrophages located at the CNS “borders”: between the parenchyma and blood vessels (perivascular macrophages, PVMs), within the meninges (meningeal macrophages, MMs) and at the choroid plexus (choroid plexus macrophages, ChPMs) (Utz and Greter, 2019). In physiological conditions, BAMs display scavenger functions, by clearing cellular debris from the CNS (Kida *et al.*, 1993; Mendes-Jorge *et al.*, 2009) and by presenting antigens to lymphocytes (Fabrick *et al.*, 2005). However, their roles in pathological conditions are less known. PVMs have been identified as modulators of neurovascular coupling in models of chronic hypertension (Faraco *et al.*, 2016), and Alzheimer disease (Park *et al.*, 2017). It has been demonstrated that PVMs can produce reactive oxygen species and cytokines, linking them to the inflammatory response (Faraco *et al.*, 2016). In addition to this, BAMs and particularly PVMs could play a major role in post-stroke inflammation because of their strategic location at the interface between the bloods vessels, the brain parenchyma and the circulating immune system. Accordingly to this, they have been described as modulators of granulocyte infiltration and blood-brain barrier integrity after stroke (Pedragosa *et al.*, 2018). Also, we have previously shown that BAMs modulate the post-stroke inflammatory responses in a context of neuroinflammatory priming induced by excessive alcohol consumption, known as a preeminent modifiable risk factor of stroke (Drieu *et al.*, 2020).

Most of the preclinical studies on stroke have been conducted in young male rodents. However, age is the most significant non-modifiable risk factor for many human diseases, and the single most important risk factor for ischemic stroke (Sacco *et al.*, 1997; Popa-Wagner *et al.*, 2020; Virani *et al.*, 2020). With

every decade of life, the incidence of stroke more than doubles (Mozaffarian *et al.*, 2016). Advanced age is associated with profound pathophysiological changes in both the CNS and the periphery, which underlie the increased susceptibility of the brain to ischemic injury (Candelario-Jalil and Paul, 2021). In spite of all these facts, most of the preclinical stroke research (including stroke-induced inflammatory responses and the role of BAMs in stroke) have been conducted in young, healthy animals.

Based on previous studies (Drieu *et al.*, 2020), we hypothesized that BAMs could shift stroke outcome and the stroke-induced inflammatory responses in a different manner depending on the inflammatory status of the brain prior stroke onset, and particularly during aging. To test this hypothesis, we compared stroke outcome in young and aged mice with or without a previous BAMs depletion. Our results showed that stroke functional outcome was worsened in aged BAMs-depleted mice and was accompanied by (i) an increased endothelial P-selectin expression, (ii) an increased leukocyte rolling and adhesion to the vessel wall, and (iii) an increased leukocyte infiltration in the injured hemisphere. Interestingly, these exacerbated inflammatory responses were not accompanied by changes in lesion volume. Finally, by using RNAseq analysis from isolated BAMs, we show that BAMs change their transcriptomic phenotype during aging to overexpress genes implicated in the regulation of both innate and adaptive immune response and antigen presentation. Taken together, our results unmask a new role of BAMs following stroke as central coordinators of the neuroimmune response, especially during aging.

Results

Identification of BAMs and characterization of their depletion.

For this study, we wanted to focus on the migration of immune cells across the blood brain barrier (BBB) after stroke. For this reason, we first focused our IHC experiments exclusively on PVMs (which surround brain blood vessels and are located in the perivascular space). Sub-meningeal PVMs are positive for the scavenger receptor CD206 (**Figure 1A-D**), whereas microglia is negative for CD206 but positive for P2Ry12 (**Figure 1B**) and Iba1 (**Figure 1F**). PVMs are located in the perivascular space around blood vessels, between the basal lamina and the *glia limitans* formed by the astrocytic end-feet (**Figure 1C, D**).

To determine the roles of PVMs, we depleted them by injecting clodronate-encapsulated liposomes (Clodronate-liposomes; CLO) in the lateral ventricle (control mice received PBS-encapsulated liposomes; Vehicle). When injected into the lateral ventricle, clodronate liposomes diffuse into the CSF, around the brain through the subarachnoid space, as well as into the perivascular spaces. When the liposomes meet the macrophages they are phagocytosed and the clodronate is then released in the cell, which induces its death by apoptosis (Polfliet *et al.*, 2001; Moriyama and Nomura, 2018). Thus, this method makes it possible to deplete all the BAMs present in the CSF.

We assessed the depletion of BAMs 5 days after CLO or Vehicle injection using IHC and flow cytometry (**Figure 1E**). As previously described in other studies (Polfliet *et al.*, 2001; Drieu *et al.*, 2020), the injection of CLO liposomes reduces by at least 80% the number of PVMs (measured by IHC in the sub-meningeal areas) compared to the vehicle group (**Figure 1G**). The depletion induced by CLO injection is specific for BAMs and does not affect the microglia (**Figure 1G**). It is important to note that in the flow cytometry experiments meninges were maintained when extracting the brains, so the whole BAMs population (including PVMs, MMs and ChPMs) was detected. We confirm that 5 days after CLO injection, there is a specific depletion of BAMs (CD11b⁺ CD45⁺ CD206⁺ cells) which does not affect the microglia (CD11b⁺ CD45^{low}) (**Figures 1H, 1I**). No increase in microglial activation (CD11b⁺ CD45^{high}) or in the number of neutrophils (CD11b⁺ CD45⁺ Ly6G⁺) was observed, which indicates that 5 days after its injection, there is no inflammatory reaction induced by CLO itself (**Figures 1H, 1I**).

Inflammatory priming in the brain of aged mice is not accompanied by changes in the number or the morphology of BAMs.

In a previous study, we showed that alcohol exposure induces an inflammatory priming in the brain of mice that was characterized by an increase of the microglial activation and of PVMs numbers (Drieu *et al.*, 2020). It is well admitted that aging could correspond to a certain kind of neuroinflammatory priming (Niraula, Sheridan and Godbout, 2017). For this reason, we decided to study the inflammatory status of elderly brains in mice (18 months old) compared to young ones (2 months old). We observed by flow cytometry that there was no difference in the number of PVMs between young and old mice (**Figure 2A-C**). However, we observed a significant increase in activated microglia ($p < 0.01$, $n = 6$ mice/group; **Figure 2B-D**), in the number of neutrophils ($p < 0.01$, $n = 6$ mice/group; **Figure 2B-D**), $CD4^+$ T cells ($p < 0.05$; $n = 5$ mice/group; **Figure 2E, F**) and $CD8^+$ T cells ($p < 0.01$; $n = 5$ mice/group; **Figure 2E, F**) in the brain of old mice compared to young mice. These results were confirmed by IHC analyses, in which we did not observe a difference in the number of $CD206^+$ BAMs (**Figure 2G-H**). We confirmed the increase in activated microglia expressing the lysosomal marker CD68, characteristic of phagocytosis (6.2 ± 0.9 vs 49.5 ± 6.4 $Iba1^+CD68^+$ cells per mm^2), while the total number of microglia did not change ($Iba1^+$; **Figure 2I-J**). We therefore confirm an increased inflammatory status in the apparently healthy brains of aged mice, without changes in the number or morphology of BAMs.

BAMs depletion worsens stroke functional outcome in aged mice but not in young mice.

We performed thromboembolic stroke 5 days after the injection of CLO or Vehicle in young and old mice. Functional recovery tests and MR imaging examinations were performed 24h after stroke onset (**Figure 3A**). In young mice, the depletion of BAMs had no impact on the functional deficit (**Figure 3B, C**), the distribution of the lesion (**Figure 3D**), the ischemic lesion volume (**Figure 3F**), the recanalization rate (**Figure 3H**) or the hemorrhagic transformation score (**Figure 3J**).

Interestingly, aged mice subjected to thromboembolic stroke showed a significantly higher functional deficit specifically in the BAMs-depleted group. This deficit was observed by measuring both the overall strength of the two forepaws ($p < 0.001$; $n = 10$ mice PBS group/ 15 mice CLO group; 10.3 ± 1.8 vs 25.4 ± 2.2 % deficit respectively; **Figure 3B**) and the specific strength of the left paw (the side affected by

the stroke) ($p < 0.05$; $n = 10$ mice PBS group/ 15 mice CLO group; 16.1 ± 3.7 vs 28.3 ± 3.3 % deficit respectively; **Figure 3C**). This difference in the functional deficit was neither due to a difference in lesion distribution or volume (**Figure 3E, F**) nor the recanalization score (**Figure 3H**). No significant difference was found in the hemorrhagic score, although more petechial hemorrhages or small subarachnoid bleeds (Score 1) were observed in the CLO group compared to Vehicle (37.5 % in the aged-depleted mice vs 12.5 % in aged-control mice; **Figure 3J**).

BAMs depletion increases the expression of the P-selectin adhesion molecule after stroke in aged mice but not in young mice.

In order to study the role of PVMs on endothelial activation and possible associated inflammatory reactions after ischemic stroke, we performed molecular imaging and immunohistological analyses of P-selectin (P-sel), an adhesion molecule responsible of leukocyte rolling on the vessel wall (**Figure 4A**), which is one of the first steps of leukocyte infiltration across the blood-brain-barrier (BBB). The expression of P-sel was *in vivo* detected by using specific anti-P-sel coupled microparticles of iron oxide (MPIOs). Thus, when P-sel is expressed by activated endothelial cells, the antibodies fixed to the MPIOs recognize and bind to P-sel molecules (**Figure 4B**). MPIOs then reveal a hypointense signal on MRI and are thus visible on a T2-star sequence (**Figure 4C**).

MPIOs signal was significantly increased in the cortex ipsilateral to the ischemia in aged mice previously depleted of their BAMs compared to aged mice not depleted (22.8 ± 5.5 vs 37.6 ± 2.9 % cortex area; $p < 0.05$, $n = 7$ mice/group; **Figure 4D**). There was no difference between the two groups in young mice. We also measured P-selectin signal by IHC on brain sections. No difference was observed in the number of P-sel⁺ vessels twenty-four hours after stroke onset between the vehicle and CLO-treated groups in young or aged mice (**Figure 4G**). By contrast, 5 days after the stroke, the number of P-sel⁺ vessels and the P-sel⁺ signal area was significantly increased in aged mice with a previous depletion of BAMs ($p < 0.05$, $n = 5$ mice/group; **Figures 4G, 4H**).

BAMs influence the intracerebral trafficking of leukocytes following ischemic stroke.

We used intravital two-photon microscopy to study the role of PVMs in leukocyte adhesion to the vessel wall, and to determine the functional impact of the increased expression of P-selectin. We measured

leukocyte adhesion and rolling in both young and aged mice previously treated with Vehicle or CLO, 24h after stroke onset (**Figure 5A**). We performed intravenous injection of FITC-Dextran (70 kDa) (**Figure 5B**) allowing blood vessels visualization and Rhodamine-6G (4 kDa) for leukocytes staining (**Figure 5C**). We observed a significant decrease in the number of leukocytes adhered to the vessel wall in young BAMS-depleted mice, but no difference in the number of rolling leukocytes ($p < 0.05$, $n = 5$ mice/group). By contrast, in aged mice previously depleted of BAMS, we detected a significant increase in both the number of rolling and adherent leukocytes ($p < 0.05$, $n = 5$ mice/group; 0.5 ± 0.2 vs 1.39 ± 0.2 rolling leukocytes; 1.34 ± 0.5 vs 3.87 ± 1.65 adherent leukocytes; **Figures 5E, F**).

BAMS depletion exacerbates neuroinflammation and infiltration of peripheral immune cells after stroke in aged mice.

We next wanted to test whether the increased vascular inflammation observed in aged BAMS-depleted mice was accompanied by a higher infiltration of immune cells into the brain parenchyma. We studied the cellular immune responses triggered at different time points after stroke onset by flow cytometry (**Figure 6, 7**) and IHC (**Figure 8, 9**). In agreement with the results on vascular inflammation, we observed a significant increase in all of the immune cell types studied in aged BAMS-depleted mice (**Figure 7, Figure 9**), with an increase in the infiltration of neutrophils (**Figure 7C, Figure 9J**) and CD4⁺ T cells (**Figure 7E, Figure 9L**) from 24h to 5 days after stroke by both IHC and flow cytometry. We also observe an increase in microglial activation in aged-depleted mice (**Figure 7C**).

Using flow cytometry, we observed in young BAMS-depleted mice a slight but significant increase in CD4⁺ T cells 2 days after stroke onset ($p < 0.05$, $n = 7$ mice/group; **Figure 6E**) followed by a decrease in the number of these same cells in the perilesional area and in the ischemic core at 5 days when measured by IHC ($p < 0.01$, $n = 7$ mice/group; **Figure 8L**). We also observed in young BAMS-depleted mice an increase in microglia and microglial activation in the perilesional area 24h after stroke onset ($p < 0.05$, $n = 7$ mice/group; **Figure 8D, H**). This increase is not found in the quantification of the ipsilateral hemisphere by cytometry 48 hours after the stroke (**Figure 6C**).

BAMs change their transcriptomic phenotype during aging by overexpressing genes implicated in the regulation of both innate and adaptive immune responses, including cell adhesion and cytokine-mediated signaling pathways.

Given the differences in the immune and inflammatory responses observed specifically in aged BAMs-depleted mice subjected to stroke, the next step was to determine whether BAMs gene expression was influenced by aging. In other words, we wanted to know if the different impact, after stroke, of the depletion of BAMs observed between young and aged mice could be due to a different phenotype of BAMs acquired during aging, making them become master regulators of the neuroinflammatory response.

We therefore sorted BAMs from young and aged mouse brains and performed RNAseq analysis (**Figure 10A**). Out of all the 9143 genes detected in BAMs, 30 genes are downregulated and 90 are upregulated in the BAMs of aged mice compared to young mice (**Figure 10B, C**). The Gene Set Enrichment Analysis (GSEA) aggregates the per gene statistics across genes within a gene set, therefore making it possible to detect situations where all genes in a predefined set change in a small but coordinated way. The GSEA analysis was started on the Gene sets derived from the GO Biological Process ontology database. We have thus demonstrated 58 upregulated pathways in BAMs of old mice compared to young. In the list of the 30 most regulated biological pathways, we found a large majority of pathways involved in regulation of the innate and adaptive immune response. (**Figure 10D**). The clueGO tool (Bindea *et al.*, 2009) was used to visualize pathway groupings according to the terms used in the gene ontology database. Pathways with a p-value <0.05 in the GSEA analysis based on GO biological process data are grouped into four clusters: the “innate and adaptive immunity” cluster containing 72.97% of the pathways, the “antigen presentation” cluster containing 16.22% of the pathways, the “cellular response to heat” cluster contains 5.41% of the pathways, and the “regulation of fibroblast proliferation” cluster containing 5.41% of the pathways (**Figure 10E**). We thus show that BAMs change their transcriptomic phenotype during aging and overexpress genes implicated in the regulation of innate and adaptive immune responses.

Discussion

In this study we aimed to study the specific role of PVMs on acute ischemic stroke, with a particular focus on the inflammatory response in both young and aged mice. We hypothesized that aging, by driving a primed neuroinflammatory state, could shift BAMs phenotype, giving them a more important role in the modulation of the neuroinflammatory responses to stroke. To study this, we compared young and old control with corresponding BAMs-depleted mice at the acute and sub-acute phases of ischemic stroke. Next, we isolated BAMs from young and old mice and performed transcriptomic analyses. Our results show that BAMs in old mice overexpress genes implicated in the regulation of both innate and adaptive immune responses, including cell adhesion and cytokine-mediated signaling pathways.

Our present results in young mice show that BAMs do modulate the neuroinflammatory response, but that this does not influence the final ischemic lesion size or neurological deficits after thromboembolic stroke. These data are in agreement with a previous report from our group in a model of thromboembolic stroke in young mice subjected to an inflammatory priming (induced by excessive alcohol consumption), including a previous depletion of BAMs (Drieu *et al.*, 2020). Interestingly, another study performed in a model of transient (filament) ischemic stroke in young mice described that the previous depletion of BAMs showed less granulocyte infiltration and increased permeability of blood vessels but was also not associated to changes in lesion volume. However, in this study, the authors report that a depletion of BAMs contributed to exacerbated neurological dysfunctions at the acute phase of ischemia/reperfusion (Pedragosa *et al.*, 2018). The discrepancies between these studies might be due to the experimental model of stroke used in each case, on which the inflammatory response timing is different and processes like secondary microthrombosis after the filament removal are inexistent in thromboembolic models (Gauberti *et al.*, 2014; Levard *et al.*, 2020). However, when we used aged mice subjected to the same paradigms of thromboembolic stroke with or without previous depletion of BAMs, we observed that although stroke damages such as lesion volume were not significantly affected by BAMs depletion, their neurological deficits were worsened. Thus, these data suggest that aging acts as a neuroimmune “primer” that changes BAMs phenotype, and play a critical role in the influence of final outcome following ischemic stroke.

Our results also show that after stroke, and specifically in aged mice, the depletion of BAMs is associated to (i) a significant increase in the endothelial adhesion molecule P-selectin; (ii) a significant increase in leukocyte rolling and adhesion; and (iii) an increased parenchymal infiltration of neutrophils, macrophages, as well as CD4⁺ and CD8⁺ T cells. Importantly, these exacerbated immune responses are present not only at the acute phase after stroke, but also at the sub-acute phase (up to 5 days after stroke onset), thus suggesting that the presence of BAMs ensures a long-term control of the immune response after stroke.

Interestingly, the numbers of BAMs do not seem to be important on regulating the neuroimmune responses to stroke, but the reprogramming of the gene expression profile of BAMs seems to be crucial for the stroke-induced immune responses. This reprogramming has been described in the context of stroke by Pedragosa *et al.* (2018), where the authors describe transcriptomic changes that have a rapid impact on leukocyte chemotaxis and blood-brain barrier integrity, and promote neurological impairment in the acute phase of stroke. A similar effect on the reprogramming of BAMs seems to take place during aging, where BAMs seem to acquire a more important role on orchestrating the inflammatory responses triggered by stroke.

In the CNS, inflammatory priming mainly describes the phenotype and reactivity of microglial cells: after undergoing an initial stimulus, microglial cells exhibit an exaggerated inflammatory response to a second stimulus (Haley *et al.*, 2019). Subsequent studies have since shown that inflammatory brain priming can also be triggered by chronic stimuli, including stress, diabetes, hypertension, chronic alcohol use, and even aging (Muriach *et al.*, 2014; Norden, Muccigrosso and Godbout, 2015; Winklewski *et al.*, 2015; Drieu *et al.*, 2020). A previous study of high-dimensional single-cell mapping of CNS myeloid cells showed that during aging, there was an increase in the number of BAMs expressing major histocompatibility complex class II (MHC II), suggesting an increased role in antigen presentation (Mrdjen *et al.*, 2018). In our study, by focusing specifically on the transcriptomic changes of BAMs during aging, we confirm this observation. Indeed, we show that aging also induces a series of transcriptomic changes in BAMs, affecting genes involved in innate and adaptive immune response, antigen presentation, cellular response to heat and fibroblast proliferation.

Interestingly, and apart from phenomena related to the immune response, our transcriptomic results reveal that BAMs overexpress during aging genes linked to the regulation of fibroblast proliferation. Recent studies have begun to shine light on the fibroblasts present in the meninges, choroid plexus and perivascular spaces of the brain and spinal cord, i.e. in direct contact with BAMs. Although the origins and functions of CNS fibroblasts are still being described, recent work has revealed that fibroblasts play crucial roles in fibrotic scar formation in the CNS after injury, including stroke (Dorrier *et al.*, 2021). In Col1a1-GFP mice, both PDGFR β ⁺ and GFP⁺ cells, which were referred as stromal cells, increased in number in the lesion core surrounded by fibrotic proteins following a middle cerebral artery occlusion by filament (Fernández-Klett *et al.*, 2013). With regard to neurodegeneration, in the pre-symptomatic stages of amyotrophic lateral sclerosis (ALS), the fibroblast marker genes *SPPI* and *COLA6A1* are enriched and their protein products accumulate in the perivascular spaces. Increased expression levels of these genes predicted shorter survival times in patients with ALS, indicating that perivascular fibroblasts contribute to early dysfunction during the disease progression (Månberg *et al.*, 2021). Thus, future studies could investigate the existing links between BAMs and fibroblasts, especially in the case of post-stroke scars or neurodegenerative pathologies.

A limitation of our study is the lack of very long-term measurements. Indeed, we focused on the acute and sub-acute inflammatory reactions, 24 hours to 5 days after the stroke. It would have been interesting to question the role of BAMs on the resolution of inflammation and long-term functional recovery. The thromboembolic model of stroke used in this study seems to be one of the closest to human pathophysiology and may thus provide an opportunity to study not only fibrinolytic drugs but also strategies targeting inflammation and immune responses triggered after the onset of stroke (Levard *et al.*, 2020); however, our study could be improved by comparing our data with other experimental model of stroke. The other limitation of the study is the use of liposomes containing clodronate. Indeed, the initial study focused on the role of PVMs which, due to their strategic location, could modulate leukocyte transmigration through the BBB. However, it is clear that the clodronate liposomes injected into the cerebral lateral ventricle in this study target all BAMs (i.e. PVMs, MMs, ChPMs) without distinction, due to their common location in the CSF. We therefore cannot determine the specific roles of each

subpopulation of BAMs on the inflammatory reaction induced after stroke. It is a safe bet that ChPMs and MMs play a major role, with the appearance of many recent studies describing the meninges and choroid plexuses as major entry routes to the CNS for inflammatory cells (Llovera *et al.*, 2014; Benakis, Llovera and Liesz, 2018; Alves de Lima, Rustenhoven and Kipnis, 2020).

Taken together, our results reveal that BAMs acquire, during aging, a central role in orchestrating the neuroimmune responses triggered by stroke, and that BAMs guarantee a long-term fine-tuning of the immune responses after stroke.

Methods

Animals

Two months-old male (Young group) and 18 months-old male (Aged group) C57/BL6J (Janvier Labs) mice were housed (Centre Universitaire de Ressources Biologiques, Normandy University, Caen, France) at 21° C in a 12 h light/dark cycle with food and water *ad libitum*. All mice were checked daily for health and abnormal behavior. For intravital two-photon imaging, male C57BL/6J CX3CR1-GFP^{+/-} mice were used.

All the procedures needing anesthesia were performed by an initial exposure to 5% isoflurane followed by a maintaining phase of 1.5-2% isoflurane 30%O₂/70%N₂O during experiments.

Depletion of border-associated macrophages (BAMs)

Anesthetized mice were placed in a stereotaxic device. Then the skin was removed and a small craniotomy was performed (coordinates: -0.2mm anteroposterior; +1mm lateral; -2mm depth from the Bregma). A glass micropipette containing 10µl PBS-liposomes (Vehicle-liposomes group) or clodronate-encapsulated liposomes (Clodronate-liposomes group; CLO) (purchased at clodronateliposomes.com) was inserted and the product was gently injected in the left lateral ventricle during 20 minutes. CLO liposomes injected into the cerebral ventricles are phagocytized by BAMs and, once in the cytosol, CLO acts as a cytotoxic ATP analog, which impairs mitochondrial oxygen consumption leading to cell death (Lehenkari *et al.*, 2002). In order to minimize the pro-inflammatory effects of CLO *per se*, the intracerebroventricular (icv) injection of CLO was performed 5 days before the stroke.

Thromboembolic stroke

We used the *in situ* thromboembolic stroke model consisting in the injection of thrombin directly into the middle cerebral artery (MCA) as described before (Orset *et al.*, 2007). Briefly, anesthetized mice were placed in a stereotaxic device, a small craniotomy was performed, the dura was excised, and the MCA was exposed. A pulled glass micropipette was introduced into the lumen of the MCA and 1 µL

(1.5 UI/ μ l for C57BL/6J mice) of purified murine alpha-thrombin (Enzyme Research Labs, USA) was pneumatically injected to induce MCA occlusion (MCAo) by the *in situ* formation of a clot. Lesion volumes were quantified by Magnetic Resonance Imaging (MRI) on Image J software 24 hours after stroke onset. The pipette was removed 10 minutes after, when the clot had stabilized. Cerebral blood flow was monitored before and up to 20 min after MCAo.

Intravital two-photon microscopy

Anesthetized mice were placed in a stereotaxic device and aqueous medium was deposited between the thin-skull window and the X25 immersive objective. One hundred μ l of Rhodamine 6G (1mg/kg) and 100 μ l of 70kDa FITC-Dextran (5mg/ml) (Sigma Aldrich, France) were injected in the tail vein to stain circulating leukocytes and to visualize the lumen of blood vessels, respectively. Acquisitions were performed using a Leica TCS SP5 MP microscope at 840 nm two-photon excitation wavelength (Coherent Chameleon, USA). Photomultiplier (PMT) 2 (recorded capacity: 500-550nm; gain 850V; offset 0) and PMT3 (recorded capacity: 565-605nm; gain 850V; offset 0) were used. The pulsing laser characteristics were: gain 23%; trans 17%; offset 50%.

Leukocyte rolling/adhesion counting

Leukocyte adhesion and rolling to venular endothelium were measured after the intravenous injection of 100 μ l of Rhodamine 6G (1mg/kg) and 100 μ l of 70kDa FITC-Dextran (5mg/ml) (Sigma Aldrich, France) to stain circulating leukocytes and visualize the lumen of blood vessels, respectively.

For adherent leukocyte quantification, the images obtained by time-lapse (2 minutes, 7.7 frames per second, 256x256 pixel resolution, 1000Hz frequency) were compiled and red spots, corresponding to adherent leukocytes, were counted for each group. For rolling leukocytes, we used the Kymograph plugin on ImageJ software (developed by J. Rietdorf and A. Seitz) (line width perpendicular to vessel lumen: 10; size pixel² after threshold: (2-5)-infinity). Leukocytes that were too fast were considered as background and not counted as rolling leukocytes.

Magnetic Resonance Imaging

Mice were deeply anesthetized with 5% isoflurane and maintained with 1.5-2% isoflurane 30%O₂/70%N₂O during the acquisitions. Experiments were carried out on a Pharmascan 7T (Bruker, Germany). T2-weighted images were acquired using a multislice multiecho sequence: TE/TR 33 ms/2500 ms. Lesion sizes were quantified on these images using ImageJ software. Mice showing lesions <6mm³ at 24h post MCAo were considered as surgical failure and excluded from the analyses.

T2*-weighted sequences were used to control if animals underwent hemorrhages events. Two-dimensional time-of-flight angiographies (TE/TR 12 ms/7 ms) were acquired and analyses of the MCA angiogram were also performed to control the recanalization status of the MCA. The angiographic score is inspired on the TIC1 grade flow scoring. Score 0 refers to the absence of any anterograde flow beyond the MCA. Score 1 is incomplete filling of the distal bed. Score 2 is almost complete filling of the distal territory. Score 3 is complete filling of the distal territory.

Molecular Imaging of P-Selectin

Micro-sized particles of iron oxide (MPIOs) (diameter 1.08 μm) (Invitrogen) covalently conjugated to purified polyclonal goat anti-mouse antibodies for P-selectin (R&D Systems, clone AF737) were prepared as previously described. The quality of conjugated MPIOs was systematically checked in a naive mouse, by stereotaxic injection of lipopolysaccharide (1 μl, 1mg/kg) in the striatum (0.5mm anterior, 2.0mm lateral, -3mm ventral to the Bregma).

Three-dimensional T2*- weighted gradient echo imaging with flow compensation (spatial resolution of 70 μm x 70 μm x 70 μm interpolated to an isotropic resolution of 70 μm), TE/TR 13.2ms/200 ms and a flip angle of 21° was performed to visualize MPIOs. MRI acquisitions started immediately after the intravenous injection of MPIOs (200 μl of 2 mg Fe/kg of conjugated MPIOs). All T2*-weighted images presented are minimum intensity projections of six consecutive slices. The signal void quantification of MPIOs on 3D T2*-weighted images was measured by using automatic triangle threshold in ImageJ software and results presented as MPIOs-induced signal void on the contralateral cortex divided by the signal void on the structure of interest (in percent).

Immunohistochemistry

Terminally anesthetized mice were transcardially perfused with cold heparinized saline (15 mL/min) and fixed with 50 mL of 4% paraformaldehyde phosphate buffer (pH 7.4). Brains were post-fixed with 4% paraformaldehyde phosphate buffer (18 hours; 4°C) and cryoprotected (sucrose 20% in PBS; 24 hours; 4°C) before freezing in Tissue-Tek (Miles Scientific, Naperville, IL, USA). Cryostat-cut sections (10 µm) were collected on poly-lysine slides and stored at – 80°C before processing.

Sections were co-incubated overnight with goat anti-mouse Collagen-IV (1:1000, SouthernBiotech 1340), rat anti-mouse CD206 (1:500, Serotec, clone MR5D3), rabbit anti-mouse Iba1 (1:1000, Wako 019-19741), rat anti-mouse CD68 (1:800, Abcam 53444), goat anti-mouse P-selectin (1:1000, RD System AF737), rabbit anti-mouse Aquaporin 4 (sc 20812, Santa Cruz), rabbit anti-mouse Laminin (1:1500, Abcam 11575), rat anti-mouse Ly6G (1:500, clone 1A8, StemCell 60031), rabbit anti-mouse CD3 (1:25, Abcam 5690), rat anti-mouse CD4 (1:25, eBiosciences 14-0042-86) and P2Ry12 (1:500, Anaspec). Primary antibodies were revealed by using Fab'2 fragments of donkey anti-rabbit linked to FITC, anti-rat linked to Cy3, anti-goat IgG linked to Cy5 (1:600, Jackson ImmunoResearch, West Grove, USA). Washed sections were coverslipped with antifade medium containing DAPI. Fluorescence images were digitally captured using a Leica DM6000 epifluorescence microscope-coupled coolsnap camera, or using a Leica DMI8 microscope equipped with a confocal head Yokogawa CSU-X1 and a Hamamatsu Orca Flash 4.0 camera. This system was controlled by Metamorph software (molecular devices). Images were visualized with Leica MM AF 2.2.0 software (Molecular Devices, USA) and further processed using ImageJ 1.52k software.

Flow Cytometry

After transcardiac perfusion with PBS, brains were roughly minced and homogenized with a potter tissue grinder in Hanks' balanced salt solution (HBSS) containing 15 mM HEPES buffer and 0.54% glucose. Whole brain homogenate was separated by 37% Percoll gradient centrifugation at 800g for 30 min at 4 °C (no brake). The pellet containing CNS leukocytes at the bottom of the tube was then collected and washed once with PBS containing 2% FCS before staining.

Fc receptors were blocked with CD16/32 (553142, BD Biosciences) for 10 min at 4 °C before incubation with the primary antibodies. Cells were stained with antibodies directed against CD11b (M1/70, BioLegend), CD45 (30-F11, BD Biosciences), Ly6G (1A8, BD Biosciences), CD3e (145-2C11, BD Biosciences), CD4 (RM4-5, BD Biosciences), CD8a (53-6.7, BD Biosciences) and CD206 (C068C2, BioLegend) for 45 min at 4 °C. After washing, samples were analyzed by a FACSVerser flow cytometer or sorted by a FACSAria (BD Biosciences). Appropriate isotype control antibodies were used to establish sorting parameters. Data were analyzed with the FlowJo 7.6.5 software (TreeStar Inc.). Data are expressed as percent.

Total RNA extraction

Total RNA was extracted from FACS sorted mouse brain macrophages stabilized in RNAProtect buffer according to the “Purification of total RNA from animal and human cells” protocol of the RNeasy Plus Micro Kit (QIAGEN, Hilden, Germany). In brief, cells were stored and shipped in buffer RNAProtect at 2-8 °C. After pelleting by centrifugation for 5 minutes at 5,000 x g, the RNAProtect was replaced by 350 µl buffer RLT Plus and the samples were homogenized by vortexing for 30 seconds. Genomic DNA contamination was removed by using gDNA Eliminator spin columns. Next one volume of 70 % ethanol was added and the samples were applied to RNeasy MinElute spin columns followed by several wash steps. Finally the total RNA was eluted in 12 µl of nuclease free water. Purity and integrity of the RNA was assessed on the Agilent 2100 Bioanalyzer with the RNA 6000 Pico LabChip reagent set (Agilent, Palo Alto, CA, USA).

RNAseq

The SMARTer Ultra Low Input RNA Kit for Sequencing v4 (Clontech Laboratories, Inc., Mountain View, CA, USA) was used to generate first strand cDNA from approximately 500 pg total-RNA. Double stranded cDNA was amplified by LD PCR (13 cycles) and purified *via* magnetic bead clean-up. Library preparation was carried out as described in the Illumina Nextera XT Sample Preparation Guide (Illumina, Inc., San Diego, CA, USA). Thereby 150 pg of input cDNA were tagmented (tagged and fragmented) by the Nextera XT transposome. The products were purified and amplified *via* a limited-

cycle PCR program to generate multiplexed sequencing libraries. For the PCR step 1:5 dilutions of the unique dual indexing (i7 and I5) adapters were used. The libraries were quantified using the KAPA Library Quantification Kit - Illumina/ABI Prism User Guide (Roche Sequencing Solutions, Inc., Pleasanton, CA, USA). Equimolar amounts of each library were sequenced on an Illumina NextSeq 2000 instrument controlled by the NextSeq 2000 Control Software (NCS) v1.2.0.36376, using two 100 cycles P2 Flow Cell with the dual index, single-read (SR) run parameters. Image analysis and base calling were done by the Real Time Analysis Software (RTA) v3.7.17. The resulting .bcl files were converted into .fastq files with the bcl2fastq v2.20 software.

RNA extraction, library preparation and RNAseq were performed at the Genomics Core Facility “KFB - Center of Excellence for Fluorescent Bioanalytics” (University of Regensburg, Regensburg, Germany; www.kfb-regensburg.de).

RNAseq analysis

The GSEA analysis was started on the Gene sets derived from the GO Biological Process ontology (BP) database using the ClusterProfiler package, gseGO function. Then the Simplify function was used *via* GOSemSim to eliminate the redundant GO terms (Yu *et al.*, 2012).

ClueGO is a Cytoscape plug-in that visualizes the non-redundant biological terms for large clusters of genes in a functionally grouped network. ClueGO performs single cluster analysis and comparison of several clusters (lists of genes). From the ontology sources used, the terms are selected by different filter criteria. The related terms which share similar associated genes can be fused to reduce redundancy. The ClueGO network is created with kappa statistics and reflects the relationships between the terms based on the similarity of their associated genes (Bindea *et al.*, 2009).

Statistical analyses

Results are the mean \pm SEM. Statistical analyses were performed using the Graphpad Prism 9.0 software. The Kolmogorov-Smirnov test was used to assess normality. Proportions were compared using the chi-square or Fisher test, while the continuous variables between groups were compared with

the Student's t or the Mann-Whitney test depending on whether their distribution was normal or not.

Mann-Whitney test was used when independent experiments were compared between two groups.

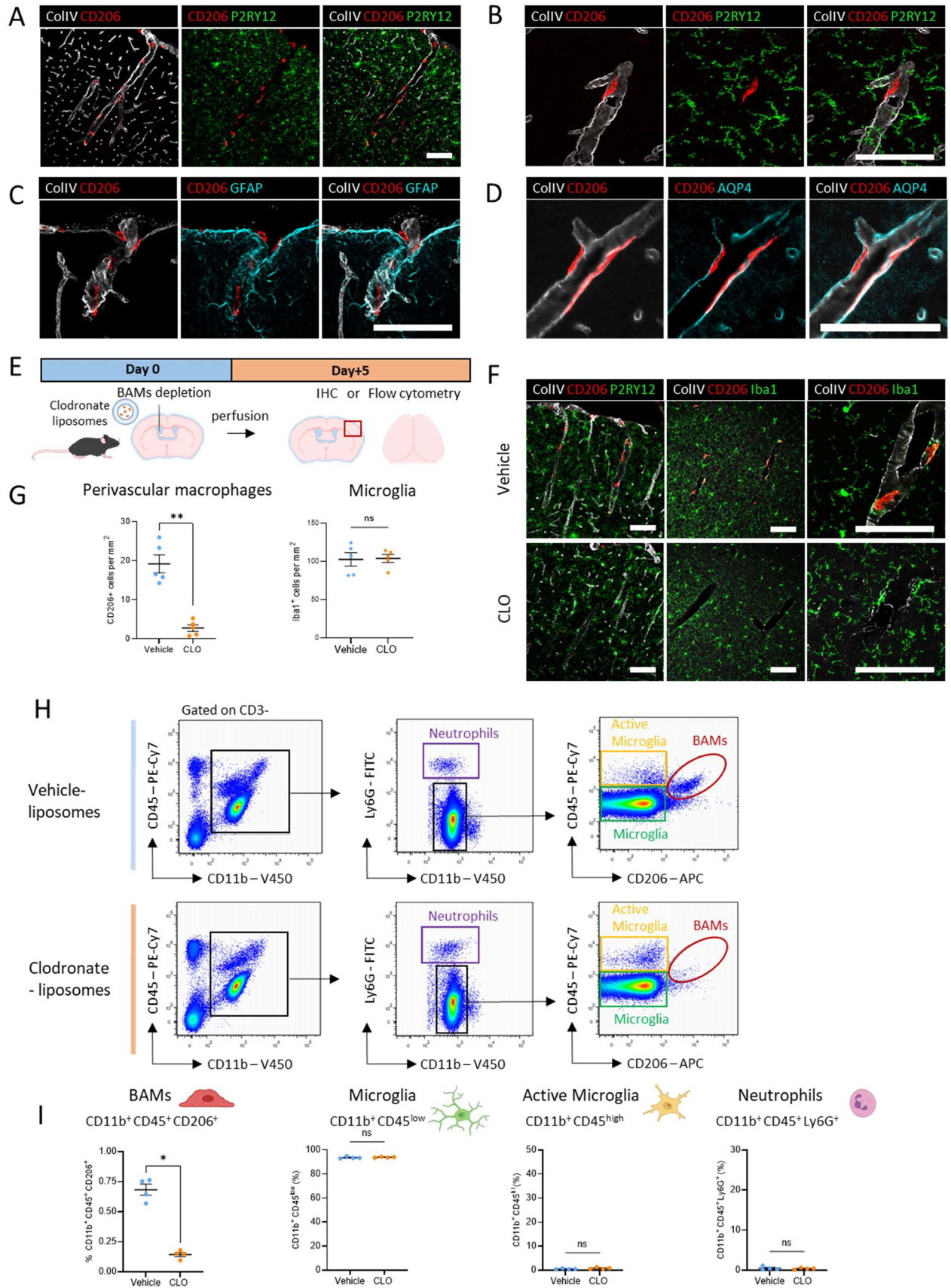


FIGURE 1

Figure 1: Immunohistological description of border-associated macrophages in the mouse brain, and characterization of their depletion by intracerebroventricular injection of clodronate-liposomes. **A)** Representative immunofluorescence images of CD206⁺ border-associated macrophages (BAMs) (red), P2RY12⁺ microglia (green) and collagen IV in the basal lamina of blood vessels (gray) in mice brain cortex. Scale bar: 100 μ m. **B)** Representative immunofluorescence images of CD206⁺ BAMs (red), P2RY12⁺ microglia (green) and collagen IV in the basal lamina of blood vessels (gray) in mice brain cortex. Scale bar: 100 μ m. **C)** Representative immunofluorescence images of CD206⁺ BAMs (red), GFAP⁺ astrocytes (cyan) and collagen IV in the basal lamina of blood vessels (gray) in mice brain cortex. Scale bar: 100 μ m. **D)** Representative immunofluorescence images of CD206⁺ BAMs (red), AQP4⁺ astrocytes endfeet (cyan) and collagen IV in the basal lamina of blood vessels (gray) in mice brain cortex. Scale bar: 100 μ m. **E)** Schematic representation of the experimental protocol for BAMs depletion and quantification. **F)** Representative immunofluorescence images of CD206⁺ BAMs (red), Iba1⁺ microglia (green) and collagen IV in the basal lamina of blood vessels (gray), in vehicle or clodronate-liposomes treated mice cortex. Scale bar: 100 μ m. **G)** Immunohistological quantification of CD206⁺ perivascular macrophages (PVMs) and Iba1⁺ microglia in vehicle or clodronate-liposomes treated mice cortex. n=5, * p<0.05, Mann-Whitney U test. **H)** Representative flow cytometry dot-plots and gating strategy used for quantification of BAMs, microglia, active microglia and neutrophils from mice brain treated with vehicle or clodronate-liposomes. **I)** Flow cytometry quantification of BAMs, microglia, active microglia and neutrophils from mice brain treated with vehicle or clodronate-liposomes. n=4, * p<0.05, Mann-Whitney U test.

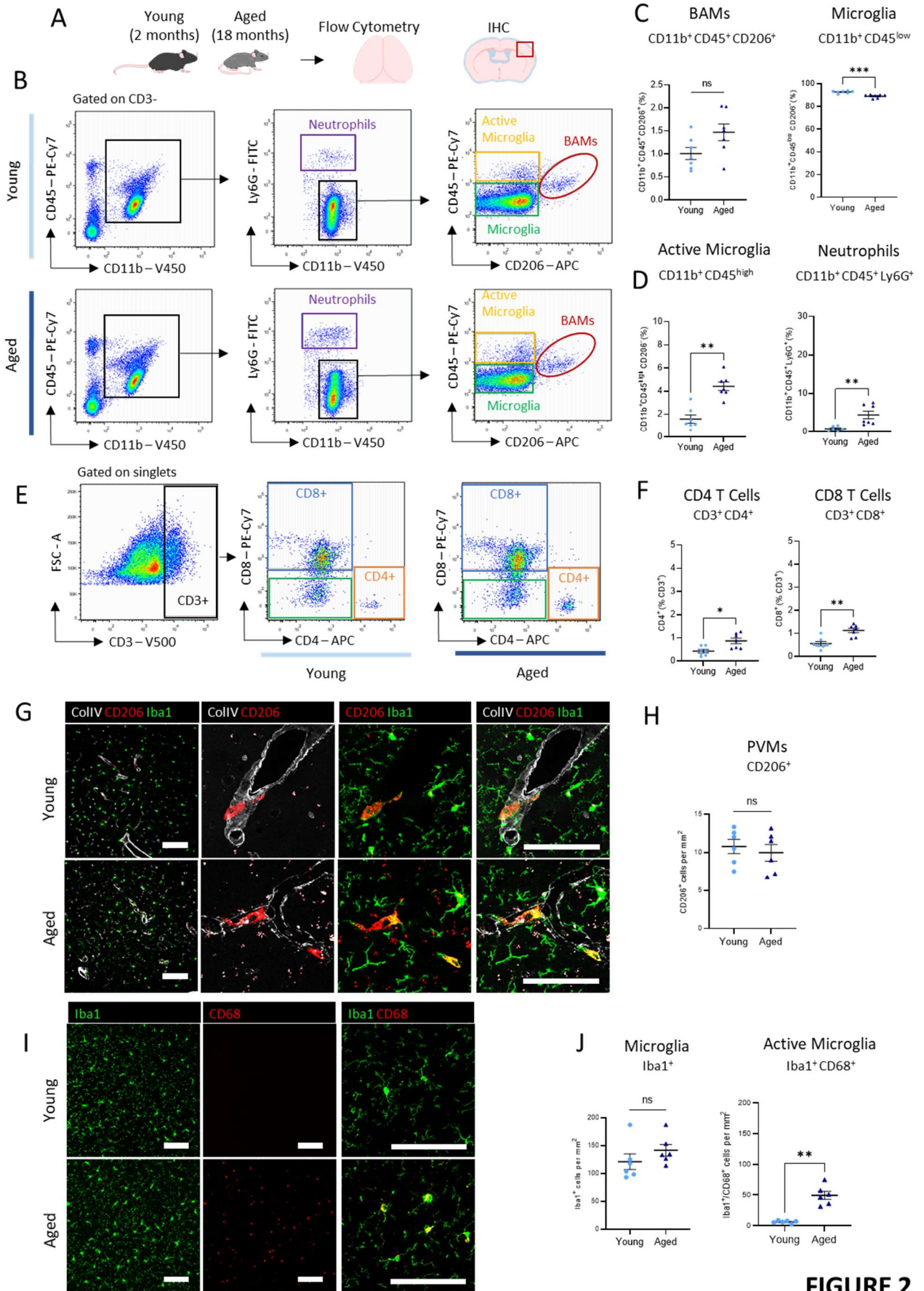


FIGURE 2

Figure 2: Inflammatory priming in the brain of aged mice, with no apparent change in the BAMs population. **A)** Schematic representation of the experimental protocol for immune cells quantification in young or aged mice brain. **B)** Representative flow cytometry dot-plots and gating strategy used for quantification of BAMs, microglia, active microglia and neutrophils from young or aged mice brain. **C, D)** Flow cytometry quantification of BAMs, microglia, active microglia and neutrophils from young or aged mice brain. $n=7$, ** $p<0.01$, *** $p<0.001$ Mann-Whitney U test. **E)** Representative flow cytometry dot-plots and gating strategy used for quantification of T cells from young or aged mice brain. **F)** Flow cytometry quantification of T cells from young or aged mice brain. $n=7$, * $p<0.05$, ** $p<0.01$, Mann-Whitney U test. **G)** Representative immunofluorescence images of CD206⁺ BAMs (red), Iba1⁺ microglia (green) and collagen IV in the basal lamina of blood vessels (gray) in young or aged mice brain cortex. Scale bar: 100 μm . **H)** Immunohistological quantification of CD206⁺ perivascular macrophages in young or aged mice brain cortex. $n=6$, * $p<0.05$, Mann-Whitney U test. **I)** Representative immunofluorescence images of Iba1⁺ microglia (green) and CD68⁺ macrophage/active microglia (red) in young or aged mice brain cortex. Scale bar: 100 μm . **J)** Immunohistological quantification of Iba1⁺ microglia and Iba1⁺/CD68⁺ active microglia in young or aged mice brain cortex. $n=6$, ** $p<0.01$, Mann-Whitney U test.

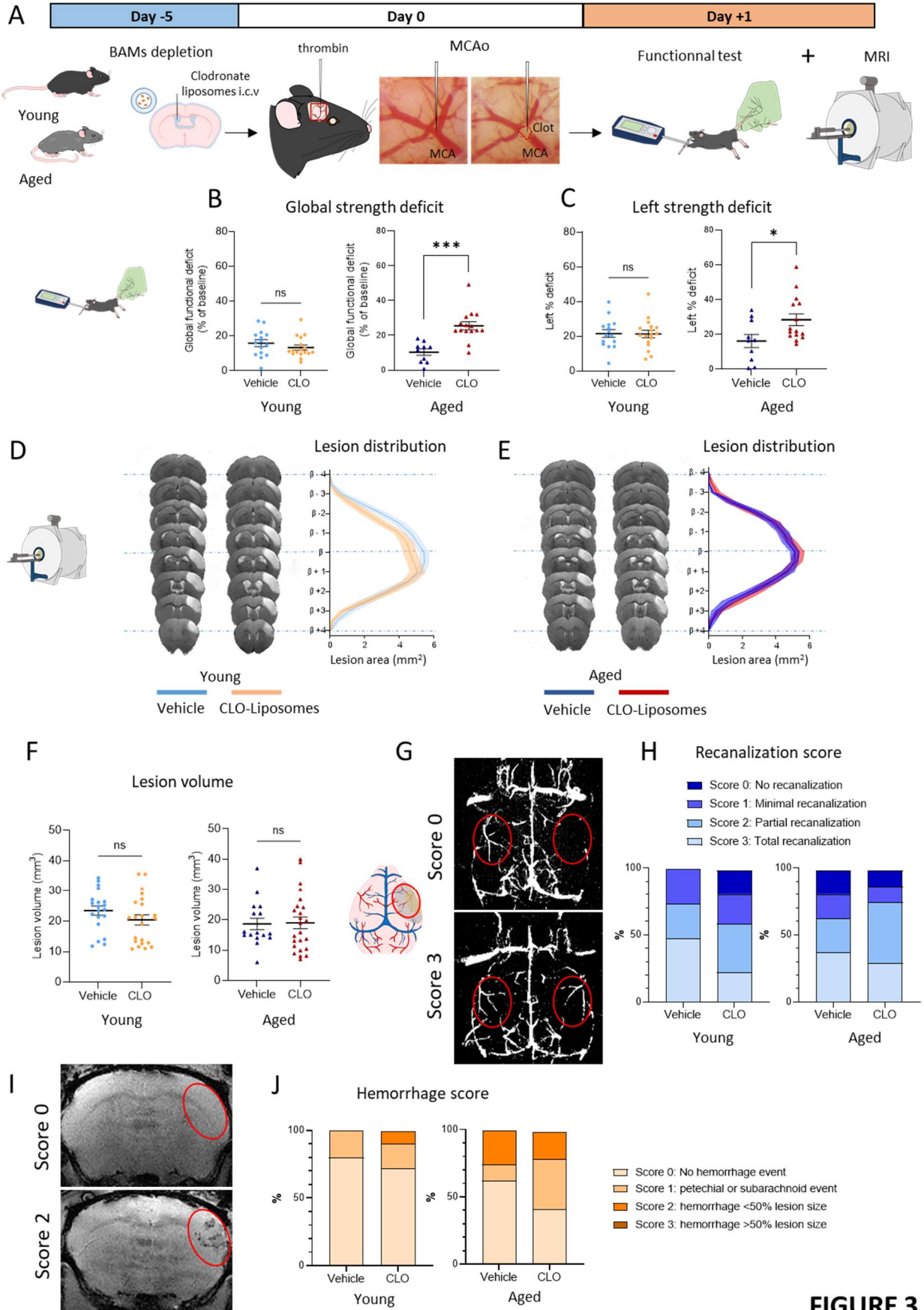


FIGURE 3

Figure 3: BAMs depletion increases functional deficit after stroke in aged mice but not in young mice. **A)** Schematic representation of the experimental protocol. **B)** Quantification of the global strength deficit measured by grip test at 24 hours after stroke onset in vehicle or clodronate-treated young (left) or aged (right) mice. n=20 vehicle, young /n=22 clodronate, young /n=16 vehicle, aged /n=24 clodronate, aged; *** p<0.001; Mann-Whitney U test. **C)** Quantification of the specific left paw strength deficit measured by grip test at 24 hours after stroke onset in vehicle or clodronate-treated young (left) or aged (right) mice. n=20 vehicle, young /n=22 clodronate, young /n=16 vehicle, aged /n=24 clodronate, aged; * p<0.05; Mann-Whitney U test. **D)** Representative T2-weighted MRI brain images of the ischemic lesion at 24 hours after stroke (left) and representation of the lesion distribution around the bregma (right) in vehicle or clodronate-treated young and **E)** aged mice. **F)** Quantification of ischemic lesion volume at 24 hours after stroke in vehicle or clodronate-treated young (left) or aged (right) mice. n=20 vehicle, young /n=22 clodronate, young /n=16 vehicle, aged /n=24 clodronate, aged. Mann-Whitney U test. **G)** Representative 3D-reconstructed angiographies illustrating recanalization score 0 (top) or score 3 (bottom) after stroke. **H)** Percentage of recanalization score at 24 hours after stroke onset in vehicle or clodronate-treated young (left) or aged (right) mice. n=20 vehicle, young /n=22 clodronate, young /n=16 vehicle, aged /n=24 clodronate, aged. Score 0 = complete occlusion; Score 1 = incomplete filling of the distal territory; Score 2 = almost complete filling of the distal territory; Score 3 = complete recanalization. **I)** Representative T2* weighted MRI brain images illustrating hemorrhage score 0 (top) or score 3 (bottom) after stroke. **J)** Percentage of hemorrhage score at 24 hours after stroke onset in vehicle or clodronate-treated young (left) or aged (right) mice. n=20 vehicle, young /n=22 clodronate, young /n=16 vehicle, aged /n=24 clodronate, aged. Score 0 = no hemorrhage event; Score 1 = petechial (small bleeding spots from small bleeding areas) or subarachnoid event; Score 2 = hemorrhage <50% of the lesion size; Score 3 = hemorrhage >50% of the lesion size (not observed).

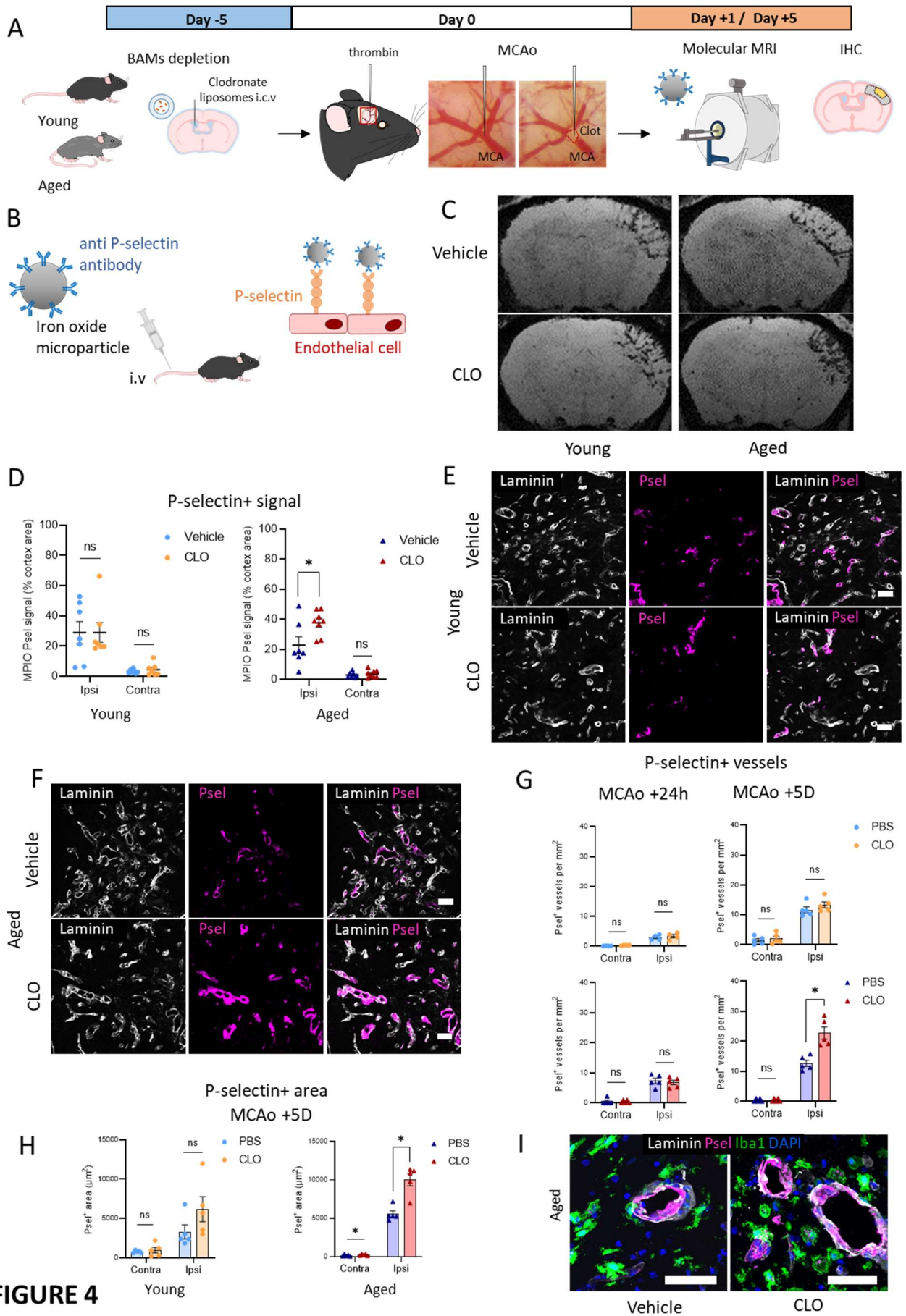


FIGURE 4

Figure 4: BAMs depletion increases the expression of the P-selectin adhesion molecule after stroke in aged mice but not in young mice. **A)** Schematic representation of the experimental protocol. **B)** Schematic representation of microparticles of iron oxide (MPIOs) coupled to anti-P-selectin antibodies to reveal vascular inflammation by magnetic resonance imaging (MRI). **C)** Representative T2*-weighted MRI brain images of the MPIOs signal at 24 hours after stroke in vehicle or clodronate-treated young and aged mice. **D)** Quantification of MPIOs hyposignal in the cortex. n=7 vehicle, young /n=7 clodronate, young /n=7 vehicle, aged /n=8 clodronate, aged. * p<0.05, Mann-Whitney U test. **E)** Representative immunofluorescence images of Psel⁺ blood vessels in mice brain cortex at 5 days after stroke in vehicle or clodronate-treated young mice. Scale bar: 50 μm. **F)** Representative immunofluorescence images of Psel⁺ blood vessels in mice brain cortex at 5 days after stroke in vehicle or clodronate-treated aged mice. Scale bar: 50 μm. **G)** Immunohistological quantification of the number of Psel⁺ blood vessels in mice brain cortex at 24 hours/5 days after stroke. n=5; * p<0.05; Mann-Whitney U test. **H)** Immunohistological quantification of the Psel⁺ area in mice brain cortex at 5 days after stroke. n=5; * p<0.05; Mann-Whitney U test. **I)** Immunofluorescence images of Psel⁺ (magenta) blood vessels (gray) and Iba1⁺ microglia (green) in mice brain cortex at 5 days after stroke in vehicle or clodronate-treated aged mice. Scale bar: 50 μm.

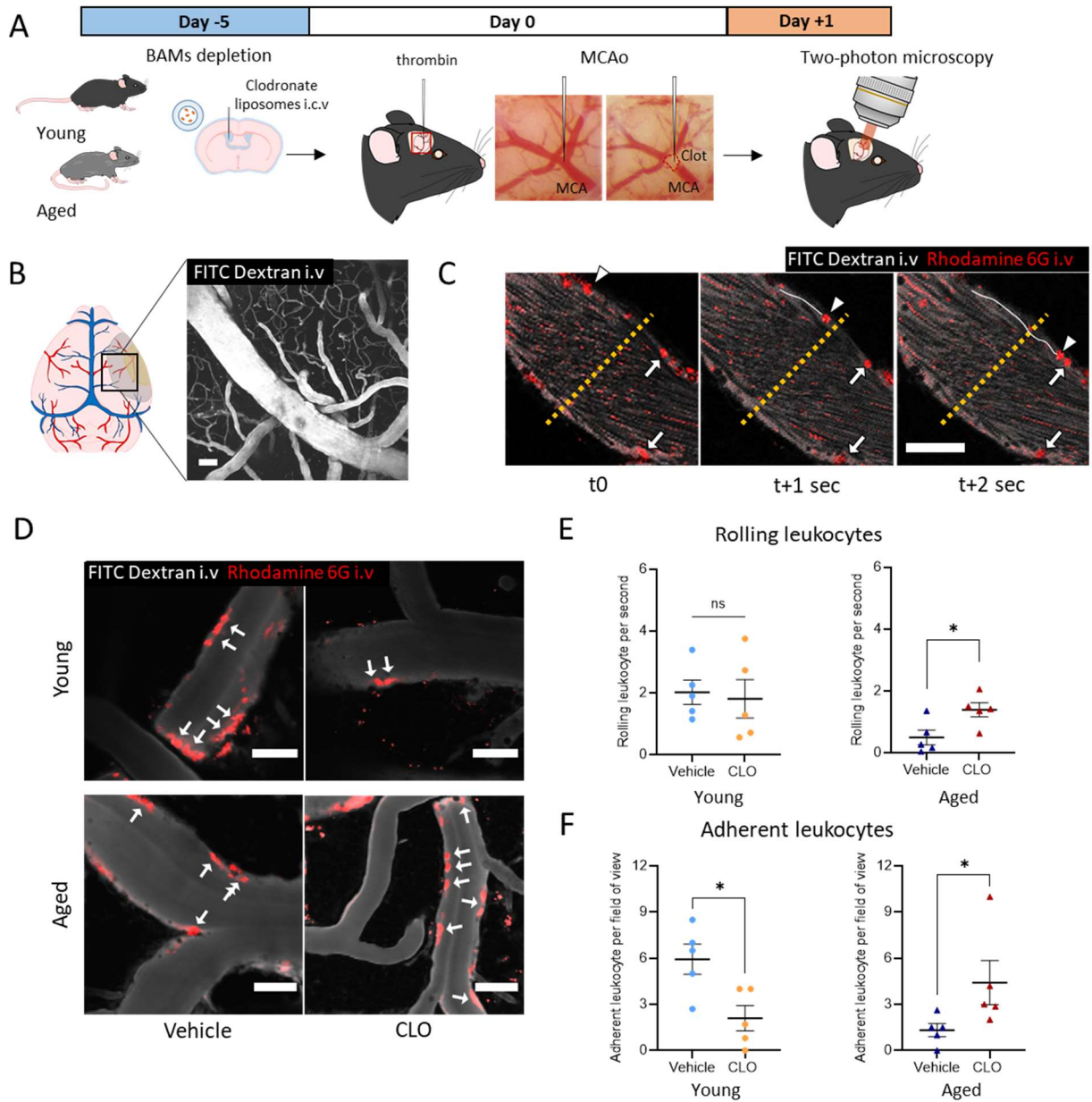


FIGURE 5

Figure 5: BAMs depletion differentially modulates leukocyte trafficking in cerebral vessels after stroke. **A)** Schematic representation of the experimental protocol. **B)** Left: schematic view of the brain seen from above, the shaded area corresponds to the ischemic area, the black square represents the imaging area through the thinned cranial window. Right: Two-photon z-projection of cortical blood vessels labelled with intravenously injected FITC-Dextran 70kDa (gray). Scale bar: 50 μm . **C)** Time-lapse images acquired with two-photon microscope, illustrating the quantification of rolling leukocytes using the kymograph plugin. Circulating leukocytes are labelled with intravenously injected Rhodamine-6G (red). The yellow dotted line represents the kymograph line in order to quantify the number of leukocytes passing through it. The white arrowhead shows a leukocyte rolling on the vessel wall. The white line represents its path between t_0 and $t + 2\text{sec}$. White arrows show adherent leukocytes, which do not move between t_0 and $t + 2\text{sec}$. Scale bar: 50 μm . **D)** Representative compilation images of 2 minutes time-lapse showing leukocyte adhesion to the walls of cerebral vessels 24 hours after stroke. White arrows show adherent leukocytes. Scale bar: 50 μm . **E)** Quantification of leukocyte rolling 24 hours after stroke in vehicle or clodronate-treated young and aged mice. $n=5$; * $p<0.05$; Mann-Whitney U test. **F)** Quantification of leukocyte adhesion 24 hours after stroke in vehicle or clodronate-treated young and aged mice. $n=5$; * $p<0.05$; Mann-Whitney U test.

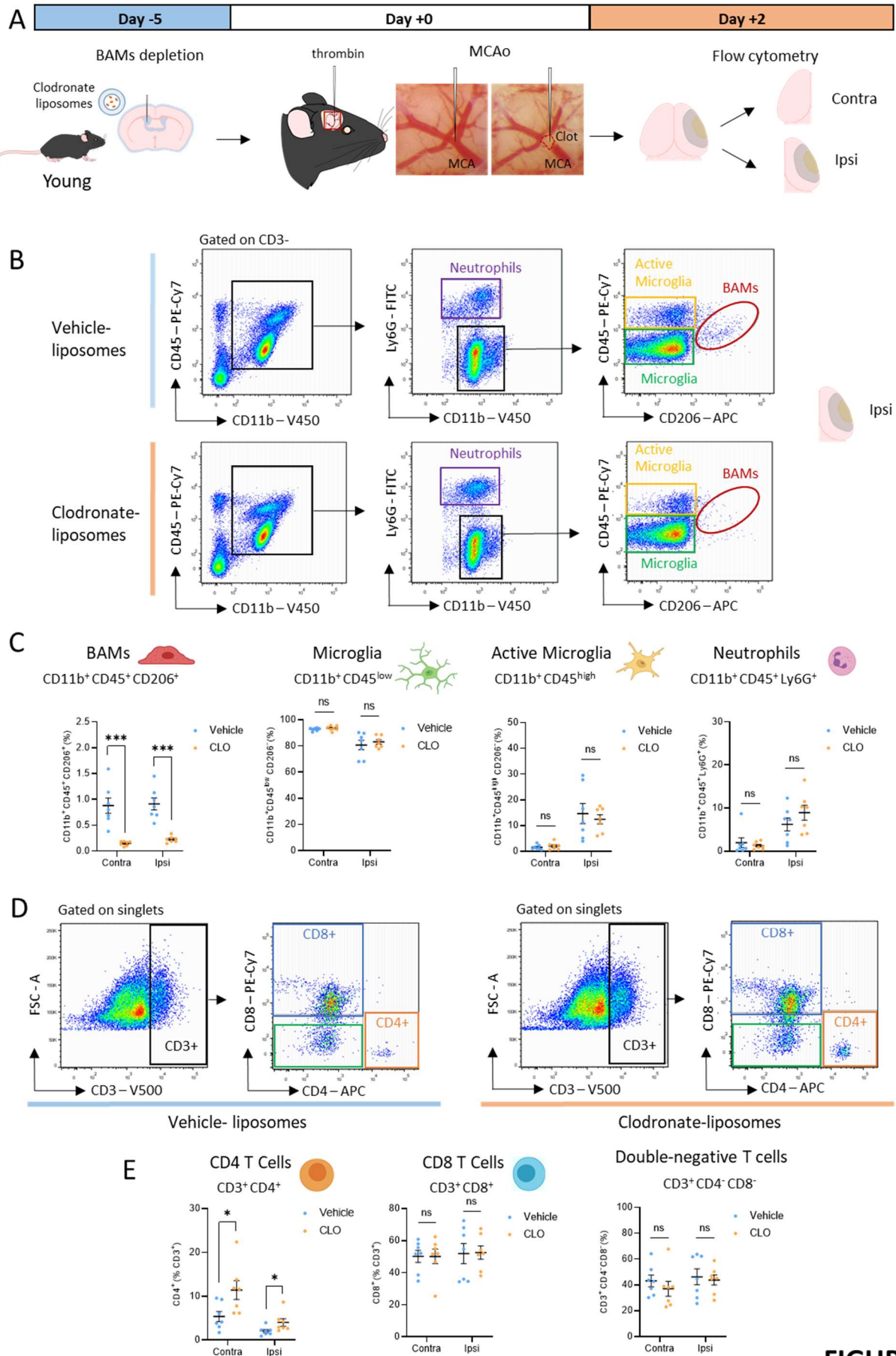


FIGURE 6

Figure 6: BAMs depletion slightly increases CD4⁺ T cells infiltration 2 days after stroke in young mice. **A)** Schematic representation of the experimental protocol. **B)** Representative flow cytometry dot-plots and gating strategy used for quantification of BAMs, microglia, active microglia and neutrophils 2 days after stroke in vehicle or clodronate-treated young mice brain. **C)** Flow cytometry quantification of BAMs, microglia, active microglia and neutrophils 2 days after stroke in vehicle or clodronate-treated young mice brain. n=7; *** p<0.001; Mann-Whitney U test. **D)** Representative flow cytometry dot-plots and gating strategy used for quantification of T cells 2 days after stroke in vehicle or clodronate-treated young mice brain. **E)** Flow cytometry quantification of T cells 2 days after stroke in vehicle or clodronate-treated young mice brain. n=7; * p<0.05; Mann-Whitney U test.

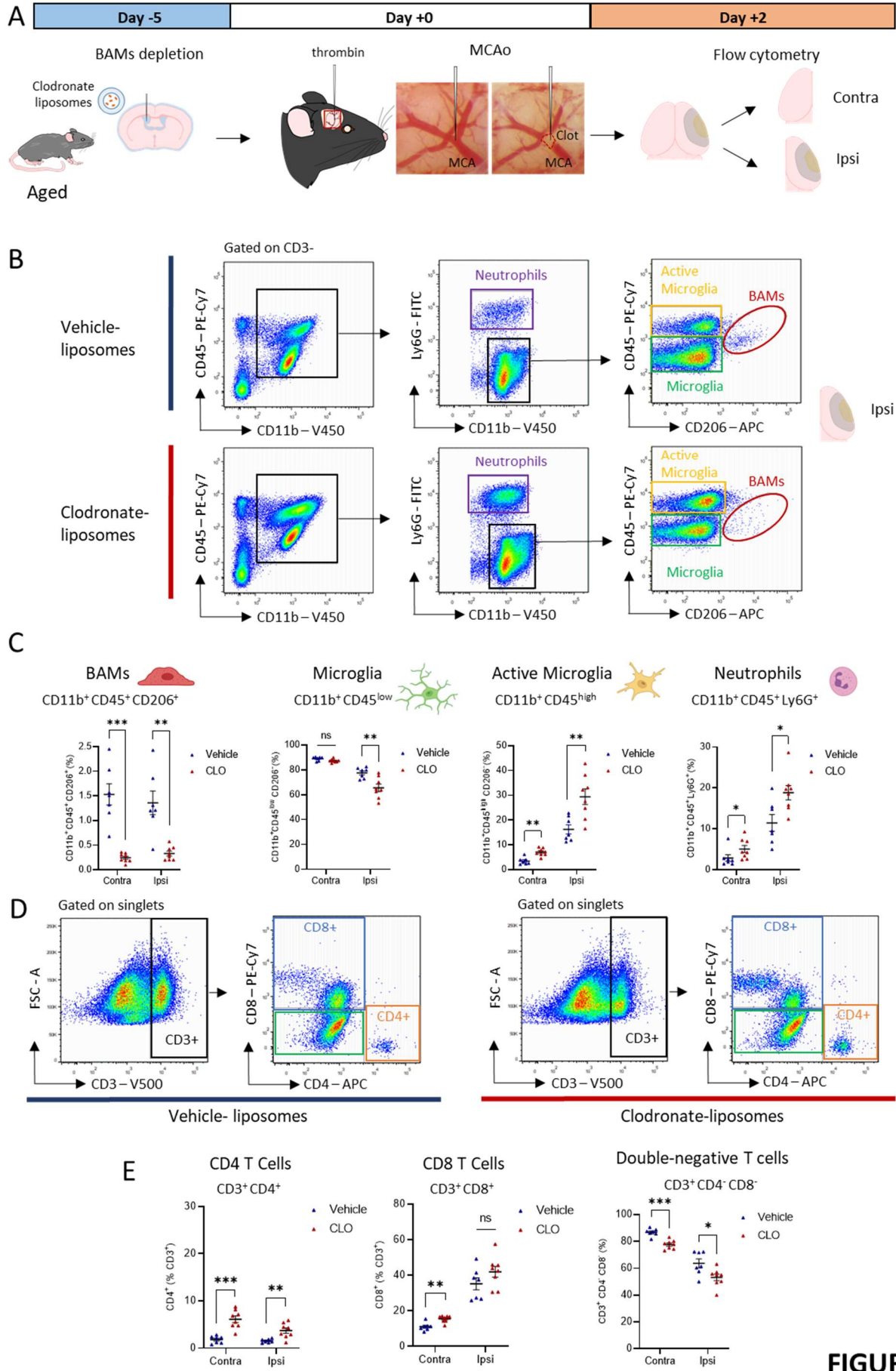


FIGURE 7

Figure 7: BAMs depletion dramatically increases microglial activation and neutrophils, CD4⁺ and CD8⁺ T cells infiltration 2 days after stroke in aged mice. **A)** Schematic representation of the experimental protocol. **B)** Representative flow cytometry dot-plots and gating strategy used for quantification of BAMs, microglia, active microglia and neutrophils 2 days after stroke in vehicle or clodronate-treated aged mice brain. **C)** Flow cytometry quantification of BAMs, microglia, active microglia and neutrophils 2 days after stroke in vehicle or clodronate-treated aged mice brain. n=7; * p<0.05; ** p<0.01; *** p<0.001; Mann-Whitney U test. **D)** Representative flow cytometry dot-plots and gating strategy used for quantification of T cells 2 days after stroke in vehicle or clodronate-treated aged mice brain. **E)** Flow cytometry quantification of T cells 2 days after stroke in vehicle or clodronate-treated aged mice brain. n=7; * p<0.05; ** p<0.01; *** p<0.001; Mann-Whitney U test.

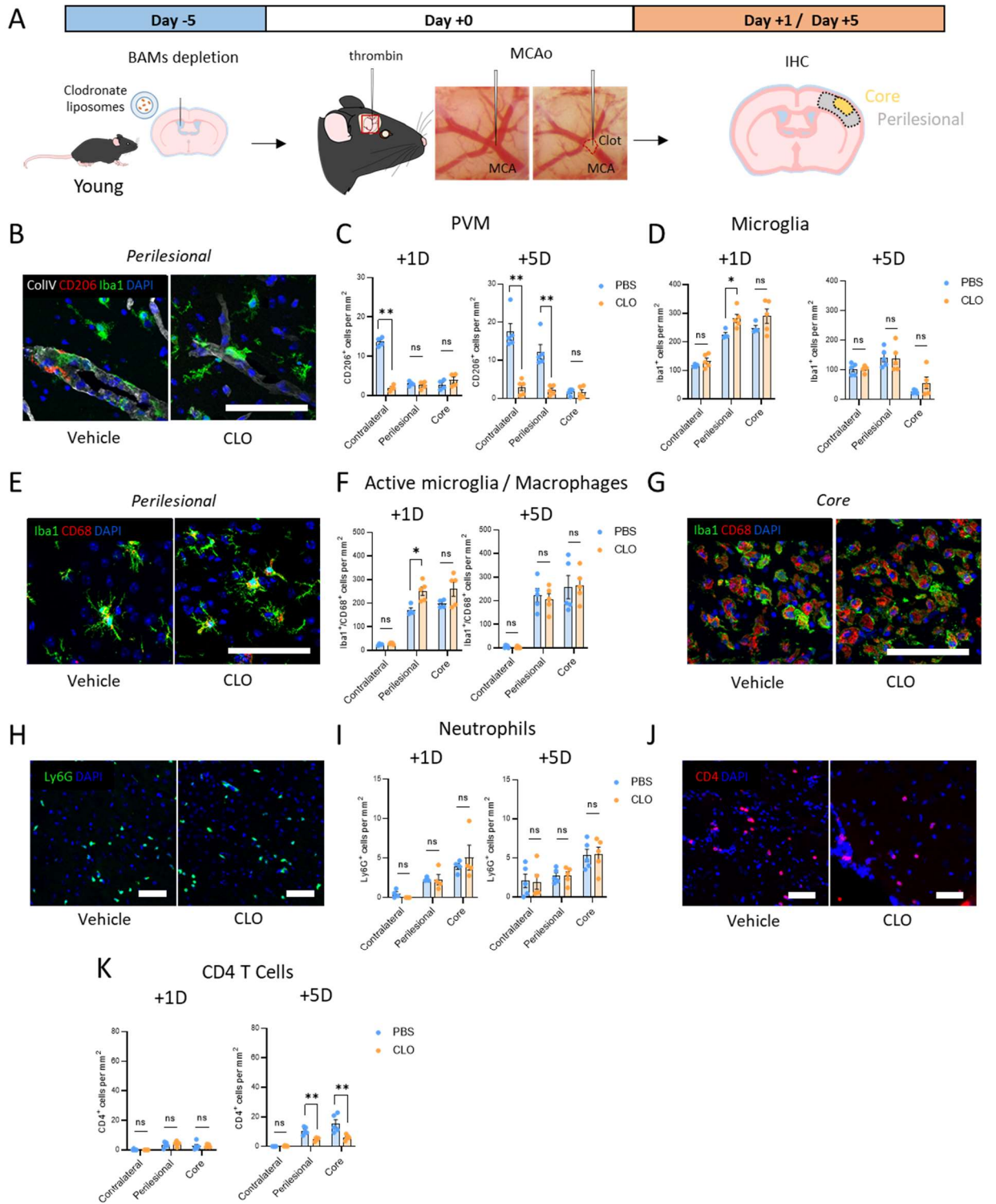


FIGURE 8

Figure 8: Immunohistological characterization of stroke-induced inflammation 1 day and 5 days after stroke in vehicle and clodronate-treated young mice. **A)** Schematic representation of the experimental protocol. **B)** Representative immunofluorescence images of CD206⁺ PVMs and Iba1⁺ microglia in brain cortex at 5 days after stroke in vehicle or clodronate-treated young mice. Scale bar: 100 μ m. **C)** Immunohistological quantification of CD206⁺ PVMs 1 day (left) and 5 days (right) after stroke. n=5; ** p<0.01; Mann-Whitney U test. **D)** Immunohistological quantification of Iba1⁺ microglia 1 day (left) and 5 days (right) after stroke. n=5; * p<0.05; ** p<0.01; Mann-Whitney U test. **E)** Representative immunofluorescence images of Iba1⁺/CD68⁺ active microglia in perilesional area 1 day after stroke in vehicle or clodronate-treated young mice. Scale bar: 100 μ m. **F)** Immunohistological quantification of Iba1⁺/CD68⁺ active microglia/macrophages 1 day (left) and 5 days (right) after stroke. n=5; * p<0.05; Mann-Whitney U test. **G)** Representative immunofluorescence images of Iba1⁺/CD68⁺ microglia/macrophages in ischemic core at 5 days after stroke in vehicle or clodronate-treated young mice. Scale bar: 100 μ m. **H)** Representative immunofluorescence images of Ly6G⁺ neutrophils in brain cortex at 5 days after stroke in vehicle or clodronate-treated young mice. **I)** Immunohistological quantification of Ly6G⁺ neutrophils 1 day (left) and 5 days (right) after stroke. n=5. **J)** Representative immunofluorescence images of CD4⁺ T cells in brain cortex at 5 days after stroke in vehicle or clodronate-treated young mice. **K)** Immunohistological quantification of CD4⁺ T cells 1 day (left) and 5 days (right) after stroke. n=5; ** p<0.01; Mann-Whitney U test.

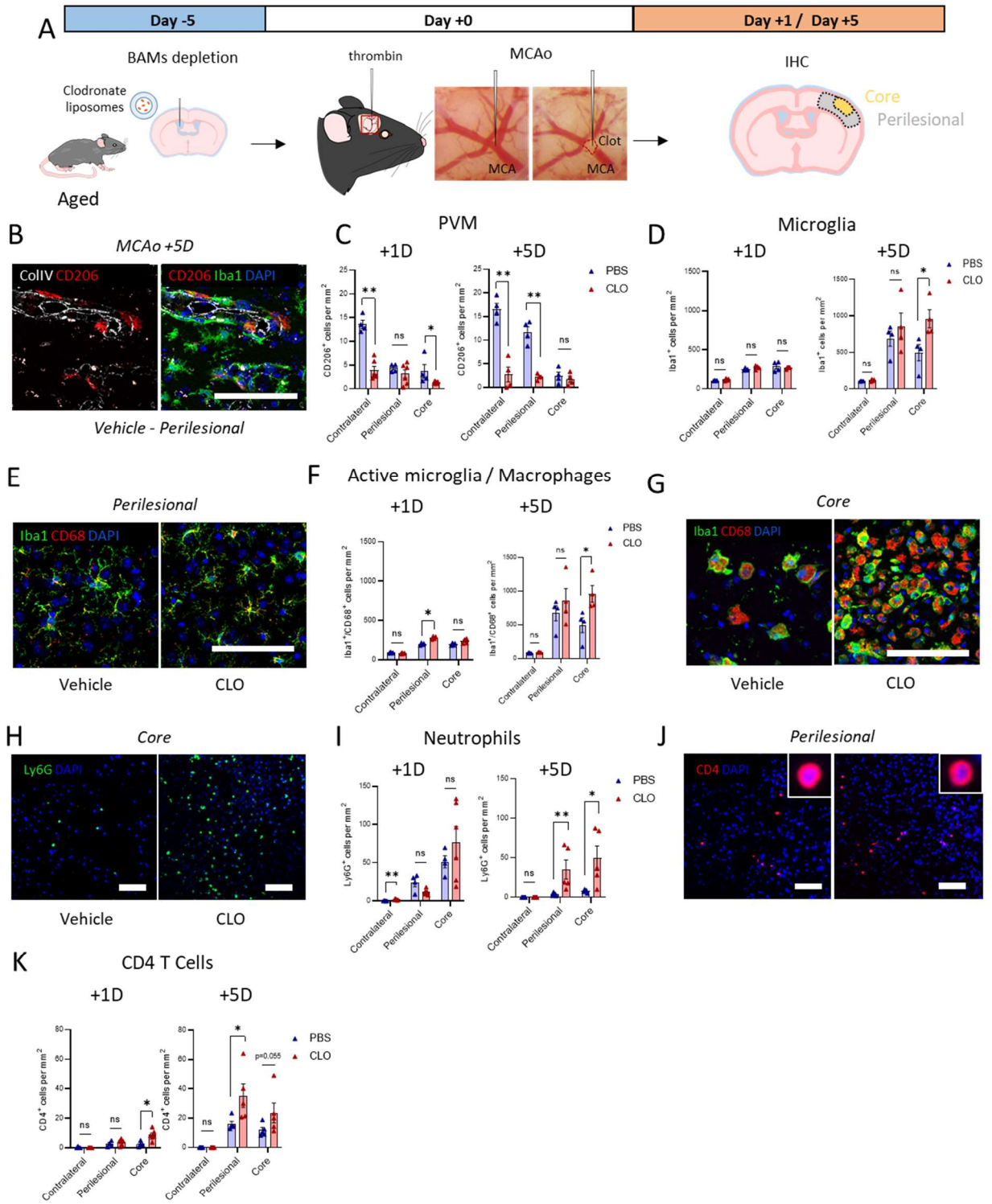
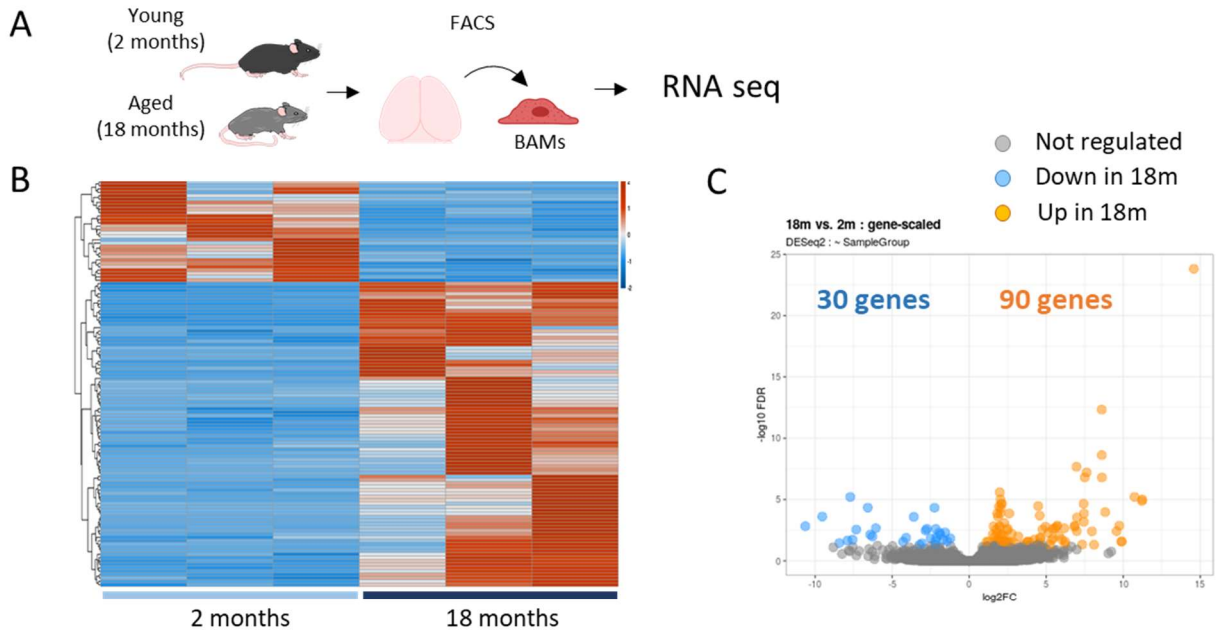
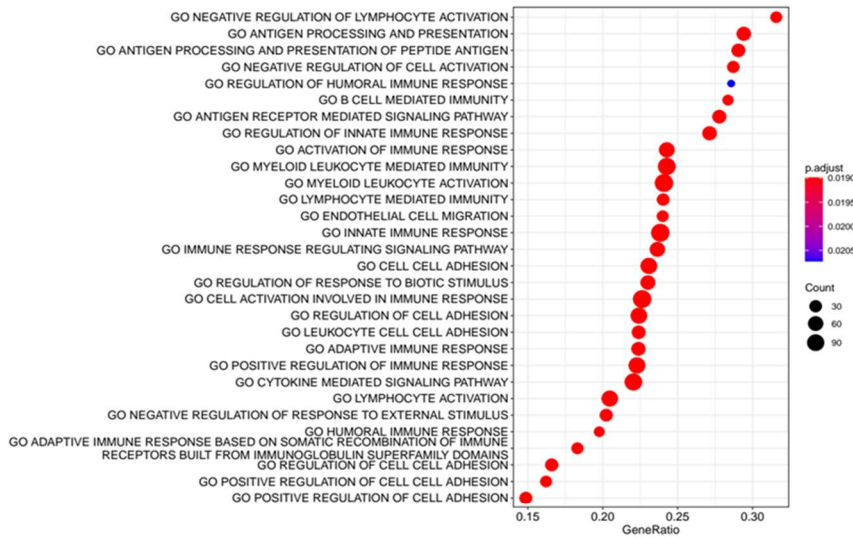


FIGURE 9

Figure 9: Immunohistological characterization of stroke-induced inflammation 1 day and 5 days after stroke in vehicle and clodronate-treated aged mice. **A)** Schematic representation of the experimental protocol. **B)** Representative immunofluorescence images of CD206⁺ PVMs and Iba1⁺ microglia in perilesional area at 5 days after stroke in vehicle aged mice. Scale bar: 100 μ m. **C)** Immunohistological quantification of CD206⁺ PVMs 1 day (left) and 5 days (right) after stroke. n=5; * p<0.05; ** p<0.01; Mann-Whitney U test. **D)** Immunohistological quantification of Iba1⁺ microglia 1 day (left) and 5 days (right) after stroke. n=5; * p<0.05; Mann-Whitney U test. **E)** Representative immunofluorescence images of Iba1⁺/CD68⁺ active microglia in perilesional area at 1 day after stroke in vehicle or clodronate-treated aged mice. Scale bar: 100 μ m. **F)** Immunohistological quantification of Iba1⁺/CD68⁺ active microglia 1 day (left) and 5 days (right) after stroke. n=5; * p<0.05; Mann-Whitney U test. **G)** Representative immunofluorescence images of Iba1⁺/CD68⁺ microglia/macrophages in ischemic core at 5 days after stroke in vehicle or clodronate-treated aged mice. Scale bar: 100 μ m. **H)** Representative immunofluorescence images of Ly6G⁺ neutrophils in brain cortex at 5 days after stroke in vehicle or clodronate-treated aged mice. **I)** Immunohistological quantification of Ly6G⁺ neutrophils 1 day (left) and 5 days (right) after stroke. n=5; * p<0.05; **p<0.01; Mann-Whitney U test. **J)** Representative immunofluorescence images of CD4⁺/CD8⁺ T cells in brain cortex at 5 days after stroke in vehicle or clodronate-treated aged mice. Scale bar: 100 μ m. **K)** Immunohistological quantification of CD4⁺ T cells 1 day (left) and 5 days (right) after stroke. n=5; * p<0.05; Mann-Whitney U test.



D Gene-set: GO biological process – top 30 regulated pathways



E

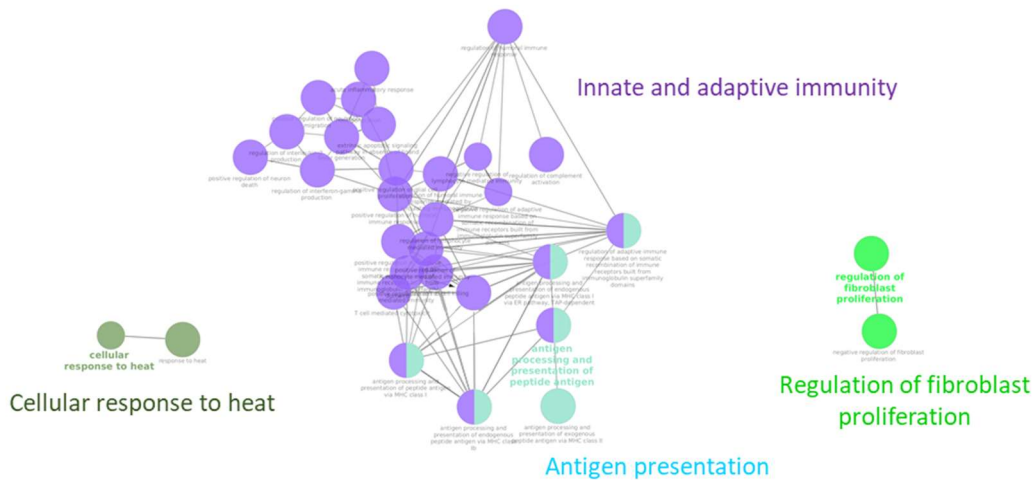


FIGURE 10

Figure 10: BAMs change their transcriptomic phenotype during aging and overexpress genes implicated in the regulation of cell adhesion, regulation of both innate and adaptive immune responses and cytokine-mediated signaling pathways. **A)** Schematic representation of the experimental protocol to isolate CD11b⁺ CD45⁺ CD206⁺ BAMs by fluorescence activated cell sorting (FACS) from young and aged mice brain to analyse the RNA expression profile. **B)** Heatmap of differentially expressed genes determined by whole-transcriptome RNA-seq of BAMs from young and aged mice brain. Normalized Z score values (high, red; low, blue) were calculated for each differentially expressed gene. **C)** Volcano plot showing significantly differentiated genes (upregulated, orange; downregulated, blue). **D)** Dotplot representing the 30 most upregulated pathways according to the gene set enrichment analysis (GSEA) analysis from the Biological Process ontology. **E)** Clustering of significantly regulated GO biological process pathways. Pathways are grouped into four clusters: the “T-cell mediated immunity” cluster (purple), the “antigen presentation” cluster (turquoise), the “cellular response to heat” cluster (khaki), and the “regulation of fibroblast proliferation” cluster (light green).

- Alves de Lima, K., Rustenhoven, J. and Kipnis, J. (2020) 'Meningeal Immunity and Its Function in Maintenance of the Central Nervous System in Health and Disease', *Annual Review of Immunology*, 38(1), pp. 597–620. doi:10.1146/annurev-immunol-102319-103410.
- Amki, M.E. *et al.* (2020) 'Neutrophils Obstructing Brain Capillaries Are a Major Cause of No-Reflow in Ischemic Stroke', *Cell Reports*, 33(2). doi:10.1016/j.celrep.2020.108260.
- Anrather, J. and Iadecola, C. (2016) 'Inflammation and Stroke: An Overview', *Neurotherapeutics: The Journal of the American Society for Experimental NeuroTherapeutics*, 13(4), pp. 661–670. doi:10.1007/s13311-016-0483-x.
- Benakis, C., Llovera, G. and Liesz, A. (2018) 'The meningeal and choroidal infiltration routes for leukocytes in stroke', *Therapeutic Advances in Neurological Disorders*, 11, p. 1756286418783708. doi:10.1177/1756286418783708.
- Bindea, G. *et al.* (2009) 'ClueGO: a Cytoscape plug-in to decipher functionally grouped gene ontology and pathway annotation networks', *Bioinformatics (Oxford, England)*, 25(8), pp. 1091–1093. doi:10.1093/bioinformatics/btp101.
- Candelario-Jalil, E. and Paul, S. (2021) 'Impact of aging and comorbidities on ischemic stroke outcomes in preclinical animal models: A translational perspective', *Experimental Neurology*, 335, p. 113494. doi:10.1016/j.expneurol.2020.113494.
- Dorrier, C.E. *et al.* (2021) 'Emerging roles for CNS fibroblasts in health, injury and disease', *Nature Reviews Neuroscience*, pp. 1–12. doi:10.1038/s41583-021-00525-w.
- Drieu, A. *et al.* (2018) 'Anti-inflammatory treatments for stroke: from bench to bedside', *Therapeutic Advances in Neurological Disorders*, 11, p. 1756286418789854. doi:10.1177/1756286418789854.
- Drieu, A. *et al.* (2020) 'Alcohol exposure-induced neurovascular inflammatory priming impacts ischemic stroke and is linked with brain perivascular macrophages', *JCI insight* [Preprint]. doi:10.1172/jci.insight.129226.
- Fabriek, B.O. *et al.* (2005) 'CD163-positive perivascular macrophages in the human CNS express molecules for antigen recognition and presentation', *Glia*, 51(4), pp. 297–305. doi:10.1002/glia.20208.
- Faraco, G. *et al.* (2016) 'Perivascular macrophages mediate the neurovascular and cognitive dysfunction associated with hypertension', *Journal of Clinical Investigation*, 126(12), pp. 4674–4689. doi:10.1172/JCI86950.
- Fernández-Klett, F. *et al.* (2013) 'Early loss of pericytes and perivascular stromal cell-induced scar formation after stroke', *Journal of Cerebral Blood Flow & Metabolism*, 33(3), p. 428. doi:10.1038/jcbfm.2012.187.
- Gauberti, M. *et al.* (2014) 'Lack of Secondary Microthrombosis After Thrombin-Induced Stroke in Mice and Non-Human Primates', *Journal of thrombosis and haemostasis: JTH*, 12(3), pp. 409–414. doi:10.1111/jth.12487.
- Haley, M.J. *et al.* (2019) 'Microglial Priming as Trained Immunity in the Brain', *Neuroscience*, 405, pp. 47–54. doi:10.1016/j.neuroscience.2017.12.039.
- Katan, M. and Luft, A. (2018) 'Global Burden of Stroke', *Seminars in Neurology*, 38(2), pp. 208–211. doi:10.1055/s-0038-1649503.

- Kida, S. *et al.* (1993) 'Perivascular cells act as scavengers in the cerebral perivascular spaces and remain distinct from pericytes, microglia and macrophages', *Acta Neuropathologica*, 85(6), pp. 646–652.
- Lehenkari, P.P. *et al.* (2002) 'Further insight into mechanism of action of clodronate: inhibition of mitochondrial ADP/ATP translocase by a nonhydrolyzable, adenine-containing metabolite', *Molecular Pharmacology*, 61(5), pp. 1255–1262.
- Levard, D. *et al.* (2020) 'Filling the gaps on stroke research: focus on inflammation and immunity', *Brain, Behavior, and Immunity* [Preprint]. doi:10.1016/j.bbi.2020.09.025.
- Llovera, G. *et al.* (2014) 'Modeling Stroke in Mice: Permanent Coagulation of the Distal Middle Cerebral Artery', *Journal of Visualized Experiments : JoVE* [Preprint], (89). doi:10.3791/51729.
- Månberg, A. *et al.* (2021) 'Altered perivascular fibroblast activity precedes ALS disease onset', *Nature Medicine*, 27(4), pp. 640–646. doi:10.1038/s41591-021-01295-9.
- Mendes-Jorge, L. *et al.* (2009) 'Scavenger function of resident autofluorescent perivascular macrophages and their contribution to the maintenance of the blood-retinal barrier', *Investigative Ophthalmology & Visual Science*, 50(12), pp. 5997–6005. doi:10.1167/iovs.09-3515.
- Moriyama, Y. and Nomura, M. (2018) 'Clodronate: A Vesicular ATP Release Blocker', *Trends in Pharmacological Sciences*, 39(1), pp. 13–23. doi:10.1016/j.tips.2017.10.007.
- Mozaffarian, D. *et al.* (2016) 'Heart Disease and Stroke Statistics-2016 Update: A Report From the American Heart Association', *Circulation*, 133(4), pp. e38-360. doi:10.1161/CIR.0000000000000350.
- Mrdjen, D. *et al.* (2018) 'High-Dimensional Single-Cell Mapping of Central Nervous System Immune Cells Reveals Distinct Myeloid Subsets in Health, Aging, and Disease', *Immunity*, 48(2), pp. 380-395.e6. doi:10.1016/j.immuni.2018.01.011.
- Muriach, M. *et al.* (2014) 'Diabetes and the brain: oxidative stress, inflammation, and autophagy', *Oxidative Medicine and Cellular Longevity*, 2014, p. 102158. doi:10.1155/2014/102158.
- Niraula, A., Sheridan, J.F. and Godbout, J.P. (2017) 'Microglia Priming with Aging and Stress', *Neuropsychopharmacology*, 42(1), pp. 318–333. doi:10.1038/npp.2016.185.
- Norden, D.M., Muccigrosso, M.M. and Godbout, J.P. (2015) 'Microglial priming and enhanced reactivity to secondary insult in aging, and traumatic CNS injury, and neurodegenerative disease', *Neuropharmacology*, 96, pp. 29–41. doi:10.1016/j.neuropharm.2014.10.028.
- Orset, C. *et al.* (2007) 'Mouse model of in situ thromboembolic stroke and reperfusion', *Stroke*, 38(10), pp. 2771–2778. doi:10.1161/STROKEAHA.107.487520.
- Park, L. *et al.* (2017) 'Brain Perivascular Macrophages Initiate the Neurovascular Dysfunction of Alzheimer A β Peptides', *Circulation Research*, 121(3), pp. 258–269. doi:10.1161/CIRCRESAHA.117.311054.
- Pedragosa, J. *et al.* (2018) 'CNS-border associated macrophages respond to acute ischemic stroke attracting granulocytes and promoting vascular leakage', *Acta Neuropathologica Communications*, 6(1), p. 76. doi:10.1186/s40478-018-0581-6.
- Polfliet, M.M. *et al.* (2001) 'A method for the selective depletion of perivascular and meningeal macrophages in the central nervous system', *Journal of Neuroimmunology*, 116(2), pp. 188–195.

Popa-Wagner, A. *et al.* (2020) 'Ageing as a risk factor for cerebral ischemia: Underlying mechanisms and therapy in animal models and in the clinic', *Mechanisms of Ageing and Development*, 190, p. 111312. doi:10.1016/j.mad.2020.111312.

Quenault, A. *et al.* (2017) 'Molecular magnetic resonance imaging discloses endothelial activation after transient ischaemic attack', *Brain*, 140(1), pp. 146–157. doi:10.1093/brain/aww260.

Sacco, R.L. *et al.* (1997) 'American Heart Association Prevention Conference. IV. Prevention and Rehabilitation of Stroke. Risk factors', *Stroke*, 28(7), pp. 1507–1517. doi:10.1161/01.str.28.7.1507.

Sadler, R. *et al.* (2019) 'Short-chain fatty acids improve post-stroke recovery via immunological mechanisms', *The Journal of Neuroscience: The Official Journal of the Society for Neuroscience* [Preprint]. doi:10.1523/JNEUROSCI.1359-19.2019.

Utz, S.G. and Greter, M. (2019) 'Checking macrophages at the border', *Nature Neuroscience*, 22(6), pp. 848–850. doi:10.1038/s41593-019-0411-6.

Virani, S.S. *et al.* (2020) 'Heart Disease and Stroke Statistics-2020 Update: A Report From the American Heart Association', *Circulation*, 141(9), pp. e139–e596. doi:10.1161/CIR.0000000000000757.

Winklewski, P.J. *et al.* (2015) 'Brain inflammation and hypertension: the chicken or the egg?', *Journal of Neuroinflammation*, 12, p. 85. doi:10.1186/s12974-015-0306-8.

Yu, G. *et al.* (2012) 'clusterProfiler: an R Package for Comparing Biological Themes Among Gene Clusters', *OMICS: a Journal of Integrative Biology*, 16(5), p. 284. doi:10.1089/omi.2011.0118.

DISCUSSION

Les BAMs acquièrent au cours du vieillissement un rôle central en tant que régulateurs de la réponse neuroinflammatoire

Dans cette étude, nous avons étudié le rôle des PVM dans la physiopathologie de l'AVC ischémique aiguë, et particulièrement la réaction inflammatoire, chez des souris jeunes et âgées. Nous avons émis l'hypothèse que le vieillissement, en entraînant un *priming* neuroinflammatoire, pourrait modifier le phénotype des BAMs, leur conférant un rôle plus important dans la modulation des réponses neuroinflammatoires aux AVC. Pour étudier cela, nous avons comparé des souris témoins jeunes et âgées à des souris dépourvues de BAMs, durant les phases aiguë et subaiguë de l'AVC ischémique.

Nous avons observé que les dommages causés par l'AVC (lésions, déficits neurologiques, et réponses inflammatoires) n'étaient pas significativement affectés par la déplétion des BAMs chez les jeunes souris. En revanche, chez les souris âgées, les déficits neurologiques étaient aggravés spécifiquement chez les souris déplétées en BAMs, et cette aggravation s'accompagnait d'une exacerbation des réponses inflammatoires dans les compartiments vasculaires et parenchymateux. Afin de mieux comprendre les mécanismes biologiques sous-jacents à cette différence entre souris jeunes et âgées, nous avons d'abord étudié l'état neuroinflammatoire basal du cerveau de souris âgées. Nous avons observé une augmentation de la neuroinflammation basale (microglie activée, présence de neutrophiles et de lymphocytes) dans le cerveau de souris âgées, qui ne s'accompagnait pas de changement dans le nombre de BAMs. Ensuite, nous avons isolé les BAMs de souris jeunes et âgées et effectué des analyses transcriptomiques. Nos résultats montrent que les BAMs chez les souris âgées surexpriment des gènes impliqués dans la régulation des réponses immunitaires innées et adaptatives, y compris l'adhésion cellulaire et les voies de signalisation médiées par les cytokines.

Nos résultats chez les souris jeunes montrent que les BAMs semblent intervenir dans la réponse neuroinflammatoire, mais que cela n'impacte significativement ni la taille finale de la lésion ischémique ni les déficits neurologiques aiguë après un AVC thromboembolique. En revanche, une étude réalisée dans un modèle d'AVC ischémique transitoire (avec filament) chez des souris naïves a décrit que les souris déplétées en BAMs présentaient moins d'infiltration de granulocytes et une perméabilité accrue de la BHE. De façon intéressante, ces

effets n'étaient pas associés à des changements de volume de lésion, mais contribuaient à un dysfonctionnement neurologique dans la phase aiguë d'un modèle d'AVC avec reperfusion (Pedragosa *et al.*, 2018). Les divergences entre ces études pourraient être dues au modèle expérimental d'AVC utilisé dans chaque cas, dans lesquels les profils de réponse inflammatoire induite sont différents. De plus, la microthrombose secondaire induite après le retrait du filament dans ce modèle est inexistante dans les modèles thromboemboliques (Gauberti *et al.*, 2014; Levard *et al.*, 2020). Ces études mettent en évidence la nécessité de combiner plusieurs modèles expérimentaux pour affiner notre connaissance de physiopathologie de l'AVC ischémique.

Nos résultats montrent qu'après l'AVC, et plus particulièrement chez les souris âgées, la déplétion des BAMs est associée (i) à une augmentation significative de la molécule d'adhésion endothéliale Psel ; (ii) à une augmentation significative du *rolling* et de l'adhésion des leucocytes à la paroi vasculaire ; (iii) et à une infiltration parenchymateuse accrue des neutrophiles, des macrophages ainsi que des cellules T CD4⁺ et CD8⁺. Ces réponses immunitaires exacerbées sont présentes non seulement à la phase aiguë après l'AVC, mais également à la phase subaiguë (jusqu'à 5 jours après l'AVC) suggérant ainsi que la présence des BAMs assure un contrôle à long terme de la réponse immunitaire.

Les BAMs changent de phénotype durant le vieillissement

De façon intéressante, le nombre de BAMs ne semble pas être l'élément primordial pour réguler les réponses neuroimmunes après AVC, mais c'est la reprogrammation du profil d'expression génique des BAMs qui semble être cruciale. Cette reprogrammation a été décrite dans le cadre de l'AVC par Pedragosa et collaborateurs (Pedragosa *et al.*, 2018; Rajan *et al.*, 2020), où les auteurs décrivent des changements transcriptomiques qui ont un impact rapide sur la chimiotaxie des leucocytes et l'intégrité de la BHE. Ces modifications favorisent ainsi les troubles neurologiques dans la phase aiguë de l'AVC. Un effet similaire sur la reprogrammation des BAMs semble avoir lieu au cours du vieillissement, où les BAMs semblent acquérir un rôle plus important dans l'orchestration des réponses inflammatoires déclenchées par l'AVC.

Dans le SNC, le *priming* inflammatoire décrit principalement le phénotype et la réactivité des cellules microgliales : après un stimulus initial, les cellules microgliales

présentent une réponse inflammatoire exacerbée à un deuxième stimulus (Haley *et al.*, 2019). Des études ultérieures ont depuis montré que le *priming* cérébral inflammatoire peut également être déclenché par des stimuli chroniques, notamment le stress, le diabète, l'hypertension, la consommation chronique d'alcool, mais également le vieillissement (on parle alors d'*inflammaging*) (Muriach *et al.*, 2014; Norden, Muccigrosso and Godbout, 2015; Winklewski *et al.*, 2015; Drieu *et al.*, 2020). Une étude précédente de cytométrie de masse couplée au séquençage ARN des cellules myéloïdes du SNC a montré qu'au cours du vieillissement, il y avait une augmentation du nombre de BAMs exprimant le MHC II, suggérant un rôle renforcé dans la présentation d'antigènes (Mrdjen *et al.*, 2018).

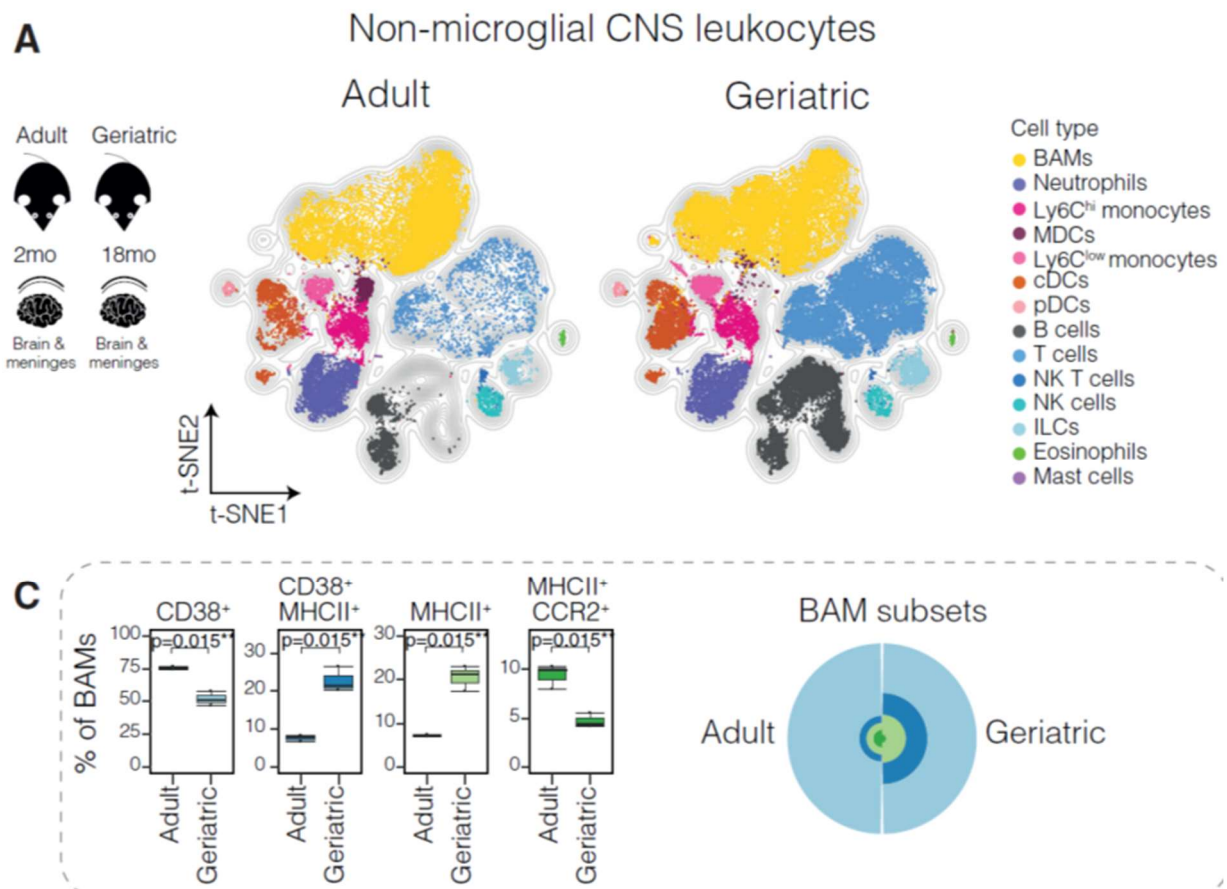


Figure 32 : Altérations des différentes populations de leucocytes du SNC (hors microglie) lors du vieillissement

Le nombre de BAMs exprimant le MHC II est augmenté chez les souris âgées, suggérant un rôle accru dans la présentation d'antigènes.

D'après "High-Dimensional Single-Cell Mapping of Central Nervous System Immune Cells Reveals Distinct Myeloid Subsets in Health, Aging, and Disease" (Mrdjen et al., 2018)

De plus, Masao Mato avait déjà observé en 1982 une augmentation de la phagocytose des graisses circulantes avec l'âge par les PVM, alors appelés « *fluorescent granular perithelial cells* », suggérant un changement d'activité de ces cellules au cours du vieillissement (Mato et al., 1982). Dans notre étude, en étudiant les modifications transcriptomiques des BAMs au cours du vieillissement, nous confirmons que les PVM acquièrent de nouveaux rôles au cours du vieillissement, et peuvent s'adapter en fonction du contexte physiologique les entourant. En effet, nous montrons que le vieillissement induit une série de changements transcriptomiques dans les BAMs, affectant les gènes impliqués dans la réponse immunitaire

innée et adaptative, la présentation d'antigènes, mais aussi la réponse cellulaire à la chaleur et la prolifération des fibroblastes.

Timing de mesure des déficits post-AVC et limite du modèle

Une des limites de cette étude est le manque de mesures au-delà d'une semaine post-AVC. En effet, la réaction inflammatoire intervient en phase aiguë dès les premières minutes après le début de l'AVC, mais s'étend également à long terme sur plusieurs semaines, intervenant également dans la réparation tissulaire et la récupération fonctionnelle. Or, nous nous sommes ici concentrés sur la neuroinflammation aiguë et subaiguë, de 24 heures à 5 jours après l'AVC. Il aurait été intéressant de s'interroger sur le rôle des BAMs sur la résolution de l'inflammation et la récupération à long terme. En effet, dans le modèle thromboembolique d'AVC utilisé dans notre étude, actuellement seuls des déficits fonctionnels mineurs peuvent être détectés et la récupération se produit seulement quelques jours suivants l'AVC. Cela rend donc difficile l'évaluation de la récupération fonctionnelle à long terme. Des études sont en cours au sein du laboratoire afin de mieux caractériser les déficits fonctionnels moteurs et sensitifs mesurables dans ce modèle.

En effet, le *timing* d'évaluation des fonctions neurologiques post-AVC est un autre facteur pouvant contribuer aux résultats contradictoires entre les études précliniques et les résultats chez les patients. Alors que dans la plupart des études cliniques le score neurologique est mesuré chez les patients jusqu'à plusieurs mois après l'AVC (généralement 90 jours), une grande majorité des études précliniques chez la souris se concentrent principalement sur les premiers jours après l'AVC (Veltkamp and Gill, 2016; Dreikorn *et al.*, 2018). Nous devrions donc utiliser des tests comportementaux qui mesurent la récupération fonctionnelle sur des temps plus longs si nous voulons obtenir une plus grande transposabilité de nos résultats à la clinique. Comme mentionné précédemment, le principal obstacle est que chez la souris il est plus difficile d'obtenir des déficits observables sur le long terme, surtout dans des modèles incluant des animaux jeunes avec des lésions corticales bien standardisées. En effet, alors que les processus de récupération chez les rongeurs sont achevés en quelques jours, ils se produisent dans les 3 mois environs chez l'Homme et peuvent même se poursuivre sur des années (Cassidy and Cramer, 2017; Sommer, 2017).

Malgré ces difficultés, des études récentes ont montré des résultats encourageants pour la translation préclinique-clinique. Par exemple, Sadler et collaborateurs ont démontré l'impact fonctionnel à long terme des acides gras à chaîne courte sur l'activation microgliale et le recrutement des lymphocytes T dans le cerveau ischémié (Sadler *et al.*, 2019). En utilisant un système automatisé pour l'entraînement et l'évaluation de la fonction des membres antérieurs (Becker *et al.*, 2016) dans un modèle murin d'AVC par photothrombose, des déficits moteurs ont été observés jusqu'à 56 jours après le début de l'AVC. Une autre étude à récemment montré que le ciblage de l'intégrine alpha-9-bêta-1 (fortement exprimée sur les neutrophiles activés) améliorait significativement les résultats fonctionnels à court et long terme (jusqu'à 4 semaines) dans deux modèles d'AVC ischémiques avec des comorbidités préexistantes (Dhanesha *et al.*, 2020).

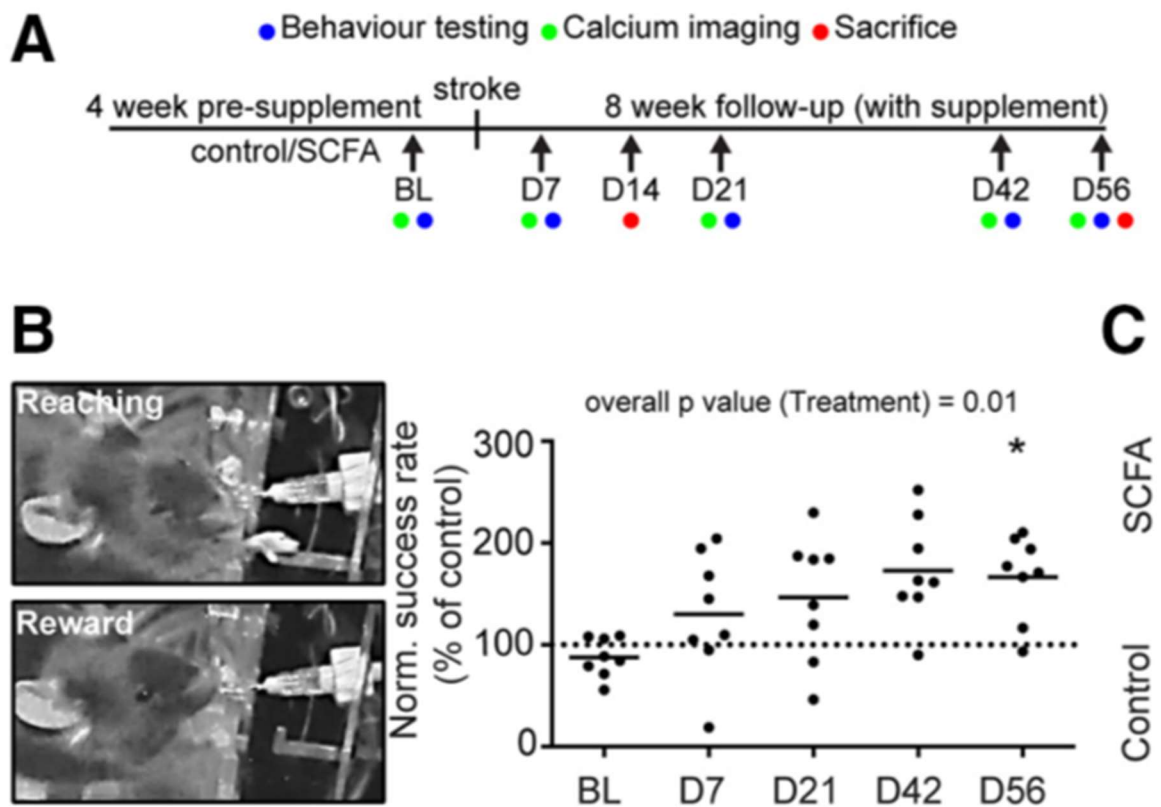


Figure 33 : Déficiences fonctionnelles mesurées à l'aide d'un test de préhension automatisé

Les souris sont entraînées à tirer un levier isométrique à l'aide du membre antérieur contralésionnel, chaque réussite étant récompensée par une goutte d'huile d'arachide. B, Images représentatives obtenues lors du test de traction du levier d'une souris entraînée atteignant avec succès le levier et obtenant la récompense de l'huile d'arachide. À droite, taux de réussite normalisé pour les tractions de levier par le membre antérieur affecté. Les valeurs relatives sont indiquées par point de temps normalisé par rapport à la moyenne du groupe témoin.

D'après "Short-Chain Fatty Acids Improve Poststroke Recovery via Immunological Mechanisms" (Sadler et al., 2020).

Liens entre réaction inflammatoire, volume de lésion ischémique et déficits neurologiques

L'hypothèse longtemps répandue était que, lors d'un AVC ischémique, l'adhésion et l'infiltration des leucocytes durant la réaction inflammatoire participent à l'établissement de la lésion ischémique et aux déficits neurologiques. Les leucocytes adhérant à la paroi des vaisseaux sanguins s'infiltrent dans le parenchyme et sécrètent des cytokines pro-inflammatoires, causant des dommages cérébraux supplémentaires. La conséquence de cette infiltration serait donc une majoration de la lésion ischémique ainsi que des déficits observables (Fu *et al.*, 2015).

On peut alors penser qu'une variation de l'adhésion et de l'infiltration leucocytaire suite à l'ischémie impacterait de la même façon le volume de lésion ischémique, et c'est pourquoi, depuis de nombreuses années, une bonne partie de la recherche clinique et préclinique sur les AVC a tenté de cibler spécifiquement l'infiltration leucocytaire (par exemple les essais cliniques avec Enlimomab, Fingolimod ou Natalizumab) pour réduire les lésions ischémiques. De manière plus large, des dizaines d'études précliniques (utilisant dans la vaste majorité le modèle filament d'AVC) sur des traitements anti-inflammatoires ont aussi montré des liens directs entre la réponse inflammatoire et les lésions ischémiques. Or, dans notre étude nous observons que la déplétion des BAMs induit des altérations de la réaction inflammatoire, tels que l'expression des molécules d'adhésion et infiltration des leucocytes, sans que cela n'impacte le volume de lésion ischémique. Ces résultats, ainsi que d'autres études sur l'infiltration leucocytaire et la réponse inflammatoire post-AVC (Llovera *et al.*, 2017; Pedragosa *et al.*, 2018) dans lesquelles les changements de la réponse immunitaire ne sont pas associés à des modifications du volume de lésion, soulèvent de nouvelles questions concernant l'impact réel de la réponse inflammatoire sur le volume de lésion ischémique final.

Plus précisément, plusieurs facteurs négligés dans le passé peuvent fortement influencer la réponse inflammatoire et les conséquences de l'AVC. On peut mentionner notamment (i) les caractéristiques du processus de recanalisation artérielle et ses réponses inflammatoires dérivées qui sont extrêmement dépendantes du modèle expérimental utilisé, (ii) les voies d'entrées alternatives des leucocytes dans le parenchyme cérébral, (iii) le *timing* des analyses menées dans les modèles précliniques et (iv) l'importance des comorbidités

affectant l'état inflammatoire basal, qui devrait être pris en compte. Afin de clarifier d'une part les liens entre l'infiltration leucocytaire et le devenir de la lésion ischémique et d'autre part les liens entre la lésion et la traduction de cette lésion tissulaire en déficits fonctionnels, il est impératif de tenir compte de ces facteurs dans les études précliniques et cliniques sur l'AVC.

Limite de la méthode de déplétion et différentes voies d'entrées dans le SNC des leucocytes périphériques

Une autre limite de l'étude est l'utilisation de liposomes contenant du clodronate afin de dépléter les BAMS. En effet, l'étude initiale s'est focalisée sur le rôle des PVM qui, de par leur localisation stratégique, pourraient moduler la transmigration leucocytaire à travers la BHE. Cependant, il est clair que les liposomes de clodronate injectés dans le ventricule latéral cérébral dans cette étude ciblent tous les BAMS (i.e. PVM, MM, ChPM) sans distinction, en raison de leur localisation commune dans le LCR. Nous ne pouvons donc pas déterminer les rôles spécifiques de chaque sous-population de BAMS sur la réaction inflammatoire induite après un AVC. Il y a d'ailleurs fort à parier que les ChPMs et les MM jouent un rôle majeur, avec l'apparition de nombreuses études récentes décrivant les méninges et les plexus choroïdes comme des voies d'entrée majeures vers le SNC pour les cellules inflammatoires (Llovera *et al.*, 2014; Benakis, Llovera and Liesz, 2018; Alves de Lima, Rustenhoven and Kipnis, 2020).

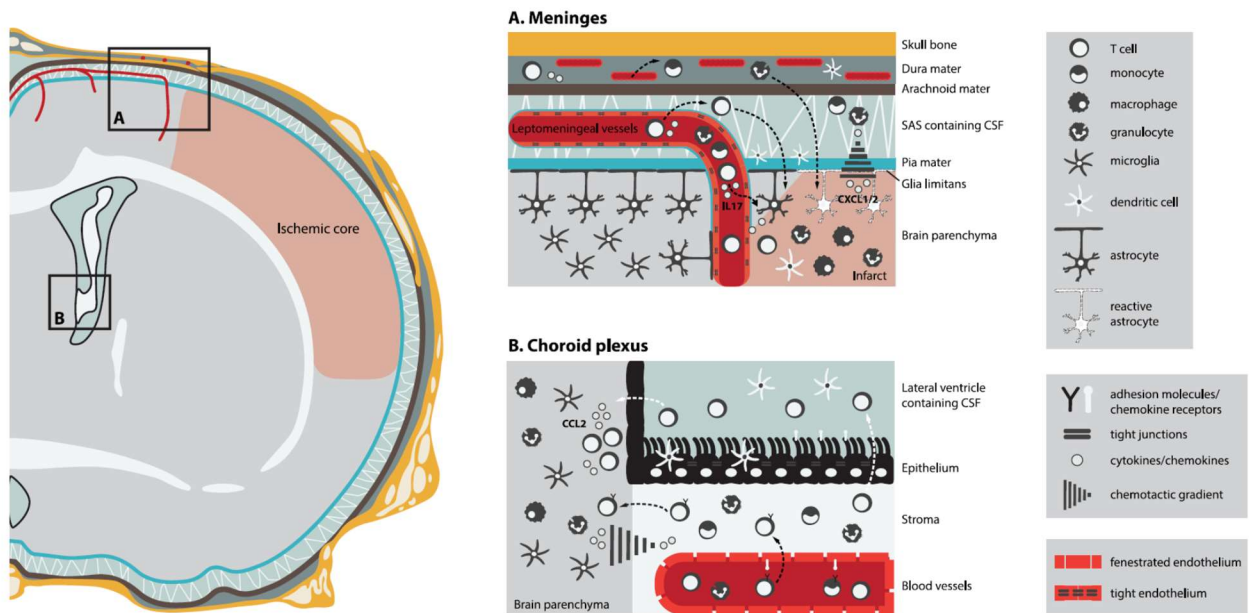


Figure 34 : Voies d'infiltration cérébrale méningée et par les plexus choroïdes pour les leucocytes dans la neuroinflammation post-AVC.

L'ischémie cérébrale induit la libération de chemokines, tels que CXCL1/2 et CCL2, par des cellules parenchymateuses, conduisant au recrutement de leucocytes via les méninges et les plexus choroïdes dans la zone ischémisée. Les flèches indiquent les voies de migration possible des leucocytes à partir (A) des méninges : vaisseaux sanguins de la dure-mère et vaisseaux leptoméningés (flèches noires) et (B) les plexus choroïdes. D'après « The meningeal and choroidal infiltration routes for leukocytes in stroke » (Benakis et al., 2018).

Interaction entre les BAMs et les fibroblastes du SNC

En dehors des phénomènes liés à la réponse immunitaire, nos résultats transcriptomiques révèlent que les BAMs surexpriment au cours du vieillissement un ensemble de gènes liés à la régulation de la prolifération des fibroblastes. Leurs rôles au sein du SNC sont peu connus, mais des études récentes commencent à mettre en lumière l'existence de fibroblastes dans les méninges, les plexus choroïdes et les espaces périvasculaires, à savoir au voisinage direct des BAMs. Bien que les origines et fonctions des fibroblastes du SNC soient encore en cours de description, des travaux récents ont révélé que les fibroblastes jouent un rôle crucial dans la formation de cicatrices fibreuses dans le SNC après une blessure tissulaire, y compris dans le cas d'un AVC (Dorrier *et al.*, 2021). Chez des souris Col1a1-GFP⁺, le nombre de fibroblastes PDGFR β ⁺ et GFP⁺, alors appelés cellules stromales, augmente dans le noyau de la lésion suite à une occlusion transitoire de l'artère cérébrale moyenne dans un modèle filament (Fernández-Klett *et al.*, 2013). Concernant la neurodégénérescence, dans les stades pré-symptomatiques de la sclérose latérale (SLA) amyotrophique, les gènes SPP1 et COLA6A1 des fibroblastes sont enrichis et leurs produits protéiques s'accumulent dans les espaces périvasculaires. Des niveaux d'expression accrus de ces gènes prédisent des temps de survie plus courts chez les patients atteints de SLA, indiquant que les fibroblastes périvasculaires contribuent au début de la progression de la maladie (Månberg *et al.*, 2021). Ainsi, de futures études pourraient s'intéresser aux liens entre les BAMs et les fibroblastes du SNC, notamment dans le cas des cicatrices tissulaires post-AVC ou dans les pathologies neurodégénératives.

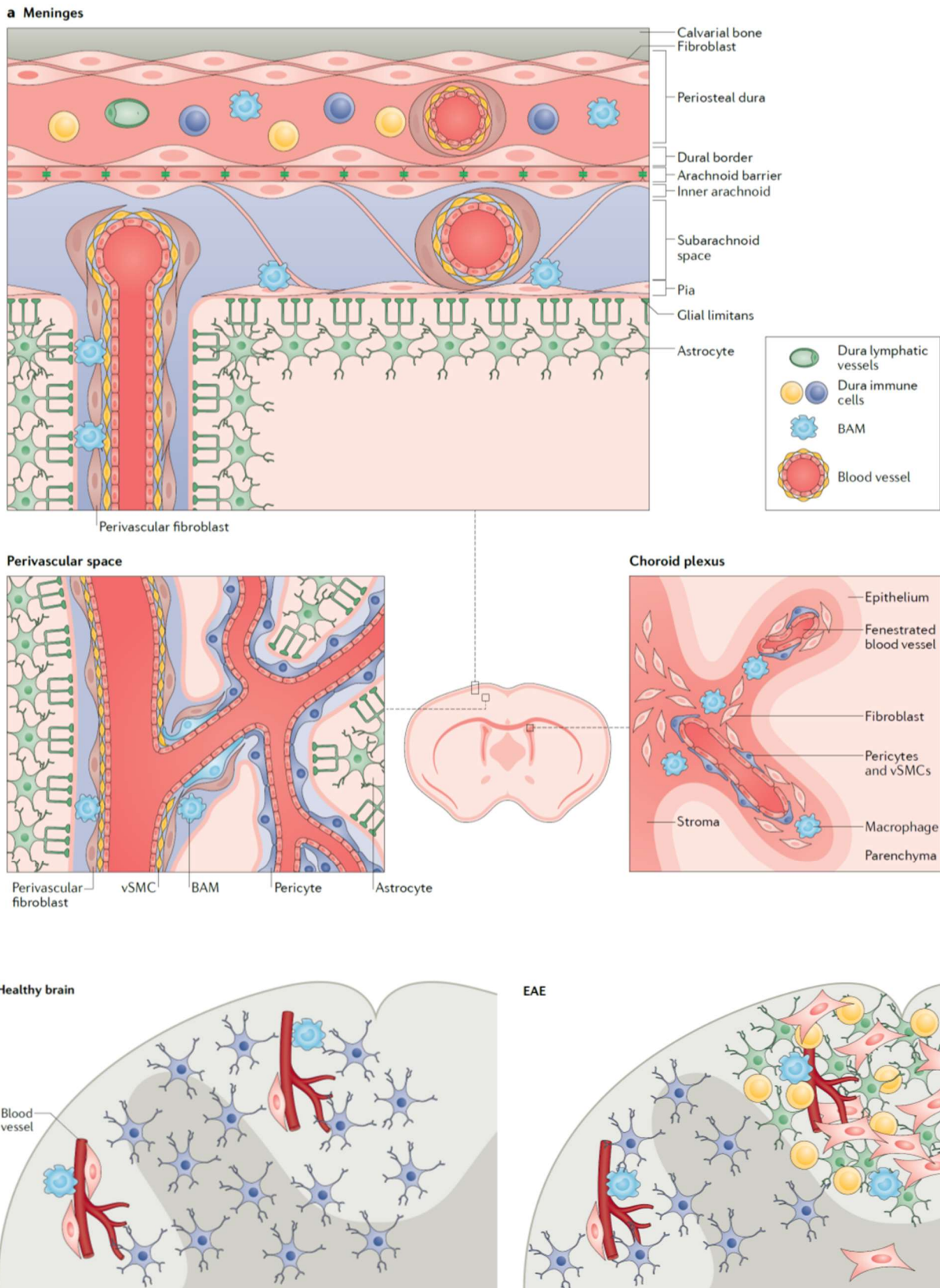


Figure 35 : Localisation des fibroblastes dans le cerveau de souris adulte et organisation des cicatrices gliales et fibrotiques.

Les fibroblastes sont présents dans les méninges, le plexus choroïde et les espaces périvasculaires, à proximité des BAM. Les lésions de l'EAE comprennent des cellules immunitaires infiltrantes, telles que des cellules T, et une cicatrice constituée de fibroblastes voisins et d'astrocytes réactifs. D'après "Emerging roles for CNS fibroblasts in health, injury and disease" (Dorrier et al., 2021)

Conclusion

Dans cette étude, nous avons cherché à étudier le rôle spécifique des PVM dans la réaction inflammatoire induite par l'AVC ischémique, chez les souris jeunes et âgées. Notre hypothèse, basée sur les études décrites précédemment et sur la localisation privilégiée des PVM à l'interface entre le compartiment vasculaire et le parenchyme cérébral, était que les PVM pouvaient jouer un rôle majeur dans la réponse inflammatoire déclenchée par l'AVC, *via* la médiation du recrutement et l'infiltration des leucocytes. De plus, sur la base d'études précédentes, nous avons fait l'hypothèse que les PVM pourraient moduler l'AVC et les réponses inflammatoires induites par l'AVC de manière différente en fonction de l'état inflammatoire basal du cerveau, en particulier au cours du vieillissement.

Pour tester cette hypothèse, nous avons étudié l'AVC chez des souris jeunes et âgées avec ou sans déplétion antérieure des BAM. Nos résultats ont montré que le déficit fonctionnel de l'AVC était aggravé chez les souris âgées déplétées en BAMs et s'accompagnait d'une inflammation accrue dans les compartiments vasculaires, périvasculaires et parenchymateux de l'hémisphère ischémié. Il est intéressant de noter que ces réponses inflammatoires exacerbées n'étaient pas accompagnées de modifications du volume de lésion. Enfin, en utilisant le séquençage ARN à partir de BAMs isolés, nous montrons que les BAMs modifient leur phénotype transcriptomique au cours du vieillissement pour surexprimer les gènes impliqués dans la régulation de la réponse immunitaire innée et adaptative et de la présentation des antigènes.

Pour conclure, l'ensemble de nos résultats montre que les BAMs acquièrent au cours du vieillissement un rôle central dans l'orchestration de la réponse neuroinflammatoire déclenchée par un AVC, et que leur présence garantit une bonne régulation de la réponse immunitaire à long terme.

AUTRES TRAVAUX











Received: 22 September 2020 | Accepted: 24 May 2021

DOI: 10.1111/jth.15414



ORIGINAL ARTICLE

Factor XII protects neurons from apoptosis by epidermal and hepatocyte growth factor receptor-dependent mechanisms

Eugénie Garnier¹ | Damien Levard¹   | Carine Ali¹ | Izaskun Buendia¹ |
Yannick Hommet¹ | Maxime Gauberti¹  | Tiziana Crepaldi^{2,3} | Paolo Comoglio² |
Marina Rubio¹ | Denis Vivien^{1,4}  | Fabian Docagne¹   |
Sara Martinez de Lizarrondo¹  

¹Normandie Univ, Unicaen, Inserm, Physiopathology and imaging of neurological disorders (PhIND), Caen, France

²Candiolo Cancer Institute FPO-IRCCS, Candiolo, Italy

³Department of Oncology, University of Torino Medical School, Candiolo, Italy

⁴CHU Caen, Department of Clinical Research, CHU Caen Côte de Nacre, Caen, France

Correspondence

Sara Martinez de Lizarrondo, Fabian Docagne and Izaskun Buendia, Inserm U1237, "Physiopathology and Imaging for Neurological Disorders (PhIND)," Centre Cyeron. BP5229. 14074 Caen Cedex, France.

Emails: smartinez@cyeron.fr (SML); docagne@cyeron.fr (FD); izaskunendia@hotmail.com (IB)

Funding information

This work was supported by the "Institut National de la Santé Et de la Recherche Médicale" (INSERM) and the "Etablissement Français du Sang" (EFS) and the Normandy Regional Council. T.C. and P.C were supported by FISM Onlus-"Fondazione Italiana Sclerosi Multipla".

Abstract

Background: Factor XII (FXII) is a serine protease that participates in the intrinsic coagulation pathway. Several studies have shown that plasma FXII exerts a deleterious role in cerebral ischemia and traumatic brain injury by promoting thrombo-inflammation. Nevertheless, the impact of FXII on neuronal cell fate remains unknown.

Objectives: We investigated the role of FXII and FXIIa in neuronal injury and apoptotic cell death.

Methods: We tested the neuroprotective roles of FXII and FXIIa in an experimental model of neuronal injury induced by stereotaxic intracerebral injection of N-methyl-D-aspartic acid (NMDA) *in vivo* and in a model of apoptotic death of murine primary neuronal cultures through serum deprivation *in vitro*.

Results: Here, we found that exogenous FXII and FXIIa reduce brain lesions induced by NMDA injection *in vivo*. Furthermore, FXII protects cultured neurons from apoptosis through a growth factor-like effect. This mechanism was triggered by direct interaction with epidermal growth factor (EGF) receptor and subsequent activation of this receptor. Interestingly, the "proteolytically" active and two-chain form of FXII, FXIIa, exerts its protective effects by an alternative signaling pathway. FXIIa activates the pro-form of hepatocyte growth factor (HGF) into HGF, which in turn activated the HGF receptor (HGFR) pathway.

Conclusion: This study describes two novel mechanisms of action of FXII and identifies neurons as target cells for the protective effects of single and two-chain forms of FXII. Therefore, inhibition of FXII in neurological disorders may have deleterious effects by preventing its beneficial effects on neuronal survival.

KEYWORDS

apoptosis, contact pathway, intrinsic pathway, neuroprotection, thromboinflammation

Garnier, Levard, Docagne, and Martinez de Lizarrondo made equal contributions to this work.

Manuscript handled by: Joost Meijers

Final decision: Joost Meijers, 24 May 2021

© 2021 International Society on Thrombosis and Haemostasis

1 | INTRODUCTION

Factor XII (FXII), is a 80 kDa chymotrypsin-like serine protease with various effects in the circulation, ranging from activation of the phase contact ("intrinsic") coagulation pathway to pro-inflammatory actions.¹ FXII is primarily produced as a zymogen single-chain enzyme, secondarily activated to its two-chain form, FXIIa, by plasma kallikrein or by auto-activation when bound to some negatively charged and anionic surfaces.²⁻⁴ Although most of the reported actions of FXII are due to the proteolytic activity of its active form FXIIa, proteolytic and non-proteolytic actions of the zymogen FXII have also been reported.⁵⁻⁷ Several receptors, including urokinase plasminogen activator surface receptor (uPAR) and epidermal growth factor (EGF) receptor (EGFR)^{5,6,8} have been suggested to mediate these non-proteolytic effects, mediating proliferative responses in endothelial cells.

Several studies have shown that circulating FXII can exert detrimental effects in cerebral ischemia⁹ and traumatic brain injury¹⁰ by promoting thrombo-inflammation. Nevertheless, the question remains open whether FXII may impact neuronal cell fate within the brain parenchyma, independently of its effects on vascular injury. This question is important considering the recent discovery that a short isoform of FXII is expressed by neurons in the brain.¹¹

Chymotrypsin-like serine proteases form a family of multi-domain proteins with mosaic structures. In addition to similarities in their trypsin-like protease domains, these proteins share non-proteolytic domains such as Kringle or EGF-like domains. These structural similarities suggest that, beyond their common protease activity, serine proteases can present similarities in their non-proteolytic actions. In particular, the domain composition of the serine protease tissue-type plasminogen activator (t-PA), is similar to that of FXII: t-PA displays two Kringle domains and one EGF-like domain, while FXII displays one Kringle domain and two EGF-like domains. In earlier studies, we have shown that t-PA, by virtue of its EGF-like domain, induces anti-apoptotic effects in oligodendrocytes and neurons by binding to EGFR.^{12,13} In light of the above, we hypothesized that FXII could promote anti-apoptotic effects in neurons by activating the EGFR signaling pathway.

Apoptosis of neurons is considered to play a significant role in several neurovascular disorders including stroke, Alzheimer's disease, Parkinson's disease, Huntington's disease, or amyotrophic lateral sclerosis.¹⁴⁻¹⁶ In these pathological conditions, apoptosis can result from oxidative stress, exposure to pro-apoptotic factors such as apoptosis stimulating fragment (Fas) or tumor necrosis factor (TNF), or starvation from trophic factors.¹² This latter condition can be mimicked *in vitro* by removing trophic support from cultured neurons in a classical paradigm termed serum deprivation (SD).¹³

Here, we report that both forms of inactive and active FXII (FXII and FXIIa) protect from neuronal injury induced by stereotaxic intracerebral injection of N-methyl-D-aspartic acid (NMDA) *in vivo*. In addition, we show that FXII rescues cultured neurons from apoptosis by non-protease actions involving direct binding to EGFR and subsequent activation of the Erk1/2 intracellular

Essentials

- Several studies have shown that plasma factor XII (FXII) exerts a deleterious role in cerebral ischemia and traumatic brain injury by promoting thrombo-inflammation.
- Nevertheless, the impact of FXII on neuronal cell fate remains unknown.
- Factor XII and FXIIa exert neuroprotective effects in the brain parenchyma *in vivo*.
- This anti-apoptotic effect of FXII is mediated by epidermal and hepatocyte growth factor receptor--dependent mechanisms.

pathway. Pharmacological inhibition of Erk1,2 phosphorylation quenches the FXII-mediated protection. Interestingly, we observe that FXIIa also protects neurons by indirect trophic effects: it cleaves the pro-form of hepatocyte growth factor (HGF) into HGF, which in turn protects neurons from apoptosis by HGFR pathway activation. Together, these data indicate that both forms of FXII promote survival of neurons by EGFR- and HGFR-dependent mechanisms.

2 | MATERIALS AND METHODS

2.1 | Materials

Corn trypsin inhibitor (CTI) and all FXII forms (single-chain FXII, FXIIa, and β -FXIIa) were purchased from Enzyme Research Laboratories (UK) and presented with a certificate of analysis. As detailed by the supplier, all proteins were purified from human plasma. FXII content was determined to be >95% as judged by sodium dodecyl sulphate polyacrylamide gel electrophoresis (SDS-PAGE) and showed no reduction upon incubation with 2-mercaptoethanol. FXIIa β -FXIIa were activated from homogeneous FXII using dextran sulfate (unknown concentration) that was removed thereafter. Complete activation was observed on SDS-PAGE.

NMDA, EGF receptor kinase inhibitor (AG1478), and NMDA receptor antagonist (MK801) were obtained from Tocris Bioscience. FXII chromogenic substrate (S-2302) was obtained from Werfen. Rabbit anti-pErk1/2 (#9102), anti-Erk1/2 (#9101) and anti-EGFR (#4267) antibodies were purchased from Cell Signaling. Anti-HGF (SBF5) antibody and recombinant HGF (PHG0254) were obtained from Invitrogen. Anti-HGF (sc1356) and anti-kininogen (sc-59581) antibodies were obtained from Santacruz. Anti-Actin (A2066) antibody was purchased from Sigma. PPACK (H-D-Pro-Phe-Arg-Chloromethylketone trifluoroacetate salt) was obtained from Bachem. The biotinylation kit, EZ-link[®] Sulfo-NHS-LC-Biotinylation kit was purchased from Thermo Scientific. Blocking anti-HGF (AF2207) and recombinant human HGF Propeptide (pro-HGF, 7057-HG-010) were obtained from R&D Systems. Erk Inhibitor

(SCH772984) was obtained from Selleckchem. JNJ-38877605 was kindly provided by Janssen Pharmaceuticals. Rabbit anti-mouse plasminogen polyclonal antibody was kindly provided by HR Lijnen (University of Leuven, Belgium). Mouse FXII total antigen assay ELISA kit came from Molecular Innovations.

2.2 | Animals

Studies were conducted in male Swiss mice (DAP #2889; age 12 weeks, weight 35–45 g; Centre Universitaire de Ressources Biologiques, Normandy University, Caen, France). Mice were housed with food and water *ad libitum* access. Animals were randomized to treatment groups, and all analyses were performed by investigators blinded to group allocation. All animal experiments were performed and reported in accordance with the Animal Research: Reporting of In Vivo Experiments (ARRIVE) guidelines (<https://arriveguidelines.org/>).

2.3 | NMDA-induced cerebral injury

Mice were deeply anesthetized with 5% isoflurane and maintained with 1.5–2% isoflurane 30% O₂/70% N₂O during the experiment. Anesthetized mice were placed in a stereotaxic device. Then the skin was removed, and a small craniotomy was performed. A glass micropipette containing 1 µl of FXII or FXIIa (1 µg; FXII and FXIIa groups, respectively) or control buffer (vehicle group) was inserted (coordinates: –1 mm anteroposterior; +3.3 mm lateral; –0.8 mm depth from the Bregma) in the cortex. The pipette was left in place for 2 min before injection. Then, the solution was pneumatically injected in the right cortex for 2 min (by applying positive pressure with a syringe connected to the pipette through a catheter). After the injection, the pipette was left in place again for 2 min to ensure adequate diffusion of the solution.

Ten minutes after the injection of vehicle or FXII, a glass micropipette was inserted at the aforementioned coordinates, and 0.5 µl of NMDA (40 nmol/µl; 20 nmol) was injected as described above. Lesion volumes were quantified by magnetic resonance imaging (MRI) on ImageJ software 24 h after injection.

2.4 | Magnetic resonance imaging

Mice were deeply anesthetized with 5% isoflurane and maintained with 1.5–2% isoflurane 30% O₂/70% N₂O during the acquisitions. Experiments were carried out on a Pharmascan 7T (Bruker). T2-weighted images were acquired using a multislice multiecho sequence: TE/TR 33 ms/2500 ms. Apoptotic lesion sizes were manually segmented on each section of T2-weighted images to calculate the total volume of brain lesions. These images were analyzed using ImageJ software by a blinded investigator. T2*-weighted sequences were used to control for brain hemorrhage.

2.5 | TUNEL immunofluorescence analyses

TdT-mediated biotin-dUTP nick end labeling (TUNEL) immunofluorescence analyses were performed in control (vehicle) and FXII treated-mice (*n* = 5/group); 6 h after NMDA cortical injections deeply anesthetized mice were transcardially perfused with cold heparinized saline (15 ml/min) followed by 150 ml of fixative (phosphate-buffered saline 0.1 M, pH 7.4 containing 2% paraformaldehyde and 0.2% picric acid). Brains were post-fixed (24 h; 4°C) and cryoprotected (sucrose 20% in veronal buffer; 24 h; 4°C) before freezing in Tissue-Tek (Miles Scientific). Cryomicrotome-cut sections (10 µm) were collected on poly-lysine slides and stored at –80°C before processing. Sections were permeabilized and stained with In Situ Cell Death Detection Kit, Fluorescein (Sigma Aldrich), as stated by the manufacturer instructions. For detection, washed sections were coverslipped with antifade medium containing DAPI and images were digitally captured using a Leica DM6000 microscope-coupled coolsnap camera and visualized with Metavue 5.0 software (Molecular Devices) and further processed using ImageJ 1.45r software (NIH). TUNEL+cells were calculated in both ipsilateral and contralateral cortical areas for both groups.

2.6 | Primary murine neuronal cortical cultures

Murine neuronal cultures were prepared as previously described in Liot et al.¹³ Neuronal cortical cultures were obtained from fetal mice at E15–E16. Cortices were dissociated and plated on 24-well plates coated with poly-D-lysine (0.1 mg/ml) and laminin (0.02 mg/ml). Cells were cultured in Dulbecco's modified Eagle medium (DMEM) supplemented with 2 mM glutamine, 5% horse serum, and 5% fetal bovine serum. Cultures were maintained at 37°C in a humidified 5% CO₂ atmosphere. Cytosine β-D-arabinoside (10 µM) was added after 3 days *in vitro* (DIV) to inhibit non-neuronal proliferation. All experiments were performed at DIV7.

2.7 | Serum deprivation-induced apoptosis

SD was induced by the exposure of neuronal cultures (DIV7) to a serum-free DMEM as previously described.¹³ This condition enables us to eliminate all exogenous FXII coming from the serum. Controls were maintained in serum-containing medium and allow calibrating as the 0% of death. MK801 (1 µM) was added to prevent secondary NMDA receptor activation. Cells under SD were treated with FXII, FXIIa, or FXIIa-PPACK. Inhibitors were added simultaneously to treatments (unless otherwise stated in the text). Before fixation on 4% paraformaldehyde, cells were stained with 0.4% trypan blue for 15 min after 24 h of SD. Neuronal cell injury was quantified by counting trypan blue positive cells in four random fields per well. The percentage of neuronal death was determined as the number of trypan blue-positive neurons after SD compared with the total neuron number. The mean values of trypan blue-positive neurons

in sham washed control conditions were subtracted from experimental values to yield the specific effect of the tested conditions.

2.8 | Western blot

After solubilization in a lysis buffer (50 mM Tris-HCl, 150 mM NaCl, 0.5% Triton X-100) containing protease and phosphatase inhibitor cocktails (1/100), cell lysates were centrifuged for 20 min at 12,000 g and supernatants were harvested. Protein concentrations were calculated using the BCA Protein Assay Reagent (Pierce). Protein samples (20 µg) or media supernatants (20 µl) were separated using a SDS-PAGE and transferred into a polyvinylidene difluoride membrane. Membranes were blocked for 2 h in Tween 20-Tris Base Solution with 1% BSA and incubated overnight at 4°C with the specific primary antibody at the following concentrations: for anti-αEGFR, anti-pErk, anti-Erk total, anti-kininogen, anti-HGF (AF2207) and anti-Actin at 1/1000; anti-αHGF (s1256) at 1/500, anti-plasminogen 1/1500. After washes and 1 h of incubation with the corresponding peroxidase secondary antibody, proteins were revealed with a chemiluminescence ECL select immunoblotting detection system (GE Healthcare).

2.9 | EGFR crossed immunoprecipitation assay

Biotinylated FXII and FXIIa (Biot-FXII and Biot-FXIIa, respectively) were produced following manufacturer's kit (EZ-link® Sulfo-NHS-LC-Biotinylation). After treatment during 24 h with 125 nM of Biot-FXII and Biot-FXIIa, lysed cultured cortical neurons (DIV 7; 100 µg of total protein) were incubated overnight at 4°C with an antibody anti-EGFR (6 µg, Cell Signaling, #4267) and then coupled to protein G-Sepharose. Then, immunoprecipitated proteins were separated by 7.5% SDS-PAGE, and immunoblots were revealed with ExtrAvidin peroxidase (1/2000).¹²

2.10 | FXIIa-PPACK generation

To inhibit FXIIa proteolytic activity, 250 nM of FXIIa was incubated with PPACK (H-D-phe-pro-arg-chloromethylketone; 1000 nM) for 30 min at room temperature in HEPES-buffer (25 mM HEPES, pH = 7.4, 150 mM NaCl, 1 mg/ml BSA). After incubation, free PPACK was extensively dialyzed. We then used FXII chromogenic substrate s-2302 to confirm the complete blockade of FXIIa-PPACK proteolytic activity.

2.11 | FXII autoactivation by neurons during SD

To measure the possible activation of FXII into FXIIa *in vitro*, neurons under SD were treated with 125 nM of FXII over time (1 h, 4 h, 6 h, and 24 h). Then, the supernatants were harvested. The possible

activation of FXII into FXIIa was determined in supernatants by two techniques. FXII immunoblotting under non-reduced conditions (using FXII and FXIIa as controls), and by measuring FXIIa-mediated hydrolysis of chromogenic substrate S-2302 at 800 µM. Changes in OD 405 nm were continuously monitored on a microplate reader for 2 h. FXIIa at 125 nM was used as control.

2.12 | Artificial activation of FXII by the glass micropipette

To measure the possible FXII auto-activation into FXIIa *in vivo* through contact with the glass micropipette 1 µg of FXII was processed through the glass micropipette following the same protocol performed in the *in vivo* injection. Then the sample was retrieved and migrated in non-reduced conditions and Coomassie staining was performed. FXII and FXIIa were used as negative and positive controls, respectively.

2.13 | Cleavage of pro-HGF in HGF in recombinant purified conditions

To study activation of pro-HGF into HGF, the recombinant form of pro-HGF (52 nM) was incubated with either 5.2 nM of FXII, FXIIa, β-FXIIa, and FXIIa-PPACK for 4 h at 37°C. At the end of the incubation, HGF western blot, which discriminates both forms of HGF, was performed.

2.14 | Statistical analysis

All results are expressed as mean ± standard deviation unless otherwise stated. For *in vitro* experiments, the *n* value corresponds to *n* different well pools derived from independent dissections. For group comparison, Kruskal-Wallis tests were used followed by Mann-Whitney *U*-tests as post-hoc tests. For *in vivo* experiments, Dunn's multiple comparison tests were performed.

3 | RESULTS

3.1 | FXII and FXIIa reduce brain lesion induced by stereotaxic injection of NMDA

Our first objective was to explore the potential role of FXII in the brain parenchyma, independently of its effects on vascular injury, known to be detrimental. With this aim, a classical model of brain injury induced by the stereotaxic injection of NMDA (1 µl at 40 mM) in the cortex (Figure 1A) was performed. We observed that the administration of FXII and FXIIa 10 min before the injection (1 µg in 1 µl) significantly reduced the mean lesion volume (by 45% and 37% compared to control group) 24 h after, measured by MRI (Figure 1B

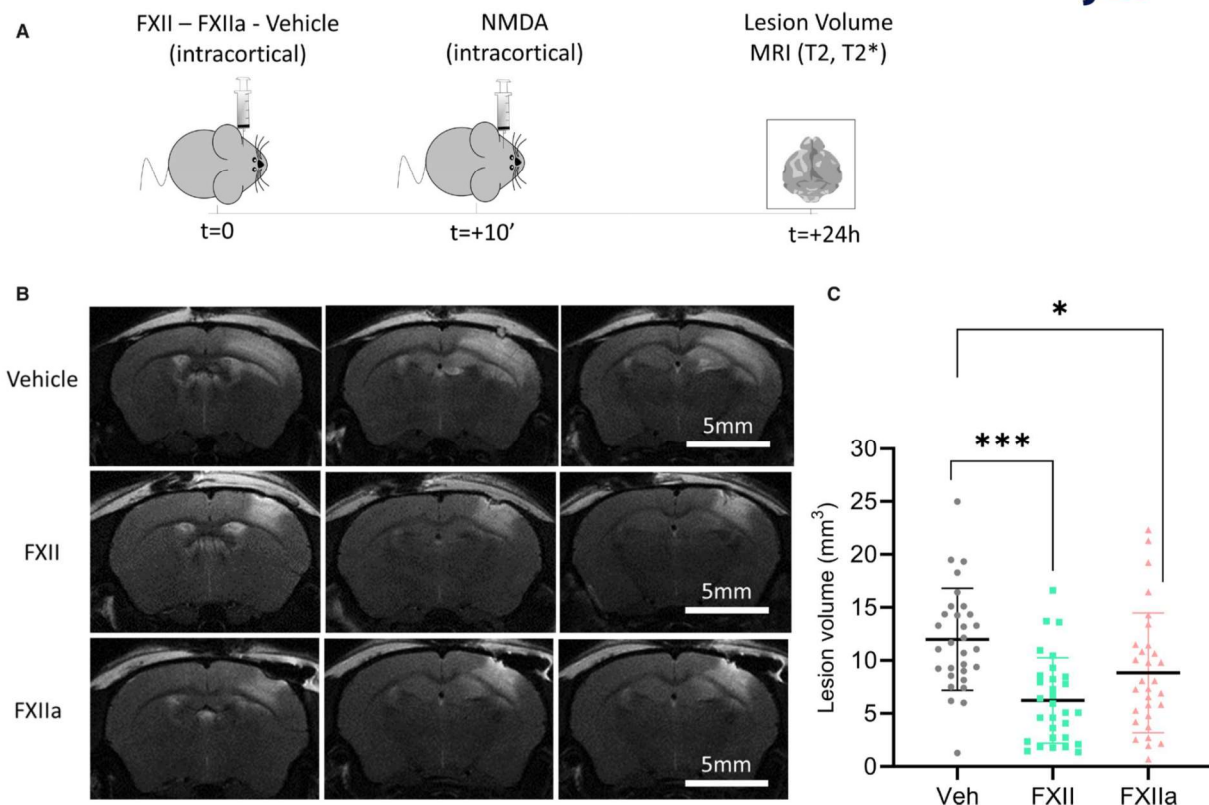


FIGURE 1 Factor XII and Factor XIIa (FXII and FXIIa, respectively) reduce brain lesions induced by stereotaxic injection of N-Methyl-D-Aspartate (NMDA). A, Experimental design. B, Representative T2-weighted (top) and T2*-weighted magnetic resonance imaging (MRI) images, showing, respectively, the NMDA-induced lesion in vehicle and FXII/FXIIa treated mice 24 h after NMDA intracortical injection. T2 (top) and T2* (bottom). C, Lesion volume quantification. $n = 30$ mice per group. Data are presented as mean \pm standard deviation and individual values. Dunn's multiple comparisons test, *** $P < .001$, * $P < .05$

and corresponding quantification, Figure 1C). These data indicate that both forms of FXII exert neuroprotective effects in the brain parenchyma.

It is well described in the literature that NMDA injection promotes apoptotic lesions that can be measured by TUNEL immunofluorescence analyses.¹⁷ Therefore, we performed TUNEL immunofluorescence analyses in a new set-up of experiments in control and FXII-treated mice, confirming the anti-apoptotic effect by histological feature at an early time point (6 h). As observed in Figure S1 in supporting information, FXII significantly reduces apoptotic neuronal cell death in the ipsilateral cortex as compared to vehicle-treated mice (* $P < .05$). Contralateral cortical brains were used as controls, showing a lack of significant apoptosis in both groups due to NMDA injection (Figure S1).

3.2 | FXII protects neurons from apoptosis by activating EGFR and subsequent signaling pathway

Our next step was to investigate whether both forms of FXII also display neuroprotective effects *in vitro*. We first tested the effect of zymogen FXII in cortical neurons subjected to SD, a classical and

standardized model of apoptosis.¹³ Interestingly, we observed that FXII exerted a dose-dependent anti-apoptotic effect (0–250 nM) compared to control (SD; Figure 2). Our hypothesis to explain this effect was that FXII could act, at least in part, due to the binding to EGFR and its activation, such as previously reported for t-PA,^{12,13} a serine protease that presents homologous EGF-like domains. To address this question, we treated cortical neurons with biotinylated FXII, extracted the proteins and subjected them to immunoprecipitation (IP) using an anti-EGFR antibody (Figure 3A). We detected biotinylated FXII among the EGFR-immunoprecipitated proteins as a ~80 kDa band revealed by peroxidase-coupled avidin (Figure 3A), at the same molecular weight as biotinylated FXII ran in parallel. FXII was absent in untreated cells (SD). These data show that FXII and EGFR are part of a same protein complex in FXII-treated neurons.

Then, we asked whether the interaction of FXII with EGFR, and its subsequent activation, could be responsible for the anti-apoptotic effect of FXII on neurons. In line with this hypothesis, the inhibitor of the EGFR kinase, AG1478 (5 μ M), reversed the effect of FXII on neurons during SD, while it showed no effect when applied alone (Figure 3B). EGFR activation can trigger several signaling cascades, including mitogen-activated protein kinase/extracellular regulated kinase (MAPK/Erk). Moreover, Tyr1068 in EGFR, the residue

phosphorylated upon FXII treatment, is involved in the transduction of EGF signal through Erk pathway.¹⁸ We first confirmed that Erk-phosphorylated levels were not significantly modified after SD compared to controls (Figure S2 in supporting information). Then,

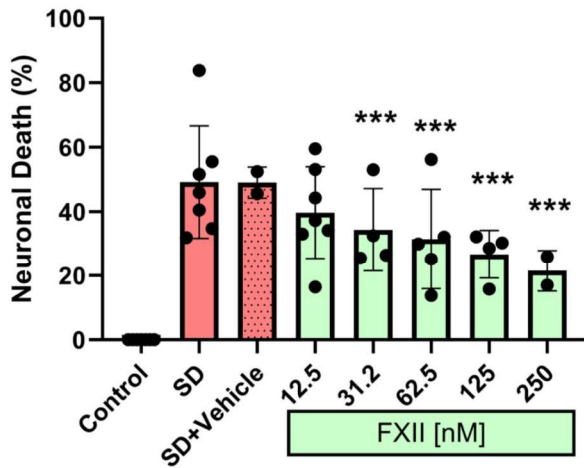


FIGURE 2 Factor XII (FXII) rescues neurons from serum deprivation--induced apoptosis. Quantification of neuronal death following 24 h of serum deprivation (SD) alone or in the presence of recombinant FXII (12.5–250 nM). Error bars represent the mean \pm standard deviation. Symbols indicate significantly different from serum deprivation by Mann Whitney (***) $P < .001$, $n = 16$ –28 from 4–7 different experiments). CTRL, control

we studied Erk phosphorylation levels after FXII administration in SD conditions at different time-points. In this case, we observed that FXII (125 nM) induced the rapid (within 5 min) and transient (<1 h) phosphorylation of Erk1/2 (Figure 4A). Accordingly, the pre-treatment with MEK/Erk $\frac{1}{2}$ inhibitor (SCH7772984, 5 μ M) reversed the anti-apoptotic effect of FXII (Figure 4B). Together, these data show that the activation of EGFR by FXII triggers Erk activation, and that this pathway actively participates in the anti-apoptotic effects of FXII in neurons.

3.3 | FXIIa also protects neurons from apoptosis by binding EGFR but not activating downstream signaling

We know that once FXII is activated from its single-chain form (FXII) it changes into a proteolytically active two-chain form (FXIIa). Because FXIIa also significantly reduced brain lesion *in vivo* induced by injection of intracortical-NMDA (Figure 1C), our next step was to investigate if FXIIa showed the same anti-apoptotic effects as FXII *in vitro*. When applied to cortical neurons during SD, FXIIa exerted an anti-apoptotic effect in a dose-dependent manner, although at slightly higher doses than FXII (Figure 5A). It is noteworthy that in contrast to what we observed for FXII, the anti-apoptotic effect of FXIIa was not reversed by the inhibitor of EGFR activation, AG1478 (5 nM, Figure 5B). Moreover, we observed that proteolytically inactive FXIIa (FXIIa-PPACK) retained residual anti-apoptotic capacity that was blocked by AG1478 (Figure S3A,B in supporting information).

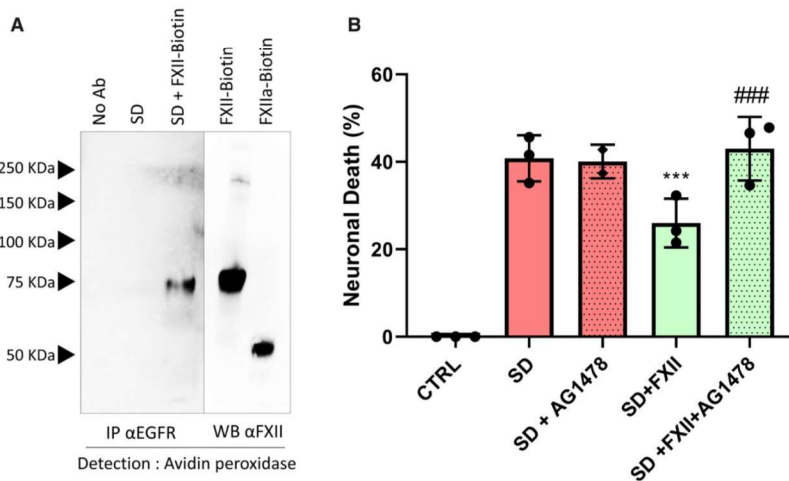


FIGURE 3 Factor XII (FXII) interacts with and activates epithelial growth factor receptor (EGFR) to mediate its antiapoptotic effects in neurons. A, 100 μ g of total proteins from lysates of untreated (serum deprivation [SD]) or biotinylated FXII (Biotin-FXII)-treated mouse neurons (125 nM) or purified Biotin-FXII were subjected to immunoprecipitation (IP) using α -EGFR antibody followed by detection with either peroxidase-coupled avidin or with α -EGFR. As a control, the same procedure was performed by omitting the α -EGFR (No Ab). Factor XII and Factor XIIa are indicated as FXII or FXIIa, respectively. Representative images of immunoblots from three individual experiments are presented. Numbers indicate molecular mass of standard proteins in kilodaltons (KDa). B, Quantification of neuronal death following 24 h of either SD alone or SD in the presence of 125 nM FXII with or without 5 μ M of the EGFR kinase inhibitor, AG1478 (mean \pm standard deviation; $n = 12$ in 3 different experiments). *** and ### $P < .001$ significantly different from SD and FXII, respectively. CTRL, control

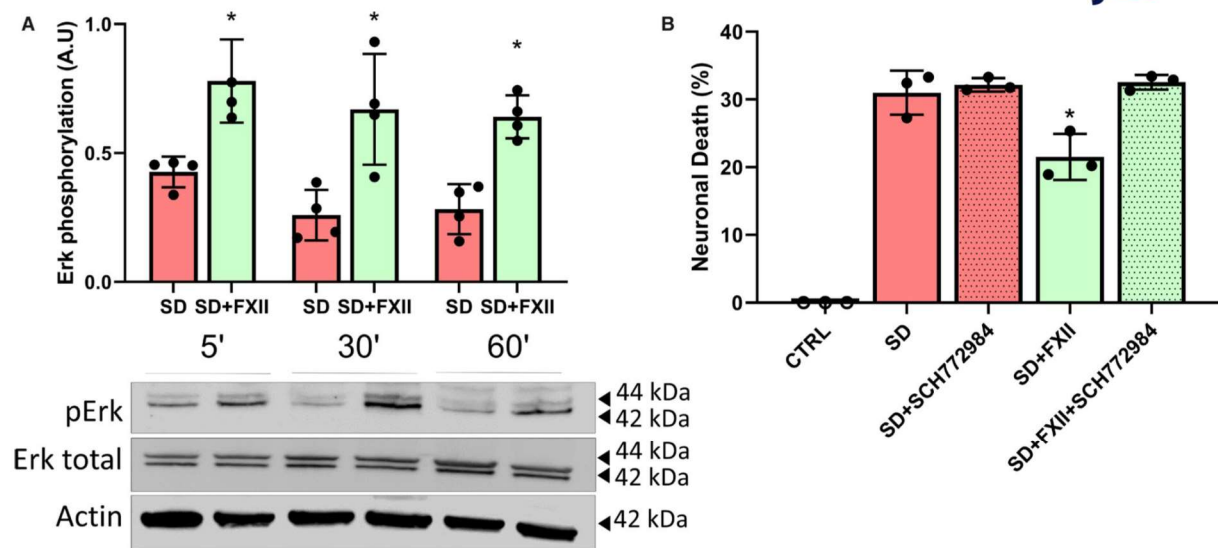


FIGURE 4 Antiapoptotic effect of factor XII (FXII) implicates activation of Erk1/2 intracellular pathway. **A**, Immunodetection of total and phosphorylated Erk1/2 forms (denoted with a prefix, pErk and Erk total, respectively) in 20 μ g of total proteins from lysates of neurons subjected to serum deprivation (SD) in the presence of 125 nM FXII after 5', 30', and 1 h of incubation. Actin was used as a loading control. Total forms of Erk1/2 were used as a control. Representative images of four independent experiments are presented. * $P < .05$ significantly different from corresponding SD. **B**, Quantification of neuronal death following 24 h of either SD alone or SD in the presence of 125 nM FXII with or without 5 μ M Erk1/2 inhibitor, SCH72984 (mean \pm standard deviation; $n = 12$ in 3 different experiments). * $P < .05$ significantly different from SD

To test whether FXIIa can bind to EGFR, we repeated the immunoprecipitation studies with biotinylated FXIIa. As observed in Figure 5C, biotinylated FXIIa is present among the EGFR-immunoprecipitated proteins as a ~50 kDa band revealed by peroxidase-coupled avidin (Figure 5C), at the same molecular weight as biotinylated FXIIa ran in parallel. Similarly, the above immunoprecipitated material showed a band at approximately 175 kDa corresponding to EGFR, when revealed with anti-EGFR antibodies (Figure 5C). These data show that FXIIa and EGFR are part of the same protein complex in FXIIa-treated neurons and confirm that FXIIa binds to EGFR, as previously shown for FXII. Interestingly, the blockade of EGFR by AG1478 is not sufficient to block FXIIa. Because FXIIa differs from FXII by its proteolytic activity, we wondered whether this activity could be involved in its anti-apoptotic function. To address this question, we co-treated neurons subjected to SD with FXIIa and CTI (at 10 μ M) an inhibitor of its proteolytic activity. Interestingly, CTI reversed the anti-apoptotic effect of FXIIa (Figure 5D). Together, these results suggest that FXIIa exerts anti-apoptotic effect on neurons mainly by a proteolytic effect.

3.4 | FXIIa protects neurons from apoptosis by promoting pro-HGF cleavage, leading to HGFR-mediated anti-apoptotic effect

The proteolytic activity of FXIIa is known, among other actions, to induce the cleavage and activation of HGF from its pro-form

to its active form,¹⁹ which in turn can activate its receptor, HGFR (also known as c-Met). We thus hypothesized that the effect of FXIIa could be mediated by the proteolytic activation of HGF and a subsequent stimulation of HGFR. When we co-treated neurons subjected to SD with FXIIa and an anti-HGF blocking antibody (2.5 μ g/ml) that prevents HGF and pro-HGF binding to the cells' surface,^{20,21} the anti-apoptotic effect of FXIIa was completely reversed (Figure 6A). An isotype of anti-HGF was used as control antibody showing no effect when added with FXIIa (Figure 6A). Interestingly, as shown in Figure 6B, the blocking anti-HGF antibody completely reverted the anti-apoptotic effect of FXIIa. Moreover, it increased the quantity of free pro-HGF and HGF in the medium of SD neurons, supporting that it prevented their binding to the cellular surface (Figure 6B). JNJ, an inhibitor of HGFR phosphorylation (Figure 6C) also prevented FXIIa protective effect but had no effect on free pro-HGF and HGF in the medium (Figure S4A in supporting information). These results were confirmed when adding FXIIa with another anti-HGF antibody (SC1356)²² (Figure S4B) whereas the anti-apoptotic effect of FXIIa-PPACK was not reversed when blocking HGF with SC1356 (Figure S3D), showing that the serine protease domain activity is required for HGF signaling pathway. We also confirmed that only FXII forms that present active serine protease (FXIIa and β -FXIIa) can efficiently convert pro-HGF into HGF, compared to FXII and FXIIa-PPACK (Figure S5 in supporting information).

These data show that FXIIa triggers the activation of pro-HGF into HGF, which in turn binds and activates HGFR pathway to provide anti-apoptotic effects in neurons.

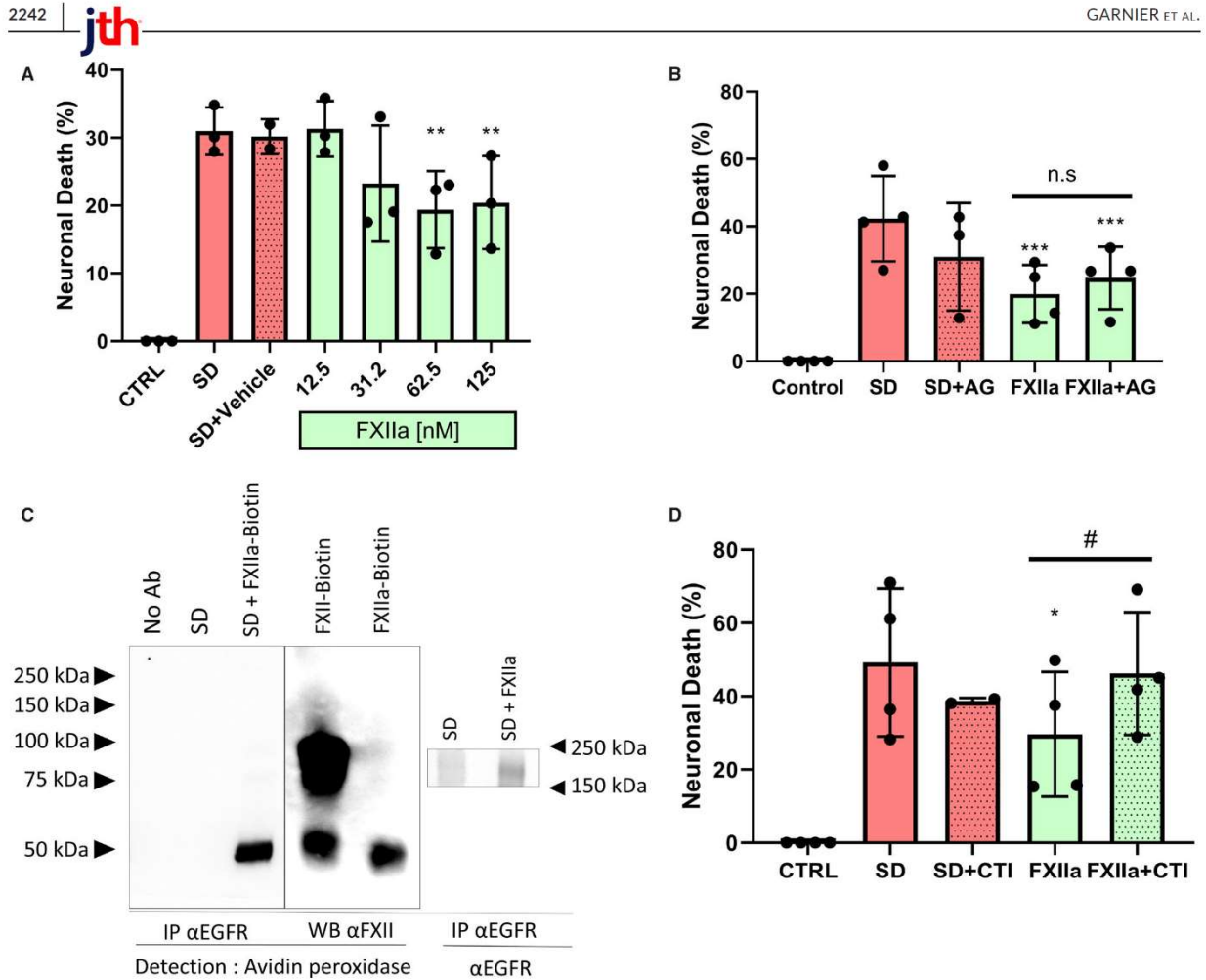


FIGURE 5 Factor XIIa (FXIIa) rescues neurons from serum deprivation-induced apoptosis. The mechanism is dependent on epidermal growth factor receptor (EGFR) binding but not EGFR signaling pathway activation. **A**, Quantification of neuronal death following 24 h of either serum deprivation (SD) alone or SD in the presence of recombinant FXIIa (12.5–125 nM). Error bars represent the mean \pm standard deviation. Symbols indicate significantly different from SD by Mann Whitney (** $P < .01$, $n = 12$ in 3 different experiments). **B**, Quantification of neuronal death following 24 h of either SD alone or SD in the presence of 125 nM FXIIa with or without 5 μ M EGFR kinase inhibitor, AG1478 (mean \pm standard deviation; $n = 16$ in 4 different experiments). *** $P < .001$ and no significantly different from SD and FXIIa, respectively. **C**, 100 μ g of total proteins from lysates of untreated (SD) or biotinylated FXIIa (Biot-FXIIa)-treated mouse neurons (125 nM) or purified Biot-FXIIa were subjected to immunoprecipitation (IP) using α -EGFR antibody followed by detection with either peroxidase-coupled avidin or with α -EGFR. As a control, the same procedure was performed by omitting the α -EGFR (No Ab). Representative images of immunoblots from three individual experiments are presented. Numbers indicate molecular mass of standard proteins in kilodaltons. **D**, Quantification of neuronal death following 24 h of either SD alone or SD in the presence of 125 nM FXIIa with or without 10 μ M FXIIa inhibitor, corn trypsin inhibitor (CTI; mean \pm standard deviation; $n = 16$ in 4 different experiments). * $P < .05$ and # $P < .05$ significantly different from SD and FXIIa, respectively. CTRL, control

Last, we know that FXII-driven contact systems start coagulation and inflammatory mechanisms via the intrinsic pathway of coagulation and the bradykinin-producing kallikrein-kinin system. Thus, we analyzed by western blot the levels of plasminogen and high molecular weight kininogen (HK), both precursors of the fibrinolytic and contact pathways that are activated by FXIIa in the supernatant of neurons in control, SD and SD+FXIIa conditions compared to controls. As shown in Figure S6 in supporting information, plasminogen and HK are not readily detectable in the SD conditions. In addition, there is no apparent activation of plasminogen into plasmin nor HK

cleavage in FXIIa conditions. Our results show that neither fibrinolytic nor contact pathway systems have an impact on FXIIa protective effects (Figure S6).

Factor XII activation into FXIIa can occur either by the action of proteases,¹ or by surface-mediated auto-activation in certain conditions, such as anionic surfaces.¹⁻⁴ Thus, we wanted to study whether FXII could be auto-activated during the injection with the contact of the glass-micropipette in our *in vivo* experiments, as well as at the surface of neurons during our SD experiments in our *in vitro* set of data. For the *in vivo* experiments, we performed a control

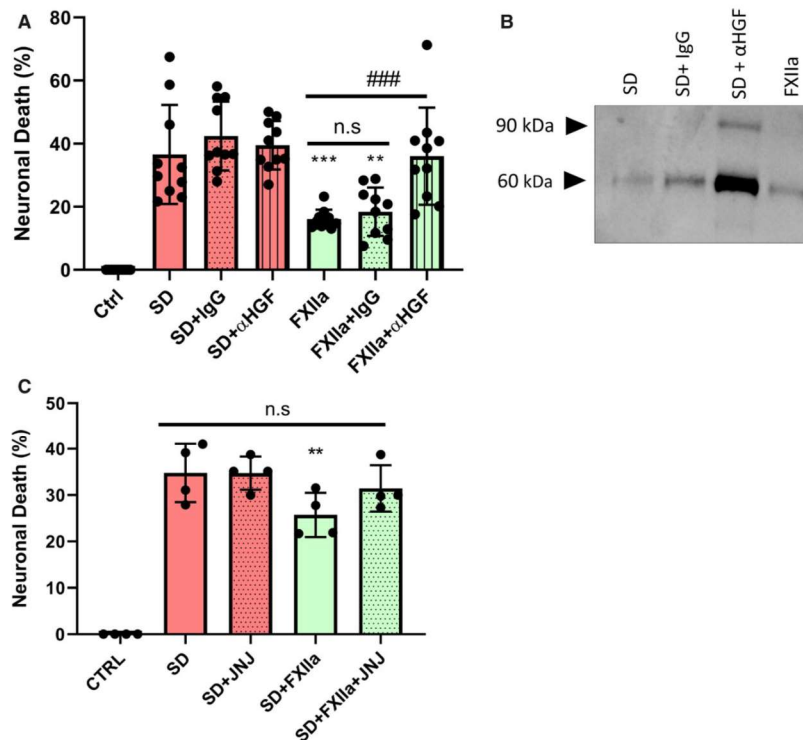


FIGURE 6 The antiapoptotic effect of FXIIa is also dependent on hepatocyte growth factor (HGF) conversion and hepatocyte growth factor receptor (HGFR) activation. A, Quantification of neuronal death following 24 h of either serum deprivation (SD) alone or SD in the presence of 125 nM FXIIa with or without an IgG and/or blocking antibody of HGF (mean + standard deviation; $n = 10$ in 4 different experiments). $***P < .001$, $**P < .01$ and $###P < .001$ significantly different from SD and FXIIa, respectively. B, Representative western blot image of the HGF conversion blocking in the supernatants by the treatment of cells with 125 nM FXIIa with or without an IgG and/or blocking antibody of HGF (4 different experiments). C, Quantification of neuronal death following 24 h of either SD alone or SD in the presence of 125 nM FXIIa with or without 500 nM JNJ, an inhibitor of HGFR phosphorylation (mean \pm standard deviation; $n = 16$ in 4 different experiments). $**P < .01$ significantly different from SD

experiment to confirm that there was no auto-activation of zymogen FXII into FXIIa during the injection through the glass micro-pipette (Figure S7 in supporting information). Then, we tested if FXII (at 125 nM) would be activated at the surface of neurons during the 24 h of SD at different time points (1 h, 4 h, 6 h, and 24 h) *in vitro*. As observed in Figure 7A, FXII is only marginally converted into FXIIa at the surface of neurons at 24 h by FXII immunoblot (Figure 7A). No FXIIa is present at 1 h, 4 h, and 6 h incubation nor in the SD control condition (0 h). When looking at the proteolytic activity assay, FXII from supernatants also presented residual (below 4 A.U.) proteolytic activity when monitoring s-2302 cleavage compared to FXIIa used at the same dose (>70 AU; Figure 7B). These results confirm that there is no significant auto-activation of FXII into FXIIa at the surface of neurons in SD conditions in 24 h.

4 | DISCUSSION

This study reveals the neuroprotective roles of FXII and FXIIa *in vivo* and describes the anti-apoptotic effects of both forms of FXII against SD-induced apoptosis in neurons. We report that their effect is due

to either “growth factor-like” activity via EGFR binding (for FXII) or proteolytic activity via the activation of the HGF/HGFR pathway (for FXIIa). We propose a model in which FXII induces its effects via the direct binding to EGFR, the subsequent activation of this receptor, the triggering of Erk pathways that would lead to modulation of gene balance toward anti-apoptotic effects in neurons. In parallel, FXII, once activated into FXIIa, will activate pro-HGF into HGF secreted from neurons under serum deprivation. HGF can thus bind and activate its receptor HGFR to induce anti-apoptotic effects (Figure 8).

As far as we know, this is the first description that FXII, in addition to its largely described effects in thrombosis and inflammation, can induce anti-apoptotic effects on neurons. It adds to previous reports on anti-apoptotic effects of the structurally related serine protease t-PA on neurons¹³ and oligodendrocytes.¹² While non-proteolytic, growth factor-like effects were reported before for t-PA in neurons,²³ the present work is the first one to show such effects for both forms of FXII in neurons. The presence of EGF-like domains in both proteins (one in t-PA, two in FXII) could explain why both proteins can induce these similar trophic effects by directly binding to and activating EGFR. Apoptosis is regulated by a balance between pro- and anti-apoptotic factors

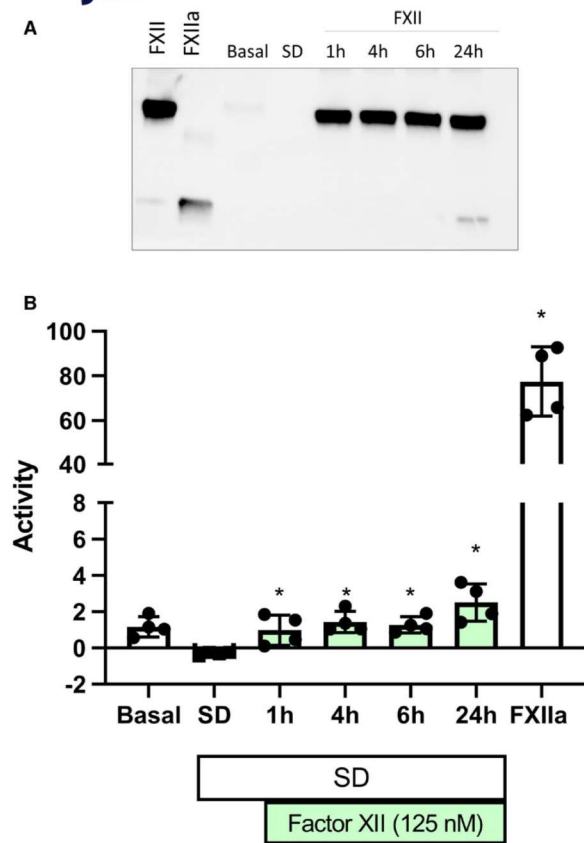


FIGURE 7 Factor XII is not activated into FXIIa by neurons during serum deprivation (SD). A, Representative FXII immunoblot of supernatants of neurons subjected to SD in the presence of 125 nM FXII at different time points (1 h, 4 h, 6 h, and 24 h). FXII and FXIIa were used as controls. Four independent experiments are presented. B, FXII proteolytic activity measured in those same samples after incubation with 800 μ M chromogenic substrate S-2302. Changes in OD 405 nm were continuously monitored on a microplate reader for 2 h. FXIIa at 125 nM was used as control. $P < .05$ compared to SD condition. 4 independent experiments are presented

that control downstream protease activity of effector caspases and subsequent cell death.

We report here that FXII activates the MAPK/Erk pathway in neurons by a growth factor-like effect, which corroborates previous studies in endothelial cells⁶ and aortic smooth muscle cells.²⁴ In line with this, t-PA, via EGFR activation, activates Bcl-2 and inhibits Bax.¹² Together, these studies seem to indicate that growth factor-like activity of serine proteases such as FXII and t-PA trigger in neurons the same anti-apoptotic pathways as genuine growth factors. Nevertheless, the signaling pathways underlining the neuroprotective effect of FXII and FXIIa, such as the regulation of pro- and anti-apoptotic genes, remain to be studied.

We have confirmed that FXII and FXIIa forms bind EGFR by co-immunoprecipitation studies. Our data suggest that FXIIa binds EGFR, but in contrast to FXII, its neuroprotective effects are not

dependent on the EGFR signaling pathway. Maybe the change of the 3D structure of FXIIa is sufficient to block its ability to activate EGFR without blocking its ability to bind it. Nevertheless, this hypothesis remains to be confirmed. The determination of the affinity or kinetics of this interaction remains to be assessed in further studies, for instance by surface plasmon resonance, to help understanding the nature of the binding at the molecular level. In addition, because it has been shown that FXII activates EGFR signaling through uPAR,⁶ it remains to be tested in further studies if our results are dependent on uPAR activation or directly operated by EGFR binding.

In addition to this direct growth factor-like effect due to binding to EGFR, we report that FXII, in its proteolytic form FXIIa, displays anti-apoptotic effects by promoting the activation of pro-HGF into HGF, which in turn activates its receptor, HGFR. HGF is linked to the blood coagulation and fibrinolytic system not only structurally but also functionally. In fact HGF is structurally similar to plasminogen, it contains four Kringle domains and a serine protease homology domain that lacks proteolytic activity.²⁵ It stimulates migration and survival of endothelial cells to repair blood vessels.²⁶ Here, we provide evidence on a proteolytic action of FXII on HGF/HGFR leading to neuroprotection against cell death. Similar indirect trophic effects have been reported for t-PA, although in a different context in which by the activation of plasmin t-PA can convert heparin-bound HGF into free HGF, leading to subsequent HGFR signaling.

Overall, these aforementioned studies suggest that serine proteases with growth factor-like domains could, in specific conditions, substitute trophic molecules such as cytokines or growth factors to promote survival of brain cells.

In addition to t-PA and FXII, several other serine proteases contain growth-factor like domains, such as urokinase or HGF activator (HGFA).²⁷ The conservation of these domains in several of these mosaic proteins is intriguing on an evolutionary point of view. Some of the functions of these proteases are redundant, while others are specific, which may explain their maintenance over evolution. Strikingly, these different studies point out the fact that serine proteases such as t-PA or FXII, and growth factors such as EGF or HGF, are redundant and pleiotropic actors that take part in interrelated networks, in which serine proteases can facilitate growth factor maturation and activate their receptors to induce trophic effects.

Of note, it has previously been demonstrated that the ligand/receptor binding ability of FXII relies on sufficiently high ambient concentration of free Zinc (Zn).^{4,8} Nevertheless, we were not able to test this hypothesis because Zn is toxic to neurons at concentrations relevant for FXII activity.²⁸⁻³⁰

On the other hand, a deleterious role was attributed to circulating FXII/FXIIa in models of cerebral ischemia⁹ and brain trauma,¹⁰ in which thromboses are, respectively, a primary or a secondary cause of brain damage. In contrast, both forms of FXII turned out to be neuroprotective in the brain lesion model used in our study, probably because thrombosis plays limited if any role in the development of lesions. Together, these sets of studies suggest a dual role of FXII in acute brain diseases such as stroke or head trauma: a deleterious pro-thrombotic activity in the circulation and a beneficial

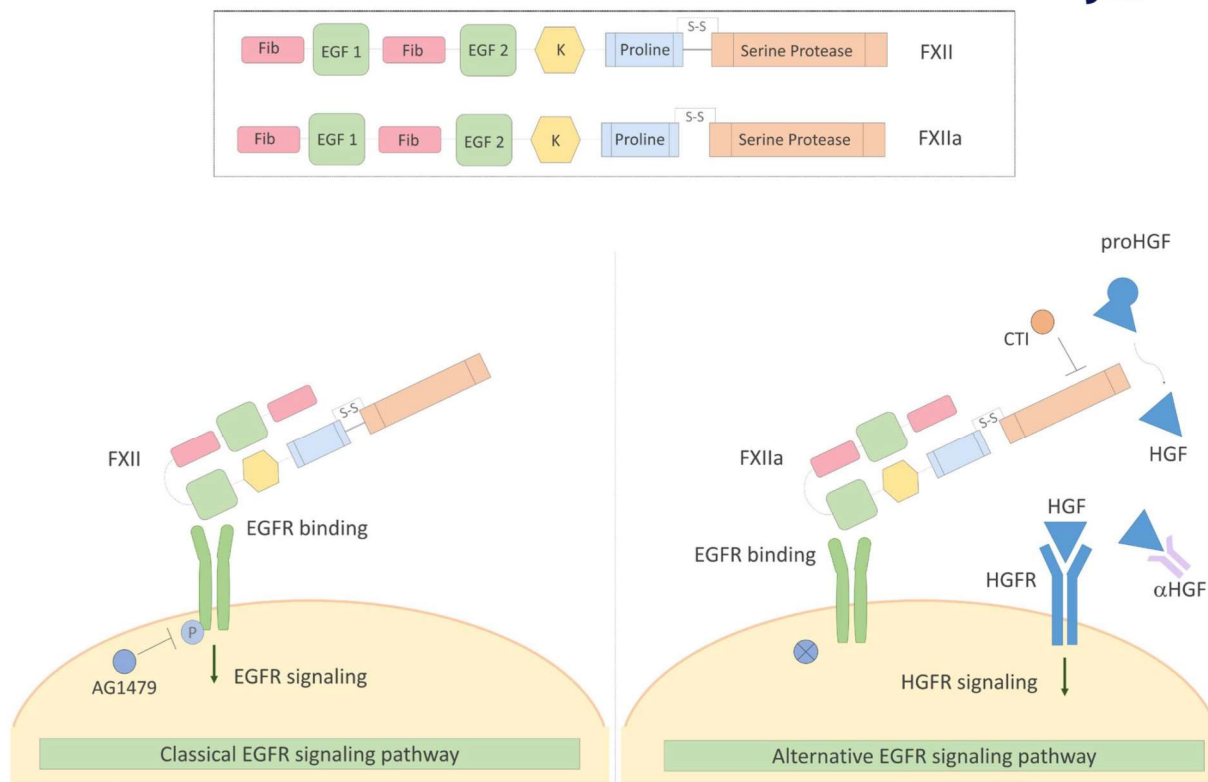


FIGURE 8 Factor XII and FXIIa protect neurons from apoptosis by epidermal growth factor receptor (EGFR)- and hepatocyte growth factor receptor (HGFR)-dependent mechanisms

anti-apoptotic effect within the brain parenchyma. These opposite effects not only occur at distinct sites but are also likely to appear with distinct timings in the injured brain.

While the pro-thrombotic activity is commonly attributed to liver-derived FXII, it is tempting to hypothesize that its anti-apoptotic effects may be due to an isoform so far only identified in neurons.¹¹ This isoform (FXII₂₉₇₋₅₉₆) is shorter than the liver-derived form and contains the proline-rich domain and the catalytic domain of FXII.¹¹ Interestingly, it can convert pro-HGF in mature HGF,¹¹ and may thus display the proteolytic, HGFR/c-Met-mediated anti-apoptotic effects described here in cultured neurons.

Neuron-derived FXII₂₉₇₋₅₉₆ does not contain EGF domain and is therefore unlikely to display the "growth factor"-like effect mediated by direct EGFR activation described here. However, the full-length form of FXII, able to display this effect, may reach the central nervous system (CNS) parenchyma by at least two ways: First, its structure and size are compatible with its transport through the blood-brain barrier (BBB) via either active processes or passive transfer, as previously described for other serine proteases.^{31,32} Second, FXII is produced by neutrophils⁵ and these cells are known to infiltrate the injured CNS. In addition, it cannot be ruled out that CNS cells other than neurons are able to produce isoforms of FXII containing the EGF domain. In line with these results, we detected

low levels of FXII in the brain cortex by ELISA but not by immunoblotting (Figure S8 in supporting information). Notably, in pathological conditions involving BBB leakage, FXII that is present in the plasma at higher concentrations could reach the brain and increase the local parenchymal concentration. This point should be addressed in future studies. In addition, further cell-specific FXII knock-out mice may help deciphering the respective roles of the distinct cellular origins of FXII during brain injury.

In neuronal-cell culture system, we have observed that FXII exerts anti-apoptotic effects by binding to EGFR and FXIIa by activating pro-HGF. Nevertheless, especially *in vivo*, we cannot exclude that the neuroprotective effect is also mediated by other pathways.

Factor XII has been referred to as a "mysterious" protease, and the question of the real function of FXII has not even been asked.³³ In addition to the two major physiological functions attributed to FXII—maintenance of thrombus stability and regulation of vascular permeability—its anti-apoptotic action should emerge as an important function and may help explain the evolutionary maintenance of this protease.

In addition to apoptosis, our *in vivo* results suggest that FXII and FXIIa protect from NMDA-induced neuronal cell death. This might be relevant to several neurological diseases involving excitotoxicity such as ischemic stroke, Alzheimer's disease, or multiple sclerosis.³⁴⁻³⁶

First, a thorough description of FXII expression in brain cells is still lacking and should be the purpose of further studies using appropriate and reliable tools. Considering that it exerts common mechanisms of action with t-PA, FXII may induce protective effects in models in which t-PA has already been shown to do so. Indeed, the growth factor--like effects of t-PA (produced by brain cells or exogenously administered) have been shown to induce protection to brain cells in several *in vivo* animal models of brain injury^{12,23,37,38} independently of its effect in the bloodstream. Several studies in animal models of brain diseases have reported deleterious effects of FXII.^{9,10,39,40} It is noteworthy that these deleterious effects are attributed to pro-thrombotic or pro-inflammatory effects of FXII. The protective effects of FXII described here may have been masked in those conditions. Nevertheless, it is important to note that the doses used in this study are well below the plasma concentrations of FXII (12.5 nM to 125 nM in the present study, vs. 375 nM in plasma).⁴¹ Thus, in the case of BBB leakage, the deleterious effects of FXII observed in different brain models could be modulated by its beneficial effects. In addition, the FXII benefits may be unveiled in models in which the impact of apoptosis is superior to those of thrombosis or inflammation. These studies should thus help further understanding on how FXII acts in brain diseases as a unique serine-protease at the interface of thrombosis, inflammation, and cell survival.

ACKNOWLEDGMENT

The authors thank Dr. Elodie Hedou for her help in pro-HGF conversion experiments.

CONFLICTS OF INTEREST

The authors have no conflicts to disclose.

AUTHOR CONTRIBUTIONS

E.G. and D.L. performed experiments, analyzed the data, and participated in manuscript redaction; I.B., M.R., C.A., S.M.D.L. performed experiments and analyzed the data; C.A., Y.H., M.G., T.C., P.C., M.R., and D.V. participated in data acquisition, provided reagents, and critically reviewed the manuscript; D.V. and F.D. secured funding of the study; I.B., F.D., and S.M.D.L. designed the study, analyzed the data, and wrote the manuscript.

ORCID

Damien Levard  <https://orcid.org/0000-0002-7275-3170>
 Maxime Gauberti  <https://orcid.org/0000-0003-0752-7342>
 Fabian Docagne  <https://orcid.org/0000-0003-1745-0625>
 Sara Martinez de Lizarrondo  <https://orcid.org/0000-0003-2303-3895>

TWITTER

Damien Levard  @Damien_Levard
 Denis Vivien  @ViviensLab1
 Fabian Docagne  @fabian_docagne
 Sara Martinez de Lizarrondo  @S_MartinezDeLiz

REFERENCES

1. Maas C, Renné T. Coagulation factor XII in thrombosis and inflammation. *Blood*. 2018;131:1903-1909.
2. Samuel M, Pixley RA, Villanueva MA, Colman RW, Villanueva GB. Human factor XII (Hageman factor) autoactivation by dextran sulfate. Circular dichroism, fluorescence, and ultraviolet difference spectroscopic studies. *J Biol Chem*. 1992;267:19691-19697.
3. Long AT, Kenne E, Jung R, Fuchs TA, Renné T. Contact system revisited: an interface between inflammation, coagulation, and innate immunity. *J Thromb Haemost*. 2016;14:427-437.
4. Schmaier AH, Stavrou EX. Factor XII - What's important but not commonly thought about. *Res Pract Thromb Haemost*. 2019;3:599-606.
5. Stavrou EX, Fang C, Bane KL, et al. Factor XII and uPAR upregulate neutrophil functions to influence wound healing. *J Clin Invest*. 2018;128:944-959.
6. LaRusch GA, Mahdi F, Shariat-Madar Z, et al. Factor XII stimulates ERK1/2 and Akt through uPAR, integrins, and the EGFR to initiate angiogenesis. *Blood*. 2010;115:5111-5120.
7. Ivanov I, Matafonov A, Sun MF, et al. Proteolytic properties of single-chain factor XII: a mechanism for triggering contact activation. *Blood*. 2017;129:1527-1537.
8. Mahdi F, Madar ZS, Figueroa CD, Schmaier AH. Factor XII interacts with the multiprotein assembly of urokinase plasminogen activator receptor, gC1qR, and cytokeratin 1 on endothelial cell membranes. *Blood*. 2002;99:3585-3596.
9. Kleinschnitz C, Stoll G, Bendtszus M, et al. Targeting coagulation factor XII provides protection from pathological thrombosis in cerebral ischemia without interfering with hemostasis. *J Exp Med*. 2006;203:513-518.
10. Hopp S, Albert-Weissenberger C, Mencil S, et al. Targeting coagulation factor XII as a novel therapeutic option in brain trauma. *Ann Neurol*. 2016;79:970-982.
11. Zamolodchikov D, Bai Y, Tang Y, McWhirter JR, Macdonald LE, Alessandri-Haber N. A short isoform of coagulation factor XII mRNA is expressed by neurons in the human brain. *Neuroscience*. 2019;413:294-307.
12. Correa F, Gauberti M, Parcq J, et al. Tissue plasminogen activator prevents white matter damage following stroke. *J Exp Med*. 2011;208:1229-1242.
13. Liot G, Roussel BD, Lebeurrier N, et al. Tissue-type plasminogen activator rescues neurons from serum deprivation-induced apoptosis through a mechanism independent of its proteolytic activity. *J Neurochem*. 2006;98:1458-1464.
14. Radi E, Formichi P, Battisti C, Federico A. Apoptosis and oxidative stress in neurodegenerative diseases. *J Alzheimers Dis*. 2014;42(Suppl 3):S125-S152.
15. Radak D, Katsiki N, Resanovic I, et al. Apoptosis and acute brain ischemia in ischemic stroke. *Curr Vasc Pharmacol*. 2017;15:115-122.
16. Behrens MI, Koh JY, Muller MC, Choi DW. NADPH diaphorase-containing striatal or cortical neurons are resistant to apoptosis. *Neurobiol Dis*. 1996;3:72-75.
17. Lam TT, Abler AS, Kwong JM, Tso MO. N-methyl-D-aspartate (NMDA)-induced apoptosis in rat retina. *Invest Ophthalmol Vis Sci*. 1999;40:2391-2397.
18. Rojas M, Yao S, Lin YZ. Controlling epidermal growth factor (EGF)-stimulated Ras activation in intact cells by a cell-permeable peptide mimicking phosphorylated EGF receptor. *J Biol Chem*. 1996;271:27456-27461.
19. Shimomura T, Miyazawa K, Komiyama Y, et al. Activation of hepatocyte growth factor by two homologous proteases, blood-coagulation factor XIIIa and hepatocyte growth factor activator. *Eur J Biochem*. 1995;229:257-261.
20. Finisguerra V, Di Conza G, Di Matteo M, et al. MET is required for the recruitment of anti-tumoural neutrophils. *Nature*. 2015;522:349-353.

21. Vogel S, Trapp T, Börger V, et al. Hepatocyte growth factor-mediated attraction of mesenchymal stem cells for apoptotic neuronal and cardiomyocytic cells. *Cell Mol Life Sci*. 2010;67:295-303.
22. Nayeri F, Nayeri T, Aili D, Brudin L, Liedberg B. Clinical impact of real-time evaluation of the biological activity and degradation of hepatocyte growth factor. *Growth Factors*. 2008;26:163-171.
23. Vivien D, Gauberti M, Montagne A, Defer G, Touzé E. Impact of tissue plasminogen activator on the neurovascular unit: from clinical data to experimental evidence. *J Cereb Blood Flow Metab*. 2011;31:2119-2134.
24. Gordon EM, Venkatesan N, Salazar R, et al. Factor XII-induced mitogenesis is mediated via a distinct signal transduction pathway that activates a mitogen-activated protein kinase. *Proc Natl Acad Sci USA*. 1996;93:2174-2179.
25. Trusolino L, Bertotti A, Comoglio PM. MET signalling: principles and functions in development, organ regeneration and cancer. *Nat Rev Mol Cell Biol*. 2010;11:834-848.
26. Bussolino F, Di Renzo MF, Ziche M, et al. Hepatocyte growth factor is a potent angiogenic factor which stimulates endothelial cell motility and growth. *J Cell Biol*. 1992;119:629-641.
27. Shia S, Stamos J, Kirchhofer D, et al. Conformational lability in serine protease active sites: structures of hepatocyte growth factor activator (HGFA) alone and with the inhibitory domain from HGFA inhibitor-1B. *J Mol Biol*. 2005;346:1335-1349.
28. Yokoyama M, Koh J, Choi DW. Brief exposure to zinc is toxic to cortical neurons. *Neurosci Lett*. 1986;71:351-355.
29. Bozym RA, Chimienti F, Giblin LJ, et al. Free zinc ions outside a narrow concentration range are toxic to a variety of cells in vitro. *Exp Biol Med (Maywood)*. 2010;235:741-750.
30. Li YV, Frederickson CJ. Zinc-secreting neurons, gluzincergic and zincergic neurons. In: Kretsinger RH, Uversky VN, Permyakov EA, eds. *Encyclopedia of metalloproteins*. New York, NY: Springer New York; 2013:2565-2571.
31. Benchenane K, Berezowski V, Ali C, et al. Tissue-type plasminogen activator crosses the intact blood-brain barrier by low-density lipoprotein receptor-related protein-mediated transcytosis. *Circulation*. 2005;111:2241-2249.
32. Benchenane K, Berezowski V, Fernández-Monreal M, et al. Oxygen glucose deprivation switches the transport of tPA across the blood-brain barrier from an LRP-dependent to an increased LRP-independent process. *Stroke*. 2005;36:1065-1070.
33. de Maat S, Maas C. Factor XII: form determines function. *J Thromb Haemost*. 2016;14:1498-1506.
34. Wu QJ, Tymianski M. Targeting NMDA receptors in stroke: new hope in neuroprotection. *Molecular Brain*. 2018;11:15.
35. Macrez R, Ortega MC, Bardou I, et al. Neuroendothelial NMDA receptors as therapeutic targets in experimental autoimmune encephalomyelitis. *Brain*. 2016;139:2406-2419.
36. Liu J, Chang L, Song Y, Li H, Wu Y. The role of NMDA receptors in Alzheimer's disease. *Front Neurosci*. 2019;13:43.
37. Lemarchand E, Maubert E, Haelewyn B, Ali C, Rubio M, Vivien D. Stressed neurons protect themselves by a tissue-type plasminogen activator-mediated EGFR-dependent mechanism. *Cell Death Differ*. 2016;23:123-131.
38. Fredriksson L, Lawrence DA, Medcalf RL. tPA modulation of the blood-brain barrier: a unifying explanation for the pleiotropic effects of tPA in the CNS. *Semin Thromb Hemost*. 2017;43:154-168.
39. Zamolodchikov D, Chen ZL, Conti BA, Renné T, Strickland S. Activation of the factor XII-driven contact system in Alzheimer's disease patient and mouse model plasma. *Proc Natl Acad Sci USA*. 2015;112:4068-4073.
40. Chen ZL, Revenko AS, Singh P, MacLeod AR, Norris EH, Strickland S. Depletion of coagulation factor XII ameliorates brain pathology and cognitive impairment in Alzheimer disease mice. *Blood*. 2017;129:2547-2556.
41. Stavrou E, Schmaier AH. Factor XII: what does it contribute to our understanding of the physiology and pathophysiology of hemostasis & thrombosis. *Thromb Res*. 2010;125:210-215.

SUPPORTING INFORMATION

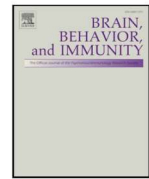
Additional supporting information may be found online in the Supporting Information section.

How to cite this article: Garnier E, Levard D, Ali C, et al. Factor XII protects neurons from apoptosis by epidermal and hepatocyte growth factor receptor-dependent mechanisms. *J Thromb Haemost*. 2021;19:2235-2247. <https://doi.org/10.1111/jth.15414>



Contents lists available at ScienceDirect

Brain, Behavior, and Immunity

journal homepage: www.elsevier.com/locate/ybrbi

Filling the gaps on stroke research: Focus on inflammation and immunity

Damien Levard^{a,1}, Izaskun Buendia^{a,1}, Anastasia Lanquetin^a, Martina Glavan^a, Denis Vivien^{a,b}, Marina Rubio^{a,*}^a Normandie Univ, UNICAEN, INSERM, GIP Cyceron, Institut Blood and Brain @Caen-Normandie (BB@C), UMR-S U1237, Physiopathology and Imaging of Neurological Disorders (PhIND), Caen, France^b CHU Caen, Department of Clinical Research, Caen University Hospital, Avenue de la Côte de Nacre, Caen, France

ARTICLE INFO

Keywords:

Ischemic stroke
Inflammation
Immune response
Clinical trials
Translational research
Experimental models

ABSTRACT

For the last two decades, researchers have placed hopes in a new era in which a combination of reperfusion and neuroprotection would revolutionize the treatment of stroke. Nevertheless, despite the thousands of papers available in the literature showing positive results in preclinical stroke models, randomized clinical trials have failed to show efficacy. It seems clear now that the existing data obtained in preclinical research have depicted an incomplete picture of stroke pathophysiology. In order to ameliorate bench-to-bed translation, in this review we first describe the main actors on stroke inflammatory and immune responses based on the available pre-clinical data, highlighting the fact that the link between leukocyte infiltration, lesion volume and neurological outcome remains unclear. We then describe what is known on neuroinflammation and immune responses in stroke patients, and summarize the results of the clinical trials on immunomodulatory drugs. In order to understand the gap between clinical trials and preclinical results on stroke, we discuss in detail the experimental results that served as the basis for the summarized clinical trials on immunomodulatory drugs, focusing on (i) experimental stroke models, (ii) the timing and selection of outcome measuring, (iii) alternative entry routes for leukocytes into the ischemic region, and (iv) factors affecting stroke outcome such as gender differences, ageing, comorbidities like hypertension and diabetes, obesity, tobacco, alcohol consumption and previous infections like Covid-19.

We can do better for stroke treatment, especially when targeting inflammation following stroke. We need to re-think the design of stroke experimental setups, notably by (i) using clinically relevant models of stroke, (ii) including both radiological and neurological outcomes, (iii) performing long-term follow-up studies, (iv) conducting large-scale preclinical stroke trials, and (v) including stroke comorbidities in preclinical research.

1. Introduction

Stroke is the second leading cause of death for people older than 60 years and the first cause of disability. It is estimated that by 2050, more than 1.5 billion people will be over 65, increasing therefore stroke prevalence (Krishnamurthi et al., 2010). Taking into account the tremendous socio-economic impact of this fact, the better understanding of the pathophysiology in order to finally develop new treatments for patients is crucial. This is especially important considering that for the moment there are only two approved treatments for acute ischemic stroke (AIS): (i) clot thrombolysis through the intravenous administration of tissue plasminogen activator (tPA, Actilyse), which is limited in clinical practice due to a short therapeutic window (4.5 h) and a risk of intracerebral hemorrhage; and (ii) clot removal by endovascular

thrombectomy up to 24 h after stroke onset depending on imaging criteria (Casetta et al., 2020; Thomalla and Gerloff, 2019). Additional agents to combine with tPA administration and/or thrombectomy to enlarge the therapeutic window of the current therapies, enhance their efficacy and improve outcomes associated with stroke are needed.

Insights into the consequences of glucose and oxygen deprivation concerning oxidative, excitotoxic and microvasculature injuries, blood brain barrier (BBB) disruption, oedema and neuronal death have been possible thanks to the efforts of hundreds of research groups that have dedicated the past decades to the better understanding of the mechanisms underlying stroke. However, there are two more recently described key players, which will be the focus of this review: neuroinflammation and immune responses to stroke. Neuroinflammation is defined as an inflammatory response within the central nervous system

* Corresponding author.

E-mail address: rubio@cyceron.fr (M. Rubio).¹ These co-authors equally contributed to this work.<https://doi.org/10.1016/j.bbi.2020.09.025>

Received 29 June 2020; Received in revised form 10 September 2020; Accepted 23 September 2020

Available online 02 October 2020

0889-1591/© 2020 Published by Elsevier Inc.

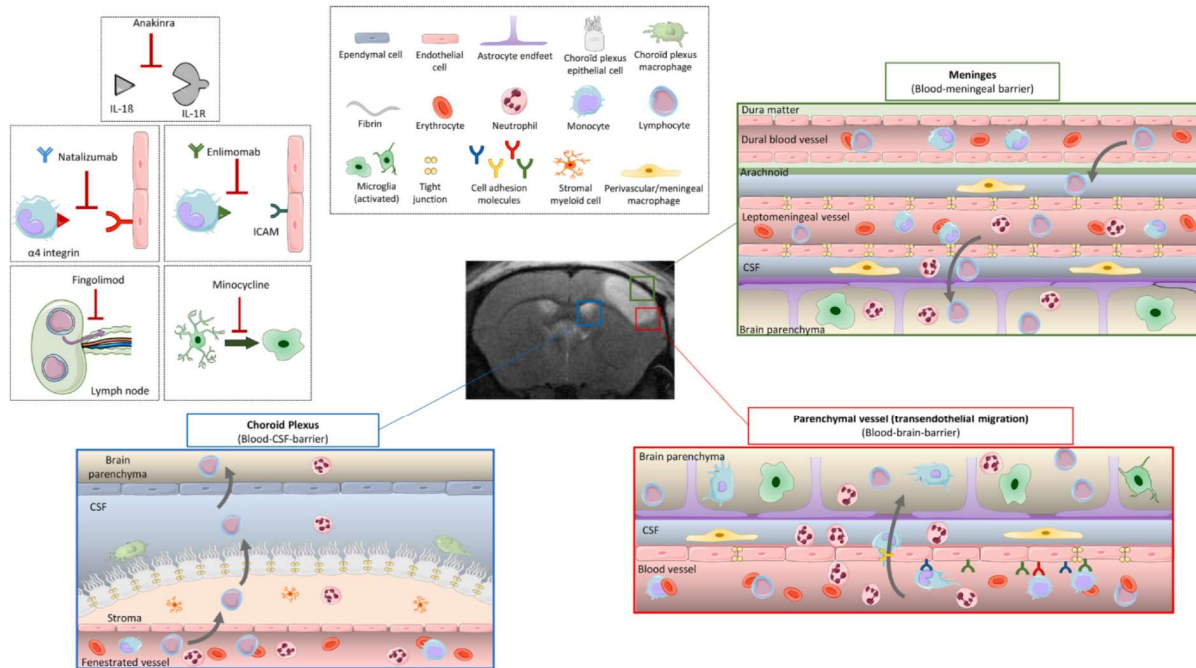


Fig. 1. Inflammatory/immune responses after ischemic stroke, and targets of the immunomodulatory drugs tested on clinical trials. In the healthy brain, three main barriers protect the parenchyma from external pathogens: the blood–brain barrier (BBB) around the cerebral vessels, the blood-meningeal barrier in the meninges, and the blood-CSF barrier of the choroid plexus. Immune cells circulate freely in the blood, and a few lymphocytes patrol the CSF to do immunosurveillance. In the brain parenchyma resting microglia survey the environment with their processes. After stroke, microglia switches from a resting form to an activated state, adopting a phagocytic phenotype and secreting pro-inflammatory factors. The BBB is disrupted, local ECs are activated and express CAMs. The tight junctions between ECs disappear. This allows leukocyte rolling and adhesion at the luminal side of the blood vessel and then transmigration from the vascular compartment to the brain parenchyma. Leukocytes can also invade the brain through blood-meningeal and blood-CSF barriers. Once infiltrated in the tissue, neutrophils secrete pro-inflammatory factors that will recruit monocytes/macrophages, and later lymphocytes to the parenchyma. Immunomodulatory drugs tested on clinical trials and discussed in this review include (i) Anakinra, an antagonist of the proinflammatory cytokine interleukin-1, (ii) Natalizumab, which acts by blocking the binding of integrin $\alpha 4$ to the adhesion molecule VCAM to reduce leukocyte infiltration. (iii) Enlimomab is an antibody targeting the adhesion molecule ICAM. (iv) Minocycline inhibits microglial activation among other anti-inflammatory properties. (v) Fingolimod is a high-affinity agonist for several of the sphingosine-1-phosphate receptors that prevents the egress of lymphocytes from lymph nodes, thus limiting the infiltration of lymphocytes to the brain. BBB, blood–brain barrier; CAM, cellular adhesion molecule; CSF: cerebrospinal fluid; EC, endothelial cell.

(CNS), thus, the brain or spinal cord. This process is due to the production of different mediators such as cytokines, chemokines, reactive oxygen species, and secondary messengers by resident CNS glia, endothelial cells, and peripherally derived immune cells. On the other hand, immune response combines the terms of innate and adaptive immune responses, involved in regular brain development but also in different pathologic conditions, such as neurodegenerative diseases or stroke (Ransohoff et al., 2015). Briefly, immune cells classically involved in innate responses include natural killer cells, neutrophils, dendritic cells and macrophages that participate in the selective recognition and the clearance of pathogens and toxic cell debris during infection or tissue injury (Medzhitov and Janeway, 2002). However, it is now evident that resident cells, glial cells, ependymal cells and even neurons are capable of mounting innate immune responses on their own (Nguyen et al., 2002; Ransohoff et al., 2015).

Although many aspects of postischemic inflammation, that is, the response of the immune system to disruption of tissue homeostasis, manifest themselves days and weeks after the event, the inflammatory cascade is activated immediately after the vessel occlusion (Anrather and Iadecola, 2016). A secondary huge cascade of inflammatory responses is orchestrated within minutes and persists among days or even weeks after. This process, especially during the first 48 h hours after stroke onset, has been deeply studied and reviewed during the last decades (Anrather and Iadecola, 2016; Shi et al., 2019; Chamorro et al., 2016; Drieu et al., 2018). The immune response is initiated immediately

after the cell injury, by the release of different damage-associated molecular patterns (DAMPs), such as heat shock proteins, high mobility group box 1 and interleukin-33, purines (ATP, UTP, and their catabolites), peroxiredoxins, and mitochondrial-derived N-formyl peptides. These molecules activate pattern recognition receptors on microglia, the brain resident immune cells, and astrocytes. Later on, activation of endothelial cells aggravates the BBB breakdown allowing peripheral leukocytes to arrive to the injured area (Gadani et al., 2015; Shi et al., 2019). Due to the disruption of the BBB, cytokines and DAMPs enter the circulation and induce a systemic immune response, with an increase in pro-inflammatory cytokines and circulating leukocytes during the first hours after stroke (Anrather and Iadecola, 2016). However, after this early activation of the immune system, a state of systemic immunodepression that predisposes to poststroke infections occurs. Indeed, complications from pulmonary or urinary tract infections have been observed in ~ 20% of patients with stroke (Meisel et al., 2005; Prass et al., 2003; Langhorne et al., 2000). Thus, an ambition to understand the role of the immune system and the potential of immunomodulatory drugs to act as a treatment for the stroke, have been a driving force for the extensive research in the past decade.

After a brief description of the main actors of the inflammatory/immune responses after stroke, in this review we will first focus on clinical data, obtained in stroke patients and randomized clinical trials (RCT), and we will then compare and summarize the preclinical findings that served as a basis support for clinical trials. Next, we will

discuss aspects that are often neglected yet important to be considered in preclinical research, in order to give light to the unfortunate bench-to-bed translational gap in ischemic stroke research concerning immunomodulatory drugs. In particular, we will discuss about (i) the selection of the best experimental model(s; in terms of the nature of arterial occlusion and its potential recanalization) for a given experimental design, (ii) the timing and selection of outcome measuring, (iii) the existence of alternative entry routes for leukocytes into the ischemic region, and (iv) factors affecting stroke outcome (gender differences, ageing, comorbidities like hypertension diabetes and previous infections, and external factors related to daily life like obesity, tobacco and alcohol consumption).

2. Main actors on stroke inflammatory and immune responses

A schematized, non-exhaustive overview of the inflammatory and immune responses after stroke is depicted in Fig. 1. Microglial response is one of the first steps before the innate immune responses triggered after stroke. These cells can adopt a large spectrum of phenotypes ranging from pro- to anti-inflammatory and are known to rapidly respond to neuronal injury in the boundary zone of the infarct after stroke (Szalay et al., 2016). Due to the lack of nutrients, differences in ion gradients and altered neuronal activity, microglial responses start minutes after stroke in both the core and the penumbra regions. Microglial cells detect with their processes purinergic metabolites and changes in ionic gradients in surrounding suffering cells (Cserep, 2020). At the acute phase after stroke onset, microglial cells at the core of the lesion detect DAMPs and HMGB1 via their receptors -mainly belonging to the Toll-like Receptor family (TLR). This ligand-receptor link leads to the activation of the NF- κ B pathway and thus, to the activation of microglial cells. Once activated after stroke onset, microglial cells increase their expression of CD11b, CD45 and CD68 corresponding to a phagocytic phenotype responsible for the clearance of cellular debris, as well as TNF and the pro-inflammatory interleukins IL-1 and IL-6 that exacerbate astrocyte and endothelial cell (EC) activation (Xu et al., 2020). Afterwards, DAMPs and cytokines expressed during the early phase of ischemic injury can access to the systemic circulation through the disrupted BBB or the cerebrospinal fluid drainage system that includes venous and lymphatic outflows (Anrather and Iadecola, 2016).

Following ischemia and lasting from hours to weeks after, astrocytes are other key players. It is well-known that cytokines from neurons and glial cells lead to astrocyte reactivity hyperplasia. Astrocytes endfeet are in close interaction with brain capillary endothelial cells and pericytes that form BBB. During ischemia, MMP-9 disrupts the connection between astrocyte endfeet and endothelial cells by degrading basal lamina (del Zoppo, 2010). Astrocyte proliferation results in the synthesis of inflammatory factors such as monocyte chemoattractant protein-1, IL-1 β , glial fibrillary acidic protein (GFAP), vimentin, and nestin that can lead to reactive gliosis and later scar formation (Jayaraj et al., 2019). Hence, it has been classically assumed that the ruptured BBB acts as a major gateway for the invasion of peripheral leukocytes through their trans-endothelial migration. As discussed afterwards, alternative entry routes for leukocytes have been described in recent years.

Activated cerebral microvessels become more permeable to molecules that are normally prevented from crossing the blood–brain barrier. In particular, the immunological BBB is substantially altered after ischemia. Together with the secretion of chemokines, the successive entry of systemic leukocytes including neutrophils, macrophages, and lymphocytes is promoted (Veltkamp and Gill, 2016). Corresponding to the upregulation of adhesion molecules on EC, integrins exhibit similar functions on activated leukocytes. Leukocytes start to roll on the vessel wall with the help of selectins expressed by activated EC. After rolling, leukocytes adhere to the vessel wall by strong links with intercellular adhesion molecule-1 (ICAM-1) and vascular cell adhesion molecule-1 (VCAM-1). Similar to other inflammatory cells, leukocytes release proinflammatory factors in the ischemic region of the brain.

Leukocytosis has been described as a marker of inflammatory response after stroke. Neutrophils are the first bloodborne immune cells to invade the ischemic tissue, followed by monocytes. The sequence of leukocyte recruitment into the brain after experimental stroke has been well characterized (Gelderblom et al., 2009; Drieu et al., 2020a, 2020b), whereas the temporal and spatial profile of the immune cell recruitment after stroke in humans requires better characterization (Veltkamp and Gill, 2016).

Neutrophils enhance leukocyte recruitment by degranulation of their content, rich in cytokines/chemokines, proteolytic enzymes and activated-complement system (Mayadas et al., 2014). In addition to this, neutrophils could contribute to brain injury after ischemic stroke by obstructing microvessel circulation, damaging EC and extracellular matrix by hydrolytic enzymes and free radicals, promoting intravascular thrombus formation together with platelet activation, and releasing cytokines and chemotactic factors that could promote extension of the inflammatory response. Moreover, neutrophil extracellular traps (NETs; networks of DNA, histones and proteolytic enzymes) secreted by neutrophils are capable of activating platelets and contribute to the thrombotic processes (Rayasam et al., 2018). Clinical data and experimental models of stroke have shown that neutrophils infiltrate the brain parenchyma within hours of stroke onset (Gelderblom et al., 2009; Drieu et al., 2020a, 2020b; Cai et al., 2020). Furthermore, clinical studies demonstrated that the neutrophil-to-lymphocyte ratio might be a strong prognostic marker in acute ischemic stroke (Xue et al., 2017) and that the NETs are increased in patients with stroke (Vallés et al., 2017).

The consequences of the adaptive immune response on ischemic stroke are still debated, as both beneficial and deleterious results have been reported depending on the type of lymphocyte subpopulation. Infiltrating $\gamma\delta$ T, CD8⁺ T, and NK cells contribute to the acute brain injury after stroke onset, while regulatory T and B cells are reported to be protective (Feng et al., 2017). Experimental models of stroke have shown that lymphocyte infiltration into the ischemic tissue comes later after stroke onset, starting at day 3 (Drieu et al., 2020a, 2020b). Post-mortem human samples have shown that lymphocyte infiltration into the ischemic area occurs from day 3 and can be present up to 53 years after stroke (Mena et al., 2004).

Neuroinflammation is also considered necessary for the reparation phase that persists after the initial brain insult. Initial inflammation is self-limiting and ultimately gives a way to structural remodeling and functional reorganization. After the acute phase of ischemic stroke, the inflammatory response gradually decreases, and ischemic stroke enters another stage during which tissue repair dominates the infarction region (Xu et al., 2020). The end of the acute phase is characterized by removal of dead cells/tissue debris, creation of an anti-inflammatory milieu and production of pro-survival factors (Malone et al., 2019). This phase aims to restore tissue integrity and involves matrix remodeling, neurogenesis, axon sprouting, dendritogenesis and oligodendrogenesis (Peruzzotti-Jametti et al., 2014) carried out in concert by many cell types, ranging from immune cells to neurons and astrocytes. Together, these cells produce growth factors and proteases, allowing the remodeling of the ischemic site (Iadecola and Anrather, 2011).

3. What do we know about neuroinflammation and immune responses in stroke patients?

Unfortunately, due to the lack of specificity of biomarkers for imaging patients *in vivo* and the reduced number of *post-mortem* analyses, studying inflammation/immune responses in humans is limited. As aforementioned, glial cells are one of the main key players in the inflammatory responses triggered after ischemic stroke. Long-term imaging or additional *post-mortem* pathological studies would be crucial to definitely confirm whether global glial activation after stroke is persistent in humans (Shi et al., 2019). However, different groups have been able to perform short term studies by using *in vivo* imaging

techniques. Focusing on microglial cells, by using the PK11195-PET radioactive ligand of the translocator protein, highly expressed by activated microglia, and diffusion tensor imaging MRI, the involvement of this cell-type is clearer. In this manner, activated microglia have demonstrated to accumulate focally within a week after stroke and can be detected in distal regions several months after (Gerhard et al., 2005; Thiel et al., 2010; Radlinska et al., 2009). In addition, in another study positive signals have been observed in the subacute phase (6 to 21 weeks after the lesion) in non-infarcted ipsilateral areas (Morris et al., 2018).

However, it is worth to mention that translocator protein is also expressed by monocytes or macrophages and to a lesser extent, by astrocytes, reducing the specificity of the technique (Dupont et al., 2017). Furthermore, the absence of a specific astrocyte biomarker feasible for *in vivo* imaging in patients leads to a tremendous gap in clinical evidence supporting a role for astrocytes in brain inflammation after stroke. Therefore, it becomes crucial to improve and to develop these techniques for the future.

In addition, clinical evidences regarding peripheral immune cells mobilization and vascular inflammation are scarce (Shi et al., 2019). We encourage researchers within the field to increase the clinical research, so the promising results obtained in preclinical models aforementioned can be confirmed and better therapeutic targets/manipulations can be suggested.

4. Results of the clinical trials on immunomodulatory agents

Given that mechanisms of immune-mediated neuronal injury have relatively recently gained increasing attention, few drugs with the primary aim of modulating inflammatory/immune pathways have reached the Phase II or Phase III RCT stage in acute stroke. In this review, we will focus on RCT aiming to address neuroinflammation/immunomodulation, setting aside any RCT involving tPA or thrombectomy by itself (see (Chamorro et al., 2016; Smith et al., 2015). A schematic view of the immunomodulatory drug targets tested in clinical trials is shown in Fig. 1.

There have been several RCT pursuing the modulation of pro-inflammatory cytokine interleukin-1, by the use of recombinant interleukin-1 receptor antagonist (IL-1Ra) (Anakinra). This compound, historically used to treat rheumatoid arthritis and similar inflammatory diseases, showed a good safety profile. Besides the promising results obtained in preclinical studies, in human studies, a phase II trial in 2005 showed Anakinra to be safe and well tolerated in AIS patients (Emsley et al., 2005). With the replacement of the intravenous formulation by a subcutaneous injection, the effects of the drug have been re-investigated at a twice-daily dose since (Sobowale et al., 2016). However, even though Anakinra significantly decreased plasma levels of pro-inflammatory IL-6 and C-reactive protein, patients did not show a reduction in disability levels at 3 months compared to placebo. A possible negative interaction between IL and 1Ra and tPA has been revealed (Smith et al., 2015) and has been suggested to mask the potential beneficial effect of Anakinra. Thus, further preclinical and clinical studies are required to confirm its use as stroke treatment.

Minocycline, a tetracycline derivative, is a well-documented protective compound in preclinical stroke models. It exerts anti-inflammatory properties by inhibiting the expression of polyadenosine diphosphate ribose polymerase 1 and matrix metalloproteinases, and inhibiting microglial activation. It has shown an acceptable safety profile in an open-label, dose-escalation study in patients treated within 6 h after the symptoms onset, including a subset of patients who also received alteplase. A small pilot study confirmed the safety of intravenous minocycline administered within 24 h of stroke onset, but did not show efficacy of the drug by improving the proportion of patients free of disability at 90 days (Kohler et al., 2013). However, the meta-analysis of previous RCT demonstrated the efficacy and minocycline has been suggested as a promising neuroprotective agent in AIS patients

(Malhotra et al., 2018).

Several options have been followed pursuing the avoidance of invasion of peripheral cells to the CNS. Among them, we can find **Natalizumab**, a humanized CD49d antibody that blocks α 4-integrin, attenuating leucocytic infiltration. Promising results were obtained in animal and in a first clinical trial in which Natalizumab did not have an effect on the infarct volume growth on brain MRI at day 5 (primary outcome), but the therapy was safe and provided global clinical gains on the Stroke Clinical Impact-16 scale and in cognitive function at 90 days (Elkins et al., 2017). Disappointingly, the follow-up phase IIb trial (“ACTION2”) did not meet its primary or secondary endpoints. As a result, further development of Natalizumab in AIS will not be pursued (Malone et al., 2019).

A role of the endothelial β 2-integrin ligand ICAM-1 in neutrophil recruitment across the BBB in stroke was proposed as an alternative pharmacological target. Although positive results were obtained in preclinical research, a phase III clinical trial of anti-ICAM-1 antibody **Enlimomab**, failed to replicate these results, with the antibody-treated group reporting higher mortality (Enlimomab Acute Stroke Trial Investigators, 2001).

Fingolimod is a high-affinity agonist for several of the sphingosine-1-phosphate receptors that prevents the egress of lymphocytes from lymph nodes, limiting the infiltration of lymphocytes into the brain, and inhibiting local activation of microglia and macrophages. Preclinical studies using several rodent models of brain ischemia have shown that Fingolimod can reduce infarct size, neurological deficit, oedema, and the number of dying cells in the core and *peri*-infarct area (Liu et al., 2013). In stroke patients, when administered within 72 h after stroke onset, oral Fingolimod caused no severe adverse effects and had efficacy in limiting secondary tissue injury, in decreasing microvascular permeability, attenuating neurological deficits, and in promoting recovery (Zhang et al., 2017). In addition to this, the combination of Fingolimod with alteplase resulted in fewer circulating lymphocytes, smaller lesion volumes, less hemorrhages, and attenuated neurological deficits (Zhu et al., 2015; Zhang et al., 2017). However, while Fingolimod remains one of the most compelling stroke immunotherapies, further large-scale clinical trials are required (Malone et al., 2019).

5. Experimental basis for the clinical trials on immunomodulatory drugs: Translational gaps on stroke.

The existing preclinical data on immunomodulatory drugs discussed in this review is summarized in Table 1. As aforementioned, in spite of the beneficial effects shown in preclinical research, RCT have shown disappointing results. To overcome this gap, the Stroke Therapy Academic Industry Roundtable (STAIR) recommendations and guidelines have been proposed. However, there are still some important factors which are often neglected, that could explain -at least in part- the bench to bedside translational failure. We will particularly focus here on (i) the characteristics of the arterial recanalization process and its derived inflammatory responses, which are extremely dependent on the experimental model used, (ii) alternative entry routes for leucocytes to the brain parenchyma, (iii) the appropriate timing of measurements in preclinical models and (iv) the vital importance of concomitant factors affecting stroke that needs to be taken into account.

- i) Characteristics of the arterial occlusion and recanalization processes: the importance of choosing the appropriate experimental model

Preclinical models of ischemic stroke are necessary for investigating pathogenic processes triggered after the ischemic insult, as well as to screen for candidate therapeutic strategies. This section aims to highlight the importance of an element that could partially explain the translational gap in stroke research in general and in the

Table 1
Existing preclinical data on the immunomodulatory drugs discussed in this review: Anakinra, Natalizumab, Enlimomab, Minocycline and Fingolimod.

Drug	Experimental model	Animal species (*)	Administration route/timing	Lesion volume	Neuromotor deficit	Main results	Ref.
Anakinra	pMCAO	Rat	Central, 30' before and 10' after	24 h	No	Reduced infarct volume.	(Relton and Rothwell, 1992)
	pMCAO	Rat	Subcut., before and up to 7 days	24 h, 7 days	Neurological score at 24 h and 7 days	Decreased the number of necrotic neurons and the number of PMN leukocytes. Improved neurological scores.	(Garcia et al., 1995)
	pMCAO	Rat	ICV, 30' after	24 h, 7 days	No	Reduced total and cortical infarct volume. 24 h and 7 days post.	(Lodwick and Rothwell, 1996)
	tMCAO (60')	Rat	ICV, 1,2 or 3 h after	24 h and 48 h	No	Reduced brain damage, when administered 3 h after.	(Mulcahy et al., 2003)
	tMCAO (60')	Rat	Subcut, just after and 24 h after	24,48 h and 28 days	Gross neurological score and functional recovery, motor tasks, days 6–9 and 25–28	Enhanced functional recovery and protected against sociability defect and depression.	(Girard et al., 2014)
	tMCAO (70 or 90')	Rats, young and aged and Corpulent	Subcut, 3 and 6 h after	24 h and 7 days	Motor, behavioral and cylinder tests, 24 h and 7 days	Improved stroke outcome and promotes neurogenesis in both young and aged/co-morbid rats.	(Pradillo et al., 2017)
	tMCAO (45')	Mouse	Subc.,30' and 3 h after	24 h and 7 days	Bederson and Corner tests, 24 h and 7 days	Preclinical cross-laboratory stroke trial supporting the therapeutic potential of interleukin 1 receptor antagonist.	(Maysami et al., 2016)
	Permanent (electrocoag.)	Mouse (10 months)	Subc., 30' and 3 h after	3 and 28 days	Catwalk test 3,14,21,18 days		
	Permanent (electrocoag.)	Mouse	Subc., 30' and 3 h after	24 h and 7 days	Hunter and corner tests, 24 h, 2, 7 and 28 days		
	tMCAO (30')	Mouse	Subc., 30' and 3 h after	24 h	Neurological Score, 24 h		
	tMCAO (Thrombin)	Mouse	Subc., 30' and 3 h after	7 days	No		
	Permanent (Electrocoag.)	Mouse	Subc., 30' and 3 h after	7 days	Corner test, 1,2 and 7 days		

(continued on next page)

Table 1 (continued)

Drug	Experimental model	Animal species (*)	Administration route/timing	Lesion volume	Neuromotor deficit	Main results	Ref.
Minocycline	tMCAO (90')	Rat	I.P., every day, up to 3	24 h	No	Decreased infarct volume and inflammation.	(Vrjähelkki et al., 1999)
	tMCAO (90')	Rat	IV, 4.5, and 6 h after	24 h	Neurological Score, 24 h	Decreased infarct volume and improved neurological deficits.	(Xu et al., 2004)
	pBCCAO	Rat	I.P., just after, twice a day, up to 14 days	No	No	Decreased neuronal and myelin damage and inflammation.	(Cho et al., 2006)
	tBCCAO(30')	Rat	I.P., 12 h before, just after and every 24 h up to 3 days	No	No	Enhanced neuronal viability, decreased inflammation.	(Cai et al., 2006)
	tMCAO (60')	Rat	I.P., 4 days after up to 3 weeks	No	Motor function and learning and memory tests, 6 weeks after	Promoted neurogenesis, improved motor function and memory.	(Liu et al., 2007)
	tMCAO (60')	Rat	I.P., 30' and 2 h after up to 3 days	3 days	Neurological deficit scores, 3 days	Improved neurological deficits, decreased infarct volume.	(Chu et al., 2007)
	pBCCAO	Female rat	Oral, once a day up to 16 weeks	No	Morris and openfield tests, 4, 8, 12 and 16 weeks	Improved memory, decreased infarct volume, iNOS and inflammation.	(Cai et al., 2008)
	tMCAO(30')	Rat	I.V., 60' after	3 days	Body swing and Bederson test, 3 days	Improved neurological deficits and decreased infarct volume.	(Matsukawa et al., 2009)
	tMCAO (2 h)	Rat	I.V., 1 h after, once per day up to 6	7 days	No	Decreased infarct volume and inflammation.	(Martin et al., 2011)
	pBCCAO	Female Wistar rat	Oral, once per day up to 16 weeks	No	No	Decreased neuroinflammation.	(Cai et al., 2010)
	tBCCAO	Rat	I.P., just after and every 12 h up to 3 days	24 h and 3 days	Water maze 24 h and 3 days	Improved memory, decreased infarct volume.	(Zheng et al., 2013)
	tMCAO (2 h)	Rat	I.V., just after and up to 14 days	No	Neurological severity scores and the staircase test, 2 days, 1, 2 and 4 weeks	Reduced BBB permeability and improved sensorimotor deficits.	(Tao et al., 2013)
	Endothelin	Rat	I.P., twice a day up to 48 h	No	Modified sticky-tape test, 24 h, 3 and 7 days	Improved sensorimotor deficits, inflammation and neuronal viability.	(Cardoso et al., 2013)
	tBCCAO (20')	Rat	Oral, 48, 24 h and 1 h before	No	No	Reduced neuronal degeneration.	(Aras et al., 2013)
	pBCCAO	Female rat	Oral, 4 days after ischemia, daily up to 4 weeks	No	Water maze 1, 2, 3, 4 and 5 days	Improved memory, enhanced neuronal plasticity.	(Zhao et al., 2015)
	tMCAO (90')	Hypertens. rat	I.V., just after	48 h, 1, 2 and 4 weeks	No	Decreased infarct volume, inflammation, improved BBB permeability.	(Yang et al., 2015)
	tMCAO (90')	Rat	I.V., just after	14 days	Bederson, beam walk, rotarod performance and grip test, 1, 3, 7 and 14 days	Decreased infarct volume, improved neurobehavioural and motor functions.	(Soliman et al., 2015)
	tMCAO (30')	Rat	I.V., 30' before	7 days	Adhesive removal test, 1 and 7 days	Decreased infarct volume, improved neurobehavioural functions.	(Park et al., 2015)
	tBCCAO (20')	Rat	I.P., once per day up to 7	No	Morris water-maze 7 days	Improved memory, enhanced neuronal viability.	(Naderi et al., 2017)
	Photothromb.	Rat	I.P., 1 h, 12, 24, 36 and 48 h after	3 and 24 h, 2, 3 and 7 days	The forelimb placing response and cylinder tests, 3 and 24 h, 2, 3 and 7 days	Improved motor function and decreased phagocytic cells.	(Yew et al., 2019)

(continued on next page)

Table 1 (continued)

Drug	Experimental model	Animal species (%)	Administration route/timing	Lesion volume	Neuromotor deficit	Main results	Ref.
	tMCAO (60')	Rat	I.V, just after	24 h	No	Reduced infarct size, microglial activation and white matter injury.	(Fahnestock et al., 2019)
	pMCAO	Mouse	I.P., 60' before, 30' and 4 h after	24 h	Neurological score, 24 h	Decreased infarct volume, oxidative stress and improved neurological deficits.	(Morimoto et al., 2005)
	pMCAO	Mouse	I.P., 12 h before or 2 h after	24 h and 72 h	No	Decreased infarct volume.	(Koistinaho et al., 2005)
	tMCAO (45')	Mouse	I.P., 30' and 12 h after, twice per day up to 7	1, 3, 7 and 30 days	Corner and ladder tests, 3, 7 and 30 days	Decreased infarct volume and improved sensorimotor deficits.	(Tang et al., 2007)
	tMCAO (4 h)	Mouse	I.P., once per day up to 14	24 h	Neurologic score 4 h and 1, 7, and 14 days after	Decreased infarct volume and improved neurological deficits.	(Hayakawa et al., 2008)
	Photothromb. Thromboemb.	Mouse	Subcut., 30' before and 2 h after	24 h	No	Decreased infarct volume.	(Park et al., 2011)
	tMCAO (2 h)	Male and female mouse	60' after	48 h	Neurological deficit score and adhesive tape test, 48 h	Decreased infarct volume and improved neurological deficits.	(Hoda et al., 2014)
	tMCAO (1 h)	Mouse	I.P., 12 h before or after	48 h	Bederson test, 48 h	Decreased infarct volume and inflammation and improved neurological deficits.	(Jin et al., 2015)
	pMCAO	Mouse	I.P., 1 h after, once per day up to 3 days	72 h	Neurological score, 72 h	Decreased infarct volume and inflammation and improved neurological deficits.	(Lu et al., 2016)
	Tromboembol. (Thrombin)	ICR mouse	I.P., 60' before	24 h	No	Decreased infarct volume.	(Tanaka et al., 2018)
	tMCAO (3 h)	Mouse	I.P., 1 h or 48 h after	24 h and 5 days	Grip test, 24 h and 5 days	Early treatment reduced infarct volume and improved behavior	(Orieu et al., 2020a)
Natalizumab	tMCAO (3 h)	Rat	I.P., 2 h after	48 h after	Bederson test, 2, 3, 4, 5, 6, 24, and 48 h	peripheral leukocytosis, improves neurological outcome, and decreases infarct volume.	(Becker et al., 2001)
	tMCAO (90')	Rat	I.V, just after	24 h after	No	Improved functional outcome and decreased infarct volume.	(Relton, 2001)
	tMCAO (60')	Hypertens. Rat	I.V, 24 h before	24 h after	No	Decreased infarct volume.	(Relton et al., 2001)
	tMCAO (30' and 60') and pMCAO	Mouse	I.P., 24 h before and 3 h after	1,3 and 7 days	Corner test, 1,3 and 7 days	Improved functional outcome and decreased infarct volume.	(Liesz et al., 2011b)
	tMCAO (30') and pMCAO (electrocog.)	Mouse	I.P., 24 h before and 3 h after	1 and 7 days	Bederson, grip and corner test 1 and 7 days.	No effect	(Langhauser et al., 2014)
	tMCAO (60') and pMCAO (electrocog.)	Mouse	I.P., 3 h after	7 days or 4 days	Rotarod and adhesive removal tests 1,3 and 7 days; or 2 and 4 days.	Reduced leukocyte invasion and infarct volume after pMCAO, no effect after tMCAO.	(Llovera et al., 2015)
	tMCAO (45') and pMCAO (electrocog.)	LysM-eGFP and CXCR1-eGFP mouse	I.V, just after and 24 h after	4 and 7 days	No	Reduced infarct volume and improved functional outcome.	(Llovera et al., 2015)
	Tromboembol. (Thrombin)	Mouse	I.P., 1 h or 48 h after	24 h and 5 days	Grip test 24 h and 5 days	No effect on lesion volume or neurological deficit.	(Orieu et al., 2020a)

(continued on next page)

Table 1 (continued)

Drug	Experimental model	Animal species (*)	Administration route/timing	Lesion volume	Neuromotor deficit	Main results	Ref.
Fingolimod	tMCAO (2 h)	Rat	I.P., just after	1 and 3 days	Neurological score, 1 and 3 days	Reduction in infarct volume and functional deficits.	(Hasegawa et al., 2010)
	tMCAO (1 h)	Rat	I.P., 24 h before and once daily every 2 days	7 days after	Passive avoidance test and neurological score (24 h, 3 and 7 days)	Reduced oedema and neurological score 24 h, 3 and 7 days after.	(Nazari et al., 2016)
	tMCAO (90')	Mouse	I.P. before	24 h	Neurological test, 24 h	Reduction in stroke volume and functional deficits	(Czech et al., 2009)
	tMCAO (60')	Swiss-Webster ND4 mouse	I.P. 30' or 48 h before	24 h	Neurological test, 24 h	Reduction in infarct volume and functional deficits.	(Wacker et al., 2009)
	tMCAO (60')	Mouse	I.P., 5' before and once per day for 3 days	24 h and 4 days	Neurological test, 24 h and 4 days	Reduction in infarct volume.	(Shichita et al., 2009)
	tMCAO (90' and 3 h)	Mouse	I.P. 2 h after	24 h	Neurological test, 24 h	Reduced infarct volume	(Pfeilschifter et al., 2011)
	tMCAO (60') and pMCAO	Mouse	Oral, 48 h before and 3 h after; and I.P. once daily 48 h before	24 h	Croner test, 1, 3 and 7 days	No differences.	(Liesz et al., 2011a)
	tMCAO (90' and 2 h) and pMCAO	Mouse and rats	I.P. 30' after; 1 h or 2, 24 and 48 h after; 2 h or 4 h after in pMCAO	48 h	Wire grip test, 1, 3, 7, 10 and 14 days	Reduced infarct volume; improved neurological function.	(Wei et al., 2011)
	tMCAO (30')	Mouse	I.P., before and after 2 days	1 and 7 days	Ladder rung walking test, 1 and 7 days	Reduced infarct volume and improved neurological function 1 day after.	(Schuhmann et al., 2016)
	tMCAO (60 and 90')	C57 and Rag 1 ^{-/-} mouse	I.P., just before	24 h and 3 days	Bederson and grip test, 1 day	Reduced infarct size and functional improvement 1 day after	(Kraft et al., 2013)
	Thromboemb. (thrombin)	Mouse	I.P. 30', 24 and 48 h after; I.V. 3 h, 24 and 48 h after	3 days	Grid and cylinder test, 3 days	Reduced infarct volume and improved functional outcome.	(Campos et al., 2013)
	tMCAO (180')	Mouse	I.P., before	No	Neurological score 1 day	Higher mortality. Association with IPA performed.	(Cai et al., 2013)
	Photothromb.	Mouse	I.P., twice per day beginning 3 days after up to 5 days	No	Grid and cylinder test, 7, 14, 21 and 31 days	Improvement in functional outcome on day 7 and day 31.	(Brunkhorst et al., 2013)
	Photothromb.	Mouse	I.P., 2 h after and daily	1 and 3 days	Modified neurological severity scores, 7 days	Decreased infarct volume, improved neurological deficits and attenuates autophagic activity.	(Li et al., 2017)
	tMCAO (45')	Mouse	I.P., after	No	Neurological test, 48 h	Attenuated haemorrhagic transformation after ischemia	(Salas-Perdomo et al., 2019)
	Photothromb.	Mouse	I.P., 24 h after and 1, 7 or 14 days	No	Modified neurological severity score up to 14 days	Promoted angiogenesis via microglial M2 polarization and exerted neuroprotection.	(Shang et al., 2020)

(*) Unless specified, animals were young and healthy males.

Table 2
Comparison of the different experimental models of stroke in terms of (i) resemblance to human stroke usually included in randomized clinical trials on stroke, and (ii) experimental advantages and disadvantages.

	Similarities to stroke patients included in RCT*	Differences with stroke patients included in RCT*	Experimental advantages	Experimental disadvantages
Intraluminal monofilament MCAO	<ul style="list-style-type: none"> • No craniotomy needed • Massive ischemic lesion • Localization of ischemic lesion (cortical + subcortical) • High mortality • No clot • Reperfusion injury after filament removal • Rapid, sudden recanalization after filament removal • Ischemic lesion location equivalent to human stroke included in RCT 	<ul style="list-style-type: none"> • Small craniotomy needed 	<ul style="list-style-type: none"> • Control of the duration of the occlusion • Behavioral deficits easily quantifiable 	<ul style="list-style-type: none"> • Transection of the external carotid artery needed (ischemic damages in the unirrigated territories) • Secondary microthrombosis after filament removal • High mortality
Electrocoagulation MCAO	<ul style="list-style-type: none"> • No reperfusion injury • Ischemic lesion location equivalent to human stroke included in RCT 	<ul style="list-style-type: none"> • Small craniotomy needed 	<ul style="list-style-type: none"> • No secondary microthrombosis • Low mortality 	<ul style="list-style-type: none"> • Not suitable for testing thrombolytic drugs • Slight behavioral deficits, not long-lasting
Thromboembolic MCAO- Thrombin injection- FeCl ₃ contact	<ul style="list-style-type: none"> • No reperfusion injury • Ischemic lesion location equivalent to human stroke included in RCT • Real clot (fibrin-rich or platelet-rich) into the lumen of the artery • Possible spontaneous recanalization within 24 h after stroke onset (thrombin model) • Similar time-window response to intravenous tPA (thrombin model) 	<ul style="list-style-type: none"> • Small craniotomy needed 	<ul style="list-style-type: none"> • Good models for testing thrombolytics • No secondary microthrombosis • Low mortality 	<ul style="list-style-type: none"> • Possible uncontrolled early spontaneous recanalization (in situ thrombin injection model) • Slight behavioral deficits, not long-lasting

*RCT (randomized clinical trials) on immunomodulatory/anti-inflammatory drugs; MCAO, Middle Cerebral Artery Occlusion

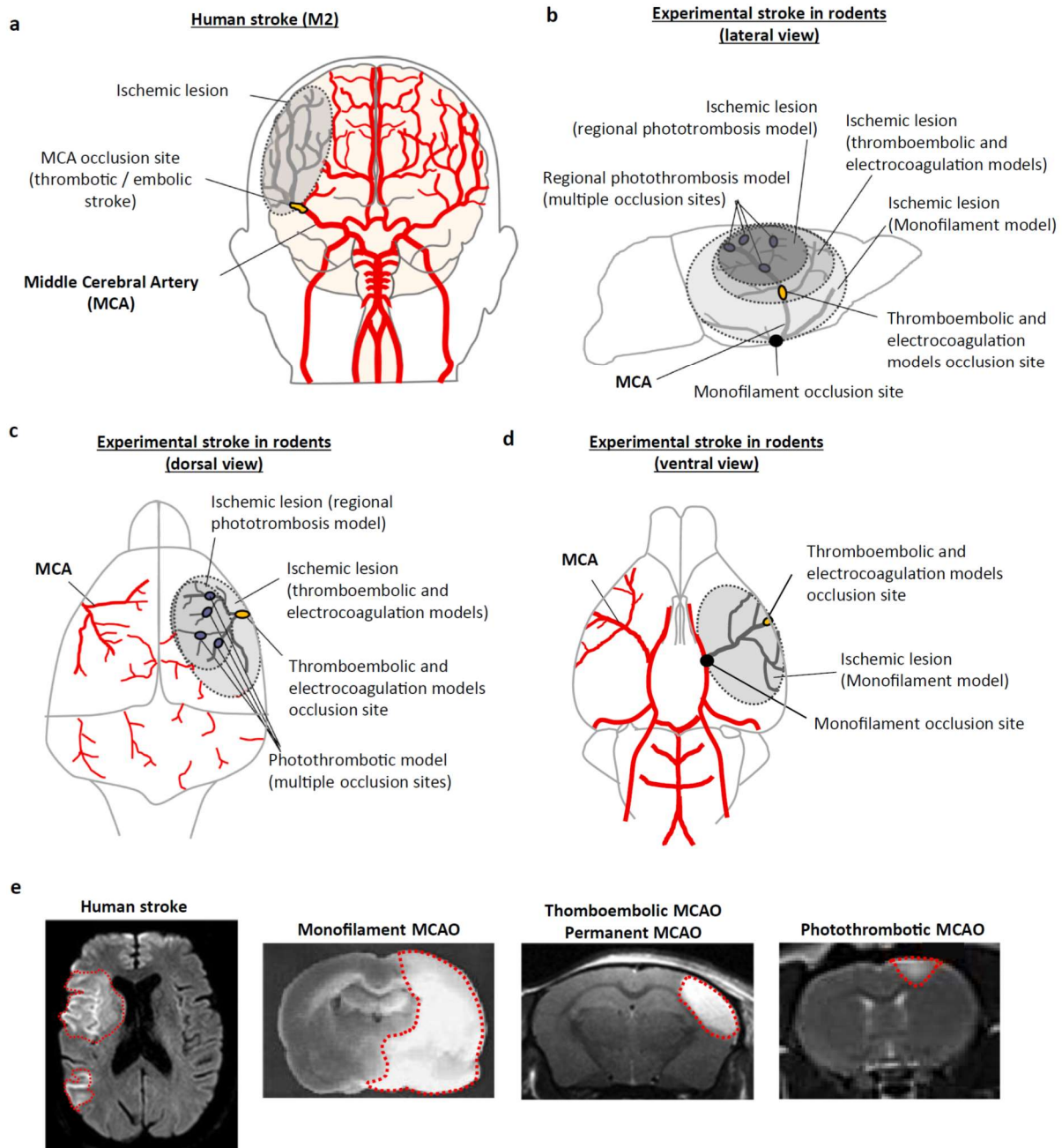


Fig. 2. Comparison of human stroke and experimental models of stroke in rodents. a) Schematic view of the human brain vasculature with one of the most frequent stroke subtypes, a thrombotic/embolic occlusion of the M2 segment of the middle cerebral artery (MCA), usually included in randomized clinical trials (RCT) on immunomodulatory/anti-inflammatory drugs for stroke treatment. b) Schematic view of the rodent brain vasculature (lateral view). In thromboembolic and electrocoagulation experimental stroke models, there is only one site of MCA occlusion, whereas in regional photothrombotic stroke there are multiple occlusion sites within the area illuminated by the laser. In both cases, lesions are limited to the brain cortex. The occlusion site in the monofilament experimental model is located at the origin of the MCA, leading to a bigger ischemic volume including both cortical and subcortical brain regions. c) Schematic view of the rodent brain vasculature (dorsal view). d) Schematic view of the rodent brain vasculature (ventral view). e) Comparison of ischemic lesions (delimited area) visualized by MRI in human stroke (M1-M2 occlusion) and different experimental models of stroke.

neuroinflammation domain in particular, as is the choice of clinically relevant experimental models. We will briefly discuss the main models of middle cerebral artery occlusion (MCAO) used in preclinical research (mechanical occlusion by an intraluminal filament, permanent electrocoagulation, photothrombosis and thromboembolic models).

Attention should be paid on the selection of the most adapted experimental model and the best combination of models for future studies, not only when testing new anti-inflammatory/immunomodulatory drugs, but also in the description of the cellular and molecular mechanisms involved in the pathogenesis of stroke. Each stroke model has

experimental advantages and disadvantages, and shows more or less resemblance to the clinical reality, which have been resumed in Table 2. A descriptive scheme comparing the blockade of the MCA in patients (the MCA being the most common occlusion site in AIS patients) and in experimental models of stroke discussed in this review, as well as the comparison of the corresponding ischemic lesions visualized by MRI, are shown in Fig. 2. In our opinion, and following the STAIR recommendations, the use of several clinically relevant experimental models for a given drug is one of the critical improvements that researchers can implement to ameliorate the translation between pre-clinical and clinical stroke research.

5.1. Mechanical MCAO by an intraluminal filament

The most frequently used experimental model of ischemic stroke in rodents is the intraluminal filament model (Sommer, 2017). To induce MCAO, a nylon filament is introduced into the internal carotid artery and advanced until the origin of the MCA, occluding the blood flow. The filament model does not require craniotomy and can be used to either model permanent ischemia (Chu et al., 2014; Pedragosa et al., 2018) or transient ischemia by withdrawal of the filament, allowing reperfusion at different time points, from 30 min to 120 min (Yan et al., 2015; Buscemi et al., 2019). This model is characterized by a large infarct volume, and longer durations of occlusion usually resulting in larger infarcts involving both the cortex and striatum (see Fig. 2), and may be associated with some mortality (Hata et al., 2000). It often induces hypothalamus damage that rarely occurs in human stroke (Uzdensky, 2018). While researchers see fewer infiltrating leukocytes in general after transient MCAO in compared with some permanent models of occlusion (Zhou et al., 2013), the inflammatory response, especially once BBB injury occurs is substantial in this model and includes excessive leukocyte recruitment and production of inflammatory cytokines. Thousands of anti-inflammatory molecules have been tested in this model and have shown beneficial effects on ischemic volume and/or neurological outcome. Unfortunately, very few, if any, have so far shown real clinical benefit so far.

This model typically shows a prompt recovery of a primary core, whereas a sudden and rapid reperfusion results in a secondary, delayed injury, known as “ischemia–reperfusion injury”. Indeed, it has been shown that 70% of the lesion volume in this experimental model is in fact due to the formation of microthrombi after to the withdrawal of the filament (Gauberti et al., 2014a, 2014b). This delayed injury evolves after a free interval of as long as 6 to 12 h, which confers to this experimental setup a longer therapeutic window compared to the human pathophysiology or to other experimental stroke models.

The prompt reperfusion of the MCA after the removal of the filament contrasts with the gradual reperfusion occurs in many non-treated human ischemic stroke (Hossmann, 2012); however, even after mechanical thrombectomy the secondary damage has not been observed in patients. Using the data from one randomized trial, Gauberti et al. (Gauberti et al., 2018) measured the impact of abrupt reperfusion on infarct growth in patients that benefited from mechanical thrombectomy. No growth in ischemic lesion after abrupt reperfusion was observed. Moreover, in most of the patients the impact of ischemia–reperfusion injury on the lesion growth was limited during the first 24 h. Considering the fact that reperfusion injury plays a prominent role in the mechanical MCAO models, this discovery questions the relevance of the filament model as well as the current understanding of the human stroke pathophysiology.

5.2. MCAO by electrocoagulation

The MCAO by electrocoagulation is another of the most frequently used stroke models (Howells et al., 2010). This model consists of the permanent occlusion of the MCA using electrical stimulation, which induces the coagulation of the artery. It is usually followed by the

dissection of the artery to avoid any risk of recanalization. A craniotomy is necessary in order to access the MCA. This experimental model does not induce the presence of a penumbra area. The lesion is smaller than in the monofilament model and is confined to the cortical area (see Fig. 2). The resulting infarct volume and localization after permanent MCA coagulation corresponds to ischemic brain lesions in the majority of human strokes in proportion to brain size (Llovera et al., 2014).

The inflammatory reaction described in this model is greater than in the filament model, although it could be overestimated due to the confounding effects of electrocoagulation. The microglial activation is more important, as is leukocyte infiltration. This inflammatory response is also exacerbated in terms of pro-inflammatory cytokines and adhesion molecules expression (Zhou et al., 2013). However, only minor behavioral deficits can be detected in behavioral tests and functional recovery appears within the first days after stroke. That makes it difficult to assess long-term functional outcome in this model (Llovera et al., 2014).

5.3. Photothrombosis model

Photothrombosis stroke model involves the focal illumination of cerebral vessels through the skull after intravenous injection of a photosensitive dye (Watson et al., 1985). The photosensitive dye (Rose Bengal or erythrosin B) is first administered intraperitoneally in mice or intravenously in rats. Then, photo activation of the dye leads to formation of oxygen free radicals, such as singlet oxygen and superoxide, resulting in endothelial damage and platelet activation and aggregation in all the vessels within the illuminated area (Kim et al., 2000). This model does not require a craniotomy, since the light source can be applied directly and passes through the skull. It produces a small-size and well-defined cortical lesion (Labat-gest and Tomasi, 2013) (Fig. 2). Moreover, it does not require mechanical manipulations with blood vessel such as ligation or filament insertion, which carry the risk of side lesions.

It was shown in this model microglial activation, lymphocyte infiltration and an increase in the level of pro-inflammatory cytokines up to 14 days after the occurrence of ischemic stroke (Feng et al., 2017). Moreover, this model induces long-term sensorimotor deficits with high survival (Lunardi Baccetto and Lehmann, 2019), which may be useful to study late inflammatory process involved in recovery and regeneration after stroke.

However, disadvantages of this stroke model are major differences from the ischemic stroke pathology. The injury caused by photothrombosis presents simultaneously early acute cytotoxic and vasogenic edema, microvascular injury and blood–brain barrier breakdown (Lee et al., 1996). Additionally, this model causes well-defined ischemic lesion without the penumbra area typically present in stroke pathology.

5.4. Thromboembolic models

Several thromboembolic models exist. A previously formed clot (by autologous or heterologous blood) can be directed to the base of the MCA (Ansar et al., 2014). A clot can also be created by the application of iron or aluminum chloride to the artery (Bonnard and Hagemeyer, 2015). Another model of thromboembolic stroke consists in injecting thrombin directly into the MCA by using a micropipette, which causes the *in situ* formation of a fibrin-rich clot (Orset et al., 2007; Le Behot et al., 2014). These fibrin-rich clots may be spontaneously lysed (partially or completely), as occurs in non-treated patients (Drieu et al., 2020a, 2020b). Infarct volume and localization after both ferric chloride and thrombin models correspond to ischemic brain lesions in the majority of human strokes in proportion to brain size. As in humans, the lesion is mostly cortical and well defined (see Fig. 2), with the presence of a *peri*-lesional area that can be saved by early-tPA fibrinolysis in the thrombin-induced thromboembolic model (Orset et al.,

2007; Macrez et al., 2011; Orset et al., 2016). The thrombin model is the only one to have shown a similar profile of time-to-treatment-related benefit after tPA administration (Orset et al., 2007; Macrez, 2011; Orset et al., 2016). By contrast, clots formed by the ferric chloride thromboembolic model are platelet-rich and cannot be lysed by tPA (Martinez de Lizarrondo et al., 2017).

We have recently provided a detailed longitudinal description of the inflammatory response following the thrombin-induced stroke experimental model consisting in an early myeloid response peaking at 48 h after stroke onset and still present (although to a lesser extent) 5 days after stroke onset. T-lymphocytes infiltrate later on (from 48 h after stroke onset). These cellular responses are accompanied by EC activation at 24 h–48 h that is not present later on (5 days after stroke onset). Whereas ischemic lesions are maximal at 24–48 h after stroke onset, BBB leakage progressively increases with time, being maximal at 5 days after stroke (Drieu et al., 2020a, 2020b).

Regarding translational issues, thromboembolic models are, in many aspects, closer to the human pathophysiology (see table 2) and may thus provide an opportunity to investigate not only fibrinolytic drugs but also strategies targeting inflammation and immune responses triggered after stroke onset. In this regard, the thrombin-induced stroke model has shown similarities with the results obtained in several RCT. In addition to the aforementioned results on tPA, Natalizumab, which has shown its effectiveness in several other models before failing in the clinic, is not beneficial in the thrombin model of stroke (Drieu et al., 2020a, 2020b), but minocycline has shown promising results (Drieu et al., 2020a, 2020b) as in humans (Malhotra et al., 2018). Apart from this, there is not hindsight enough on the use of the thrombin model to demonstrate a better translation into the clinic compared to other experimental models. For this reason, and as recommended by the STAIR roundtable, several stroke models should be tested in multicenter studies for a given drug before its translation into randomized clinical trials.

Similar to the electrocoagulation model, one drawback of these models is the low behavioral deficits. Only minor behavioral deficits can be detected in the first days after stroke with behavioral tests and functional recovery appears after few days. This currently makes it difficult to assess long-term functional results. It would be necessary to further characterize the functional deficits of this model over the long term, especially in the context of the study of late inflammatory response and recovery.

ii) Timing and selection of outcome measuring

The timing of outcome assessment is another factor that contributes to contradictory results between mouse and human studies. While in most clinical studies the neurological outcome is measured in patients up to several months after the stroke (usually 90 days), a vast majority of preclinical studies in mice focus only on the first days after the stroke (Veltkamp and Gill, 2016; Dreikorn et al., 2018).

The inflammatory reaction participates in each stage of stroke pathophysiology. It takes place from the first minutes after occlusion and lasts until the late phase, including the recovery and regeneration processes. This is why we should use behavioral tests, which measure functional recovery at longer time points, if we want preclinical studies to be more transposable to the clinic. As aforementioned, the main obstacle is that in mice it is difficult to obtain observable neurological deficits for a long time, in models with young animals with cortical well-standardized lesions. Furthermore, while recovery processes in rodents can be completed 4 weeks post-stroke, in humans they occur within about 3 months and may continue for years (Sommer, 2017; Cassidy and Cramer, 2017).

In spite of these difficulties, recent studies have shown encouraging results for mouse to human translation. For example, Sadler and collaborators (Sadler et al., 2020) have demonstrated the impact of short-chain fatty acids on microglial activation, which depended on the

recruitment of T cells to the infarcted brain. Using an automated task for the training and assessment of distal forelimb function (Becker et al., 2016) in a mouse model of photothrombotic stroke, differences in motor deficit were observed up to 56 days after stroke onset. Another study has recently shown that targeting integrin alpha-9-beta-1 (highly expressed on activated neutrophils during ischemic stroke) significantly improved short and long-term functional outcomes (up to 4 weeks) in two different stroke models with pre-existing comorbidity (Dhanesha et al., 2020).

This being said, the STAIR X recommendations have highlighted that the time point of the standard 90-day functional outcome may be reconsidered for different reasons. First, it may result in enrollment bias, as socioeconomic and other factors may involve recruitment of only certain individuals into prospective trials. Furthermore, evaluation at later time points exclude patients that might succumb due to the other illnesses. Also, the impact of acute stroke interventions may be more efficiently revealed by early improvements in clinical deficits. Early National Institutes of Health Stroke Scale improvement or the serial change in neurological deficits from baseline to 24 h provides an early indication of what might ensue at 90 days, although early evaluation may raise challenges in some cases, as intubated or other patients may not be evaluable (Liebeskind et al., 2018).

An additional issue on the translation between preclinical and clinical studies is to deal with the discrepancies between the very specific and sensitive outcome measurements (histological, different imaging techniques and/or specific and sophisticated behavior tests) in preclinical research versus the well-established but yet less sensitive standardized clinical scores (composite scores, mRS, etc). In fact, it is possible that some of the positive results found in preclinical research are not strong enough to be detected in the neurological or functional outcome measurements in clinical practice. This is why it is important, in our opinion, to perform several outcome measurements for every drug tested. In addition, multicenter studies may help to increase the relevance of the preclinical results.

iii) Entry routes for leukocytes into the ischemic region.

In the past few years, research on anti-inflammatory strategies for stroke has focused on limiting the transendothelial migration of peripheral immune cells into the brain parenchyma, aiming to reduce stroke severity. These studies are based on the idea of endothelial transmigration of peripheral immune cells through the BBB, but new evidence suggests that there are other pathways at least just as important (if not more): migration through the meninges and choroid plexus (ChP), (for a complete review, see (Benakis et al., 2018).

The ChP is originally known as the main producer of CSF, which fills all brain ventricles, subarachnoid spaces and perivascular spaces and thereby reaches a large surface area of the CNS. This highly vascularized brain structure resides in the brain ventricles and consists of an epithelial layer forming a tight blood-cerebrospinal fluid barrier (BCSFB), which surrounds a core of fenestrated capillaries and connective tissue. However, data is accumulating that CNS specific immune processes like immune surveillance are regulated by the ChP (Ghersin-Gege et al., 2018). First, it has been demonstrated by Ge and collaborators that ChP responds to a cortical ischemic lesion by elevated adhesion molecules and chemokines, and that monocytes-derived macrophages can invade ischemic hemisphere through ChP and CSF (Ge et al., 2017). Furthermore, it has been shown the ChP is a key invasion route for T-cell to the cortex in a permanent electrocoagulation stroke model, via a CCR2-ligand dependent mechanism (Llovera et al., 2017).

In addition to this, several recent studies have shown that the meninges could be a major player in leukocyte infiltration into the brain parenchyma. Immunohistochemistry and flow cytometry analysis revealed that $\gamma\delta$ T cells increased in the meninges early after stroke onset (Benakis et al., 2016) and preceded their accumulation in the ischemic

area (Gelderblom et al., 2014). Moreover, ischemic injury can induce the growth of meningeal lymphatic vessels (LVs) and the absence of these LVs impact post-stroke outcomes. Interestingly, only photo-thrombotic stroke (and not transient MCAO) induce lymphangiogenesis. However, removal of meningeal lymphatics exacerbates severity of stroke, only in the transient MCAO model (Yanev et al., 2020). These data indicate that the meninges could orchestrate leukocyte infiltration into the brain parenchyma.

Taken together, these recent studies reveal the previously unrecognized diversity of selective invasion routes for leukocyte sub-populations after stroke. Understanding how immune cells migrate to the brain via these alternative pathways may help us to develop more effective approaches for anti-inflammatory/immunomodulatory stroke therapies. As discussed above, several clinical trials have been initiated using Enlimomab (anti-ICAM-1 antibody), Natalizumab (anti-CD49d) or Fingolimod (FTY720). While Fingolimod (FTY720) could reduce the infarct volume and improve recovery, Natalizumab and enlimomab failed to show an effect on their primary endpoints (Fu et al., 2015; Elkins et al., 2017; Enlimomab Acute Stroke Trial Investigators, 2001). One of the reasons for these discrepancies might be due to the incomplete concept that lymphocytes infiltrate the brain mainly via the transendothelial route of parenchymal capillaries, without considering the meninges and ChP. Natalizumab and Enlimomab aimed to block the lymphocyte entrance to the CNS by blocking specific adhesion molecules required for transendothelial migration across parenchymal vessels. However, VCAM as well as ICAM-1 are not expressed on ChP EC (Steffen et al., 1996). Hence, lymphocytes in the ChP vasculature have no access to these adhesion molecules and blocking of these will not affect the ChP infiltration route (Benakis et al., 2018). In contrast, Fingolimod works by promoting lymphocyte retention in the thymus and lymph nodes (Mandala et al., 2002) and thus reduces the number of circulating lymphocytes independently of adhesion molecules expression at the various migration routes, which might explain why currently the only positive results on treatment efficacy are obtained with this drug in patients with stroke (Benakis et al., 2018). This could also explain the promising results obtained with minocycline treatment. Indeed, minocycline exerts anti-inflammatory effects on several targets, notably microglial activation, which do not depend on the migration route of peripheral immune cells (Malhotra et al., 2018). Thus, therapeutic targets should then be identified by focusing on compounds which act directly on circulating immune cells rather than on the different adhesion molecules, to maximize effectiveness across all of the entry pathways.

iv) Factors affecting stroke outcome

Last, but not less important, several factors affecting stroke outcome are usually neglected in stroke preclinical research from an inflammatory perspective. In this review, we are going to summarize some of them: gender differences, ageing, pre-stroke infections, comorbidities such as hypertension and diabetes, and external factors related to daily life e.g. obesity, tobacco and alcohol consumption. In our opinion, inclusion of these comorbidities in preclinical research would increase the value, robustness and translational potential of the results.

As can be seen in the literature reviewed in this paper, the vast majority of the preclinical data has been obtained in young male mice/rats. However, while stroke in general is more common in men than women within the young and middle-aged population, women have a higher lifetime risk of stroke than men (20–21% versus 14–17%) with poorer functional outcomes (Guzik and Bushnell, 2017). Furthermore, the risk of stroke in women is correlated with ageing, particularly after 65 years compared to men (Appelros et al., 2009). This could partially explain women having more severe ischemic stroke in addition to age-related factors such as atrial fibrillation (Phan et al., 2019; Marzona et al., 2018).

Regarding the preclinical data, it has been shown in rodents, that premenopausal females exhibit smaller infarct sizes than age-matched males. Estrogen, the primary ovarian hormone has been described as a key element as the treatment with this hormone in the male or ovariectomized animals has shown to reduce infarct and neuronal death following ischemia and to decrease proinflammatory cytokines (Wise et al., 2001; Liu et al., 2012). Thus, besides the hormonal changes observed with estrus cycle, evidence as well as the STAIR recommendations (Fisher, 2003), indicate gender as an important biological variable to be addressed in stroke research.

As aforementioned, most of the preclinical stroke data has been obtained in young and healthy animals and to date, studies on the effectiveness of anti-inflammatory/immunomodulatory drugs in co-morbid animals are limited. Concerning the drugs reviewed here (see Table 1), there is only one study on the effects of Anakinra in young vs aged and Corpulent rats (a model of atherosclerosis, obesity and insulin resistance) (Pradillo et al., 2017), and another one on Minocycline in hypertensive rats (Yang et al., 2015), and one on Natalizumab in hypertensive rats (Relton et al., 2001). These studies have been performed on the transient MCAO model of stroke and have shown beneficial effects of the tested drug in these co-morbid animals.

With the life expectancy increase of the population, ageing has become a principal risk factor for ischemic stroke, with incidence rates accelerating exponentially above 70 years (Sandu et al., 2017). Interestingly, the neuroprotection has been related to anti-inflammation in young brain but related to proinflammation in the aged brain, with reduced microglial proliferation, attenuated macrophage cytokine production, and recruitment of macrophages in ischemic injury (Kim and Cho, 2016). Ageing has impact on immune cells; it is well known that aging is associated with an increase in basal inflammation in the CNS, overall decline in cognitive function, and poorer recovery following injury. Aged rodents had increased brain injury and increased CD8 + T cells in the aged CNS were associated with compromised proinflammatory functions in microglia. The primed microglia increased the inflammation and leukocyte recruitment in the brain following stroke in a gender independent manner (Ritzel et al., 2016). Consistent with this evidence, several *in vivo* studies have shown that brain of aged mice have increased proinflammatory and decreased anti-inflammatory profiles (Tang et al., 2014) or increased numbers of M2 macrophages in lymph nodes, bone marrow and spleen (Jackaman et al., 2013; Kim and Cho, 2016).

Another risk factor related to stroke is infection preceding stroke. Thromboinflammatory (platelet-mediated) processes beyond infection are likely to be an important contributor to stroke pathophysiology. Although several infections are documented to increase stroke risk, such as *Herpes simplex* 1 and 2, cytomegalovirus, Epstein-Barr virus, *Hemophilus influenzae*; or *Mycoplasma pneumoniae* and *Helicobacter pylori*, controversial results are also found. For instance, by the results obtained in the Northern Manhattan Study, it is described that patients with high chronic infectious burden showed 1.4-fold increased risk of stroke (Elkind et al., 2010). However, others have not replicated the results (Palm et al., 2016; Parikh et al., 2020). More recently, although additional research is required, Covid-19 infection has been shown to increase the risk (or probability) of stroke as well. Several studies have been conducted in China. For instance, a retrospective study of data from the Covid-19 outbreak in Wuhan, China, showed that the incidence of stroke among hospitalized Covid-19 patients was approximately 5%. Another retrospective study has shown that among 221 patients with Covid-19, 13 (5.9%) developed cerebrovascular diseases after the infection. Out of these patients, 11 (84.6%) were diagnosed with ischemic stroke. Another study has reported that cryptogenic stroke was confirmed in 32 of 3556 hospitalized patients with positive Covid-19 test. (Qin et al., 2020; Oxley et al., 2020; Mao et al., 2020). Other countries have shown evidences on this line as well, like the observational study conducted in New York, in which 32 (0.9%), out of 3556 hospitalized patients with diagnosis of Covid-19 infection, had

imaging-proven ischemic stroke (Yaghi et al., 2020). A retrospective cohort study from two New York City academic hospitals, approximately 1.6% of adults with COVID-19 who visited the emergency department or were hospitalized experienced ischemic stroke (Merkler et al., 2020). Other study conducted in Italy has shown that among 388 patients with confirmed COVID-19, 9 patients experienced ischemic stroke (Lodigiani et al., 2020). Data from a Spanish hospital has shown that the incidence of CVD among the patients with COVID-19 infection was 1.4% of which the 73.9% were classified as cerebral ischemia (Hernández-Fernández et al., 2020). Thus, even if more research in the field is needed, the presence of infectious diseases seems to be a factor to be taken into account as well, while working in stroke therapies.

Besides gender and aging, there are several modifiable comorbidities related to stroke that should also be considered. For instance, hypertension is the most common modifiable risk factor for stroke, affecting about one-third of US adults over 20 years. Although most of them are aware, only about half have blood pressure controlled regularly (Guzik and Bushnell, 2017). Hypertension increases endothelial oxidative stress and inflammation, and it leads to worse stroke outcomes and higher mortality. Studies investigating the underlying pathophysiology of hypertension indicate the involvement of neuroimmune interactions (Kim and Cho, 2016), but mechanisms linking the immune responses to hypertension are still vague. The inclusion of rodent models of hypertension, such as spontaneously hypertensive rats (SHR), salt-induced hypertension model, or Angiotensin II-induced hypertension model (Lopez Gelston and Mitchell, 2017), in stroke preclinical research would help to correct translation of the data to RCT.

Similarly, disorders of glucose metabolism are major risk factors for stroke, including type 1 and type 2 diabetes mellitus (Guzik and Bushnell, 2017). These disorders are highly prevalent in patients with stroke: 25–45% of the patients have diabetes mellitus (Kernan et al., 2014). Data on diabetic patients in stroke clinical trials are missing. Meta-analysis of prospective studies showed a hazard ratio of 2.27 for ischemic stroke in diabetics compared to non-diabetics (Emerging Risk Factors Collaboration et al., 2010). Furthermore, diabetes has also shown a Hazard Ratio of 1.59 for stroke recurrence (Kaplan et al., 2005). In animal models, acute hyperglycemia immediately before or during ischemia exacerbates the ischemic brain injury. Elevated proinflammatory cytokines; tumor necrosis factor- α (TNF- α), interleukin-1 (IL-1), interleukin-6 (IL-6), and interferon- γ (IFN- γ), as well as altered activation of macrophages, T cells, natural killer cells, and other immune cell populations are associated with major comorbidities (including diabetes) for stroke (Shukla et al., 2017).

Regarding the life style of the actual society, there are several habits that influence on stroke risk from the inflammatory point of view, which cannot be neglected. Obesity, characterized by a body mass index (BMI) of at least 30 kg/m², is largely a consequence of fat-rich diet and physical inactivity and is associated with several risk factors including inflammation, metabolic syndrome, hypertension, diabetes and hypercholesterolaemia (Sandu et al., 2017). It has been demonstrated that obesity increases levels of pro-inflammatory mediators such as Interleukin 6 or C-reactive protein, causing a chronic inflammation, which is linked to a higher stroke risk and worse outcome (Haley and Lawrence, 2016). Efforts are being done to improve the stroke translational research. For instance, Pradillo et al (Pradillo et al., 2017) reported the improvement of stroke outcome through the administration of the IL-1Ra after stroke in control and overweight Wistar rats.

Other life-style risk factors are tobacco and alcohol consumption. It is well known that current smokers have more than doubled risk of stroke, with an apparent dose–response relationship seen (Guzik and Bushnell, 2017). Focusing on alcohol consumption, alcohol has emerged as a potentially important factor with a J- or U-shaped association to stroke risk. Epidemiological studies suggest that low-moderate ethanol intake lowers the incidence of ischemic stroke, reduces mortality and infarct volume from ischemic stroke, whereas heavy

ethanol consumption increases the incidence of ischemic stroke and worsens the prognosis of ischemic stroke. Chronic ethanol consumption dose-dependently affects both incidence and prognosis of stroke (Xu et al., 2019). Although the association between alcohol and cardiovascular diseases has been a point of interest since 3 decades ago, there are still considerable gaps in this area. Heavy alcohol consumption > 2 drinks/day on average in midlife increases stroke risk, especially shortly after baseline (on average 50 years) until the age of 75 years, and may shorten time to stroke by \approx 5 years regardless of familial and other common confounds. Although often neglected as a risk factor, heavy drinking in midlife is at least comparable with well-known risk factors of stroke such as diabetes mellitus or hypertension (Kadlecová et al., 2015). Studies in animal models have shown that ethanol may affect both basal and post-ischemic inflammatory profile in the brain (Drieu et al., 2020a, 2020b). In a recent translational study, the chronic exposure to alcohol in both humans and mice has shown to exacerbate ischemic lesions (Drieu et al., 2020a, 2020b). The preclinical results of this study have shown that alcohol consumption itself provokes a neurovascular inflammatory priming. The term “priming” is used to describe the propensity of a particular cell type to make an exaggerated response to a secondary stimulus at the parenchymal, perivascular and vascular levels whose consequence could be the exacerbated response to the ischemic injuries. In humans, chronic alcohol drinking (\geq 6 drinks/day in the last 5 years) has been independently associated (a) to stroke severity baseline, (b) to early neurological deterioration (END, defined as the increase of NIHSS in \geq 4 in the first 48 h after admission), and (c) to higher infarct volume in stroke patients. Beyond the significance of these results on alcohol consumption and stroke outcome, these results highlight the decisive impact of the “basal” inflammatory state preceding stroke.

6. Conclusions

We must acknowledge that we are still far from the complete understanding of the role of inflammation and immune responses to stroke. Several studies have described the inflammatory and immune responses after stroke in different experimental models (Gelderblom et al., 2009; Zhou et al., 2013; Drieu et al., 2020a, 2020b) and humans and it is undeniable that neuroinflammation and immune responses are present minutes after stroke onset and last for months or even years. Moreover, anti-inflammatory and immunomodulatory therapies have shown beneficial effects in some of the experimental models (in particular, in the intraluminal filament model). Some of these molecules have been tested in RCT but have failed to show positive results in stroke patients. This fact suggests that the mechanisms through which inflammatory processes contribute to injury after stroke are not well understood and could reflect a mismatch between the burden of inflammation in these particular experimental models and in stroke patients. It is also possible that the different experimental approaches actually model different aspects of the disease, which highlights the importance of testing drugs in several clinically relevant experimental models before their translation to clinical trials. In the past years, several studies have followed this guideline (Martinez de Lizarrondo et al., 2017; Llovera et al., 2015). Furthermore, the development of multicenter preclinical studies would help to definitely confirm the potential preclinical positive results before proceeding to clinical trials. Moreover, the burden of comorbidities (ageing, inflammatory states preceding stroke, etc) is often neglected in experimental studies and, thus, far from the clinical reality of stroke patients. Therefore, we encourage scientists to increase the knowledge in this field, before going ahead to clinical research.

We need to better understand the involvement of inflammation/immune system in stroke with the final aim of modulating it and improving the pharmacological approaches available. For this, the choice of clinically relevant experimental models of stroke; the inclusion of measurements including acute but also long-term quantification of

infarct volume and behavioral outcome; performing multicenter studies; and the inclusion of coexisting risk factors, are mandatory before considering the translation of a new stroke therapy into randomized clinical trials. In conclusion, in our opinion, as well as other authors', (Chamorro et al., 2016; Shi et al., 2019), all the above-mentioned parameters should be considered when working in the stroke preclinical and clinical research field. This will improve the liability and translational strength of the results.

Acknowledgements

MG is a PhD student from the European Union's Horizon 2020 research and innovation programme under the Marie Skłodowska-Curie grant agreement No. 813294. DL and AL are PhD students from the Region Normandie.

Appendix A. Supplementary data

Supplementary data to this article can be found online at <https://doi.org/10.1016/j.bbi.2020.09.025>.

References

- Anrather, J., Iadecola, C., 2016. Inflammation and stroke: an overview. *Neurother. J. Am. Soc. Exp. Neurother.* 13, 661–670. <https://doi.org/10.1007/s13311-016-0483-x>.
- Ansar, S., Chatzikonstantinou, E., Wistuba-Schier, A., Mirau-Weber, S., Fatar, M., Hennerici, M.G., Meairs, S., 2014. Characterization of a new model of thromboembolic stroke in C57 black/6J mice. *Transl. Stroke Res.* 5, 526–533. <https://doi.org/10.1007/s12975-013-0315-9>.
- Appelros, P., Stegmayr, B., Terént, A., 2009. Sex differences in stroke epidemiology: a systematic review. *Stroke* 40, 1082–1090. <https://doi.org/10.1161/STROKEAHA.108.540781>.
- Aras, M., Urfali, B., Serarslan, Y., Ozgür, T., Ulutaş, K.T., Urfali, S., Altaş, M., Yılmaz, N., 2013. Protective effects of minocycline against short-term ischemia-reperfusion injury in rat brain. *Pediatr. Neurosurg.* 49, 172–178. <https://doi.org/10.1159/000362202>.
- Becker, A.M., Meyers, E., Sloan, A., Rennaker, R., Kilgard, M., Goldberg, M.P., 2016. An automated task for the training and assessment of distal forelimb function in a mouse model of ischemic stroke. *J. Neurosci. Methods* 258, 16–23. <https://doi.org/10.1016/j.jneumeth.2015.10.004>.
- Becker, K., Kindrick, D., Relton, J., Harlan, J., Winn, R., 2001. Antibody to the alpha4 integrin decreases infarct size in transient focal cerebral ischemia in rats. *Stroke* 32, 206–211. <https://doi.org/10.1161/01.str.32.1.206>.
- Benakis, C., Brea, D., Caballero, S., Faraco, G., Moore, J., Murphy, M., Sita, G., Racchumi, G., Ling, L., Pamer, E.G., Iadecola, C., Anrather, J., 2016. Commensal microbiota affects ischemic stroke outcome by regulating intestinal $\gamma\delta$ T cells. *Nat. Med.* 22, 516–523. <https://doi.org/10.1038/nm.4068>.
- Benakis, C., Llovera, G., Liesz, A., 2018. The meningeal and choroidal infiltration routes for leukocytes in stroke. *Ther. Adv. Neurol. Disord.* 11. <https://doi.org/10.1177/1756286418783708>.
- Bonnard, T., Hagemeyer, C.E., 2015. Ferric chloride-induced thrombosis mouse model on carotid artery and mesentery vessel. *J. Vis. Exp. JoVE* e52838. <https://doi.org/10.3791/52838>.
- Brunkhorst, R., Kanaan, N., Koch, A., Ferreiros, N., Mirceska, A., Zeiner, P., Mittelbronn, M., Derouiche, A., Steinmetz, H., Foerch, C., Pfeilschifter, J., Pfeilschifter, W., 2013. FTY720 treatment in the convalescence period improves functional recovery and reduces reactive astrogliosis in photothrombotic stroke. *PLoS One* 8, e70124. <https://doi.org/10.1371/journal.pone.0070124>.
- Buscemi, L., Price, M., Bezzi, P., Hirt, L., 2019. Spatio-temporal overview of neuroinflammation in an experimental mouse stroke model. *Sci. Rep.* 9, 507. <https://doi.org/10.1038/s41598-018-36598-4>.
- Cai, A., Schlunk, F., Bohmann, F., Kashefiolasi, S., Brunkhorst, R., Foerch, C., Pfeilschifter, W., 2013. Coadministration of FTY720 and rt-PA in an experimental model of large hemispheric stroke-no influence on functional outcome and blood-brain barrier disruption. *Exp. Transl. Stroke Med.* 5, 11. <https://doi.org/10.1186/2040-7378-5-11>.
- Cai, W., Liu, S., Hu, M., Huang, F., Zhu, Q., Qiu, W., Hu, X., Colello, J., Zheng, S.G., Lu, Z., 2020. Functional dynamics of neutrophils after ischemic stroke. *Transl. Stroke Res.* 11, 108–121. <https://doi.org/10.1007/s12975-019-00694-y>.
- Cai, Z., Lin, S., Fan, L.-W., Pang, Y., Rhodes, P.G., 2006. Minocycline alleviates hypoxic-ischemic injury to developing oligodendrocytes in the neonatal rat brain. *Neuroscience* 137, 425–435. <https://doi.org/10.1016/j.neuroscience.2005.09.023>.
- Cai, Z.-Y., Yan, Y., Chen, R., 2010. Minocycline reduces astrocytic reactivation and neuroinflammation in the hippocampus of a vascular cognitive impairment rat model. *Neurosci. Bull.* 26, 28–36. <https://doi.org/10.1007/s12264-010-0818-2>.
- Cai, Z.-Y., Yan, Y., Sun, S.-Q., Zhang, J., Huang, L.-G., Yan, N., Wu, F., Li, J.-Y., 2008. Minocycline attenuates cognitive impairment and restrains oxidative stress in the hippocampus of rats with chronic cerebral hypoperfusion. *Neurosci. Bull.* 24, 305–313. <https://doi.org/10.1007/s12264-008-0324-y>.
- Campos, F., Qin, T., Castillo, J., Seo, J.H., Arai, K., Lo, E.H., Waerber, C., 2013. Fingolimod reduces hemorrhagic transformation associated with delayed tissue plasminogen activator treatment in a mouse thromboembolic model. *Stroke* 44, 505–511. <https://doi.org/10.1161/STROKEAHA.112.679043>.
- Cardoso, M.M., Franco, E.C.S., de Souza, C.C., da Silva, M.C., Gouveia, A., Gomes-Leal, W., 2013. Minocycline treatment and bone marrow mononuclear cell transplantation after endothelin-1 induced striatal ischemia. *Inflammation* 36, 197–205. <https://doi.org/10.1007/s10753-012-9535-5>.
- Casetta, I., Fainardi, E., Saia, V., Pracucci, G., Padroni, M., Renieri, L., Nencini, P., Inzitari, D., Morosetti, D., Sallustio, F., Vallone, S., Bigliardi, G., Zini, A., Longo, M., Francalanza, I., Bracco, S., Vallone, I.M., Tassi, R., Bergui, M., Naldi, A., Saletti, A., De Vito, A., Gasparotti, R., Magoni, M., Castellán, L., Serrati, C., Menozzi, R., Scoditti, U., Causin, F., Pieroni, A., Puglielli, E., Casalena, A., Sanna, A., Ruggiero, M., Cordici, F., Di Maggio, L., Duc, E., Cosottini, M., Giannini, N., Sanfilippo, G., Zappoli, F., Cavallini, A., Cavin, N., Critelli, A., Ciceri, E., Plebani, M., Cappellari, M., Chiumarulo, L., Petruzzellis, M., Terrana, A., Cariddi, L.P., Burdi, N., Tinelli, A., Auteri, W., Silvagni, U., Biraschi, F., Nicolini, E., Padolecchia, R., Tassinari, T., Filauri, P., Sacco, S., Pavia, M., Invernizzi, P., Nuzzi, N.P., Marcheselli, S., Amistà, P., Russo, M., Galesio, I., Craparo, G., Mannino, M., Mangiafico, S., Toni, D., Registry of Endovascular Treatment in Acute Stroke, I., 2020. Endovascular thrombectomy for acute ischemic stroke beyond 6 hours from onset: a real-world experience. *Stroke* 51, 2051–2057. <https://doi.org/10.1161/STROKEAHA.119.027974>.
- Cassidy, J.M., Cramer, S.C., 2017. Spontaneous and therapeutic-induced mechanisms of functional recovery after stroke. *Transl. Stroke Res.* 8, 33–46. <https://doi.org/10.1007/s12975-016-0467-5>.
- Chamorro, Á., Dirnagl, U., Urra, X., Planas, A.M., 2016. Neuroprotection in acute stroke: targeting excitotoxicity, oxidative and nitrosative stress, and inflammation. *Lancet Neurol.* 15, 869–881. [https://doi.org/10.1016/S1474-4422\(16\)00114-9](https://doi.org/10.1016/S1474-4422(16)00114-9).
- Cho, K.-O., La, H.O., Cho, Y.-J., Sung, K.-W., Kim, S.Y., 2006. Minocycline attenuates white matter damage in a rat model of chronic cerebral hypoperfusion. *J. Neurosci. Res.* 83, 285–291. <https://doi.org/10.1002/jnr.20727>.
- Chu, H.X., Kim, H.A., Lee, S., Moore, J.P., Chan, C.T., Vinh, A., Gelderblom, M., Arumugam, T.V., Broughton, B.R.S., Drummond, G.R., Sobey, C.G., 2014. Immune cell infiltration in malignant middle cerebral artery infarction: comparison with transient cerebral ischemia. *J. Cereb. Blood Flow Metab. Off. J. Int. Soc. Cereb. Blood Flow Metab.* 34, 450–459. <https://doi.org/10.1038/jcbfm.2013.217>.
- Chu, L.-S., Fang, S.-H., Zhou, Y., Yu, G.-L., Wang, M.-L., Zhang, W.-P., Wei, E.-Q., 2007. Minocycline inhibits 5-lipoxygenase activation and brain inflammation after focal cerebral ischemia in rats. *Acta Pharmacol. Sin.* 28, 763–772. <https://doi.org/10.1111/j.1745-7254.2007.00578.x>.
- Cserep, 2020. Microglia monitor and protect neuronal function through specialized somatic purinergic junctions. *Science*.
- Czech, B., Pfeilschifter, W., Mazaheri-Omrani, N., Strobel, M.A., Kahles, T., Neumann-Haefelin, T., Rami, A., Huwiler, A., Pfeilschifter, J., 2009. The immunomodulatory sphingosine 1-phosphate analog FTY720 reduces lesion size and improves neurological outcome in a mouse model of cerebral ischemia. *Biochem. Biophys. Res. Commun.* 389, 251–256. <https://doi.org/10.1016/j.bbrc.2009.08.142>.
- del Zoppo, G.J., 2010. The neurovascular unit in the setting of stroke. *J. Intern. Med.* 267, 156–171. <https://doi.org/10.1111/j.1365-2796.2009.02199.x>.
- Dhanesha, N., Jain, M., Tripathi, A., Daddapattar, P., Chorawala, M., Bathla, G., Nayak, M.K., Ghatge, M., Lentz, S.R., Kon, S., Chauhan, A.K., 2020. Targeting Myeloid-Specific Integrin $\alpha 9 \beta 1$ Improves Short and Long-Term Stroke Outcomes in Murine Models With Preexisting Comorbidities by Limiting Thrombosis And Inflammation. *Circ. Res.* <https://doi.org/10.1161/CIRCRESAHA.120.316659>.
- Dreikorn, M., Milacic, Z., Pavlovic, V., Meuth, S.G., Kleinschmitt, C., Kraft, P., 2018. Immunotherapy of experimental and human stroke with agents approved for multiple sclerosis: a systematic review. *Ther. Adv. Neurol. Disord.* 11. <https://doi.org/10.1177/1756286418770626>.
- Drieu, A., Buendia, I., Levard, D., Hélie, P., Brodin, C., Vivien, D., Rubio, M., 2020a. Immune responses and anti-inflammatory strategies in a clinically relevant model of thromboembolic ischemic stroke with reperfusion. *Transl. Stroke Res.* 11, 481–495. <https://doi.org/10.1007/s12975-019-00733-8>.
- Drieu, A., Lanquatin, A., Levard, D., Glavan, M., Campos, F., Quenault, A., Lemarchand, E., Naveau, M., Pitel, A.L., Castillo, J., Vivien, D., Rubio, M., 2020b. Alcohol exposure-induced neurovascular inflammation priming impacts ischemic stroke and is linked with brain perivascular macrophages. *JCI Insight* 5. <https://doi.org/10.1172/jci.insight.129226>.
- Drieu, A., Levard, D., Vivien, D., Rubio, M., 2018. Anti-inflammatory treatments for stroke: from bench to bedside. *Ther. Adv. Neurol. Disord.* 11. <https://doi.org/10.1177/1756286418789854>.
- Dupont, A.-C., Largeau, B., Santiago Ribeiro, M.J., Guilloteau, D., Tronel, C., Arlicot, N., 2017. Translocator protein-18 kDa (TSPO) positron emission tomography (PET) imaging and its clinical impact in neurodegenerative diseases. *Int. J. Mol. Sci.* 18. <https://doi.org/10.3390/ijms18040785>.
- Elkind, M.S.V., Ramakrishnan, P., Moon, Y.P., Boden-Albala, B., Liu, K.M., Spitalnik, S.L., Rundek, T., Sacco, R.L., Paik, M.C., 2010. Infectious burden and risk of stroke: the northern Manhattan study. *Arch. Neurol.* 67, 33–38. <https://doi.org/10.1001/archneurol.2009.271>.
- Elkins, J., Veltkamp, R., Montaner, J., Johnston, S.C., Singhal, A.B., Becker, K., Lansberg, M.G., Tang, W., Chang, I., Muralidharan, K., Gheuens, S., Mehta, L., Elkind, M.S.V., 2017. Safety and efficacy of natalizumab in patients with acute ischaemic stroke (ACTION): a randomised, placebo-controlled, double-blind phase 2 trial. *Lancet Neurol.* 16, 217–226. [https://doi.org/10.1016/S1474-4422\(16\)30357-X](https://doi.org/10.1016/S1474-4422(16)30357-X).
- Collaboration, Emerging Risk Factors, Sarwar, N., Gao, P., Seshasai, S.R.K., Gobin, R., Kaptoge, S., Di Angelantonio, E., Ingelsson, E., Lawlor, D.A., Selvin, E., Stampfer, M., Stehouwer, C.D.A., Lewington, S., Pennells, L., Thompson, A., Sattar, N., White, I.R., Ray, K.K., Danesh, J., 2010. Diabetes mellitus, fasting blood glucose concentration,

- and risk of vascular disease: a collaborative meta-analysis of 102 prospective studies. *Lancet Lond. Engl.* 375, 2215–2222. [https://doi.org/10.1016/S0140-6736\(10\)60484-9](https://doi.org/10.1016/S0140-6736(10)60484-9).
- Emmsley, H.C.A., Smith, C.J., Georgiou, R.F., Vail, A., Hopkins, S.J., Rothwell, N.J., Tyrrell, P.J., Investigators, Acute Stroke, 2005. A randomised phase II study of interleukin-1 receptor antagonist in acute stroke patients. *J. Neurol. Neurosurg. Psychiatry* 76, 1366–1372. <https://doi.org/10.1136/jnnp.2004.054882>.
- Enlimomab Acute Stroke Trial Investigators, 2001. Use of anti-ICAM-1 therapy in ischemic stroke: results of the Enlimomab Acute Stroke Trial. *Neurology* 57, 1428–1434. <https://doi.org/10.1212/wnl.57.8.1428>.
- Faheem, H., Mansour, A., Elkordy, A., Rashad, S., Shebl, M., Madi, M., Elwy, S., Niizuma, K., Tomiina, T., 2019. Neuroprotective effects of minocycline and progesterone on white matter injury after focal cerebral ischemia. *J. Clin. Neurosci. Off. J. Neurosurg. Soc. Australas.* 64, 206–213. <https://doi.org/10.1016/j.jocn.2019.04.012>.
- Feng, Y., Liao, S., Wei, C., Jia, D., Wood, K., Liu, Q., Wang, X., Shi, F.-D., Jin, W.-N., 2017. Infiltration and persistence of lymphocytes during late-stage cerebral ischemia in middle cerebral artery occlusion and photothrombotic stroke models. *J. Neuroinflammation* 14, 248. <https://doi.org/10.1186/s12974-017-1017-0>.
- Fisher, Stroke Therapy Academic Industry Roundtable, 2003. Recommendations for advancing development of acute stroke therapies: Stroke Therapy Academic Industry Roundtable 3. Stroke.
- Fu, Y., Liu, Q., Anrather, J., Shi, F.-D., 2015. Immune interventions in stroke. *Nat. Rev. Neurol.* 11, 524–535. <https://doi.org/10.1038/nrneurol.2015.144>.
- Gadani, S.P., Walsh, J.T., Lukens, J.R., Kipnis, J., 2015. Dealing with danger in the CNS: the response of the immune system to injury. *Neuron* 87, 47–62. <https://doi.org/10.1016/j.neuron.2015.05.019>.
- Garcia, J.H., Liu, K.F., Relton, J.K., 1995. Interleukin-1 receptor antagonist decreases the number of necrotic neurons in rats with middle cerebral artery occlusion. *Am. J. Pathol.* 147, 1477–1486.
- Gauberti, M., Lapergue, B., Martinez de Lizarrondo, S., Vivien, D., Richard, S., Bracad, S., Piotin, M., Gory, B., 2018. Ischemia-reperfusion injury after endovascular thrombectomy for ischemic stroke. *Stroke* 49, 3071–3074. <https://doi.org/10.1161/STROKEAHA.118.022015>.
- Gauberti, M., Martinez de Lizarrondo, S., Orset, C., Vivien, D., 2014a. Lack of secondary microthrombosis after thrombin-induced stroke in mice and non-human primates. *J. Thromb. Haemost.* 14, 409–414. <https://doi.org/10.1111/jth.12487>.
- Gauberti, Maxime, Montagne, A., Quenault, A., Vivien, D., 2014b. Molecular magnetic resonance imaging of brain-immune interactions. *Front. Cell. Neurosci.* 8, 389. <https://doi.org/10.3389/fncel.2014.00389>.
- Ge, R., Tornero, D., Hirota, M., Monni, E., Laterza, C., Lindvall, O., Kokaia, Z., 2017. Chorioid plexus-cerebrospinal fluid route for monocyte-derived macrophages after stroke. *J. Neuroinflammation* 14, 153. <https://doi.org/10.1186/s12974-017-0909-3>.
- Gelderblom, M., Arunachalam, P., Magnus, T., 2014. $\gamma\delta$ T cells as early sensors of tissue damage and mediators of secondary neurodegeneration. *Front. Cell. Neurosci.* 8, 368. <https://doi.org/10.3389/fncel.2014.00368>.
- Gelderblom, M., Leyboldt, F., Steinbach, K., Behrens, D., Choe, C.-U., Siler, D.A., Arumugam, T.V., Orthey, E., Gerloff, C., Tolosa, E., Magnus, T., 2009. Temporal and spatial dynamics of cerebral immune cell accumulation in stroke. *Stroke* 40, 1849–1857. <https://doi.org/10.1161/STROKEAHA.108.534503>.
- Gerhard, A., Schwarz, J., Myers, R., Wise, R., Banati, R.B., 2005. Evolution of microglial activation in patients after ischemic stroke: a [11C](R)-PK11195 PET study. *NeuroImage* 24, 591–595. <https://doi.org/10.1016/j.neuroimage.2004.09.034>.
- Gherzi-Egea, J.-F., Strazielle, N., Catala, M., Silva-Vargas, V., Voetsch, F., Engelhardt, B., 2018. Molecular anatomy and functions of the chorioid blood-cerebrospinal fluid barrier in health and disease. *Acta Neuropathol. (Berl.)* 135, 337–361. <https://doi.org/10.1007/s00401-018-1807-1>.
- Girard, S., Murray, K.N., Rothwell, N.J., Metz, G.A.S., Allan, S.M., 2014. Long-term functional recovery and compensation after cerebral ischemia in rats. *Behav. Brain Res.* 270, 18–28. <https://doi.org/10.1016/j.bbr.2014.05.008>.
- Guzik, A., Bushnell, C., 2017. Stroke epidemiology and risk factor management. *Contin. Minn.* 23, 15–39. <https://doi.org/10.1212/CON.00000000000000416>.
- Haley, M.J., Lawrence, C.B., 2016. Obesity and stroke: Can we translate from rodents to patients? *J. Cereb. Blood Flow Metab. Off. J. Int. Soc. Cereb. Blood Flow Metab.* 36, 2007–2021. <https://doi.org/10.1177/0271678X16670411>.
- Hasegawa, Y., Suzuki, H., Sozen, T., Rolland, W., Zhang, J.H., 2010. Activation of sphingosine 1-phosphate receptor-1 by FTY720 is neuroprotective after ischemic stroke in rats. *Stroke* 41, 368–374. <https://doi.org/10.1161/STROKEAHA.109.568899>.
- Hata, R., Maeda, K., Hermann, D., Mies, G., Hossmann, K.A., 2000. Evolution of brain infarction after transient focal cerebral ischemia in mice. *J. Cereb. Blood Flow Metab. Off. J. Int. Soc. Cereb. Blood Flow Metab.* 20, 937–946. <https://doi.org/10.1097/00004647-200006000-00006>.
- Hayakawa, K., Mishima, K., Nozako, M., Hazeckawa, M., Mishima, S., Fujioka, M., Orito, K., Egashira, N., Iwasaki, K., Fujiwara, M., 2008. Delayed treatment with minocycline ameliorates neurologic impairment through activated microglia expressing a high-mobility group box1-inhibiting mechanism. *Stroke* 39, 951–958. <https://doi.org/10.1161/STROKEAHA.107.495820>.
- Hernández-Fernández, F., Valencia, H.S., Barbella-Aponte, R.A., Collado-Jiménez, R., Ayo-Martín, O., Barrena, C., Molina-Nuevo, J.D., García-García, J., Lozano-Setién, E., Alcahut-Rodríguez, C., Martínez-Martín, A., Sánchez-López, A., Segura, T., 2020. Cerebrovascular disease in patients with COVID-19: neuroimaging, histological and clinical description. *Brain J. Neurol.* <https://doi.org/10.1093/brain/awaa239>.
- Hoda, M.N., Fagan, S.C., Khan, M.B., Vaibhav, K., Chaudhary, A., Wang, P., Dhandapani, K.M., Waller, J.L., Hess, D.C., 2014. A 2 × 2 factorial design for the combination therapy of minocycline and remote ischemic preconditioning: efficacy in a preclinical trial in murine thromboembolic stroke model. *Exp. Transl. Stroke Med.* 6, 10. <https://doi.org/10.1186/2040-7378-6-10>.
- Hossmann, K.A., 2012. The two pathophysiologicals of focal brain ischemia: implications for translational stroke research. *J. Cereb. Blood Flow Metab. Off. J. Int. Soc. Cereb. Blood Flow Metab.* 32, 1310–1316. <https://doi.org/10.1038/jcbfm.2011.186>.
- Howells, D.W., Porritt, M.J., Rewell, S.S.J., O'Collins, V., Sena, E.S., van der Worp, H.B., Traystman, R.J., Macleod, M.R., 2010. Different strokes for different folks: the rich diversity of animal models of focal cerebral ischemia. *J. Cereb. Blood Flow Metab. Off. J. Int. Soc. Cereb. Blood Flow Metab.* 30, 1412–1431. <https://doi.org/10.1038/jcbfm.2010.66>.
- Iadecola, C., Anrather, J., 2011. The immunology of stroke: from mechanisms to translation. *Nat. Med.* 17, 796–808. <https://doi.org/10.1038/nm.2399>.
- Jackaman, C., Radley-Crabb, H.G., Soffe, Z., Shavlakadze, T., Grounds, M.D., Nelson, D.J., 2013. Targeting macrophages rescues age-related immune deficiencies in C57BL/6J geriatric mice. *Aging Cell* 12, 345–357. <https://doi.org/10.1111/acel.12572>.
- Jayaraj, R.L., Azimullah, S., Beiram, R., Jalal, F.Y., Rosenberg, G.A., 2019. Neuroinflammation: friend and foe for ischemic stroke. *J. Neuroinflamm.* 16, 142. <https://doi.org/10.1186/s12974-019-1516-2>.
- Jin, Z., Liang, J., Wang, J., Kolattukudy, P.E., 2015. MCP-induced protein 1 mediates the minocycline-induced neuroprotection against cerebral ischemia/reperfusion injury in vitro and in vivo. *J. Neuroinflamm.* 12, 39. <https://doi.org/10.1186/s12974-015-0264-1>.
- Kadlecová, P., Anđel, R., Mikulík, R., Handing, E.P., Pedersen, N.L., 2015. Alcohol consumption at midlife and risk of stroke during 43 years of follow-up: cohort and twin analyses. *Stroke* 46, 627–633. <https://doi.org/10.1161/STROKEAHA.114.006724>.
- Kaplan, R.C., Tirschwell, D.L., Longstreth, W.T., Manolio, T.A., Heckbert, S.R., Lefkowitz, D., El-Saed, A., Psaty, B.M., 2005. Vascular events, mortality, and preventive therapy following ischemic stroke in the elderly. *Neurology* 65, 835–842. <https://doi.org/10.1212/01.wnl.0000176058.09848.bb>.
- Kernan, W.N., Ovbiagele, B., Black, H.R., Bravata, D.M., Chimowitz, M.I., Ezekowitz, M.D., Fang, M.C., Fisher, M., Furie, K.L., Heck, D.V., Johnston, S.C.C., Kasner, S.E., Kittner, S.J., Mitchell, P.H., Rich, M.W., Richardson, D., Schwamm, L.H., Wilson, J.A., Council on Cardiovascular and Stroke Nursing, Council on Clinical Cardiology, and Council on Peripheral Vascular Disease, American Heart Association Stroke, 2014. Guidelines for the prevention of stroke in patients with stroke and transient ischemic attack: a guideline for healthcare professionals from the American Heart Association/American Stroke Association. *Stroke* 45, 2160–2236. <https://doi.org/10.1161/STR.0000000000000024>.
- Kim, E., Cho, S., 2016. Microglia and monocyte-derived macrophages in stroke. *Neurother. J. Am. Soc. Exp. Neurother.* 13, 702–718. <https://doi.org/10.1007/s13311-016-0463-1>.
- Kim, G.W., Sugawara, T., Chan, P.H., 2000. Involvement of oxidative stress and caspase-3 in cortical infarction after photothrombotic ischemia in mice. *J. Cereb. Blood Flow Metab. Off. J. Int. Soc. Cereb. Blood Flow Metab.* 20, 1690–1701. <https://doi.org/10.1097/00004647-200012000-00008>.
- Köhler, E., Prentice, D.A., Bates, T.R., Hankey, G.J., Claxton, A., van Heerden, J., Blacker, D., 2013. Intravenous minocycline in acute stroke: a randomized, controlled pilot study and meta-analysis. *Stroke* 44, 2493–2499. <https://doi.org/10.1161/STROKEAHA.113.000780>.
- Koistinaho, M., Malm, T.M., Kettunen, M.I., Goldsteins, G., Starckx, S., Kauppinen, R.A., Odenakker, G., Koistinaho, J., 2005. Minocycline protects against permanent cerebral ischemia in wild type but not in matrix metalloproteinase-9-deficient mice. *J. Cereb. Blood Flow Metab. Off. J. Int. Soc. Cereb. Blood Flow Metab.* 25, 460–467. <https://doi.org/10.1038/sj.jcbfm.9600040>.
- Kraft, P., Göb, E., Schuhmann, M.K., Göbel, K., Deppermann, C., Thielmann, I., Herrmann, A.M., Lorenz, K., Brede, M., Stoll, G., Meuth, S.G., Nieswandt, B., Pfeilschifter, W., Kleinschnitz, C., 2013. FTY720 ameliorates acute ischemic stroke in mice by reducing thrombo-inflammation but not by direct neuroprotection. *Stroke* 44, 3202–3210. <https://doi.org/10.1161/STROKEAHA.113.002880>.
- Krishnamurthy, R.V., Feigin, V.L., Forouzanfar, M.H., Mensah, G.A., Connor, M., Bennett, D.A., Moran, A.E., Sacco, R.L., Anderson, L.M., Truelsen, T., O'Donnell, M., Venketasubramanian, N., Barker-Collins, S., Lawes, C.M.M., Wang, W., Shinohara, Y., Witt, E., Ezziati, M., Naghavi, M., Murray, C., Global Burden of Diseases, Injuries, Risk Factors Study 2010 (GBD 2010), GBD Stroke Experts Group, 2013. Global and regional burden of first-ever ischaemic and haemorrhagic stroke during 1990–2010: findings from the Global Burden of Disease Study 2010. *Lancet Glob. Health* 1, e259–281. [https://doi.org/10.1016/S2214-109X\(13\)70089-5](https://doi.org/10.1016/S2214-109X(13)70089-5).
- Labat-gest, V., Tomasi, S., 2013. Photothrombotic ischemia: a minimally invasive and reproducible photochemical cortical lesion model for mouse stroke studies. *J. Vis. Exp. JoVE*. <https://doi.org/10.3791/50370>.
- Langhauser, F., Kraft, P., Göb, E., Leinweber, J., Schuhmann, M.K., Lorenz, K., Gelderblom, M., Bittner, S., Meuth, S.G., Wiendl, H., Magnus, T., Kleinschnitz, C., 2014. Blocking of $\alpha 4$ integrin does not protect from acute ischemic stroke in mice. *Stroke* 45, 1799–1806. <https://doi.org/10.1161/STROKEAHA.114.005000>.
- Langhorne, P., Stott, D.J., Robertson, L., MacDonald, J., Jones, L., McAlpine, C., Dick, F., Taylor, G.S., Murray, G., 2000. Medical complications after stroke: a multicenter study. *Stroke* 31, 1223–1229. <https://doi.org/10.1161/01.str.31.6.1223>.
- Le Behot, A., Gauberti, M., Martinez De Lizarrondo, S., Montagne, A., Lemarchand, E., Repesse, Y., Guillou, S., Denis, C.V., Maubert, E., Orset, C., Vivien, D., 2014. Gplb-VWF blockade restores vessel patency by dissolving platelet aggregates formed under very high shear rate in mice. *Blood* 123, 3354–3363. <https://doi.org/10.1182/blood-2013-12-543074>.
- Lee, V.M., Burdett, N.G., Carpenter, A., Hall, L.D., Pambakian, P.S., Patel, S., Wood, N.I., James, M.F., 1996. Evolution of photochemically induced focal cerebral ischemia in the rat. Magnetic resonance imaging and histology. *Stroke* 27, 2110–2118; discussion 2118–2119. <https://doi.org/10.1161/01.str.27.11.2110>.
- Li, X., Wang, M.-H., Qin, C., Fan, W.-H., Tian, D.-S., Liu, J.-L., 2017. Fingolimod

D. Levard, et al.

Brain, Behavior, and Immunity 91 (2021) 649–667

- suppresses neuronal autophagy through the mTOR/p70S6K pathway and alleviates ischemic brain damage in mice. *PLoS One* 12, e0188748. <https://doi.org/10.1371/journal.pone.0188748>.
- Liebeskind, D.S., Derdeyn, C.P., Wechsler, L.R., STAIR X Consortium, 2018. STAIR X: Emerging Considerations in Developing and Evaluating New Stroke Therapies. *Stroke* 49, 2241–2247. <https://doi.org/10.1161/STROKEAHA.118.021424>.
- Liesz, A., Sun, L., Zhou, W., Schwarting, S., Mracko, E., Zorn, M., Bauer, H., Sommer, C., Veltkamp, R., 2011a. FTY720 reduces post-ischemic brain lymphocyte influx but does not improve outcome in permanent murine cerebral ischemia. *PLoS ONE* 6, e21312. <https://doi.org/10.1371/journal.pone.0021312>.
- Liesz, A., Zhou, W., Mracko, E., Karcher, S., Bauer, H., Schwarting, S., Sun, L., Bruder, D., Stegemann, S., Cerwenka, A., Sommer, C., Dalpke, A.H., Veltkamp, R., 2011b. Inhibition of lymphocyte trafficking shields the brain against deleterious neuroinflammation after stroke. *Brain J. Neurol.* 134, 704–720. <https://doi.org/10.1093/brain/awr008>.
- Liu, F., Benashski, S.E., Xu, Y., Siegel, M., McCullough, L.D., 2012. Effects of chronic and acute oestrogen replacement therapy in aged animals after experimental stroke. *J. Neuroendocrinol.* 24, 319–330. <https://doi.org/10.1111/j.1365-2826.2011.02248.x>.
- Liu, J., Zhang, C., Tao, W., Liu, M., 2013. Systematic review and meta-analysis of the efficacy of sphingosine-1-phosphate (S1P) receptor agonist FTY720 (Fingolimod) in animal models of stroke. *Int. J. Neurosci.* 123, 163–169. <https://doi.org/10.3109/00207454.2012.749255>.
- Liu, Z., Fan, Y., Won, S.J., Neumann, M., Hu, D., Zhou, L., Weinstein, P.R., Liu, J., 2007. Chronic treatment with minocycline preserves adult new neurons and reduces functional impairment after focal cerebral ischemia. *Stroke* 38, 146–152. <https://doi.org/10.1161/01.STR.0000251791.64910.cd>.
- Llovera, G., Benakis, C., Enzmann, G., Cai, R., Arzberger, T., Ghasemigharagoz, A., Mao, X., Malik, R., Lazarevic, I., Liebscher, S., Ertürk, A., Meissner, L., Vivien, D., Haffner, C., Plesnila, N., Montaner, J., Engelhardt, B., Liesz, A., 2017. The choroid plexus is a key cerebral invasion route for T cells after stroke. *Acta Neuropathol. (Berl.)* 134, 851–868. <https://doi.org/10.1007/s00401-017-1758-y>.
- Llovera, G., Hofmann, K., Roth, S., Salas-Pédomo, A., Ferrer-Ferrer, M., Perego, C., Zanier, E.R., Mamrak, U., Rex, A., Party, H., Agin, V., Fauchon, C., Orset, C., Haelewyn, B., De Simon, M.-G., Dirnagl, U., Grittner, U., Planas, A.M., Plesnila, N., Vivien, D., Liesz, A., 2015. Results of a preclinical randomized controlled multicenter trial (pRCT): Anti-CD49d treatment for acute brain ischemia. *Sci. Transl. Med.* 7, 299ra121. <https://doi.org/10.1126/scitranslmed.aaa9853>.
- Llovera, G., Roth, S., Plesnila, N., Veltkamp, R., Liesz, A., 2014. Modeling stroke in mice: permanent coagulation of the distal middle cerebral artery. *J. Vis. Exp. JoVE* e51729. <https://doi.org/10.3791/51729>.
- Loddick, S.A., Rothwell, N.J., 1996. Neuroprotective effects of human recombinant interleukin-1 receptor antagonist in focal cerebral ischaemia in the rat. *J. Cereb. Blood Flow Metab. Off. J. Int. Soc. Cereb. Blood Flow Metab.* 16, 932–940. <https://doi.org/10.1097/00004647-199609000-00017>.
- Lodigiani, C., Iapichino, G., Careno, L., Cecconi, M., Ferrazzi, P., Sebastian, T., Kucher, N., Studd, J.-D., Sacco, C., Alexia, B., Sandri, M.T., BarcoHumanitas COVID-19 Task Force, S., 2020. Venous and arterial thromboembolic complications in COVID-19 patients admitted to an academic hospital in Milan, Italy. *Thromb. Res.* 191, 9–14. <https://doi.org/10.1016/j.thromres.2020.04.024>.
- Lopez Gelston, C.A., Mitchell, B.M., 2017. Recent advances in immunity and hypertension. *Am. J. Hypertens.* 30, 643–652. <https://doi.org/10.1093/ajh/hpx011>.
- Lu, Y., Xiao, G., Luo, W., 2016. Minocycline suppresses NLRP3 inflammasome activation in experimental ischemic stroke. *Neuroimmunomodulation* 23, 230–238. <https://doi.org/10.1159/000452172>.
- Lunardi Baccetto, S., Lehmann, C., 2019. Microcirculatory changes in experimental models of stroke and CNS-injury induced immunodepression. *Int. J. Mol. Sci.* 20. <https://doi.org/10.3390/ijms2005184>.
- Macrez, Richard, et al., 2011. Antibodies preventing the interaction of tissue-type plasminogen activator with N-methyl-D-aspartate receptors reduce stroke damages and extend the therapeutic window of thrombolysis. *Stroke*.
- Malhotra, K., Chang, J.J., Khunger, A., Blacker, D., Switzer, J.A., Goyal, N., Hernandez, A.V., Pasupuleti, V., Alexandrov, A.V., Tsvigoulis, G., 2018. Minocycline for acute stroke treatment: a systematic review and meta-analysis of randomized clinical trials. *J. Neurol.* 265, 1871–1879. <https://doi.org/10.1007/s00415-018-8935-3>.
- Malone, K., Amu, S., Moore, A.C., Waeber, C., 2019. The immune system and stroke: from current targets to future therapy. *Immunol. Cell Biol.* 97, 5–16. <https://doi.org/10.1111/imcb.12191>.
- Mandala, S., Hajdu, R., Bergstrom, J., Quackenbush, E., Xie, J., Milligan, J., Thornton, R., Shei, G.-J., Card, D., Keohane, C., Rosenbach, M., Hale, J., Lynch, C.L., Rupprecht, K., Parsons, W., Rosen, H., 2002. Alteration of lymphocyte trafficking by sphingosine-1-phosphate receptor agonists. *Science* 296, 346–349. <https://doi.org/10.1126/science.1070238>.
- Mao, L., Jin, H., Wang, M., Hu, Y., Chen, S., He, Q., Chang, J., Hong, C., Zhou, Y., Wang, D., Miao, X., Li, Y., Hu, B., 2020. Neurologic Manifestations of Hospitalized Patients With Coronavirus Disease 2019 in Wuhan, China. *JAMA Neurol.* <https://doi.org/10.1001/jama.2020.1127>.
- Martín, A., Boisgard, R., Kassou, M., Dollé, F., Tavittian, B., 2011. Reduced PBR/TSP0 expression after minocycline treatment in a rat model of focal cerebral ischemia: a PET study using [(18)F]DPA-714. *Mol. Imaging Biol.* 13, 10–15. <https://doi.org/10.1007/s11307-010-0324-y>.
- Martinez de Lizarondo, S., Gakuba, C., Herbig, B.A., Repessé, Y., Ali, C., Denis, C.V., Lenting, P.J., Touzé, E., Diamond, S.L., Vivien, D., Gauberti, M., 2017. Potent Thrombolytic Effect of N-Acetylcysteine on Arterial Thrombi. *Circulation* 136, 646–660. <https://doi.org/10.1161/CIRCULATIONAHA.117.027290>.
- Marziona, I., Proietti, M., Farcomeni, A., Romiti, G.F., Romanazzi, I., Raparelli, V., Basili, S., Lip, G.Y.H., Nobili, A., Roncaglioni, M.C., 2018. Sex differences in stroke and major adverse clinical events in patients with atrial fibrillation: a systematic review and meta-analysis of 993,600 patients. *Int. J. Cardiol.* 269, 182–191. <https://doi.org/10.1016/j.ijcard.2018.07.044>.
- Matsukawa, N., Yasuhara, T., Hara, K., Xu, L., Maki, M., Yu, G., Kaneko, Y., Ojika, K., Hess, D.C., Borlongan, C.V., 2009. Therapeutic targets and limits of minocycline neuroprotection in experimental ischemic stroke. *BMC Neurosci.* 10, 126. <https://doi.org/10.1186/1471-2202-10-126>.
- Mayadas, T.N., Cullere, X., Lowell, C.A., 2014. The multifaceted functions of neutrophils. *Annu. Rev. Pathol.* 9, 181–218. <https://doi.org/10.1146/annurev-pathol-020712-164023>.
- Maysami, S., Wong, R., Pradillo, J.M., Denes, A., Dhungana, H., Malm, T., Koistinaho, J., Orset, C., Rahman, M., Rubio, M., Schwanning, M., Vivien, D., Bath, P.M., Rothwell, N.J., Allan, S.M., 2016. A cross-laboratory preclinical study on the effectiveness of interleukin-1 receptor antagonist in stroke. *J. Cereb. Blood Flow Metab. Off. J. Int. Soc. Cereb. Blood Flow Metab.* 36, 596–605. <https://doi.org/10.1177/0271678X15606714>.
- Medzhitov, R., Janeway, C.A., 2002. Decoding the patterns of self and nonself by the innate immune system. *Science* 296, 298–300. <https://doi.org/10.1126/science.1068883>.
- Meisel, C., Schwab, J.M., Prass, K., Meisel, A., Dirnagl, U., 2005. Central nervous system injury-induced immune deficiency syndrome. *Nat. Rev. Neurosci.* 6, 775–786. <https://doi.org/10.1038/nrn1765>.
- Mena, H., Cadavid, D., Rushing, E.J., 2004. Human cerebral infarct: a proposed histopathologic classification based on 137 cases. *Acta Neuropathol. (Berl.)* 108, 524–530. <https://doi.org/10.1007/s00401-004-0918-z>.
- Merkler, A.E., Parikh, N.S., Mir, S., Gupta, A., Kamel, H., Lin, E., Lantos, J., Schenck, E.J., Goyal, P., Bruce, S.S., Kahan, J., Lansdale, K.N., LeMoss, N.M., Murthy, S.B., Stieg, P.E., Fink, M.E., Iadecola, C., Segal, A.Z., Cusick, M., Campion, T.R., Diaz, J., Zhang, C., Navi, B.B., 2020. Risk of Ischemic Stroke in Patients With Coronavirus Disease 2019 (COVID-19) vs Patients With Influenza. *JAMA Neurol.* <https://doi.org/10.1001/jama.2020.2730>.
- Morimoto, N., Shimazawa, M., Yamashita, T., Nagai, H., Hara, H., 2005. Minocycline inhibits oxidative stress and decreases in vitro and in vivo ischemic neuronal damage. *Brain Res.* 1044, 8–15. <https://doi.org/10.1016/j.brainres.2005.02.062>.
- Morris, R.S., Simon Jones, P., Alawneh, J.A., Hong, Y.T., Fryer, T.D., Aigbirhio, F.I., Warburton, E.A., Baron, J.-C., 2018. Relationships between selective neuronal loss and microglial activation after ischaemic stroke in man. *Brain J. Neurol.* 141, 2098–2111. <https://doi.org/10.1093/brain/awy121>.
- Mulcahy, N.J., Ross, J., Rothwell, N.J., Loddick, S.A., 2003. Delayed administration of interleukin-1 receptor antagonist protects against transient cerebral ischaemia in the rat. *Br. J. Pharmacol.* 140, 471–476. <https://doi.org/10.1038/sj.bjp.0705462>.
- Naderi, Y., Sabetkasaei, M., Parvardeh, S., Moini Zanjani, T., 2017. Neuroprotective effects of pretreatment with minocycline on memory impairment following cerebral ischemia in rats. *Behav. Pharmacol.* 28, 214–222. <https://doi.org/10.1097/FBP.0000000000000297>.
- Nazari, M., Keshavarz, S., Rafati, A., Namavar, M.R., Haghani, M., 2016. Fingolimod (FTY720) improves hippocampal synaptic plasticity and memory deficit in rats following focal cerebral ischemia. *Brain Res. Bull.* 124, 95–102. <https://doi.org/10.1016/j.brainresbull.2016.04.004>.
- Nguyen, M.D., Julien, J.-P., Rivest, S., 2002. Innate immunity: the missing link in neuroprotection and neurodegeneration? *Nat. Rev. Neurosci.* 3, 216–227. <https://doi.org/10.1038/nrn752>.
- Orset, C., Haelewyn, B., Allan, S.M., Ansar, S., Campos, F., Cho, T.H., Durand, A., El Amki, M., Fatar, M., Garcia-Yébenes, I., Gauberti, M., Grudzenski, S., Lizasoain, I., Lo, E., Macrez, R., Margaill, I., Maysami, S., Meairs, S., Nighoghossian, N., Orbe, J., Paramo, J.A., Parienti, J.-J., Rothwell, N.J., Rubio, M., Waeber, C., Young, A.R., Touzé, E., Vivien, D., 2016. Efficacy of alteplase in a mouse model of acute ischemic stroke: a retrospective pooled analysis. *Stroke* 47, 1312–1318. <https://doi.org/10.1161/STROKEAHA.116.012238>.
- Orset, C., Macrez, R., Young, A.R., Panthou, D., Angles-Cano, E., Maubert, E., Agin, V., Vivien, D., 2007. Mouse model of in situ thromboembolic stroke and reperfusion. *Stroke* 38, 2771–2778. <https://doi.org/10.1161/STROKEAHA.107.487520>.
- Oxley, T.J., Mocco, J., Majidi, S., Kellner, C.P., Shoirah, H., Singh, I.P., De Leacy, R.A., Shigematsu, T., Ladner, T.R., Yaeger, K.A., Skliut, M., Weinberger, J., Dangayach, N.S., Bederson, J.B., Tuhim, S., Fifi, J.T., 2020. Large-vessel stroke as a presenting feature of covid-19 in the young. *N. Engl. J. Med.* 382, e60. <https://doi.org/10.1056/NEJMc2009787>.
- Palm, F., Pussinen, P.J., Aigner, A., Becher, H., Bugge, F., Bauer, M.F., Grond-Ginsbach, C., Safer, A., Urbanek, C., Grau, A.J., 2016. Association between infectious burden, socioeconomic status, and ischemic stroke. *Atherosclerosis* 254, 117–123. <https://doi.org/10.1016/j.atherosclerosis.2016.10.008>.
- Parikh, N.S., Merkler, A.E., Iadecola, C., 2020. Inflammation, autoimmunity, infection, and stroke: epidemiology and lessons from therapeutic intervention. *Stroke* 51, 711–718. <https://doi.org/10.1161/STROKEAHA.119.024157>.
- Park, C.H., Shin, T.K., Lee, H.Y., Kim, S.J., Lee, W.S., 2011. Matrix metalloproteinase inhibitors attenuate neuroinflammation following focal cerebral ischemia in mice. *Korean J. Physiol. Pharmacol. Off. J. Korean Physiol. Soc. Korean Soc. Pharmacol.* 15, 115–122. <https://doi.org/10.4196/kjpp.2011.15.2.115>.
- Park, S.I., Park, S.K., Jang, K.S., Han, Y.M., Kim, C.H., Oh, S.J., 2015. Preischemic neuroprotective effect of minocycline and sodium ozagrel on transient cerebral ischemic rat model. *Brain Res.* 1599, 85–92. <https://doi.org/10.1016/j.brainres.2014.12.051>.
- Pedragosa, J., Salas-Pédomo, A., Gallizioli, M., Cugota, R., Miró-Mur, F., Briand, F., Justicia, C., Pérez-Asensio, F., Marquez-Kisinousky, L., Urra, X., Gieryng, A., Kaminska, B., Chamorro, A., Planas, A.M., 2018. CNS-border associated macrophages respond to acute ischemic stroke attracting granulocytes and promoting vascular leakage. *Acta Neuropathol. Commun.* 6, 76. <https://doi.org/10.1186/s40478-018->

D. Levard, et al.

Brain, Behavior, and Immunity 91 (2021) 649–667

- 0581-6.
Peruzzotti-Jametti, L., Donegá, M., Giusto, E., Mallucci, G., Marchetti, B., Pluchino, S., 2014. The role of the immune system in central nervous system plasticity after acute injury. *Neuroscience* 283, 210–221. <https://doi.org/10.1016/j.neuroscience.2014.04.036>.
- Pfeilschifter, W., Czech-Zechmeister, B., Sujak, M., Foerch, C., Wichelhaus, T.A., Pfeilschifter, J., 2011. Treatment with the immunomodulator FTY720 does not promote spontaneous bacterial infections after experimental stroke in mice. *Exp. Transl. Stroke Med.* 3, 2. <https://doi.org/10.1186/2040-7378-3-2>.
- Phan, H.T., Reeves, M.J., Blizzard, C.L., Thrift, A.G., Cadilhac, D.A., Sturm, J., Otahal, P., Rothwell, P., Bejot, Y., Cabral, N.L., Appelros, P., Körv, J., Vibo, R., Minelli, C., Gall, S.L., 2019. Sex differences in severity of stroke in the INSTRUCT study: a meta-analysis of individual participant data. *J. Am. Heart Assoc.* 8, e010235. <https://doi.org/10.1161/JAHA.118.010235>.
- Pradillo, J.M., Murray, K.N., Coutts, G.A., Moraga, A., Oroz-Gonjar, F., Boutin, H., Moro, M.A., Lizasoain, I., Rothwell, N.J., Allan, S.M., 2017. Reparative effects of interleukin-1 receptor antagonist in young and aged/co-morbid rodents after cerebral ischemia. *Brain Behav. Immun.* 61, 117–126. <https://doi.org/10.1016/j.bbi.2016.11.013>.
- Prass, K., Meisel, C., Höflich, C., Braun, J., Halle, E., Wolf, T., Ruscher, K., Victorov, I.V., Priller, J., Dirnagl, U., Volk, H.-D., Meisel, A., 2003. Stroke-induced immunodeficiency promotes spontaneous bacterial infections and is mediated by sympathetic activation reversal by poststroke T helper cell type 1-like immunostimulation. *J. Exp. Med.* 198, 725–736. <https://doi.org/10.1084/jem.20021098>.
- Qin, C., Zhou, L., Hu, Z., Yang, S., Zhang, S., Chen, M., Yu, H., Tian, D.-S., Wang, W., 2020. Clinical Characteristics and Outcomes of COVID-19 Patients With a History of Stroke in Wuhan, China. *Stroke* 51, 2219–2223. <https://doi.org/10.1161/STROKEAHA.120.030365>.
- Radlinska, B.A., Ghinani, S.A., Lyon, P., Jolly, D., Soucy, J.-P., Minuk, J., Schirmacher, R., Thiel, A., 2009. Multimodal microglia imaging of fiber tracts in acute subcortical stroke. *Ann. Neurol.* 66, 825–832. <https://doi.org/10.1002/ana.21796>.
- Ransohoff, R.M., Schafer, D., Vincent, A., Blachère, N.E., Bar-Or, A., 2015. Neuroinflammation: ways in which the immune system affects the brain. *Neurother. J. Am. Soc. Exp. Neurother.* 12, 896–909. <https://doi.org/10.1007/s13311-015-0385-3>.
- Rayasam, A., Hsu, M., Kijak, J.A., Kissel, L., Hernandez, G., Sandor, M., Fabry, Z., 2018. Immune responses in stroke: how the immune system contributes to damage and healing after stroke and how this knowledge could be translated to better cures? *Immunology* 154, 363–376. <https://doi.org/10.1111/imm.12918>.
- Relton, J., 2001. Inhibition of alpha4 integrin to protect the brain against ischemic injury. *Drug News Perspect.* 14, 346–352.
- Relton, J.K., Rothwell, N.J., 1992. Interleukin-1 receptor antagonist inhibits ischaemic and excitotoxic neuronal damage in the rat. *Brain Res. Bull.* 29, 243–246. [https://doi.org/10.1016/0361-9230\(92\)90033-t](https://doi.org/10.1016/0361-9230(92)90033-t).
- Relton, J.K., Sloan, K.E., Frew, E.M., Whalley, E.T., Adams, S.P., Lobb, R.R., 2001. Inhibition of alpha4 integrin protects against transient focal cerebral ischemia in normotensive and hypertensive rats. *Stroke* 32, 199–205. <https://doi.org/10.1161/01.str.32.1.199>.
- Ritzel, R.M., Crapsier, J., Patel, A.R., Verma, R., Grenier, J.M., Chauhan, A., Jellison, E.R., McCullough, L.D., 2016. Age-associated resident memory CD8 T cells in the central nervous system are primed to potentiate inflammation after ischemic brain injury. *J. Immunol. Baltim. Md 1950 (196)*, 3318–3330. <https://doi.org/10.4049/jimmunol.1502021>.
- Sadler, R., Cramer, J.V., Heindl, S., Kostidis, S., Betz, D., Zuurbier, K.R., Northoff, B.H., Hejink, M., Goldberg, M.P., Plautz, E.J., Roth, S., Malik, R., Dichgans, M., Holdt, L.M., Benakis, C., Giera, M., Stowe, A.M., Liesz, A., 2020. Short-chain fatty acids improve poststroke recovery via immunological mechanisms. *J. Neurosci. Off. J. Soc. Neurosci.* 40, 1162–1173. <https://doi.org/10.1523/JNEUROSCI.1359-19.2019>.
- Salas-Perdomo, A., Miró-Mur, F., Gallizioli, M., Brait, V.H., Justicia, C., Meissner, A., Urrea, X., Chamorro, A., Planas, A.M., 2019. Role of the S1P pathway and inhibition by Fingolimod in preventing hemorrhagic transformation after stroke. *Sci. Rep.* 9, 8309. <https://doi.org/10.1038/s41598-019-44845-5>.
- Sandu, R.E., Dumbra, D., Surugiu, R., Glavan, D.-G., Gresita, A., Petcu, E.B., 2017. Cellular and molecular mechanisms underlying non-pharmaceutical ischemic stroke therapy in aged subjects. *Int. J. Mol. Sci.* 19. <https://doi.org/10.3390/ijms19010099>.
- Schuhmann, M.K., Krstic, M., Kleinschmitz, C., Fluri, F., 2016. Fingolimod (FTY720) reduces cortical infarction and neurological deficits during ischemic stroke through potential maintenance of microvascular patency. *Curr. Neurovasc. Res.* 13, 277–282. <https://doi.org/10.2174/1567202613666160823152446>.
- Shang, K., He, J., Zou, J., Qin, C., Lin, L., Zhou, L.-Q., Yang, L.-L., Wu, L.-J., Wang, W., Zhan, K.-B., Tian, D.-S., 2020. Fingolimod promotes angiogenesis and attenuates ischemic brain damage via modulating microglial polarization. *Brain Res.* 1726, 146509. <https://doi.org/10.1016/j.brainres.2019.146509>.
- Shi, K., Tian, D.-C., Li, Z.-G., Ducruet, A.F., Lawton, M.T., Shi, F.-D., 2019. Global brain inflammation in stroke. *Lancet Neurol.* 18, 1058–1066. [https://doi.org/10.1016/S1474-4422\(19\)30078-X](https://doi.org/10.1016/S1474-4422(19)30078-X).
- Shichita, T., Sugiyama, Y., Ooboshi, H., Sugimori, H., Nakagawa, R., Takada, I., Iwaki, T., Okada, Y., Iida, M., Cua, D.J., Iwakura, Y., Yoshimura, A., 2009. Pivotal role of cerebral interleukin-17-producing gamma-delta T cells in the delayed phase of ischemic brain injury. *Nat. Med.* 15, 946–950. <https://doi.org/10.1038/nm.1999>.
- Shukla, V., Shukya, A.K., Perez-Pinzon, M.A., Dave, K.R., 2017. Cerebral ischemic damage in diabetes: an inflammatory perspective. *J. Neuroinflamm.* 14, 21. <https://doi.org/10.1186/s12974-016-0774-5>.
- Smith, C.J., Denes, A., Tyrrell, P.J., Di Napoli, M., 2015. Phase II anti-inflammatory and immune-modulating drugs for acute ischaemic stroke. *Expert Opin. Investig. Drugs* 24, 623–643. <https://doi.org/10.1517/13543784.2015.1020110>.
- Sobowale, O.A., Parry-Jones, A.R., Smith, C.J., Tyrrell, P.J., Rothwell, N.J., Allan, S.M., 2016. Interleukin-1 in stroke: from bench to bedside. *Stroke* 47, 2160–2167. <https://doi.org/10.1161/STROKEAHA.115.010001>.
- Soliman, S., Ishrat, T., Fouda, A.Y., Patel, A., Pillai, B., Fagan, S.C., 2015. Sequential therapy with minocycline and candesartan improves long-term recovery after experimental stroke. *Transl. Stroke Res.* 6, 309–322. <https://doi.org/10.1007/s12975-015-0408-8>.
- Sommer, C.J., 2017. Ischemic stroke: experimental models and reality. *Acta Neuropathol. (Berl.)* 133, 245–261. <https://doi.org/10.1007/s00401-017-1667-0>.
- Steffen, B.J., Breier, G., Butcher, E.C., Schulz, M., Engelhardt, B., 1996. ICAM-1, VCAM-1, and MADCAM-1 are expressed on choroid plexus epithelium but not endothelium and mediate binding of lymphocytes *in vitro*. *Am. J. Pathol.* 148, 1819–1838.
- Szalay, G., Martincz, B., Lénárt, N., Környei, Z., Orsolits, B., Judák, L., Császár, E., Fekete, R., West, B.L., Katona, G., Rózsa, B., Dénes, Á., 2016. Microglia protect against brain injury and their selective elimination dysregulates neuronal network activity after stroke. *Nat. Commun.* 7, 11499. <https://doi.org/10.1038/ncomms11499>.
- Tanaka, M., Ishihara, Y., Mizuno, S., Ishida, A., Vogel, C.F., Tsuji, M., Yamazaki, T., Itoh, K., 2018. Progression of vasogenic edema induced by activated microglia under permanent middle cerebral artery occlusion. *Biochem. Biophys. Res. Commun.* 496, 582–587. <https://doi.org/10.1016/j.bbrc.2018.01.094>.
- Tang, X.N., Wang, Q., Koike, M.A., Cheng, D., Goris, M.L., Blankenberg, F.G., Yenari, M.A., 2007. Monitoring the protective effects of minocycline treatment with radiolabeled annexin V in an experimental model of focal cerebral ischemia. *J. Nucl. Med. Off. Publ. Soc. Nucl. Med.* 48, 1822–1828. <https://doi.org/10.2967/jnumed.107.041335>.
- Tang, Y., Li, T., Li, J., Yang, J., Liu, H., Zhang, X.J., Le, W., 2014. Jmd3 is essential for the epigenetic modulation of microglia phenotypes in the immune pathogenesis of Parkinson's disease. *Cell Death Differ.* 21, 369–380. <https://doi.org/10.1038/cdd.2013.159>.
- Tao, T., Xu, G., Si Chen, C., Feng, J., Kong, Y., Qin, X., 2013. Minocycline promotes axonal regeneration through suppression of RGMa in rat MCAO/reperfusion model. *Synapse* N. Y. N 67, 189–198. <https://doi.org/10.1002/syn.21620>.
- Thiel, A., Radlinska, B.A., Paquette, C., Sidel, M., Soucy, J.-P., Schirmacher, R., Minuk, J., 2010. The temporal dynamics of poststroke neuroinflammation: a longitudinal diffusion tensor imaging-guided PET study with 11C-PK11195 in acute subcortical stroke. *J. Nucl. Med. Off. Publ. Soc. Nucl. Med.* 51, 1404–1412. <https://doi.org/10.2967/jnumed.110.076612>.
- Thomalla, G., Gerloff, C., 2019. Acute imaging for evidence-based treatment of ischemic stroke. *Curr. Opin. Neurol.* 32, 521–529. <https://doi.org/10.1097/WCO.0000000000000716>.
- Uzdensky, A.B., 2018. Photothrombotic stroke as a model of ischemic stroke. *Transl. Stroke Res.* 9, 437–451. <https://doi.org/10.1007/s12975-017-0593-8>.
- Vallés, J., Lago, A., Santos, M.T., Latorre, A.M., Tembl, J.I., Salom, J.B., Nieves, C., Moscardó, A., 2017. Neutrophil extracellular traps are increased in patients with acute ischemic stroke: prognostic significance. *Thromb. Haemost.* 117, 1919–1929. <https://doi.org/10.1160/TH17-02-0130>.
- Veltkamp, R., Gill, D., 2016. Clinical trials of immunomodulation in ischemic stroke. *Neurother. J. Am. Soc. Exp. Neurother.* 13, 791–800. <https://doi.org/10.1007/s13311-016-0458-y>.
- Wacker, B.K., Park, T.S., Gidday, J.M., 2009. Hypoxic preconditioning-induced cerebral ischemic tolerance: role of microvascular sphingosine kinase 2. *Stroke* 40, 3342–3348. <https://doi.org/10.1161/STROKEAHA.109.560714>.
- Watson, B.D., Dietrich, W.D., Busto, R., Wachtel, M.S., Ginsberg, M.D., 1985. Induction of reproducible brain infarction by photochemically initiated thrombosis. *Ann. Neurol.* 17, 497–504. <https://doi.org/10.1002/ana.410170513>.
- Wei, Y., Yemisci, M., Kim, H.-H., Yung, L.M., Shin, H.K., Hwang, S.-K., Guo, S., Qin, T., Alsharif, N., Brinkmann, V., Liao, J.K., Lo, E.H., Waerber, C., 2011. Fingolimod provides long-term protection in rodent models of cerebral ischemia. *Ann. Neurol.* 69, 119–129. <https://doi.org/10.1002/ana.22186>.
- Wise, P.M., Dubal, D.B., Wilson, M.E., Rau, S.W., Böttner, M., Rosewell, K.L., 2001. Estradiol is a protective factor in the adult and aging brain: understanding of mechanisms derived from *in vivo* and *in vitro* studies. *Brain Res. Brain Res. Rev.* 37, 313–319. [https://doi.org/10.1016/S0165-0173\(01\)00136-9](https://doi.org/10.1016/S0165-0173(01)00136-9).
- Xu, G., Li, C., Parsiola, A.L., Li, J., McCarter, K.D., Shi, R., Mayhan, W.G., Sun, H., 2019. Dose-dependent influences of ethanol on ischemic stroke: role of inflammation. *Front. Cell. Neurosci.* 13, 6. <https://doi.org/10.3389/fncel.2019.00006>.
- Xu, L., Fagan, S.C., Waller, J.L., Edwards, D., Borlongan, C.V., Zheng, J., Hill, W.D., Feuerstein, G., Hess, D.C., 2004. Low dose intravenous minocycline is neuroprotective after middle cerebral artery occlusion-reperfusion in rats. *BMC Neurol.* 4, 7. <https://doi.org/10.1186/1471-2377-4-7>.
- Xu, S., Lu, J., Shao, A., Zhang, J.H., Zhang, J., 2020. Glial cells: role of the immune response in ischemic stroke. *Front. Immunol.* 11, 294. <https://doi.org/10.3389/fimmu.2020.00294>.
- Xue, J., Huang, W., Chen, X., Li, Q., Cai, Z., Yu, T., Shao, B., 2017. Neutrophil-to-lymphocyte ratio is a prognostic marker in acute ischemic stroke. *J. Stroke Cerebrovasc. Dis. Off. J. Natl. Stroke Assoc.* 26, 650–657. <https://doi.org/10.1016/j.jstrokecerebrovasdis.2016.11.010>.
- Yaghi, S., Ishida, K., Torres, J., Mac Grory, B., Raz, E., Humbert, K., Henninger, N., Trivedi, T., Lillemo, K., Alam, S., Sanger, M., Kim, S., Scher, E., Dehkharghani, S., Wachs, M., Tanweer, O., Volpicelli, F., Bosworth, B., Lord, A., Frontera, J., 2020. SARS-CoV-2 and Stroke in a New York healthcare system. *Stroke* 51, 2002–2011. <https://doi.org/10.1161/STROKEAHA.120.030335>.
- Yan, T., Chopp, M., Chen, J., 2015. Experimental animal models and inflammatory cellular changes in cerebral ischemic and hemorrhagic stroke. *Neurosci. Bull.* 31, 717–734. <https://doi.org/10.1007/s12264-015-1567-z>.

D. Levard, et al.

Brain, Behavior, and Immunity 91 (2021) 649–667

- Yanev, P., Poinatte, K., Hominick, D., Khurana, N., Zuurbier, K.R., Berndt, M., Plautz, E.J., Dellinger, M.T., Stowe, A.M., 2020. Impaired meningeal lymphatic vessel development worsens stroke outcome. *J. Cereb. Blood Flow Metab Off. J. Int. Soc. Cereb. Blood Flow Metab.* 40, 263–275. <https://doi.org/10.1177/0271678X18822921>.
- Yang, Yirong, Salayandia, V.M., Thompson, J.F., Yang, L.Y., Estrada, E.Y., Yang, Yi, 2015. Attenuation of acute stroke injury in rat brain by minocycline promotes blood-brain barrier remodeling and alternative microglia/macrophage activation during recovery. *J. Neuroinflamm.* 12, 26. <https://doi.org/10.1186/s12974-015-0245-4>.
- Yew, W.P., Djukic, N.D., Jayaseelan, J.S.P., Walker, F.R., Roos, K.A.A., Chataway, T.K., Muyderman, H., Sims, N.R., 2019. Early treatment with minocycline following stroke in rats improves functional recovery and differentially modifies responses of peri-infarct microglia and astrocytes. *J. Neuroinflamm.* 16, 6. <https://doi.org/10.1186/s12974-018-1379-y>.
- Yrjänheikki, J., Tikka, T., Keinänen, R., Goldsteins, G., Chan, P.H., Koistinaho, J., 1999. A tetracycline derivative, minocycline, reduces inflammation and protects against focal cerebral ischemia with a wide therapeutic window. *Proc. Natl. Acad. Sci. U. S. A.* 96, 13496–13500. <https://doi.org/10.1073/pnas.96.23.13496>.
- Zhang, S., Zhou, Y., Zhang, R., Zhang, M., Campbell, B., Lin, L., Shi, F.-D., Lou, M., 2017. Rationale and design of combination of an immune modulator fingolimod with alteplase bridging with mechanical thrombectomy in acute ischemic stroke (FAMTAIS) trial. *Int. J. Stroke Off. J. Int. Stroke Soc.* 12, 906–909. <https://doi.org/10.1177/1747493017710340>.
- Zhao, Y., Xiao, M., He, W., Cai, Z., 2015. Minocycline upregulates cyclic AMP response element binding protein and brain-derived neurotrophic factor in the hippocampus of cerebral ischemia rats and improves behavioral deficits. *Neuropsychiatr. Dis. Treat.* 11, 507–516. <https://doi.org/10.2147/NDT.S73836>.
- Zheng, Y., Xu, L., Yin, J., Zhong, Z., Fan, H., Li, X., Chang, Q., 2013. Effect of minocycline on cerebral ischemia-reperfusion injury. *Neural Regen. Res.* 8, 900–908. <https://doi.org/10.3969/j.issn.1673-5374.2013.10.004>.
- Zhou, W., Liesz, A., Bauer, H., Sommer, C., Lahrmann, B., Valous, N., Grabe, N., Veltkamp, R., 2013. Postischemic brain infiltration of leukocyte subpopulations differs among murine permanent and transient focal cerebral ischemia models. *Brain Pathol. Zurich Switz.* 23, 34–44. <https://doi.org/10.1111/j.1750-3639.2012.00614.x>.
- Zhu, Z., Fu, Y., Tian, D., Sun, N., Han, W., Chang, G., Dong, Y., Xu, X., Liu, Q., Huang, D., Shi, F.-D., 2015. Combination of the immune modulator fingolimod with alteplase in acute ischemic stroke: a pilot trial. *Circulation* 132, 1104–1112. <https://doi.org/10.1161/CIRCULATIONAHA.115.016371>.

Alcohol exposure–induced neurovascular inflammatory priming impacts ischemic stroke and is linked with brain perivascular macrophages

Antoine Drieu, ... , Denis Vivien, Marina Rubio

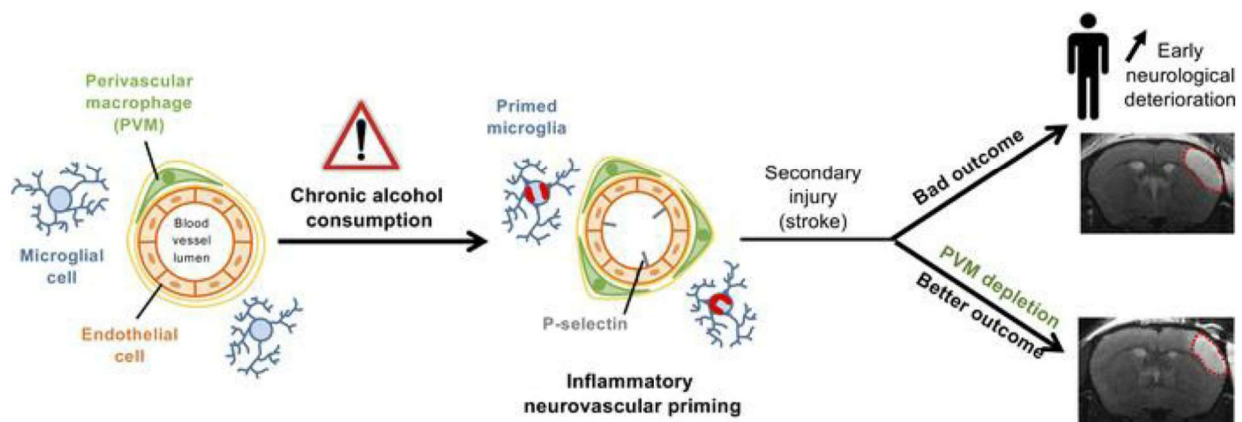
JCI Insight. 2020;5(4):e129226. <https://doi.org/10.1172/jci.insight.129226>.

Research Article

Inflammation

Neuroscience

Graphical abstract



Find the latest version:

<https://jci.me/129226/pdf>



Alcohol exposure–induced neurovascular inflammatory priming impacts ischemic stroke and is linked with brain perivascular macrophages

Antoine Drieu,¹ Anastasia Lanquetin,¹ Damien Levard,¹ Martina Glavan,¹ Francisco Campos,² Aurélien Quenault,¹ Eloïse Lemarchand,¹ Mikaël Naveau,³ Anne Lise Pitel,⁴ José Castillo,² Denis Vivien,¹ and Marina Rubio¹

¹INSERM, Physiopathology and Imaging of Neurological Disorders, UMR-S 1237, Normandie Université, Caen, France.

²Clinical Neurosciences Research Laboratory, Health Research Institute of Santiago de Compostela (IDIS), Santiago de

Compostela, Spain. ³CNRS, UMR-S 3408, GIP Cyceron, Normandie Université, Caen, France. ⁴INSERM, Neuropsychologie et Imagerie de la Mémoire Humaine, UMR-S 1077, Université Paris Sciences et Lettres, Caen, France.

Alcohol abuse is a major public health problem worldwide, causing a wide range of preventable morbidity and mortality. In this translational study, we show that heavy drinking (HD) (≥ 6 standard drinks/day) is independently associated with a worse outcome for ischemic stroke patients. To study the underlying mechanisms of this deleterious effect of HD, we performed an extensive analysis of the brain inflammatory responses of mice chronically exposed or not to 10% alcohol before and after ischemic stroke. Inflammatory responses were analyzed at the parenchymal, perivascular, and vascular levels by using transcriptomic, immunohistochemical, in vivo 2-photon microscopy and molecular MRI analyses. Alcohol-exposed mice show, in the absence of any other insult, a neurovascular inflammatory priming (i.e., an abnormal inflammatory status including an increase in brain perivascular macrophages [PVM]) associated with exacerbated inflammatory responses after a secondary insult (ischemic stroke or LPS challenge). Similar to our clinical data, alcohol-exposed mice showed larger ischemic lesions. We show here that PVM are key players on this aggravating effect of alcohol, since their specific depletion blocks the alcohol-induced aggravation of ischemic lesions. This study opens potentially new therapeutic avenues aiming at blocking alcohol-induced exacerbation of the neurovascular inflammatory responses triggered after ischemic stroke.

Introduction

Alcohol abuse is a major public health problem worldwide, causing a wide range of preventable morbidity and mortality. In the European Union, 89% of men and 82% of women are current drinkers; among them, 15.3% of men and 3.4% of women are heavy drinkers (>6 drinks/day) (1). In the United States, excessive alcohol use is known to kill about 88,000 people each year, and the cost of excessive alcohol use reached \$249 billion in 2010 (<http://www.cdc.gov/features/costsofdrinking>). Alcohol modifies the risk of stroke: light and moderate alcohol consumption (0–2 drinks/day) are associated with a lower risk of ischemic stroke, whereas higher doses of alcohol are associated with an increased risk (2). Importantly, stroke risk associated with high and heavy drinking (HD) in midlife (<75 years) predominates over well-known stroke risk factors like hypertension and diabetes (3). However, the impact of alcohol consumption on stroke outcome is less known. Current clinical studies are controversial and have described either an aggravating effect (4) or no effect of HD (5) on stroke severity. Preclinical reports have also described either a protective effect of low alcohol consumption on ischemic stroke (6, 7) or larger infarcts in rodents exposed to higher alcohol dose (6, 8). However, the mechanisms mediating this aggravation are not well understood. Our previous results on the impact of alcohol consumption on ischemic stroke, obtained in a clinically relevant thromboembolic model of stroke (9, 10), have shown that the aggravating effect of excessive drinking is not due to alcohol-induced changes in hemodynamic

Conflict of interest: The authors have declared that no conflict of interest exists.

Copyright: © 2020, American Society for Clinical Investigation.

Submitted: March 29, 2019

Accepted: January 15, 2020

Published: February 27, 2020.

Reference information: *JCI Insight*. 2020;5(4):e129226.

<https://doi.org/10.1172/jci.insight.129226>.

parameters (clot formation, stability, or sensitivity to fibrinolysis) (8). On the other hand, clinical and preclinical data have shown that alcohol consumption may have an impact on inflammation (11–13).

Perivascular macrophages (PVM) are a subpopulation of myeloid cells residing in the CNS. PVM surround brain blood vessels and are located at the perivascular space (14, 15). In physiological conditions, PVM have scavenger functions, revealing a role of clearing debris from the CNS (16–18), and can also present antigens to lymphocytes (19). Recent data implicate PVM in several pathological contexts, including brain infections, immune activation, Alzheimer's disease, or multiple sclerosis, suggesting that PVM are a key component of the brain-resident immune system, with broad implications for the pathogenesis of major brain diseases (20). PVM can produce reactive oxygen species and cytokines, linking them to the inflammatory response (21). Due to the major role of inflammation in stroke pathobiology and outcome (22), in this translational study, we aimed at investigating the role of inflammation in the aggravating effect of chronic alcohol drinking on ischemic stroke.

Results

HD stroke patients show higher stroke baseline severity and worse neurological outcome. A total of 3,645 ischemic stroke patients were included in the retrospective analysis (Figure 1A). HD stroke patients ($n = 424$, 11.6%; drinking ≥ 6 drinks/day in the last 5 years) were significantly younger, were more frequently men, and presented a history of hypertension and higher smoking habits than non-HD stroke patients. In addition, HD stroke patients had more severe ischemic strokes, with a higher infarct volume, higher mortality during hospitalization, worse prognosis at 3 months, and higher levels of markers associated with the inflammatory response. Mortality during hospitalization was significantly increased in HD stroke patients (11.7% vs. 9.7%, $P < 0.0001$; Table 1).

The NIH Stroke Scale (NIHSS) scores at admission, 24 hours, and 48 hours after stroke onset were significantly higher in HD stroke patients (Figure 1B and Table 1). Interestingly, significantly more HD stroke patients presented early neurological deterioration (END), defined as the increase of NIHSS in 4 or more points in the first 48 hours after admission (19.2% vs. 4.4%; Table 1 and Figure 1B).

HD is independently associated with an increased risk of END. Based on the first univariate analysis, END was used as the main variable to analyze the cohort of stroke patients included in this study (Table 2). In this second univariate analysis, a total 3352 patients were included (3146 without END and 206 with END; 293 fewer patients than for the descriptive analysis, since NIHSS data were not recorded or were lost between the admission and the 48 hours). As expected, patients with END showed significantly higher hemorrhagic transformation, higher infarct volume, and worse prognosis at 3 months. Moreover, patients with END presented higher inflammatory response at admission, characterized by higher leukocyte numbers, as well as C-reactive protein (CRP) levels. Interestingly, significantly more END patients had HD habits (36.9% vs. 10.2%, $P < 0.0001$; Table 2).

The inflammatory response is associated with the risk of END in HD stroke patients. We then performed multivariate analysis of END adjusted by HD (Model A, Figure 1C and Supplemental Table 1; supplemental material available online with this article; <https://doi.org/10.1172/jci.insight.129226DS1>) or by HD and inflammatory markers (Model B, Figure 1D and Supplemental Table 1). Model A showed that HD is independently associated with an increased risk of END (OR = 4.49; 95% CI, 2.94–6.86; $P < 0.0001$) (Figure 1C and Supplemental Table 1). When inflammatory markers (axillary temperature, leukocyte numbers and CRP) were included in the analysis (Model B, Figure 1D and Supplemental Table 1), the impact of HD on the END OR decreased from 4.49 (obtained on the Model A) to 2.45 (OR = 2.45; 95% CI, 1.01–5.91; $P < 0.0001$), showing that the inflammatory response is associated with the risk of END in HD stroke patients. Age and sex do not have a relevant impact on END (Supplemental Table 2).

Finally, we studied the effect of HD on infarct volume. After adjusting for those variables that can interfere with the variable “infarct volume” (age, sex, axillary temperature, leukocyte levels, fibrinogen levels, CRP levels, tissue-type plasminogen activator (tPA) treatment, thrombectomy, hemorrhagic transformation, NIHSS on admission, END, Trial of ORG 10172 in Acute Stroke Treatment (TOAST) classification, and HD; Supplemental Table 3), linear regression analysis of infarct volume showed that the predictor value of HD was 19.66 (B = 19.66 rate of change; 95% CI, 8.03–31.30; $P < 0.001$; Supplemental Table 4).

HD patients without stroke show high levels of inflammatory markers. Data from the independent cohort of HD patients without stroke showed that the levels of circulating monocytes are significantly increased compared with control healthy subjects (0.73 ± 0.27 vs. 0.2 ± 0.17 , respectively, $P = 0.003$; Table 3). In addition to this, 61.8% of HD showed increased high-sensitivity CRP (hs-CRP) levels (Table 3).

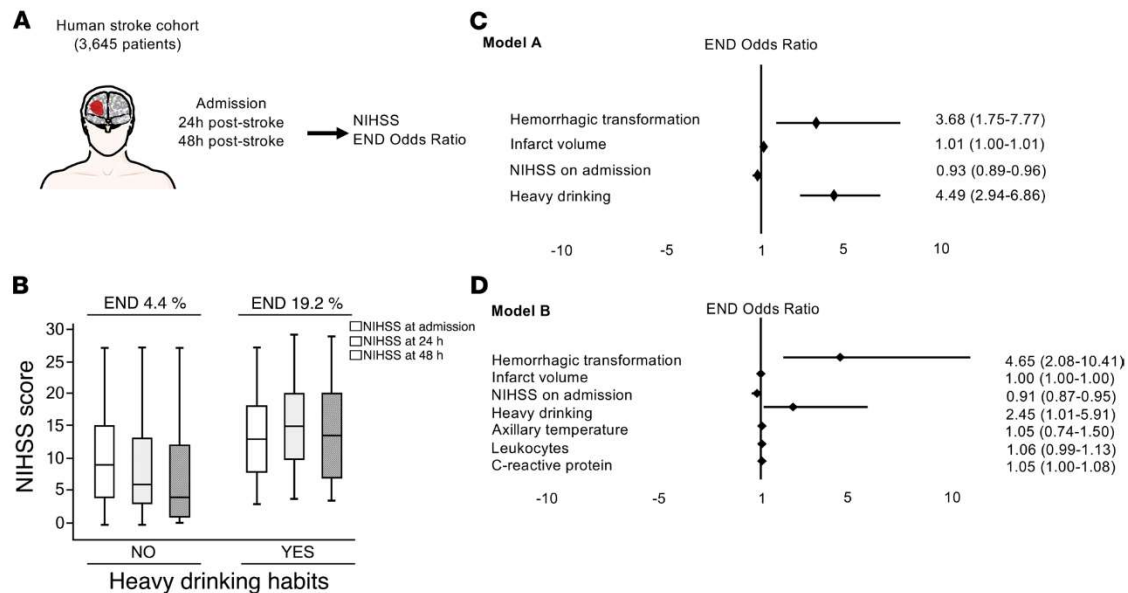


Figure 1. Heavy drinking (HD) aggravates ischemic stroke baseline severity and outcome, and it increases early neurological deterioration (END) risk. Inflammatory markers are independently associated to the alcohol-induced increased risk of END. **(A)** Schema of the study. **(B)** Representation of neurological stroke severity determined by the NIH Stroke Scale (NIHSS) at admission and 24 and 48 hours in stroke patients with and without heavy drinking habits. Early neurological deterioration (END) is defined as an increase of NIHSS in 4 or more points in the first 48 hours after admission. **(C)** Forest plot of the multivariate analysis including variables predicting END ($n = 206$) such as hemorrhagic transformation, infarct volume, NIHSS on admission, and HD habits (Model A). **(D)** Forest plot of the multivariate analysis of the variables included in the Model A and inflammatory biomarkers (axillary temperature, number of leukocytes levels, and C-reactive protein levels) (Model B).

Alcohol exposure induces a neurovascular inflammatory priming in mice. The first set of experiments aimed to analyze the inflammatory status in the brain of mice drinking 10% alcohol for 6 weeks (~5 g/kg/day), in the absence of any other insult (Figure 2A). To study microglial cells, brain samples were stained with Iba1, a constitutive marker of microglial cells, and with the lysosomal marker CD68, present in activated microglial cells (23). We found that, whereas the total number of activated microglial (Iba1⁺CD68⁺) cells remained unchanged (Figure 2, B–D), the total area of CD68⁺ staining was significantly increased in alcohol-exposed mice ($P < 0.05$ vs. control; Figure 2, C and E), suggestive of an alcohol-induced increase in microglial activation. Alcohol exposure did not change microglial cell numbers (total number of Iba1⁺ cells) (Figure 2, B and F; $n = 4$ mice/group). In terms of microglial morphology, alcohol exposure did not change the number of main processes (starting from the soma) (Figure 2, C and G) or the mean area of microglial cells (Figure 2, C and H).

The alcohol-induced increase in microglial activation was demonstrated by an *in vivo* functional measurement of microglial phagocytosis after the injection of nonionic latex beads in the brain cortex of control and alcohol-exposed mice (Figure 2, I–L). Eight hours after the intracortical injection of the beads, alcohol-exposed mice showed significantly more phagocytosed beads (surrounded by Iba1⁺ staining) than control mice (Figure 2, I–K and M; $n = 4$ mice/group; $P < 0.05$ vs. control), demonstrating that microglia in alcohol-exposed mice is more prone for phagocytosis. These results show an alcohol-induced microglial priming characterized by a morphological “resting” state — accompanied, however, by an increase in both microglial activation status and phagocytic capacity.

In this study, we also wanted to examine potential inflammatory effects of alcohol exposure on the brain vasculature (Figure 3, A and B). For this reason, we analyzed the endothelial levels of the adhesion molecule P-selectin (CD62P marker), responsible of leukocyte tethering and rolling on the vessel wall. At the vascular level, alcohol-exposed mice showed significantly increased P-selectin⁺ blood vessels (152% increase; 1.03 ± 0.31 CD62P⁺ blood vessels/mm²; $n = 4$ mice/group; $P < 0.05$ vs. control; Figure 3B), whereas, in control mice, very low levels of P-selectin (0.31 ± 0.11 CD62P⁺ blood vessels/mm²) were detected, demonstrating an alcohol-induced endothelial activation in the absence of any other brain injury.

Table 1. Univariate analysis of stroke patients with and without heavy drinking habits (>6 standard drinks/day)

	Heavy drinking		
	No <i>n</i> = 3221	Yes <i>n</i> = 424	
Age (years)	72.60 ± 14.06	66.79 ± 11.87	<0.0001
Men (%)	50.5	85.8	<0.0001
History of hypertension (%)	64.6	52.4	<0.0001
History of diabetes (%)	24.7	22.6	0.368
History of smoking (%)	12.5	56.1	<0.0001
History of dyslipemia (%)	34.0	32.3	0.513
History of ischemic heart disease (%)	11.5	11.3	0.491
Axillary temperature at admission (°C)	36.3 ± 0.6	36.6 ± 0.6	<0.0001
Leukocytes on admission (× 10 ³ /mL)	8.8 ± 3.1	9.9 ± 3.2	0.135
Fibrinogen on admission (mg/dL)	416.9 ± 97.6	439.5 ± 87.1	<0.0001
C-reactive protein on admission (mg/L)	2.7 ± 4.2	3.5 ± 3.1	<0.0001
Sedimentation rate (mm)	21.9 ± 23.6	24.1 ± 23.5	0.05
tPA treatment (%)	22.9	21.0	0.206
Trombectomy (%)	3.2	1.4	0.025
Hemorrhagic transformation (%)	8.8	10.5	0.147
Infarct volume (mL), <i>n</i> = 2121	40.1 ± 70.4	46.9 ± 64.8	0.021
NIHSS on admission, <i>n</i> = 3645	9 (5–15 NIHSS)	14 (11–19 NIHSS)	<0.0001
NIHSS at 24 hours, <i>n</i> = 3277	6 (3–10 NIHSS)	18 (9–20 NIHSS)	<0.0001
NIHSS at 48 hours, <i>n</i> = 3352	4 (1–10 NIHSS)	14 (7–20 NIHSS)	<0.0001
END (%), <i>n</i> = 3352	4.4	19.2	<0.0001
mRS at 3 months, <i>n</i> = 2935	2 (1–4 mRS)	3 (2–4 mRS)	<0.0001
Poor outcome at 3 months (%), <i>n</i> = 2935	53.6	65.1	<0.0001
TOAST			0.286
Atherothrombotic (%)	23.2	26.7	
Cardioembolic (%)	37.1	32.8	
Small vessel disease (%)	7.3	6.1	
Indeterminate (%)	31.2	33.3	
Others (%)	1.1	1.2	
Mortality during hospitalization (%)	9.1	11.7	<0.0001

Analyses were retrospectively performed from data of the stroke registry at the Stroke Unit of the University Clinical Hospital of Santiago de Compostela (Spain). tPA, tissue-type plasminogen activator; NIHSS, National Institute of Health Stroke Scale; mRS, modified Rankin Scale; END, Early Neurological Deterioration (defined as the increase of NIHSS in ≥4 points in the first 48 hours after admission); TOAST, Trial of ORG 10172 in Acute Stroke Treatment classification.

To determine the functional impact of the increase in P-selectin expression, we performed *in vivo* 2-photon microscopy analyses to measure venular leukocyte adhesion and rolling in mice exposed or not to alcohol, after the *i.v.* injection of FITC-Dextran (allowing blood vessels visualization) and Rhodamine-6G (staining leukocytes). Alcohol-exposed mice showed significantly more adherent (Figure 3, C and D) and rolling (Figure 3, E and F) leukocytes compared with control mice (317% and 724% increase, respectively; *n* = 6 mice/group; *P* < 0.05 vs. control).

Concerning mRNA expression of inflammatory markers, alcohol-exposed mice showed a significant increase in TGF-β mRNA levels (*P* < 0.05; *n* = 6 mice/group) compared with control mice that was not accompanied by changes in proinflammatory cytokines such as IL-1β, TNF, IL-6, P-selectin, TLR4, or VCAM1 (Table 4).

We also studied blood-brain barrier (BBB) integrity after alcohol exposure by using 3 different methods. Our results showed that chronic alcohol exposure does not seem to alter BBB integrity, since neither Evans Blue extravasation measured by near-infrared fluorescence (NIRF) imaging (Supplemental Figure 1, A–D; *n* = 4 mice/group), positive signals of gadolinium extravasation measured by T1-weighted (T1-w) MRI (Supplemental Figure 1, E–H; *n* = 4 mice/group) or fibrinogen deposits (Supplemental Figure 1I; *n* = 4 mice/group) were found in alcohol-exposed mice.

Concerning the potential alcohol-induced neuronal death, we did not find any fluoro-jade C-positive staining in alcohol-exposed mice (Supplemental Figure 1B; *n* = 4 mice/group).

Table 2. Univariate analysis of stroke patients with and without early neurological deterioration

	Early neurological deterioration		
	No <i>n</i> = 3146	Yes <i>n</i> = 206	
Age (years)	72.1 ± 13.4	73.8 ± 11.9	0.977
Men (%)	54.7	59.2	0.219
History of hypertension (%)	62.8	62.6	0.509
History of diabetes (%)	24.5	23.3	0.384
History of smoking (%)	17.4	20.2	0.193
History of dyslipemia (%)	33.8	35.4	0.339
History of ischemic heart disease (%)	11.3	14.1	0.135
Axillary temperature at admission (°C)	36.3 ± 0.6	36.4 ± 0.8	0.005
Leukocytes on admission (× 10 ³ /mL)	8.9 ± 3.3	10.4 ± 4.2	0.019
Fibrinogen on admission (mg/dL)	426.7 ± 102.8	422.8 ± 120.5	0.255
C-reactive protein on admission (mg/L)	3.2 ± 4.3	4.6 ± 4.9	<0.0001
Sedimentation rate (mm)	27.7 ± 25.6	28.5 ± 26.1	0.695
tPA treatment (%)	23.5	22.3	0.389
Trombectomy (%)	2.7	3.9	0.210
Hemorrhagic transformation (%)	9.4	17.1	<0.0001
Infarct volume (mL)	50.3 ± 77.1	107.7 ± 107.8	<0.0001
NIHSS at admission	12 (NIHSS 7–17)	13 (NIHSS 8–15)	0.017
mRS at 3 months	3 (mRS 1–4)	5 (mRS 3–6)	<0.0001
Poor outcome at 3 months (%)	51.0	81.2	<0.0001
TOAST			0.613
Atherothrombotic (%)	24.3	25.2	
Cardioembolic (%)	35.8	38.3	
Small vessel disease (%)	7.2	4.4	
Indeterminate (%)	31.6	31.1	
Others (%)	1.1	1.0	
Heavy drinking (%)	10.2	36.9	<0.0001

Alcohol exposure exacerbates brain neurovascular inflammatory reactions after an acute systemic insult. Alcohol-exposed mice showed a global exacerbated inflammatory response in the brain 24 hours after an acute i.p. injection of LPS compared with control mice (Figure 4A). At the parenchymal level, alcohol-exposed mice receiving LPS showed a significant increase in (a) total microglial cells (Iba1⁺ cells) (Figure 4, B and C; *n* = 5 mice/group; *P* < 0.05 vs. control), (b) activated microglia (Iba1⁺CD68⁺ cells) (Figure 4, B and D; *n* = 5 mice/group; *P* < 0.05 vs. control), and (c) CD68⁺Iba1⁻ cells that we considered as macrophages (Figure 4, B and E) compared with LPS-injected control mice.

At the vascular level, P-selectin immunostaining (Figure 4, F and G) was significantly increased in alcohol-exposed mice receiving LPS compared with control mice (*n* = 5 mice/group; *P* < 0.05 vs. control). Molecular MRI also showed a significantly increased number of P-selectin-coupled microsized particles of iron oxide-positive (MPIO⁺) blood vessels in alcohol-exposed mice receiving LPS (Figure 4, H and I; *n* = 5 mice/group; *P* < 0.05 vs. control). Consequently, venular leukocyte adhesion (Figure 4, J and K) and rolling (Figure 4, L and M), measured by intravital 2-photon microscopy, were significantly increased in alcohol-exposed mice receiving LPS compared with control mice (*n* = 5 mice/group; *P* < 0.05 vs. control).

Alcohol exposure aggravates stroke lesions and exacerbates neurovascular inflammatory responses after ischemic stroke in mice. Alcohol-exposed mice showed significantly larger ischemic lesions than control mice (drinking only water) 24 hours after stroke onset (Figure 5, A–C; *n* = 8 mice/group; *P* < 0.05 vs. control) (8). These data on lesion volume are part of a previously published figure (8). No hemorrhagic transformation was detected in any mice (data not shown).

Table 3. Heavy drinkers have higher levels of inflammatory markers, in the absence of any other injury

	Control subjects <i>n</i> = 21	Heavy drinkers <i>n</i> = 34	<i>P</i>
Age	43.8 ± 7.4 (29–55 years)	45.7 ± 9.2 (33–66 years)	0.29
Women/Men Ratio	5/21	9/34	0.83
BMI	25.3 ± 4.4 ^a (19.5–35.5 BMI)	23.9 ± 4.4 (17.3–39.8 BMI)	0.32
AUDIT	2.9 ± 1.6 (scores 0–6)	28.9 ± 7.7 (scores 4–40)	<0.001
Leucocytes (g/L)	6.4 ± 1.7 (3.7–9.7 g/L)	7.0 ± 2.1 (3.5–12.3 g/L)	0.24
Neutrophils (g/L)	3.6 ± 1.4 (1.7–7.2 g/L)	4.1 ± 1.7 (1.7–8.6 g/L)	0.28
Eosinophils (g/L)	0.17 ± 0.08 (0.04–0.31 g/L)	0.18 ± 0.13 (0–0.53 g/L)	0.80
Basophils (g/L)	0.03 ± 0.02 (0.01–0.07 g/L)	0.04 ± 0.02 (0.01–0.1 g/L)	0.09
Lymphocytes (g/L)	1.95 ± 0.72 (1.03–3.85 g/L)	1.93 ± 0.75 (0.93–3.88 g/L)	0.96
Monocytes (g/L)	0.52 ± 0.17 (0.27–0.99 g/L)	0.73 ± 0.27 (0.11–1.42 g/L)	0.003
C Reactive protein >3 mg/L		61.8% (21 of 34)	

Demographic and clinical characteristics, leukocyte cell counting, and C-reactive Protein (CRP) levels in an independent cohort of healthy control participants and heavy drinkers recruited in the Addiction Unit of the University Hospital of Caen (Normandy, France) while they were receiving withdrawal treatment as inpatients. Data are expressed as mean ± SD; parenthesis data correspond to interval. AUDIT, Alcohol Use Disorders Identification Test.

^aMissing data. *N* = 20.

Microglial/macrophage reaction after stroke (Figure 5, D–K) was exacerbated in the ipsilateral cortex of alcohol-exposed mice, with significant increases in (a) the total number of Iba1⁺ cells in the peri-infarct area (Figure 5F; *n* = 3 mice/group; *P* < 0.05 vs. control), (b) the number of CD68⁺Iba1⁺ cells in the peri-infarct area and the ischemic core (Figure 5G; *n* = 3 mice/group; *P* < 0.05 vs. control), and (c) the area of lysosomal CD68 staining in the ipsilateral hemisphere of alcohol-exposed mice compared with control (Figure 5H; *n* = 3 mice/group; *P* < 0.05 vs. control). The number of processes starting from the soma was significantly decreased in the ipsilateral cortex of alcohol-exposed mice compared with control mice (Figure 5I; *n* = 3 mice/group; *P* < 0.05 vs. control), suggestive of an increased microglial phagocytic phenotype induced by alcohol exposure. Whole cell area of Iba1⁺ cells remained unchanged between groups (Figure 5J; *n* = 3 mice/group). The number of CD68⁺Iba1⁻ cells was significantly increased in the peri-infarct area of alcohol-exposed mice 24 hours after stroke onset (Figure 5K; *n* = 3 mice/group; *P* < 0.05 vs. control).

Vascular activation was exacerbated in alcohol-exposed mice after stroke (Figure 6, A–F). The area of P-selectin in blood vessels was significantly increased in alcohol-exposed mice 24 hours after stroke onset (Figure 6C; *n* = 3 mice/group; *P* < 0.05 vs. control), although the number of P-selectin⁺ blood vessels showed no changes between groups (Figure 6B). Similarly, molecular MRI (Figure 6D) showed significantly increased hyposignals corresponding to P-selectin–coupled MPIOs adhering to blood vessels in the ipsilateral cortex of alcohol-exposed mice 24 hours after stroke onset (Figure 6E; *n* = 5–6 mice/group; *P* < 0.05 vs. control), with no changes in the total number of P-selectin MPIO⁺ blood vessels (Figure 6F).

Venular leukocyte adhesion (Figure 6, H and I) and rolling (Figure 6, J and K) were both significantly increased in alcohol-exposed mice compared with control mice (317% and 724% increase, respectively; *n* = 6 mice/group; *P* < 0.05 vs. control) 24 hours after stroke. Schemas in Figure 6G show the relative position of the middle cerebral artery (MCA) occlusion site and the thinned-skull cranial window where in vivo 2-photon imaging was performed.

mRNA levels of IL-1β, P-selectin, and TNF were significantly increased in alcohol-exposed mice in the ipsilateral cortex 24 hours after stroke onset compared with control mice (*P* < 0.05; *n* = 6 mice/group; Table 4).

PVM depletion prevents the aggravating effect of chronic alcohol consumption on ischemic stroke. In addition to the neurovascular priming profile found in alcohol-exposed mice, we also detected a significant increase in

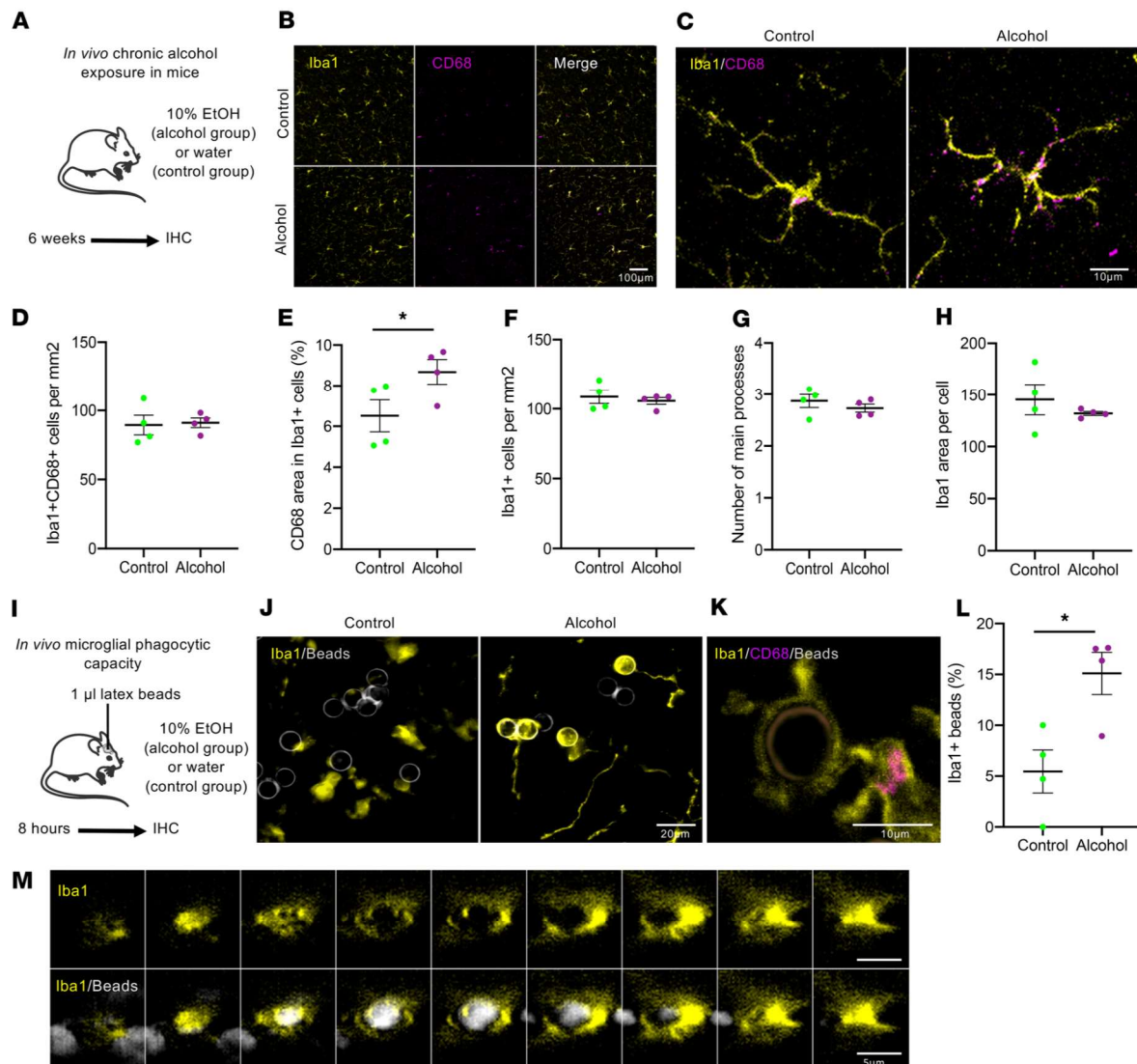


Figure 2. Alcohol exposure provokes a microglial priming in mice. (A) Experimental design to study the effects of chronic alcohol exposure on microglia. (B) Representative photomicrographs of microglial cells stained with Iba1 and CD68. Scale bar: 100 μm . (C) High-magnification representative photomicrographs of microglial cells in control and alcohol-exposed mice. Scale bar: 10 μm . (D) Quantification of Iba1⁺CD68⁺ cells. (E) Quantification of CD68 area on Iba1⁺ microglial cells. (F) Quantification of Iba1⁺ cells. (G) Quantification of the number of processes starting from the soma. (H) Quantification of the area of microglial cells. $n = 4$ mice per group. (I) Experimental design to in vivo study the microglial phagocytic capacity: 1 μL of latex beads were injected in the cortex of control and alcohol-exposed mice. Eight hours later, phagocytosed latex beads were quantified by immunohistochemical analyses. (J) Representative photomicrographs of Iba1⁺ microglial cells and latex beads. Scale bar: 20 μm . (K) Detail of a latex bead phagocytosed by a microglial cell in an alcohol-exposed mouse. Note the lysosomal activation (CD68, red) at the apex of microglial process. Scale bar: 10 μm . (L) Quantification of phagocytosed latex beads/total number of beads. $n = 4$ mice per group; * $P < 0.05$ versus Control, Mann-Whitney U test. (M) Sequential confocal photomicrographs of a phagocytosed latex bead.

the number of brain PVM (Figure 7, A–C; $n = 4$ mice/group; $P < 0.05$ vs. control). PVM are a subpopulation of resident brain macrophages located at the perivascular space (Supplemental Figures 2, A–E). In this study, we have measured only submeningeal signals on IHC and in vivo imaging experiments to focus on PVM and no other border-associated macrophages. In addition to their specific shape and location surrounding brain blood vessels (Supplemental Figure 2), in naive conditions, PVM can be distinguished from microglia since they are very low positive for Iba1. PVM can be stained with both CD68 and CD206 (Supplemental Figure 2 and Figure 7, B and C). Concerning the origin of the increased number of PVM

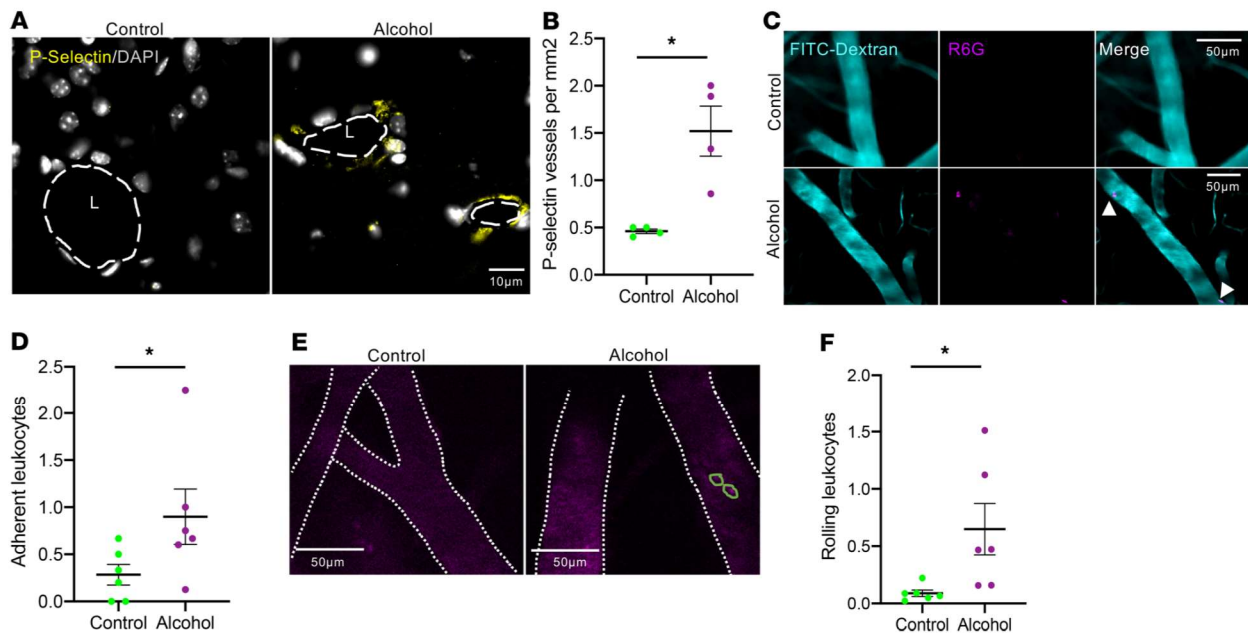


Figure 3. Alcohol exposure provokes endothelial activation in the brain. (A) Representative photomicrographs of P-selectin⁺ vessels in control and alcohol-exposed mice (note the absence of positive staining in control mice). Dotted lines represent the lumen (L) of the blood vessel. Scale bar: 10 μ m. (B) Quantification of P-selectin signal in the brain cortex of control and alcohol-exposed mice. $n = 4$ mice per group. (C) Compilation of in vivo time-lapse images obtained by 2-photon microscopy showing Rhodamine-6G (R6G)⁺ leukocyte adhesion (arrowheads) in control and alcohol-exposed mice (note the absence of R6G⁺ cells in control mice). Scale bars: 50 μ m. (D) Quantification of adherent leukocytes. (E) Representative time-lapse images of leukocyte rolling (green circles). Scale bars: 50 μ m. (F) Quantification of rolling leukocytes per second. $n = 4$ mice per group. * $P < 0.05$ versus control, Mann-Whitney U test.

after alcohol exposure, the longitudinal study of peripheral macrophage accumulation in the brain suggest the absence of a marked peripheral PVM recruitment (Supplemental Figure 3, A–F). Proliferation measurements by Ki67 staining were performed in harvested brains at the end of the alcohol exposure and have not shown positive signals of PVM proliferation (Supplemental Figure 3, G and H), perhaps because the measurements have been done at a single time point at the end of the alcohol exposure period.

To determine the specific role of brain PVM on ischemic stroke outcome in both healthy (naive) and primed mice (chronically exposed to alcohol), we depleted PVM by injecting clodronate-encapsulated (CLO-encapsulated) liposomes to mice exposed or not to 10% ethanol for 6 weeks (Figure 7D); control mice received PBS-encapsulated liposomes. In the adult brain, the i.c.v. injection of CLO depletes PVM (as well as meningeal macrophages) without affecting microglial cells or peripheral mononuclear cells (21), except for a transient reduction in the number of Kupffer cells in the liver (24). In our study, we have observed that the i.c.v. injection of CLO efficiently depletes PVM, but also provokes a series of inflammatory responses per se. Our data show that CLO acutely induced, per se, an inflammatory response in the ventricle area at 2 days after injection, which was not visible anymore at 6 days by molecular MRI imaging (P-selectin-coupled MPIOs) (Supplemental Figure 4, A and B; $n = 4$ mice/group). Our IHC data, focused on the injection site (the ventricle area), confirmed the data obtained by MRI and showed the absence of P-selectin⁺ staining (Supplemental Figure 4C), as well as no neutrophil infiltration (Ly6G⁺ staining) at that time (Supplemental Figure 4D). Microglia was not affected by the injection of CLO (Supplemental Figure 4D; $n = 4$ mice/group).

Flow cytometry experiments were performed at 5 days after injection, to respect the same timing profile as the one used in the stroke study. Our data show that there were no differences in the numbers of CD45^{lo}/CD11b⁺ cells (considered as resting microglia; Supplemental Figure 5B), CD45^{hi}/CD11b⁺ cells (considered as infiltrated macrophages; Supplemental Figure 5C), CD11c⁺CD11b⁺ cells (considered as DCs; Supplemental Figure 5E), or Ly6G⁺ cells (considered as granulocytes; Supplemental Figure 5F) between PBS- and CLO-treated mice. However, the numbers of CD45^{int}CD11b⁺ cells (considered as activated microglia; Supplemental Figure 5D), CD3⁺ (considered as total lymphocytes; Supplemental Figure 5G), CD4⁺ (Supplemental Figure 5H), and CD8⁺ (Supplemental Figure 5I) lymphocytes were increased in CLO-treated mice 5 days after CLO injection.

Table 4. Alcohol exposure alters the gene expression of inflammatory markers in the brain of mice, both in the absence of any other insult and after ischemic stroke

			IL-1b	IL-6	P-selectin	TGF-β	TLR4	TNF	VCAM1
Basal	C		0.19 ± 0.05	0.67 ± 0.28	1.89 ± 1.38	0.69 ± 0.11	0.80 ± 0.20	0.44 ± 0.18	0.78 ± 0.15
	A		0.54 ± 0.22	1.25 ± 0.33	0.44 ± 0.14	1.00 ± 0.14^A	1.27 ± 0.24	0.19 ± 0.01	1.02 ± 0.21
MCAo + 24 hours	Contro	C	0.14 ± 0.03	0.25 ± 0.07	0.22 ± 0.06	0.99 ± 0.20	0.77 ± 0.18	0.06 ± 0.02	0.97 ± 0.24
		A	0.15 ± 0.05	0.11 ± 0.03	0.13 ± 0.07	0.82 ± 0.14	0.64 ± 0.12	0.08 ± 0.00	0.73 ± 0.13
	Ipsi	C	3.01 ± 0.99	14.00 ± 4.04	9.32 ± 1.93	1.90 ± 0.17	1.77 ± 0.28	1.45 ± 0.23	1.39 ± 0.21
		A	5.51 ± 0.94^A	20.54 ± 3.11	17.52 ± 2.21^A	2.17 ± 0.26	2.31 ± 0.21	2.51 ± 0.38^A	1.29 ± 0.22

Gene expression was calculated using 2 housekeeping genes. The increase of the inflammatory markers expression was exacerbated in alcohol-exposed mice after thromboembolic stroke (basal, $n = 4$ mice per group; MCAo + 24 hours, $n = 5$ mice per group; ^A $P < 0.05$ vs. Control basal by Mann-Whitney U test). MCAo, middle cerebral artery occlusion.

The depletion of PVM was confirmed in vivo 24 hours after the i.c.v. injection of TRITC-Dextran (Figure 7, E–J). To assess the harmlessness of CLO injection on microglial cell numbers, we used CX3CR1-GFP^{+/−} mice in which TRITC-Dextran⁺ PVM can be distinguished in vivo from GFP⁺ microglial cells, since PVM are very low-positive for GFP (Figure 7, E and G). PVM depletion did not alter microglial cell numbers (GFP⁺ cells, Figure 7J). The phagocytosis of TRITC-Dextran by PVM was confirmed by IHC; the TRITC-Dextran⁺ cells were costained with CD206 (Figure 7F). PVM depletion was confirmed in vivo by 2-photon imaging (Figure 7, E and H; $P < 0.01$ vs. PBS) and by IHC analyses (CD206 staining; Figure 7, G and I; $P < 0.01$ vs. PBS).

The specific depletion of PVM by CLO prevented the aggravating effect of chronic alcohol exposure on ischemic lesions (Figure 7, K and L; $P < 0.05$ vs. PBS; $n = 5–6$ mice/group), whereas CLO treatment did not modify ischemic lesions in control mice (not exposed to alcohol) (Figure 7, K and L; $n = 5–6$ mice/group).

In order to explore the mechanisms of the beneficial effect of PVM depletion on stroke in alcohol-exposed mice, we studied the immune responses triggered 24 hours after stroke ($n = 4$ mice/group). We analyzed microglial/macrophage cell numbers (Iba1⁺ staining; Figure 8, A and B) and neutrophil infiltration (Figure 8, C and D) in PBS- and CLO-injected mice (PVM-depleted) exposed or not to alcohol. Microglial/macrophage numbers (Figure 8B), P-selectin protein levels (Figure 8, E and F), and VCAM1 protein levels (Figure 8, G and H) were significantly increased after stroke in PBS alcohol-exposed mice compared with PBS-control mice (Figures 8, A and B; $P < 0.05$ vs. PBS-treated control mice; $n = 4$ mice/group).

The effects of PVM depletion were different between control and alcohol-exposed mice. PVM-depleted control mice showed significantly more microglia/macrophages (Figure 8B; $P < 0.05$ vs. PBS control; $n = 4$ mice/group), as well as more neutrophils (Figure 8D; $P < 0.05$ vs. naive PBS; $n = 4$ mice/group) and increased VCAM1 protein levels (Figure 8H, $P < 0.05$ vs. naive PBS; $n = 4$ mice/group) in the ipsilateral hemisphere compared with PBS-treated control mice. By contrast, in PVM-depleted alcohol-exposed mice, microglia/macrophage (Figure 8B) and neutrophil (Figure 8D) infiltration — as well as VCAM levels (Figure 8H) — remained unchanged. We only found a significant decrease in P-selectin protein levels between PBS- and CLO-treated alcohol-exposed mice (Figure 8, E and F; $P < 0.05$ vs. PBS alcohol-exposed mice; $n = 4$ mice/group).

Interestingly, by intravital 2-photon microscopy, we observed that the number of adherent leukocytes was significantly decreased in PVM-depleted mice, independently of alcohol exposure (Figure 8, I, J, L, and M; $P < 0.05$ vs. PBS-treated mice; $n = 4$ mice/group). This effect was specific of leukocyte adhesion, since no difference was detected in the number of rolling or circulating leukocytes in any of the groups (Figure 8, K and N).

Discussion

We have performed here a translational study to investigate the effects of chronic alcohol consumption on ischemic stroke outcome. Our clinical results show that HD (≥ 6 drinks/day in the last 5 years) is independently associated (a) to END, (b) to stroke severity baseline, and (c) to higher infarct volume in stroke patients. The baseline characteristics of the study population, and outcomes at 3 months, were similar to those of large multicenter registries, suggesting good external validity of our results (25).

Our results show that the inflammatory response is associated with the risk of END in HD stroke patients. In order to elucidate the role of inflammation on the deleterious effect of HD after stroke, we

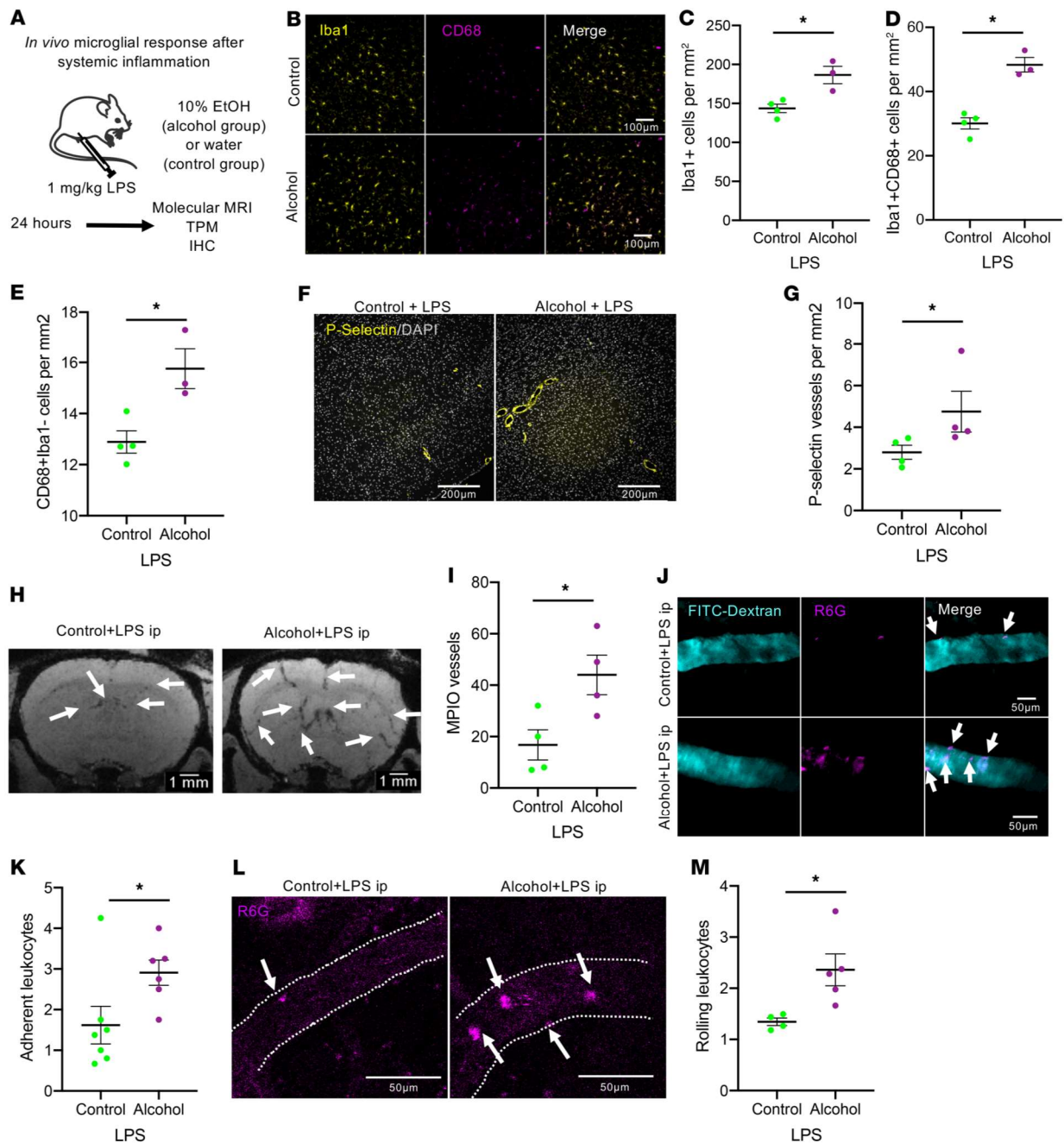


Figure 4. Alcohol exposure exacerbates brain neurovascular inflammatory reactions after an acute systemic insult in mice. (A) Experimental design to study whether chronic alcohol exposure provokes exacerbated inflammatory responses after a secondary injury (peripheral acute LPS injection). (B) Representative photomicrographs of the brain cortex of control and alcohol-exposed mice 24 hours after the acute systemic injection of LPS. Scale bars: 100 μ m. $n = 5-6$ mice per group. (C) Quantification of total microglia (Iba1⁺ cells). (D) Quantification of activated microglia (Iba1⁺/CD68⁺ cells). (E) Quantification of macrophages (CD68⁺/Iba1⁻ cells). (F) Representative photomicrographs of P-selectin staining in control and alcohol-exposed mice 24 hours after the acute systemic injection of LPS. Scale bars: 200 μ m. (G) Quantification of the number of P-selectin⁺ blood vessels. (H) Representative T2*-weighted images showing P-selectin-coupled MPIO in vivo accumulation in the brain of control and alcohol-exposed mice after the acute injection of LPS. Arrows show positive MPIO signals. (I) Quantification of MPIO + blood vessels. (J) Compilation of time-lapse images showing representative in vivo leukocyte adhesion (arrows) obtained by 2-photon microscopy. Scale bars: 50 μ m. (K) Quantification of leukocyte adhesion. (L) Representative time-lapse images of in vivo leukocyte rolling (see also Supplemental Videos 1 and 2). Scale bars: 50 μ m. (M) Quantification of rolling leukocytes per second. * $P < 0.05$ versus control, Mann-Whitney U test.

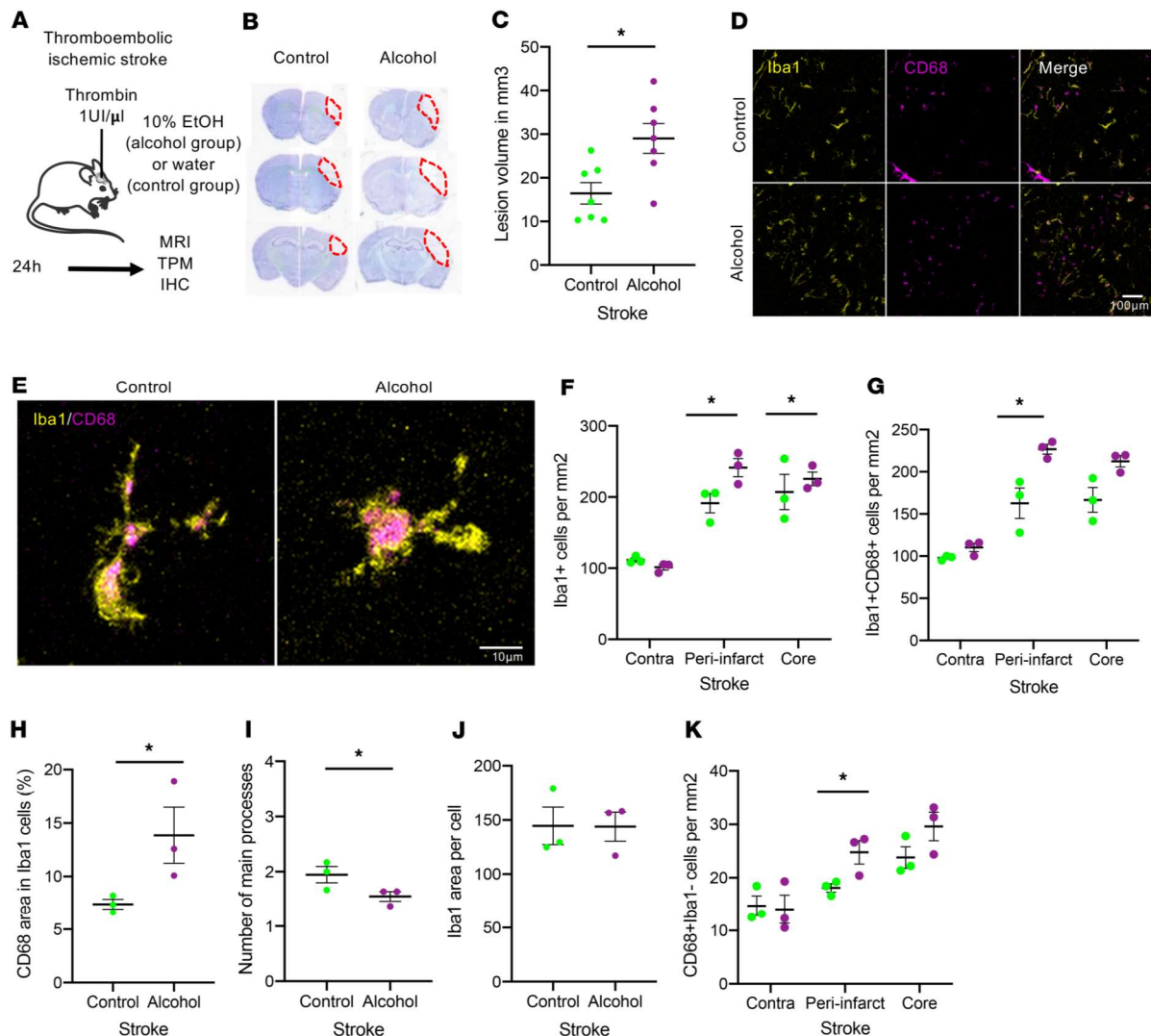


Figure 5. Alcohol exposure increases lesion volume and parenchymal inflammatory responses after ischemic stroke in mice. (A) Experimental design to study whether chronic alcohol exposure worsens ischemic stroke outcome. (B and C) Representative brain lesions (B) and corresponding quantifications (C) in control and alcohol-exposed mice 24 hours after stroke onset ($n = 8$ mice/group; $*P < 0.05$ vs. control mice). (D) Representative photomicrographs of microglial cells and infiltrated macrophages in the ipsilateral cortex 24 hours after stroke onset. Scale bar: 100 μm . $n = 4$ mice per group. (E) High-magnification photomicrographs of microglial cells at the peri-infarct area. Scale bar: 10 μm . (F) Quantification of Iba1⁺ cells. (G) Quantification of Iba1⁺CD68⁺ cells. (H) Quantification of CD68 area in Iba1⁺ cells. (I) Quantification of the number of processes starting from the soma. (J) Quantification of the mean whole cell area of Iba1⁺ cells. (K) Quantification of CD68⁺Iba1⁻ cells. $*P < 0.05$. Mann-Whitney U test.

performed preclinical experiments in mice exposed to 10% ethanol in drinking water during 6 weeks. Our preclinical findings show that chronic alcohol consumption by itself provokes a neurovascular inflammatory priming. The term “priming” is used to describe the propensity of a particular cell type to make an exaggerated response to a secondary stimulus (26) such as intracerebral or systemic LPS injection (27). Microglial priming was first described in the ME7 model of prion disease (28) but has been replicated in other models of chronic neuroinflammatory pathologies, including Alzheimer’s disease (29) and Parkinson’s disease (30).

To our knowledge, this is the first study defining a neurovascular inflammatory priming induced by chronic alcohol consumption. This alcohol-driven priming affects the brain parenchyma, as well as the perivascular and vascular compartments. In the parenchyma, it is characterized by (a) an unconventional activation profile of microglial cells, in accordance with results described by Cruz et al. (31), and (b) an increase in the expression of TGF- β mRNA not accompanied by changes in proinflammatory

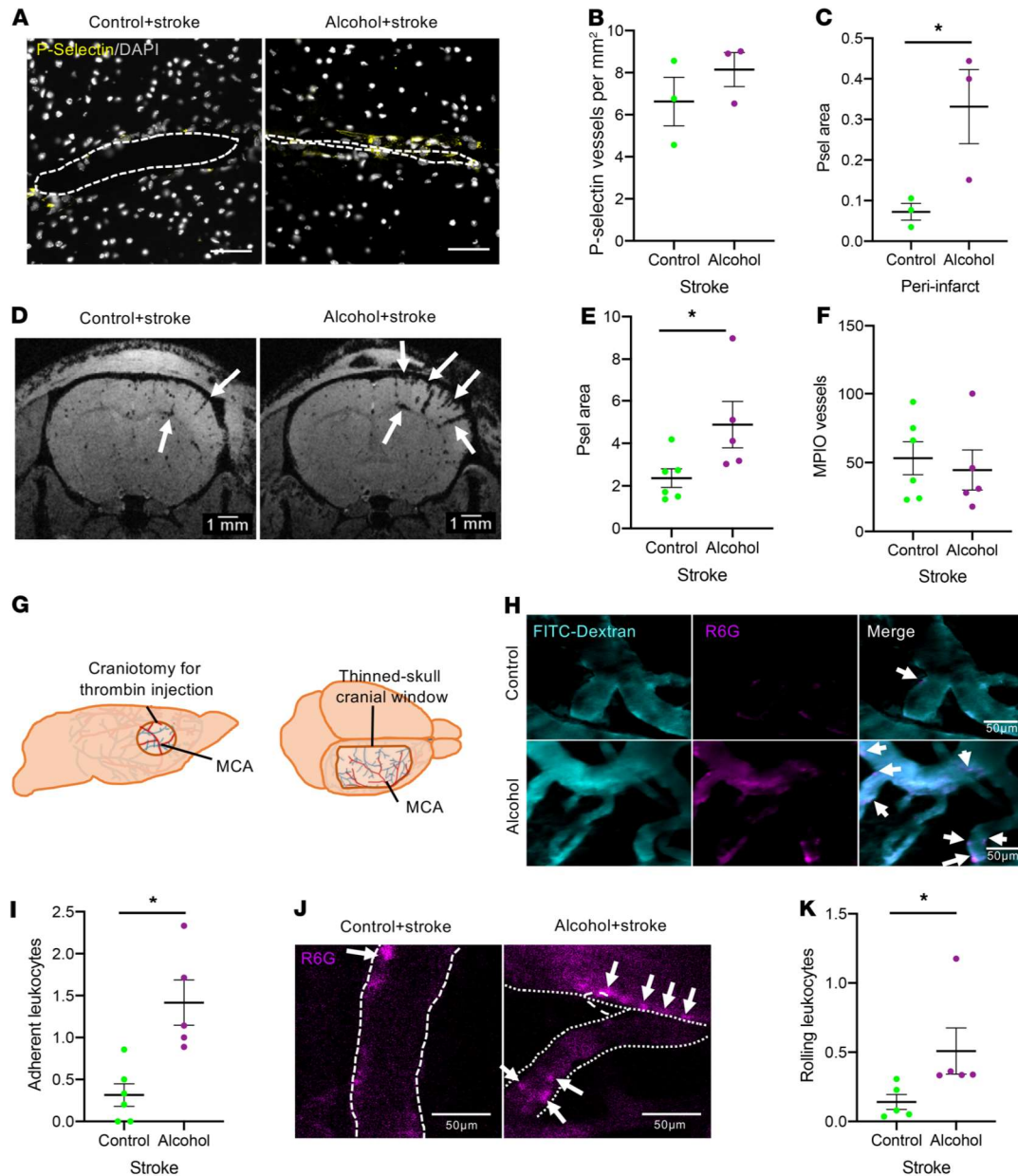


Figure 6. Alcohol exposure increases vascular inflammatory responses after ischemic stroke in mice. (A) Representative photomicrographs of P-selectin immunostaining in control and alcohol-exposed mice 24 hours after stroke onset. Scale bars: 50 μ m. (B) Quantification of the number of P-selectin⁺ vessels. (C) Quantification of P-selectin⁺ immunostaining area. (D) Representative T2*-weighted images of in vivo P-selectin molecular imaging. Arrows show MPIO⁺ blood vessels ($n = 5-6$ mice/group). (E) Quantification of MPIO⁺ area. (F) Quantification of MPIO⁺ blood vessels. (G) Schematic view of the craniotomy performed for thrombin injection, which leads to the occlusion of the MCA and the thinned-skull window for intravital 2-photon imaging. (H) Compilation of representative time-lapse images showing in vivo leukocyte adhesion (arrows) obtained by 2-photon microscopy. Scale bars: 50 μ m. (I) Quantification of leukocyte adhesion. (J) Representative time-lapse images of in vivo leukocyte rolling. Scale bars: 50 μ m. (K) Quantification of leukocyte rolling (see also Supplemental Videos 3 and 4). $n = 4$ mice per group. * $P < 0.05$ versus control, Mann-Whitney U test.

cytokines, thus following a similar profile as in priming-driving diseases such as prion disease (32). At the brain perivascular compartment, alcohol provokes an increase in the number of PVM. Finally, at the vascular level, alcohol-induced priming is characterized by increased levels of P-selectin at the endothelial surface, accompanied by an increase in the number of adherent and rolling leukocytes in the brain blood vessels.

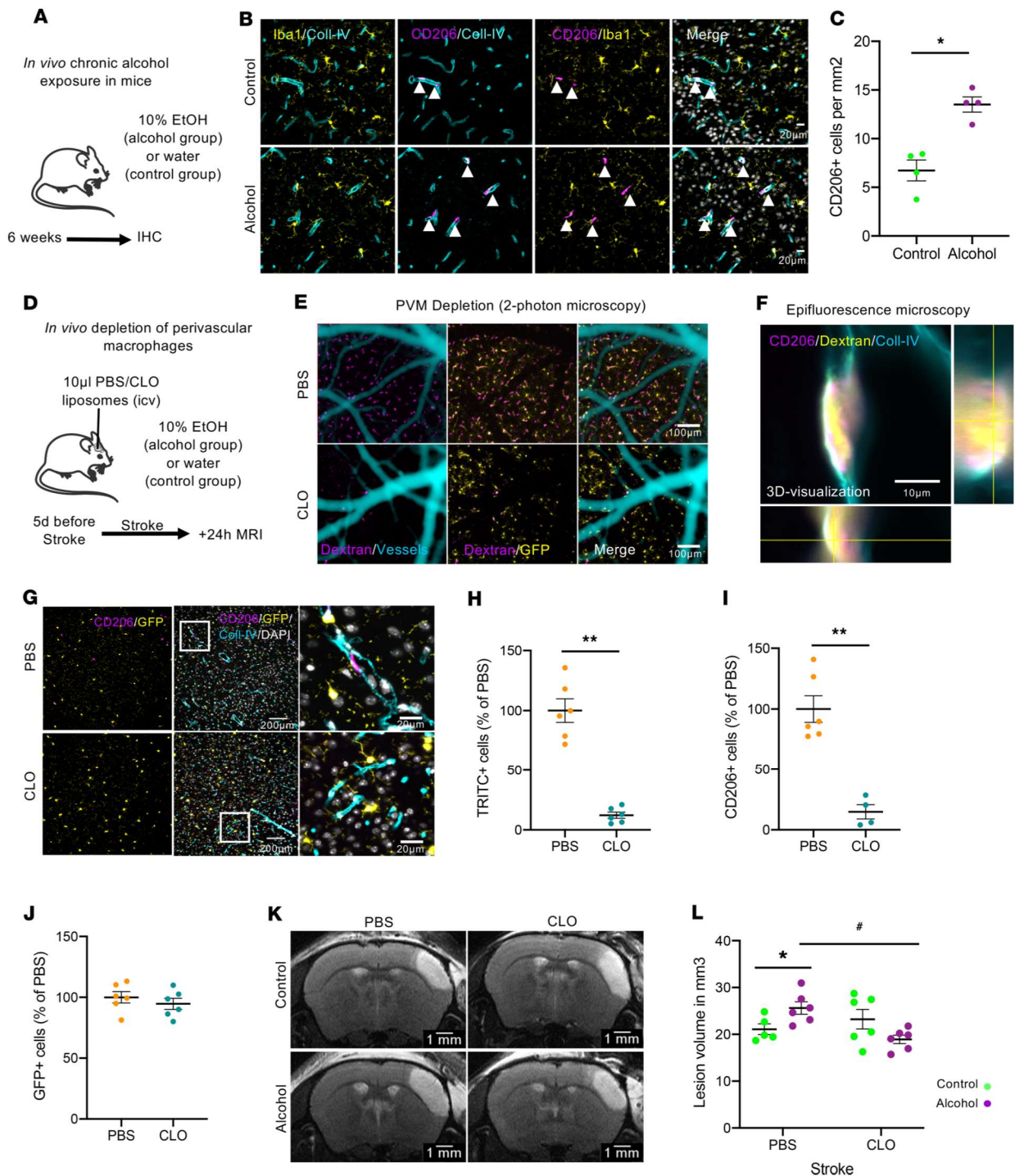


Figure 7. Perivascular macrophages (PVM) mediate the aggravating effect of chronic alcohol consumption on ischemic stroke in mice. (A) Experimental design to study the effects of chronic alcohol exposure on PVM. (B) Representative photomicrographs of PVM CD206⁺Iba1⁻ (arrowheads) cells in control and alcohol-exposed mice. (C) Quantification of PVM (CD206⁺ cells). Scale bars: 20 μ m. (D) Experimental design to deplete PVM in control and alcohol-exposed mice. (E) Representative in vivo Z stack of CX3CR1^{GFP/+} PBS/CLO-injected mice. Blood vessels are visualized through the i.v. injection of FITC-Dextran. Twenty-four hours after the i.c.v. injection of TRITC-Dextran, PVM can be in vivo visualized (note the absence of TRITC-Dextran signals in CLO-treated mice). Microglia are positive for GFP in CX3CR1^{GFP/+} mice. Scale bar: 100 μ m. (F) Colocalization of CD206 and phagocytosed TRITC-Dextran in PVM (epifluorescence microscopy). Three-dimensional visualization of a double-positive TRITC-Dextran and CD206 PVM for. Scale bar: 10 μ m. (G) Representative photomicrographs of GFP⁺ microglial cells and CD206⁺ PVMs in PBS- and CLO-treated mice.

Scale bar: 20 μm . (H and I) Quantification of PVM depletion by TRITC⁺ cell counting (H) and CD206⁺ counting (I). (J) The number of microglial cells remained unchanged after CLO treatment. (K) Representative T2-weighted MRI images showing ischemic lesions in PBS- and CLO-treated naive and alcohol-exposed mice 24 hours after stroke onset. (L) Quantification of lesion volumes. $n = 5\text{--}6$ mice per group; ** $P < 0.01$, * $P < 0.05$ versus PBS; # $P < 0.05$ versus control. Mann-Whitney U test.

We demonstrate here that alcohol provokes a brain inflammatory priming in mice by using 2 different approaches. First, we intracortically injected inert latex beads to control and alcohol-exposed mice. Eight hours after the injection, alcohol-exposed mice showed significantly more phagocytosed beads than control mice, thus demonstrating that chronic alcohol exposure makes microglia more prone to phagocytosis. Second, we systemically injected a single dose of LPS to control and alcohol-exposed mice and studied the subsequent parenchymal, perivascular, and vascular inflammatory responses 24 hours later. In accordance with our priming hypothesis, mice exposed to alcohol showed increased total microglial and activated microglial cell numbers; increased levels of P-selectin in the brain vasculature, characteristic of increased endothelial activation; and significantly increased rolling and adhering leukocyte numbers after the injection of LPS. Previous studies have reported that the exposure of C57BL/6J mice to 10 daily doses of ethanol followed by a LPS or Poly I:C challenge results in a sustained increase of proinflammatory cytokines in the brain compared with control-challenged animals (33, 34).

In accordance with our inflammatory priming hypothesis, our data show that inflammatory responses at the parenchymal, perivascular, and vascular levels were exacerbated in alcohol-exposed mice also after stroke. More precisely, microglial numbers and phagocytic capacity, brain PVM/infiltrated macrophages numbers, P-selectin levels at the brain endothelium, and leukocyte rolling and adhesion to brain vasculature were all exacerbated in alcohol-exposed mice after stroke. Inflammatory responses participate in the progression of ischemic lesions (35), but the causality or consequence relationship between the exacerbation of inflammatory responses and the increased lesion volume is difficult to determine. For this reason, our data on the inflammatory status before the ischemic injury are crucial and show that, even in the absence of stroke, HD alters the inflammatory status in both humans and mice. It has been proposed that inflammatory priming could have significant implications for acute sterile inflammatory insults, such as stroke and traumatic brain injury occurring on a background of aging or neurodegeneration (26). Our data show that chronic HD triggered a similar generalized heightened inflammatory sensitivity than in the aforementioned models of neurodegenerative diseases, and that alcohol-induced inflammatory priming had extremely deleterious consequences in stroke, not only in mice, but also in humans.

Importantly, we show here that PVM are determinant for the exacerbation of ischemic lesions, since their specific depletion by CLO blocks the aggravating effect of chronic alcohol exposure on stroke. Interestingly, the beneficial effect of PVM depletion on lesion volume is exclusive of alcohol-exposed mice, in which PVM numbers are significantly increased. Indeed, PVM accumulation at the perivascular space seems to be deleterious for ischemic stroke outcome, as it has been described in other neurological pathologies such as multiple sclerosis or Alzheimer's disease (for review, see ref. 20). It is also possible that alcohol exposure provokes not only an increase in PVM numbers, but also a shift of PVM phenotype and function from a scavenger, "buffer" cell (16, 17) to a proinflammatory, ROS-producing cell in "primed" conditions (36). In accordance with this hypothesis, it has recently been described that homeostatic subsets of CNS endogenous tissue macrophages are able to quickly change their phenotypes and generate context- and time-dependent subsets (37). An additional question that deserves future studies is whether PVM could drive microglial priming during chronic alcohol exposure, or instead, if microglial cells are responsible for the accumulation of PVM, at the perivascular spaces and the activation of brain endothelial cells.

Concerning the hypothesis of a role of PVM on mediating the stroke-induced inflammatory responses, our data show that, in naive mice, PVM do modulate stroke-induced inflammatory responses such as microglial activation/macrophage infiltration, neutrophil infiltration, endothelial activation, and leukocyte rolling/adhesion *in vivo*. It is important to take into account the effects of CLO, *per se*, found in our study, especially concerning lymphoid cells, which could also modify the post-stroke inflammatory responses. Surprisingly, these altered inflammatory responses are not associated with changes in the final lesion volume between PBS- and CLO-treated naive mice. These data are in accordance with the results reported by Pedragosa et al. (38), in which modifications of granulocyte infiltration in PVM-depleted mice are observed but are not accompanied by changes in final lesion volume in a model of ischemia/reperfusion. These results are in agreement with previous studies showing

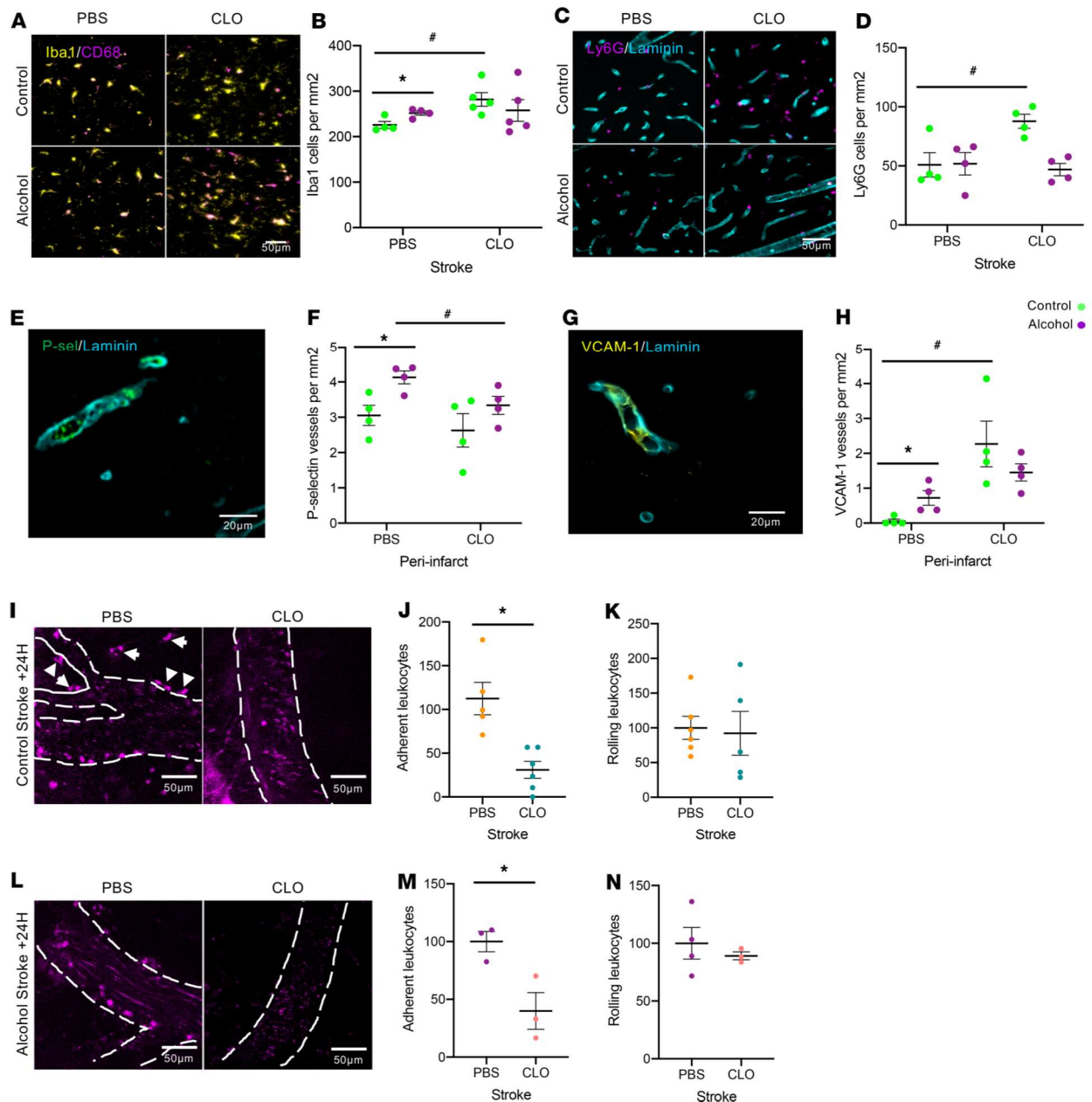


Figure 8. PVM modulate inflammatory responses to stroke in naive mice but not in alcohol-exposed mice. (A) Representative photomicrographs of different subsets of microglia/macrophages 24 hours after stroke onset at the core of the lesion. Scale bar: 50 μ m. (B) Quantification of Iba1⁺ cells. (C) Representative photomicrographs of Ly6G⁺ neutrophils at the core of the lesion. Scale bar: 50 μ m. (D) Quantification of neutrophil numbers. (E) Representative photomicrographs of P-selectin staining 24 hours after stroke onset. Scale bar: 20 μ m. (F) Quantification of P-selectin⁺ blood vessels. (G) Representative photomicrograph of VCAM1⁺ blood vessel 24 hours after stroke onset. Scale bar: 20 μ m. (H) Quantification of VCAM1⁺ blood vessels. (I) Representative photomicrographs obtained by 2-photon microscopy of leukocytes (in magenta, Rhodamine-6G) in PBS- and CLO-treated mice (not exposed to alcohol) 24 hours after stroke onset. Scale bars: 50 μ m. (J) Quantification of adherent leukocytes. (K) Quantification of circulating/rolling leukocytes. (L) Representative photomicrographs obtained by 2-photon microscopy of leukocytes (in magenta, Rhodamine-6G) in PBS- and CLO-treated mice (exposed to alcohol) 24 hours after stroke onset. Scale bars: 50 μ m. (M) Quantification of adherent leukocytes. (N) Quantification of circulating/rolling leukocytes. $n = 4$ mice per group, * $P < 0.05$ versus PBS; # $P < 0.05$ versus control PBS (B, D, H) and versus alcohol PBS (F). Mann-Whitney U test.

no impact of leukocyte recruitment on ischemic stroke volume (39, 40). Further studies are needed to better understand the links between final lesion volume and leukocyte infiltration at the ischemic area.

Our data suggest that the previous inflammatory status is critical for the ischemic stroke outcome. In the context of alcohol-induced inflammatory priming, PVM are linked to the aggravating effects of alcohol on stroke lesion volumes, since PVM-depleted mice show smaller lesion volumes. This aggravating effect of alcohol in lesion volume is associated with an increased inflammatory response in which PVM seem to play a critical role, since PVM-depleted mice show an attenuated inflammatory response compared with alcohol-exposed mice with intact PVM. One possible hypothesis to explain this differential role of PVM upon naive conditions and alcohol exposure could be a phenotypic change in PVM during alcohol exposure, as it has been described for other neuroinflammatory conditions (37), that could be crucial in case of a secondary CNS injury such as ischemic stroke.

Although research on PVM has intensified in recent times, we still have many unanswered questions concerning PVM phenotype and origin in pathological contexts. Also, since CLO depletes both meningeal macrophages and PVM, the observed effects cannot be attributed exclusively to PVM. In any case, PVM seem to be potential therapeutic targets for limiting the aggravating effects of risk factors on stroke outcome.

A potential limitation of this study is that we cannot exclude an impact of alcohol withdrawal on the worsening outcome of HD stroke patients and mice. Alcohol-withdrawn neurons are more sensitive to excitotoxic injuries (41) characteristic of early phases of ischemic stroke. Indeed, we cannot exclude that this mechanism also participates to the aggravation of stroke lesions observed in our study, making the exacerbated inflammatory responses observed after stroke the consequence and not the cause of the aggravated stroke outcome. However, our preclinical data obtained on mice not subjected to alcohol withdrawal (the intracortical latex bead-injected mice and the systemic LPS-injected mice) demonstrate that the exacerbated inflammatory response to both latex beads and acute LPS is present even in the absence of alcohol withdrawal. Other mechanisms that could contribute to the aggravation of stroke severity could be an endothelial dysfunction induced by chronic alcohol consumption (42, 43), which could have an impact by itself on microglial priming and PVM accumulation.

Interestingly, our data and the recently published data on the beneficial effect of low-dose alcohol consumption on inflammation following transient focal cerebral ischemia in rats (7) suggest that, similarly to the biphasic effects of alcohol on the risk of ischemic stroke (2), alcohol consumption also could have a biphasic effect on the consequences of ischemic stroke. These data, thus, help to clarify the apparently controversial clinical results found on the impact of alcohol consumption on stroke (4, 5).

In conclusion, we show that chronic alcohol consumption provokes, by itself, a neurovascular inflammatory priming in mice and inflammatory responses in HD patients. We experimentally demonstrate that this priming, notably involving PVM, drives the exacerbation of the damages provoked by a secondary insult such as an ischemic stroke. Our study opens potentially new avenues for the study of strategies targeting the alcohol-induced inflammatory priming before any neurological insult, in order to prevent a worsened neurological outcome in heavy drinkers.

Methods

Stroke cohort study population and patient characteristics. We retrospectively analyzed a cohort of 3,645 ischemic stroke patients from the stroke registry of the Stroke Unit of the Neurology Department of the University Clinical Hospital of Santiago de Compostela (Spain) included from January 2010 to December 2016. Acute management (diagnostic and treatment) of patients with stroke was performed according to the protocol described by the European Stroke Organization.

Stroke outcome variables. To evaluate the influence of chronic alcohol consumption on the outcome of stroke patients, the following primary outcomes variables were considered: (a) neurological stroke severity determined by the NIHSS at admission, 24 hours, and 48 hours; (b) END; (c) infarct volume determined by CT scan between the 4th and 7th day after admission; (d) degree of disability at 3 months assessed by modified Rankin scale (mRS); and (e) percentage of patients with good outcome at 3 months (mRS \leq 2).

To determine the association between chronic alcohol consumption and inflammatory response, the following biological variables were included in the analysis: (a) leukocyte numbers, (b) fibrinogen, (c) CRP, and (d) sedimentation rate. Axillary temperature over 37.5°C at admission was also considered as a marker of hyperthermia.

History of arterial hypertension was considered when the blood pressure was more than 140/90 mmHg at least 2 different days before stroke onset, if the patient was diagnosed for hypertension, or when

the patient was under antihypertensive treatment. History of diabetes disease was defined as serum glucose levels of 7.0 or more mmol/L, if the patient was diagnosed of diabetes, or when the patients was under diabetic medication. Smoking patients were defined as those patients who presented smoking habits in the last 5 years. HD habits were defined as a daily alcohol consumption of 6 or more drinks/day in the last 5 years.

Stroke cohort statistical analyses are detailed in the Supplementary Methods.

HD patients without stroke. We retrospectively analyzed data from an independent cohort including 34 patients with a DSM-5 (Diagnostic and Statistical Manual of Mental Disorders, 5th edition) diagnostic of severe Alcohol Use Disorder (AUD) (HD patients) and 21 healthy control subjects. All the participants were informed about the study, approved by the local ethics committee (CPP Nord Ouest III, IDRCB: 2011-A00495-36), and provided their written informed consent before their inclusion.

Blood samples were collected from fasted participants, either at inclusion (control subjects) or the day after admission to hospital (HD patients). Immune cell counts (leukocytes, neutrophils, eosinophils, basophils, lymphocytes, and monocytes) were measured in all participants. CRP levels were measured only in HD patients.

Additional information about this cohort and statistical analyses are detailed in the Supplemental Methods.

Experimental study design. The goal of this study was to investigate the impact of HD on stroke outcome and describe the underlying mechanisms in an experimental model of ischemic stroke in mice.

Animals were randomized to treatment groups, and all analyses were performed by investigators blinded to group allocation. Unblinding was performed after completion of statistical analysis. All animal experiments were performed and reported in accordance with the Animal Research: Reporting of In Vivo Experiments (ARRIVE) guidelines (<http://www.nc3rs.org.uk>).

Animals. Two-month-old male Swiss mice (35–45 g) (Centre Universitaire de Ressources Biologiques, Normandy University, Caen, France) were housed at 21°C in a 12-hour light/dark cycle with food and water (control group) or a 10% (v/v) alcohol solution (alcohol group) with ad libitum access for 6 weeks. All mice were checked daily for fluid consumption, health, and abnormal behavior. The average daily liquid intake and weight gain were similar between both groups (~6 mL of liquid intake/mouse/day and a weight gain of ~6 g between the beginning and the end of the alcohol exposure period; final weight ~40 g in both groups). Blood alcohol levels (BAL) were measured at the pharmacology unit of Caen University Hospital (Caen, France) in mice at the end of the 6 weeks of alcohol exposure ($n = 10$ mice). At the moment of the blood extraction, only 3 of 10 mice showed positive BAL values (0.39, 0.54, and 0.63 g/L); the rest of the mice showed nondetectable values (<0.1 g/L).

For intravital 2-photon imaging of PVM, male C57BL/6J CX3CR1-GFP^{+/−} mice (The Jackson Laboratory and in-house) were used ($n = 6$ mice/group).

All the procedures needing anesthesia of the mice were performed by an initial exposure to 5% isoflurane, followed by a maintaining phase of 1.5%–2% isoflurane 30%O₂/70%N₂O.

Thromboembolic focal cerebral ischemia. We used the in situ thromboembolic stroke model consisting of the injection of thrombin directly into the middle cerebral artery as described before (9). In order to mimic clinical conditions, alcohol solutions were changed by water after stroke onset and until killing. Additional information is provided in the Supplementary Methods.

I.p. LPS injection. A subset of control and alcohol-exposed mice ($n = 5–6$ mice per group) were i.p. injected with a single dose of the bacterial endotoxin LPS (1 mg/kg) (Sigma-Aldrich) (44) and underwent 2-photon imaging and molecular MRI 24 hours after the injection of LPS. Alcohol-exposed mice maintained free access to the alcohol solution after LPS injection and until killing.

In vivo microglial phagocytic capacity measurement. The protocol consisted of the injection of 1 μL of nonionic latex beads in the brain cortex and was modified from Hughes et al. (45). Details are provided in the Supplemental Methods.

Vascular adhesion molecular imaging. MPIOs (diameter 1.08 μm) (Invitrogen) covalently conjugated to purified polyclonal goat anti-mouse antibodies for P-selectin (R&D Systems, clone AF737) were prepared as previously described (46). Details are provided in the Supplemental Methods.

In vivo detection of BBB leakage. Three-dimensional T1 FLASH sequences (spatial resolution 70 μm × 70 μm; Echo time/repetition time (TE/TR) 4.46/15; 3 averages; 4 minutes, 2 seconds) were used before and 15 minutes after the i.v. injection of 200 μL of a solution containing 50 μL of Gadolinium chelate (DOTAREM) diluted in saline, as previously described (47). Additional information is provided in the Supplemental Methods.

Near-infrared detection of BBB leakage. NIRF imaging experiments were performed using a PhotonIMAGER (Biospace), as previously described (48). Additional information is provided in the Supplemental Methods.

Depletion of PVM. A total of 10 μ L of PBS-liposomes (PBS group) or CLO-encapsulated liposomes (CLO group) were injected in the left lateral ventricle. Additional information is provided in the Supplemental Methods.

In order to minimize the proinflammatory effects of CLO, per se, the i.c.v. injection of CLO was performed 5 days before the stroke.

In vivo macrophage labeling for the follow-up study of macrophage accumulation in the brain. A total of 200 μ L of 2 mg Fe/kg of nude MPIOs were injected i.v. to naive mice and T2*-w acquisitions were performed at different times after its injection to detect peripheral macrophage accumulation at the brain perivascular spaces. Additional details are provided in the Supplemental Methods.

Intravital 2-photon microscopy. Intravital 2-photon microscopy was performed through a thin-skull cranial window to measure leukocyte rolling and adhesion, as well as PVM visualization. Details are provided in the Supplemental Methods.

Flow cytometry analysis. Five days after the i.c.v. injection of PBS or CLO, mice were deeply anesthetized with isoflurane 5% and intracardially perfused with $1\times$ PBS (Sigma-Aldrich). Cell isolation from brains (without the cerebellum) and flow cytometry acquisition were performed as previously described (47) to obtain 2 separate panels for myeloid cells or lymphoid cells (see Supplemental Table 6 and Supplemental Figure 5A). Data were analyzed with the FlowJo 7.6.5 software (TreeStar Inc.). Data are expressed as total cell count for each sample.

Quantitative PCR analyses. Details on the methods for quantitative PCR (qPCR) analyses are provided in the Supplemental Methods. Primers used for this study are detailed in Supplemental Table 5.

IHC. Epifluorescence and confocal microscopy analyses were performed in brain sections and isolated brain vessels. Details on the protocol and methods are provided in the Supplemental Methods.

Statistics. Results are the mean \pm SEM. Statistical analyses were performed by the Mann-Whitney *U* test using the Statview software.

Study approval. Stroke patient registry was approved by the Ethics Committee of Galicia (CEIC) (Spain, protocol code 201/516). Signed informed consent was obtained from patients or a relative before study inclusion. Experimental studies were approved by the French ministry of education and research (Project 3748; Center agreement D14118001). All the participants were informed about the study, approved by the local ethics committee (CPP Nord Ouest III, IDRCB 2011-A00495-36) and provided their written informed consent before their inclusion. All animal experiments were performed and reported in accordance with the Animal Research: Reporting of In Vivo Experiments (ARRIVE) guidelines (<http://www.nc3rs.org.uk>), in accordance with French laws (act no. 87-848; Ministère de l'Agriculture et de la Forêt) and European Communities Council Directives of November 24, 1986 (86/609/EEC) guidelines, and they have been approved by the ethical committee (affiliation 3748).

Author contributions

MR designed and coordinated the study and was responsible for stroke model surgeries. AD and DL performed histological and transcriptional analyses, as well as in vivo functional analyses of microglial phagocytosis. AD, DL, AQ, and EL were responsible for molecular MRI. AD and MR were responsible for 2-photon microscopy. AD, DL, and MN analyzed immunohistochemical samples. MG and MR analyzed flow cytometry. AL and ALP analyzed data from the ALCOBRAIN cohort of HD patients. FC and JC analyzed data and writing of results from the stroke cohort of patients. DV supervised the study. MR wrote the manuscript with the revision and approval of all authors.

Acknowledgments

The authors are grateful to Carine Ali and Fabian Docagne for their valuable scientific suggestions, as well as Laurent Coulbaut for the analyses of human samples from the ALCOBRAIN cohort. The authors thank Véronique Lelong-Boulouard for the BAL measurements. This study was funded by the Fondation pour la Recherche en Alcoologie (MR), the AXA Research Found (MR), INSERM, Caen-Normandy University, the Regional Council of Normandy, the ANR grant RHU MARVELOUS (ANR-16-RHUS-0009) (DV), and ANR "Retour jeune chercheur" (ALP).

Address correspondence to: Marina Rubio, PHIND Boulevard Henri Becquerel 14074 Caen Cedex, Caen, France. Phone: 33.2.31.47.01.55; Email: rubio@cyceron.fr.

1. Rehm J, et al. Defining substance use disorders: do we really need more than heavy use? *Alcohol Alcohol*. 2013;48(6):633–640.
2. Larsson SC, Wallin A, Wolk A, Markus HS. Differing association of alcohol consumption with different stroke types: a systematic review and meta-analysis. *BMC Med*. 2016;14(1):178.
3. Kadlecová P, Anđel R, Mikulík R, Handing EP, Pedersen NL. Alcohol consumption at midlife and risk of stroke during 43 years of follow-up: cohort and twin analyses. *Stroke*. 2015;46(3):627–633.
4. Ducroquet A, et al. Influence of chronic ethanol consumption on the neurological severity in patients with acute cerebral ischemia. *Stroke*. 2013;44(8):2324–2326.
5. Gattringer T, et al. IV thrombolysis in patients with ischemic stroke and alcohol abuse. *Neurology*. 2015;85(18):1592–1597.
6. Zhao H, Mayhan WG, Arrick DM, Xiong W, Sun H. Dose-related influence of chronic alcohol consumption on cerebral ischemia/reperfusion injury. *Alcohol Clin Exp Res*. 2011;35(7):1265–1269.
7. McCarter KD, et al. Effect of Low-Dose Alcohol Consumption on Inflammation Following Transient Focal Cerebral Ischemia in Rats. *Sci Rep*. 2017;7(1):12547.
8. Lemarchand E, et al. Impact of alcohol consumption on the outcome of ischemic stroke and thrombolysis: role of the hepatic clearance of tissue-type plasminogen activator. *Stroke*. 2015;46(6):1641–1650.
9. Orset C, et al. Mouse model of in situ thromboembolic stroke and reperfusion. *Stroke*. 2007;38(10):2771–2778.
10. Orset C, et al. Efficacy of Alteplase in a Mouse Model of Acute Ischemic Stroke: A Retrospective Pooled Analysis. *Stroke*. 2016;47(5):1312–1318.
11. Imhof A, Froehlich M, Brenner H, Boeing H, Pepys MB, Koenig W. Effect of alcohol consumption on systemic markers of inflammation. *Lancet*. 2001;357(9258):763–767.
12. Alho H, Sillanaukee P, Kalela A, Jaakkola O, Laine S, Nikkari ST. Alcohol misuse increases serum antibodies to oxidized LDL and C-reactive protein. *Alcohol Alcohol*. 2004;39(4):312–315.
13. He J, Crews FT. Increased MCP-1 and microglia in various regions of the human alcoholic brain. *Exp Neurol*. 2008;210(2):349–358.
14. Goldmann T, et al. Origin, fate and dynamics of macrophages at central nervous system interfaces. *Nat Immunol*. 2016;17(7):797–805.
15. He H, et al. Perivascular Macrophages Limit Permeability. *Arterioscler Thromb Vasc Biol*. 2016;36(11):2203–2212.
16. Kida S, Steart PV, Zhang ET, Weller RO. Perivascular cells act as scavengers in the cerebral perivascular spaces and remain distinct from pericytes, microglia and macrophages. *Acta Neuropathol*. 1993;85(6):646–652.
17. Mendes-Jorge L, et al. Scavenger function of resident autofluorescent perivascular macrophages and their contribution to the maintenance of the blood-retinal barrier. *Invest Ophthalmol Vis Sci*. 2009;50(12):5997–6005.
18. Mato M, et al. Involvement of specific macrophage-lineage cells surrounding arterioles in barrier and scavenger function in brain cortex. *Proc Natl Acad Sci USA*. 1996;93(8):3269–3274.
19. Fabrick BO, et al. CD163-positive perivascular macrophages in the human CNS express molecules for antigen recognition and presentation. *Glia*. 2005;51(4):297–305.
20. Faraco G, Park L, Anrather J, Iadecola C. Brain perivascular macrophages: characterization and functional roles in health and disease. *J Mol Med*. 2017;95(11):1143–1152.
21. Faraco G, et al. Perivascular macrophages mediate the neurovascular and cognitive dysfunction associated with hypertension. *J Clin Invest*. 2016;126(12):4674–4689.
22. Anrather J, Iadecola C. Inflammation and Stroke: An Overview. *Neurotherapeutics*. 2016;13(4):661–670.
23. Perego C, Fumagalli S, De Simoni MG. Temporal pattern of expression and colocalization of microglia/macrophage phenotype markers following brain ischemic injury in mice. *J Neuroinflammation*. 2011;8:174.
24. Polfliet MM, Goede PH, van Kesteren-Hendriks EM, van Rooijen N, Dijkstra CD, van den Berg TK. A method for the selective depletion of perivascular and meningeal macrophages in the central nervous system. *J Neuroimmunol*. 2001;116(2):188–195.
25. Dávalos A et al. Citicoline in the treatment of acute ischaemic stroke: an international, randomised, multicentre, placebo-controlled study (ICTUS trial). *Lancet*. 2012;380(9839):349–357.
26. Hennessy E, Griffin EW, Cunningham C. Astrocytes Are Primed by Chronic Neurodegeneration to Produce Exaggerated Chemokine and Cell Infiltration Responses to Acute Stimulation with the Cytokines IL-1 β and TNF- α . *J Neurosci*. 2015;35(22):8411–8422.
27. Cunningham C, Wilcockson DC, Champion S, Lunnon K, Perry VH. Central and systemic endotoxin challenges exacerbate the local inflammatory response and increase neuronal death during chronic neurodegeneration. *J Neurosci*. 2005;25(40):9275–9284.
28. Perry VH, Cunningham C, Boche D. Atypical inflammation in the central nervous system in prion disease. *Curr Opin Neurol*. 2002;15(3):349–354.
29. Sly LM, et al. Endogenous brain cytokine mRNA and inflammatory responses to lipopolysaccharide are elevated in the Tg2576 transgenic mouse model of Alzheimer's disease. *Brain Res Bull*. 2001;56(6):581–588.
30. Pott Godoy MC, Tarelli R, Ferrari CC, Sarchi MI, Pitossi FJ. Central and systemic IL-1 exacerbates neurodegeneration and motor symptoms in a model of Parkinson's disease. *Brain*. 2008;131(Pt 7):1880–1894.
31. Cruz SA, et al. Loss of IRF2BP2 in Microglia Increases Inflammation and Functional Deficits after Focal Ischemic Brain Injury. *Front Cell Neurosci*. 2017;11:201.
32. Cunningham C, Boche D, Perry VH. Transforming growth factor beta1, the dominant cytokine in murine prion disease: influence on inflammatory cytokine synthesis and alteration of vascular extracellular matrix. *Neuropathol Appl Neurobiol*. 2002;28(2):107–119.
33. Qin L, He J, Hanes RN, Pluzarev O, Hong JS, Crews FT. Increased systemic and brain cytokine production and neuroinflammation by endotoxin following ethanol treatment. *J Neuroinflammation*. 2008;5:10.
34. Qin L, Crews FT. Chronic ethanol increases systemic TLR3 agonist-induced neuroinflammation and neurodegeneration. *J Neuroinflammation*. 2012;9:130.
35. Iadecola C, Anrather J. The immunology of stroke: from mechanisms to translation. *Nat Med*. 2011;17(7):796–808.
36. Capone C, Faraco G, Park L, Cao X, Davisson RL, Iadecola C. The cerebrovascular dysfunction induced by slow pressor doses of angiotensin II precedes the development of hypertension. *Am J Physiol Heart Circ Physiol*. 2011;300(1):H397–H407.
37. Jordão MJC, et al. Single-cell profiling identifies myeloid cell subsets with distinct fates during neuroinflammation. *Science*.

- 2019;363(6425):eaat7554.
38. Pedragosa J, et al. CNS-border associated macrophages respond to acute ischemic stroke attracting granulocytes and promoting vascular leakage. *Acta Neuropathol Commun.* 2018;6(1):76.
 39. Harris AK, Ergul A, Kozak A, Machado LS, Johnson MH, Fagan SC. Effect of neutrophil depletion on gelatinase expression, edema formation and hemorrhagic transformation after focal ischemic stroke. *BMC Neurosci.* 2005;6:49.
 40. Schmidt A, et al. Targeting Different Monocyte/Macrophage Subsets Has No Impact on Outcome in Experimental Stroke. *Stroke.* 2017;48(4):1061–1069.
 41. Rubio M, et al. Pharmacological activation/inhibition of the cannabinoid system affects alcohol withdrawal-induced neuronal hypersensitivity to excitotoxic insults. *PLoS ONE.* 2011;6(8):e23690.
 42. Mayhan WG. Responses of cerebral arterioles during chronic ethanol exposure. *Am J Physiol.* 1992;262(3 Pt 2):H787–H791.
 43. Sun H, Patel KP, Mayhan WG. Tetrahydrobiopterin, a cofactor for NOS, improves endothelial dysfunction during chronic alcohol consumption. *Am J Physiol Heart Circ Physiol.* 2001;281(5):H1863–H1869.
 44. Montagne A, et al. Ultra-sensitive molecular MRI of cerebrovascular cell activation enables early detection of chronic central nervous system disorders. *Neuroimage.* 2012;63(2):760–770.
 45. Hughes MM, Field RH, Perry VH, Murray CL, Cunningham C. Microglia in the degenerating brain are capable of phagocytosis of beads and of apoptotic cells, but do not efficiently remove PrPSc, even upon LPS stimulation. *Glia.* 2010;58(16):2017–2030.
 46. Quenault A, et al. Molecular magnetic resonance imaging discloses endothelial activation after transient ischaemic attack. *Brain.* 2017;140(1):146–157.
 47. Drieu A et al. Immune Responses and Anti-inflammatory Strategies in a Clinically Relevant Model of Thromboembolic Ischemic Stroke with Reperfusion. *Transl Stroke Res.* September 2019.
 48. Marcos-Contreras OA, et al. Hyperfibrinolysis increases blood-brain barrier permeability by a plasmin- and bradykinin-dependent mechanism. *Blood.* 2016;128(20):2423–2434.



Immune Responses and Anti-inflammatory Strategies in a Clinically Relevant Model of Thromboembolic Ischemic Stroke with Reperfusion

Antoine Drieu¹ · Izaskun Buendia² · Damien Levard¹ · Pauline Hélie¹ · Camille Brodin¹ · Denis Vivien^{1,3} · Marina Rubio¹ 

Received: 19 March 2019 / Revised: 20 August 2019 / Accepted: 23 August 2019
© Springer Science+Business Media, LLC, part of Springer Nature 2019

Abstract

The poor clinical relevance of experimental models of stroke contributes to the translational failure between preclinical and clinical studies testing anti-inflammatory molecules for ischemic stroke. Here, we (i) describe the time course of inflammatory responses triggered by a thromboembolic model of ischemic stroke and (ii) we examine the efficacy of two clinically tested anti-inflammatory drugs: Minocycline or anti-CD49d antibodies (tested in stroke patients as Natalizumab) administered early (1 h) or late (48 h) after stroke onset. Radiological (lesion volume) and neurological (grip test) outcomes were evaluated at 24 h and 5 days after stroke. Immune cell responses peaked 48 h after stroke onset. Myeloid cells (microglia/macrophages, dendritic cells, and neutrophils) were already increased 24 h after stroke onset, peaked at 48 h, and remained increased—although to a lesser extent—5 days after stroke onset. CD8⁺ and CD4⁺ T-lymphocytes infiltrated the ipsilateral hemisphere later on (only from 48 h). These responses occurred together with a progressive blood-brain barrier leakage at the lesion site, starting 24 h after stroke onset. Lesion volume was maximal 24–48 h after stroke onset. Minocycline reduced both lesion volume and neurological deficit only when administered early after stroke onset. The blockade of leukocyte infiltration by anti-CD49d had no impact on lesion volume or long-term neurological deficit, independently of the timing of treatment. Our data are in accordance with the results of previous clinical reports on the use of Minocycline and Natalizumab on ischemic stroke. We thus propose the use of this clinically relevant model of thromboembolic stroke with recanalization for future testing of anti-inflammatory strategies for stroke.

Keywords Inflammation · Ischemic stroke · Leukocytes · Microglia · Experimental models · Translational research

Introduction

Ischemic stroke is the second leading cause of death and the first cause of acquired long-term disability worldwide with one stroke occurring every 2 s in the world [1] (stroke.org.uk). Ischemic stroke (80–85% of strokes) is described as the sudden interruption of blood flow in a particular brain region leading to rapid neuronal death [2]. Stroke-induced neuronal loss is envisioned to be a multiphasic process involving excitotoxicity, apoptosis, and inflammation [3]. In spite of promising results in experimental models of stroke, no treatment targeting these mechanisms has shown a clear beneficial effect in clinical practice. Indeed, the only successful and approved therapies for ischemic stroke nowadays are thrombolysis (i.e., the intravenous injection of tissue-type plasminogen activator (tPA)) within 4.5 h after stroke onset [4] and

Electronic supplementary material The online version of this article (<https://doi.org/10.1007/s12975-019-00733-8>) contains supplementary material, which is available to authorized users.

✉ Marina Rubio
rubio@cyceron.fr

¹ Normandie Univ, UNICAEN, INSERM, U1237, PhIND “Physiopathology and Imaging of Neurological Disorders”, Institut Blood and Brain @ Caen-Normandie, Cyceron, 14000 Caen, France, Normandie Université, 14000 Caen, France

² Servicio de Farmacología Clínica, Hospital Universitario de la Princesa, Instituto de Investigación Sanitaria, Madrid, Spain

³ Department of Clinical Research, CHU de Caen Normandy, 14000 Caen, France

thrombectomy (i.e., the mechanical removal of the clot) up to 24 h after stroke onset [5].

The poor clinical relevance of experimental models of stroke has been suggested as a contributor to the dichotomy between promising experimental results and the limited success of clinical trials testing immunomodulatory molecules for ischemic stroke [6]. Although the majority of untreated stroke patients show progressive spontaneous arterial recanalization after stroke, pre-clinical studies testing the efficacy of immunomodulatory drugs for stroke have been performed in models in which the middle cerebral artery (MCA) is either permanently or transiently occluded respectively by electrocoagulation or by a monofilament. In the case of transient mechanical occlusions, recanalization of the artery is sudden and associated to ischemic/reperfusion injuries [7]. Kinetics, localization, and intensity of the inflammatory responses differ among these models [8–11]. In an attempt to improve translational research on the stroke field, we conceived in the past years a new experimental murine model of stroke consisting in the injection of thrombin directly into the MCA. This model leads to the formation of a fibrin-rich clot in the lumen of the MCA [12, 13]. Similar to clinical reports [14, 15], in this experimental model, tissue-type plasminogen activator is able to reduce ischemic volume when injected early after stroke onset but not when injected late [12, 16, 17]. The first objective of this study was to describe the time course of inflammatory responses triggered by this experimental model of ischemic stroke. Our second objective was to study the efficacy of two anti-inflammatory drugs previously tested in stroke patients: minocycline or anti-CD49d antibodies. We chose these drugs in order to compare the results obtained in this model to the results reported in clinical trials, with the aim of testing the predictive potential of this experimental model and to ultimately improve translational research in the stroke field.

Material and Methods

Animals and Treatments

Studies were conducted in male Swiss mice (age 12 weeks, weight 35–45 g). Mice were housed with food and water *ad libitum* access. All experiments were performed following the ARRIVE guidelines (www.nc3rs.org.uk), including blind analyses of the samples. Minocycline (a single dose of 30 mg/kg IP; Sigma-Aldrich) or the rat anti-mouse CD49d antibody (Clone R1-2; BD Biosciences; a single dose of 250 µg iv) was administered either 1 h or 48 h after the middle cerebral artery occlusion (MCAo).

Thromboembolic Stroke Model

Mice were placed in a stereotaxic device, a small craniotomy was performed, the dura was excised, and the MCA was

exposed. A customer-made glass micropipette was introduced into the lumen of the MCA and 1 µL of purified murine alpha-thrombin (1 UI; Enzyme Research Labs) was pneumatically injected to induce the in situ formation of a clot. The pipette was removed 10 min after, when the clot had stabilized. Cerebral blood flow was monitored by laser Doppler flowmetry using a fiber-optic probe (Oxford Optronix) before and up to 45 min after the MCAo to check and exclude of the study early spontaneous recanalization (no mouse was excluded for this reason). The number of mice included, excluded, and dead on each experiment is indicated in Supplementary Table 1. Twenty-four hours after stroke onset, mice lost around 5% of their weight (retrospective analysis of laboratory internal data including 63 mice).

Magnetic Resonance Imaging

Mice were deeply anesthetized with 5% isoflurane and maintained with 1.5–2% isoflurane 30%O₂/70%N₂O during the acquisitions. Experiments were carried out on a Phamscan 7T (Bruker, Germany). T2-weighted images were acquired using a multislice multiecho sequence: TE/TR 33 ms/2500 ms. Lesion sizes were quantified on these images using ImageJ software. Mice showing lesions < 6 mm³ at 24 h post-MCAo were considered as surgical failure and excluded from the analyses.

T2*-weighted sequences were used to control if animals underwent hemorrhages events. Two-dimensional time-of-flight angiographies (TE/TR 12 ms/7 ms) were acquired, and analyses of the MCA angiogram were also performed to control the recanalization status of the MCA. The angiographic score is inspired on the TICI grade flow scoring. Score 0 refers to the absence of any antegrade flow beyond the MCA. Score 1 is incomplete filling of the distal bed. Score 2 is almost complete filling of the distal territory. Score 3 is complete filling of the distal territory.

In Vivo Detection of BBB Leakage

Three dimensional T1 FLASH sequences (spatial resolution 70 mm × 70 mm; TE/TR 4.46/15; 3 averages; 4 min 2 s) were used, 15 min after the iv injection of 200 µL of a solution containing 50 µL of gadolinium chelate (DOTAREM) diluted in saline. Blood-brain barrier (BBB) leakage was measured before and 6, 24, 48, and 120 h (5 days) after stroke.

In Vivo Molecular Imaging of Macrophage Infiltration

Two hundred microliters of 2 mg Fe/kg of nude micro-sized particles of iron oxide (MPIOs) (diameter 1.08 µm) (Invitrogen) was injected iv 1 day before stroke (*n* = 6). Three-dimensional T2*-weighted (T2*-w) gradient echo imaging of flow compensation (spatial resolution 70 mm³ isotropic, TE/TR 13.2 ms/200 ms, and a flip angle of 21°) was

performed every day starting from the day before the MCAo to detect MPIOs. Images were analyzed by Fiji software. Signal void quantification was performed by using image threshold, and results presented as MPIO-induced signal void on the contralateral cortex divided by the signal void on the structure of interest in percent.

In Vivo Molecular Imaging of Endothelial Activation

MPIOs covalently conjugated to purified polyclonal goat anti-mouse antibodies for P-selectin (R&D Systems, clone AF737) were prepared as previously described [18]. The quality of conjugated MPIOs was checked in a naive mouse, by stereotaxic injection of lipopolysaccharide (1 μ l, 1 mg/kg) in the striatum (0.5 mm anterior, 2.0 mm lateral, –3 mm ventral to the Bregma) (data not shown).

MRI acquisitions (same 3D T2*-w sequence than the one used for nude MPIO detection) started immediately after the intravenous injection of MPIOs (200 μ l of 2 mg Fe/kg of α -P-selectin conjugated MPIOs). All T2*-w scans presented are minimum intensity projections of six consecutive slices. Signal void quantification on 3D T2*-weighted images was measured by using automatic triangle threshold in ImageJ software, and results presented as MPIO-induced signal void on the contralateral cortex divided by the signal void on the structure of interest (in percent).

Immunohistochemistry

For all groups, mice were deeply anesthetized and transcardially perfused with cold heparinized saline (15 mL) followed by 100 mL of fixative (PBS 0.1 M, pH 7.4 containing 2% paraformaldehyde and 0.2% picric acid). The brains were post-fixed (18 h; 4 °C) and cryoprotected (sucrose 20% in PBS; 24 h; 4 °C) before freezing in Tissue-Tek (Miles Scientific, Naperville, IL, USA). Cryomicrotome-cut sections (10 μ m) were collected on poly-lysine slides and stored at –80 °C before processing.

Sections were co-incubated overnight with rabbit anti-mouse Iba1 (1:1000, Wako 019-19741), rat anti-mouse CD68 (1:800, Abcam 53444), rat anti-mouse Ly6G (1:500, clone 1A8, StemCell 60031), goat anti-mouse type-IV collagen (1:1000, SouthernBiotech 1340), rabbit anti-mouse CD3 (1:25, Abcam 5690), rat anti-mouse CD4 (1:25, eBiosciences 14-0042-86), rabbit anti-mouse laminin (1:1000, Abcam 14055-50), and sheep anti-mouse fibrinogen (1:10,000). Primary antibodies were revealed by using Fab'2 fragments of Donkey anti-rabbit linked to FITC, anti-sheep linked to FITC, anti-rat linked to Cy3, anti-rabbit linked to Cy5, and anti-goat IgG linked to Cy5 (1:600, Jackson ImmunoResearch, West Grove, USA). Washed sections were coverslipped with anti-fade medium containing DAPI, and images were digitally captured using a Leica DM6000 epifluorescence microscope-coupled coolsnap camera and

visualized with Leica MM AF 2.2.0 software (Molecular Devices, USA) and further processed using ImageJ 1.51k software.

Leukocyte Isolation for Flow Cytometry Analysis

Cell Isolation from Brain Hemispheres

At each corresponding time point, mice were deeply anesthetized with isoflurane 5% and intracardially perfused with 1 \times PBS (Sigma-Aldrich). The brains were harvested, and hemispheres (ipsi and contralateral) were separated. Hemispheres were washed with 1X PBS, filtered across a 40 μ M filter (Corning) with 1 \times PBS, washed by centrifugation, and resuspended in 30% Percoll. Cells were then loaded onto a 70% Percoll phase for a 30/70% Percoll gradient protocol as follows: after a centrifugation at 1200 \times g for 30 min, myelin was removed from the top of the gradient and cells were harvested, filtered, and washed with sterile staining buffer (PBS supplemented with 2% fetal bovine serum (from Gibco)). At this step, immune cells from each sample were measured by Malassez cell counting.

Flow Cytometry Acquisition

Cells were then resuspended in 50 μ l of staining buffer, and fc receptors were blocked for 15 min at 4 °C with anti-CD16/CD32 antibodies (10 μ g/mL, BD Biosciences). After the blocking phase, cells were labeled for 20 min at 4 °C with corresponding fluorochrome-conjugated monoclonal antibodies (BD Biosciences) (see Table 1) corresponding to two separated panels (for myeloid cells or lymphoid cells). Harvested cells were then washed with staining buffer by centrifugation at 250 \times g for 10 min at room temperature, resuspended in 500 μ L of 1 \times PBS, and finally, samples were assayed by a FACSVerse flow cytometer (Beckton Dickinson). Data were analyzed with the FlowJo 7.6.5 software (TreeStar Inc.). Data are expressed as total cell count after Malassez cell counting for each sample.

Functional Recovery Assessment by Grip Strength Test

The grip strength test (BIOSEB, France) assesses neuromuscular functions in mice by determining the strength displayed by the animal relative to the forepaw-grasping reflex. Mice, holding by the tail, were dropped on a T-like-bar and gently removed by the experimenter. Measurements of forepaws strength were picked up the day before MCAo (baseline acquisition), 24 h and 5 days after MCAo. To reduce variability, five assays per mouse are performed, with 1 min of rest between each assay to obtain the mean strength. Data are expressed as percentage of strength deficit with respect to the baseline strength (each mouse being its own control).

Table 1 List of antibodies used for flow cytometry analyses

	Clone	Isotype	Quantity per test	Supplier/reference
Antibody				
-Lymphoid cell panel-				
BV510 hamster anti-mouse CD3e	145-2C11	Armenian hamster IgG1, κ	0.6 μ g	BD Biosciences/563024
APC rat anti-mouse CD4	RM4-5	Rat (DA) IgG2a, κ	0.6 μ g	BD Biosciences/553051
PE-Cy7 rat anti-mouse CD8a	53-6.7	Rat (LOU) IgG2a, κ	0.6 μ g	BD Biosciences/552877
Antibody				
-Myeloid cell panel -				
BV510 hamster anti-mouse CD3e	145-2C11	Armenian hamster IgG1, κ	0.6 μ g	BD Biosciences/563024
BV421 rat anti-mouse CD11b	M1/70	Rat (DA) IgG2b, κ	0.6 μ g	BD Biosciences/562605
APC rat anti-mouse CD11c	HL3	Armenian Hamster IgG1, 2	0.6 μ g	BD Biosciences/550261
PE-Cy7 rat anti-mouse CD45	30-F11	Rat (LOU) IgG2b, κ	0.6 μ g	BD Biosciences/561868
FITC rat anti-mouse Ly-6G	1A8	Rat (LEW) IgG2a, κ	1 μ g	BD Biosciences/551460
Antibody				
-Fc Blocking-				
Purified rat anti-mouse CD16/CD32 (mouse BD Fc block)	2.4G2	Rat IgG2b, κ	0.5 μ g	BD Biosciences/553142

Statistical Analyses

Results are the mean \pm SEM. Statistical analyses were performed using the Statview software. The Wilcoxon test was used to compare values between ipsi- and contralateral cortex, as well as longitudinal evaluation of BBB leakage; the Mann-Whitney test was used for the remaining analyses.

Results

Characterization of Thrombin-Induced Vascular Occlusion

The MCA was occluded through the injection of 1 μ l of thrombin (1 UI/ μ l), which provoked the formation of a clot in the lumen of the artery (Fig. 1a). Using T2-w MRI sequences, we revealed ischemic brain lesions 6 h after the occlusion of the MCA, extending at 24 h ($p < 0.05$ vs 6 h), stabilizing at 48 h ($p < 0.05$ vs 6 h), and starting to reduce in size after 5 days (Fig. 1b, c; $n = 6$ mice/group). In the absence of comorbidities, in this model, hemorrhagic transformation occurs in less than 1% of mice (internal data).

Concerning the longitudinal study of BBB leakage, gadolinium hypersignal was slightly detectable from 6 h after MCAo and continuously increased and was maximal at 48 h (Fig. 1b, d; $p < 0.05$ vs 6 h). Gadolinium extravasation was clearly located at the lesion site. The gadolinium signal ratio between the lesion site and the contralateral cortex exponentially increased up to 5 days after stroke (Fig. 1b, e; $p < 0.05$ vs 6 h).

Fibrin(ogen) deposits associated to BBB leakage were not detected before 48 h post-stroke (Fig. 1f). Slight signals were found at 48 h, and clear fibrin(ogen) deposits were found at the lesion core 5 days after stroke onset (Fig. 1f).

Similar to untreated stroke patients, in this experimental model, clots are progressively and spontaneously lysed: 24 h after MCAo 50% of mice show a total (score 3) recanalization of the MCA (Fig. 1g, h). These angiographic analyses were obtained from an independent series of mice ($n = 18$).

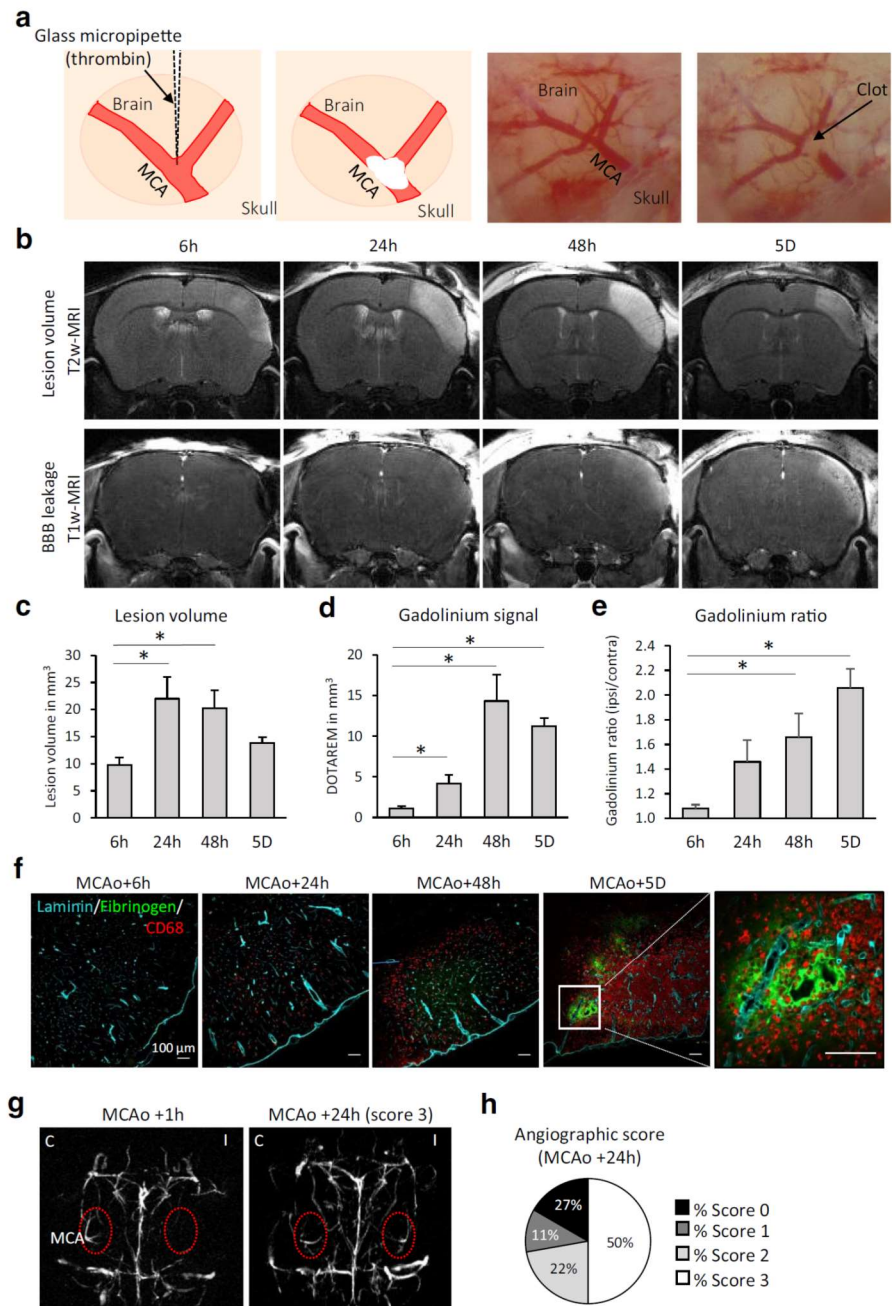
Microglial Activation/Macrophage Recruitment

The macroscopic profile of microglia/macrophage responses after MCAo has been schematized in Fig. 2a. The shape of microglia and the characteristic immunostaining for Iba1 and CD68 markers are shown in Fig. 2b.

Six hours after ischemic stroke onset, the number of Iba1⁺ microglial cells (Fig. 2c) increased in the ipsilateral cortex (peri-infarct zone 191.73 ± 10.96 cells/mm², +176% vs before; core = 202.26 ± 15.65 cells/mm², +185%), and this number considerably increased 5 days after stroke onset. The total number CD68⁺ cells (Fig. 2d) (CD68 being a lysosomal marker present in activated microglial cells and macrophages) also continuously increased from 6 h (peri-infarct zone 144.98 ± 0.69 cells/mm², +161% vs basal; core 156.97 ± 7.39 cells/mm², +174%) to 5 days after stroke onset (peri-infarct zone 334.57 ± 25.23 cells/mm², +371% vs basal; core 1638.99 ± 90.63 cells/mm², +1818%).

Furthermore, we also counted the number of a subset of activated microglial cells/infiltrated macrophages negative for the Iba1 marker (CD68⁺Iba1⁻ cells; Fig. 2e). The number of

Fig. 1 Murine model of thromboembolic stroke by thrombin injection. **a** One microliter of thrombin is directly injected into the middle cerebral artery (MCA) by using a glass micropipette. **b** Representative T2w and T1w MRI scans showing respectively lesion volume and gadolinium extravasation at different time points after stroke onset. **c** Quantification of lesion volumes based on T2w MRI scans at different time points. *N* = 6 mice/group at 6, 24, and 48 h; *N* = 5 mice/group at 5 days; **p* < 0.05 vs 6 h. **d** Quantification of gadolinium volume based on T1-weighted MRI images. *N* = 6 mice/group at 6, 24, and 48 h; *N* = 5 mice/group at 5 days. **e** Ratio of gadolinium signal intensity between the ipsilateral and contralateral cortex. **f** Representative photomicrographs of fibrin(ogen) deposits obtained by immunohistochemistry. *N* = 3–5 mice/group. **g** Representative 3D-reconstructed angiographies showing the complete occlusion of the MCA 1 h after the occlusion and its spontaneous recanalization after 24 h. **h** Percentage of angiographic scores 24 h after MCAo from an independent series of mice (*n* = 18). Score 0 = complete occlusion; score 1 = incomplete filling of the distal bed; score 2 = almost complete filling of the distal territory; score 3 = complete filling of the distal bed

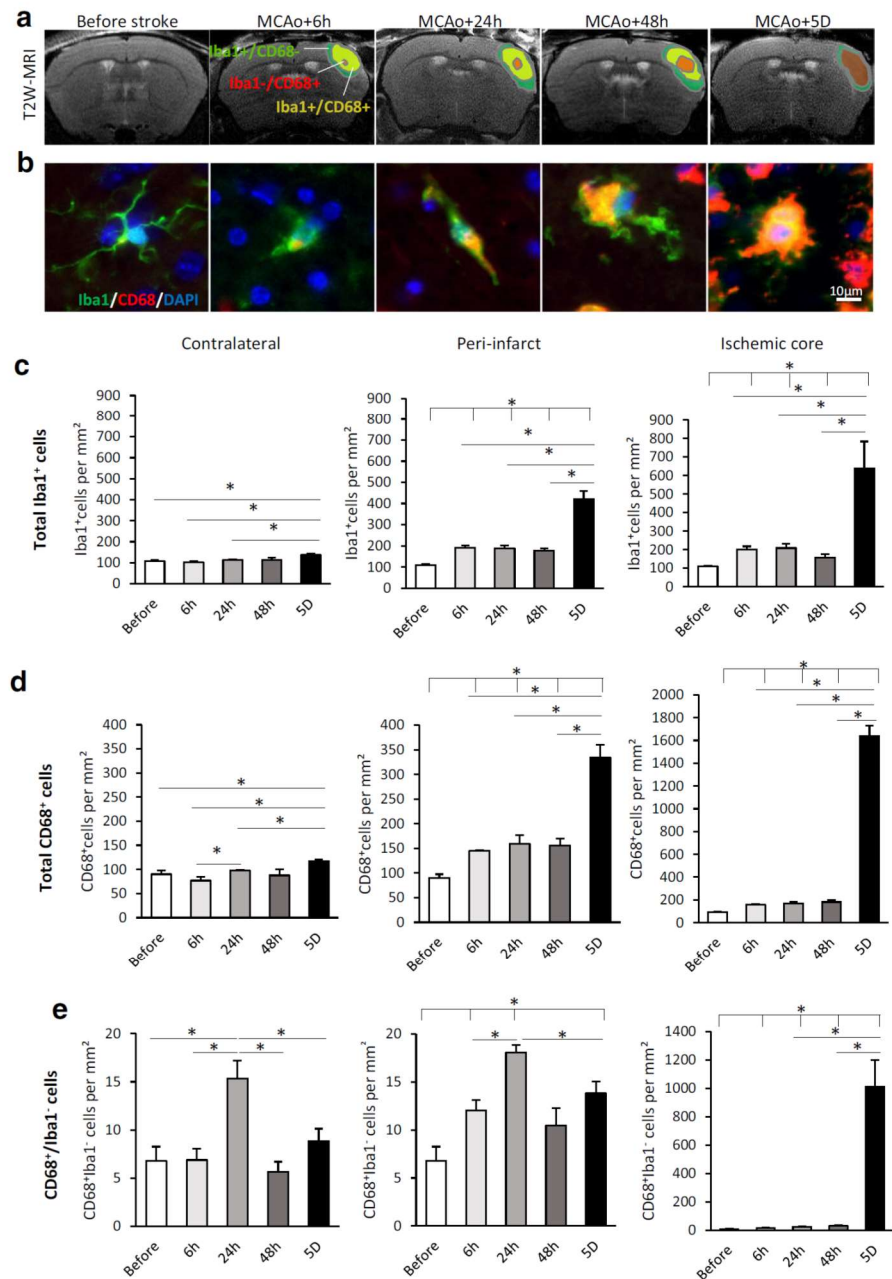


CD68⁺Iba1⁻ cells increased from 6 h (peri-infarct zone 12.01 ± 1.08 cells/mm², + 177% vs basal; core 16.28 ± 2.25 cells/mm², + 240%) to 48 h (peri-infarct zone 10.47 ± 1.81 cells/mm², + 154% vs basal; core 28.95 ± 6.69 cells/mm², + 427%) after stroke onset. This number markedly increased 5 days after stroke onset in the core of the lesion (peri-infarct zone 13.79 ± 1.23 cells/mm², + 203% vs basal; core 1011.23 ± 187.02 cells/mm², + 14,906%).

In Vivo Visualization of Macrophage Recruitment

In vivo longitudinal 3D-T2* acquisitions allowed the specific detection of hyposignals corresponding to phagocytosed MPIOs by peripheral macrophages (Fig. 3b). Hyposignals were rarely observed at 24 and 48 h after stroke onset and markedly increased at 5 days (Fig. 3c–e).

Fig. 2 Quantification of total microglia and activated microglia/macrophages at different time points after thromboembolic stroke. **a** Schematic representation of the immunostainings found in the ipsilateral cortex, superposed on a T2w MRI scan: Iba1⁺/CD68⁻ (non-activated microglia, as found before stroke, in green), colocalized Iba1⁺/CD68⁺ (activated microglia/macrophages, in yellow), or Iba1⁻/CD68⁺ (macrophages, in red). **b** Characteristic shape of microglia and characteristic staining of Iba1 and CD68 markers found in the ipsilateral cortex. All the quantifications were done on contralateral cortex, peri-infarct zone and core of the lesion at 6, 24, 48 h, and 5 days after MCAo. **c** Quantification of total microglia (Iba1⁺ cells). **d** Quantification of Iba1⁺CD68⁺ cells. **e** Quantification of Iba1⁻CD68⁺ cells. (*N* = 3–5 mice per group; *p* < 0.05; Mann-Whitney test)



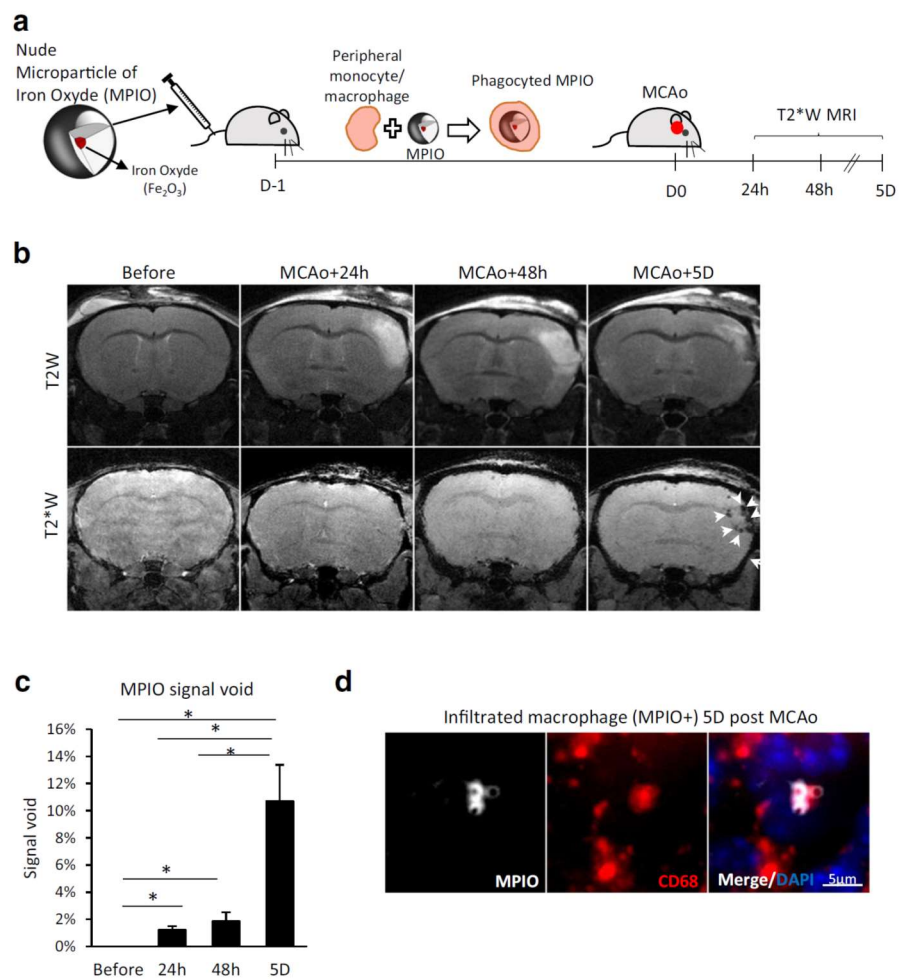
P-Selectin Expression at the Endothelial Surface

The expression of the adhesion molecule P-selectin was detected in vivo by specific α -P-selectin-coupled MPIO (schematized in Fig. 4a). P-selectin levels were significantly increased at the endothelial surface at 24 h and were maximal 48 h after stroke onset (Fig. 4b, c; *p* < 0.05 vs 6 h; *n* = 6).

Neutrophils and Lymphocytes

A small number of Ly6G⁺ neutrophils were found at 48 h after stroke onset (Fig. 4d–f; peri-infarct zone 2.39 ± 0.78 cells/mm²; core 29.58 ± 3.88 cells/mm²). The number of neutrophils markedly increased at 5 days after stroke onset on the core as well as on the peri-infarct zone of the lesion (peri-infarct zone 46.72 ± 15.86 cells/mm²; core 54.85 ± 17.66 cells/mm²; Fig. 4e). At

Fig. 3 Macrophage infiltration after thromboembolic stroke. **a** Schema of the experimental design to detect specifically blood-derived macrophage infiltration after stroke. The day before stroke, nude MPIOs are peripherally injected to mice. Peripheral monocyte/macrophage phagocyte nude MPIOs that can be detected as hyposignals on T2*w MRI sequences once macrophages have infiltrated the ischemic area. **c** Representative T2w and T2*w MRI scans. Arrows, MPIO hyposignals corresponding to infiltrated macrophages at the ischemic area. **d** Quantification of MPIO signal at each time point. $N = 6$ mice per group, * $p < 0.05$, Wilcoxon test. **e** Representative photomicrographs of infiltrated macrophages positive for CD68 and containing MPIO 5 days after MCAo



both time points, neutrophils were found beside blood vessels and within the brain parenchyma (Fig. 4d). No neutrophils were found before stroke (data not shown).

CD3⁺ and CD4⁺ lymphocytes (Fig. 4g–j) were found in the brain only at 5 days after stroke onset. Lymphocytes were found in the peri-infarct zone (CD3⁺ cells 85.55 ± 17.88 cells/mm²; Fig. 4i) (CD4⁺ cells 17.61 ± 1.25 cells/mm²; Fig. 4j) and in the core of the lesion (CD3⁺ cells 213.53 ± 31.71 cells/mm²; Fig. 4i) (CD4⁺ cells 79.91 ± 9.2 cells/mm²; Fig. 4j). In both cases, lymphocytes were found beside blood vessels and within the brain parenchyma (Fig. 4g). No lymphocytes were found before stroke (data not shown).

Flow Cytometry Analyses of Immune Responses After Stroke

The presence of stroke lesions was systematically verified by MRI 24 after MCAo (mean lesion volume of 19.2 ± 1.6 mm³

for the 24 h group ($n = 5$ mice), 20.1 ± 2.8 mm³ for the 48 h group ($n = 5$ mice), 19.4 ± 3.9 mm³ for the 5 days group ($n = 6$ mice)).

Globally, the myeloid response (Fig. 5) was present in the ipsilateral hemisphere from 24 h, peaked at 48 h and remained increased—although to a lesser extent—up to 5 days after stroke onset. We subdivided CD45⁺/CD11b⁺ cells into three categories: CD45^{high}/CD11b⁺ were considered as infiltrated macrophages [19], CD45^{intermediate}/CD11b⁺ (CD45^{int}/CD11b⁺) were considered as activated microglial cells, and CD45^{low}/CD11b⁺ were considered as resting microglial cells. Percentage of each cell type in the ipsilateral and contralateral hemispheres is indicated in Fig. 6e.

An early, long-lasting significant increase of CD45^{high}/CD11b⁺ cells (Fig. 5b; $n = 5–6$ mice/group) and CD11b⁺/CD11c⁺ cells (considered as dendritic cells; (Fig. 5d; $n = 5–6$ mice/group)) was detected from 24 h and was still present—although to a lesser extent—5 days after stroke onset in the

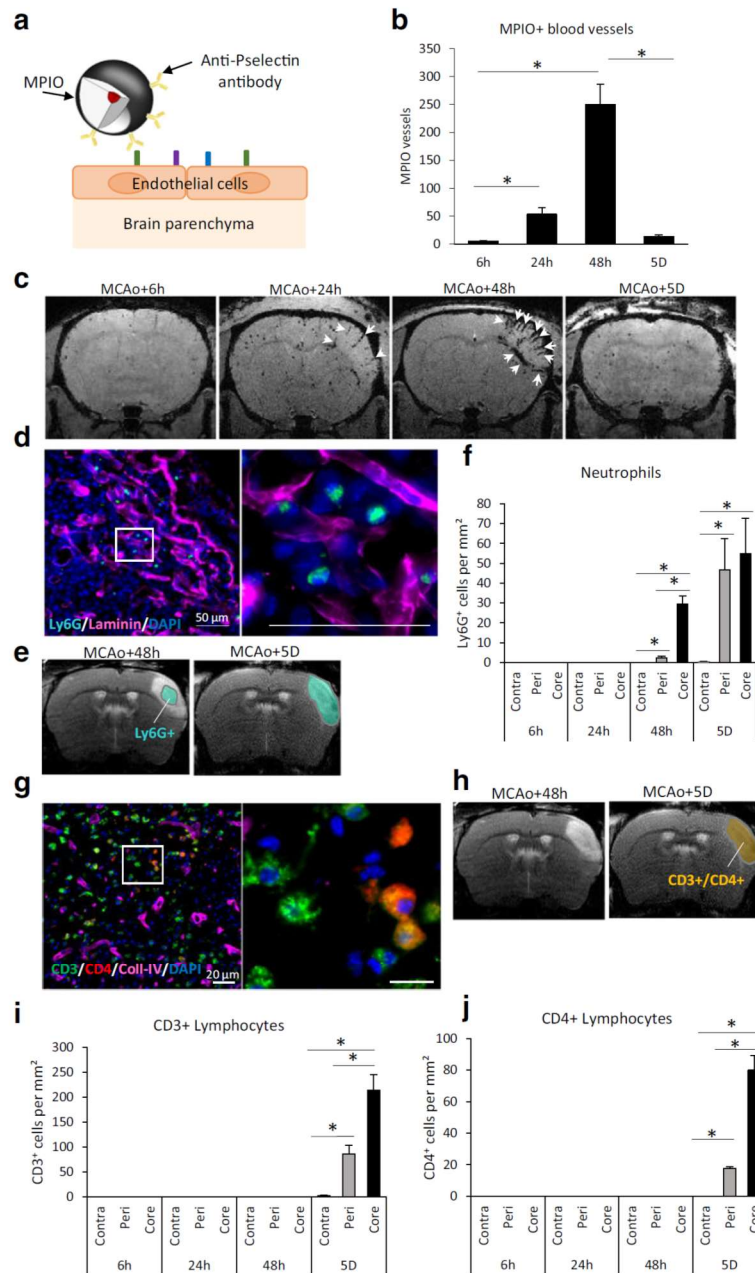


Fig. 4 Endothelial P-selectin expression, neutrophil, and lymphocyte infiltration after thromboembolic stroke. **a** To in vivo detect the expression of P-selectin at the endothelial surface, MPIOs were coupled to an antibody targeting P-selectin. P-selectin-coupled MPIOs were injected iv before each MRI acquisition. **b** Quantification of MPIO hyposignals. $N = 6$ mice/group. **c** Representative T2*_w scan. Arrows, hyposignals corresponding to P-selectin-coupled MPIOs. **d** Representative photomicrographs of neutrophil (Ly6G⁺) cells infiltration at the ischemic core 5 days after thromboembolic stroke. No Ly6G⁺ cells were found at 6 or 24 h after MCAo. **e** Schematic representation of the Ly6G⁺ immunostaining distribution found in the ipsilateral cortex at 48 h and 5 days after MCAo superposed on a T2w MRI scan. **f** Quantification of neutrophils

by ICH on the contralateral cortex, peri-infarct zone, and the ischemic core at 6, 24, 48 h, and 5 days after MCAo. $N = 3-5$ mice per group, $*p < 0.05$, Mann-Whitney test. **g** Representative photomicrographs of CD3⁺ and CD4⁺ lymphocytes at the ischemic core 5 days after thromboembolic stroke. No CD3⁺ or CD4⁺ cells were found by IHC at 6, 24, and 48 h after MCAo. **h** Schematic representation of the CD3⁺ and CD4⁺ cell distribution 5 days after MCAo. **i** Quantification of total lymphocytes (CD3⁺ cells). **j** Quantification of CD4⁺ lymphocytes. All the quantifications were done on the contralateral cortex, peri-infarct area, and core of the lesion at 6, 24, 48 h, and 5 days after MCAo. $N = 3-5$ mice/group, $*p < 0.05$, Mann-Whitney test

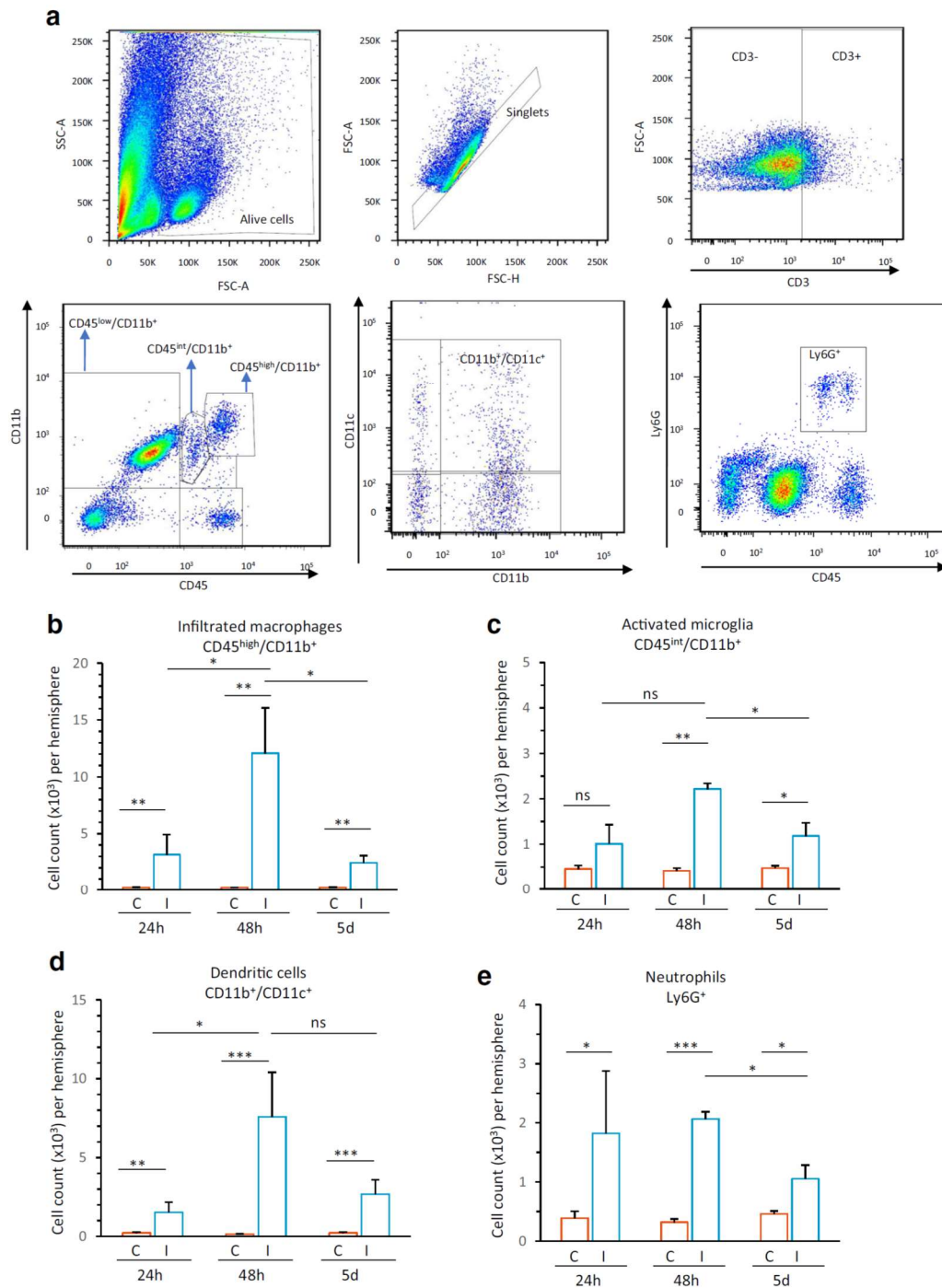


Fig. 5 Myeloid responses after thromboembolic stroke. **a** Representative gating strategy for absolute cell count analysis of leukocyte subsets in brain homogenates of the entire ischemic hemisphere. CD3⁻ leukocytes were gated for subpopulation analysis after using scattergram gates for viable leukocytes. **b–e** Flow cytometric analysis of absolute cell counts of

macrophages (CD45^{high}/CD11b⁺, **b**), activated microglia (CD45^{int}/CD11b⁺, **c**), dendritic cells (CD11b⁺/CD11c⁺, **d**), and neutrophils (Ly6G⁺, **e**). Data are expressed as total cell count (mean ± SEM) after Malassez cell counting for each hemisphere. *N* = 5–6 mice/group; ns non-significant, **p* < 0.05; ***p* < 0.01; ****p* < 0.001 (Mann-Whitney test)

ipsilateral hemisphere. CD45^{int}/CD11b⁺ cells peaked at 48 h and remained significantly increased 5 days after stroke onset (Fig. 5c; $n = 5-6$ mice/group).

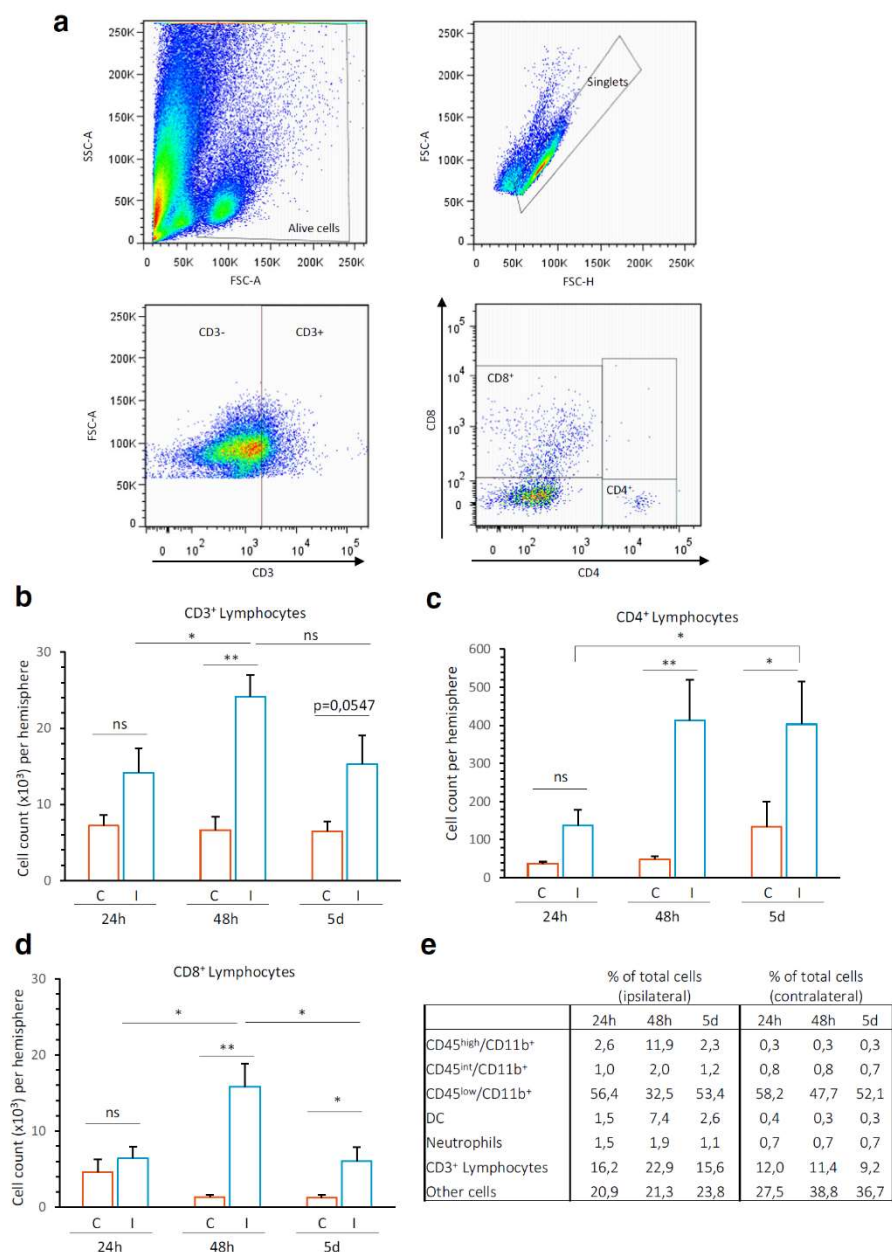
Compared to the myeloid response, T lymphocyte responses in the ipsilateral hemisphere were present only later on (from 48 h after stroke onset). Among CD3⁺ lymphocytes, the most abundant subtype was CD8⁺ T cells. The number of CD8⁺ cells was significantly increased at 48 h and decreased at 5 days after stroke onset, although it was still significantly increased compared to the contralateral hemisphere (Fig. 6d;

$n = 5-6$ mice/group). CD4⁺ lymphocytes were significantly increased in the ipsilateral hemisphere at 48 h and remained increased at 5 days, suggesting a more durable CD4 response (Fig. 6c; $n = 5-6$ mice/group).

Minocycline Effects on Radiological and Neurological Outcomes

The early (1 h post-MCAo) administration of minocycline was able to reduce ischemic lesions at 24 h after stroke onset

Fig. 6 Lymphoid responses after thromboembolic stroke. **a** Representative gating strategy for absolute cell count analysis of leukocyte subsets in brain homogenates of the entire ischemic hemisphere. CD3⁺ leukocytes were gated for subpopulation analysis after using scattergram gates for viable leukocytes. **b-d** Flow cytometric analysis of absolute cell counts of CD3⁺ lymphocytes, CD4⁺ lymphocytes, and CD8⁺ lymphocytes. **e** Percentage of cell subsets in the ipsilateral and contralateral hemispheres at different time points after stroke onset. Data are expressed as total cell count (mean \pm SEM) after Malassez cell counting for each hemisphere (**b, c**) or as percentage of total cells (**e**). $N = 5-6$ mice/group; ns non-significant, * $p < 0.05$; ** $p < 0.01$ (Mann-Whitney test)



Transl. Stroke Res.

Fig. 7 Early minocycline reduces ischemic volume and ameliorates neurological outcome after stroke.

a Experimental design. **b** Representative T2w scans at 24 h or 5 days after stroke from saline-, early Mino (+ 1 h post-MCAo)-, or late Mino (+ 48 h post-MCAo)-treated mice. **c** Quantification of lesion volume at 24 h after stroke onset. **d** Quantification of lesion volume at 5 days after stroke onset. **e** Stroke-induced forepaw strength loss at 24 h after stroke onset. **f** Stroke-induced forepaw strength loss at 5 days after stroke onset. *N* = 9 mice/group (all the time points); **p* < 0.05 vs saline, Mann-Whitney test

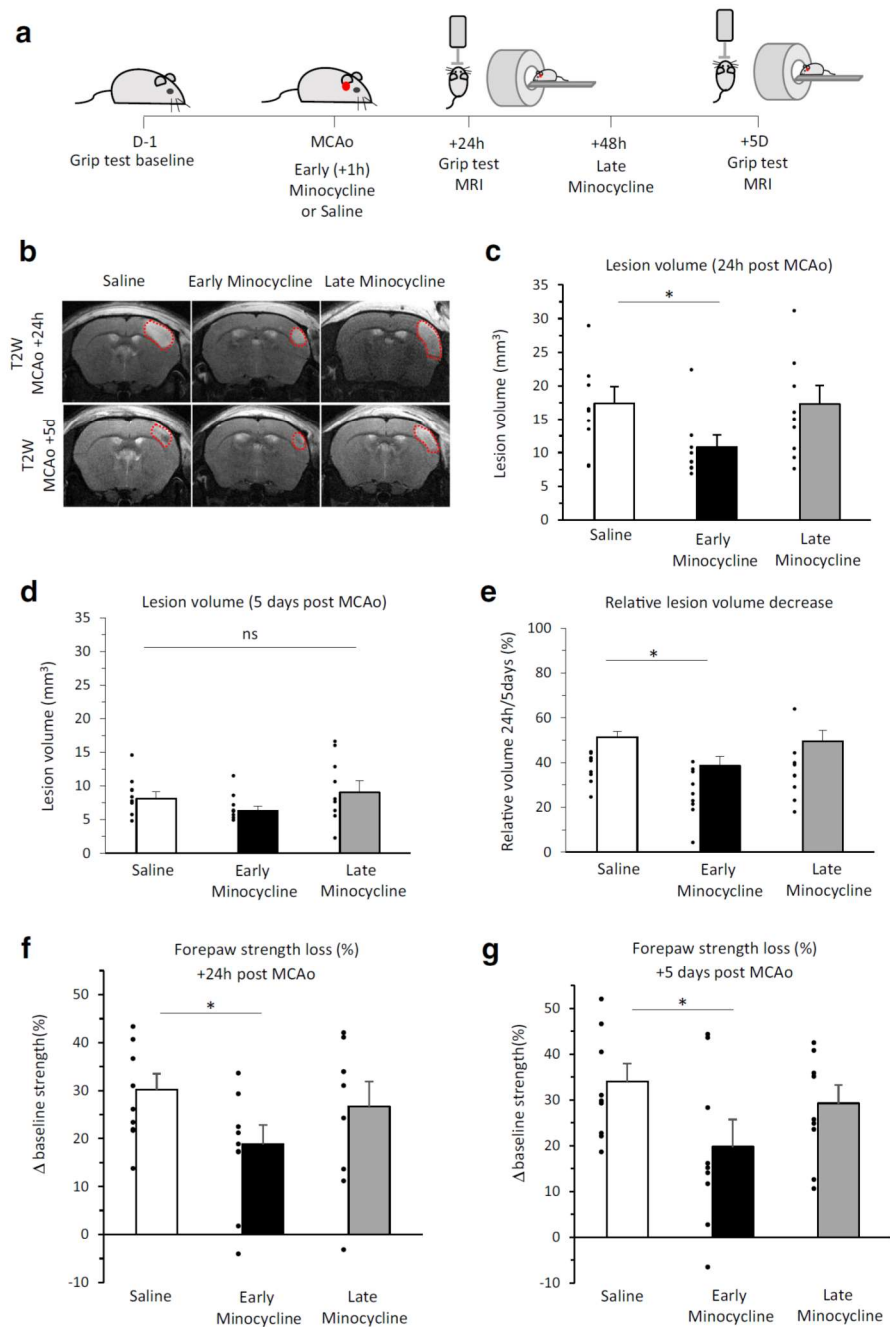


(Fig. 7a–c; *n* = 9 mice/group; *p* < 0.05 vs saline). This difference was not present at 5 days (Fig. 7b, d; *n* = 9 mice/group; *p* < 0.05 vs saline). One possible explanation to this could be that spontaneous clot lysis led to a reduction in lesion size, even in the saline-treated group, between 24 h and 5 days, reducing the impact of the treatment. Another possible hypothesis to explain this reduction of the impact of minocycline at 5 days could be that small lesions (i.e., lesions involving less edema

at 24 h) decrease proportionally less between 24 h and 5 days than bigger lesions, although this hypothesis should be further studied in future investigations. The late (48 h after stroke onset) administration of minocycline did not impact lesion volume at any tested time (Fig. 7b–d).

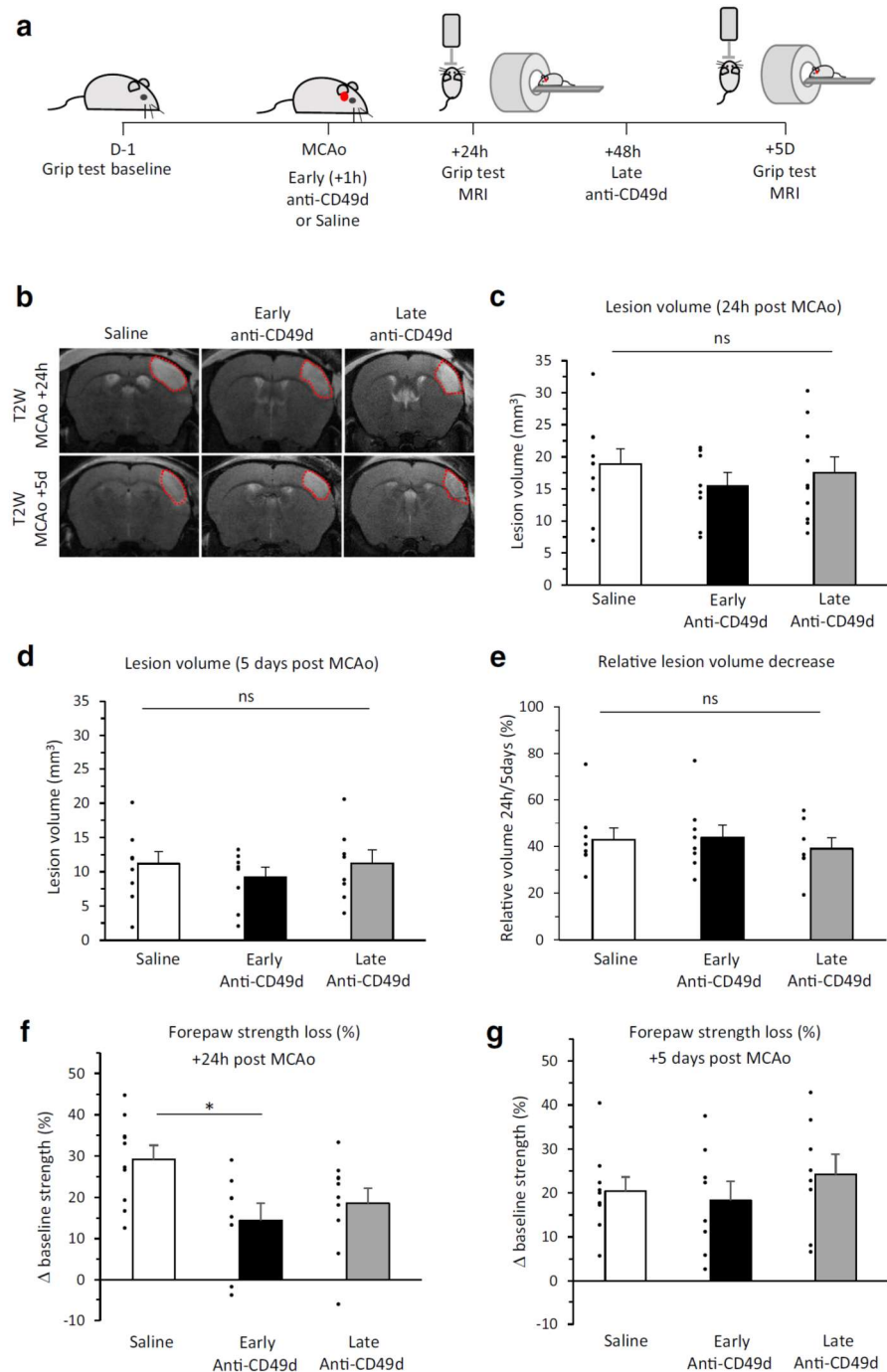
Concerning neurological outcome, the early administration of minocycline significantly ameliorated forepaws strength loss at both 24 h (38% deficit amelioration; Fig. 7f; *p* < 0.05 vs saline;

$n = 9$ mice/group) and 5 days (42% deficit amelioration; Fig. 7g; $p < 0.05$ vs saline; $n = 9$ mice/group) after stroke onset. In contrast, the late administration of minocycline did not ameliorate neurological outcome (Fig. 7f–g; $n = 9$ mice/group) at 24 h or 5 days after stroke.

Anti-CD49d Effects on Radiological and Neurological Outcomes

Neither the early (+ 1 h post-MCAo) nor the late (+ 48 h post-MCAo) blockade of leukocyte infiltration by anti-CD49d

Fig. 8 Anti-CD49d antibodies do not change ischemic volume or long-term neurological outcome after stroke. **a** Experimental design. **b** Representative T2w scans at 24 h or 5 days after stroke from saline-, early anti-CD49d (+ 1 h post-MCAo)-, or late anti-CD49d (+ 48 h post-MCAo)-treated mice. **c** Quantification of lesion volume at 24 h after stroke onset ($N = 8–10$ mice/group). **d** Quantification of lesion volume at 5 days after stroke onset ($N = 8–9$ mice/group). **e** Stroke-induced forepaw strength loss at 24 h after stroke onset ($N = 8–10$ mice/group). **f** Stroke-induced forepaw strength loss at 5 days after stroke onset ($N = 8–9$ mice/group). * $p < 0.05$ vs saline, Mann-Whitney test



were able to reduce ischemic lesions at any time point (Fig. 8a–d; $n = 8–10$ mice/group at 24 h; $n = 8–9$ mice/group at 5 days) or to change lesion progression between 24 h and 5 days after stroke onset (Fig. 8e). Only the early administration (+ 1 h after stroke onset) of anti-CD49d temporarily ameliorated forepaw strength loss at 24 h after stroke onset (Fig. 8f; $p < 0.05$ vs saline; $n = 8–10$ mice/group), although this difference disappeared 5 days after stroke onset (Fig. 8g).

Discussion

The first aim of this study was to describe the time course of the inflammatory responses triggered in an experimental model of thromboembolic stroke consisting in the in situ formation of a fibrin-rich clot into the MCA. This experimental model shows two important similarities to the human pathology: (i) the early administration of tPA is beneficial and reduces lesion size, as previously reported [4, 12, 17, 20], and, as shown in this study, (ii) in the absence of any treatment, spontaneous recanalization occurs in a high proportion of mice within the first 24 h after MCAo. It is important to note that, in our hands, there is no correlation between angiographic score at 24 h and maximal lesion volume.

Our study shows that in this experimental model, there is a global peak of immune cell responses at 48 h after stroke onset that decreases later on (except for CD4⁺ lymphocytes, which remain increased at 5 days). The adhesion molecule P-selectin is present at the endothelial surface from 24 h and is maximal at 48 h after stroke onset. Simultaneous to the increase of P-selectin expression, BBB leakage in the ischemic area appears from 24 h and progressively increases later on (48 h–5 days), which suggests the facilitated transmigration of leukocytes across damaged BBB in the ischemic area. Further studies at later time points after stroke could determine whether chronic BBB leakage and leukocyte infiltration (notably CD4⁺ cells) may act as contributors and predictors for long-term cognitive impairment or other post-stroke neurological symptoms.

It was not the aim of our study to directly compare the inflammatory responses triggered in the thrombin model versus other “classical” models of ischemic stroke (notably the transient middle cerebral artery occlusion (tMCAO) by a monofilament, or the permanent MCAO (pMCAO) by electrocoagulation). Nevertheless, it is interesting to note that the extent, the time course, and the proportion of immune cell responses to stroke can notably vary depending on the experimental model used [8, 9, 11]. Indeed, the efficacy of immunomodulatory drugs varies depending on the stroke model used [21]. As an example of a potential source of variation of the immune responses in experimental models of stroke, secondary microthrombosis is a major pathophysiological mechanism leading to brain damage occurring in tMCAO model, but not in other models based on clot-induced ischemic

stroke like the thrombin model used here [7]. One could hypothesize that the beneficial effects of immunomodulatory agents reported in tMCAO models (and that provided the basis of clinical trials on immunomodulatory therapies for stroke) could be due to their action on thromboinflammation and/or secondary microthrombosis. Since it is unclear whether thromboinflammation is a universal pathophysiological mechanism in human stroke [22, 23], experimental models of stroke that do not induce secondary thromboinflammation (such as the thrombin model) should be considered when testing immunomodulatory drugs, in order to increase the potential success of translational stroke research.

The second aim of our study was to assess the effects of two anti-inflammatory treatments already tested in stroke clinical trials: minocycline and the anti-CD49d antibody Natalizumab®. These treatments were administered at two time-points after ischemic onset: early (1 h) and late (48 h) after MCAo. We studied the impact of these treatments on both radiological (lesion volume by MRI) and neurological (grip test) outcomes, which were determined at 24 h and 5 days after stroke.

Minocycline is an anti-infective agent of the tetracycline family, highly lipophilic and able to cross the BBB. Among other anti-inflammatory actions and by acting through different pathways, minocycline is able to inhibit microglial activation [24–27]. More specifically, minocycline selectively inhibits the microglia polarization to a pro-inflammatory state [28]. This specificity is important, since total microglial depletion seems to have, on the contrary, a deleterious impact on ischemic stroke [29]. Our results show that only the early administration of minocycline (1 h after stroke onset) is able to reduce ischemic lesions and to ameliorate neurological outcome after stroke. Three randomized clinical trials have reported the efficacy of minocycline, alone or in combination with tPA, among small cohorts of ischemic stroke patients by demonstrating the improvement of NIHSS score at 90 days [30–32], mRS score [30, 31], and Barthel Index [30, 31]. A fourth trial performed in a small sample of acute stroke patients [33] has shown that minocycline showed that minocycline was safe but not efficacious. Nevertheless, this study was underpowered to analyze the treatment effect of minocycline [27]. It has been suggested that further clinical trials testing minocycline in ischemic stroke are needed, and our data support the use of minocycline in the acute phase of ischemic stroke to reduce ischemic lesions and ameliorate neurological outcome.

Natalizumab®, an anti-CD49d antibody used to block the leukocyte-endothelium adhesion by antagonism of the leukocyte integrin $\alpha 4$ (Very Late Antigen-4, VLA-4), has been tested in experimental models and clinical trials for stroke treatment. In spite of the first promising experimental results [34], a preclinical randomized controlled multicenter trial has reported that the benefits of the anti-CD49d treatment in

reducing infarct volume and leukocyte invasion were dependent on the experimental model of stroke and limited to small cortical lesions [21]. Our results do not support this hypothesis, since the thrombin model also provokes such kind of cortical lesions and the anti-CD49d antibody is not able to reduce ischemic volume, independently of the timing of administration. Although we found an initial improvement in forepaw strength loss in early treated mice, blocking leukocyte infiltration does not seem to promote long-lasting beneficial effect on neurological outcome in this experimental model. Concerning clinical results, Natalizumab® has not shown beneficial effects on infarct growth or neurological score at 90 days after stroke (ACTION [35] and ACTION II (NCT02730455) trials) and further development of Natalizumab® in acute ischemic stroke will not be pursued by the company (<https://www.businesswire.com/news/home/20180207005645/en/Biogen-Reports-Top-Line-Results-Phase-2b-Study>).

Our study has several limits. First, data have been obtained in young, healthy mice, and we acknowledge that immune responses can substantially vary in time and intensity in comorbid conditions, which occur in 90% of stroke events [36]. Second, minocycline is known to have many other potentially beneficial mechanisms in acute ischemic stroke including anti-apoptotic effects, MMP inhibition, and others that have not been explored here. Third, the 5 day end point is a limitation since inflammation is known to occur long after this and can impact ultimate neurologic outcome. Finally, even if the grip test is a validated test, we could also have tested additional neurological tests. Future studies are needed to in-depth study other measures of sensorimotor and cognitive outcomes.

Summary/Conclusions

The thrombin model of acute ischemic stroke triggers an early myeloid response peaking at 48 h after stroke onset and still present (although to a lesser extent) 5 days after stroke onset. T-lymphocytes infiltrate later on (from 48 h after stroke onset). These cellular responses are accompanied by endothelial activation at 24–48 h. BBB leakage propagates and expands from 24 h up to 5 days after stroke. Ischemic lesions are maximal at 24–48 h after stroke onset. The early (but not late) administration of minocycline is able to reduce ischemic volume and to ameliorate neurological outcome. In contrast, the blockade of leukocyte infiltration by anti-CD49d antibodies does not reduce ischemic volume or ameliorate neurological outcome, regardless of the timing of administration. The results obtained in this experimental model of ischemic stroke are in accordance with clinical reports on the use of minocycline and Natalizumab®. We propose that this clinically relevant model of stroke may be efficient in predicting the potential benefits

of anti-inflammatory stroke therapies and may thus improve the translation of preclinical stroke research to clinical trials.

Acknowledgments The authors thank Dr. Fabian Docagne for his diligent English editing of the manuscript.

Authors' contributions - Surgeries: MR, CB
 - Immunohistochemical analyses: AD, DL
 - MRI acquisition and analyses: AD, IB, DL, MR
 - Flow cytometry experiments: IB, MR, PH
 - Behavioral analyses: IB, DL
 - Study design and manuscript writing: AD, MR, DV

Funding Information This work was supported by the RHU MARVELOUS (ANR-16-RHUS-0009) of l'Université Claude Bernard Lyon 1 (UCBL), within the program "Investissements d'Avenir" operated by the French National Research Agency (ANR), the INSERM (Institut National de la Santé et de la Recherche Médicale), the French Ministry of Higher Education and Research, and the University of Caen Normandie.

Compliance with Ethical Standards

Conflict of Interest The authors declare that they have no conflict of interest.

Ethical Approval All applicable international, national, and/or institutional guidelines for the care and use of animals were followed.

References

1. Feigin VL, Nguyen G, Cercy K, Johnson CO, Alam T, Parmar PG, et al. Global, regional, and country-specific lifetime risks of stroke, 1990 and 2016. The GBD 2016 Lifetime Risk of Stroke Collaborators. *N Engl J Med.* 2018;379:2429–2437. <https://doi.org/10.1056/NEJMoal804492>
2. Rha J-H, Saver JL. The impact of recanalization on ischemic stroke outcome: a meta-analysis. *Stroke.* 2007;38:967–73.
3. Dimagl U, Iadecola C, Moskowitz MA. Pathobiology of ischaemic stroke: an integrated view. *Trends Neurosci.* 1999;22:391–7.
4. Hacke W, Kaste M, Bluhmki E, Brozman M, Dávalos A, Guidetti D, et al. Thrombolysis with alteplase 3 to 4.5 hours after acute ischemic stroke. *N Engl J Med.* 2008;359:1317–29.
5. Nogueira RG, Jadhav AP, Haussen DC, Bonafé A, Budzik RF, Bhuva P, et al. Thrombectomy 6 to 24 hours after stroke with a mismatch between deficit and infarct. *N Engl J Med.* 2018;378:11–21.
6. Drieu A, Levard D, Vivien D, Rubio M. Anti-inflammatory treatments for stroke: from bench to bedside. *Ther Adv Neurol Disord.* 2018;11:1756286418789854.
7. Gauberti M, Martinez de Lizarrondo S, Orset C, Vivien D. Lack of secondary microthrombosis after thrombin-induced stroke in mice and non-human primates. *J Thromb Haemost.* 2014;12:409–14.
8. Zhou W, Liesz A, Bauer H, Sommer C, Lahrmann B, Valous N, et al. Postischemic brain infiltration of leukocyte subpopulations differs among murine permanent and transient focal cerebral ischemia models. *Brain Pathol.* 2013;23:34–44.
9. Gelderblom M, Leypoldt F, Steinbach K, Behrens D, Choe C-U, Siler DA, et al. Temporal and spatial dynamics of cerebral immune cell accumulation in stroke. *Stroke.* 2009;40:1849–57.
10. Chu HX, Kim HA, Lee S, Moore JP, Chan CT, Vinh A, et al. Immune cell infiltration in malignant middle cerebral artery

- infarction: comparison with transient cerebral ischemia. *J Cereb Blood Flow Metab.* 2014;34:450–9.
11. Cai, W., Liu, S., Hu, M. et al. Functional dynamics of neutrophils after ischemic stroke. *Transl Stroke Res.* 2019. <https://doi.org/10.1007/s12975-019-00694-y>
 12. Orset C, Macrez R, Young AR, Panthou D, Angles-Cano E, Maubert E, et al. Mouse model of in situ thromboembolic stroke and reperfusion. *Stroke.* 2007;38:2771–8.
 13. Le Behot A, Gauberti M, Martinez De Lizarrondo S, Montagne A, Lemarchand E, Repesse Y, et al. GpIb α -VWF blockade restores vessel patency by dissolving platelet aggregates formed under very high shear rate in mice. *Blood.* 2014;123:3354–63.
 14. Kimura K, Sakamoto Y, Iguchi Y, Shibazaki K. Serial changes in ischemic lesion volume and neurological recovery after t-PA therapy. *J Neurol Sci.* 2011;304:35–9.
 15. Pialat J-B, Wiart M, Nighoghossian N, Adeleine P, Derex L, Hemmier M, et al. Evolution of lesion volume in acute stroke treated by intravenous t-PA. *J Magn Reson Imaging.* 2005;22:23–8.
 16. Effect of intravenous recombinant tissue plasminogen activator on ischemic stroke lesion size measured by computed tomography. The National Institute of Neurological Disorders and Stroke (NINDS) rt-PA Stroke Study Group. *Stroke.* 2000;31(12):2912–9. <https://doi.org/10.1161/01.str.31.12.2912>
 17. Orset C, Haelewyn B, Allan SM, Ansar S, Campos F, Cho TH, et al. Efficacy of alteplase in a mouse model of acute ischemic stroke: a retrospective pooled analysis. *Stroke.* 2016;47:1312–8.
 18. Quenault A, Martinez de Lizarrondo S, Etard O, Gauberti M, Orset C, Haelewyn B, et al. Molecular magnetic resonance imaging discloses endothelial activation after transient ischaemic attack. *Brain.* 2017;140:146–57.
 19. Greter M, Lelios I, Croxford AL. Microglia versus myeloid cell nomenclature during brain inflammation. *Front Immunol.* 2015;6:249.
 20. Macrez R, Obiang P, Gauberti M, Roussel B, Baron A, Parcq J, et al. Antibodies preventing the interaction of tissue-type plasminogen activator with N-methyl-D-aspartate receptors reduce stroke damages and extend the therapeutic window of thrombolysis. *Stroke.* 2011;42:2315–22.
 21. Llovera G, Hofmann K, Roth S, Salas-Pédomo A, Ferrer-Ferrer M, Perego C, et al. Results of a preclinical randomized controlled multicenter trial (pRCT): anti-CD49d treatment for acute brain ischemia. *Sci Transl Med.* 2015;7:299ra121.
 22. De Meyer SF, Denorme F, Langhauser F, Geuss E, Fluri F, Kleinschnitz C. Thromboinflammation in stroke brain damage. *Stroke.* 2016;47:1165–72.
 23. Gauberti M, Potzeha F, Vivien D, Martínez de Lizarrondo S. Impact of bradykinin generation during thrombolysis in ischemic stroke. *Front Med (Lausanne).* 2018;5:195.
 24. Machado LS, Sazonova IY, Kozak A, Wiley DC, El-Remessy AB, Ergul A, et al. Minocycline and tissue-type plasminogen activator for stroke: assessment of interaction potential. *Stroke.* 2009;40:3028–33.
 25. Morimoto N, Shimazawa M, Yamashima T, Nagai H, Hara H. Minocycline inhibits oxidative stress and decreases in vitro and in vivo ischemic neuronal damage. *Brain Res.* 2005;1044:8–15.
 26. Plane JM, Shen Y, Pleasure DE, Deng W. Prospects for minocycline neuroprotection. *Arch Neurol.* 2010;67:1442–8.
 27. Malhotra K, Chang JJ, Khunger A, Blacker D, Switzer JA, Goyal N, et al. Minocycline for acute stroke treatment: a systematic review and meta-analysis of randomized clinical trials. *J Neurol.* 2018;265:1871–9.
 28. Kobayashi K, Imagama S, Ohgomori T, Hirano K, Uchimura K, Sakamoto K, et al. Minocycline selectively inhibits M1 polarization of microglia. *Cell Death Dis.* 2013;4:e525.
 29. Szalay G, Martincz B, Lénárt N, Környei Z, Orsolits B, Judák L, et al. Microglia protect against brain injury and their selective elimination dysregulates neuronal network activity after stroke. *Nat Commun.* 2016;7:11499.
 30. Lampl Y, Boaz M, Gilad R, Lorberboym M, Dabby R, Rapoport A, et al. Minocycline treatment in acute stroke: an open-label, evaluator-blinded study. *Neurology.* 2007;69:1404–10.
 31. Padma Srivastava MV, Bhasin A, Bhatia R, Garg A, Gaikwad S, Prasad K, et al. Efficacy of minocycline in acute ischemic stroke: a single-blinded, placebo-controlled trial. *Neurol India.* 2012;60:23–8.
 32. Amiri-Nikpour MR, Nazarboghi S, Hamdi-Holasou M, Rezaei Y. An open-label evaluator-blinded clinical study of minocycline neuroprotection in ischemic stroke: gender-dependent effect. *Acta Neurol Scand.* 2015;131:45–50.
 33. Kohler E, Prentice DA, Bates TR, Hankey GJ, Claxton A, van Heerden J, et al. Intravenous minocycline in acute stroke: a randomized, controlled pilot study and meta-analysis. *Stroke.* 2013;44:2493–9.
 34. Liesz A, Zhou W, Mraesko É, Karcher S, Bauer H, Schwarting S, et al. Inhibition of lymphocyte trafficking shields the brain against deleterious neuroinflammation after stroke. *Brain.* 2011;134:704–20.
 35. Elkins J, Veltkamp R, Montaner J, Johnston SC, Singhal AB, Becker K, et al. Safety and efficacy of natalizumab in patients with acute ischaemic stroke (ACTION): a randomised, placebo-controlled, double-blind phase 2 trial. *Lancet Neurol.* 2017;16:217–26.
 36. O'Donnell MJ, Xavier D, Liu L, Zhang H, Chin SL, Rao-Melacini P, et al. Risk factors for ischaemic and intracerebral haemorrhagic stroke in 22 countries (the INTERSTROKE study): a case-control study. *Lancet.* 2010;376:112–23.

Publisher's Note Springer Nature remains neutral with regard to jurisdictional claims in published maps and institutional affiliations.

Anti-inflammatory treatments for stroke: from bench to bedside

Antoine Drieu, Damien Levard, Denis Vivien and Marina Rubio 

Ther Adv Neurol Disord

2018, Vol. 11: 1–15

DOI: 10.1177/
1756286418789854

© The Author(s), 2018.
Reprints and permissions:
[http://www.sagepub.co.uk/
journalsPermissions.nav](http://www.sagepub.co.uk/journalsPermissions.nav)

Abstract: So far, intravenous tissue-type plasminogen activator (tPA) and mechanical removal of arterial blood clot (thrombectomy) are the only available treatments for acute ischemic stroke. However, the short therapeutic window and the lack of specialized stroke unit care make the overall availability of both treatments limited. Additional agents to combine with tPA administration or thrombectomy to enhance efficacy and improve outcomes associated with stroke are needed. Stroke-induced inflammatory processes are a response to the tissue damage due to the absence of blood supply but have been proposed also as key contributors to all the stages of the ischemic stroke pathophysiology. Despite promising results in experimental studies, inflammation-modulating treatments have not yet been translated successfully into the clinical setting. This review will (a) describe the timing of the stroke immune pathophysiology; (b) detail the immune responses to stroke sift-through cell type; and (c) discuss the pitfalls on the translation from experimental studies to clinical trials testing the therapeutic pertinence of immune modulators.

Keywords: clinical trial, immunomodulatory drugs, inflammation, stroke models, translation

Received: 23 March 2018; revised manuscript accepted: 19 June 2018.

Introduction

Every year, 15 million people worldwide suffer a stroke. Of these, 5 million die and another 5 million are left permanently disabled, placing a burden on family and community (http://www.who.int/cardiovascular_diseases/en/cvd_atlas_15_burden_stroke.pdf?ua=1). In the United States a stroke event happens every 40 seconds, and every 4 minutes, someone dies of stroke (American Stroke Association). Ischemic stroke is provoked by an arterial occlusion in the brain that leads to the rapid death of the brain tissue irrigated by that particular artery. So far, intravenous tissue-type plasminogen activator (tPA) is the only available pharmacological agent for acute ischemic stroke, but this agent is frequently underutilized due to its limited therapeutic window (4.5 h) and increased risk of intracerebral hemorrhage. Recently, mechanical thrombectomy has demonstrated beneficial effects on ischemic stroke in selected patients¹ and has become the standard of care for patients with large-vessel occlusion up to 24 h of stroke onset.^{2,3} Additional agents to combine with tPA administration or thrombectomy to

improve efficacy and ameliorate outcomes associated with stroke are needed, in particular, for those patients not eligible for thrombolysis or thrombectomy, or with no access to specialized stroke unit care. Easily administrable agents reducing tissue damage even modestly would drastically decrease the burden of stroke on society and would ameliorate patient outcomes and quality of life.⁴

Stroke-induced inflammatory processes, which include mechanisms of innate and adaptive immunity, are a response to tissue damage due to the absence of blood supply but have also been proposed as key contributors to all the stages of the ischemic stroke pathophysiology.⁵ However, despite promising results in experimental studies, inflammation-modulating treatments have not yet been translated successfully into the clinical setting. This review will focus on the innate and adaptive immune responses participating in ischemic brain injury and their impact on tissue damage and repair in both experimental models of stroke and available clinical data. It has been

Correspondence to:

Marina Rubio
Pathophysiology and
Imaging of Neurological
Disorders, Normandy
University, Boulevard
Henri Becquerel BP 5229,
Caen Cedex, 14000, France
rubio@cyceron.fr

Antoine Drieu
Damien Levard
Pathophysiology and
Imaging of Neurological
Disorders, Normandy
University, Caen, France

Denis Vivien
Pathophysiology and
Imaging of Neurological
Disorders, Normandy
University, Caen, France
Pathophysiology and
Imaging of Neurological
Disorders, Centre
Hospitalier Universitaire
de Caen, Caen, France



structured in three parts: a first part describing the timing of the stroke pathophysiology from an immunological point of view (Figure 1); a second part detailing the immune responses to stroke sift-through cell type; and a third part discussing the pitfalls on the translation from preclinical to clinical stroke research of immunomodulating therapeutic agents.

Timeline of inflammatory events after stroke

Basically, inflammatory responses after stroke can be decomposed in three phases.⁵ The acute phase (first hours after stroke onset) corresponds to the clearing of dead cells mainly by resident phagocytic cells such as microglia/macrophages and a first entry of leukocytes, mainly neutrophils. The subacute phase (first days after stroke) corresponds to resolution of inflammation. The late phase (days and weeks after stroke) corresponds to tissue repair by astrocytes and microglia (glial scar).

The acute phase of stroke: tissue injury, microglial and endothelial activation

The arterial occlusion at the origin of ischemic stroke leads to deprivation of oxygen and nutrients that are essential for neuronal survival, leading to rapid neuronal death in the core of the lesion site only minutes after stroke onset. The absence of blood supply into the tissue is followed by a cascade of events starting with a reduction in cellular adenosine triphosphate (ATP) that is required to maintain ionic gradients. The disruption of ionic gradients leads to an influx of Na^+ and Ca^{2+} , cellular depolarization and release of neurotransmitters, including the excitatory neurotransmitter glutamate.⁶ As energy-dependent removal of glutamate is impaired, glutamate accumulation leads to overactivation and opening of monovalent ion channels followed by water influx, thus resulting in cellular swelling and death.⁷ Dying neurons at the core of the lesion express free radicals, damage-associated molecular patterns (DAMPs) and high-mobility group box 1 (HMGB1) protein that lead to inflammatory reactivity by microglia. Edaravone, a free radical scavenger, has shown beneficial properties in stroke patients with large-vessel occlusion, especially when combined with recombinant tissue-type plasminogen activator, but not in combination with thrombectomy.⁸ Activated microglia

adopt a pro-inflammatory status, expressing pro-inflammatory cytokines [interleukin 1 (IL-1), IL-6] that are released into blood circulation.⁹

Pro-inflammatory cytokines exacerbate endothelial cell (EC) activation contributing to leukocyte rolling, adhesion and infiltration in brain tissue. Leukocytes start to roll on the vessel wall with the help of selectins expressed by activated EC. After rolling, leukocytes strongly adhere to the vessel wall by strong links with intercellular adhesion molecule (ICAM-1) and vascular cell adhesion molecule (VCAM-1).^{10,11} Into the brain, there is almost no way for leukocytes to pass through the blood–brain barrier (BBB) in nonpathological conditions.¹² However, the BBB integrity is disrupted after stroke onset and tight junctions between EC disappear, allowing leukocyte infiltration into the injured brain tissue.¹³ Clinical data and experimental models of stroke have shown that neutrophils infiltrate within hours of stroke onset.^{14,15}

The subacute phase: resolution of inflammation

In the first days after stroke, different leukocyte populations, including macrophages and lymphocytes, infiltrate the brain.^{14,15} The infiltration of leukocyte subpopulations differs among murine permanent and transient mechanical focal cerebral ischemia models¹⁶ and the inflammatory response seems to be more pronounced after permanent electrocoagulatory middle cerebral artery occlusion (MCAO) compared with 30-min and 90-min transient mechanical vascular occlusion (TMVO).¹⁶ Descriptive data on the timeline inflammatory responses in thrombus-induced experimental stroke models are missing.

Preclinical studies performed on TMVO models of ischemic stroke have shown a secondary injury after reperfusion (i.e. cerebral ischemia/reperfusion injury). While mechanical thrombectomy also promotes rapid reperfusion, it does not seem to provoke such a secondary injury in patients with proximal middle-cerebral-artery or internal-carotid-artery occlusion and a penumbral region of tissue (i.e. a brain region that is ischemic but not infarcted yet, which is therefore salvageable). This is probably due to a better collateral circulation and slower infarct growth in these patients and is associated to a higher proportion of good functional outcomes at 3 months after stroke, compared with patients with little or no penumbra,

even when performed late (16–24 h) after stroke onset.^{2,3,17} In the DEFUSE 2 study, patients with little or no penumbra had a greater lesion growth despite reperfusion. This greater lesion growth could be the result of reperfusion-related edema based on the larger infarct core volumes in the no penumbra group.¹⁷

The late phase: tissue repair and glial scar

Neuroinflammation is also considered necessary for the reparation phase that persists after the initial brain insult.^{18–20} This phase aims at restoring tissue integrity and involves matrix remodeling, neurogenesis, axon sprouting, dendritogenesis and oligodendrogenesis.²¹ All these processes are common to acute brain injuries (including ischemia, hemorrhage, and trauma), neuroinflammatory (including multiple sclerosis) and neurodegenerative disorders,²² that initiate an extensive glial response known as reactive gliosis. Reactive gliosis involves an enhanced expression of specific markers, such as various extracellular matrix molecules (ECM) like chondroitin sulfate proteoglycans (CSPG) and glial fibrillary acidic protein (GFAP) for astrocytes. Glial scar formation is crucial for sealing the lesion site to remodel the injured tissue, in order to spatially and temporally control the local immune response and revascularization of blood capillaries. Nonetheless, the glial scar also acts as an obstacle to axon regeneration and thus avoids the recovery of central nervous system (CNS) function in the chronic phase after stroke. Experimental studies on the glial response to ischemic stroke have been performed in animal models using variations of permanent or focal transient MCAO and photothrombosis.^{23–25} The human brain after ischemic injury seems to share similar properties to these experimental models of stroke.²⁶

Immunomodulating therapeutic strategies for stroke: sift-through cell type

Clinical trials on stroke immunology have targeted both innate and adaptive immune responses, by reducing microglial activation, inhibiting leukocyte or lymphocyte migration to the brain parenchyma, and blocking the IL-1 receptor. The increasing number of immunomodulatory treatments that are already established for other indications in humans have provided a good opportunity to fast-track innovative proof-of-concept trials in stroke. However, and despite promising preclinical results,

immunomodulatory drugs have not shown clear benefits in large clinical trials on stroke. Another strategy has been the induction of hypothermia to reduce inflammatory responses and apoptosis triggered after stroke (among other mechanisms). Several trials have shown its safety and feasibility, alone or in combination with thrombolysis;^{27–30} however, its efficacy in the treatment of ischemic stroke is still debatable, especially because of increased pneumonia incidence and mortality in the hypothermia group.³¹ New clinical trials on the effects of the combination of thrombolysis/thrombectomy plus hypothermia are ongoing.³² Figure 2 summarizes the results of clinical trials targeting the immune responses triggered after ischemic stroke.

Microglial cells

Pathophysiology. Microglial cells constitute 10–15% of the brain cells and are the resident mononuclear phagocytes of the brain parenchyma.³³ As aforementioned, microglial response is one of the first steps of the innate immune responses triggered after stroke. Microglial cells are in close contact with neurons and constantly survey the environment with their processes.³⁴ These cells can adopt a large spectrum of phenotypes ranging from pro-inflammatory to anti-inflammatory and neuroprotective. At the acute phase after stroke onset, microglial cells at the core of the lesion detect DAMPs and HMGB1 *via* their receptors mainly belonging to the Toll-like receptor (TLR) family.^{13,35–37} This ligand–receptor link leads to internalization of nuclear factor of kappa light polypeptide gene enhancer in B-cells inhibitor ($\text{I}\kappa\text{B}$) kinase into the nucleus and the subsequent activation of the nuclear factor of kappa light chain enhancer of activated B-cells (NF- κB) pathway and thus to the activation of microglial cells. Also, loss of the constitutively expressed neuronal ligand CX3CL1 (fractalkine) after neuronal death results in enhanced microglial activation through their receptors CX3CR1.³⁸ Experimental models of both transient and permanent ischemic stroke have shown an increase in the number of microglial cells on the ipsilateral cortex in the first 24 h after stroke onset.^{14,16} Once activated, microglial cells express high levels of CD11b, CD45 and CD68 corresponding to a phagocytic phenotype responsible for the clearance of cellular debris,⁹ as well as tumor necrosis factor and the pro-inflammatory interleukins IL-1 and IL-6 that are released into blood circulation.⁹ IL-1 has been targeted to

reduce further cerebral injury mediated by inflammation. A meta-analysis showed that IL-1 receptor antagonist (IL-1Ra) administration was associated with a 38.2% reduction in mean infarct volume across 16 published preclinical studies.³⁹ In a phase II clinical study, recombinant human IL-1Ra (rhIL-1Ra; anakinra) administered at hospital arrival has shown beneficial effects in patients with cortical infarcts, with better clinical outcomes after 3 months in the treated group.⁴⁰ However, the recently published results of a second phase II study on the effect of subcutaneous IL-1Ra administration (SCIL-STROKE) has shown that, in spite of a significant reduction in plasma inflammatory markers associated with a worse outcome after ischemic stroke, IL-1Ra treatment was not associated with a favorable outcome on modified Rankin Scale (mRS).⁴¹

Recently developed techniques of total microglial depletion have shown that microglia seem essential to the limitation of stroke damages, since microglia-depleted mice show larger infarct volumes than nondepleted mice.⁴²

Therapeutic strategies targeting microglia. Minocycline, an anti-infective agent of the tetracycline family used for the treatment of infections caused by a wide range of organisms, has been tested for the treatment of stroke. It is highly lipophilic and crosses the blood-brain barrier. Minocycline, by acting through different pathways, is able to inhibit microglial activation, decrease migration of T cells, reduce neuronal apoptosis, block free radical production, decrease CNS expression of chemokines and their associated receptors, and inhibit matrix metalloproteinases, particularly matrix metalloproteinase-9.^{43–58} In preclinical stroke studies, minocycline ameliorated behavioral function and decreased lesion volume and hemorrhagic transformation.^{44–47} It did not alter the fibrinolytic effect of rtPA⁴⁶ and could enlarge the time window for thrombolysis.⁴⁹ Two phase II clinical trials have shown minocycline to be safe and potentially effective in acute ischemic stroke, alone or in combination with tPA, when administered in the first 24 h after stroke onset and for 5 days.^{59,60} However, a third pilot study performed in a small sample of acute stroke patients has shown that minocycline administration in the first 24 h was safe but not efficacious.⁴³ The authors acknowledged that this third study was not powered to identify reliably or exclude a modest but clinically important treatment effect of minocycline.⁴³ Larger clinical trials

are thus needed to study the effect of minocycline in stroke patients.

Recently, preclinical studies have focused also on the switch of microglial cell phenotype from M1 to M2 as a potential target to improve stroke outcome, by administering IL-33⁶¹ or IL-4.⁶²

Endothelial cells

Pathophysiology. In the brain, the functional unit formed by tightly joined ECs and astrocytic endfeet constitute the BBB, a strong protective blood-tissue barrier against pathogens. A few minutes after stroke onset, the BBB is disrupted, and local ECs are activated.^{63,64} When activated, ECs express cellular adhesion molecules (CAMs) which allow leukocyte rolling and adhesion to the luminal side of the EC and eventually leukocyte transmigration toward the brain parenchyma.⁵ After their activation, the first adhesion molecules expressed by ECs are the selectins (E- and P-selectins). They are constitutively produced by ECs and stored in Weibel-Palade bodies until EC activation. The initial adhesive interactions between leukocytes and selectins expressed on the luminal side of the venular endothelium are tethering (capture) and rolling. These low-affinity (weak) interactions are subsequently strengthened as a result of the sequential activation of different families of adhesion molecules that are located on the surface of leukocytes and ECs.⁶⁵ A few hours after stroke onset, ECs start to express the VCAM-1 and the ICAM-1,^{63,66} allowing leukocytes to adhere and remain stationary on the vessel wall. Finally, ECs express the platelet endothelial cell adhesion molecule (PECAM-1), responsible for leukocyte transmigration into the brain parenchyma.¹¹

Therapeutic strategies targeting selectins. Strategies for the blockade of CAMs through the intravenous injection of antibodies have failed in ameliorating stroke outcome both in clinical and preclinical trials.

Enlimomab, a murine ICAM-1 antibody, reduces leukocyte adhesion and infarct size in experimental stroke studies.⁶⁷ However, the clinical trial performed in stroke patients showed that the administration of enlimomab within 6 h after stroke onset is not an effective treatment for ischemic stroke and, indeed, significantly worsened stroke outcome and increased adverse events.⁶⁸ One of the possible explanations for this

failure is the murine origin of the injected antibody to stroke patients.⁶⁹

Induction of mucosal tolerance to E-selectin to minimize inflammation and risk of further cerebral insult has been tested in a phase I clinical trial, but results have not been disclosed.⁷⁰

L-selectin, a CAM located in the surface of leukocytes, has also been targeted in an experimental stroke model in rabbits by using a humanized monoclonal antibody (HuDREG200). This strategy, alone or in combination with alteplase, failed to significantly ameliorate stroke outcome.⁷¹

Neutrophils

Pathophysiology. The principal role of neutrophils is to enhance leukocyte recruitment by degranulation of their content, rich in cytokines/chemokines, proteolytic enzymes and activated-complement system.⁷² The extent of neutrophil infiltration after stroke is still debated, being described either limited to the perivascular space or infiltrating the brain tissue in preclinical stroke models (permanent or mechanical transient occlusion of the MCA) and human postmortem samples.^{73–75}

It was postulated that neutrophils could contribute to brain injury after ischemic stroke by obstructing microvessel circulation, damaging endothelial cells and ECM by hydrolytic enzymes and free radicals, promoting intravascular thrombus formation together with platelet activation, and releasing cytokines and chemotactic factors that could promote extension of the inflammatory response.⁷⁶

Therapeutic strategies targeting neutrophils. Preclinical and clinical studies aiming at blocking neutrophil infiltration have targeted CD11/CD18 (LFA-1 for lymphocyte function-associated antigen 1), located at the surface of neutrophils, to prevent their adhesion to ICAM-1 (expressed at the luminal surface of ECs). Preclinical studies have shown that CD11/CD18 monoclonal antibodies are not beneficial in permanent stroke models,^{77,78} but are beneficial on a transient mechanical ischemic stroke model.⁷⁹ In spite of this, two clinical trials have been performed to prevent neutrophil recruitment after stroke onset and have shown no beneficial effect. On the HALT phase III trial, the humanized antibody

Hu23F2G, administered twice daily, appeared to produce an improvement in mRS score in a phase II study. However, the sponsor terminated a subsequent phase III study when a ‘futility analysis’ advised that no benefit of the treatment would occur if the study was completed. No public information regarding the database, outcomes, safety issues, or relative number of adverse events has appeared.⁷⁶ On the ASTIN (Acute Stroke Therapy by Inhibition of Neutrophils) study, UK-279,276 (another CD18 antagonist) was administered within 6 h of stroke symptom onset, but, similar to the HALT study, the trial was stopped early due to futility.⁸⁰

Lymphocytes

Pathophysiology. Adaptive immunity also plays an important role during stroke. Lymphocytes consist of distinct subpopulations with diverse functions and can be subdivided into two groups: pro- and anti-inflammatory lymphocytes. The consequences of the adaptive immune response on ischemic stroke are still debated, as both beneficial and deleterious results have been reported depending on the type of T-helper (Th) immune response set in motion after the activation of lymphocytes.^{81–83} Both transient (mechanical) and permanent experimental models of stroke have shown that lymphocyte infiltration into the ischemic tissue comes later after stroke onset (starting at 3 days).^{14,16} Postmortem human samples have shown that lymphocyte infiltration into the ischemic area occur from day 3 and can be present up to 53 years after stroke.¹⁵

The choroid plexuses (CP) have recently been proposed as the preferential route for lymphocyte infiltration into the lesion site after experimental stroke. Indeed, CP infarction reduces lymphocyte infiltration after stroke onset; however, the ischemic volume is not modified in these mice, even if lymphocyte infiltration is actually reduced.⁸⁴ These intriguing results raise important questions about the role of lymphocytes on the development of the ischemic lesion.

Therapeutic strategies targeting lymphocytes. Therapeutic strategies targeting lymphocytes would be desirable because they focus the delayed phase of the injury and thus could have a particularly wide therapeutic window. Several preclinical studies have shown that pro-inflammatory lymphocytes, such as TH1, TH17, and $\gamma\delta$ T

cells worsen stroke outcome, and that blocking of their brain invasion is neuroprotective.^{85–87}

Contrary to pro-inflammatory lymphocytes, regulatory T cells (Treg) and B cells have been characterized as anti-inflammatory and as disease-limiting protective cells. Targeting Tregs as the endogenous orchestrators of the postischemic immune response has been proposed as a more effective therapy than blocking only a particular inflammatory pathway.^{5,13} However, because of the complex function of regulatory cells in immune homeostasis and disease, as well as partially divergent findings using different stroke models, the pathophysiologic function of regulatory lymphocytes in stroke remains uncertain. As an example, among nine studies using Treg-depletion paradigms, three of the studies revealed an increase in infarct volume^{88–90} whereas five studies did not detect any effect on stroke outcome^{88,89,91–93} and one study even observed a reduction of infarct size in Treg-deficient mice.⁹⁴ To explain this, the experimental model used (permanent *versus* transient mechanical) and more particularly, the resulting volume of the ischemic lesion, has been proposed as a determinant on the overall effect of Treg depletion that seems to provide a benefit only on small lesion volumes provoked on the permanent stroke model.⁹⁵

Another strategy for Treg modulation has been the administration of enhancers of Treg function by adoptive cell transfer of purified Treg to wild-type animals to increase circulating Treg numbers, or by the administration of a CD28 superagonist (CD28SA), which provokes *in vivo* expansion of Tregs and amplification of their suppressive function. However, the obtained results are again controversial, with some studies describing an improvement of stroke outcome⁹⁶ and other studies describing an increase of ischemic volume.⁹⁷ Once again, it has been proposed that stroke severity might predict the net biological effect of Tregs.⁹⁵

It has been proposed that Tregs have a deleterious role on ischemic stroke not related to their established immunoregulatory characteristics but to a specific effect on microvascular thrombus formation in a model of transient mechanical occlusion.⁹⁴ Secondary microthrombosis arises within minutes after reperfusion in transient mechanical models of stroke once the occluding filament has been removed. It provokes delayed cerebral blood flow (CBF) reduction, secondary ischemia and

lesion growth, which is responsible for ~70% of the final ischemic lesion size.⁹⁸ However, clinical studies have shown that secondary ischemia and lesion growth are modest or nonexistent after reperfusion in selected patients,^{2,17,99,100} and concerns have been raised about the clinical relevance of transient mechanical vascular occlusion stroke models.¹⁰¹ For these reasons, it would be interesting to test the role of Tregs in nonmechanical models of ischemic stroke, where secondary microthrombosis is absent.¹⁰²

To increase the complexity of this question, fingolimod (FTY720), an immunomodulatory drug currently approved by the US Food and Drug Administration for the treatment of multiple sclerosis that inhibits lymphocyte circulation and brain immigration, has been tested in models of permanent and transient mechanical ischemia. As in the case of the aforementioned CP infarction,⁸⁴ although a reduction of lymphocyte brain invasion was detected using fingolimod, no effect was observed on infarct volumes and behavioral dysfunction in any of the models. This lack of neuroprotection despite effective lymphopenia was attributed to a divergent impact of fingolimod on cytokine expression and possible activation of innate immune cells after brain ischemia.⁸⁶ A phase II clinical trial using fingolimod (administered within 6 h after the onset of symptoms) combined with alteplase and mechanical thrombectomy on ischemic stroke (FAMTAIS) is ongoing.¹⁰³

Two clinical pilot studies have tested fingolimod, alone and later than 4.5 h after stroke onset for 3 days,¹⁰⁴ or in combination with tPA (thus before 4.5 h after stroke onset) for 3 days.¹⁰⁵ These two studies have shown a beneficial effect of the oral administration of fingolimod within 72 h of stroke onset, especially when combined with tPA, where patients who received the combination exhibited smaller lesion volumes, less hemorrhage, and a better recovery at day 90.

Therapeutic strategies targeting global leukocyte infiltration. The transendothelial migration of leukocytes through the interaction between the molecules VLA-4 (leukocyte very late antigen-4) (present at the surface of neutrophils, monocytes, and T and B lymphocytes among other blood cell types) and VCAM-1 (vascular cell adhesion molecule-1) has been targeted in several studies. Antibodies against the alpha chain of VLA-4 (anti-CD49d antibodies) have shown efficacy in several models of autoimmune diseases, and the

humanized antibody natalizumab is currently one of the most effective therapies for patients with multiple sclerosis.¹⁰⁶ However, preclinical data have shown conflicting results from four positive and one inconclusive studies on the use of anti-CD49d antibodies on ischemic stroke.^{86,107–110} Recently, a preclinical randomized controlled multicenter trial highlighted the importance of testing new therapies in different experimental stroke models (discussed further on), since the administration of CD49d-antibodies reduced both leukocyte invasion and infarct volume after the permanent distal occlusion of the MCA (which causes a small cortical infarction), whereas it did not reduce leukocyte invasion or infarct volume after transient proximal mechanical occlusion of the MCA (which induces large lesions).¹¹¹ These results could suggest that the benefits of immune-targeted therapies may be dependent on infarct localization and severity.

The recently published results of the administration of one dose of natalizumab in patients with acute ischemic stroke (ACTION trial) have shown that natalizumab administered up to 9 h after stroke onset did not reduce infarct growth (primary endpoint of the study), but more patients in the natalizumab group than in the placebo group had mRS scores of 0 or 1 at day 30, although this beneficial effect disappeared 90 days after stroke.¹¹² These results reinforce the need of new studies to understand (a) how natalizumab exerts a positive effect on functional outcome without reducing the infarct volume at 30 days, and (b) why this beneficial effect on functional outcome is lost at 90 days. Additionally, the ACTION II trial has been recently completed. Its primary objective was to assess the effects of natalizumab on functional independence and activities of daily living.¹¹³ Results have not been published yet.

Immunomodulating therapies in stroke: a gap between our expectations and reality

The reasons for the failure of immunomodulatory therapies in clinical trials are multifactorial. As discussed, one of the main issues of the bench-to-bed translation of immunomodulatory therapies for stroke is the huge gap between human pathophysiology and the stroke models that have mainly been used to study stroke immunology. In experimental stroke models, preclinical stroke research nowadays disposes of a wide range of experimental models including permanent and transient arterial

occlusions. In addition to this, the origin of the occlusion may also vary from a transient mechanical occlusion to real blood clots located in the lumen of the artery. In the case of clot-induced stroke models, researchers can even adopt different strategies to determine the nature of clots (fibrin-rich or platelet-rich) and, consequently, clot susceptibility to thrombolytic agents^{114–116} to mimic the heterogeneity of human thrombi subtypes. It is important to note that despite the variety of available stroke models, the vast majority of preclinical data on transient models of ischemic stroke has been obtained on mechanical occlusion models that provoke thromboinflammation and secondary microthrombosis. This secondary microthrombosis is a major pathophysiologic mechanism leading to brain damage which does not occur in other models based on clot-induced ischemic stroke like the thrombin-induced stroke model.^{102,116} As in the aforementioned case of Treg-targeted drugs, immunomodulatory agents that have clearly shown beneficial effects on mechanical occlusion models of stroke could actually be targeting thromboinflammation and secondary microthrombosis. Since it is unclear whether thromboinflammation is a universal pathophysiological mechanism of human stroke, immunomodulatory drugs deserve to be evaluated or re-evaluated in experimental stroke models not inducing secondary thromboinflammation before trying to apply them in clinical practice.

Other reasons for the failure in the translation of immunomodulatory therapies from bench to bedside may include poorly designed preclinical and clinical studies, and underpowered clinical trials with overambitious and pathophysiologically irrelevant therapeutic windows.^{117,118} In addition, a biased selection of substances for clinical testing may partially explain the slow progress in developing treatments.¹¹⁸

It is also possible that the positive results seen with immunomodulatory drugs in experimental studies are not transposable to the complexity and the variability of the immunologic response in human stroke, which may depend on different parameters including prestroke status of the patient and the natural history of the disease.^{63,93} In most animal studies, complete occlusion is induced and is either maintained or followed by complete reperfusion. In human stroke, however, only a few patients are likely to experience both complete occlusion and complete reperfusion (excepting thrombectomized patients). The

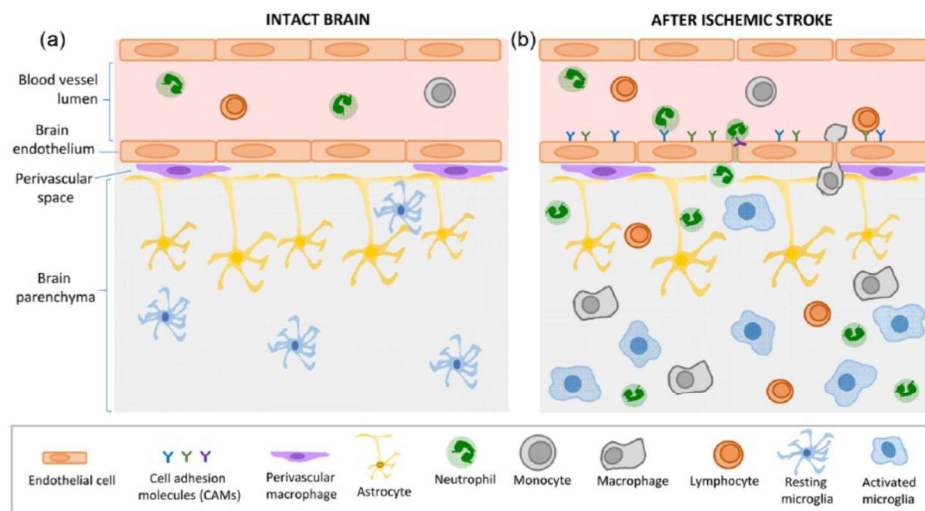


Figure 1. Immune reactions after ischemic stroke.

(a) In the intact brain, the functional unit formed by tightly jointed ECs and astrocytic endfeet constitute the BBB, a strong protective blood–tissue barrier from pathogens. Immune cells circulate freely in the blood, and in the brain parenchyma, resting microglia survey the environment with their processes. (b) A few minutes after stroke onset, the BBB is disrupted and local ECs are activated. The tight junctions between ECs disappear and activated ECs express CAMs. This allows white cell rolling and adhesion at the luminal side of the blood vessel and then transmigration from the vascular compartment to the brain parenchyma. Once infiltrated in the tissue, neutrophils secrete pro-inflammatory factors that will recruit monocytes/macrophages, and later lymphocytes to the parenchyma. After stroke, microglia switches from a resting form to an activated state, adopting a phagocytic phenotype and secreting pro-inflammatory factors. BBB, blood–brain barrier; CAM, cellular adhesion molecule; EC, endothelial cell.

unlimited variety of outcomes seen in stroke patients suggests that stroke itself, as well as the body's response to ischemic stroke represents a seamless continuum of exigencies rather than the definitive scenario employed in animal studies.⁶⁸ In addition, stroke risk factors such as diet, smoking, aging, atherosclerosis, hypertension, alcohol consumption and stress cannot be replicated well in the laboratory; actually, most of the preclinical studies are performed in healthy mice. Moreover, although stroke remains the third cause of death in women,¹¹⁹ most of the preclinical studies are performed on male animals. Inflammatory cells such as microglia, dendritic cells, neutrophils and lymphocytes show variations between sex, and so may play different roles in the pathophysiology of stroke.^{120–123}

The failure of immunomodulatory drugs clinically tested on stroke to date may also indicate that the inflammatory response after stroke is an important aspect of the regenerative process triggered after stroke and only becomes detrimental when exaggerated, perhaps in relation to the severity of ischemic injury (as shown in preclinical stroke models) or to concomitant disease states or risk factors. However, many of the preclinical

studies examining immunomodulation were targeted at the acute phase, not during the phases where recovery is expected to occur. Thus, this hypothesis needs to be addressed in future studies.

Another important element to be considered when testing immunomodulatory drugs for stroke is that postischemic systemic immunomodulation and infectious complications are some of the main comorbidities after stroke. In experimental models, the systemic immune responses differ substantially among stroke models and infarct volume.^{89,124} Translational studies of immunomodulatory therapies for stroke must account for this heterogeneity, especially in the case of drugs with long-term effects such as natalizumab, that blocks the α -4 integrin for at least 4 weeks.¹²⁵

Conclusion

Factors contributing to the failure in the translation of therapies targeting stroke-induced immune responses to clinical practice include nonmodifiable factors (differences in the cerebrovascular system in humans and rodents, variability in the immune response in patients depending on their



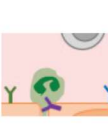

 <p>IL-1 receptor antagonist IL-1 receptor</p>	<p>Therapeutic strategies targeting IL-1-induced inflammation</p> <p>Recombinant human IL-1 receptor antagonist, rhIL1-Ra</p> <p>Positive results in a Phase II clinical trial (intravenous administration) (Emsley <i>et al.</i>, 2005)</p> <p>Not beneficial in a Phase II clinical trial (subcutaneous administration) (SCIL-STROKE) (Smith <i>et al.</i>, 2018)</p>
	<p>Therapeutic strategies targeting microglial activation</p> <p>Minocycline</p> <p>Positive results in two Phase II clinical trials (Lampl <i>et al.</i>, 2007; Padma Srivastava <i>et al.</i>, 2012)</p> <p>Phase IV clinical trial stopped for futility (NeuMAST) (Kohler <i>et al.</i>, 2013)</p>
	<p>Therapeutic strategies targeting endothelial selectins</p> <p>Enlimomab (mouse anti-ICAM-1)</p> <p>Worse stroke outcome in a Phase III clinical trial (Enlimomab Acute Stroke Trial Investigators, 2001)</p> <p>E-selectin tolerance</p> <p>Results from Phase II clinical trial not disclosed (http://clinicaltrials.gov/show/NCT00012454)</p>
	<p>Therapeutic strategies targeting leukocyte infiltration</p> <p>UK-279, 276 (Recombinant neutrophil inhibitory factor, blocking its interaction with ICAM-1) (ASTIN)</p> <p>Phase II clinical trial stopped for futility (Krams <i>et al.</i>, 2003)</p> <p>Hu23F2G (Humanized monoclonal antibody against neutrophil CD11/CD18, blocking its interaction with ICAM-1) (HALT)</p> <p>Phase III clinical trial stopped for futility (results not disclosed) (del Zoppo, 2010)</p> <p>Fingolimod (sphingosine-1-phosphate receptor on lymphocytes)</p> <p>Positive results in two pilot studies (Fu <i>et al.</i>, 2014; Zhu <i>et al.</i>, 2015)</p> <p>Natalizumab (humanized antibody against the VCAM-1 leukocyte ligand VLA-4) (ACTION)</p> <p>Not beneficial in a Phase II clinical trial (Elkins <i>et al.</i>, 2017)</p>

Figure 2. Summary of clinical trials targeting the immune responses triggered after ischemic stroke. CD11/CD18, LFA-1 for lymphocyte function-associated antigen 1; IL-1, interleukin 1; rhIL1-Ra, recombinant human interleukin 1 receptor antagonist; ICAM-1, intercellular adhesion molecule; VCAM-1, vascular cell adhesion molecule; VLA-4, leukocyte very late antigen-4.

prestroke inflammatory status, which is extremely difficult to mimic in animal models of stroke...) that need to be considered when interpreting results. However, most of these factors are modifiable and include, among others, the use of clinically relevant stroke models and therapeutic time windows, the comparison of a same molecule in different stroke models, the improvement in the experimental designs and the inclusion of females and comorbidities in preclinical studies.

Now that we are in the age of acute revascularization, one might wonder if we can do better than thrombectomy for patients with penumbra. If the answer is 'no' then there is probably no need for immunomodulatory treatments for these patients. If the answer is 'yes,' and also for all the other patients, immunomodulation will retain therapeutic interest. Preclinical studies should be conceived according to the targeted stroke subpopulation. In any case, a strictly linear bench-to-bedside

paradigm is probably not optimal for translating basic scientific findings into clinically effective stroke therapies, and a bedside-back-to-bench paradigm will help in this translation.

In spite of the limitations of experimental stroke models, our knowledge about the inflammatory responses triggered after stroke onset exponentially increases thanks to preclinical and clinical studies, and gives rise to novel therapeutic targets and improved strategies, with the hope of ameliorating stroke outcome in patients.

Funding

This research received no specific grant from any funding agency in the public, commercial, or not-for-profit sectors.

Conflict of interest statement

The authors declare that there is no conflict of interest.

ORCID iD

Marina Rubio  <https://orcid.org/0000-0002-6120-4053>

References

- Jovin TG, Chamorro A, Cobo E, *et al.* Thrombectomy within 8 hours after symptom onset in ischemic stroke. *N Engl J Med* 2015; 372: 2296–2306.
- Nogueira RG, Jadhav AP, Haussen DC, *et al.* Thrombectomy 6 to 24 hours after stroke with a mismatch between deficit and infarct. *N Engl J Med* 2018; 378: 11–21.
- Albers GW, Marks MP, Kemp S, *et al.* Thrombectomy for stroke at 6 to 16 hours with selection by perfusion imaging. *N Engl J Med* 2018; 378: 708–718.
- Fagan SC, Cronin LE and Hess DC. Minocycline development for acute ischemic stroke. *Transl Stroke Res.* 2011; 2: 202–208.
- Iadecola C and Anrather J. The immunology of stroke: from mechanisms to translation. *Nat Med* 2011; 17: 796–808.
- Choi DW. Glutamate neurotoxicity in cortical cell culture is calcium dependent. *Neurosci Lett* 1985; 58: 293–297.
- Koistinaho M and Koistinaho J. Interactions between Alzheimer's disease and cerebral ischemia—focus on inflammation. *Brain Res Brain Res Rev* 2005; 48: 240–250.
- Miyaji Y, Yoshimura S, Sakai N, *et al.* Effect of edaravone on favorable outcome in patients with acute cerebral large vessel occlusion: subanalysis of RESCUE-Japan Registry. *Neurol Med Chir (Tokyo)* 2015; 55: 241–247.
- Perego C, Fumagalli S and De Simoni M-G. Temporal pattern of expression and colocalization of microglia/macrophage phenotype markers following brain ischemic injury in mice. *J Neuroinflammation* 2011; 8: 174.
- Huang J, Upadhyay UM and Tamargo RJ. Inflammation in stroke and focal cerebral ischemia. *Surg Neurol* 2006; 66: 232–245.
- Muller WA. Leukocyte-endothelial cell interactions in the inflammatory response. *Lab Investig J Tech Methods Pathol* 2002; 82: 521–533.
- Engelhardt B and Ransohoff RM. The ins and outs of T-lymphocyte trafficking to the CNS: anatomical sites and molecular mechanisms. *Trends Immunol* 2005; 26: 485–495.
- Eltzschig HK and Eckle T. Ischemia and reperfusion—from mechanism to translation. *Nat Med* 2011; 17: 1391–1401.
- Gelderblom M, Leypoldt F, Steinbach K, *et al.* Temporal and spatial dynamics of cerebral immune cell accumulation in stroke. *Stroke* 2009; 40: 1849–1857.
- Mena H, Cadavid D and Rushing EJ. Human cerebral infarct: a proposed histopathologic classification based on 137 cases. *Acta Neuropathol (Berl)* 2004; 108: 524–530.
- Zhou W, Liesz A, Bauer H, *et al.* Postischemic brain infiltration of leukocyte subpopulations differs among murine permanent and transient focal cerebral ischemia models: infiltration differs among cerebral ischemia. *Brain Pathol* 2013; 23: 34–44.
- Lansberg MG, Straka M, Kemp S, *et al.* MRI profile and response to endovascular reperfusion after stroke (DEFUSE 2): a prospective cohort study. *Lancet Neurol* 2012; 11: 860–867.
- Kyritsis N, Kizil C, Zocher S, *et al.* Acute inflammation initiates the regenerative response in the adult zebrafish brain. *Science* 2012; 338: 1353–1356.
- Macrez R, Ali C, Toutirais O, *et al.* Stroke and the immune system: from pathophysiology to new therapeutic strategies. *Lancet Neurol* 2011; 10: 471–480.
- Tobin MK, Bonds JA, Minshall RD, *et al.* Neurogenesis and inflammation after ischemic stroke: what is known and where we go from here. *J Cereb Blood Flow Metab Off J Int Soc Cereb Blood Flow Metab* 2014; 34: 1573–1584.
- Peruzzotti-Jametti L, Donegá M, Giusto E, *et al.* The role of the immune system in central nervous system plasticity after acute injury. *Neuroscience* 2014; 283: 210–221.
- Schwartz M, Kipnis J, Rivest S, *et al.* How do immune cells support and shape the brain in health, disease, and aging? *J Neurosci Off J Soc Neurosci* 2013; 33: 17587–17596.
- Nowicka D, Rogozinska K, Aleksy M, *et al.* Spatiotemporal dynamics of astroglial and microglial responses after photothrombotic stroke in the rat brain. *Acta Neurobiol Exp (Warsz)* 2008; 68: 155–168.
- Lively S, Moxon-Emre I and Schlichter LC. SC1/hevin and reactive gliosis after transient ischemic stroke in young and aged rats. *J Neuropathol Exp Neurol* 2011; 70: 913–929.
- Morioka T, Kolehua AN and Streit WJ. Characterization of microglial reaction after

- middle cerebral artery occlusion in rat brain. *J Comp Neurol* 1993; 327: 123–132.
26. Huang L, Wu Z-B, Zhuge Q, *et al.* Glial scar formation occurs in the human brain after ischemic stroke. *Int J Med Sci* 2014; 11: 344–348.
 27. Krieger DW, Georgia MAD, Abou-Chebl A, *et al.* Cooling for Acute Ischemic Brain Damage (COOL AID): an open pilot study of induced hypothermia in acute ischemic stroke. *Stroke* 2001; 32: 1847–1854.
 28. De Georgia MA, Krieger DW, Abou-Chebl A, *et al.* Cooling for Acute Ischemic Brain Damage (COOL AID): a feasibility trial of endovascular cooling. *Neurology* 2004; 63: 312–317.
 29. Lyden PD, Allgren RL, Ng K, *et al.* Intravascular Cooling in the Treatment of Stroke (ICTuS): early clinical experience. *J Stroke Cerebrovasc Dis Off J Natl Stroke Assoc* 2005; 14: 107–114.
 30. Hemmen TM, Raman R, Guluma KZ, *et al.* Intravenous thrombolysis plus hypothermia for acute treatment of ischemic stroke (ICTuS-L): final results. *Stroke* 2010; 41: 2265–2270.
 31. Lyden P, Hemmen T, Grotta J, *et al.* Results of the ICTuS 2 trial (Intravascular Cooling in the Treatment of Stroke 2). *Stroke* 2016; 47: 2888–2895.
 32. van der Worp HBI, Macleod MR, Bath PM, *et al.* Trial of therapeutic cooling in patients with acute ischaemic stroke. *Int J Stroke* 2014; 9(5): 642–645. doi: 10.1111/ijss.12294. <https://www.eurohyp1.eu/> (accessed 15 May 2018).
 33. Lawson LJ, Perry VH and Gordon S. Turnover of resident microglia in the normal adult mouse brain. *Neuroscience* 1992; 48: 405–415.
 34. Kettenmann H, Hanisch U-K, Noda M, *et al.* Physiology of microglia. *Physiol Rev* 2011; 91: 461–553.
 35. Chen GY and Nuñez G. Sterile inflammation: sensing and reacting to damage. *Nat Rev Immunol* 2010; 10: 826–837.
 36. Fernandez-Fernandez S, Almeida A and Bolaños JP. Antioxidant and bioenergetic coupling between neurons and astrocytes. *Biochem J* 2012; 443: 3–11.
 37. Fernandez-Lizarbe S, Pascual M and Guerri C. Critical role of TLR4 response in the activation of microglia induced by ethanol. *J Immunol* 2009; 183: 4733–4744.
 38. Cardona AE, Piro EP, Sasse ME, *et al.* Control of microglial neurotoxicity by the fractalkine receptor. *Nat Neurosci* 2006; 9: 917–924.
 39. Banwell V, Sena ES and Macleod MR. Systematic review and stratified meta-analysis of the efficacy of interleukin-1 receptor antagonist in animal models of stroke. *J Stroke Cerebrovasc Dis Off J Natl Stroke Assoc* 2009; 18: 269–276.
 40. Emsley HCA, Smith CJ, Georgiou RF, *et al.* A randomised phase II study of interleukin-1 receptor antagonist in acute stroke patients. *J Neurol Neurosurg Psychiatry* 2005; 76: 1366–1372.
 41. Smith CJ, Hulme S, Vail A, *et al.* SCIL-STROKE (Subcutaneous Interleukin-1 Receptor Antagonist in Ischemic Stroke): a randomized controlled phase 2 trial. *Stroke* 2018; 49: 1210–1216.
 42. Szalay G, Martinecz B, Lénárt N, *et al.* Microglia protect against brain injury and their selective elimination dysregulates neuronal network activity after stroke. *Nat Commun* 2016; 7: 11499.
 43. Kohler E, Prentice DA, Bates TR, *et al.* Intravenous minocycline in acute stroke: a randomized, controlled pilot study and meta-analysis. *Stroke* 2013; 44: 2493–2499.
 44. Lapchak PA, Chapman DF and Zivin JA. Metalloproteinase inhibition reduces thrombolytic (tissue plasminogen activator)-induced hemorrhage after thromboembolic stroke. *Stroke* 2000; 31: 3034–3040.
 45. Lee CZ, Xue Z, Zhu Y, *et al.* Matrix metalloproteinase-9 inhibition attenuates vascular endothelial growth factor-induced intracerebral hemorrhage. *Stroke* 2007; 38: 2563–2568.
 46. Machado LS, Sazonova IY, Kozak A, *et al.* Minocycline and tissue-type plasminogen activator for stroke: assessment of interaction potential. *Stroke* 2009; 40: 3028–3033.
 47. Matsukawa N, Yasuhara T, Hara K, *et al.* Therapeutic targets and limits of minocycline neuroprotection in experimental ischemic stroke. *BMC Neurosci* 2009; 10: 126.
 48. Morimoto N, Shimazawa M, Yamashita T, *et al.* Minocycline inhibits oxidative stress and decreases in vitro and in vivo ischemic neuronal damage. *Brain Res* 2005; 1044: 8–15.
 49. Murata Y, Rosell A, Scannevin RH, *et al.* Extension of the thrombolytic time window with minocycline in experimental stroke. *Stroke* 2008; 39: 3372–3377.
 50. Plane JM, Shen Y, Pleasure DE, *et al.* Prospects for minocycline neuroprotection. *Arch Neurol* 2010; 67: 1442–1448.

51. Power C, Henry S, Del Bigio MR, *et al.* Intracerebral hemorrhage induces macrophage activation and matrix metalloproteinases. *Ann Neurol* 2003; 53: 731–742.
52. Sanchez Mejia RO, Ona VO, Li M, *et al.* Minocycline reduces traumatic brain injury-mediated caspase-1 activation, tissue damage, and neurological dysfunction. *Neurosurgery* 2001; 48: 1393–1399; discussion 1399–1401.
53. Stirling DP, Khodarahmi K, Liu J, *et al.* Minocycline treatment reduces delayed oligodendrocyte death, attenuates axonal dieback, and improves functional outcome after spinal cord injury. *J Neurosci Off J Soc Neurosci* 2004; 24: 2182–2190.
54. Teng YD, Choi H, Onario RC, *et al.* Minocycline inhibits contusion-triggered mitochondrial cytochrome c release and mitigates functional deficits after spinal cord injury. *Proc Natl Acad Sci U S A* 2004; 101: 3071–3076.
55. Wang CX, Yang T, Noor R, *et al.* Delayed minocycline but not delayed mild hypothermia protects against embolic stroke. *BMC Neurol* 2002; 2: 2.
56. Wells JEA, Hurlbert RJ, Fehlings MG, *et al.* Neuroprotection by minocycline facilitates significant recovery from spinal cord injury in mice. *Brain J Neurol* 2003; 126(Pt 7): 1628–1637.
57. Xu L, Fagan SC, Waller JL, *et al.* Low dose intravenous minocycline is neuroprotective after middle cerebral artery occlusion-reperfusion in rats. *BMC Neurol* 2004; 4: 7.
58. Yong VW, Wells J, Giuliani F, *et al.* The promise of minocycline in neurology. *Lancet Neurol* 2004; 3: 744–751.
59. Lampl Y, Boaz M, Gilad R, *et al.* Minocycline treatment in acute stroke: an open-label, evaluator-blinded study. *Neurology* 2007; 69: 1404–1410.
60. Padma Srivastava MV, Bhasin A, Bhatia R, *et al.* Efficacy of minocycline in acute ischemic stroke: a single-blinded, placebo-controlled trial. *Neurol India* 2012; 60: 23–28.
61. Yang Y, Liu H, Zhang H, *et al.* ST2/IL-33-dependent microglial response limits acute ischemic brain injury. *J Neurosci Off J Soc Neurosci* 2017; 37: 4692–4704.
62. Liu X, Liu J, Zhao S, *et al.* Interleukin-4 is essential for microglia/macrophage M2 polarization and long-term recovery after cerebral ischemia. *Stroke* 2016; 47: 498–504.
63. Gauberti M, Montagne A, Marcos-Contreras OA, *et al.* Ultra-sensitive molecular MRI of vascular cell adhesion molecule-1 reveals a dynamic inflammatory penumbra after strokes. *Stroke* 2013; 44: 1988–1996.
64. Montagne A, Gauberti M, Macrez R, *et al.* Ultra-sensitive molecular MRI of cerebrovascular cell activation enables early detection of chronic central nervous system disorders. *NeuroImage* 2012; 63: 760–770.
65. Granger DN and Senchenkova E. *Inflammation and the microcirculation*. San Rafael (CA): Morgan & Claypool Life Sciences, <http://www.ncbi.nlm.nih.gov/books/NBK53373/> (2010, accessed 12 March 2018).
66. Gauberti M, Fournier AP, Docagne F, *et al.* Molecular magnetic resonance imaging of endothelial activation in the central nervous system. *Theranostics* 2018; 8: 1195–1212.
67. Bowes MP, Rothlein R, Fagan SC, *et al.* Monoclonal antibodies preventing leukocyte activation reduce experimental neurologic injury and enhance efficacy of thrombolytic therapy. *Neurology* 1995; 45: 815–819.
68. Enlimomab Acute Stroke Trial Investigators. Use of anti-ICAM-1 therapy in ischemic stroke: results of the Enlimomab Acute Stroke Trial. *Neurology* 2001; 57: 1428–1434.
69. DeGraba TJ. The role of inflammation after acute stroke: utility of pursuing anti-adhesion molecule therapy. *Neurology* 1998; 51(3 Suppl 3): S62–S68.
70. Cayce Onks. *E-selectin nasal spray to prevent stroke recurrence*. <https://clinicaltrials.gov/ct2/show/NCT00012454> (accessed 22 March 2018).
71. Bednar M, Gross C, Russell S, *et al.* Humanized anti-L-selectin monoclonal antibody DREC200 therapy in acute thromboembolic stroke. *Neurol Res* 1998; 20: 403–408.
72. Nathan C. Neutrophils and immunity: challenges and opportunities. *Nat Rev Immunol* 2006; 6: 173–182.
73. Enzmann G, Mysiorek C, Gorina R, *et al.* The neurovascular unit as a selective barrier to polymorphonuclear granulocyte (PMN) infiltration into the brain after ischemic injury. *Acta Neuropathol (Berl)* 2013; 125: 395–412.
74. Chu HX, Kim HA, Lee S, *et al.* Immune cell infiltration in malignant middle cerebral artery infarction: comparison with transient cerebral


- ischemia. *J Cereb Blood Flow Metab Off J Int Soc Cereb Blood Flow Metab* 2014; 34: 450–459.
75. Perez-de-Puig I, Miró-Mur F, Ferrer-Ferrer M, *et al.* Neutrophil recruitment to the brain in mouse and human ischemic stroke. *Acta Neuropathol (Berl)* 2015; 129: 239–257.
 76. Del Zoppo GJ. Acute anti-inflammatory approaches to ischemic stroke. *Ann N Y Acad Sci* 2010; 1207: 143–148.
 77. Garcia JH, Liu KF and Bree MP. Effects of CD11b/18 monoclonal antibody on rats with permanent middle cerebral artery occlusion. *Am J Pathol* 1996; 148: 241–248.
 78. Jiang N, Chopp M and Chahwala S. Neutrophil inhibitory factor treatment of focal cerebral ischemia in the rat. *Brain Res* 1998; 788: 25–34.
 79. Prestigiacomo CJ, Kim SC, Connolly ES, *et al.* CD18-mediated neutrophil recruitment contributes to the pathogenesis of reperfused but not nonreperfused stroke. *Stroke* 1999; 30: 1110–1117.
 80. Krams M, Lees KR, Hacke W, *et al.* Acute Stroke Therapy by Inhibition of Neutrophils (ASTIN): an adaptive dose-response study of UK-279,276 in acute ischemic stroke. *Stroke* 2003; 34: 2543–2548.
 81. Gee JM, Kalil A, Shea C, *et al.* Lymphocytes: potential mediators of postischemic injury and neuroprotection. *Stroke* 2007; 38(2 Suppl): 783–788.
 82. Hallenbeck J, Del Zoppo G, Jacobs T, *et al.* Immunomodulation strategies for preventing vascular disease of the brain and heart: workshop summary. *Stroke* 2006; 37: 3035–3042.
 83. Schwartz M and Kipnis J. Autoimmunity on alert: naturally occurring regulatory CD4(+) CD25(+) T cells as part of the evolutionary compromise between a « need » and a « risk ». *Trends Immunol* 2002; 23: 530–534.
 84. Llovera G, Benakis C, Enzmann G, *et al.* The choroid plexus is a key cerebral invasion route for T cells after stroke. *Acta Neuropathol (Berl)* 2017; 134: 851–868.
 85. Gelderblom M, Weymar A, Bernreuther C, *et al.* Neutralization of the IL-17 axis diminishes neutrophil invasion and protects from ischemic stroke. *Blood* 2012; 120: 3793–3802.
 86. Liesz A, Zhou W, Mracsó É, *et al.* Inhibition of lymphocyte trafficking shields the brain against deleterious neuroinflammation after stroke. *Brain J Neurol* 2011; 134(Pt 3): 704–720.
 87. Shichita T, Sugiyama Y, Ooboshi H, *et al.* Pivotal role of cerebral interleukin-17-producing gammadeltaT cells in the delayed phase of ischemic brain injury. *Nat Med* 2009; 15: 946–950.
 88. Liesz A, Zhou W, Na S-Y, *et al.* Boosting regulatory T cells limits neuroinflammation in permanent cortical stroke. *J Neurosci Off J Soc Neurosci* 2013; 33: 17350–17362.
 89. Liesz A, Suri-Payer E, Veltkamp C, *et al.* Regulatory T cells are key cerebroprotective immunomodulators in acute experimental stroke. *Nat Med* 2009; 15: 192–199.
 90. Xie L, Sun F, Wang J, *et al.* mTOR signaling inhibition modulates macrophage/microglia-mediated neuroinflammation and secondary injury via regulatory T cells after focal ischemia. *J Immunol Baltim Md* 1950 2014; 192: 6009–6019.
 91. Li P, Gan Y, Sun B-L, *et al.* Adoptive regulatory T-cell therapy protects against cerebral ischemia. *Ann Neurol* 2013; 74: 458–471.
 92. Ren X, Akiyoshi K, Vandenbark AA, *et al.* CD4+FoxP3+ regulatory T-cells in cerebral ischemic stroke. *Metab Brain Dis* 2011; 26: 87–90.
 93. Stubbe T, Ebner F, Richter D, *et al.* Regulatory T cells accumulate and proliferate in the ischemic hemisphere for up to 30 days after MCAO. *J Cereb Blood Flow Metab Off J Int Soc Cereb Blood Flow Metab* 2013; 33: 37–47.
 94. Kleinschnitz C, Kraft P, Dreykluft A, *et al.* Regulatory T cells are strong promoters of acute ischemic stroke in mice by inducing dysfunction of the cerebral microvasculature. *Blood* 2013; 121: 679–691.
 95. Liesz A, Hu X, Kleinschnitz C, *et al.* Functional role of regulatory lymphocytes in stroke: facts and controversies. *Stroke* 2015; 46: 1422–1430.
 96. Na S-Y, Mracsó E, Liesz A, *et al.* Amplification of regulatory T cells using a CD28 superagonist reduces brain damage after ischemic stroke in mice. *Stroke* 2015; 46: 212–220.
 97. Schuhmann MK, Kraft P, Stoll G, *et al.* CD28 superagonist-mediated boost of regulatory T cells increases thrombo-inflammation and ischemic neurodegeneration during the acute phase of experimental stroke. *J Cereb Blood Flow Metab Off J Int Soc Cereb Blood Flow Metab* 2015; 35: 6–10.

98. Pham M, Kleinschnitz C, Helluy X, *et al.* Enhanced cortical reperfusion protects coagulation factor XII-deficient mice from ischemic stroke as revealed by high-field MRI. *NeuroImage* 2010; 49: 2907–2914.
99. Davis SM, Donnan GA, Parsons MW, *et al.* Effects of alteplase beyond 3 h after stroke in the Echoplanar Imaging Thrombolytic Evaluation Trial (EPITHET): a placebo-controlled randomised trial. *Lancet Neurol* 2008; 7: 299–309.
100. Delgado-Mederos R, Rovira A, Alvarez-Sabín J, *et al.* Speed of tPA-induced clot lysis predicts DWI lesion evolution in acute stroke. *Stroke* 2007; 38: 955–960.
101. Gauberti M and Vivien D. Letter by Gauberti and Vivien regarding article, « amplification of regulatory T cells using a CD28 superagonist reduces brain damage after ischemic stroke in mice ». *Stroke* 2015; 46: e50–e51.
102. Gauberti M, Montagne A, Quenault A, *et al.* Molecular magnetic resonance imaging of brain-immune interactions. *Front Cell Neurosci* 2014; 8: 389.
103. Min Lou. *Combining fingolimod with alteplase bridging with mechanical thrombectomy in acute ischemic stroke*, <https://clinicaltrials.gov/ct2/show/NCT02956200> (2016, accessed 15 May 2018).
104. Fu Y, Zhang N, Ren L, *et al.* Impact of an immune modulator fingolimod on acute ischemic stroke. *Proc Natl Acad Sci U S A*. 2014; 111: 18315–18320.
105. Zhu Z, Fu Y, Tian D, *et al.* Combination of the immune modulator fingolimod with alteplase in acute ischemic stroke: a pilot trial. *Circulation* 2015; 132: 1104–1112.
106. Rudick R, Polman C, Clifford D, *et al.* Natalizumab: bench to bedside and beyond. *JAMA Neurol* 2013; 70: 172–182.
107. Becker K, Kindrick D, Relton J, *et al.* Antibody to the alpha4 integrin decreases infarct size in transient focal cerebral ischemia in rats. *Stroke* 2001; 32: 206–211.
108. Langhauser F, Kraft P, Göb E, *et al.* Blocking of $\alpha 4$ integrin does not protect from acute ischemic stroke in mice. *Stroke* 2014; 45: 1799–1806.
109. Neumann J, Riek-Burchardt M, Herz J, *et al.* Very-late-antigen-4 (VLA-4)-mediated brain invasion by neutrophils leads to interactions with microglia, increased ischemic injury and impaired behavior in experimental stroke. *Acta Neuropathol (Berl)* 2015; 129: 259–277.
110. Relton JK, Sloan KE, Frew EM, *et al.* Inhibition of alpha4 integrin protects against transient focal cerebral ischemia in normotensive and hypertensive rats. *Stroke* 2001; 32: 199–205.
111. Llovera G, Hofmann K, Roth S, *et al.* Results of a preclinical randomized controlled multicenter trial (pRCT): anti-CD49d treatment for acute brain ischemia. *Sci Transl Med* 2015; 7: 299ra121.
112. Elkins J, Veltkamp R, Montaner J, *et al.* Safety and efficacy of natalizumab in patients with acute ischaemic stroke (ACTION): a randomised, placebo-controlled, double-blind phase 2 trial. *Lancet Neurol* 2017; 16: 217–226.
113. Jake Elkins. *Safety and efficacy of intravenous natalizumab in acute ischemic stroke*, <https://clinicaltrials.gov/ct2/show/NCT02730455> (accessed 31 May 2018.)
114. Martinez de Lizarrondo S, Gakuba C, Herbig BA, *et al.* Potent thrombolytic effect of n-acetylcysteine on arterial thrombi. *Circulation* 2017; 136: 646–660.
115. Orset C, Haelewyn B, Allan SM, *et al.* Efficacy of alteplase in a mouse model of acute ischemic stroke: a retrospective pooled analysis. *Stroke* 2016; 47: 1312–1318.
116. Orset C, Macrez R, Young AR, *et al.* Mouse model of in situ thromboembolic stroke and reperfusion. *Stroke* 2007; 38: 2771–2778.
117. Hossmann K-A. The two pathophysiologies of focal brain ischemia: implications for translational stroke research. *J Cereb Blood Flow Metab Off J Int Soc Cereb Blood Flow Metab* 2012; 32: 1310–1316.
118. O'Collins VE, Macleod MR, Donnan GA, *et al.* 1,026 experimental treatments in acute stroke. *Ann Neurol* 2006; 59: 467–477.
119. Spychala MS, Honarpisheh P and McCullough LD. Sex differences in neuroinflammation and neuroprotection in ischemic stroke. *J Neurosci Res* 2017; 95(1–2): 462–471.
120. Ginhoux F, Greter M, Leboeuf M, *et al.* Fate mapping analysis reveals that adult microglia derive from primitive macrophages. *Science* 2010; 330: 841–845.
121. Yilmaz G and Granger DN. Leukocyte recruitment and ischemic brain injury. *Neuro Molecular Med* 2010; 12: 193–204.

A Drieu, D Levard *et al.*

122. Felger JC, Abe T, Kaunzner UW, *et al.* Brain dendritic cells in ischemic stroke: time course, activation state, and origin. *Brain Behav Immun* 2010; 24: 724–737.
123. Liu F and McCullough LD. Middle cerebral artery occlusion model in rodents: methods and potential pitfalls. *J Biomed Biotechnol* 2011; 2011: 464701.
124. Hug A, Dalpke A, Wiczorek N, *et al.* Infarct volume is a major determiner of post-stroke immune cell function and susceptibility to infection. *Stroke* 2009; 40: 3226–3232.
125. Veltkamp R and Gill D. Clinical trials of immunomodulation in ischemic stroke. *Neurother J Am Soc Exp Neurother* 2016; 13: 791–800.

Visit SAGE journals online
[journals.sagepub.com/
home/tan](http://journals.sagepub.com/home/tan)

 SAGE journals

RÉFÉRENCES BIBLIOGRAPHIQUES

Ahn, J.H. *et al.* (2019) 'Meningeal lymphatic vessels at the skull base drain cerebrospinal fluid', *Nature*, p. 1. doi:10.1038/s41586-019-1419-5.

Ainslie, P.N. *et al.* (2008) 'Elevation in cerebral blood flow velocity with aerobic fitness throughout healthy human ageing', *The Journal of Physiology*, 586(16), pp. 4005–4010. doi:10.1113/jphysiol.2008.158279.

Ajami, B. *et al.* (2007) 'Local self-renewal can sustain CNS microglia maintenance and function throughout adult life', *Nature Neuroscience*, 10(12), pp. 1538–1543. doi:10.1038/nn2014.

Alho, H. *et al.* (2004) 'Alcohol misuse increases serum antibodies to oxidized LDL and C-reactive protein', *Alcohol and Alcoholism (Oxford, Oxfordshire)*, 39(4), pp. 312–315. doi:10.1093/alcalc/agh059.

Alves de Lima, K., Rustenhoven, J. and Kipnis, J. (2020) 'Meningeal Immunity and Its Function in Maintenance of the Central Nervous System in Health and Disease', *Annual Review of Immunology*, 38(1), pp. 597–620. doi:10.1146/annurev-immunol-102319-103410.

Amann, L. and Prinz, M. (2020) 'The origin, fate and function of macrophages in the peripheral nervous system-an update', *International Immunology*, 32(11), pp. 709–717. doi:10.1093/intimm/dxaa030.

Amarenco, P. *et al.* (2009) 'Classification of stroke subtypes', *Cerebrovascular Diseases (Basel, Switzerland)*, 27(5), pp. 493–501. doi:10.1159/000210432.

Amki, M.E. *et al.* (2020) 'Neutrophils Obstructing Brain Capillaries Are a Major Cause of No-Reflow in Ischemic Stroke', *Cell Reports*, 33(2). doi:10.1016/j.celrep.2020.108260.

Anrather, J. and Iadecola, C. (2016) 'Inflammation and Stroke: An Overview', *Neurotherapeutics: The Journal of the American Society for Experimental NeuroTherapeutics*, 13(4), pp. 661–670. doi:10.1007/s13311-016-0483-x.

Ansar, S. *et al.* (2014) 'Characterization of a New Model of Thromboembolic Stroke in C57 black/6J mice', *Translational Stroke Research*, 5(4), pp. 526–533. doi:10.1007/s12975-013-0315-9.

Appelros, P., Stegmayr, B. and Terént, A. (2009) 'Sex differences in stroke epidemiology: a systematic review', *Stroke*, 40(4), pp. 1082–1090. doi:10.1161/STROKEAHA.108.540781.

Barton, G.M. (2008) 'A calculated response: control of inflammation by the innate immune system', *The Journal of Clinical Investigation*, 118(2), pp. 413–420. doi:10.1172/JCI34431.

Beal, C.C. (2010) 'Gender and stroke symptoms: a review of the current literature', *The Journal of Neuroscience Nursing: Journal of the American Association of Neuroscience Nurses*, 42(2), pp. 80–87.

Bechmann, I. *et al.* (2001) 'Turnover of rat brain perivascular cells', *Experimental Neurology*, 168(2), pp. 242–249. doi:10.1006/exnr.2000.7618.

Becker, A.M. *et al.* (2016) 'An automated task for the training and assessment of distal forelimb function in a mouse model of ischemic stroke', *Journal of Neuroscience Methods*, 258, pp. 16–23. doi:10.1016/j.jneumeth.2015.10.004.

Béjot, Y. *et al.* (2014) 'Trends in the incidence of ischaemic stroke in young adults between 1985 and 2011: the Dijon Stroke Registry', *Journal of Neurology, Neurosurgery, and Psychiatry*, 85(5), pp. 509–513. doi:10.1136/jnnp-2013-306203.

Benakis, C. *et al.* (2016) 'Commensal microbiota affects ischemic stroke outcome by regulating intestinal $\gamma\delta$ T cells', *Nature Medicine*, 22(5), pp. 516–523. doi:10.1038/nm.4068.

Benakis, C., Llovera, G. and Liesz, A. (2018) 'The meningeal and choroidal infiltration routes for leukocytes in stroke', *Therapeutic Advances in Neurological Disorders*, 11, p. 1756286418783708. doi:10.1177/1756286418783708.

Bonnard, T. and Hagemeyer, C.E. (2015) 'Ferric Chloride-induced Thrombosis Mouse Model on Carotid Artery and Mesentery Vessel', *Journal of Visualized Experiments: JoVE*, (100), p. e52838. doi:10.3791/52838.

Broekaart, D.W.M. *et al.* (2018) 'Activation of the innate immune system is evident throughout epileptogenesis and is associated with blood-brain barrier dysfunction and seizure progression', *Epilepsia*, 59(10), pp. 1931–1944. doi:10.1111/epi.14550.

Brown, A.W., Marlowe, K.J. and Bjelke, B. (2003) 'Age effect on motor recovery in a post-acute animal stroke model', *Neurobiology of Aging*, 24(4), pp. 607–614. doi:10.1016/S0197-4580(02)00129-X.

Buscemi, L. *et al.* (2019) 'Spatio-temporal overview of neuroinflammation in an experimental mouse stroke model', *Scientific Reports*, 9. doi:10.1038/s41598-018-36598-4.

Cai, W. *et al.* (2019) 'Functional Dynamics of Neutrophils After Ischemic Stroke', *Translational Stroke Research* [Preprint]. doi:10.1007/s12975-019-00694-y.

Calvillo, L. *et al.* (2019) 'Neuroimmune crosstalk in the pathophysiology of hypertension', *Nature Reviews Cardiology*, 16(8), pp. 476–490. doi:10.1038/s41569-019-0178-1.

Candelario-Jalil, E. and Paul, S. (2021) 'Impact of aging and comorbidities on ischemic stroke outcomes in preclinical animal models: A translational perspective', *Experimental Neurology*, 335, p. 113494. doi:10.1016/j.expneurol.2020.113494.

Carare, R.O. *et al.* (2008) 'Solutes, but not cells, drain from the brain parenchyma along basement membranes of capillaries and arteries: significance for cerebral amyloid angiopathy and neuroimmunology', *Neuropathology and Applied Neurobiology*, 34(2), pp. 131–144. doi:10.1111/j.1365-2990.2007.00926.x.

Casetta, I. *et al.* (2020) 'Endovascular Thrombectomy for Acute Ischemic Stroke Beyond 6 Hours From Onset: A Real-World Experience', *Stroke*, 51(7), pp. 2051–2057. doi:10.1161/STROKEAHA.119.027974.

Cassidy, J.M. and Cramer, S.C. (2017) 'Spontaneous & Therapeutic-Induced Mechanisms of Functional Recovery After Stroke', *Translational stroke research*, 8(1), pp. 33–46. doi:10.1007/s12975-016-0467-5.

Chagnot, A., Barnes, S.R. and Montagne, A. (2021) 'Magnetic Resonance Imaging of Blood-Brain Barrier Permeability in Dementia', *Neuroscience* [Preprint]. doi:10.1016/j.neuroscience.2021.08.003.

Chakrabarti, L. *et al.* (1991) 'Early viral replication in the brain of SIV-infected rhesus monkeys', *The American Journal of Pathology*, 139(6), pp. 1273–1280.

Chamorro, Á. *et al.* (2016) 'Neuroprotection in acute stroke: targeting excitotoxicity, oxidative and nitrosative stress, and inflammation', *The Lancet Neurology*, 15(8), pp. 869–881. doi:10.1016/S1474-4422(16)00114-9.

Cherian, I. *et al.* (2016) 'Exploring the Virchow-Robin spaces function: A unified theory of brain diseases', *Surgical Neurology International*, 7(Suppl 26), pp. S711–S714. doi:10.4103/2152-7806.192486.

Chung, J.-W. *et al.* (2014) 'Trial of ORG 10172 in Acute Stroke Treatment (TOAST) Classification and Vascular Territory of Ischemic Stroke Lesions Diagnosed by Diffusion-Weighted Imaging', *Journal of the American Heart Association* [Preprint]. doi:10.1161/JAHA.114.001119.

Claassen, J.A.H.R. *et al.* (2021) 'Regulation of cerebral blood flow in humans: physiology and clinical implications of autoregulation', *Physiological Reviews* [Preprint]. doi:10.1152/physrev.00022.2020.

Clarke, A.G. (1944) 'The Anatomy of the Meninges', *Postgraduate Medical Journal*, 20(220), pp. 74–78. doi:10.1136/pgmj.20.220.74.

Coles, J.A. *et al.* (2017) 'Where are we? The anatomy of the murine cortical meninges revisited for intravital imaging, immunology, and clearance of waste from the brain', *Progress in Neurobiology*, 156, pp. 107–148. doi:10.1016/j.pneurobio.2017.05.002.

Collins, R. *et al.* (2016) 'Interpretation of the evidence for the efficacy and safety of statin therapy', *The Lancet*, 388(10059), pp. 2532–2561. doi:10.1016/S0140-6736(16)31357-5.

Crapser, J. *et al.* (2016) 'Ischemic stroke induces gut permeability and enhances bacterial translocation leading to sepsis in aged mice', *Aging*, 8(5), pp. 1049–1063. doi:10.18632/aging.100952.

Croese, T., Castellani, G. and Schwartz, M. (2021) 'Immune cell compartmentalization for brain surveillance and protection', *Nature Immunology*, 22(9), pp. 1083–1092. doi:10.1038/s41590-021-00994-2.

Cserép, C. *et al.* (2019) 'Microglia monitor and protect neuronal function via specialized somatic purinergic junctions', *Science* [Preprint]. doi:10.1126/science.aax6752.

Cugurra, A. *et al.* (2021) 'Skull and vertebral bone marrow are myeloid cell reservoirs for the meninges and CNS parenchyma', *Science* [Preprint]. doi:10.1126/science.abf7844.

Cui, J., Xu, H. and Lehtinen, M.K. (2021) 'Macrophages on the margin: choroid plexus immune responses', *Trends in Neurosciences* [Preprint]. doi:10.1016/j.tins.2021.07.002.

Cunningham, C. *et al.* (2005) 'Central and Systemic Endotoxin Challenges Exacerbate the Local Inflammatory Response and Increase Neuronal Death during Chronic Neurodegeneration', *Journal of Neuroscience*, 25(40), pp. 9275–9284. doi:10.1523/JNEUROSCI.2614-05.2005.

Daneman, R. and Engelhardt, B. (2017) 'Brain barriers in health and disease', *Neurobiology of Disease*, 107, pp. 1–3. doi:10.1016/j.nbd.2017.05.008.

De Vis, J. b. *et al.* (2015) 'Age-related changes in brain hemodynamics; A calibrated MRI study', *Human Brain Mapping*, 36(10), pp. 3973–3987. doi:10.1002/hbm.22891.

Del Río Hortega, P. (1918) 'Noticia de un nuevo y fácil método para la coloración de la neuroglia y el tejido conjuntivo', *Trab. Lab. Invest. Biol.* 15, pp. 367–378.

Dhanesha, N. *et al.* (2020) 'Targeting Myeloid-Specific Integrin $\alpha 9\beta 1$ Improves Short and Long-Term Stroke Outcomes in Murine Models With Preexisting Comorbidities by Limiting Thrombosis And Inflammation', *Circulation Research* [Preprint]. doi:10.1161/CIRCRESAHA.120.316659.

DiNapoli, V.A. *et al.* (2008) 'Early disruptions of the blood–brain barrier may contribute to exacerbated neuronal damage and prolonged functional recovery following stroke in aged rats', *Neurobiology of Aging*, 29(5), pp. 753–764. doi:10.1016/j.neurobiolaging.2006.12.007.

Dorrier, C.E. *et al.* (2021) 'Emerging roles for CNS fibroblasts in health, injury and disease', *Nature Reviews Neuroscience*, pp. 1–12. doi:10.1038/s41583-021-00525-w.

Dreikorn, M. *et al.* (2018) 'Immunotherapy of experimental and human stroke with agents approved for multiple sclerosis: a systematic review', *Therapeutic Advances in Neurological Disorders*, 11, p. 1756286418770626. doi:10.1177/1756286418770626.

Drieu, A. *et al.* (2018) 'Anti-inflammatory treatments for stroke: from bench to bedside', *Therapeutic Advances in Neurological Disorders*, 11, p. 1756286418789854. doi:10.1177/1756286418789854.

Drieu, A. *et al.* (2019) 'Immune Responses and Anti-inflammatory Strategies in a Clinically Relevant Model of Thromboembolic Ischemic Stroke with Reperfusion', *Translational Stroke Research* [Preprint]. doi:10.1007/s12975-019-00733-8.

Drieu, A. *et al.* (2020) 'Alcohol exposure-induced neurovascular inflammatory priming impacts ischemic stroke and is linked with brain perivascular macrophages', *JCI insight* [Preprint]. doi:10.1172/jci.insight.129226.

Ducroquet, A. *et al.* (2013) 'Influence of chronic ethanol consumption on the neurological severity in patients with acute cerebral ischemia', *Stroke*, 44(8), pp. 2324–2326. doi:10.1161/STROKEAHA.113.001355.

El Khoury, J. *et al.* (2007) 'Ccr2 deficiency impairs microglial accumulation and accelerates progression of Alzheimer-like disease', *Nature Medicine*, 13(4), pp. 432–438. doi:10.1038/nm1555.

El Khoury, J.B. *et al.* (2003) 'CD36 mediates the innate host response to beta-amyloid', *The Journal of Experimental Medicine*, 197(12), pp. 1657–1666. doi:10.1084/jem.20021546.

Elkins, J. *et al.* (2017) 'Safety and efficacy of natalizumab in patients with acute ischaemic stroke (ACTION): a randomised, placebo-controlled, double-blind phase 2 trial', *The Lancet. Neurology*, 16(3), pp. 217–226. doi:10.1016/S1474-4422(16)30357-X.

Emsley, H.C.A. *et al.* (2005) 'A randomised phase II study of interleukin-1 receptor antagonist in acute stroke patients', *Journal of Neurology, Neurosurgery, and Psychiatry*, 76(10), pp. 1366–1372. doi:10.1136/jnnp.2004.054882.

Engelhardt, B. (2006) 'Regulation of immune cell entry into the central nervous system', *Results and Problems in Cell Differentiation*, 43, pp. 259–280. doi:10.1007/400_020.

Engelhardt, B. *et al.* (2016) 'Vascular, glial, and lymphatic immune gateways of the central nervous system', *Acta Neuropathologica*, 132(3), pp. 317–338. doi:10.1007/s00401-016-1606-5.

Engelhardt, E. (2017) 'Apoplexy, cerebrovascular disease, and stroke: Historical evolution of terms and definitions', *Dementia & Neuropsychologia*, 11(4), p. 449. doi:10.1590/1980-57642016dn11-040016.

Enlimomab Acute Stroke Trial Investigators (2001) 'Use of anti-ICAM-1 therapy in ischemic stroke: results of the Enlimomab Acute Stroke Trial', *Neurology*, 57(8), pp. 1428–1434. doi:10.1212/wnl.57.8.1428.

Erickson, M.A. and Banks, W.A. (2018) 'Neuroimmune Axes of the Blood-Brain Barriers and Blood-Brain Interfaces: Bases for Physiological Regulation, Disease States, and Pharmacological Interventions', *Pharmacological Reviews*, 70(2), pp. 278–314. doi:10.1124/pr.117.014647.

Excessive Drinking is Draining the U.S. Economy (2020). Available at: <https://www.cdc.gov/alcohol/features/excessive-drinking.html> (Accessed: 19 October 2021).

Fabriek, B.O. *et al.* (2005) 'CD163-positive perivascular macrophages in the human CNS express molecules for antigen recognition and presentation', *Glia*, 51(4), pp. 297–305. doi:10.1002/glia.20208.

Fabriek, B.O. *et al.* (2007) 'The macrophage CD163 surface glycoprotein is an erythroblast adhesion receptor', *Blood*, 109(12), pp. 5223–5229. doi:10.1182/blood-2006-08-036467.

Faraco, G. *et al.* (2016) 'Perivascular macrophages mediate the neurovascular and cognitive dysfunction associated with hypertension', *The Journal of Clinical Investigation*, 126(12), pp. 4674–4689. doi:10.1172/JCI86950.

Faraco, G. *et al.* (2017) 'Brain perivascular macrophages: characterization and functional roles in health and disease', *Journal of molecular medicine (Berlin, Germany)*, 95(11), pp. 1143–1152. doi:10.1007/s00109-017-1573-x.

Feng, Y. *et al.* (2017) 'Infiltration and persistence of lymphocytes during late-stage cerebral ischemia in middle cerebral artery occlusion and photothrombotic stroke models', *Journal of Neuroinflammation*, 14(1), p. 248. doi:10.1186/s12974-017-1017-0.

Fernández-Klett, F. *et al.* (2013) 'Early loss of pericytes and perivascular stromal cell-induced scar formation after stroke', *Journal of Cerebral Blood Flow & Metabolism*, 33(3), p. 428. doi:10.1038/jcbfm.2012.187.

Fleischhauer, K. (1964) '[ON FLUORESCENCE OF PERIVASCULAR CELLS IN THE CAT BRAIN]', *Zeitschrift Fur Zellforschung Und Mikroskopische Anatomie (Vienna, Austria: 1948)*, 64, pp. 140–152.

Fu, Y. *et al.* (2015) 'Immune interventions in stroke', *Nature reviews. Neurology*, 11(9), pp. 524–535. doi:10.1038/nrneurol.2015.144.

Fuhrmann, M. *et al.* (2010) 'Microglial Cx3cr1 knockout prevents neuron loss in a mouse model of Alzheimer's disease', *Nature Neuroscience*, 13(4), pp. 411–413. doi:10.1038/nn.2511.

van Furth, R. *et al.* (1972) 'The mononuclear phagocyte system: a new classification of macrophages, monocytes, and their precursor cells', *Bulletin of the World Health Organization*, 46(6), pp. 845–852.

Furukawa, M. *et al.* (2008) 'Topographic study on nerve-associated lymphatic vessels in the murine craniofacial region by immunohistochemistry and electron microscopy', *Biomedical Research (Tokyo, Japan)*, 29(6), pp. 289–296. doi:10.2220/biomedres.29.289.

Gadani, S.P. *et al.* (2015) 'Dealing with Danger in the CNS: The Response of the Immune System to Injury', *Neuron*, 87(1), pp. 47–62. doi:10.1016/j.neuron.2015.05.019.

Galea, I. *et al.* (2005) 'Mannose receptor expression specifically reveals perivascular macrophages in normal, injured, and diseased mouse brain', *Glia*, 49(3), pp. 375–384. doi:10.1002/glia.20124.

Galea, I., Bechmann, I. and Perry, V.H. (2007) 'What is immune privilege (not)?', *Trends in Immunology*, 28(1), pp. 12–18. doi:10.1016/j.it.2006.11.004.

Gattringer, T. *et al.* (2015) 'IV thrombolysis in patients with ischemic stroke and alcohol abuse', *Neurology*, 85(18), pp. 1592–1597. doi:10.1212/WNL.0000000000002078.

Gauberti, M. *et al.* (2014) 'Lack of Secondary Microthrombosis After Thrombin-Induced Stroke in Mice and Non-Human Primates', *Journal of thrombosis and haemostasis: JTH*, 12(3), pp. 409–414. doi:10.1111/jth.12487.

Gauberti, M. *et al.* (2018) 'Ischemia-Reperfusion Injury After Endovascular Thrombectomy for Ischemic Stroke', *Stroke*, 49(12), pp. 3071–3074. doi:10.1161/STROKEAHA.118.022015.

Gauberti, M. and Martinez de Lizarrondo, S. (2021) 'Molecular MRI of Neuroinflammation: Time to Overcome the Translational Roadblock', *Neuroscience* [Preprint]. doi:10.1016/j.neuroscience.2021.08.016.

Ge, R. *et al.* (2017) 'Choroid plexus-cerebrospinal fluid route for monocyte-derived macrophages after stroke', *Journal of Neuroinflammation*, 14(1), p. 153. doi:10.1186/s12974-017-0909-3.

Gelderblom, M. *et al.* (2009) 'Temporal and Spatial Dynamics of Cerebral Immune Cell Accumulation in Stroke', *Stroke*, 40(5), pp. 1849–1857. doi:10.1161/STROKEAHA.108.534503.

Gelderblom, M., Arunachalam, P. and Magnus, T. (2014) ' $\gamma\delta$ T cells as early sensors of tissue damage and mediators of secondary neurodegeneration', *Frontiers in Cellular Neuroscience*, 8. doi:10.3389/fncel.2014.00368.

Gherzi-Egea, J.-F. *et al.* (2018) 'Molecular anatomy and functions of the choroidal blood-cerebrospinal fluid barrier in health and disease', *Acta Neuropathologica*, 135(3), pp. 337–361. doi:10.1007/s00401-018-1807-1.

Ginhoux, F. *et al.* (2010) 'Fate mapping analysis reveals that adult microglia derive from primitive macrophages', *Science (New York, N.Y.)*, 330(6005), pp. 841–845. doi:10.1126/science.1194637.

Goldmann, T. *et al.* (2016) 'Origin, fate and dynamics of macrophages at central nervous system interfaces', *Nature Immunology*, 17(7), pp. 797–805. doi:10.1038/ni.3423.

Graeber, M.B., Streit, W.J. and Kreutzberg, G.W. (1989) 'Identity of ED2-positive perivascular cells in rat brain', *Journal of Neuroscience Research*, 22(1), pp. 103–106. doi:10.1002/jnr.490220114.

Gu, L. *et al.* (2015) 'T Cells and Cerebral Ischemic Stroke', *Neurochemical Research*, 40(9), pp. 1786–1791. doi:10.1007/s11064-015-1676-0.

Guagnozzi, D. and Caprilli, R. (2008) 'Natalizumab in the treatment of Crohn's disease', *Biologics: Targets & Therapy*, 2(2), pp. 275–284.

Guzik, A. and Bushnell, C. (2017) 'Stroke Epidemiology and Risk Factor Management', *Continuum (Minneapolis, Minn.)*, 23(1, Cerebrovascular Disease), pp. 15–39. doi:10.1212/CON.0000000000000416.

Haley, M.J. *et al.* (2019) 'Microglial Priming as Trained Immunity in the Brain', *Neuroscience*, 405, pp. 47–54. doi:10.1016/j.neuroscience.2017.12.039.

Hankey, G.J. (2017) 'Stroke', *The Lancet*, 389(10069), pp. 641–654. doi:10.1016/S0140-6736(16)30962-X.

Hart, R.G., Pearce, L.A. and Aguilar, M.I. (2007) 'Meta-analysis: Antithrombotic Therapy to Prevent Stroke in Patients Who Have Nonvalvular Atrial Fibrillation', *Annals of Internal Medicine*, 146(12), pp. 857–867. doi:10.7326/0003-4819-146-12-200706190-00007.

Hashimoto, D. *et al.* (2013) 'Tissue-resident macrophages self-maintain locally throughout adult life with minimal contribution from circulating monocytes', *Immunity*, 38(4), pp. 792–804. doi:10.1016/j.immuni.2013.04.004.

Hata, R. *et al.* (2000) 'Evolution of brain infarction after transient focal cerebral ischemia in mice', *Journal of Cerebral Blood Flow and Metabolism: Official Journal of the International Society of Cerebral Blood Flow and Metabolism*, 20(6), pp. 937–946. doi:10.1097/00004647-200006000-00006.

Hawkes, C.A. and McLaurin, J. (2009) 'Selective targeting of perivascular macrophages for clearance of β -amyloid in cerebral amyloid angiopathy', *Proceedings of the National Academy of Sciences of the United States of America*, 106(4), pp. 1261–1266. doi:10.1073/pnas.0805453106.

He, H. *et al.* (2016) 'Perivascular Macrophages Limit Permeability', *Arteriosclerosis, Thrombosis, and Vascular Biology*, 36(11), pp. 2203–2212. doi:10.1161/ATVBAHA.116.307592.

He, J. and Crews, F.T. (2008) 'Increased MCP-1 and microglia in various regions of the human alcoholic brain', *Experimental Neurology*, 210(2), pp. 349–358. doi:10.1016/j.expneurol.2007.11.017.

Healy, L.M. *et al.* (2017) 'MerTK-mediated regulation of myelin phagocytosis by macrophages generated from patients with MS', *Neurology(R) Neuroimmunology & Neuroinflammation*, 4(6), p. e402. doi:10.1212/NXI.0000000000000402.

Henning, E.C. *et al.* (2009) 'Feridex preloading permits tracking of CNS-resident macrophages after transient middle cerebral artery occlusion', *Journal of Cerebral Blood Flow and Metabolism: Official Journal of the International Society of Cerebral Blood Flow and Metabolism*, 29(7), pp. 1229–1239. doi:10.1038/jcbfm.2009.48.

Heo, J.H., Han, S.W. and Lee, S.K. (2005) 'Free radicals as triggers of brain edema formation after stroke', *Free Radical Biology and Medicine*, 39(1), pp. 51–70. doi:10.1016/j.freeradbiomed.2005.03.035.

Hickey, W.F. and Kimura, H. (1988) 'Perivascular microglial cells of the CNS are bone marrow-derived and present antigen *in vivo*', *Science (New York, N.Y.)*, 239(4837), pp. 290–292. doi:10.1126/science.3276004.

Hickman, S. *et al.* (2018) 'Microglia in neurodegeneration', *Nature Neuroscience*, 21(10), pp. 1359–1369. doi:10.1038/s41593-018-0242-x.

Hickman, S.E. *et al.* (2013) 'The microglial sensome revealed by direct RNA sequencing', *Nature Neuroscience*, 16(12), pp. 1896–1905. doi:10.1038/nn.3554.

Hickman, S.E., Allison, E.K. and El Khoury, J. (2008) 'Microglial dysfunction and defective beta-amyloid clearance pathways in aging Alzheimer's disease mice', *The Journal of Neuroscience: The Official Journal of the Society for Neuroscience*, 28(33), pp. 8354–8360. doi:10.1523/JNEUROSCI.0616-08.2008.

Hoeffel, G. *et al.* (2015) 'C-Myb(+) erythro-myeloid progenitor-derived fetal monocytes give rise to adult tissue-resident macrophages', *Immunity*, 42(4), pp. 665–678. doi:10.1016/j.immuni.2015.03.011.

Hofmann, N. *et al.* (2002) 'Increased expression of ICAM-1, VCAM-1, MCP-1, and MIP-1 alpha by spinal perivascular macrophages during experimental allergic encephalomyelitis in rats', *BMC immunology*, 3, p. 11.

Hossmann, K.-A. (2006) 'Pathophysiology and Therapy of Experimental Stroke', *Cellular and Molecular Neurobiology*, 26(7), pp. 1055–1081. doi:10.1007/s10571-006-9008-1.

Hossmann, K.-A. (2012) 'The two pathophysiologies of focal brain ischemia: implications for translational stroke research', *Journal of Cerebral Blood Flow and Metabolism: Official Journal of the International Society of Cerebral Blood Flow and Metabolism*, 32(7), pp. 1310–1316. doi:10.1038/jcbfm.2011.186.

Hove, H.V. *et al.* (2019) 'A single-cell atlas of mouse brain macrophages reveals unique transcriptional identities shaped by ontogeny and tissue environment', *Nature Neuroscience*, 22(6), p. 1021. doi:10.1038/s41593-019-0393-4.

Howells, D.W. *et al.* (2010) 'Different strokes for different folks: the rich diversity of animal models of focal cerebral ischemia', *Journal of Cerebral Blood Flow and Metabolism: Official Journal of the International Society of Cerebral Blood Flow and Metabolism*, 30(8), pp. 1412–1431. doi:10.1038/jcbfm.2010.66.

Hsu, M. *et al.* (2019) 'Neuroinflammation-induced lymphangiogenesis near the cribriform plate contributes to drainage of CNS-derived antigens and immune cells', *Nature Communications*, 10(1), p. 229. doi:10.1038/s41467-018-08163-0.

Hu, M. *et al.* (2019) 'Update of inflammasome activation in microglia/macrophage in aging and aging-related disease', *CNS Neuroscience & Therapeutics*, 25(12), p. 1299. doi:10.1111/cns.13262.

Iadecola, C. and Anrather, J. (2011) 'The immunology of stroke: from mechanisms to translation', *Nature Medicine*, 17(7), pp. 796–808. doi:10.1038/nm.2399.

Imhof, A. *et al.* (2001) 'Effect of alcohol consumption on systemic markers of inflammation', *Lancet (London, England)*, 357(9258), pp. 763–767. doi:10.1016/S0140-6736(00)04170-2.

Ivan, D.C. *et al.* (2021) 'Dwellers and Trespassers: Mononuclear Phagocytes at the Borders of the Central Nervous System', *Frontiers in Immunology*, 11. doi:10.3389/fimmu.2020.609921.

Iyonaga, T. *et al.* (2019) 'Brain perivascular macrophages contribute to the development of hypertension in stroke-prone spontaneously hypertensive rats via sympathetic activation', *Hypertension Research: Official Journal of the Japanese Society of Hypertension* [Preprint]. doi:10.1038/s41440-019-0333-4.

Jayaraj, R.L. *et al.* (2019) 'Neuroinflammation: friend and foe for ischemic stroke', *Journal of Neuroinflammation*, 16(1), p. 142. doi:10.1186/s12974-019-1516-2.

Jiang, L. *et al.* (2020) 'Transcriptomic and functional studies reveal undermined chemotactic and angiostimulatory properties of aged microglia during stroke recovery', *Journal of Cerebral Blood Flow & Metabolism*, 40(1_suppl), pp. S81–S97. doi:10.1177/0271678X20902542.

Jordão, M.J.C. *et al.* (2019) 'Single-cell profiling identifies myeloid cell subsets with distinct fates during neuroinflammation', *Science (New York, N.Y.)*, 363(6425). doi:10.1126/science.aat7554.

Kadlecová, P. *et al.* (2015) 'Alcohol consumption at midlife and risk of stroke during 43 years of follow-up: cohort and twin analyses', *Stroke*, 46(3), pp. 627–633. doi:10.1161/STROKEAHA.114.006724.

Kernan, W.N. *et al.* (2014) 'Guidelines for the prevention of stroke in patients with stroke and transient ischemic attack: a guideline for healthcare professionals from the American Heart Association/American Stroke Association', *Stroke*, 45(7), pp. 2160–2236. doi:10.1161/STR.0000000000000024.

Khoshnam, S.E. *et al.* (2017) 'Pathogenic mechanisms following ischemic stroke', *Neurological Sciences: Official Journal of the Italian Neurological Society and of the Italian Society of Clinical Neurophysiology*, 38(7), pp. 1167–1186. doi:10.1007/s10072-017-2938-1.

Kida, S. *et al.* (1993) 'Perivascular cells act as scavengers in the cerebral perivascular spaces and remain distinct from pericytes, microglia and macrophages', *Acta Neuropathologica*, 85(6), pp. 646–652. doi:10.1007/BF00334675.

Kierdorf, K. *et al.* (2013) 'Microglia emerge from erythromyeloid precursors via Pu.1- and Irf8-dependent pathways', *Nature Neuroscience*, 16(3), pp. 273–280. doi:10.1038/nn.3318.

Kierdorf, K. *et al.* (2019) 'Macrophages at CNS interfaces: ontogeny and function in health and disease', *Nature Reviews. Neuroscience* [Preprint]. doi:10.1038/s41583-019-0201-x.

Kim, G.W., Sugawara, T. and Chan, P.H. (2000) 'Involvement of oxidative stress and caspase-3 in cortical infarction after photothrombotic ischemia in mice', *Journal of Cerebral Blood Flow and Metabolism: Official Journal of the International Society of Cerebral Blood Flow and Metabolism*, 20(12), pp. 1690–1701. doi:10.1097/00004647-200012000-00008.

Kim, W.-K. *et al.* (2006) 'CD163 Identifies Perivascular Macrophages in Normal and Viral Encephalitic Brains and Potential Precursors to Perivascular Macrophages in Blood', *The American Journal of Pathology*, 168(3), pp. 822–834. doi:10.2353/ajpath.2006.050215.

Knuesel, I. *et al.* (2014) 'Maternal immune activation and abnormal brain development across CNS disorders', *Nature Reviews Neurology*, 10(11), pp. 643–660. doi:10.1038/nrneurol.2014.187.

Kohler, E. *et al.* (2013) 'Intravenous minocycline in acute stroke: a randomized, controlled pilot study and meta-analysis', *Stroke*, 44(9), pp. 2493–2499. doi:10.1161/STROKEAHA.113.000780.

Kolaczowska, E. and Kubes, P. (2013) 'Neutrophil recruitment and function in health and inflammation', *Nature Reviews Immunology*, 13(3), pp. 159–175. doi:10.1038/nri3399.

Korin, B. *et al.* (2017) 'High-dimensional, single-cell characterization of the brain's immune compartment', *Nature Neuroscience*, 20(9), pp. 1300–1309. doi:10.1038/nn.4610.

Krasemann, S. *et al.* (2017) 'The TREM2-APOE Pathway Drives the Transcriptional Phenotype of Dysfunctional Microglia in Neurodegenerative Diseases', *Immunity*, 47(3), pp. 566–581.e9. doi:10.1016/j.immuni.2017.08.008.

Krishnamurthi, R.V. *et al.* (2013) 'Global and regional burden of first-ever ischaemic and haemorrhagic stroke during 1990–2010: findings from the Global Burden of Disease Study 2010', *The Lancet. Global Health*, 1(5), pp. e259–281. doi:10.1016/S2214-109X(13)70089-5.

Labat-gest, V. and Tomasi, S. (2013) 'Photothrombotic ischemia: a minimally invasive and reproducible photochemical cortical lesion model for mouse stroke studies', *Journal of Visualized Experiments: JoVE* [Preprint], (76). doi:10.3791/50370.

Lam, M.A. *et al.* (2017) 'The ultrastructure of spinal cord perivascular spaces: Implications for the circulation of cerebrospinal fluid', *Scientific Reports*, 7. doi:10.1038/s41598-017-13455-4.

Lane, J.H. *et al.* (1996) 'Neuroinvasion by simian immunodeficiency virus coincides with increased numbers of perivascular macrophages/microglia and intrathecal immune activation', *Journal of Neurovirology*, 2(6), pp. 423–432. doi:10.3109/13550289609146909.

Larsson, S.C. *et al.* (2016) 'Differing association of alcohol consumption with different stroke types: a systematic review and meta-analysis', *BMC Medicine*, 14(1), p. 178. doi:10.1186/s12916-016-0721-4.

Lawson, L.J. *et al.* (1990) 'Heterogeneity in the distribution and morphology of microglia in the normal adult mouse brain', *Neuroscience*, 39(1), pp. 151–170. doi:10.1016/0306-4522(90)90229-w.

Lee, V.M. *et al.* (1996) 'Evolution of photochemically induced focal cerebral ischemia in the rat. Magnetic resonance imaging and histology', *Stroke*, 27(11), pp. 2110–2118; discussion 2118–2119. doi:10.1161/01.str.27.11.2110.

Lehenkari, P.P. *et al.* (2002) 'Further insight into mechanism of action of clodronate: inhibition of mitochondrial ADP/ATP translocase by a nonhydrolyzable, adenine-containing metabolite', *Molecular Pharmacology*, 61(5), pp. 1255–1262. doi:10.1124/mol.61.5.1255.

Leibrand, C.R. *et al.* (2017) 'HIV-1 Tat disrupts blood-brain barrier integrity and increases phagocytic perivascular macrophages and microglia in the dorsal striatum of transgenic mice', *Neuroscience Letters*, 640, pp. 136–143. doi:10.1016/j.neulet.2016.12.073.

Levard, D. *et al.* (2020) 'Filling the gaps on stroke research: focus on inflammation and immunity', *Brain, Behavior, and Immunity* [Preprint]. doi:10.1016/j.bbi.2020.09.025.

Li, H. *et al.* (2000) 'Caspase inhibitors reduce neuronal injury after focal but not global cerebral ischemia in rats', *Stroke*, 31(1), pp. 176–182. doi:10.1161/01.str.31.1.176.

Liddel, S.A. *et al.* (2017) 'Neurotoxic reactive astrocytes are induced by activated microglia', *Nature*, 541(7638), pp. 481–487. doi:10.1038/nature21029.

Liu, F. *et al.* (2010) 'Expression of Na–K–Cl cotransporter and edema formation are age dependent after ischemic stroke', *Experimental Neurology*, 224(2), pp. 356–361. doi:10.1016/j.expneurol.2010.04.010.

Liu, F. *et al.* (2012) 'Effects of chronic and acute oestrogen replacement therapy in aged animals after experimental stroke', *Journal of Neuroendocrinology*, 24(2), pp. 319–330. doi:10.1111/j.1365-2826.2011.02248.x.

Liu, F. and McCullough, L.D. (2012) 'Interactions between age, sex, and hormones in experimental ischemic stroke', *Neurochemistry International*, 61(8), pp. 1255–1265. doi:10.1016/j.neuint.2012.10.003.

Liu, J. *et al.* (2013) 'Systematic review and meta-analysis of the efficacy of sphingosine-1-phosphate (S1P) receptor agonist FTY720 (fingolimod) in animal models of stroke', *The International Journal of Neuroscience*, 123(3), pp. 163–169. doi:10.3109/00207454.2012.749255.

Liu, Z. and Chopp, M. (2016) 'Astrocytes, therapeutic targets for neuroprotection and neurorestoration in ischemic stroke', *Progress in Neurobiology*, 144, pp. 103–120. doi:10.1016/j.pneurobio.2015.09.008.

Llovera, G. *et al.* (2014) 'Modeling Stroke in Mice: Permanent Coagulation of the Distal Middle Cerebral Artery', *Journal of Visualized Experiments: JoVE* [Preprint], (89). doi:10.3791/51729.

Llovera, G. *et al.* (2017) 'The choroid plexus is a key cerebral invasion route for T cells after stroke', *Acta Neuropathologica*, 134(6), pp. 851–868. doi:10.1007/s00401-017-1758-y.

Louveau, A. *et al.* (2017) 'Understanding the functions and relationships of the lymphatic system and meningeal lymphatics', *The Journal of Clinical Investigation*, 127(9), pp. 3210–3219. doi:10.1172/JCI90603.

Louveau, A. *et al.* (2018) 'CNS lymphatic drainage and neuroinflammation are regulated by meningeal lymphatic vasculature', *Nature Neuroscience*, 21(10), pp. 1380–1391. doi:10.1038/s41593-018-0227-9.

Lun, M.P., Monuki, E.S. and Lehtinen, M.K. (2015) 'Development and functions of the choroid plexus-cerebrospinal fluid system', *Nature Reviews. Neuroscience*, 16(8), pp. 445–457. doi:10.1038/nrn3921.

Lunardi Baccetto, S. and Lehmann, C. (2019) 'Microcirculatory Changes in Experimental Models of Stroke and CNS-Injury Induced Immunodepression', *International Journal of Molecular Sciences*, 20(20), p. 5184. doi:10.3390/ijms20205184.

Ma, J. *et al.* (2020) 'Impaired Collateral Flow in Pial Arterioles of Aged Rats During Ischemic Stroke', *Translational Stroke Research*, 11(2), p. 243. doi:10.1007/s12975-019-00710-1.

Macrez, R. *et al.* (2011) 'Antibodies preventing the interaction of tissue-type plasminogen activator with N-methyl-D-aspartate receptors reduce stroke damages and extend the therapeutic window of thrombolysis', *Stroke*, 42(8), pp. 2315–2322. doi:10.1161/STROKEAHA.110.606293.

Majno, G. and Joris, I. (2004) *Cells, Tissues, and Disease: Principles of General Pathology*. Oxford University Press.

Malhotra, K. *et al.* (2018) 'Minocycline for acute stroke treatment: a systematic review and meta-analysis of randomized clinical trials', *Journal of Neurology*, 265(8), pp. 1871–1879. doi:10.1007/s00415-018-8935-3.

Malone, K. *et al.* (2019) 'Immunomodulatory Therapeutic Strategies in Stroke', *Frontiers in Pharmacology*, 10. doi:10.3389/fphar.2019.00630.

Månberg, A. *et al.* (2021) 'Altered perivascular fibroblast activity precedes ALS disease onset', *Nature Medicine*, 27(4), pp. 640–646. doi:10.1038/s41591-021-01295-9.

Mandala, S. *et al.* (2002) 'Alteration of lymphocyte trafficking by sphingosine-1-phosphate receptor agonists', *Science (New York, N.Y.)*, 296(5566), pp. 346–349. doi:10.1126/science.1070238.

Marschallinger, J. *et al.* (2020) 'Lipid-droplet-accumulating microglia represent a dysfunctional and proinflammatory state in the aging brain', *Nature Neuroscience*, pp. 1–15. doi:10.1038/s41593-019-0566-1.

Martinez de Lizarrondo, S. *et al.* (2017) 'Potent Thrombolytic Effect of N-Acetylcysteine on Arterial Thrombi', *Circulation*, 136(7), pp. 646–660. doi:10.1161/CIRCULATIONAHA.117.027290.

Mato, M. *et al.* (1982) 'Uptake of fat by fluorescent granular perithelial cells in cerebral cortex after administration of fat rich chow', *Experientia*, 38(12), pp. 1496–1498. doi:10.1007/BF01955791.

Mato, M. *et al.* (1986) 'Tridimensional observation of fluorescent granular perithelial (FGP) cells in rat cerebral blood vessels', *The Anatomical Record*, 215(4), pp. 413–419. doi:10.1002/ar.1092150413.

Mato, M. *et al.* (1996) 'Involvement of specific macrophage-lineage cells surrounding arterioles in barrier and scavenger function in brain cortex', *Proceedings of the National Academy of Sciences of the United States of America*, 93(8), pp. 3269–3274. doi:10.1073/pnas.93.8.3269.

Mato, M., Ookawara, S. and Kurihara, K. (1980) 'Uptake of exogenous substances and marked infoldings of the fluorescent granular pericyte in cerebral fine vessels', *American Journal of Anatomy*, 157(3), pp. 329–332. doi:https://doi.org/10.1002/aja.1001570308.

Mayadas, T.N., Cullere, X. and Lowell, C.A. (2014) 'The Multifaceted Functions of Neutrophils', *Annual review of pathology*, 9, pp. 181–218. doi:10.1146/annurev-pathol-020712-164023.

McMenamin, P.G. *et al.* (2003) 'Macrophages and dendritic cells in the rat meninges and choroid plexus: three-dimensional localisation by environmental scanning electron microscopy and confocal microscopy', *Cell and Tissue Research*, 313(3), pp. 259–269. doi:10.1007/s00441-003-0779-0.

Medzhitov, R. (2008) 'Origin and physiological roles of inflammation', *Nature*, 454(7203), pp. 428–435. doi:10.1038/nature07201.

Medzhitov, R. (2010) 'Inflammation 2010: New Adventures of an Old Flame', *Cell*, 140(6), pp. 771–776. doi:10.1016/j.cell.2010.03.006.

Meisel, C. *et al.* (2005) 'Central nervous system injury-induced immune deficiency syndrome', *Nature Reviews. Neuroscience*, 6(10), pp. 775–786. doi:10.1038/nrn1765.

Mena, H., Cadavid, D. and Rushing, E.J. (2004) 'Human cerebral infarct: a proposed histopathologic classification based on 137 cases', *Acta Neuropathologica*, 108(6), pp. 524–530. doi:10.1007/s00401-004-0918-z.

Mishra, N.K. *et al.* (2010) 'Influence of Age on Outcome From Thrombolysis in Acute Stroke', *Stroke* [Preprint]. doi:10.1161/STROKEAHA.110.586206.

Mons, U. *et al.* (2015) 'Impact of smoking and smoking cessation on cardiovascular events and mortality among older adults: meta-analysis of individual participant data from

prospective cohort studies of the CHANCES consortium', *BMJ*, 350, p. h1551. doi:10.1136/bmj.h1551.

Montagne, A. *et al.* (2015) 'Blood-Brain Barrier Breakdown in the Aging Human Hippocampus', *Neuron*, 85(2), pp. 296–302. doi:10.1016/j.neuron.2014.12.032.

Mori, S. and Leblond, C.P. (1969) 'Identification of microglia in light and electron microscopy', *The Journal of Comparative Neurology*, 135(1), pp. 57–80. doi:10.1002/cne.901350104.

Mosher, K.I. and Wyss-Coray, T. (2014) 'Microglial dysfunction in brain aging and Alzheimer's disease', *Biochemical Pharmacology*, 88(4), pp. 594–604. doi:10.1016/j.bcp.2014.01.008.

Mrdjen, D. *et al.* (2018) 'High-Dimensional Single-Cell Mapping of Central Nervous System Immune Cells Reveals Distinct Myeloid Subsets in Health, Aging, and Disease', *Immunity*, 48(2), pp. 380-395.e6. doi:10.1016/j.immuni.2018.01.011.

Muriach, M. *et al.* (2014) 'Diabetes and the brain: oxidative stress, inflammation, and autophagy', *Oxidative Medicine and Cellular Longevity*, 2014, p. 102158. doi:10.1155/2014/102158.

Nabeshima, S. *et al.* (1975) 'Junctions in the meninges and marginal glia', *The Journal of Comparative Neurology*, 164(2), pp. 127–169. doi:10.1002/cne.901640202.

Nathan, C. (2006) 'Neutrophils and immunity: challenges and opportunities', *Nature Reviews. Immunology*, 6(3), pp. 173–182. doi:10.1038/nri1785.

Nikoletopoulou, V. *et al.* (2013) 'Crosstalk between apoptosis, necrosis and autophagy', *Biochimica Et Biophysica Acta*, 1833(12), pp. 3448–3459. doi:10.1016/j.bbamcr.2013.06.001.

Norden, D.M., Muccigrosso, M.M. and Godbout, J.P. (2015) 'Microglial priming and enhanced reactivity to secondary insult in aging, and traumatic CNS injury, and neurodegenerative disease', *Neuropharmacology*, 96, pp. 29–41. doi:10.1016/j.neuropharm.2014.10.028.

Oehmichen, M. (1976) 'Characterization of mononuclear phagocytes in human CSF using membrane markers', *Acta Cytologica*, 20(6), pp. 548–552.

Orset, C. *et al.* (2007) 'Mouse model of in situ thromboembolic stroke and reperfusion', *Stroke*, 38(10), pp. 2771–2778. doi:10.1161/STROKEAHA.107.487520.

Orset, C. *et al.* (2016) 'Efficacy of Alteplase in a Mouse Model of Acute Ischemic Stroke: A Retrospective Pooled Analysis', *Stroke*, 47(5), pp. 1312–1318. doi:10.1161/STROKEAHA.116.012238.

Pace, J.L. *et al.* (1983) 'Recombinant mouse gamma interferon induces the priming step in macrophage activation for tumor cell killing', *Journal of Immunology (Baltimore, Md.: 1950)*, 130(5), pp. 2011–2013.

Papadopoulos, Z., Herz, J. and Kipnis, J. (2020) 'Meningeal Lymphatics: From Anatomy to Central Nervous System Immune Surveillance', *Journal of Immunology (Baltimore, Md.: 1950)*, 204(2), pp. 286–293. doi:10.4049/jimmunol.1900838.

Park, L. *et al.* (2017) 'Brain Perivascular Macrophages Initiate the Neurovascular Dysfunction of Alzheimer A β Peptides', *Circulation Research*, 121(3), pp. 258–269. doi:10.1161/CIRCRESAHA.117.311054.

Parnes, O. (2008) 'Inflammation', *The Lancet*, 372(9639), p. 621. doi:10.1016/S0140-6736(08)61262-3.

Pedragosa, J. *et al.* (2018) 'CNS-border associated macrophages respond to acute ischemic stroke attracting granulocytes and promoting vascular leakage', *Acta Neuropathologica Communications*, 6(1), p. 76. doi:10.1186/s40478-018-0581-6.

Perez-de-Puig, I. *et al.* (2015) 'Neutrophil recruitment to the brain in mouse and human ischemic stroke', *Acta Neuropathologica*, 129(2), pp. 239–257. doi:10.1007/s00401-014-1381-0.

Perry, V.H., Nicoll, J.A.R. and Holmes, C. (2010) 'Microglia in neurodegenerative disease', *Nature Reviews. Neurology*, 6(4), pp. 193–201. doi:10.1038/nrneurol.2010.17.

Peters, S.A.E., Huxley, R.R. and Woodward, M. (2014) 'Diabetes as a risk factor for stroke in women compared with men: a systematic review and meta-analysis of 64 cohorts, including 775 385 individuals and 12 539 strokes', *The Lancet*, 383(9933), pp. 1973–1980. doi:10.1016/S0140-6736(14)60040-4.

Polfliet, M.M., Goede, P.H., *et al.* (2001) 'A method for the selective depletion of perivascular and meningeal macrophages in the central nervous system', *Journal of Neuroimmunology*, 116(2), pp. 188–195.

Polfliet, M.M., Zwijnenburg, P.J., *et al.* (2001) 'Meningeal and perivascular macrophages of the central nervous system play a protective role during bacterial meningitis', *Journal of Immunology (Baltimore, Md.: 1950)*, 167(8), pp. 4644–4650. doi:10.4049/jimmunol.167.8.4644.

Polfliet, M.M.J. *et al.* (2002) 'The role of perivascular and meningeal macrophages in experimental allergic encephalomyelitis', *Journal of Neuroimmunology*, 122(1), pp. 1–8. doi:10.1016/S0165-5728(01)00445-3.

Polman, C.H. *et al.* (2006) 'A Randomized, Placebo-Controlled Trial of Natalizumab for Relapsing Multiple Sclerosis', *New England Journal of Medicine*, 354(9), pp. 899–910. doi:10.1056/NEJMoa044397.

Postolache, T.T. *et al.* (2020) 'Inflammation in Traumatic Brain Injury', *Journal of Alzheimer's disease : JAD*, 74(1), p. 1. doi:10.3233/JAD-191150.

Prass, K. *et al.* (2003) 'Stroke-induced immunodeficiency promotes spontaneous bacterial infections and is mediated by sympathetic activation reversal by poststroke T helper

cell type 1-like immunostimulation', *The Journal of Experimental Medicine*, 198(5), pp. 725–736. doi:10.1084/jem.20021098.

Prinz, M. *et al.* (2021) 'Microglia and Central Nervous System-Associated Macrophages-From Origin to Disease Modulation', *Annual Review of Immunology* [Preprint]. doi:10.1146/annurev-immunol-093019-110159.

Prinz, M., Erny, D. and Hagemeyer, N. (2017) 'Ontogeny and homeostasis of CNS myeloid cells', *Nature Immunology*, 18(4), pp. 385–392. doi:10.1038/ni.3703.

Prinz, M., Jung, S. and Priller, J. (2019) 'Microglia Biology: One Century of Evolving Concepts', *Cell*, 179(2), pp. 292–311. doi:10.1016/j.cell.2019.08.053.

Prinz, M. and Priller, J. (2014) 'Microglia and brain macrophages in the molecular age: from origin to neuropsychiatric disease', *Nature Reviews. Neuroscience*, 15(5), pp. 300–312. doi:10.1038/nrn3722.

Püntener, U. *et al.* (2012) 'Long-term impact of systemic bacterial infection on the cerebral vasculature and microglia', *Journal of Neuroinflammation*, 9(1), pp. 1–13. doi:10.1186/1742-2094-9-146.

Rajan, W.D. *et al.* (2020) 'Defining molecular identity and fates of CNS-border associated macrophages after ischemic stroke in rodents and humans', *Neurobiology of Disease*, 137, p. 104722. doi:10.1016/j.nbd.2019.104722.

Raman, G. *et al.* (2013) 'Management Strategies for Asymptomatic Carotid Stenosis', *Annals of Internal Medicine*, 158(9), pp. 676–685. doi:10.7326/0003-4819-158-9-201305070-00007.

Ransohoff, R.M. and Brown, M.A. (2012) 'Innate immunity in the central nervous system', *The Journal of Clinical Investigation*, 122(4), pp. 1164–1171. doi:10.1172/JCI58644.

Ransohoff, R.M. and El Khoury, J. (2015) 'Microglia in Health and Disease', *Cold Spring Harbor Perspectives in Biology*, 8(1), p. a020560. doi:10.1101/cshperspect.a020560.

Ransohoff, R.M. and Engelhardt, B. (2012) 'The anatomical and cellular basis of immune surveillance in the central nervous system', *Nature Reviews Immunology*, 12(9), pp. 623–635. doi:10.1038/nri3265.

Rasmussen, M.K., Mestre, H. and Nedergaard, M. (2018) 'The glymphatic pathway in neurological disorders', *The Lancet Neurology*, 17(11), pp. 1016–1024. doi:10.1016/S1474-4422(18)30318-1.

Rayasam, A. *et al.* (2018) 'Immune responses in stroke: how the immune system contributes to damage and healing after stroke and how this knowledge could be translated to better cures?', *Immunology*, 154(3), pp. 363–376. doi:10.1111/imm.12918.

Rehm, J. *et al.* (2013) 'Defining substance use disorders: do we really need more than heavy use?', *Alcohol and Alcoholism (Oxford, Oxfordshire)*, 48(6), pp. 633–640. doi:10.1093/alcalc/agt127.

Roche, P.A. and Furuta, K. (2015) 'The ins and outs of MHC class II-mediated antigen processing and presentation', *Nature Reviews Immunology*, 15(4), pp. 203–216. doi:10.1038/nri3818.

Roy-O'Reilly, M.A. *et al.* (2020) 'Aging exacerbates neutrophil pathogenicity in ischemic stroke', *Aging (Albany NY)*, 12(1), p. 436. doi:10.18632/aging.102632.

Rustenhoven, J. *et al.* (2021) 'Functional characterization of the dural sinuses as a neuroimmune interface', *Cell*, 0(0). doi:10.1016/j.cell.2020.12.040.

Sadler, R. *et al.* (2019) 'Short-chain fatty acids improve post-stroke recovery via immunological mechanisms', *The Journal of Neuroscience: The Official Journal of the Society for Neuroscience* [Preprint]. doi:10.1523/JNEUROSCI.1359-19.2019.

Sarwar, N. *et al.* (2010) 'Diabetes mellitus, fasting blood glucose concentration, and risk of vascular disease: a collaborative meta-analysis of 102 prospective studies', *Lancet*, 375(9733), p. 2215. doi:10.1016/S0140-6736(10)60484-9.

Se, H. *et al.* (2006) 'The P2Y₁₂ receptor regulates microglial activation by extracellular nucleotides', *Nature neuroscience*, 9(12). doi:10.1038/nn1805.

Serhan, C.N. and Savill, J. (2005) 'Resolution of inflammation: the beginning programs the end', *Nature Immunology*, 6(12), pp. 1191–1197. doi:10.1038/ni1276.

Sharma, A. *et al.* (2020) 'Effect of Age on Arterial Recanalization and Clinical Outcome in Thrombolysed Acute Ischemic Stroke in CLOTBUST Cohort', *Annals of Indian Academy of Neurology*, 23(2), pp. 189–194. doi:10.4103/aian.aian_434_19.

Shi, K. *et al.* (2019) 'Global brain inflammation in stroke', *The Lancet Neurology*, 18(11), pp. 1058–1066. doi:10.1016/S1474-4422(19)30078-X.

Shi, L. *et al.* (2020) 'Genome-wide transcriptomic analysis of microglia reveals impaired responses in aged mice after cerebral ischemia', *Journal of Cerebral Blood Flow and Metabolism: Official Journal of the International Society of Cerebral Blood Flow and Metabolism*, 40(1_suppl), pp. S49–S66. doi:10.1177/0271678X20925655.

Shiple, F.B. *et al.* (2020) 'Tracking Calcium Dynamics and Immune Surveillance at the Choroid Plexus Blood-Cerebrospinal Fluid Interface', *Neuron*, 108(4), p. 623. doi:10.1016/j.neuron.2020.08.024.

Shukla, V. *et al.* (2017) 'Cerebral ischemic damage in diabetes: an inflammatory perspective', *Journal of Neuroinflammation*, 14(1), p. 21. doi:10.1186/s12974-016-0774-5.

Sierra, A. *et al.* (2016) 'The "Big-Bang" for modern glial biology: Translation and comments on Pío del Río-Hortega 1919 series of papers on microglia', *Glia*, 64(11), pp. 1801–1840. doi:10.1002/glia.23046.

Smith, C.J. *et al.* (2015) 'Phase II anti-inflammatory and immune-modulating drugs for acute ischaemic stroke', *Expert Opinion on Investigational Drugs*, 24(5), pp. 623–643. doi:10.1517/13543784.2015.1020110.

Sommer, C.J. (2017) 'Ischemic stroke: experimental models and reality', *Acta Neuropathologica*, 133(2), pp. 245–261. doi:10.1007/s00401-017-1667-0.

Steel, C.D. *et al.* (2010) 'Distinct macrophage subpopulations regulate viral encephalitis but not viral clearance in the CNS', *Journal of Neuroimmunology*, 226(1–2), pp. 81–92. doi:10.1016/j.jneuroim.2010.05.034.

Steffen, B.J. *et al.* (1996) 'ICAM-1, VCAM-1, and MAdCAM-1 are expressed on choroid plexus epithelium but not endothelium and mediate binding of lymphocytes in vitro', *The American Journal of Pathology*, 148(6), pp. 1819–1838.

Suenaga, J. *et al.* (2015) 'White matter injury and microglia/macrophage polarization are strongly linked with age-related long-term deficits in neurological function after stroke', *Experimental Neurology*, 272, pp. 109–119. doi:10.1016/j.expneurol.2015.03.021.

Szalay, G. *et al.* (2016) 'Microglia protect against brain injury and their selective elimination dysregulates neuronal network activity after stroke', *Nature Communications*, 7, p. 11499. doi:10.1038/ncomms11499.

Tay, T.L. *et al.* (2017) 'A new fate mapping system reveals context-dependent random or clonal expansion of microglia', *Nature Neuroscience*, 20(6), pp. 793–803. doi:10.1038/nn.4547.

Thanopoulou, K. *et al.* (2010) 'Scavenger receptor class B type I (SR-BI) regulates perivascular macrophages and modifies amyloid pathology in an Alzheimer mouse model', *Proceedings of the National Academy of Sciences of the United States of America*, 107(48), pp. 20816–20821. doi:10.1073/pnas.1005888107.

Thomalla, G. and Gerloff, C. (2019) 'Acute imaging for evidence-based treatment of ischemic stroke', *Current Opinion in Neurology*, 32(4), pp. 521–529. doi:10.1097/WCO.0000000000000716.

Thompson, K.A. *et al.* (2009) 'Cell-specific temporal infection of the brain in a simian immunodeficiency virus model of human immunodeficiency virus encephalitis', *Journal of Neurovirology*, 15(4), pp. 300–311. doi:10.1080/13550280903030125.

Utz, S.G. *et al.* (2020) 'Early Fate Defines Microglia and Non-parenchymal Brain Macrophage Development', *Cell*, 0(0). doi:10.1016/j.cell.2020.03.021.

Uzdensky, A.B. (2018) 'Photothrombotic Stroke as a Model of Ischemic Stroke', *Translational Stroke Research*, 9(5), pp. 437–451. doi:10.1007/s12975-017-0593-8.

Vallés, J. *et al.* (2017) 'Neutrophil extracellular traps are increased in patients with acute ischemic stroke: prognostic significance', *Thrombosis and Haemostasis*, 117(10), pp. 1919–1929. doi:10.1160/TH17-02-0130.

Vasek, M.J. *et al.* (2016) 'A complement–microglial axis drives synapse loss during virus-induced memory impairment', *Nature*, 534(7608), pp. 538–543. doi:10.1038/nature18283.

Veltkamp, R. and Gill, D. (2016) 'Clinical Trials of Immunomodulation in Ischemic Stroke', *Neurotherapeutics: The Journal of the American Society for Experimental NeuroTherapeutics*, 13(4), pp. 791–800. doi:10.1007/s13311-016-0458-y.

Virani, S.S. *et al.* (2020) 'Heart Disease and Stroke Statistics-2020 Update: A Report From the American Heart Association', *Circulation*, 141(9), pp. e139–e596. doi:10.1161/CIR.0000000000000757.

Wan, H. *et al.* (2021) 'Role of perivascular and meningeal macrophages in outcome following experimental subarachnoid hemorrhage', *Journal of Cerebral Blood Flow and Metabolism: Official Journal of the International Society of Cerebral Blood Flow and Metabolism*, p. 271678X20980296. doi:10.1177/0271678X20980296.

Watson, B.D. *et al.* (1985) 'Induction of reproducible brain infarction by photochemically initiated thrombosis', *Annals of Neurology*, 17(5), pp. 497–504. doi:10.1002/ana.410170513.

Weller, R.O. (2005) 'Microscopic morphology and histology of the human meninges', *Morphologie*, 89(284), pp. 22–34. doi:10.1016/S1286-0115(05)83235-7.

Williams, K.C. *et al.* (2001) 'Perivascular macrophages are the primary cell type productively infected by simian immunodeficiency virus in the brains of macaques: implications for the neuropathogenesis of AIDS', *The Journal of Experimental Medicine*, 193(8), pp. 905–915. doi:10.1084/jem.193.8.905.

Willis, C.L., Garwood, C.J. and Ray, D.E. (2007) 'A size selective vascular barrier in the rat area postrema formed by perivascular macrophages and the extracellular matrix', *Neuroscience*, 150(2), pp. 498–509. doi:10.1016/j.neuroscience.2007.09.023.

Wilson, E.H., Weninger, W. and Hunter, C.A. (2010) 'Trafficking of immune cells in the central nervous system', *The Journal of Clinical Investigation*, 120(5), pp. 1368–1379. doi:10.1172/JCI41911.

Winklewski, P.J. *et al.* (2015) 'Brain inflammation and hypertension: the chicken or the egg?', *Journal of Neuroinflammation*, 12, p. 85. doi:10.1186/s12974-015-0306-8.

Wise, P.M. *et al.* (2001) 'Estradiol is a protective factor in the adult and aging brain: understanding of mechanisms derived from in vivo and in vitro studies', *Brain Research. Brain Research Reviews*, 37(1–3), pp. 313–319. doi:10.1016/s0165-0173(01)00136-9.

Xu, S. *et al.* (2020) 'Glial Cells: Role of the Immune Response in Ischemic Stroke', *Frontiers in Immunology*, 11, p. 294. doi:10.3389/fimmu.2020.00294.

Xue, J. *et al.* (2017) 'Neutrophil-to-Lymphocyte Ratio Is a Prognostic Marker in Acute Ischemic Stroke', *Journal of Stroke and Cerebrovascular Diseases: The Official Journal of National Stroke Association*, 26(3), pp. 650–657. doi:10.1016/j.jstrokecerebrovasdis.2016.11.010.

Yan, T., Chopp, M. and Chen, J. (2015) 'Experimental animal models and inflammatory cellular changes in cerebral ischemic and hemorrhagic stroke', *Neuroscience Bulletin*, 31(6), pp. 717–734. doi:10.1007/s12264-015-1567-z.

Yanev, P. *et al.* (2020) 'Impaired meningeal lymphatic vessel development worsens stroke outcome', *Journal of Cerebral Blood Flow and Metabolism: Official Journal of the International Society of Cerebral Blood Flow and Metabolism*, 40(2), pp. 263–275. doi:10.1177/0271678X18822921.

Yang, T., Guo, R. and Zhang, F. (2019) 'Brain perivascular macrophages: Recent advances and implications in health and diseases', *CNS Neuroscience & Therapeutics*, n/a(n/a). doi:10.1111/cns.13263.

Zhan, Y. *et al.* (2014) 'Deficient neuron-microglia signaling results in impaired functional brain connectivity and social behavior', *Nature Neuroscience*, 17(3), pp. 400–406. doi:10.1038/nn.3641.

Zhang, C. *et al.* (2014) 'Alcohol intake and risk of stroke: A dose–response meta-analysis of prospective studies', *International Journal of Cardiology*, 174(3), pp. 669–677. doi:10.1016/j.ijcard.2014.04.225.

Zhang, D.J. *et al.* (2017) 'Culture media-based selection of endothelial cells, pericytes, and perivascular-resident macrophage-like melanocytes from the young mouse vestibular system', *Hearing research*, 345, p. 10. doi:10.1016/j.heares.2016.12.012.

Zhang, S. *et al.* (2017) 'Rationale and design of combination of an immune modulator Fingolimod with Alteplase bridging with Mechanical Thrombectomy in Acute Ischemic Stroke (FAMTAIS) trial', *International Journal of Stroke: Official Journal of the International Stroke Society*, 12(8), pp. 906–909. doi:10.1177/1747493017710340.

Zhang, W. *et al.* (2012) 'Perivascular-resident macrophage-like melanocytes in the inner ear are essential for the integrity of the intrastrial fluid-blood barrier', *Proceedings of the National Academy of Sciences of the United States of America*, 109(26), pp. 10388–10393. doi:10.1073/pnas.1205210109.

Zhang, Z. *et al.* (2011) 'Parenchymal accumulation of CD163+ macrophages/microglia in multiple sclerosis brains', *Journal of Neuroimmunology*, 237(1–2), pp. 73–79. doi:10.1016/j.jneuroim.2011.06.006.

Zhang, Z. *et al.* (2012) 'Lesional accumulation of CD163+ macrophages/microglia in rat traumatic brain injury', *Brain Research*, 1461, pp. 102–110. doi:10.1016/j.brainres.2012.04.038.

Zhou, W. *et al.* (2013) 'Postischemic brain infiltration of leukocyte subpopulations differs among murine permanent and transient focal cerebral ischemia models', *Brain Pathology (Zurich, Switzerland)*, 23(1), pp. 34–44. doi:10.1111/j.1750-3639.2012.00614.x.

Zhu, Z. *et al.* (2015) 'Combination of the Immune Modulator Fingolimod With Alteplase in Acute Ischemic Stroke: A Pilot Trial', *Circulation*, 132(12), pp. 1104–1112. doi:10.1161/CIRCULATIONAHA.115.016371.

del Zoppo, G.J. (2010) 'The neurovascular unit in the setting of stroke', *Journal of Internal Medicine*, 267(2), pp. 156–171. doi:10.1111/j.1365-2796.2009.02199.x.

Les macrophages périvasculaires cérébraux comme modulateurs de la réponse inflammatoire post-ischémique

Résumé

L'AVC ischémique est l'une des principales causes de décès et d'invalidité permanente dans le monde. Les processus inflammatoires induits par l'AVC ont été proposés comme des contributeurs clés de la physiopathologie de l'AVC ischémique. Alors que le rôle de la microglie dans l'AVC ischémique a été largement étudié, celles des macrophages associés aux bordures du SNC (BAMs) restent largement inconnues. Notre hypothèse, basée sur les études décrites précédemment et sur la localisation privilégiée des BAMs à l'interface entre le compartiment vasculaire et le parenchyme cérébral, était que les BAMs pouvaient jouer un rôle majeur dans la réponse inflammatoire déclenchée par l'AVC, *via* la médiation du recrutement et l'infiltration des leucocytes. De plus, sur la base d'études précédentes, nous avons fait l'hypothèse que les BAMs pourraient moduler les réponses inflammatoires induites par l'AVC de manière différente en fonction de l'état inflammatoire basal du cerveau, en particulier au cours du vieillissement.

Pour tester cette hypothèse, nous avons étudié l'AVC chez des souris jeunes et âgées avec ou sans déplétion antérieure des BAMs. Nos résultats ont montré que le déficit fonctionnel de l'AVC était aggravé chez les souris âgées déplétées en BAMs. Cette aggravation du résultat fonctionnel s'accompagnait (i) d'une augmentation de l'expression de la P-sélectine endothéliale, (ii) d'une augmentation du roulement et de l'adhésion des leucocytes à la paroi vasculaire, et (iii) une infiltration accrue de leucocytes dans l'hémisphère lésé. Ces réponses immunitaires exacerbées étaient présentes à la fois dans la phase aiguë et subaiguë après le début de l'AVC, suggérant ainsi que la présence de BAMs assure un contrôle à long terme de la réponse immunitaire après un AVC. En utilisant le séquençage ARN à partir de BAMs isolés, nous montrons que les BAMs modifient leur phénotype transcriptomique au cours du vieillissement pour surexprimer des gènes impliqués dans la régulation de la réponse immunitaire innée et adaptative et de la présentation des antigènes.

Nos résultats montrent que les BAMs acquièrent au cours du vieillissement un rôle central dans l'orchestration de la réponse neuroinflammatoire déclenchées par un AVC, et que leur présence garantit une bonne régulation de la réponse immunitaire

Mots-clés : Accident vasculaire cérébral, Neuroinflammation, Macrophages, Périvasculaire

Brain perivascular macrophages as modulators of the post-ischemic inflammatory response

Abstract

Ischemic stroke is one of the main causes of death and permanent disability worldwide. Stroke-induced inflammatory processes, including the activation of resident glial cells as well as the invasion of circulating leukocytes, have been proposed as key contributors of the ischemic stroke pathophysiology. While the responses of microglia to ischemic stroke have been extensively studied, those of border-associated macrophages (BAMs) remain largely unknown. In this study, we hypothesized that BAMs could influence stroke-induced inflammatory responses, particularly during aging and thus final stroke recovery.

We thus compared stroke outcome in young and old mice subjected to thromboembolic stroke with or without a previous depletion of BAMs. Our results show that functional outcome following stroke was worsened in depleted mice without modification of the lesion volumes, exclusively in aged mice. This worsening in the functional outcome was accompanied by (i) an increase of endothelial P-selectin expression, (ii) an increased leukocyte rolling and adhesion to the vessel wall, and (iii) an increased leukocyte infiltration in the injured hemisphere. These exacerbated immune responses were present at both the acute and the sub-acute phase (up to 5 days) after stroke onset, thus suggesting that the presence of BAMs ensures a long-term control of the immune response after stroke. Using cell sorted RNAseq, we show that BAMs change their transcriptomic phenotype during aging, overexpressing genes implicated in the regulation of both innate and adaptive immune responses and antigen presentation.

Taken together, our results reveal that BAMs acquire during aging a central role in orchestrating the neuroinflammatory response triggered by stroke, and that their presence guarantees good regulation of the immune response.

Key words: Stroke, Neuroinflammation, Macrophages, Perivascular